NTMS, CONNECTIVITY AND NEUROMODULATION IN BRAIN TUMOR PATIENTS

EDITED BY: Antonino F. Germano', Giovanni Raffa, András Büki and Thomas Picht

PUBLISHED IN: Frontiers in Neurology and Frontiers in Oncology

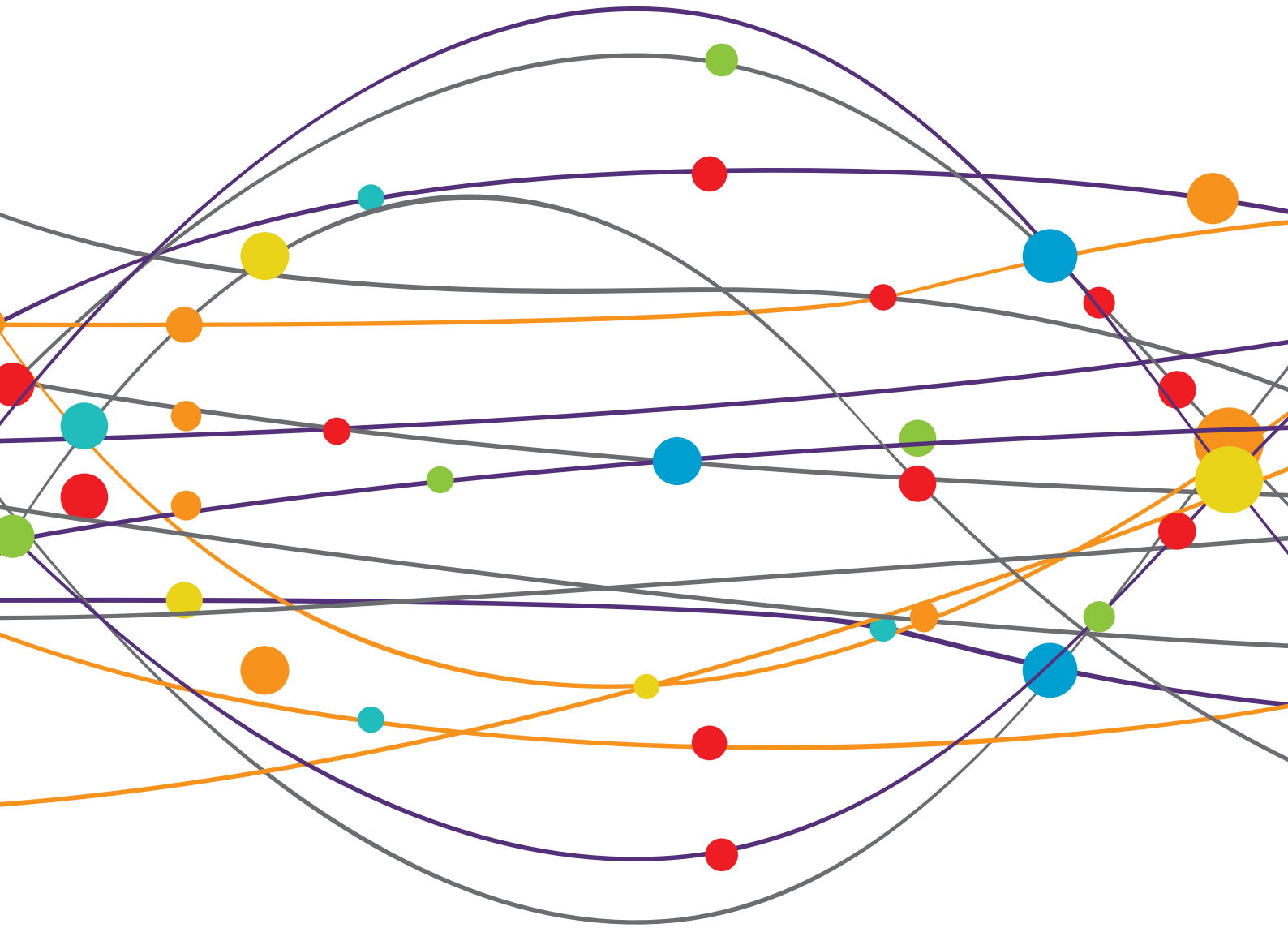

frontiers Research Topics

ISSN 1664-8714
ISBN 978-2-88976-031-2
DOI 10.3389/978-2-88976-031-2

About Frontiers

Frontiers is more than just an open-access publisher of scholarly articles: it is a pioneering approach to the world of academia, radically improving the way scholarly research is managed. The grand vision of Frontiers is a world where all people have an equal opportunity to seek, share and generate knowledge. Frontiers provides immediate and permanent online open access to all its publications, but this alone is not enough to realize our grand goals.

Frontiers Journal Series

The Frontiers Journal Series is a multi-tier and interdisciplinary set of open-access, online journals, promising a paradigm shift from the current review, selection and dissemination processes in academic publishing. All Frontiers journals are driven by researchers for researchers; therefore, they constitute a service to the scholarly community. At the same time, the Frontiers Journal Series operates on a revolutionary invention, the tiered publishing system, initially addressing specific communities of scholars, and gradually climbing up to broader public understanding, thus serving the interests of the lay society, too.

Dedication to Quality

Each Frontiers article is a landmark of the highest quality, thanks to genuinely collaborative interactions between authors and review editors, who include some of the world's best academicians. Research must be certified by peers before entering a stream of knowledge that may eventually reach the public - and shape society; therefore, Frontiers only applies the most rigorous and unbiased reviews.
Frontiers revolutionizes research publishing by freely delivering the most outstanding research, evaluated with no bias from both the academic and social point of view. By applying the most advanced information technologies, Frontiers is catapulting scholarly publishing into a new generation.

What are Frontiers Research Topics?

Frontiers Research Topics are very popular trademarks of the Frontiers Journals Series: they are collections of at least ten articles, all centered on a particular subject. With their unique mix of varied contributions from Original Research to Review Articles, Frontiers Research Topics unify the most influential researchers, the latest key findings and historical advances in a hot research area! Find out more on how to host your own Frontiers Research Topic or contribute to one as an author by contacting the Frontiers Editorial Office: frontiersin.org/about/contact

NTMS, CONNECTIVITY AND NEUROMODULATION IN BRAIN TUMOR PATIENTS

Topic Editors:
Antonino F. Germano', University of Messina, Italy
Giovanni Raffa, University of Messina, Italy
András Büki, University of Pécs, Hungary
Thomas Picht, Charité Universitätsmedizin Berlin, Germany

Citation: Germano', A. F., Raffa, G., Büki, A., Picht, T., eds. (2022). nTMS, Connectivity and Neuromodulation in Brain Tumor Patients. Lausanne: Frontiers Media SA. doi: 10.3389/978-2-88976-031-2

Table of Contents

06 ***Editorial: nTMS, Connectivity and Neuromodulation in Brain Tumor Patients***
Giovanni Raffa, Thomas Picht, András Büki and Antonino Germanò

10 ***Can Non-invasive Brain Stimulation Be Considered to Facilitate Reoperation for Low-Grade Glioma Relapse by Eliciting Neuroplasticity?***
Hugues Duffau

15 ***Preoperative Transcranial Direct Current Stimulation in Glioma Patients: A Proof of Concept Pilot Study***
Stefan Lang, Liu Shi Gan, Cael McLennan, Adam Kirton, Oury Monchi and John J. P. Kelly

28 ***Preoperative Applications of Navigated Transcranial Magnetic Stimulation***
Alexander F. Haddad, Jacob S. Young, Mitchel S. Berger and Phiroz E. Tarapore

39 ***Evaluation of Changes in Preoperative Cortical Excitability by Navigated Transcranial Magnetic Stimulation in Patients With Brain Tumor***
Iuri Santana Neville, Alexandra Gomes dos Santos, Cesar Cimonari Almeida, Cintya Yukie Hayashi, Davi Jorge Fontoura Solla, Ricardo Galhardoni, Daniel Ciampi de Andrade, Andre Russowsky Brunoni, Manoel Jacobsen Teixeira and Wellingson Silva Paiva

50 ***Detecting Corticospinal Tract Impairment in Tumor Patients With Fiber Density and Tensor-Based Metrics***
Lucius S. Fekonja, Ziqian Wang, Dogu B. Aydogan, Timo Roine, Melina Engelhardt, Felix R. Dreyer, Peter Vajkoczy and Thomas Picht

62 ***Time-Frequency Representation of Motor Evoked Potentials in Brain Tumor Patients***
Kathrin Machetanz, Alberto L. Gallotti, Maria Teresa Leao Tatagiba, Marina Liebsch, Leonidas Trakolis, Sophie Wang, Marcos Tatagiba, Alireza Gharabaghi and Georgios Naros

73 ***Perspectives on (A)symmetry of Arcuate Fasciculus. A Short Review About Anatomy, Tractography and TMS for Arcuate Fasciculus Reconstruction in Planning Surgery for Gliomas in Language Areas***
Andrea Di Cristofori, Gianpaolo Basso, Camilla de Laurentis, Ilaria Mauri, Martina Andrea Sirtori, Carlo Ferrarese, Valeria Isella and Carlo Giussani

81 ***Risk Assessment by Pre-surgical Tractography in Left Hemisphere Low-Grade Gliomas***
Tamara Ius, Teresa Somma, Cinzia Baiano, Ilaria Guarracino, Giada Pauletto, Annacarmen Nilo, Marta Maieron, Francesca Palese, Miran Skrap and Barbara Tomasino

94 ***The Frontal Aslant Tract: A Systematic Review for Neurosurgical Applications***
Emanuele La Corte, Daniela Eldahaby, Elena Greco, Domenico Aquino, Giacomo Bertolini, Vincenzo Levi, Malte Ottenhausen, Greta Demichelis, Luigi Michele Romito, Francesco Acerbi, Morgan Broggi, Marco Paolo Schiariti, Paolo Ferroli, Maria Grazia Bruzzone and Graziano Serrao

109 ***High Grade Glioma Treatment in Elderly People: Is It Different Than in Younger Patients? Analysis of Surgical Management Guided by an Intraoperative Multimodal Approach and Its Impact on Clinical Outcome***
Giuseppe Maria Vincenzo Barbagallo, Roberto Altieri, Marco Garozzo, Massimiliano Maione, Stefania Di Gregorio, Massimiliano Visocchi, Simone Peschillo, Pasquale Dolce and Francesco Certo

118 ***From Neurosurgical Planning to Histopathological Brain Tumor Characterization: Potentialities of Arcuate Fasciculus Along-Tract Diffusion Tensor Imaging Tractography Measures***
Matteo Zoli, Lia Talozzi, Matteo Martinoni, David N. Manners, Filippo Badaloni, Claudia Testa, Sofia Asioli, Micaela Mitolo, Fiorina Bartiromo, Magali Jane Rochat, Viscardo Paolo Fabbri, Carmelo Sturiale, Alfredo Conti, Raffaele Lodi, Diego Mazzatenta and Caterina Tonon

134 ***Optimizing Adjuvant Stereotactic Radiotherapy of Motor-Eloquent Brain Metastases: Sparing the nTMS-Defined Motor Cortex and the Hippocampus***
Yvonne Dzierma, Michaela Schuermann, Patrick Melchior, Frank Nuesken, Joachim Oertel, Christian Rübe and Philipp Hendrix

146 ***Brain Mapping-Aided SupraTotal Resection (SpTR) of Brain Tumors: The Role of Brain Connectivity***
Giuseppe Roberto Giammalva, Lara Brunasso, Roberta Costanzo, Federica Paolini, Giuseppe Emmanuele Umana, Gianluca Scalia, Cesare Gagliardo, Rosa Maria Gerardi, Luigi Basile, Francesca Graziano, Carlo Gulì, Domenico Messina, Maria Angela Pino, Paola Feraco, Silvana Tumbiolo, Massimo Midiri, Domenico Gerardo Iacopino and Rosario Maugeri

153 ***The Cologne Picture Naming Test for Language Mapping and Monitoring (CoNaT): An Open Set of 100 Black and White Object Drawings***
Carolin Weiss Lucas, Julia Pieczewski, Sophia Kochs, Charlotte Nettekoven, Christian Grefkes, Roland Goldbrunner and Kristina Jonas

168 ***Navigated Transcranial Magnetic Stimulation Motor Mapping Usefulness in the Surgical Management of Patients Affected by Brain Tumors in Eloquent Areas: A Systematic Review and Meta-Analysis***
Giuseppe Emmanuele Umana, Gianluca Scalia, Francesca Graziano, Rosario Maugeri, Nicola Alberio, Fabio Barone, Antonio Crea, Saverio Fagone, Giuseppe Roberto Giammalva, Lara Brunasso, Roberta Costanzo, Federica Paolini, Rosa Maria Gerardi, Silvana Tumbiolo, Salvatore Cicero, Giovanni Federico Nicoletti and Domenico Gerardo Iacopino

176 ***Middle Frontal Gyrus and Area 55b: Perioperative Mapping and Language Outcomes***
Sally Rosario Hazem, Mariam Awan, Jose Pedro Lavrador, Sabina Patel, Hilary Margaret Wren, Oeslle Lucena, Carla Semedo, Hassna Irzan, Andrew Melbourne, Sebastien Ourselin, Jonathan Shapey, Ahilan Kailaya-Vasan, Richard Gullan, Keyoumars Ashkan, Ranjeev Bhangoo and Francesco Vergani

190 ***Should Complex Cognitive Functions Be Mapped With Direct Electrostimulation in Wide-Awake Surgery? A Network Perspective***
Guillaume Herbet

195 ***Repetitive Transcranial Magnetic Stimulation for Tinnitus Treatment in Vestibular Schwannoma: A Pilot Study***
Maria Teresa Leao, Kathrin Machetanz, Joey Sandritter, Marina Liebsch, Andreas Stengel, Marcos Tatagiba and Georgios Naros

204 ***Pre-surgical fMRI Localization of the Hand Motor Cortex in Brain Tumors: Comparison Between Finger Tapping Task and a New Visual-Triggered Finger Movement Task***
Marco Ciavarro, Eleonora Grande, Luigi Pavone, Giuseppina Bevacqua, Michelangelo De Angelis, Paolo di Russo, Roberta Morace, Giorgia Committeri, Giovanni Grillea, Marcello Bartolo, Sergio Paolini and Vincenzo Esposito

213 ***Clinical Utility of Transcranial Magnetic Stimulation (TMS) in the Presurgical Evaluation of Motor, Speech, and Language Functions in Young Children With Refractory Epilepsy or Brain Tumor: Preliminary Evidence***
Shalini Narayana, Savannah K. Gibbs, Stephen P. Fulton, Amy Lee McGregor, Basanagoud Mudigoudar, Sarah E. Weatherspoon, Frederick A. Boop and James W. Wheless

231 ***Preoperative nTMS and Intraoperative Neurophysiology - A Comparative Analysis in Patients With Motor-Eloquent Glioma***
Tizian Rosenstock, Mehmet Salih Tuncer, Max Richard Münch, Peter Vajkoczy, Thomas Picht and Katharina Faust

243 ***Mapping and Preserving the Visuospatial Network by repetitive nTMS and DTI Tractography in Patients With Right Parietal Lobe Tumors***
Giovanni Raffa, Maria Catena Quattropani, Giuseppina Marzano, Antonello Curcio, Vincenzo Rizzo, Gabriella Sebestyén, Viktória Tamás, András Büki and Antonino Germanò

263 ***Novel Asleep Techniques for Intraoperative Assessment of Brain Connectivity***
Francesco Sala, Davide Giampiccolo and Luigi Cattaneo

268 ***Cortical Excitability and Connectivity in Patients With Brain Tumors***
Vincenzo Rizzo, Carmen Terranova, Giovanni Raffa, Salvatore Massimiliano Cardali, Filippo Flavio Angileri, Giuseppina Marzano, Maria Catena Quattropani, Antonino Germanò, Paolo Girlanda and Angelo Quartarone

frontiers | Frontiers in Neurology

EDITORIAL
published: 06 April 2022
doi: 10.3389/fneur.2022.885773

Editorial: nTMS, Connectivity and Neuromodulation in Brain Tumor Patients

Giovanni Raffa[1*†], *Thomas Picht*[2†], *András Büki*[3‡] *and Antonino Germanò*[1‡]

[1] *Division of Neurosurgery, BIOMORF Department, University of Messina, Messina, Italy,* [2] *Department of Neurosurgery, Charité Universitätsmedizin Berlin, Berlin, Germany,* [3] *Department of Neurosurgery, Faculty of Medicine and Health, Örebro University, Örebro, Sweden*

Keywords: **brain connectivity, brain mapping, brain tumors, neuromodulation, nTMS, preoperative planning, tractography**

Editorial on the Research Topic

nTMS, Connectivity and Neuromodulation in Brain Tumor Patients

Surgery of brain tumors still represents a challenge for neurosurgeons, especially if these lesions are located close to or eventually infiltrate functionally-eloquent brain networks (1). The goal of surgery is to achieve the maximal safe resection of the neoplastic tissue while preserving the surrounding functionally-relevant brain areas (e.g., sensorimotor, language, visual networks) (2). Such a goal can be achieved by combining technological advancements in surgical techniques with knowledge of the brain's anatomic and functional organization.

In recent years we have witnessed a paradigm shift in knowledge about how the brain works: the historical localizationist interpretation of brain functional organization has been recently replaced by the hodotopical model, in which brain functions do not correspond to fixed anatomical areas but rely on complex cortico-subcortical networks with huge plastic potential (3). Neuroplasticity is responsible for the final connectomic organization of functional brain networks and brain tumor patients usually show huge neuroplasticity phenomena. Disclosing these neuroplasticity phenomena and investigating connectomics underlying the brain functional organization in brain tumor patients is essential to plan and achieve the maximal safe resection of the tumor that is associated with improved outcome and prolonged survival (4). Several electrophysiological and neuroimaging techniques can be used before and during surgery to map the spatial relationship between the tumor and adjacent eloquent networks that must be preserved during surgery. Among these, transcranial magnetic stimulation (TMS), transcranial electrical stimulation (TES), functional MRI (fMRI), magnetoelectroencephalography (MEG), tractography, and finally awake surgery and direct electric stimulation (DES) are the most used. In addition, electrophysiological approaches have been developed to analyze and induce neuroplasticity in these patients before and after surgery, aiming to stimulate brain functional reorganization, making resection safer, and promoting postoperative functional recovery (5, 6).

All these different imaging and neurophysiological advanced techniques, or specific combinations of them, provide a unique and modern *in-vivo* connectomic analysis of the brain functional organization in every single patient. Those analyses enable a personalized strategy for surgical resection and post-operative rehabilitation and neurological recovery, resulting in a better patients' outcome and quality of life.

Nevertheless, the integration of information provided by these modern tools requires a multidisciplinary approach and a strong collaboration between different professionals, including neuroscientists, neurologists, neuroradiologists, neuropsychologists, and neurosurgeons with strong expertise in the field. A comprehensive review of the technical aspects of such a multidisciplinary approach for connectomics analysis before and during surgery of brain tumors

OPEN ACCESS

Edited and Reviewed by:
Jan Kassubek,
University of Ulm, Germany

***Correspondence:**
Giovanni Raffa
giovanni.raffa@unime.it

†These authors share first authorship
‡These authors share last authorship

Specialty section:
This article was submitted to Applied Neuroimaging, a section of the journal Frontiers in Neurology

Received: *28 February 2022*
Accepted: *02 March 2022*
Published: *06 April 2022*

Citation:
Raffa G, Picht T, Büki A and Germanò A (2022) Editorial: nTMS, Connectivity and Neuromodulation in Brain Tumor Patients. Front. Neurol. 13:885773. doi: 10.3389/fneur.2022.885773

is still lacking. The present Article Collection attempted to provide new insights into novel multidisciplinary approaches to perform advanced connectomics analysis of brain functional organization through the description of the modern pre- and intraoperative electrophysiological and neuroimaging techniques to plan and achieve the maximal safe resection of brain tumors, as well as the illustration of novel neuromodulation approaches based on advanced brain stimulation techniques used to disclose neuroplasticity phenomena, and promote neurological reorganization before surgery.

Among preoperative neurophysiological tools for connectomic analysis, navigated TMS (nTMS) is one of the most widely diffused in Neurosurgical Departments all over the world. Several studies demonstrated nTMS provides a reliable mapping of the motor cortex and language cortical areas, thus allowing neurosurgeons to plan the safest surgical strategy to remove brain tumors close to these networks (7–13). In the present Article Collection, Umana et al. performed an updated systematic review and meta-analysis of literature regarding the use of nTMS mapping before brain tumor surgery: the authors confirmed that nTMS is a safe technique that, in association with DES, improves brain mapping and the extent of tumor resection, thus favoring a better patients' postoperative outcome. Similarly, a study by Haddad et al. summarized the current evidence supporting the efficacy of preoperative nTMS mapping in improving the surgical planning, tumor resection, and postoperative outcome in brain tumor patients. However, the nTMS motor mapping is useful not only to plan tumor surgical resection but also to define a safer radiotherapy plan: Dzierma et al. demonstrated that, in patients with motor-eloquent brain metastases, the inclusion of nTMS motor information into the radiotherapy treatment planning is possible with a straightforward workflow and can achieve reduced doses to the nTMS-defined motor area without compromising coverage of the planning target volume. Finally, three different studies demonstrated that the nTMS motor mapping can also be used to reveal preoperative alterations of the cortical excitability in patients with motor-eloquent brain tumors that could be related to and predict the occurrence of motor deficits (Neville et al.; Machetanz et al.; Rizzo et al.).

However, the nTMS cortical mapping of complex functions, including language, is more difficult and reliable than mapping the motor cortex. Weiss Lucas et al. here proposed a novel robust and reliable picture naming tool, optimized for clinical use, to map and monitor language functions in brain tumor patients during preoperative nTMS mapping and awake surgery. On the other hand, Hazem et al. in their study proposed a novel target for the nTMS preoperative mapping of language cortical areas: in particular, they demonstrated that the posterior middle frontal gyrus, including the area 55b, is an important integration cortical hub for both dorsal and ventral streams of language and can be successfully used as a target for the nTMS language cortical mapping.

A few data are currently available about the possibility to use nTMS for mapping cortical areas involved in brain functions other than language. Raffa et al. submitted a paper demonstrating nTMS can be used also for mapping the cortical areas of the right parietal lobe involved in visuospatial abilities. The authors reported that the nTMS mapping of these areas, in combination with the tractography of the superior longitudinal fascicle (SLF), can be used to plan and achieve the maximal safe resection of brain tumors located in the right parietal lobe, without inducing a worsening of patients' visuospatial abilities.

All the previous studies refer to the nTMS cortical mapping in adult brain tumor patients. However, in the previous literature, only anecdotic reports analyzed the feasibility of the nTMS mapping in children. Narayana et al. performed a study demonstrating that TMS is a safe, reliable, and effective tool to map eloquent cortices also in a series of 36 young children (3 years old or younger). In this study the TMS mapping improved understanding the risk-benefit ratio prior to surgery and facilitated surgical planning aimed at preserving motor, speech, and language functions.

Nevertheless, the nTMS mapping enables only the visualization of the cortical areas of functional networks (motor/language/visuospatial) that must be preserved during the resection of the tumor. Therefore, the data from nTMS cortical mapping must be combined with the tractography of the respective subcortical pathways, aiming at the preoperative identification of the entire functional network (14–16). Rosenstock et al. demonstrated that the nTMS motor mapping can be successfully combined with the tractography of the corticospinal tract to stratify patients with motor-eloquent tumors before surgery, distinguishing between patients with a high vs. low risk of developing new postoperative motor deficits. Such a stratification is particularly useful during surgery, by helping neurosurgeons to interpret ambiguous intraoperative monitoring phenomena (such as irreversible MEP amplitude decrease $\leq$50%) and to adjust the subcortical stimulation intensity. In another study, Fekonja et al. showed that the analysis of tractography measurements along the corticospinal tract (regardless of using a deterministic or probabilistic approach) is useful to stratify patients with motor-eloquent gliomas by disclosing tumor-induced changes in the structural integrity of the tract in the affected hemisphere.

A similar preoperative patient stratification can be achieved also in cases of language-eloquent tumors by performing the tractography of fascicles involved in the language network. Ius et al. in their study, computed the tractography of the superior longitudinal fascicle (SLF) and inferior fronto-occipital fascicle (IFOF) to stratify patients with language-eloquent low-grade gliomas. In particular, the authors demonstrated that the comparison of quantitative parameters resulting from the DTI tractography between the tumoral vs. the healthy hemisphere is useful to assess the risk of post-operative transient language impairment in these patients. Moreover, Di Cristofori et al. performed a review to analyze the current literature evidence about the possible role of the preoperative assessment of the asymmetry of the arcuate fascicle (AF) by DTI tractography for the preoperative risk assessment of patients undergoing surgical resection of gliomas. They also reported the usefulness of the analysis of AF asymmetry in the health vs. affected hemisphere to predict recovery from aphasia and reorganization of the language brain network even after surgical damage. Finally, Zoli

et al. reported an interesting study demonstrating that DTI tractography of the AF is useful not only for planning the safest surgical strategy for tumor resection but also to analyze some along-tract DTI metrics that can provide useful information for differentiating low-grade and high-grade tumors. Another important subcortical white matter tract involved in the language network, the Frontal Aslant Tract (FAT), has been analyzed in the study La Corte et al. The authors performed a systematic review of the literature about the FAT anatomical connectivity and functional roles, thus providing an overview for practical neurosurgical applications in patients with brain tumors: they also eventually suggested the evaluation of FAT integrity by tractography could be useful to plan a safer surgery and to reduce post-operative deficits in patients with language-eloquent brain tumors.

Another important preoperative tool to identify functional networks before brain tumor surgery is fMRI. Nevertheless, some concerns about its accuracy, especially in comparison with nTMS, have been reported in the literature (17). In particular, some criticisms have been raised concerning the accuracy of the motor tasks used for mapping the motor network, especially in patients with brain tumor-related motor deficits (18). Ciavarro et al. performed a very interesting study proposing a novel motor task for a more accurate preoperative localization of the motor cortex in brain tumor patients: the proposed visual-triggered finger movement task (VFMT) resulted to be more reliable than the standard finger-tapping task for the identification of the hand-knob region and showed good correspondence to intraoperative DES. They concluded the VFMT could be very helpful for planning the safest surgical strategy in patients with motor-eloquent tumors.

Recently, neuromodulation by non-invasive brain stimulation (NIBS) has been proposed in the literature as a novel strategy to increase the safety of surgical resection of brain tumors. This strategy aims to promote neuroplasticity and connectivity changes in brain functional networks at surgical risk, thus allowing a "shift" of eloquent structures far away from the tumor. The father of the hodotopical revolution, Duffau, in his Editorial discussed all the potential applications of NIBS to elicit neuroplasticity and facilitate reoperation for low-grade glioma relapse. Moreover, Lang et al. performed a very interesting proof of concept pilot study demonstrating that transcranial direct current stimulation (tDCS) can be used to modify the connectivity of the sensorimotor network in glioma patients. Such a pioneering study confirms the potential usefulness of neuromodulation by NIBS even in the clinical practice, for safer surgical management of brain tumors. Finally, Leao et al. demonstrated that neuromodulation may be used also for the treatment of specific medical conditions, such as tinnitus. The authors reported that low-frequency repetitive TMS to the right dorsolateral prefrontal cortex in patients affected by vestibular schwannomas can result in a significant acute but limited long-term effect on tinnitus.

Apart from preoperative techniques, also intraoperative imaging, neurophysiological and neuropsychological tools play an important role in achieving the safe surgical resection of brain tumors. Barbagallo et al., in their study, demonstrated the importance of a multimodal approach based on different intraoperative imaging techniques (5-ALA, ultrasound, CT scan, etc.) to achieve the maximal safe resection of high-grade gliomas and to improve the patients' postoperative outcome. Giammalva et al. performed a systematic review to assess the role of preoperative connectivity analysis and intraoperative brain mapping to guide the supratotal resection (SpTR) of gliomas, also analyzing the clinical impact of SpTR. They concluded SpTR is related to a longer overall and progression-free survival along with preserving neuro-cognitive functions and quality of life. Herbet et al. reported a perspective article highlighting the possibility to map advanced cognitive functions and behaviors (e.g., multidetermined cognitions such as contextual decision-making or fast learning) during wide-awake surgery. Finally, Sala et al., propose a very interesting opinion study, suggesting novel strategies for the intraoperative assessment of brain connectivity in the anesthetized patient. The aim is to overcome the limitations of the standard neurophysiological mapping and monitoring techniques during asleep surgery and increase the safety of brain tumor resection when awake surgery is not feasible.

In conclusion, this Article Collection includes several remarkable studies summarizing the state-of-the-art of modern preoperative and intraoperative brain stimulation and neuroimaging techniques for performing connectomic analysis and promoting neuroplasticity in brain tumor patients. The scope is to highlight the most novel strategies to enhance knowledge about brain functional organization in brain tumor patients, aiming to improve their surgical treatment and outcome. We believe this Collection will encourage future clinical studies on this fascinating topic and open novel, tailored, safer, and hopefully more effective therapeutic perspectives for patients harboring brain tumors.

AUTHOR CONTRIBUTIONS

GR, TP, AB, and AG: conceptualization, collection of the data, writing of the draft, and revision of the final manuscript. All authors are accountable for the content of the work.

FUNDING

This editorial and the article collection have been funded by a grant from the European Social Fund (FSE), Call PON Ricerca e Innovazione 2014-2020—AIM Attraction and International Mobility, Activity AIM1839117-3, Line 1, Area SNSI Salute (CUP J44I18000280006), Recipient: GR, BIOMORF Department, University of Messina, Italy. TP acknowledges the support of the Cluster of Excellence *Matters of Activity. Image Space Material* funded by the Deutsche Forschungsgemeinschaft (DFG, German Research Foundation) under Germany's Excellence Strategy—EXC 2025−390648296.

REFERENCES

1. Hervey-Jumper SL, Berger MS. Role of surgical resection in low- and high-grade gliomas. *Curr Treat Options Neurol.* (2014) 16:284. doi: 10.1007/s11940-014-0284-7
2. Duffau H. Introduction. Surgery of gliomas in eloquent areas: from brain hodotopy and plasticity to functional neurooncology. *Neurosurg Focus.* (2010) 28:Intro. doi: 10.3171/2009.12.FOCUS.FEB2010.INTRO
3. De Benedictis A, Duffau H. Brain Hodotopy: From esoteric concept to practical surgical applications. *Neurosurgery.* (2011) 68:1709-23. doi: 10.1227/NEU.0b013e3182124690
4. Duffau H. *Brain Mapping - from Neural Basis of Cognition to Surgical Application*. Wien: Springer-Verlag. (2011). doi: 10.1007/978-3-7091-0723-2
5. Barcia JA, Sanz A, Gonzalez-Hidalgo M, de Las Heras C, Alonso-Lera P, Diaz P, et al. Rtms stimulation to induce plastic changes at the language motor area in a patient with a left recidivant brain tumor affecting broca's area. *Neurocase.* (2012) 18:132–8. doi: 10.1080/13554794.2011.568500
6. Rivera-Rivera PA, Rios-Lago M, Sanchez- Casarrubios S, Salazar O, Yus M, Gonzalez-Hidalgo M, et al. Cortical plasticity catalyzed by prehabilitation enables extensive resection of brain tumors in eloquent areas. *J Neurosurg.* (2017) 126:1323–33. doi: 10.3171/2016.2.JNS152485
7. Raffa G, Quattropani MC, Germano A. When imaging meets neurophysiology: the value of navigated transcranial magnetic stimulation for preoperative neurophysiological mapping prior to brain tumor surgery. *Neurosurg Focus.* (2019) 47:E10. doi: 10.3171/2019.9.FOCUS19640
8. Picht T, Krieg SM, Sollmann N, Rosler J, Niraula B, Neuvonen T, et al. A comparison of language mapping by preoperative navigated transcranial magnetic stimulation and direct cortical stimulation during awake surgery. *Neurosurgery.* (2013) 72:808–19. doi: 10.1227/NEU.0b013e3182889e01
9. Rosler J, Niraula B, Strack V, Zdunczyk A, Schilt S, Savolainen P, et al. Language mapping in healthy volunteers and brain tumor patients with a novel navigated tms system: evidence of tumor-induced plasticity. *Clin Neurophysiol.* (2014) 125:526–36. doi: 10.1016/j.clinph.2013.08.015
10. Belotti F, Tuncer MS, Rosenstock T, Ivren M, Vajkoczy P, Picht T. Predicting the extent of resection of motor-eloquent gliomas based on tms-guided fiber tracking. *Brain Sci.* (2021) 11. doi: 10.3390/brainsci11111517
11. Raffa G, Scibilia A, Conti A, Cardali SM, Rizzo V, Terranova C, et al. Multimodal surgical treatment of high grade gliomas in the motor area: the impact of the combination of navigated transcranial magnetic stimulation and fluorescein-guided resection. *World Neurosurg.* (2019). doi: 10.1016/j.wneu.2019.04.158
12. Raffa G, Scibilia A, Conti A, Ricciardo G, Rizzo V, Morelli A, et al. The role of navigated transcranial magnetic stimulation for surgery of motor-eloquent brain tumors: a systematic review and meta-analysis. *Clin Neurol Neurosurg.* (2019) 180:7–17. doi: 10.1016/j.clineuro.2019.03.003
13. Raffa G, Picht T, Angileri FF, Youssef M, Conti A, Esposito F, et al. Surgery of malignant motor-eloquent gliomas guided by sodium-fluorescein and navigated transcranial magnetic stimulation: a novel technique to increase the maximal safe resection. *J Neurosurg Sci.* (2019). doi: 10.23736/S0390-5616.19.04710-6
14. Raffa G, Scibilia A, Germanò A, Conti A. Ntms-based dti fiber tracking of motor pathways. In: Krieg S, editor. *Navigated Transcranial Magnetic Stimulation in Neurosurgery*. Cham: Springer International Publishing. (2017). p. 97–114. doi: 10.1007/978-3-319-54918-7_6
15. Raffa G, Picht T, Scibilia A, Rosler J, Rein J, Conti A, et al. Surgical treatment of meningiomas located in the rolandic area: the role of navigated transcranial magnetic stimulation for preoperative planning, surgical strategy, and prediction of arachnoidal cleavage and motor outcome. *J Neurosurg.* (2019) 1–12. doi: 10.3171/2019.3.JNS183411
16. Giampiccolo D, Howells H, Bahrend I, Schneider H, Raffa G, Rosenstock T, et al. Preoperative transcranial magnetic stimulation for picture naming is reliable in mapping segments of the arcuate fasciculus. *Brain Commun.* (2020) 2:fcaa158. doi: 10.1093/braincomms/fcaa158
17. Mangraviti A, Casali C, Cordella R, Legnani FG, Mattei L, Prada F, et al. Practical assessment of preoperative functional mapping techniques: navigated transcranial magnetic stimulation and functional magnetic resonance imaging. *Neurol Sci.* (2013) 34:1551–7. doi: 10.1007/s10072-012-1283-7
18. Krings T, Reinges MH, Erberich S, Kemeny S, Rohde V, Spetzger U, et al. Functional mri for presurgical planning: problems, artefacts, and solution strategies. *J Neurol Neurosurg Psychiatry.* (2001) 70:749–60. doi: 10.1136/jnnp.70.6.749

Conflict of Interest: The authors declare that the research was conducted in the absence of any commercial or financial relationships that could be construed as a potential conflict of interest.

frontiers in Neurology

OPINION
published: 12 November 2020
doi: 10.3389/fneur.2020.582489

Can Non-invasive Brain Stimulation Be Considered to Facilitate Reoperation for Low-Grade Glioma Relapse by Eliciting Neuroplasticity?

Hugues Duffau [1,2]*

[1] Department of Neurosurgery, Gui de Chauliac Hospital, Montpellier University Medical Center, Montpellier, France, [2] Team "Plasticity of Central Nervous System, Stem Cells and Glial Tumors," National Institute for Health and Medical Research (INSERM), U1191 Laboratory, Institute of Functional Genomics, University of Montpellier, Montpellier, France

Keywords: awake surgery, low-grade glioma, non-invasive brain stimulation, neuroplasticity, transcranial magnetic stimulation

OPEN ACCESS

Edited by:
András Büki,
University of Pécs, Hungary

Reviewed by:
Tamas Doczi,
University of Pécs, Hungary
Francesco Sala,
University of Verona, Italy

***Correspondence:**
Hugues Duffau
h-duffau@chu-montpellier.fr

Specialty section:
This article was submitted to Applied Neuroimaging, a section of the journal Frontiers in Neurology

Received: *12 July 2020*
Accepted: *19 October 2020*
Published: *12 November 2020*

Citation:
Duffau H (2020) Can Non-invasive Brain Stimulation Be Considered to Facilitate Reoperation for Low-Grade Glioma Relapse by Eliciting Neuroplasticity? Front. Neurol. 11:582489. doi: 10.3389/fneur.2020.582489

INTRODUCTION

Diffuse low-grade glioma (LGG, i.e., World Health Organization grade II glioma) is a brain primary neoplasm with a constant invasion along the cerebral connectome and with an inevitable malignant transformation, which results in functional worsening and ultimately in the death of the patient (1). To optimize the oncofunctional balance of therapeutic management, namely, to increase both the overall survival and the quality of life (QoL), the purpose is to achieve an early and maximal safe surgical resection, performed until critical neural networks have been identified by means of intraoperative corticosubcortical direct electrostimulation (DES) mapping in awake patients (2). Indeed, despite the lack of randomized controlled trials, complete LGG removal and, when functionally feasible, supracomplete resection [i.e., with an oncological margin around the FLAIR signal abnormality visible on the pre-operative magnetic resonance imaging (MRI)] led to a significant increase in median survival around 15 years (3, 4), while in parallel, electrical-guided surgery allowed a significant reduction of severe persistent deteriorations, even in the so-called "eloquent regions" (5). In fact, mechanisms of neuroplasticity induced by the slow progression of the LGG over the years, explaining why the vast majority of patients do experience only mild (or even no) neurological deficits at diagnosis (usually made because of inaugural seizures), open the door to massive surgical resection in areas deemed to be inoperable in a rigid localizationist view of brain processing, with functional recovery and return to a normal life (6–9). Such a considerable functional redeployment is possible, thanks to an actual meta-networking brain organization, based on dynamic interactions within and between neural circuits subserving sensorimotor, visuospatial, language, cognitive, emotional, and behavioral functions (10).

SURGERY FOR LOW-GRADE GLIOMA AND FUNCTIONAL REARRANGEMENT

Nonetheless, despite this major improvement of functional and oncological outcomes following LGG surgery in the two past decades (11), because of its intrinsic diffuse nature, LGG cannot be cured, as evidenced by relapse that may arise even many years after supratotal resection (4). As a consequence, reoperation(s) has been advocated in the event of LGG recurrence, with the aim of reducing again the tumor volume and then decreasing the risk of malignant transformation and prolonging overall survival (12, 13). Interestingly, in a large series with more than 1,000 patients, it has been demonstrated that repeat surgeries were significantly associated with greater

survival (3). However, preservation of QoL might seem more uncertain still in case of subsequent surgery, especially when the first resection was interrupted according to individual functional boundaries. Yet, it is worth noting that functional rearrangement has been observed between the first and second intervention, as revealed by intraoperative DES (14, 15). Remarkably, such a functional reorganization, likely elicited by the initial operation itself, the post-operative cognitive rehabilitation (16), and the glioma regrowth, enabled an optimization of the extent of resection while avoiding neurological morbidity (15, 17).

On the other hand, this reconfiguration over the years is seen only in a subgroup of LGG patients, and reoperation did not permit to perform (supra)marginal resection in all cases because of some limitations of neuroplasticity, especially related to the involvement of the "minimal common brain" (18). This "neural core," with a low interindividual variability (19) and a low plastic potential, is mainly constituted by the input systems (as the visual and somatosensory systems), the output systems (as the pyramidal system), and the subcortical connectivity [as the associative fibers, e.g., the arcuate fasciculus or the inferior fronto-occipital fasciculus (IFOF)]; see a recent probabilistic atlas of brain plasticity (8). Such a limitation of brain adaption in reaction to glioma migration explains why some degrees of cognitive disturbances may be found, despite a normal neurological examination at the standard clinical evaluation, when an objective neuropsychological assessment is performed in LGG patients. These disorders may be identified before any treatment [as semantic impairment if the left IFOF is invaded (20)], or following surgical resection—as subjective empathy changes related to the disconnection of the left cingulum bundle or the right IFOF (21), or lexical access troubles associated to damages of the left inferior longitudinal fasciculus (8). Consequently, neurosurgeons should find the optimal compromise between the dynamics of neural networks allowing compensation after glioma resection and limitations of brain reshaping based on the knowledge of critical cortical hubs and axonal pathways (22, 23). To this end, introducing the fourth dimension to optimize the oncofunctional balance over the years in LGG patients led to the proposal of an original paradigm, that is, to consider a multistage surgical approach. This new concept enables to deal with the individual capacity of the central nervous system to reallocate in reaction to slow glioma progression, at least to some extent (24, 25).

NON-INVASIVE BRAIN STIMULATION AND NEUROPLASTICITY

In this setting, the next step would be to try to promote neural redistribution before reoperation in order to increase the likelihood of achieving an improved extent of resection. This facilitation of brain functional rearrangement seems now possible for several reasons. First, mechanisms underlying neuroplasticity after a first glioma surgery start to be better understood, especially thanks to post-operative neuroimaging studies by means of task-based as well as resting functional MRI (fMRI), which showed a balance between recruitment of perilesional areas and involvement of contralesional homologous regions (26–28). Second, besides fMRI, which is based on the principle of neurovascular coupling, resulting in serious limitations as a low reliability and the impossibility to distinguish critical areas from those that can be compensated following brain insult (29), transcranial magnetic stimulation (TMS) has been proposed for functional mapping in cerebral tumor patients (30). Indeed, by evoking a magnetic field able to bypass the skull, TMS may excite neurons in a suprathresholded manner and then can elicit neuronal activity: this permits to quantify network properties such as excitability and connectivity or to cause a transitory virtual lesion disrupting ongoing task, as DES, but non-invasively (31). However, in a recent investigation that compared navigated repetitive TMS (rTMS) with intraoperative DES in glioma patients, TMS showed only 81.6% sensitivity, 59.6% specificity, 78.5% positive predictive value, and 64.1% negative predictive value for pre-operative language mapping (32), confirming that DES remains the criterion standard. Third, beyond pre-surgical planning, TMS has recently been used to study neuroplasticity before and after tumor surgery. In a recent preliminary experience with 18 patients harboring a left glioma, rTMS language mapping has been achieved before a first and then before a second surgery and confirmed a functional reallocation of language sites, with (i) more "language-negative areas" around the neoplasm during the reoperation in patients in whom critical language areas have been found during the first mapping; (ii) more functional reorganization in slow-growing tumors: in other words, these findings support that eloquent regions can leave the tumor area over time, especially in LGG (33). In agreement with fMRI studies, by generating many language disorders over the right hemisphere, rTMS investigations plead in favor of an active recruitment of the contralesional side to compensate for the glioma growth in the left side (34).

In addition, non-invasive brain stimulation (NBS) techniques by means of rTMS or anodal transcranial direct current stimulation (tDCS), which can actively generate neuromodulation by changing cortical excitability into inhibitory or excitatory direction using magnetic or electric fields, respectively, may enable both to potentiate behavioral performances in healthy volunteers and to facilitate post-lesional neuroplasticity in brain-damaged patients (35, 36). Indeed, repeated sessions of NBS over the healthy brain have significantly improved language functions such as speech, semantic fluency, word retrieval, and verbal learning (37–39). Interestingly, this functional improvement was significantly associated with a modulation of the effective connectivity, especially between the left inferior frontal gyrus and the right insula in verb learning facilitation (40). This is in line with DES mapping, which disrupts behavior by stimulating focally an entry door to a larger circuit (41, 42); even though the effects of NBS are foremost local, neural activity within the whole network is actually affected. For example, regarding movement, the interhemispheric transcallosal inhibitory effects may be modified by applying tDCS to one primary motor cortex, as it can facilitate the contralateral primary motor cortex through potentiation of interhemispheric interactions (43). The same concept has been utilized in patients with cerebral insult, in particular

for the therapy of post-stroke aphasia. Indeed, although the actual mechanisms of reorganization elicited by excitatory combined with inhibitory effects of NBS on different nodes of the injured neural networks are still matter of debate, it seems that the complex interactions between the ipsilesional, contralesional, and interhemispheric connectivity may be modulated to facilitate functional compensation (44). For instance, anodal tDCS over the left inferior frontal gyrus resulted in an improvement of speech, naming, and repetition in aphasic patients (45, 46). However, because the effect of NBS is not restricted to the stimulated region but also evokes modifications of the functional connectivity in a wider language circuit (47, 48), beyond excitatory stimulation to perilesional sites, inhibitory low-frequency rTMS has been performed over contralateral homotopic language regions to facilitate post-stroke recovery (49, 50). In the same spirit, NBS has also been used in association with speech therapy to potentiate functional compensation (51).

PERSPECTIVES

Based on these preliminary results in stroke, it could be considered to use NBS in patients who underwent brain surgery, in addition to functional rehabilitation, which is already known to participate in post-operative network rearrangement (16, 52). As mentioned, besides the improvement of QoL, the goal would be to optimize the post-operative functional redeployment and to reopen the door to subsequent surgical resection(s), especially for slow-growing LGG (15). Of note, invasive stimulation has previously been suggested by placing a grid of electrodes over the residual glioma at the end of a first partial resection, in order to perform continuous cortical electrical stimulation simultaneously with behavioral training and then to accelerate plastic reorganization prior to reoperation; however, only five patients have been reported, with a high rate of surgical complications (two infections, one subdural hematoma) due to the invasiveness of this technique (53). Moreover, these findings were not reproduced in the literature. As a consequence, a more reliable and feasible original therapeutic solution in clinical routine might be to develop specific NBS protocols that aim pushing away functional nodes to leave the glioma region. Indeed, contrary to the post-stroke aphasic patients, in whom it has been proposed to use inhibitory rTMS over the right hemisphere, particularly the inferior frontal gyrus, in order to facilitate reinforcement within the left damaged language network (51), the main purpose in brain tumor patients would be to favor the recruitment of the contralateral homologous areas, which have been demonstrated by means of fMRI as playing a pivotal role in recovery following a first surgery (26, 54). In fact, to increase the extent of resection during a reoperation, NBS could be utilized to inhibit the perilesional critical sites and to force them out of the periphery of the surgical cavity, where the tumor removal was interrupted at the end of the first operation because functional boundaries have been reached. In other words, the ultimate goal would be to change the respective weight of the nodes within a large-scale bilateral functional network, or even to modulate the interactions between brain systems—as it has been evidenced that language compensation after surgery for left LGG might involve non-language functions such as attentional resources, i.e., that picture naming recovery was correlated to the recruitment of the right frontoparietal attentional network (28). This means that such an innovative therapeutic strategy can be conceived only in a dynamic metanetworking account of neural processing, breaking with the traditional dogmatic localizationist theory (10); therefore, a stronger link should be built between cognitive neurosciences (as the new field of connectomics), technical advances in neuromodulation tools (as rTMS and tDCS), and elaboration of original management for glioma patients, based on a better understanding and guidance of interactions between tumor progression and brain adaptation. In this spirit, the next question could be to use NBS with the aim of catalyzing neuroplasticity and optimizing the extent of resection for gliomas involving critical neural networks even before the first surgery.

AUTHOR CONTRIBUTIONS

The author confirms being the sole contributor of this work and has approved it for publication.

REFERENCES

1. Duffau H, editor. *Diffuse Low-Grade Gliomas in Adults*. 2nd ed. London: Springer (2017). doi: 10.1007/978-3-319-55466-2
2. Duffau H. Diffuse low-grade glioma, oncological outcome and quality of life: a surgical perspective. *Curr Opin Oncol.* (2018) 30:383–9. doi: 10.1097/CCO.0000000000000483
3. Capelle L, Fontaine D, Mandonnet E, Taillandier L, Golmard JL, Bauchet L, et al. Spontaneous and therapeutic prognostic factors in adult hemispheric World Health Organization Grade II gliomas: a series of 1097 cases: clinical article. *J Neurosurg.* (2013) 118:1157–68. doi: 10.3171/2013.1.JNS121
4. Duffau H. Long-term outcomes after supratotal resection of diffuse low-grade gliomas: a consecutive series with 11-year follow-up. *Acta Neurochir.* (2016) 158:51–8. doi: 10.1007/s00701-015-2621-3
5. de Witt Hamer PC, Gil Robles S, Zwinderman A, Duffau H, Berger MS. Impact of intraoperative stimulation brain mapping on glioma surgery outcome: a meta-analysis. *J Clin Oncol.* (2012) 30:2559–65. doi: 10.1200/JCO.2011.38.4818
6. Duffau H. Lessons from brain mapping in surgery for low-grade glioma: insights into associations between tumour and brain plasticity. *Lancet Neurol.* (2005) 4:476–86. doi: 10.1016/S1474-4422(05)70140-X
7. Desmurget M, Bonnetblanc F, Duffau H. Contrasting acute and slow-growing lesions: a new door to brain plasticity. *Brain.* (2007) 130:898–914. doi: 10.1093/brain/awl300
8. Herbet G, Maheu M, Costi E, Lafargue G, Duffau H. Mapping neuroplastic potential in brain-damaged patients. *Brain.* (2016) 139:829–44. doi: 10.1093/brain/awv394
9. Ng S, Herbet G, Moritz-Gasser S, Duffau H. Return to work following surgery for incidental diffuse low-grade glioma: a prospective series with 74 patients. *Neurosurgery.* (2019) 87:720–9. doi: 10.1093/neuros/nyz513
10. Herbet G, Duffau H. Revisiting the functional anatomy of the human brain: toward a meta-networking theory of cerebral functions. *Physiol Rev.* (2020) 100:1181–228. doi: 10.1152/physrev.00033.2019
11. Ferracci FX, Duffau H. Improving surgical outcome for gliomas with intraoperative mapping. *Expert Rev Neurother.* (2018) 18:333–41. doi: 10.1080/14737175.2018.1451329

12. Martino J, Taillandier L, Moritz-Gasser S, Gatignol P, Duffau H. Re-operation is a safe and effective therapeutic strategy in recurrent WHO grade II gliomas within eloquent areas. *Acta Neurochir.* (2009) 151:427–36. doi: 10.1007/s00701-009-0232-6
13. Schmidt MH, Berger MS, Lamborn KR, Aldape K, McDermott MW, Prados MD, et al. Repeated operations for infiltrative low-grade gliomas without intervening therapy. *J Neurosurg.* (2003) 98:1165–9. doi: 10.3171/jns.2003.98.6.1165
14. Southwell DG, Hervey-Jumper SL, Perry DW, Berger MS. Intraoperative mapping during repeat awake craniotomy reveals the functional plasticity of adult cortex. *J Neurosurg.* (2016) 124:1460–9. doi: 10.3171/2015.5.JNS142833
15. Picart T, Herbet G, Moritz-Gasser S, Duffau H. Iterative surgical resections of diffuse glioma with awake mapping: how to deal with cortical plasticity and connectomal constraints? *Neurosurgery.* (2018) 85:105–16. doi: 10.1093/neuros/nyy218
16. Duffau H. New philosophy, clinical pearls and methods for intraoperative cognition mapping and monitoring "à la carte" in brain tumor patients. *Neurosurgery.* in press.
17. Duffau H. The huge plastic potential of adult brain and the role of connectomics: new insights provided by serial mappings in glioma surgery. *Cortex.* (2014) 58:325–37. doi: 10.1016/j.cortex.2013.08.005
18. Ius T, Angelini E, Thiebaut de Schotten M, Mandonnet E, Duffau H. Evidence for potentials and limitations of brain plasticity using an atlas of functional resectability of WHO grade II gliomas: towards a -minimal common brain. *Neuroimage.* (2011) 56:992–1000. doi: 10.1016/j.neuroimage.2011.03.022
19. Duffau H. A two-level model of interindividual anatomo-functional variability of the brain and its implications for neurosurgery. *Cortex.* (2017) 86:303–13. doi: 10.1016/j.cortex.2015.12.009
20. Almairac F, Herbet G, Moritz-Gasser S, de Champfleur NM, Duffau H. The left inferior fronto-occipital fasciculus subserves language semantics: a multilevel lesion study. *Brain Struct Funct.* (2015) 220:1983–95. doi: 10.1007/s00429-014-0773-1
21. Herbet G, Lafargue G, Moritz-Gasser S, Menjot de Champfleur N, Costi E, Bonnetblanc F, et al. A disconnection account of subjective empathy impairments in diffuse low-grade glioma patients. *Neuropsychologia.* (2015) 70:165–76. doi: 10.1016/j.neuropsychologia.2015.02.015
22. Sarubbo S, Tate M, De Benedictis A, Merler S, Moritz-Gasser S, Herbet G, et al. Mapping critical cortical hubs and white matter pathways by direct electrical stimulation: an original functional atlas of the human brain. *Neuroimage.* (2020) 205:116237. doi: 10.1016/j.neuroimage.2019.116237
23. Sarubbo S, Tate M, De Benedictis A, Merler S, Moritz-Gasser S, Herbet G, et al. A normalized dataset of 1821 cortical and subcortical functional responses collected during direct electrical stimulation in patients undergoing awake brain surgery. *Data Brief.* (2019) 28:104892. doi: 10.1016/j.dib.2019.104892
24. Duffau H, Denvil D, Capelle L. Long term reshaping of language, sensory, and motor maps after glioma resection: a new parameter to integrate in the surgical strategy. *J Neurol Neurosurg Psychiatry.* (2002) 72:511–6. doi: 10.1136/jnnp.72.4.511
25. Robles SG, Gatignol P, Lehéricy S, Duffau H. Long-term brain plasticity allowing a multistage surgical approach to World Health Organization Grade II gliomas in eloquent areas. *J Neurosurg.* (2008) 109:615–24. doi: 10.3171/JNS/2008/109/10/0615
26. Vassal M, Charroud C, Deverdun J, Le Bars E, Molino F, Bonnetblanc F, et al. Recovery of functional connectivity of the sensorimotor network after surgery for diffuse low-grade gliomas involving the supplementary motor area. *J Neurosurg.* (2017) 126:1181–90. doi: 10.3171/2016.4.JNS 152484
27. Deverdun J, van Dokkum LEH, Le Bars E, Herbet G, Mura T, D'Agata B, et al. Language reorganization after resection of low-grade gliomas: an fMRI task based connectivity study. *Brain Imaging Behav.* (2020) 14:1779–91. doi: 10.1007/s11682-019-00114-7
28. van Dokkum LEH, Moritz Gasser S, Deverdun J, Herbet G, Mura T, D'Agata B, et al. Resting state network plasticity related to picture naming in low-grade glioma patients before and after resection. *Neuroimage Clin.* (2019) 24:102010. doi: 10.1016/j.nicl.2019.102010
29. Azad TD, Duffau H. Limitations of functional neuroimaging for patient selection and surgical planning in glioma surgery. *Neurosurg Rev.* (2020) 48:E12. doi: 10.3171/2019.11.FOCUS19769
30. Krieg SM, Shiban E, Buchmann N, Gempt J, Foerschler A, Meyer B, et al. Utility of presurgical navigated transcranial magnetic brain stimulation for the resection of tumors in eloquent motor areas. *J Neurosurg.* (2012) 116:994–1001. doi: 10.3171/2011.12.JNS111524
31. Siebner HR, Hartwigsen G, Kassuba T, Rothwell JC. How does transcranial magnetic stimulation modify neuronal activity in the brain? Implications for studies of cognition. *Cortex.* (2009) 45:1035–42. doi: 10.1016/j.cortex.2009.02.007
32. Motomura K, Takeuchi H, Nojima I, Aoki K, Chalise L, Iijima K, et al. Navigated repetitive transcranial magnetic stimulation as preoperative assessment in patients with brain tumors. *Sci Rep.* (2020) 10:9044. doi: 10.1038/s41598-020-65944-8
33. Ille S, Engel L, Albers L, Schroeder A, Kelm A, Meyer B, et al. Functional reorganization of cortical language function in glioma patients-a preliminary study. *Front Oncol.* (2019) 9:446. doi: 10.3389/fonc.2019.00446
34. Rösler J, Niraula B, Strack V, Zdunczyk A, Schilt S, Savolainen P, et al. Language mapping in healthy volunteers and brain tumor patients with a novel navigated TMS system: evidence of tumor-induced plasticity. *Clin Neurophysiol.* (2014) 125:526–36. doi: 10.1016/j.clinph.2013.08.015
35. Fiori V, Coccia M, Marinelli CV, Vecchi V, Bonifazi S, Ceravolo MG, et al. Transcranial direct current stimulation improves word retrieval in healthy and nonfluent aphasic subjects. *J Cognit Neurosci.* (2011) 23:2309–23. doi: 10.1162/jocn.2010.21579
36. Schlaug G, Marchina S, Wan CY. The use of non-invasive brain stimulation techniques to facilitate recovery from post-stroke aphasia. *Neuropsychol Rev.* (2011) 21:288–301. doi: 10.1007/s11065-011-9181-y
37. Cattaneo Z, Pisoni A, Papagno C. Transcranial direct current stimulation over Broca's region improves phonemic and semantic fluency in healthy individuals. *Neuroscience.* (2011) 183:64–70. doi: 10.1016/j.neuroscience.2011.03.058
38. Holland R, Leff AP, Josephs O, Galea JM, Desikan M, Price CJ, et al. Speech facilitation by left inferior frontal cortex stimulation. *Curr Biol.* (2011) 21:1403–7. doi: 10.1016/j.cub.2011.07.021
39. Fiori V, Nitsche M, Iasevoli L, Cucuzza G, Caltagirone C, Marangolo P. Differential effects of bihemispheric and unihemispheric transcranial direct current stimulation in young and elderly adults in verbal learning. *Behav Brain Res.* (2017) 321:170–5. doi: 10.1016/j.bbr.2016.12.044
40. Fiori V, Kunz L, Kuhnke P, Marangolo P, Hartwigsen G. Transcranial direct current stimulation (tDCS) facilitates verb learning by altering effective connectivity in the healthy brain. *NeuroImage.* (2018) 181:550–9. doi: 10.1016/j.neuroimage.2018.07.040
41. Mandonnet H, Winkler WA, Duffau H. Direct electrical stimulation as an input gate into brain functional networks: principles, advantages and limitations. *Acta Neurochir.* (2010) 152:185–93. doi: 10.1007/s00701-009-0469-0
42. Duffau H. Stimulation mapping of white matter tracts to study brain functional connectivity. *Nat Rev Neurol.* (2015) 11:255–65. doi: 10.1038/nrneurol.2015.51
43. Cabibel V, Muthalib M, Teo WP, Perrey S. High-definition transcranial direct-current stimulation of the right M1 further facilitates left M1 excitability during crossed facilitation. *J Neurophysiol.* (2018) 119:1266–72. doi: 10.1152/jn.00861.2017
44. Hamilton RH, Chrysikou EG, Coslett B. Mechanisms of aphasia recovery after stroke and the role of noninvasive brain stimulation. *Brain Lang.* (2011) 118:40–50. doi: 10.1016/j.bandl.2011.02.005
45. Fiori V, Cipollari S, Di Paola M, Razzano C, Caltagirone C, Marangolo P. tDCS stimulation segregates words in the brain: evidence from aphasia. *Front Hum Neurosci.* (2013) 7:269. doi: 10.3389/fnhum.2013.00269
46. Marangolo P, Fiori V, Calpagnano M, Campana S, Razzano C, Caltagirone C, et al. tDCS over the left inferior frontal cortex improves speech production in aphasia. *Front Hum Neurosci.* (2013) 7:539. doi: 10.3389/fnhum.2013.00539
47. Meinzer M, Antonenko D, Lindenberg R, Hetzer S, Ulm L, Avirame K, et al. Electrical brain stimulation improves cognitive performance by modulating functional connectivity and task-specific activation. *J Neurosci.* (2012) 32:185–66. doi: 10.1523/JNEUROSCI.4812-11.2012
48. Holland R, Leff AP, Penny WD, Rothwell JC, Crinion J. Modulation of frontal effective connectivity during speech. *Neuroimage.* (2016) 140:126–33. doi: 10.1016/j.neuroimage.2016.01.037

49. Barwood CH, Murdoch BE, Whelan BM, Lloyd D, Riek S, O'Sullivan J, et al. The effects of low frequency repetitive transcranial magnetic stimulation (rTMS) and sham condition rTMS on behavioural language in chronic non-fluent aphasia: short term outcomes. *NeuroRehabilitation*. (2011) 28:113–28. doi: 10.3233/NRE-2011-0640
50. Weiduschat N, Thiel A, Rubi-Fessen I, Hartmann A, Kessler J, Merl P, et al. Effects of repetitive transcranial magnetic stimulation in aphasic stroke: a randomized controlled pilot study. *Stroke*. (2011) 42:409–15. doi: 10.1161/STROKEAHA.110.597864
51. Thiel A, Hartmann A, Rubi-Fessen I, Anglade C, Kracht L, Weiduschat N, et al. Effects of noninvasive brain stimulation on language networks and recovery in early poststroke aphasia. *Stroke*. (2013) 44:2240–6. doi: 10.1161/STROKEAHA.111.000574
52. Mosca C, Zoubrinetzy R, Baciub M, Aguilar L, Minotti L, Kahane P, et al. Rehabilitation of verbal memory by means of preserved nonverbal memory abilities after epilepsy surgery. *Epilepsy Behav Case Rep*. (2014) 2:167–73 doi: 10.1016/j.ebcr.2014.09.002
53. Rivera-Rivera PA, Rios-Lago M, Sanchez-Casarrubios S, Salazar O, Yus M, González-Hidalgo M, et al. Cortical plasticity catalyzed by prehabilitation enables extensive resection of brain tumors in eloquent areas. *J Neurosurg*. (2017) 126:1323–33. doi: 10.3171/2016.2.JNS152485
54. Coget A, Deverdun J, Bonafé A, van Dokkum L, Duffau H, Molino F, et al. Transient immediate postoperative homotopic functional disconnectivity in low-grade glioma patients. *Neuroimage Clin*. (2018) 18:656–62. doi: 10.1016/j.nicl.2018.02.023

Conflict of Interest: The author declares that the research was conducted in the absence of any commercial or financial relationships that could be construed as a potential conflict of interest.

frontiers in Neurology

ORIGINAL RESEARCH
published: 19 November 2020
doi: 10.3389/fneur.2020.593950

Preoperative Transcranial Direct Current Stimulation in Glioma Patients: A Proof of Concept Pilot Study

Stefan Lang[1,2,3]*, *Liu Shi Gan*[1,2,3], *Cael McLennan*[1], *Adam Kirton*[1,2,3], *Oury Monchi*[1,2,3] and *John J. P. Kelly*[1,2,4]

[1] Hotchkiss Brain Institute, University of Calgary, Calgary, AB, Canada, [2] Department of Clinical Neurosciences, University of Calgary, Calgary, AB, Canada, [3] Non-invasive Neurostimulation Network, University of Calgary, Calgary, AB, Canada, [4] Charbonneau Cancer Institute, University of Calgary, Calgary, AB, Canada

Background: Transcranial direct current stimulation (tDCS) has been used extensively in patient populations to facilitate motor network plasticity. However, it has not been studied in patients with brain tumors. We aimed to determine the feasibility of a preoperative motor training and tDCS intervention in patients with glioma. In an exploratory manner, we assessed changes in motor network connectivity following this intervention and related these changes to predicted electrical field strength from the stimulated motor cortex.

Methods: Patients with left-sided glioma (n=8) were recruited in an open label proof of concept pilot trial and participated in four consecutive days of motor training combined with tDCS. The motor training consisted of a 60-min period where the subject learned to play the piano with their right hand. Concurrently, they received 40 min of 2 mA anodal tDCS of the left motor cortex. Patients underwent task and resting state fMRI before and after this intervention. Changes in both the connectivity of primary motor cortex (M1) and general connectivity across the brain were assessed. Patient specific finite element models were created and the predicted electrical field (EF) resulting from stimulation was computed. The magnitude of the EF was extracted from left M1 and correlated to the observed changes in functional connectivity.

Results: There were no adverse events and all subjects successfully completed the study protocol. Left M1 increased both local and global connectivity. Voxel-wide measures, not constrained by a specific region, revealed increased global connectivity of the frontal pole and decreased global connectivity of the supplementary motor area. The magnitude of EF applied to the left M1 correlated with changes in global connectivity of the right M1.

Conclusion: In this proof of concept pilot study, we demonstrate for the first time that tDCS appears to be feasible in glioma patients. In our exploratory analysis, we show preoperative motor training combined with tDCS may alter sensorimotor network connectivity. Patient specific modeling of EF in the presence of tumor may contribute to understanding the dose-response relationship of this intervention. Overall, this suggests the possibility of modulating neural networks in glioma patients.

Keywords: glioma, plasticity, transcranial direct current stimulation, functional connectivity, sensorimotor network, finite element model

OPEN ACCESS

Edited by:
Antonino F. Germano, University of Messina, Italy

Reviewed by:
Simon Hanft, Westchester Medical Center, United States
Güliz Acker, Charite Universitätsklinik Berlin, Germany

***Correspondence:**
Stefan Lang
stefan.t.lang@gmail.com

Specialty section:
This article was submitted to Neuro-Oncology and Neurosurgical Oncology, a section of the journal Frontiers in Neurology

Received: *12 August 2020*
Accepted: *22 October 2020*
Published: *19 November 2020*

Citation:
Lang S, Gan LS, McLennan C, Kirton A, Monchi O and Kelly JJP (2020) Preoperative Transcranial Direct Current Stimulation in Glioma Patients: A Proof of Concept Pilot Study. Front. Neurol. 11:593950. doi: 10.3389/fneur.2020.593950

INTRODUCTION

Transcranial direct current stimulation (tDCS) is a non-invasive neuromodulation technique which passes a low amplitude electrical current into the brain. While most of the current is shunted by the scalp (1), multiple studies suggest a biologically relevant portion reaches the brain (2, 3). The effect of this is complex but may result in a polarity dependent modulation of the resting membrane potential (4), an alteration of spontaneous firing rates (4–6), a change in the local excitatory/inhibitory balance (7), an alteration of neuronal oscillatory patterns (8), and a change in the synchronization of activity in distant brain regions (9–12). This technique has been shown to facilitate motor learning (13) and cortical plasticity in healthy subjects, as well as in disease states (14). While this technique has been used extensively in the motor rehabilitation and neuropsychiatric literature (15–17), it has never been investigated in the context of brain tumors. Gliomas are the most common primary brain tumor and are associated with high rates of neurological comorbidities, including motor and language deficits, as well as neuropsychiatric conditions (18–22). This patient population may therefore benefit from investigational use of tDCS. One unique opportunity arises in the context of "eloquent" (primary motor/language) cortex tumors. Mounting evidence suggests that an aggressive surgical resection improves overall survival in glioma patients (23, 24). However, tumors located near eloquent cortex represent a particularly difficult challenge due to the high rates of neurological morbidity following surgical resection. Specifically, the risk of permanent neurological deficit reaches 40% when motor cortex lesions are resected (25). Therefore, location within these critical regions is a major limitation toward the gold standard of maximal resection. Overcoming this difficult problem will require novel and innovative strategies. One proposed strategy has arisen from the observation that patients with tumor in close proximity to these critical regions may occasionally have minimal symptoms compared to that which may be expected based on size and location alone. In these patients, it is thought that the slow growing nature of the lesion has resulted in a dramatic reorganization of cortical structure and function, such that other regions of the brain have become involved in the implementation of the critical functions (26). This remarkable plasticity can allow for aggressive resection within classically eloquent regions (27). This exemplifies the fact that critical cortical regions, such as primary motor cortex, can be removed if their function has been redistributed to alternative regions of brain. Surgeons have used this phenomenon to achieve greater resection of tumor tissue around motor and language eloquent areas. For example, Gil Robles et al. (28) performed intraoperative cortical stimulation in multiple staged surgeries of low grade glioma of motor cortex to show that increased extent of resection was possible during the second surgery. This was proposed to be due to redistribution of functional tissue away from the residual tumor. This idea was taken further in a study which attempted to facilitate this functional reorganization in-between staged surgeries (29). In this pilot study, surgeons implanted a grid of electrodes over residual tumor which contained functional tissue. These electrodes provided continuous cortical stimulation, that when combined with a physiotherapy routine, presumably facilitated the redistribution of function out of these regions without a corresponding decrease in motor ability. This allowed for more extensive resection during a second surgery. While promising, this study utilized invasive cortical electrode implantation which was associated with significant complications (infection). Further, the mechanism of this effect was not investigated. Based on these ideas, we aimed to investigate, for the first time, the use of tDCS in glioma patients with the goal of neuromodulation. Importantly, tDCS has been shown to increase functional connectivity in the sensorimotor network (30). Functional connectivity of the sensorimotor network is related to motor performance in glioma patients (31) with increased connectivity related to better performance. Therefore, we attempted to facilitate plasticity of the sensorimotor network in patients during the preoperative period. To achieve this objective, we used a motor training program combined with tDCS. Functional connectivity analyses of BOLD MRI data were used to measure changes in the sensorimotor network, and patient specific computational modeling was used to relate any changes to the magnitude of the applied electrical field (EF). We hypothesize that this intervention will facilitate cortical plasticity, measured by increased connectivity of the sensorimotor network. To examine this, we first assessed the interhemispheric primary motor cortex (M1) connection, followed by an assessment of the global and local connectivity of M1. We were also interested in examining more general connectivity changes which may not be limited to the motor network and required no assumptions about location. To accomplish this, we assessed voxel-wide measures of global and local connectivity. Overall, this research has the potential of leading to novel clinical strategies for treating tumors within or near eloquent cortex.

Abbreviations: tDCS, transcranial direct current stimulation; M1, primary motor cortex; EF, electric field; ROI, region of interest; IC, intrinsic (global) connectivity; LCOR, integrated local correlation.

METHODS

Subjects

This study was approved by the Conjoint Health Research Ethics Board of the University of Calgary, and all patients provided informed consent. Over a period of 2 years, eight adult patients (mean age $= 46.6 \pm 15.46$) with left-sided diffuse gliomas primarily of the frontal and parietal regions were recruited from the University of Calgary surgical neurooncology clinic. Inclusion criteria included the presence of a presumed glioma in an ambulatory patient and the lack of significant neurological deficits precluding participation in the training program. With the exception of one patient, the tumor was located in close proximity to the precentral gyrus. Exclusion criteria included patients requiring emergent or urgent surgery, bilateral or right-sided tumor involvement, excessive midline shift, excessive peri-tumoral edema, and poorly controlled seizure activity. Exclusion criteria for the study also included contraindications to MR imaging (e.g., claustrophobia, implanted ferromagnetic

TABLE 1 | Demographic and tumor related data.

Patient	Age	Gender	Hand	Tumor location	Presenting symptom	Tumor grade	Genetics
1	46	M	L	Left post-central	Seizure	Grade III Astrocytoma	IDH mt, ATRX loss, MGMT methylated
2	63	F	R	Left post-central	Seizure	GBM	IDH WT, ATRX retained, p53 positive, MGMT unmethylated
3	31	M	R	Left frontal	Headache	Grade III Astrocytoma	IDH1 mt, ATRX loss, MGMT methylated, p53 positive
4	64	F	R	Left post-central	Word finding difficulty, right hand sensory deficit	GBM	IDH WT, ATRX retained, MGMT methylated
5	57	M	R	Left temporal	Seizure	Oligodendroglioma	IDH mt, 1p/19q codeletion
6	32	M	R	Left frontal	Seizure	GBM	IDH mutant, ATRX loss, MGMT methylated
7	55	F	R	Left frontal	Face numbness, right hand incoordination and dysarthria	GBM	IDH WT, p53 positive, MGMT methylated
8	25	F	R	Left frontal	Seizure	Grade II Astrocytoma	IDH mt, ATRX loss, MGMT methylated

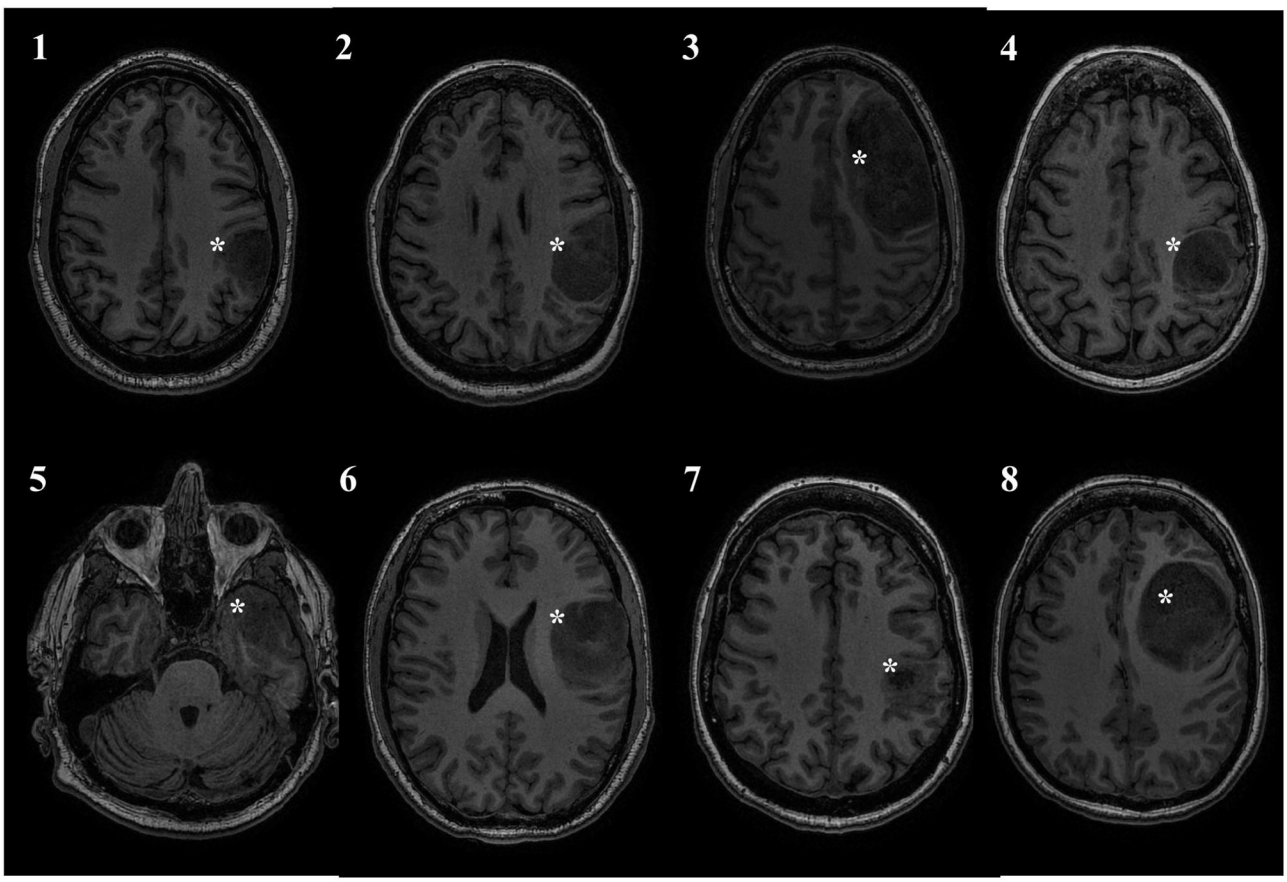

FIGURE 1 | Tumor location. All patients had left sided tumors, and 7/8 were in close proximity to the central sulcus. Tumor marked with a white asterisk.

devices, pregnancy). Demographic and tumor details are displayed in **Table 1**. **Figure 1** displays an axial T1WI in the plane of each subject's tumor.

tDCS and Motor Training

On four consecutive days, patients participated in motor training sessions combined with tDCS. tDCS was applied with the anode positioned over the left primary motor cortex and the cathode over the contralateral supraorbital area. The primary motor cortex was localized using the 10–20 Electroencephalography Electrode System (C3). All patients received active stimulation. Anodal tDCS was delivered through 35 cm^2 saline-soaked sponge electrodes using a DC Stimulator (Soterix Medical Inc., New York, USA). Current was ramped up to 2 mA over 30 s and maintained for 20 min. Immediately following application of the tDCS, subjects started training on a unilateral, right handed

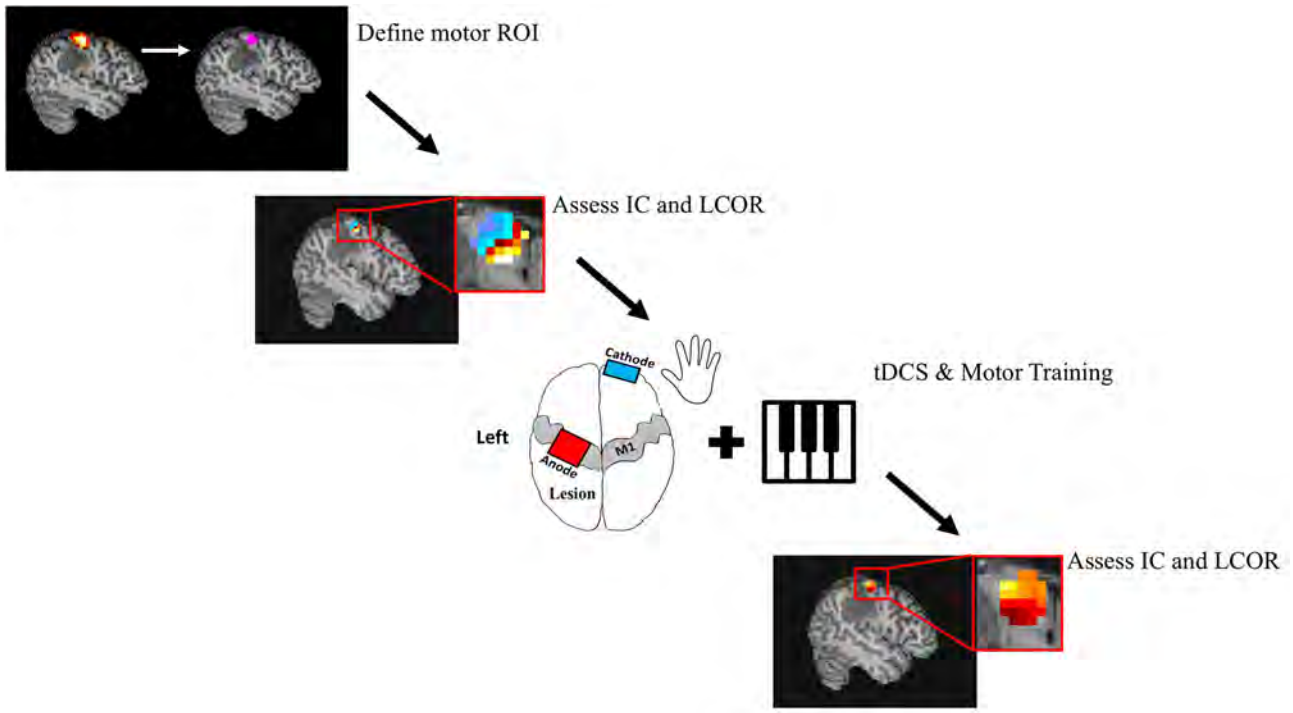

FIGURE 2 | Study Protocol. Patients underwent both task and resting state fMRI. Task fMRI was used to determine subject specific ROI's in the primary motor cortex. Resting state fMRI was used to calculate the global (Intrinsic Connectivity; IC) and local (Integrated local correlation; LCOR) connectivity of these M1 seeds. Patients then underwent 4 consecutive days of motor training and tDCS. The motor task consisted of a total of 60 min of individualized piano training, while a total of 40 min of 2 mA anodal tDCS was applied over the left motor cortex. Finally, global and local connectivity of M1 was calculated 24 h following the intervention.

music rhythm task of manual dexterity. In this task, subjects were given personalized piano playing instructions over the course of 30 min. This piano playing task was chosen because it is highly engaging for the subjects and requires focused attention. The first 20 min of this was done with concurrent stimulation. Once 30 min of training had occurred, the entire stimulation and training procedure was repeated. This resulted in a total of 40 min of stimulation and 60 min of training per day. Patients were piano naive, with the exception of one who had some experience as a child. The study protocol is displayed in **Figure 2**.

MRI Acquisition

All patients underwent both resting-state and task-based fMRI before and after the motor training/tDCS intervention. Task fMRI consisted of a hand clenching task, designed to elicit activation of the primary motor cortex. This task is routinely administered as part of a pre-surgical work-up to map motor regions. Participants open and close their hand in time with a visual cue, with each run alternating blocks of task and rest. This was performed unimanually with separate runs for each hand. The order of these runs were randomized, and each run was performed for a period of ∼4 min. All MRI data was acquired using a 3 Tesla GE Discovery MR750 whole body scanner with a receive-only 12-channel phased-array head coil (GE Healthcare, Waukesha, WI). Each participant's head was immobilized using foam cushioning, and participants had the option to terminate the study at any time during the scan using a squeeze ball placed in their hand. Resting-state fMRI was collected for two runs of 5 min using a gradient-recalled echo, echo planar imaging sequence (voxel dimensions 3.75 × 3.75 × 4 mm, 30 slices, 4-mm slice thickness, 64 × 64 matrix, TE = 30 ms, TR = 2,000 ms, flip angle = 65 degrees). Subjects were instructed to look at a fixation cross, let their mind wander freely, and to not fall asleep. T1-weighted multi-slice spoiled gradient (30 slices, 4-mm thickness, 128 × 128 matrix, minimum TE, TR = 150 ms, flip angle = 18 degrees) and 3D magnetization-prepared gradient-echo sequences (1.3 mm slices, 384 × 256 × 112 matrix, preparation time = 500 ms, minimum TE, TR = 8.9 ms, flip angle = 11 degrees) were collected for anatomical registration of the fMRI data. Task fMRI was also collected using a gradient-recalled echo, echo planar imaging sequence (voxel dimensions 3.75 × 3.74 × 4 mm, 28 slices, 4 mm slice thickness, 64 × 64 matrix, TE = 30 ms, TR = 1.5 s, flip angle = 65 degrees). Two scans were completed for each hand, for a total of four task fMRI runs.

Task fMRI Analysis

Task-fMRI data were analyzed to identify subject-specific seeds to be used in the subsequent ROI connectivity analyses. Images were preprocessed using SPM 12 software. Preprocessing steps included realignment, motion correction, co-registration of functional and structural images, non-linear normalization to MNI space, and smoothing using a 6-mm FWHM Gaussian

kernel. A time series general linear model analysis was performed on each patients' data, contrasting the motor task trial blocks with the rest blocks. The peak activation voxel from this contrast was used as the center of a 6-mm spherical ROI. This was performed separately for the data from both hands, resulting in two 6 mm spherical ROIs centered over bilateral primary motor cortex. In one subject, the peak activation voxel was located in the cerebellum and therefore the second highest voxel was chosen, which was located in the expected region of primary motor cortex. MNI coordinates for each subjects M1 ROI's can be found in **Supplementary Table 1**.

Resting State fMRI Preprocessing

Images were preprocessed and analyzed using the SPM toolbox Conn (32) (https://www.nitrc.org/projects/conn). Briefly, functional images underwent realignment, motion correction, slice-time correction, co-registration to high resolution structural images, and non-linear normalization to MNI space. The structural images were segmented into gray matter, white matter and CSF. Quality assurance, to detect outliers in motion and global signal intensity, was performed using the software *art* as implemented in Conn (https://www.nitrc.org/projects/artifact_detect). Outliers were included as regressors in the first level analysis, along with motion parameters and their first temporal derivatives. Physiological and other sources of noise from the white matter and CSF signal were estimated using the aCompcor method (32–34) and removed with the other covariates. The residual BOLD time series was high pass filtered at 0.009 Hz.

First Level Analysis

M1 Interhemispheric Connectivity

In order to specifically assess the interhemispheric connectivity within the sensorimotor network, we extracted the average residual BOLD time course (during the resting-state scans) from individualized seeds placed within left (stimulated) and right (non-stimulated) M1 regions. The Fisher Z transformed Pearson correlation coefficient was calculated between these two time courses.

M1 Global Connectivity

To assess global connectivity changes of M1, we computed a measure of network centrality known as intrinsic connectivity (IC) (35). This measure is characterized by the strength of connectivity between a given voxel and the rest of the brain. It is defined as the root mean square of correlation coefficients between each voxel and all the voxels in the brain.

$$IC\left(x\right) = \frac{\sqrt{\sum_{y \epsilon M} r(x,y)^2}}{N}$$

Where $IC(x)$ = Intrinsic Connectivity at voxel x; $r(x,y)$ = correlation coefficient between voxels x and y; and N = number of voxels. Subject specific dimensionality reduction of the voxel to voxel correlation matrices to 64 components was initially performed using singular value decomposition, followed by calculation of IC. These values are subsequently normalized. The resultant IC value was averaged over each voxel within the M1 seeds to derive a measure of M1 global connectivity.

M1 Local Connectivity

To assess local connectivity changes of M1, we next computed a measure of local coherence known as the integrated local correlation (LCOR) (36). LCOR is defined as the average of correlation coefficients between each individual voxel and a region of neighboring voxels. A full width half maximum kernel of 8 mm was used as a local weighting function.

$$LCOR\left(x\right) = \frac{\sum_{y \epsilon M} w\left(x-y\right) r(x,y)}{\sum_{y \epsilon M} w(x-y)}$$

$$w\left(z\right) = e^{\frac{-|z|^2}{2\sigma^2}}$$

Where $LCOR(x)$ = local correlation at voxel x; $r(x,y)$ = correlation coefficient between voxels x and y; and $w(z)$ = isotropic Gaussian weighting function. The LCOR measure was averaged over each voxel within the M1 seeds to derive a measure of M1 local connectivity.

M1 to Whole Brain Connectivity

To further assess the connectivity of M1, we performed a ROI to whole brain analysis using the same M1 seeds derived for each subject from the task fMRI analysis. The Fisher transformed Pearson correlation between the average BOLD signal from the left and right ROI and the signal from each voxel in the brain was calculated.

Global and Local Connectivity Across the Whole Brain

To determine if connectivity changes were occurring in regions of the brain outside of M1, we assessed changes in IC and LCOR on a voxel-wide manner, without restricting the analysis to a specific ROI.

Second Level Analysis and Statistics

The Shapiro-Wilk test was used to assess for normality of data. Changes in interhemispheric connectivity, M1 global connectivity, and M1 local connectivity were assessed with a one-tailed paired t-test, considering our hypothesis of increased M1 connectivity. Significance was determined at $p < 0.05$. Voxel-wide second level analyses (M1 to whole brain and voxel-wide global & local connectivity) were implemented in Conn using the general linear model and the likelihood ratio test to evaluate model parameters. Clusters were thresholded with a significance of $p < 0.005$ at the voxel level and $p < 0.05$ corrected for multiple comparisons with the false discovery rate at the cluster level. Linear regression was used to relate the change in global and local connectivity from right and left M1 with the average electrical field magnitude extracted from the left M1 ROI. Significance was set at $p < 0.05$.

Patient Specific Electrical Field Modeling

We performed patient specific computational modeling of the electric field resulting from the tDCS intervention, taking into consideration the anatomy and tissue components of the tumor.

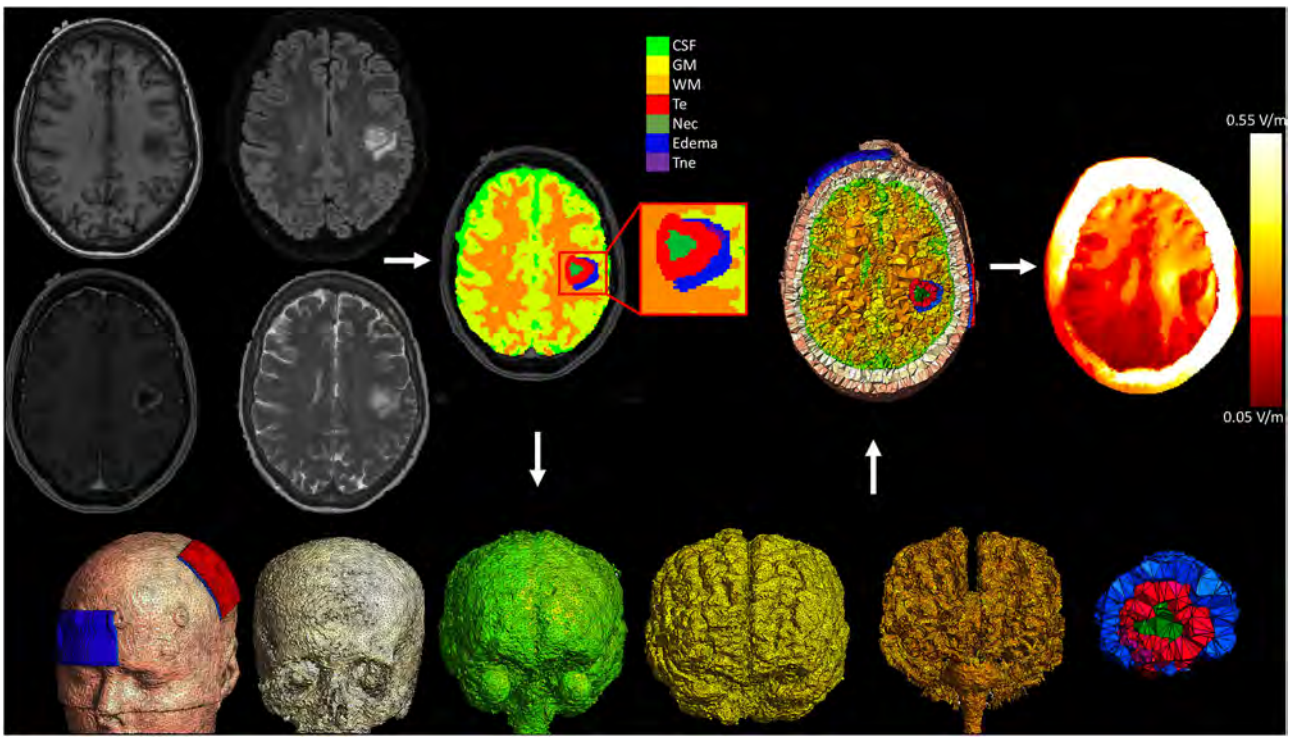

FIGURE 3 | Pipeline for patient specific electric field modeling. Each subject underwent T1WI, T2WI, T1WI with gadolinium, and FLAIR imaging as part of their routine clinical care. These images were used to segment the head, brain, and tumor into component tissue classes. A modified version of ROAST was then used to mesh the volumes and solve the finite element model. CSF, cerebrospinal fluid; GM, gray matter; WM, white matter; Te, enhancing tumor; Nec, necrosis; Tne, non-enhancing tumor.

Methodology was similar to our previous work modeling electric fields in glioma patients (37). Briefly, to perform detailed tumor segmentation, we used four MRI sequences (T1WI, T2WI, T1WI with Gadolinium and FLAIR) acquired during the routine clinical care of each patient. Using these scans as input, each subjects brain tumor was segmented into component tissues classes using an automated segmentation software [BraTumIA (38)], followed by manual correction. The tissues classes included in the model included non-enhancing tumor, enhancing tumor, necrosis, and edema. Finite element models were then created using a modified version of the Realistic vOlumetric Approach to Simulate Transcranial electrical stimulation (ROAST) pipeline (39). ROAST uses SPM12 to segment the entire head and neck and combines this with a post-processing routine to ensure continuity of CSF. A tetrahedral volume mesh is then created with iso2mesh (40), and the Laplace equation for voltage distribution is solved using getDP (41). Custom MATLAB scripts were integrated into this pipeline to allow for the addition of the tumor component masks, each with a unique conductivity. Enhancing and non-enhancing tumor were assigned conductivity values of 0.170 S/m and 0.332 S/m respectively (42, 43). Necrosis and edema tissues were assigned conductivities of 1.0 S/m, and 1.185 S/m (44, 45). The default values for conductivity of healthy tissue classes in the ROAST pipeline were used (white matter: 0.126 S/m; gray matter: 0.276 S/m; cerebrospinal fluid: 1.65 S/m; bone: 0.01 S/m; skin: 0.465 S/m; air: 2.5^{-14} S/m; gel: 0.3 S/m; electrode: 5.9^{7} S/m). Electrodes (5×7 cm^2) were placed at C3 and FP1, simulating the anodal M1 tDCS configuration performed in the study. The average electric field strength (the vector norm of the electric field) was extracted from the left M1 ROI and used in the regression with connectivity values. **Figure 3** displays the pipeline for a representative subject.

RESULTS

tDCS and Motor Training Compliance and Tolerability

All patients were examined clinically, and no motor deficits were noted prior to enrollment. Five presented with a new onset seizure, though these were under control prior to initiating the experimental paradigm. One patient was found to have sensory disturbance in the right hand, while another had minor complaints of incoordination. One subject had subjective language complaints. The clinical exam was otherwise unremarkable for all other subjects. All patients, with the exception of one, completed the study visits as designed. In each case, the follow-up fMRI was performed 24 h after the final training session. In one patient, three of the four intervention days were completed due to subject preference, and the follow-up MRI was performed 48 h following the last training session. All subjects tolerated the stimulation and there were no adverse

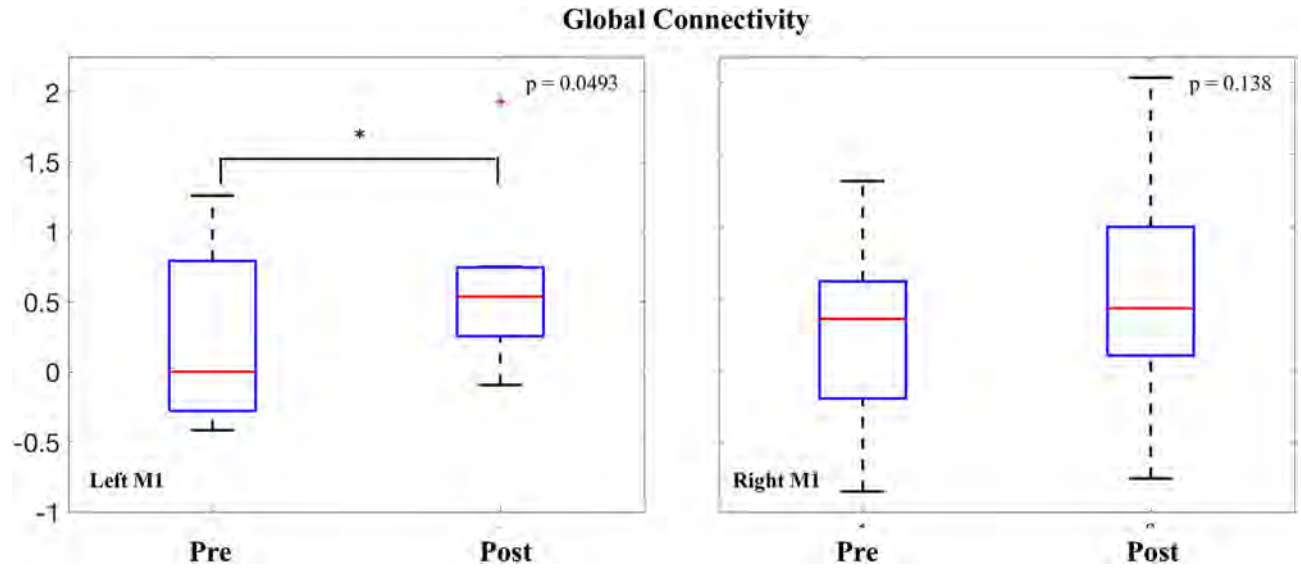

FIGURE 4 | Change in global connectivity of M1.

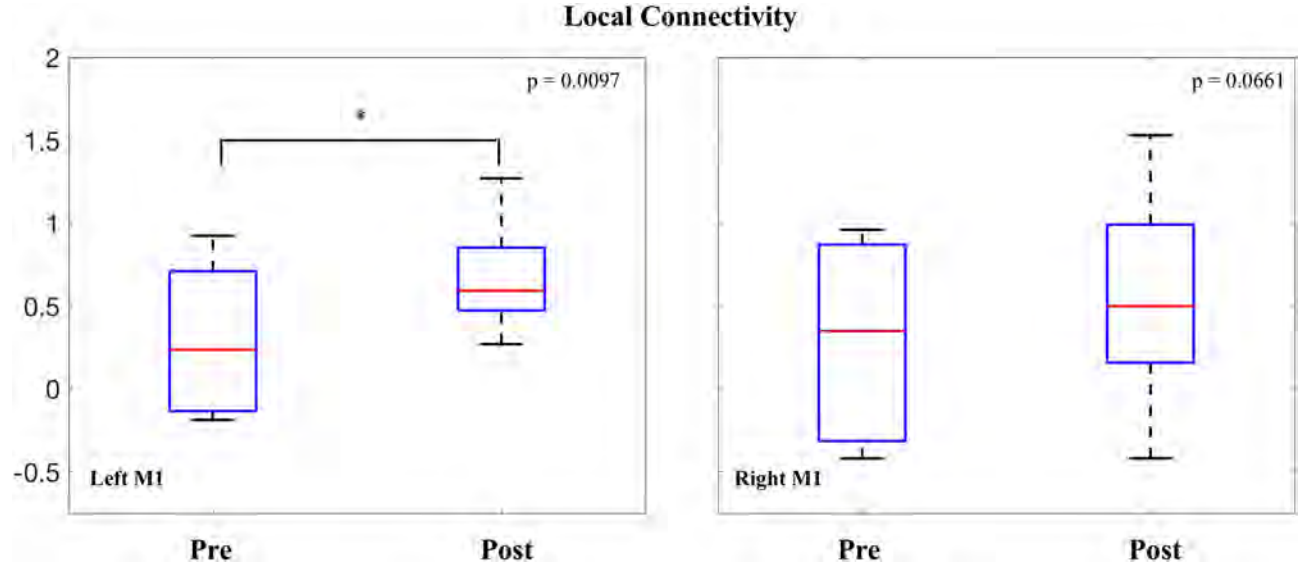

FIGURE 5 | Change in local connectivity of M1.

effects observed. No seizures were noted during the experimental period. Minor tingling and itching sensations were reported by all subjects, consistent with the vast tDCS safety literature (46). All patients subjectively improved motor performance on the task.

M1 Interhemispheric Connectivity

All connectivity and electrical field data were normally distributed as determined by the Shapiro-Wilk test. Patients on average showed an increase in interhemispheric connectivity following the intervention (0.095 ± 0.16). However, this difference did not reach threshold for statistical significance [$t_{(7)} = 1.62$, $p = 0.0743$].

M1 Global Connectivity

Intrinsic connectivity values were averaged within both the right and left M1 seeds and compared before and after the intervention. In the left (stimulated) M1, a significant increase was observed in global connectivity [0.380 ± 0.56; $t_{(7)} = 1.90$, $p = 0.0493$]. In the right (non-stimulated) M1, no difference was observed in global connectivity values before and after the intervention [0.290 ± 0.69; $t_{(7)} = 1.18$, $p = 0.138$] (**Figure 4**).

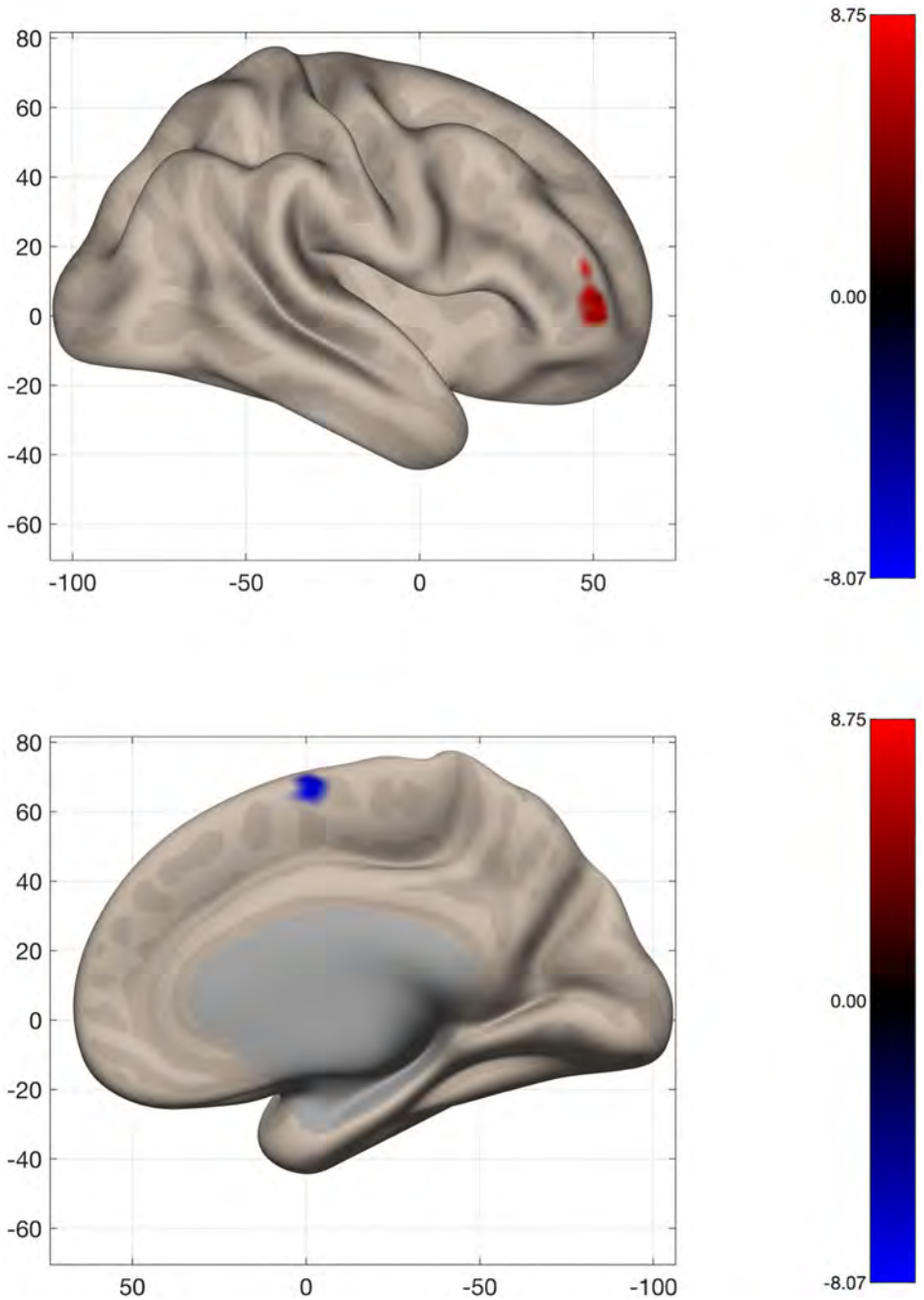

FIGURE 6 | Voxel-wide global connectivity alterations. Significant clusters are seen in the right frontal pole (increased) and supplementary motor area (decreased). Color bar represents T-score.

M1 Local Connectivity

LCOR values were also averaged within both the right and left M1 seeds and compared before and after the intervention. In the left M1, a significant increase was observed in local connectivity [0.377 ± 0.35; $t_{(7)} = 3.02$, $p = 0.0097$]. In the right M1, the change in average local connectivity did not reach threshold for statistical significance [0.257 ± 0.43; $t_{(7)} = 1.7$, $p = 0.0661$] (**Figure 5**).

M1 to Whole Brain Connectivity

To further assess the change in connectivity of M1, the time course of individualized seeds placed in left and right M1 were correlated with the time course from each voxel across the entire brain and compared before and after the intervention. No significant clusters were identified from either the left or right M1 seed.

Global and Local Connectivity Across the Whole Brain

To assess changes in connectivity which may not be limited to the sensorimotor network, we calculated IC and LCOR for every voxel in the brain and compared these values before and after the intervention. Following the intervention, patients had less global connectivity in a cluster spanning the supplementary motor cortex, while they showed increased connectivity in a cluster located in the right frontal pole (**Figure 6**). When assessed across the entire brain, no significant clusters of LCOR were observed. MNI coordinates and statistics of the significant clusters are displayed in **Table 2**.

TABLE 2 | Cluster location and statistics from voxel-wide analysis of Intrinsic Connectivity (IC).

Analysis	Cluster	MNI (x, y, z)	Size (voxels)	Peak *p*-value	Anatomical location
IC	1	42, 46, 06	76	0.000032	Right frontal pole
	2	06, −02, 62	51	0.000044	Right Supplementary Motor Area

Patient Specific Electric Field Modeling

The average electrical field strength in the brain was 0.196 ± 0.02 V/m (range 0.17–0.23 V/m), while the average EF from the left M1 ROI was 0.229 ± 0.06 V/m (range 0.16–0.33 V/m). The correlation between the average strength of the EF in left M1 and the change in global ($r^2 = 0.0257$; $p = 0.705$) and local connectivity ($r^2 = 0.0006$; $p = 0.953$) also from left M1 did not reach statistical significance. This was also true for the correlation between the change in local connectivity from right M1 with the EF magnitude from left M1 ($r^2 = 0.33$; $p = 0.136$). However, there was a significant correlation between the EF magnitude in left M1 and the change in global connectivity from the right M1 ($r^2 = 0.53$; $p = 0.0404$) (**Figure 7**).

DISCUSSION

In this proof of principle pilot study, we show for the first time that tDCS is feasible in glioma patients. Further, we demonstrate that motor training, combined with tDCS, may alter sensorimotor network connectivity in this patient population. Patients with left-sided diffuse glioma (primarily of the frontal and parietal lobes and in proximity to the central sulcus) underwent repeated motor training using a piano playing task, while anodal tDCS was applied to the motor cortex. Functional MRI was performed before and after this intervention, and changes in brain connectivity were assessed. Connectivity of the sensorimotor network, using individualized ROI's within the primary motor cortex, was computed. We assessed the interhemispheric connection between bilateral M1 as well as the global and local connectivity of M1 more broadly. We then performed voxel-wide analyses to assess for connectivity changes which did not depend on *a priori* ROIs. Interhemispheric connectivity did not change as a result of our intervention. However, the functional connectivity of M1 was altered more broadly. Patients had both increased global and local connectivity of M1 following the intervention. The seed to whole brain analysis did not show significant clusters, suggesting the increased global and local connectivity observed in M1 was not due to any particular connection. We then performed two data driven analyses in order to assess for connectivity changes occurring across the whole brain. Global connectivity increases were seen in the right frontal pole, while decreases were seen in the supplementary motor cortex. Taken together, the motor training/tDCS intervention may have resulted in increased global and local connectivity of M1, which did not appear to be due to a particular connection, while other regions showed altered global connectivity. Speculatively, decreased global connectivity of the pre-SMA may result from motor learning, as this region has been shown to decrease its contribution to motor tasks with increased practice (47). Increased right frontal global connectivity may have occurred from the cognitive demands of learning action-outcome associations required for successful task performance (48).

Patient specific models of the applied electrical field were created, taking into consideration the anatomy and conductivity of tumor tissue components. The average field strength from the stimulated (left) M1 was extracted and related to the connectivity changes of both the right and left M1. Surprisingly, there was no relationship between the applied EF and connectivity changes of the ipsilateral M1, while there appeared to be an inverse relationship with connectivity changes in the contralateral hemisphere. It is uncertain what this relationship means, though it suggests a possible dose-dependent effect of tDCS on connectivity changes. Speculatively, it suggests an inhibitory effect of the stimulation on contralateral plasticity. Further work is needed to try to elucidate this relationship.

The combination of tDCS and motor training to facilitate cortical plasticity has been studied extensively in the motor rehabilitation literature. The highest volume of data comes from adult stroke rehabilitation, where pooled analyses suggest beneficial motor effects (49), likely in a dose dependant manner (16). The novelty of our study comes from applying these insights for the first time to glioma patients and attempting to facilitate an on-going plasticity process before a planned insult occurs. The idea of attempting to prevent deficits (rather than treat deficits) derives from the concept of prehabilitation, which has gained traction in recent years. It represents a paradigm change away from the reactive model of healthcare toward a proactive approach which engages patients in their care (50). Prehabilitation of the brain presupposes that changes in functional networks are occurring that may confer resiliency against insult. Our results support the idea that periods of prehabilitation can result in connectivity changes of cortical networks, though no conclusions can be made regarding the clinical impact of these changes. Speculatively, we suggest that increased connectivity of the sensorimotor network may increase "motor reserve," a testable hypothesis which is critical to the clinical translation of this work. This idea stems from the concept of "brain reserve," which is defined as the ability to tolerate disease related pathology in the brain without developing clear clinical symptoms or signs (51, 52). This concept of "brain

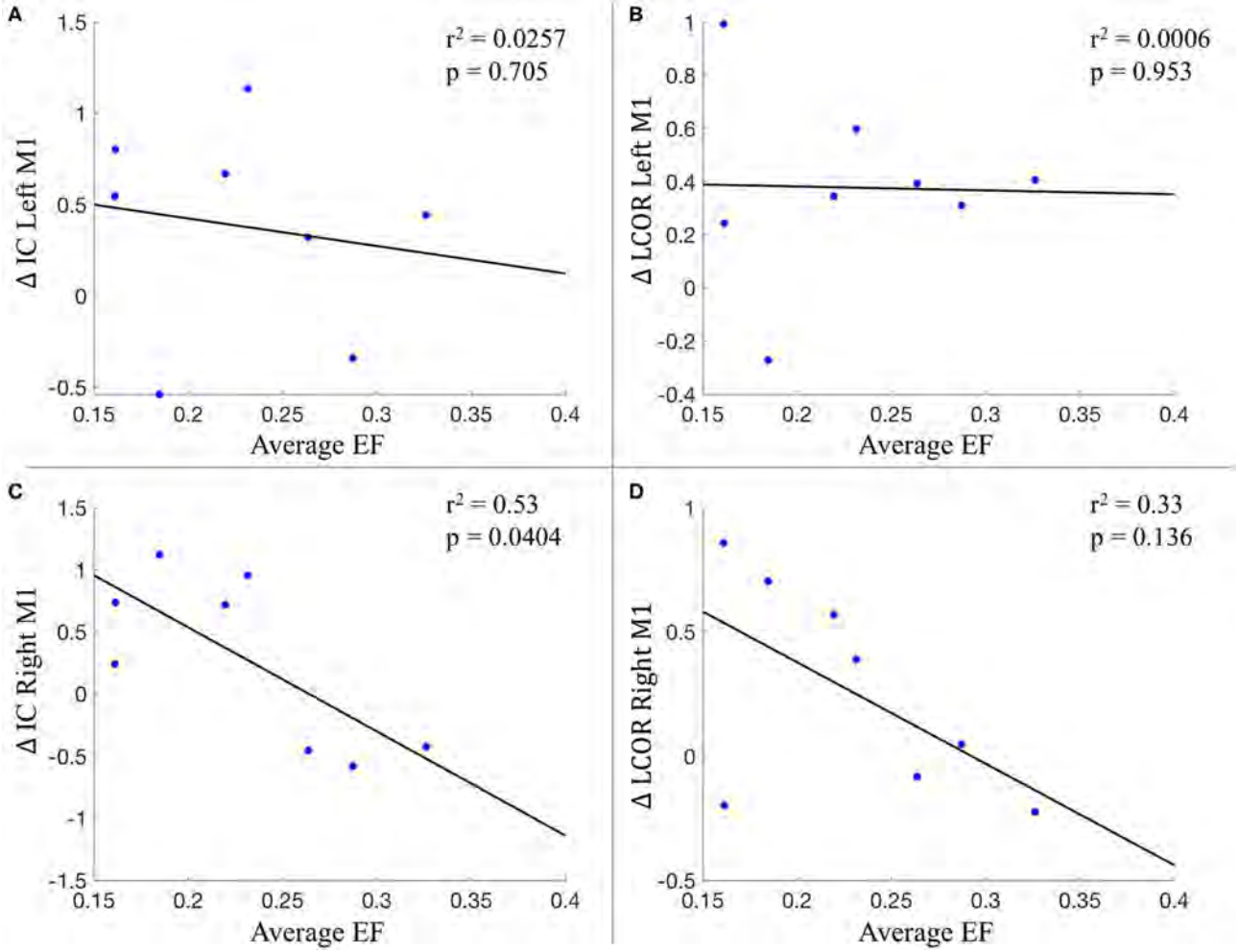

FIGURE 7 | Relationship between the average electric field from left M1 and connectivity changes**. (A)** Change in IC of left M1; **(B)** Change in LCOR of left M1; **(C)** Change in IC of right M1; **(D)** Change in LCOR of right M1. IC, intrinsic connectivity; LCOR, Integrated local correlation; EF, electric field.

reserve" is typically discussed with respect to cognition, but has also been extended to the motor domain (53). Supporting our speculation, there is some literature to suggest that increased global connectivity can contribute to "brain reserve." Here, increased global connectivity of the left frontal cortex has been shown to underlie cognitive reserve in dementia (54, 55).

One further consideration is whether tDCS is the optimal non-invasive brain stimulation technique for facilitating plasticity in brain tumor patients. Transcranial magnetic stimulation (TMS) is used frequently in glioma patients, typically with the goal of mapping eloquent cortex in the preoperative period (56, 57). TMS has a different mechanism of action, working to induce current in the brain via a rapidly changing magnetic field (58). TMS has the benefit of directly eliciting action potentials, allowing for quantifiable electrophysiological measurements of motor evoked potentials. When delivered with repetitive pulses (rTMS), the technique can modulate cortical plasticity and enhance motor performance in healthy (59) and patient populations (60). Whether or not rTMS can facilitate plasticity in glioma patients remains to be determined. Further, while there is extensive use of single pulse navigated TMS in glioma patients, the safety profile of rTMS in this patient population has not been investigated.

There are important limitations to this study that must be considered. Firstly, no conclusion can be made about the relative influence of tDCS or motor training on the connectivity results. Indeed, these results may represent an effect of motor training alone, though this also cannot be concluded from our data. Motor training has been shown to modulate connectivity in the sensorimotor network independent of tDCS (61), though tDCS can facilitate motor learning (13), and can affect motor connectivity independent of training (62). The appropriate conclusion to be drawn from the current study is that sensorimotor network connectivity likely changed as a result of the applied intervention, without specifying between tDCS or motor training. This study was designed as an open-label, proof of concept pilot trial aimed at recruiting a group of glioma patients in order to demonstrate that a tDCS/motor training intervention is feasible in this patient population. We recruited a relatively homogenous group (based on tumor

TABLE 3 | Future directions for clinical translation.

1	What is the optimal motor training paradigm for facilitating plasticity of motor networks in glioma patients?
2	What are the optimal electrode configurations and stimulation parameters?
3	What is the minimum length of time for combined motor training and NIBS to induce long-lasting changes in motor networks?
4	Does facilitating plasticity in the preoperative period lead to improved extent of resection?
5	Does facilitating plasticity in the preoperative period lead to improved motor outcomes following surgery?
6	How does the tumor affect the electric field magnitude within the brain?
7	Are there dose-response relationships between electric field magnitude and motor network plasticity?
8	What is the best measurement of network reorganization in glioma patients?
9	How does glioma grade and genetics alter response to NIBS?

NIBS, non-invasive brain stimulation.

location on the left and in proximity to the central sulcus) to explore if the sensorimotor network can undergo changes with a preoperative intervention. As such, the sample size is small, and the findings must be considered in light of this. Further, the clinical implications of these functional connectivity changes are unclear. Previous work has suggested connectivity of the sensorimotor network can track motor ability in glioma patients, with increased connectivity corresponding to increased strength (31). However, as discussed, it is unclear if increased connectivity bestows motor reserve. Importantly, the lack of a control group precludes any definitive conclusions about the effect of our intervention. However, we believe this experience is worth reporting given its high novelty and the potential to spur further investigation into this understudied patient population. We have outlined many of the unresolved questions and areas of future research in **Table 3**.

CONCLUSION

In summary, we demonstrate that tDCS is feasible in preoperative glioma subjects, and that preoperative motor training combined with tDCS may alter sensorimotor network connectivity. Patient specific modeling of the electrical field suggests there may be a dose-dependent relationship between stimulation and connectivity changes. Given the difficult problem of eloquent cortex tumors, novel and innovative strategies need to be designed to benefit patients who otherwise have limited treatment options. Our results suggest that the possibility of modulating neural networks prior to surgery in order to confer resiliency against impending insult is possible. Further work needs to be done to determine how long these changes last for, the optimal training and stimulation paradigms, including any dose-dependent effects, and whether or not modulating the functional connectivity of networks has any clinical benefit for patients. Overall, this proof of principle pilot trial is, to our knowledge, the first study attempting tDCS in glioma patients and supports future investigations into neuromodulation for patients with brain tumors.

DATA AVAILABILITY STATEMENT

The raw data supporting the conclusions of this article will be made available by the authors, without undue reservation.

ETHICS STATEMENT

The studies involving human participants were reviewed and approved by Conjoint Health Research Ethics Board of the University of Calgary. The patients/participants provided their written informed consent to participate in this study.

AUTHOR CONTRIBUTIONS

SL: conceptualization, methodology, investigation, formal analysis, writing-original draft, writing-review and editing, and visualization. LG: methodology, investigation, and writing-review and editing. CM: investigation. AK: conceptualization and writing-review and editing. OM and JK: writing-review and editing and supervision. All authors contributed to the article and approved the submitted version.

FUNDING

This work was supported by the Neurosurgery Research and Education Foundation & AANS/CNS Section on Tumors Research Fellowship Grant awarded to SL.

SUPPLEMENTARY MATERIAL

The Supplementary Material for this article can be found online at: https://www.frontiersin.org/articles/10.3389/fneur.2020.593950/full#supplementary-material

REFERENCES

1. Vöröslakos M, Takeuchi Y, Fernández-ruiz A, Kozák G, Buzsáki G, Berényi A, et al. Direct effects of transcranial electric stimulation on brain circuits in rats and humans. *Nat Commun.* (2018) 9:483. doi: 10.1038/s41467-018-02928-3
2. Huang Y, Liu AA, Lafon B, Friedman D, Dayan M, Wang X, et al. Measurements and models of electric fields in the *in vivo* human brain during transcranial electric stimulation. *Elife.* (2017) 6:e18834. doi: 10.7554/eLife.18834
3. Chhatbar PY, Kautz SA, Takacs I, Rowland NC, Revuelta GJ, George MS, et al. Evidence of transcranial direct current stimulation-generated electric fields at subthalamic level in human brain *in vivo*. *Brain Stimul.* (2018) 11:727–33. doi: 10.1016/j.brs.2018.03.006
4. Bindman LJ, Lippold OCJ, Redfearn JWT. Long-lasting changes in the level of the electrical activity of the cerebral cortex produced by polarizing currents. *Nature.* (1962) 196:584. doi: 10.1038/196584a0
5. Bindman LJ, Lippold OCJ, Redfearn JWT. The action of brief polarizing currents on the cerebral cortex of the rat (1) during current flow and (2)

in the production of long-lasting after-effects. *J Physiol.* (1964) 172:369–82. doi: 10.1113/jphysiol.1964.sp007425
6. Jamil A, Nitsche MA. What effect does tDCS have on the brain? Basic physiology of tDCS. *Curr Behav Neurosci Rep.* (2017) 4:331–40. doi: 10.1007/s40473-017-0134-5
7. Kim S, Stephenson MC, Morris PG, Jackson SR. TDCS-induced alterations in GABA concentration within primary motor cortex predict motor learning and motor memory: a 7T magnetic resonance spectroscopy study. *Neuroimage.* (2014) 99:237–43. doi: 10.1016/j.neuroimage.2014.05.070
8. Hanley CJ, Singh KD, McGonigle DJ. Transcranial modulation of brain oscillatory responses: a concurrent tDCS–MEG investigation. *Neuroimage.* (2016) 140:20–32. doi: 10.1016/j.neuroimage.2015.12.021
9. Sehm B, Schaefer A, Kipping J, Margulies D, Conde V, Taubert M, et al. Dynamic modulation of intrinsic functional connectivity by transcranial direct current stimulation. *J Neurophysiol.* (2012) 108:3253–63. doi: 10.1152/jn.00606.2012
10. Kunze T, Hunold A, Haueisen J, Jirsa V, Spiegler A. Transcranial direct current stimulation changes resting state functional connectivity: a large-scale brain network modeling study. *Neuroimage.* (2016) 140:174–87. doi: 10.1016/j.neuroimage.2016.02.015
11. Polanía R, Paulus W, Antal A, Nitsche MA. Introducing graph theory to track for neuroplastic alterations in the resting human brain: a transcranial direct current stimulation study. *Neuroimage.* (2011) 54:2287–96. doi: 10.1016/j.neuroimage.2010.09.085
12. Mancini M, Brignani D, Conforto S, Mauri P, Miniussi C, Pellicciari MC. Assessing cortical synchronization during transcranial direct current stimulation: a graph-theoretical analysis. *Neuroimage.* (2016) 140:57–65. doi: 10.1016/j.neuroimage.2016.06.003
13. Reis J, Schambra HM, Cohen LG, Buch ER, Fritsch B, Zarahn E, et al. Noninvasive cortical stimulation enhances motor skill acquisition over multiple days through an effect on consolidation. *Proc Natl Acad Sci USA.* (2009). 106:1506–5. doi: 10.1073/pnas.0805413106
14. Lefaucheur J-P, Antal A, Ayache SS, Benninger DH, Brunelin J, Cogiamanian F, et al. Evidence-based guidelines on the therapeutic use of transcranial direct current stimulation (tDCS). *Clin Neurophysiol.* (2017) 128:56–92. doi: 10.1016/j.clinph.2016.10.087
15. Allman C, Amadi U, Winkler AM, Wilkins L, Filippini N, Kischka U, et al. Ipsilesional anodal tDCS enhances the functional benefits of rehabilitation in patients after stroke. *Sci Transl Med.* (2016) 8:330re1. doi: 10.1126/scitranslmed.aad5651
16. Chhatbar PY, Ramakrishnan V, Kautz S, George MS, Adams RJ, Feng W. Transcranial direct current stimulation post-stroke upper extremity motor recovery studies exhibit a dose–response relationship. *Brain Stimul.* (2016) 9:16–26. doi: 10.1016/j.brs.2015.09.002
17. Sale M V, Mattingley JB, Zalesky A, Cocchi L. Imaging human brain networks to improve the clinical efficacy of non-invasive brain stimulation. *Neurosci Biobehav Rev.* (2015) 57:187–98. doi: 10.1016/j.neubiorev.2015.09.010
18. D'Angelo C, Mirijello A, Leggio L, Ferrulli A, Carotenuto V, Icolaro N, et al. State and trait anxiety and depression in patients with primary brain tumors before and after surgery: 1-year longitudinal study. *J Neurosurg.* (2008) 108:281–6. doi: 10.3171/JNS/2008/108/2/0281
19. Lang S, Cadeaux M, Opoku-Darko M, Gaxiola-Valdeza I, Partlo L, Goodyear BG, et al. Assessment of cognitive, emotional, and motor domains in patients with diffuse gliomas using the National Institutes of health toolbox battery. *World Neurosurg.* (2017) 99:448–56. doi: 10.1016/j.wneu.2016.12.061
20. Osoba D, Brada M, Prados MD, Yung WKA. Effect of disease burden on health-related quality of life in patients with malignant gliomas. *Neuro Oncol.* (2000) 2:221–8. doi: 10.1093/neuonc/2.4.221
21. Kushner DS, Amidei C. Rehabilitation of motor dysfunction in primary brain tumor patients†. *Neuro-Oncol Pract.* (2015) 2:185–91. doi: 10.1093/nop/npv019
22. Amidei C, Kushner DS. Clinical implications of motor deficits related to brain tumors†. *Neuro-Oncology Pract.* (2015) 2:179–84. doi: 10.1093/nop/npv017
23. Lacroix M, Abi-Said D, Fourney DR, Gokaslan ZL, Shi W, DeMonte F, et al. A multivariate analysis of 416 patients with glioblastoma multiforme: prognosis, extent of resection, and survival. *J Neurosurg.* (2001) 95:190–8. doi: 10.3171/jns.2001.95.2.0190
24. Duffau H. A new philosophy in surgery for diffuse low-grade glioma (DLGG): oncological and functional outcomes. *Neurochirurgie.* (2013) 59:2–8. doi: 10.1016/j.neuchi.2012.11.001
25. Magill ST, Han SJ, Li J, Berger MS. Resection of primary motor cortex tumors: feasibility and surgical outcomes. *J Neurosurg.* (2018) 129:961–72. doi: 10.3171/2017.5.JNS163045
26. Duffau H. The huge plastic potential of adult brain and the role of connectomics: new insights provided by serial mappings in glioma surgery. *Cortex.* (2014) 58:325–37. doi: 10.1016/j.cortex.2013.08.005
27. Benzagmout M, Gatignol P, Duffau H. Resection of World Health Organization grade II gliomas involving Broca's area: methodological and functional considerations. *Neurosurgery.* (2007) 61:741–3. doi: 10.1227/01.NEU.0000298902.69473.77
28. Robles SG, Gatignol P, Lehéricy S, Duffau H. Long-term brain plasticity allowing a multistage surgical approach to World Health Organization grade II gliomas in eloquent areas. *J Neurosurg.* (2008) 109:615–24. doi: 10.3171/JNS/2008/109/10/0615
29. Rivera-Rivera PA, Rios-Lago M, Sanchez-Casarrubios S, Salazar O, Yus M, González-Hidalgo M, et al. Cortical plasticity catalyzed by prehabilitation enables extensive resection of brain tumors in eloquent areas. *J Neurosurg.* (2017) 126:1323–33. doi: 10.3171/2016.2.JNS152485
30. Krause MR, Zanos TP, Csorba BA, Pilly PK, Choe J, Phillips ME, et al. Transcranial direct current stimulation facilitates associative learning and alters functional connectivity in the primate brain. *Curr Biol.* (2017) 27:3086–96.e3. doi: 10.1016/j.cub.2017.09.020
31. Otten ML, Mikell CB, Youngerman BE, Liston C, Sisti MB, Bruce JN, et al. Motor deficits correlate with resting state motor network connectivity in patients with brain tumours. *Brain.* (2012) 135:1017–26. doi: 10.1093/brain/aws041
32. Whitfield-Gabrieli S, Nieto-Castanon A. Conn: a functional connectivity toolbox for correlated and anticorrelated brain networks. *Brain Connect.* (2012) 2:125–41. doi: 10.1089/brain.2012.0073
33. Behzadi Y, Restom K, Liau J, Liu TT. A component based noise correction method (CompCor) for BOLD and perfusion based fMRI. *Neuroimage.* (2007) 37:90–101. doi: 10.1016/j.neuroimage.2007.04.042
34. Chai XJ, Castanon AN, Ongur D, Whitfield-Gabrieli S. Anticorrelations in resting state networks without global signal regression. *Neuroimage.* (2012) 59:1420–8. doi: 10.1016/j.neuroimage.2011.08.048
35. Martuzzi R, Ramani R, Qiu M, Shen X, Papademetris X, Constable RT. A whole-brain voxel based measure of intrinsic connectivity contrast reveals local changes in tissue connectivity with anesthetic without a priori assumptions on thresholds or regions of interest. *Neuroimage.* (2011) 58:1044–50. doi: 10.1016/j.neuroimage.2011.06.075
36. Deshpande G, LaConte S, Peltier S, Hu X. Integrated local correlation: a new measure of local coherence in fMRI data. *Hum Brain Mapp.* (2009) 30:13–23. doi: 10.1002/hbm.20482
37. Lang S, Gan LS, McLennan C, Monchi O, Kelly J. Impact of peritumoral edema during tumor treatment field therapy: a computational modelling study. *IEEE Trans Biomed Eng.* (2020). doi: 10.1109/TBME.2020.2983653. [Epub ahead of print].
38. Porz N, Bauer S, Pica A, Schucht P, Beck J, Verma RK, et al. Multi-modal glioblastoma segmentation: man versus machine. *PLoS ONE.* (2014) 9:e96873. doi: 10.1371/journal.pone.0096873
39. Huang Y, Datta A, Bikson M, Parra LC. Realistic volumetric-approach to simulate transcranial electric stimulation—ROAST—a fully automated open-source pipeline. *J Neural Eng.* (2019) 16:56006. doi: 10.1088/1741-2552/ab208d
40. Fang Q, Boas DA. Tetrahedral mesh generation from volumetric binary and grayscale images. In: *IEEE International Symposium on Biomedical Imaging: From Nano to Macro.* Boston, MA (2009). p. 1142–5.
41. Dular P, Geuzaine C, Henrotte F, Legros W. A general environment for the treatment of discrete problems and its application to the finite element method. *IEEE Trans Magn.* (1998) 34:3395–8. doi: 10.1109/20.717799
42. Latikka J, Eskola H. The resistivity of human brain tumours *in vivo*. *Ann Biomed Eng.* (2019) 47:706–13. doi: 10.1007/s10439-018-02189-7
43. Rajshekhar V. Continuous impedance monitoring during CT-guided stereotactic surgery: relative value in cystic and solid lesions. *Br J Neurosurg.* (1992) 6:439–44. doi: 10.3109/02688699208995033

44. Korshoej AR, Hansen FL, Thielscher A, von Oettingen GB, Sørensen JCH. Impact of tumor position, conductivity distribution and tissue homogeneity on the distribution of tumor treating fields in a human brain: a computer modeling study. *PLoS ONE.* (2017) 12:e0179214. doi: 10.1371/journal.pone.0179214
45. Liao Y, Oros-Peusquens A-M, Lindemeyer J, Lechea N, Weiß -Lucas C, Langen K-J, et al. An MR technique for simultaneous quantitative imaging of water content, conductivity and susceptibility, with application to brain tumours using a 3T hybrid MR-PET scanner. *Sci Rep.* (2019) 9:88. doi: 10.1038/s41598-018-36435-8
46. Aparício LVM, Guarienti F, Razza LB, Carvalho AF, Fregni F, Brunoni AR. A systematic review on the acceptability and tolerability of transcranial direct current stimulation treatment in neuropsychiatry trials. *Brain Stimul.* (2016) 9:671–81. doi: 10.1016/j.brs.2016.05.004
47. Dayan E, Cohen LG. Neuroplasticity subserving motor skill learning. *Neuron.* (2011) 72:443–54. doi: 10.1016/j.neuron.2011.10.008
48. Koechlin E. Frontal pole function: what is specifically human? *Trends Cogn Sci.* (2011) 15:241. doi: 10.1016/j.tics.2011.04.005
49. Elsner B, Kwakkel G, Kugler J, Mehrholz J. Transcranial direct current stimulation (tDCS) for improving capacity in activities and arm function after stroke: a network meta-analysis of randomised controlled trials. *J Neuroeng Rehabil.* (2017) 14:95. doi: 10.1186/s12984-017-0301-7
50. Wynter-Blyth V, Moorthy K. Prehabilitation: preparing patients for surgery. *BMJ.* (2017) 358:j3702. doi: 10.1136/bmj.j3702
51. Fratiglioni L, Wang H-X. Brain reserve hypothesis in Dementia. *J Alzheimers Dis.* (2007) 12:11–22. doi: 10.3233/JAD-2007-12103
52. Stern Y. Cognitive reserve. *Neuropsychologia.* (2009) 47:2015–28. doi: 10.1016/j.neuropsychologia.2009.03.004
53. Elbaz A, Vicente-Vytopilova P, Tavernier B, Sabia S, Dumurgier J, Mazoyer B, et al. Motor function in the elderly: evidence for the reserve hypothesis. *Neurology.* (2013) 81:417–26. doi: 10.1212/WNL.0b013e31829d8761
54. Franzmeier N, Duering M, Weiner M, Dichgans M, Ewers M. Left frontal cortex connectivity underlies cognitive reserve in prodromal Alzheimer disease. *Neurology.* (2017) 88:1054–61. doi: 10.1212/WNL.0000000000003711
55. Franzmeier N, Düzel E, Jessen F, Buerger K, Levin J, Duering M, et al. Left frontal hub connectivity delays cognitive impairment in autosomal-dominant and sporadic Alzheimer's disease. *Brain.* (2018) 141:1186–200. doi: 10.1093/brain/awy008
56. Picht T, Schmidt S, Brandt S, Frey D, Hannula H, Neuvonen T, et al. Preoperative functional mapping for rolandic brain tumor surgery: comparison of navigated transcranial magnetic stimulation to direct cortical stimulation. *Neurosurgery.* (2011) 69:581–8. doi: 10.1227/NEU.0b013e3182181b89
57. Raffa G, Quattropani MC, Germanò A. When imaging meets neurophysiology: the value of navigated transcranial magnetic stimulation for preoperative neurophysiological mapping prior to brain tumor surgery. *Neurosurg Focus FOC.* (2019) 47:e10. doi: 10.3171/2019.9.FOCUS19640
58. Hallett M. Transcranial magnetic stimulation: a primer. *Neuron.* (2007) 55:187–99. doi: 10.1016/j.neuron.2007.06.026
59. Kim Y-H, Park J-W, Ko M-H, Jang SH, Lee PKW. Facilitative effect of high frequency subthreshold repetitive transcranial magnetic stimulation on complex sequential motor learning in humans. *Neurosci Lett.* (2004) 367:181–5. doi: 10.1016/j.neulet.2004.05.113
60. Hoyer EH, Celnik PA. Understanding and enhancing motor recovery after stroke using transcranial magnetic stimulation. *Restor Neurol Neurosci.* (2011) 29:395–409. doi: 10.3233/RNN-2011-0611
61. Ma L, Narayana S, Robin DA, Fox PT, Xiong J. Changes occur in resting state network of motor system during 4weeks of motor skill learning. *Neuroimage.* (2011) 58:226–33. doi: 10.1016/j.neuroimage.2011.06.014
62. Bachtiar V, Near J, Johansen-Berg H, Stagg CJ. Modulation of GABA and resting state functional connectivity by transcranial direct current stimulation. *Elife.* (2015) 4:e08789. doi: 10.7554/eLife.08789

Conflict of Interest: The authors declare that the research was conducted in the absence of any commercial or financial relationships that could be construed as a potential conflict of interest.

frontiers in Neurology

REVIEW
published: 22 January 2021
doi: 10.3389/fneur.2020.628903

Preoperative Applications of Navigated Transcranial Magnetic Stimulation

Alexander F. Haddad[1†], *Jacob S. Young*[2†], *Mitchel S. Berger*[2] *and Phiroz E. Tarapore*[2*]

[1] School of Medicine, University of California, San Francisco, San Francisco, CA, United States, [2] Department of Neurological Surgery, University of California, San Francisco, San Francisco, CA, United States

Preoperative mapping of cortical structures prior to neurosurgical intervention can provide a roadmap of the brain with which neurosurgeons can navigate critical cortical structures. In patients undergoing surgery for brain tumors, preoperative mapping allows for improved operative planning, patient risk stratification, and personalized preoperative patient counseling. Navigated transcranial magnetic stimulation (nTMS) is one modality that allows for highly accurate, image-guided, non-invasive stimulation of the brain, thus allowing for differentiation between eloquent and non-eloquent cortical regions. Motor mapping is the best validated application of nTMS, yielding reliable maps with an accuracy similar to intraoperative cortical mapping. Language mapping is also commonly performed, although nTMS language maps are not as highly concordant with direct intraoperative cortical stimulation maps as nTMS motor maps. Additionally, nTMS has been used to localize cortical regions involved in other functions such as facial recognition, calculation, higher-order motor processing, and visuospatial orientation. In this review, we evaluate the growing literature on the applications of nTMS in the preoperative setting. First, we analyze the evidence in support of the most common clinical applications. Then we identify usages that show promise but require further validation. We also discuss developing nTMS techniques that are still in the experimental stage, such as the use of nTMS to enhance postoperative recovery. Finally, we highlight practical considerations when utilizing nTMS and, importantly, its safety profile in neurosurgical patients. In so doing, we aim to provide a comprehensive review of the role of nTMS in the neurosurgical management of a patient with a brain tumor.

Keywords: TMS, transcranial magnetic stimulation, motor mapping, language mapping, preoperative

OPEN ACCESS

Edited by:
Giovanni Raffa,
University of Messina, Italy

Reviewed by:
Cesare Zoia,
Unità di Neurochirurgia, Fondazione IRCCS Policlinico San Matteo, Italy
Giuseppe Maria Della Pepa,
Fondazione Policlinico Universitario Agostino Gemelli IRCSS, Italy

***Correspondence:**
Phiroz E. Tarapore
taraporep@neurosurg.ucsf.edu

[†] These authors have contributed equally to this work

Specialty section:
This article was submitted to Applied Neuroimaging, a section of the journal Frontiers in Neurology

Received: *13 November 2020*
Accepted: *29 December 2020*
Published: *22 January 2021*

Citation:
Haddad AF, Young JS, Berger MS and Tarapore PE (2021) Preoperative Applications of Navigated Transcranial Magnetic Stimulation. Front. Neurol. 11:628903. doi: 10.3389/fneur.2020.628903

INTRODUCTION

A primary tenet of neurosurgical oncology is to achieve maximal resection of pathologic lesions while preserving the surrounding eloquent brain and, thus, protecting a patient's functional ability. However, as we have continued to expand our knowledge of cognitive neuroscience and higher-order brain function, traditional theories regarding discrete brain regions housing critical functions and the general functional topography of the brain have been challenged (1–3). This anatomical description of functional brain regions is further complicated in the setting of architecture-distorting lesions (4), highlighting the necessity of additional modalities for determining eloquent vs. non-eloquent brain. One such modality is navigated transcranial

magnetic stimulation (nTMS). nTMS involves the use of non-invasive, image-guided stimulation of the brain to generate a functional map that differentiates eloquent from non-eloquent tissue (5). Transcranial magnetic stimulation is accomplished by using a wound copper coil (typically in a figure-of-eight configuration) to generate a strong, magnetic pulse targeted at an area of interest. By integrating the coil with a frameless stereotactic image guidance navigation system, one can achieve highly accurate maps that are specific to each subject's unique anatomy. Frequently performed in the preoperative setting, information learned from nTMS can aid with operative planning and allow for more accurate patient risk-stratification and counseling. In this review, we discuss various uses for preoperative nTMS, such as motor and language mapping, considerations surrounding patient safety, and future directions of the field.

MOTOR MAPPING WITH nTMS

The most well-established role for pre-surgical nTMS is mapping the spatial location of functional motor areas relative to the location of the tumor (6–8). The modality has a high degree of accuracy in the preoperative identification of eloquent motor cortex, with nTMS correctly identifying the primary motor cortex in 99.7% of cases (9).

Comparison With Direct Cortical Stimulation

Systematic comparisons between nTMS and direct cortical stimulation (DCS), the gold-standard technique for motor mapping, have demonstrated excellent concordance between the two modalities. Tarapore et al. found that the distance between TMS and DCS motor sites was ∼2.1 mm (10), and other groups have replicated this high degree of spatial reliability and consistency between DCS and nTMS (11, 12). Importantly, over multiple studies, there were no positive motor mapping sites identified with DCS that were unrecognized with TMS, demonstrating the high degree of sensitivity for preoperative nTMS. Conversely, sites that were deemed non-eloquent with DCS were also found to be quiet with nTMS, indicating a high degree of specificity for nTMS vs. DCS as well. As a result, nTMS based motor maps may be thought of as interchangeable with DCS based motor maps, and both positive and negative maps may be used to guide clinical care.

nTMS based motor maps have a high degree of consistency over time and between different examiners (13–15), demonstrating excellent inter-operator reliability. Moreover, the reference range of normal values for nTMS-based motor evoked potentials (MEPs) is not affected by tumor size, location, or patient clinical/socioeconomic status, which eases the interpretation of the results (16). Additionally, mapping with nTMS has been shown to be safe to perform in patients with brain tumors, although typically it is not performed in patients who are experiencing frequent seizures, with a transient headache being the most common complication reported (17). Thus, nTMS for motor mapping a straightforward technique to add to an existing workflow for neuro-oncology patients.

nTMS-Based Motor Maps in Clinical Practice

The high reliability of nTMS-based motor maps has enabled clinicians to improve the clinical management of patients with potentially eloquent brain tumors. Frey et al. found that nTMS disproved suspected involvement of the primary motor cortex by the tumor in ∼1/4 of cases, frequently altering the surgical plan and preoperative patient counseling (17). Planned surgical resection was expanded in over 1/3 of cases and the percentage of tumors where a gross total resection was achieved increased by nearly 20%. Importantly, there was a corresponding decline in the rate of postoperative deficits in the group of patients who underwent nTMS. These findings suggest that the addition of preoperative nTMS mapping data to a clinical routine of preoperative fiber tractography, intraoperative neuronavigation, and intraoperative mapping/electrophysiology improves surgical outcomes for tumors in or near the motor pathways (18).

Fiber Tracking With nTMS Motor Maps

In patients with glioma, MR signal alterations caused by vascular changes and peritumoral edema can create spurious DTI results and reduce the accuracy of the tractography. To improve accuracy, nTMS hot spots in the primary motor area can be used in conjunction with carefully selected subcortical nuclei seed voxels to improve the anatomic accuracy of the tracts. This technique is useful in patients whose tracts are closest to the tumor (19), as these patients are at highest risk of developing postoperative motor deficits due to intraoperative injury to the subcortical white matter (20–22). In addition to displaying highly accurate fiber tractography (FT) that can be used to plan the approach to surgical resection, it can also inform the surgeon when to employ intraoperative DCS. Furthermore, these nTMS-based DTI FT can be used in a predictive manner as well: patients with nTMS-generated CST fibers with lower fractional anisotropy (FA) values and higher ADC values are much more likely to have their motor function deteriorate postoperatively (23). In fact, nTMS localizer data produces better DTI corticospinal tractography results than functional MRI for patients with tumors near the cortical tract origin (i.e., primary motor cortex) (24).

Accordingly, Raffa et al. showed that nTMS-based CST mapping allowed for patients to receive smaller craniotomies (25). Phase reversal was rarely needed as the cortical nTMS information facilitated identification of the primary motor cortex (12), which likely allowed the surgeons to perform smaller craniotomies and decrease surgical time. Moreover, these patients had fewer postoperative seizures, improved EOR, and better postoperative KPS and motor performance after surgery, indicating the powerful benefit of tailoring the surgical approach with nTMS-based FT for motor-eloquent lesions. The authors demonstrate how nTMS-based tractography provides visual feedback that can guide ongoing resection of tumor in safe areas even when the DCS threshold is very low and would otherwise mandate the surgeon stop the resection. Interestingly,

nTMS-based FT appears to be more useful in high-grade tumors, as they typically displaced the tracts without infiltrating it, further highlighting the predictive nature of nTMS-based DTI for the resectability for lesions involving the CST.

Additionally, the distance from a lesion to a fiber tract defined by pre-surgical nTMS is strongly correlated with the likelihood of developing a postoperative deficit, although the proximity threshold for when a postoperative deficit is encountered may vary depending on the specific tract (e.g., corticospinal tract vs. arcuate fasciculus) in question (26). Specifically for the corticospinal tract, lesions > 8 mm from the tract have been considered low risk in some series and no new postoperative motor deficits were observed following gross total resection of the tumor (27).

Preoperative Risk Stratification

nTMS-based motor thresholds have also proven useful in pre-surgical risk stratification. Rosenstock et al. utilized a logistic regression model to identify preoperative nTMS-related variables that were associated with postoperative motor outcome. They found that three criteria were significantly associated with new postoperative deficit: tumorous infiltration of the motor cortex and/or CST; ≤8-mm distance between tumor and CST; interhemispheric resting motor threshold <90% or >110%. Of note, patients with a pre-existing motor deficit and impaired cortical excitability in the tumorous hemisphere on nTMS never showed a postoperative improvement in motor function. However, patients with equally excitable hemispheres (similar to healthy subjects) have better outcomes and may be considered lower risk (27). These findings highlight the important role of nTMS-based resting motor thresholds in measuring comparative cortical excitability. Not only does this risk-stratification strategy allow for improved surgical planning, it also improves the specificity of patient counseling with regard to perioperative risk. Accordingly, the planned extent of resection has been shown to change often in patients who undergo preoperative nTMS, with an increase in surgical aggressiveness being the most common conversion made to the surgical plan after nTMS assessment (17).

Improvement in Outcomes

Accordingly, preoperative nTMS has consistently been shown to facilitate more extensive resections while reducing functional deficits, and thus improved patient survival (6, 12, 17, 28).

Frey et al. showed that the rate of gross total resection (GTR) in patients who underwent preoperative nTMS was significantly increased compared to a control group of patients who did not undergo preoperative nTMS (17). The higher proportion of patients receiving a GTR resulted in a 7-month prolongation of progression free survival for the low-grade glioma nTMS cohort relative to the non-nTMS cohort (22.4 vs. 15.4 months, respectively). As mentioned above, the nTMS cohort also had a small drop in the rate of postoperative deficits.

Krieg et al. completed a prospective study of 100 patient with supratentorial lesions located in the motor region who underwent preoperative nTMS and compared their outcomes to a matched control group who were operated on at the same institution at a prior time without nTMS (28). Consistent with Frey's prior report, the authors found that there was a lower rate of residual tumor on the post-operative MRI and that ∼10% of patients in the nTMS group had an improvement in their motor function, which was much higher than the 1% of patients who had an improvement in motor function in the non-nTMS group. Similar to prior reports, there was a lower rate of postoperative motor decline in the nTMS group relative to the non-nTMS group (13% vs. 18%). Finally, a systematic review and meta-analysis of preoperative nTMS motor mapping by Raffa et al. demonstrated a significant reduction in new permanent postoperative motor deficits and increased GTR in patients who underwent preoperative motor mapping relative to those who did not. Although these reports are not randomized control trials, the evidence supports incorporation of nTMS into the work-flow and imaging arsenal for patients with eloquent tumors in the motor region and should be used in combination with intraoperative mapping to optimize patient outcomes. Case examples highlighting the benefit of preoperative motor mapping using nTMS can be found in **Figures 1–3**.

Prognostic Value in Recovery

nTMS motor mapping has shown promise in predicting recovery for patients with new postoperative deficits. In the first study utilizing pre- and post-operative nTMS for prognostication of recovery potential, Takakura et al. showed that when preoperative cortical hotspots (defined as cortical regions that elicited the largest EMG in the adductor hallucis brevis by nTMS) are adjacent or within 1 cm to a postoperative lesion, there is less recovery of hand grip strength compared to patients whose cortical hotspots were more distant from the postoperative lesion (29). The group with lesions adjacent to the pre-surgical nTMS hotspots had only recovered by 55% 3 months after surgery compared to patients with non-adjacent lesions who had recovered by 95% during this time. This finding is particularly important given the fact that nearly all patients will have a decline in their motor function immediately following surgery due to postoperative edema, highlighting the utility in nTMS to predict which patients are most likely to recover and the degree of that recovery. Equally importantly, there was no correlation between an intraoperative decline in MEP signaling and postoperative grip strength or recovery, highlighting the unsuitable nature of MEPs for predicting recovery from postoperative motor deficits. Finally, positive postoperative nTMS-MEPs 1 week after surgery correlated well with better recovery from an immediate postoperative deficit, which corresponds well to the post-stroke literature and represents one of the few prognostic tools that can be used to evaluate patients with new motor deficits after glioma surgery.

LANGUAGE MAPPING

While presurgical motor mapping remains the most common and well-validated application of nTMS, language mapping is also an exciting area of potential clinical utility for nTMS and has been under investigation since the early 1990s (30). In contrast to motor mapping, which uses single pulses to excite neurons

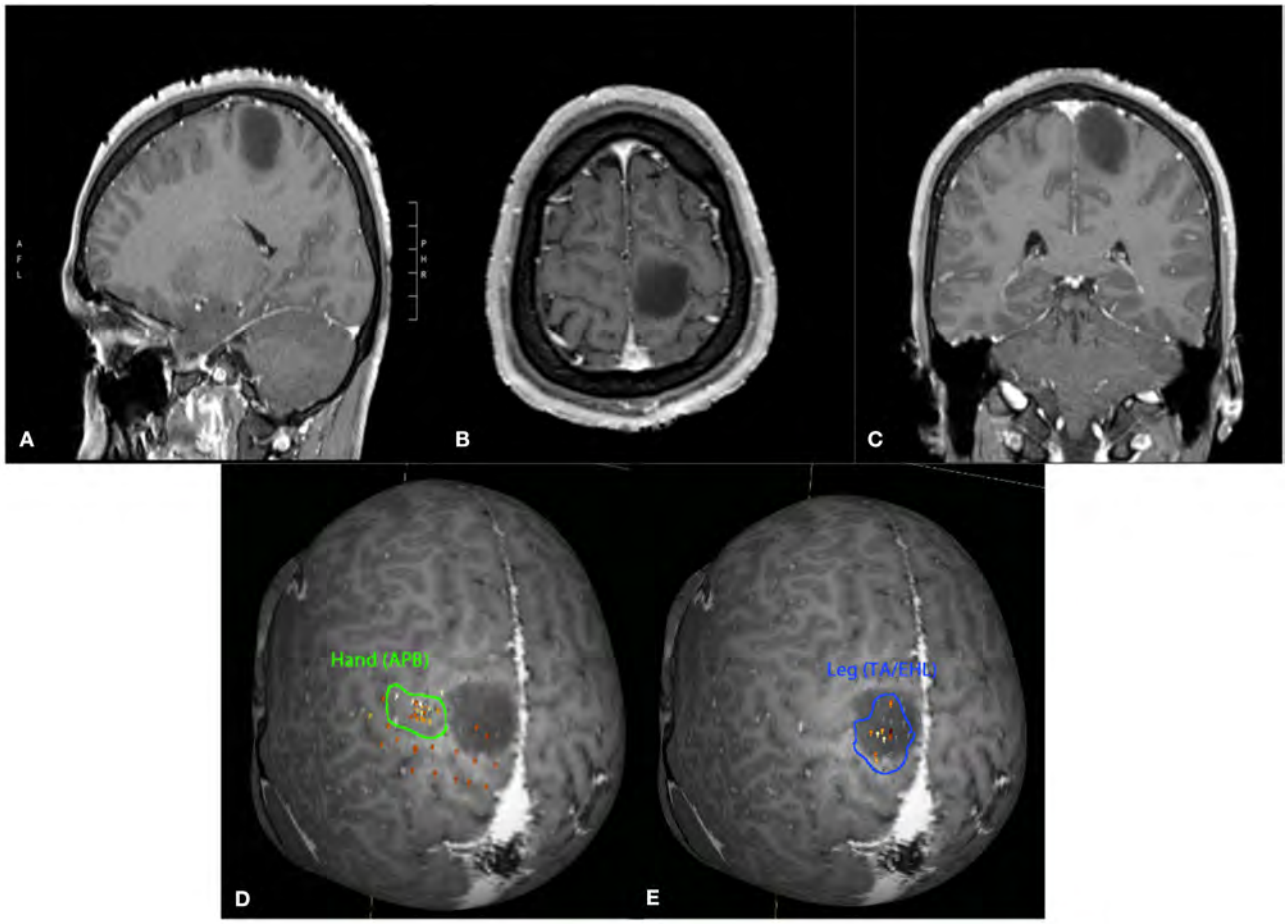

FIGURE 1 | Twenty-four-year-old male with an incidentally discovered brain lesion, presumed low grade glioma, within the left paracentral lobule (T1 post-contrast imaging, **A–C**). nTMS demonstrated hand motor responses lateral to region of the lesion, but leg responses were present throughout the lesion **(D,E)**. Surgery was deferred due to the nTMS mapping results and increased risk of potential lower extremity motor deficit following surgical intervention.

and cause downstream motor function, language mapping uses short bursts of TMS pulses, called repetitive TMS or rTMS, to cause a temporary lesion and disrupt the normal function of the brain. When these pulses are guided by neuro-navigation, they are referred to as navigated repetitive TMS (nrTMS). Although the mechanism of action is not entirely understood, synchronization of affected neurons and GABAergic inhibition are thought to contribute to the temporary brain disruption and lesion effect (31). Because of its non-invasive, reversible effect, nrTMS provides a valuable modality with which to map eloquent language regions of the cortex. Preoperative language mapping is especially valuable in brain tumor patients as, due to tumor induced plasticity and remodeling, eloquent language areas may be shifted to unexpected cortical regions (32, 33).

Initial Studies With rTMS

Early studies investigating the use of TMS in language mapping focused on determining hemispheric language dominance and utilized rTMS without navigation. Pascual-Leone et al. first highlighted the ability of rTMS to induce speech arrest in a study involving six epileptic patients, demonstrating identical lateralization results to intracarotid amobarbital tests performed on the same patient and hinting at the potential clinical utility of the technology (30). This experiment was replicated by Jennum et al. (34). However, a subsequent study by Epstein et al. in 2000 (35), highlighting inconsistencies between rTMS and intracarotid amobarbital tests, showed that the development of postoperative deficits were more effectively predicted by an intracarotid amobarbital test. This result cast some doubt on the utility of rTMS in determining hemispheric language dominance (9, 35, 36). A number of similar studies investigating rTMS alone provided unreliable results secondary to inconsistencies with intracarotid amobarbital tests, more specifically high false-positive speech arrest sites in the non-dominant hemisphere (36, 37). Studies also failed to correlate rTMS language mapping findings with DCS. These results highlighted the need for improved targeting, and controlling more specifically the perturbations of the functional landscape, and was a primary driver for integrating the rTMS system with neuro-navigation. This effort, it was hoped, would permit more detailed investigations into the relationship between TMS findings and intraoperative DCS.

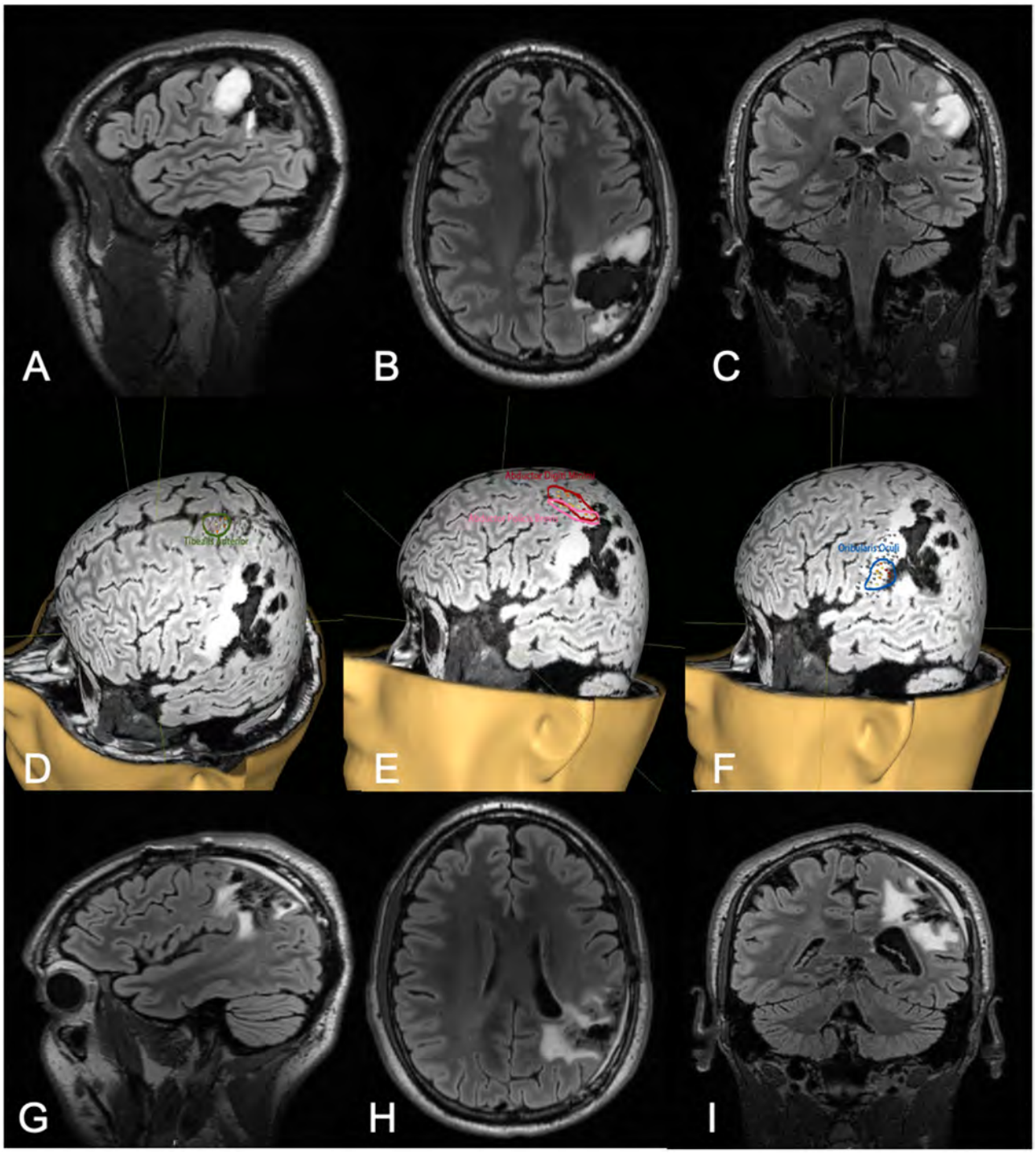

FIGURE 2 | Thirty-two-year-old male with a history of left parietal oligoastrocytoma status post prior resection, now presenting with recurrence (T2 FLAIR imaging, **A–C**). nTMS demonstrated hand motor responses anterior to the region of recurrence, face motor responses entirely within the recurrence, and leg motor responses anterior to the recurrence **(D–F)**. Intraoperative DCS identified hand and upper extremity function in close proximity to, and at times continuous with, the area of recurrence. Subtotal resection was achieved with care taken to spare hand and face motor sites intraoperatively (T2 FLAIR imaging, **G–I**). The patient had no postoperative neurological deficits on neurological examination.

Initial Language Studies With nrTMS

Fortunately, the incorporation of neuro-navigation into rTMS improved upon the results seen in previous studies using rTMS alone. Tarapore et al. sought to demonstrate the utility of nrTMS through a study of 12 brain tumor patients who also received intraoperative DCS. Using intraoperative DCS

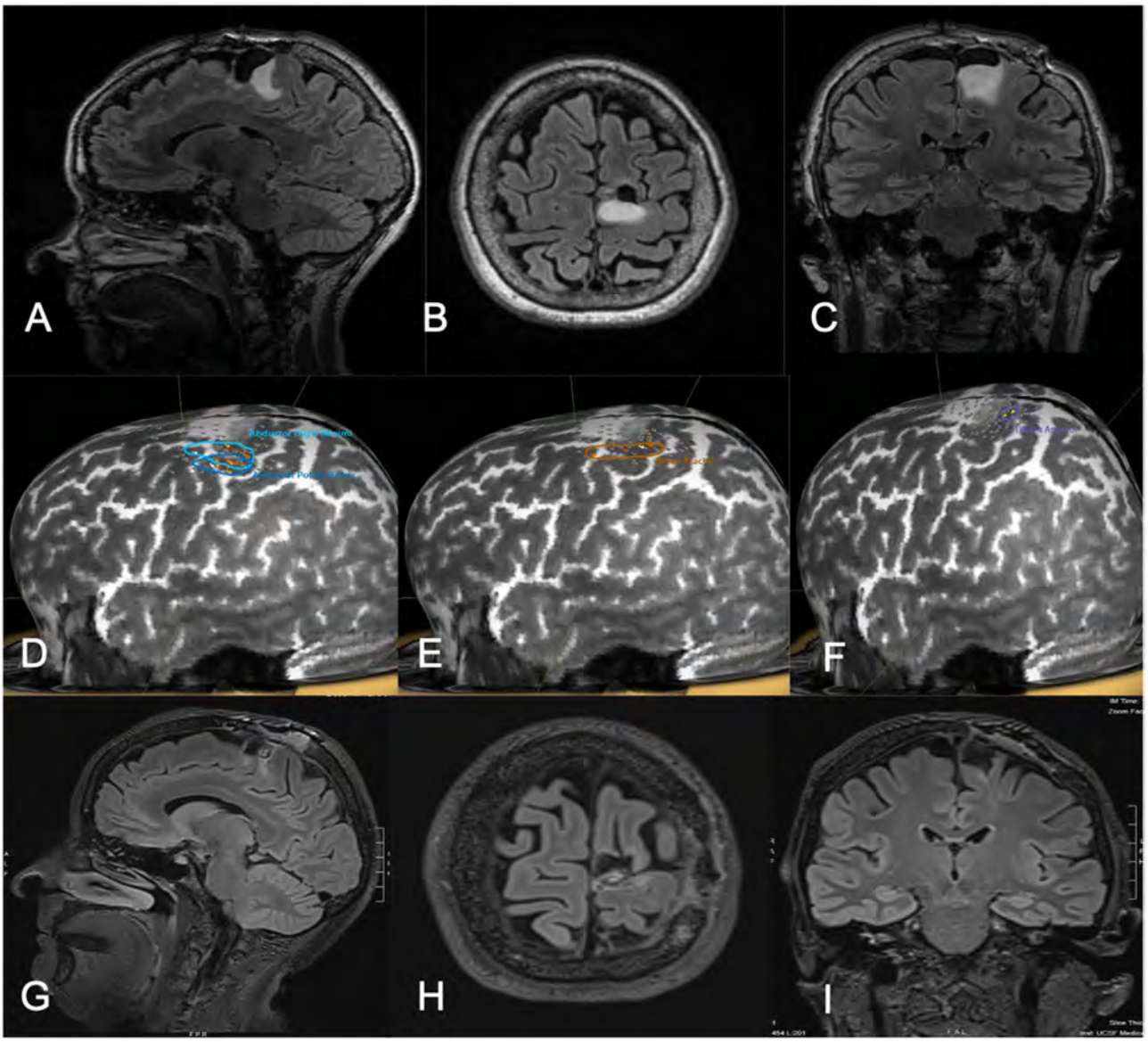

FIGURE 3 | Fifty-one-year-old female with a history of left parietal oligodendroglioma status post prior subtotal resection, now presenting with recurrence (T2 FLAIR imaging, **A–C**). nTMS demonstrated hand and lower extremity motor activity lateral and posterior to the area of prior resection and region of recurrence **(D–F)**. Intraoperative DCS identified lower extremity motor function in close proximity to the area of recurrence, as identified on preoperative nTMS. Subtotal resection was achieved with care taken to spare motor sites intraoperatively (T2 FLAIR imaging, **G–I**). The patient had no postoperative neurological deficits on neurological examination.

as the gold-standard test, they demonstrated that nrTMS had a sensitivity of 90% and a specificity of 98% for detecting speech-language disruption sites (positive predictive value of 69% and negative predictive value of 99%), highlighting the accuracy and utility of nrTMS (37). However, the predictive values reported by Tarapore et al. were significantly higher than a similar study performed by Picht et al. in 20 patients undergoing awake resection of a brain tumor. Also using DCS as a gold-standard test, they reported significantly lower predictive values: sensitivity of 90.2%, specificity of 23.8%, positive predictive value of 35.6%, and negative predictive value of 83.9% (38). Given the similarity in methodology between the two studies, a difference in the definition of a language disruption site is thought to contribute to the discordance in predictive values observed (9). Indeed, Tarapore et al. which demonstrated a higher correlation between nrTMS and DCS, utilized a slightly more stringent definition of language disruption, requiring the agreement of two blinded experts with the utilization of a third expert in the case of a disagreement (9, 37). A subsequent study by Raffa et al. took a slightly different approach, using

postoperative aphasia (determined by the Western Aphasia Battery) as a gold-standard measure to determine the accuracy of preoperative nrTMS and nrTMS-based DTI FT in brain tumor patients unable to undergo intraoperative DCS. They also demonstrated a good correlation between preoperative nrTMS and development of a postoperative deficit: sensitivity 100%, specificity 57.14%, negative predictive value 100%, positive predictive value 50%, further highlighting the promise of this technology (33). Indeed, the high negative predictive value seen by Raffa et al. especially demonstrates the value and reliability of a negative test result, which can significantly aid with preoperative planning and identifying non-eloquent regions of the brain. In the largest study to date, Sollmann et al. utilized data from 100 patients undergoing preoperative language mapping. Using deterministic tractography based on nrTMS data, they demonstrated a significant relationship between lesion to tract distance (LTD) and the development of permanent post-surgical language deficits with cutoffs of $\leq$16 mm LTD for the arcuate fasciculus and $\leq$25 mm LTD for other closest language-related tract (26). This study again highlighted the utility of nrTMS, more specifically LTD, as a preoperative risk stratification tool.

The Role of nrTMS in Multi-Modal Presurgical Language Mapping

Thus, while nrTMS is an improving technology for preoperative language mapping, it remains less accurate than when used for motor mapping, as previously discussed. This has prompted the combination of nrTMS with other non-invasive technologies, such as functional MRI (fMRI) leading to improved predictive ability of language disruption sites when the two are used together (39, 40). Additionally, a growing literature has described the benefit of seeding tractography maps with nrTMS-based language disruption sites. This is especially critical in cases requiring more accurate subcortical language mapping. Sollmann et al. demonstrated the feasibility nTMS based DTI FT of subcortical language pathways in 2016, highlighting the ability of the two technologies together to identify nine language-related subcortical tracts (41). Raffa et al. subsequently showed that nTMS combined with DTI FT allowed for a more accurate and reliable reconstruction of the subcortical language network when compared to standard DTI FT using anatomical landmarks, further demonstrating the synergistic nature of the two technologies (42). Interestingly, Sollmann et al. then demonstrated the ability to produce a function specific DTI FT when only specific language errors following nrTMS were utilized as regions of interest for DTI FT; highlighting the ability to more specifically map subcortical functions (43). In a separate study, Sollman et al. described the clinical use of nrTMS and nrTMS-based DTI FT. While the study described some clinical outcomes, including craniotomy size, extent of resection, and postoperative language deficits it lacked a control group, making it difficult to appreciate the full impact of these technologies a patient's outcome (44). Nevertheless, it was a first step toward much needed studies, such as a randomized controlled trial, in which any potential clinical benefits associated with nrTMS-based DTI FT could be more clearly described. Finally, nrTMS-based DTI FT has also demonstrated use in preoperative risk stratification of patients with tumors in language eloquent regions. Sollman et al. sought to define the LTDs on nrTMS-based DTI FT that predicted postoperative surgical deficits in 50 patients with left hemispheric language eloquent brain tumors. They demonstrated LTDs of $\leq$8 mm for the arcuate fasciculus and $\leq$11 mm other language-related tracts as cutoffs for surgery-related permanent aphasias (45). Of note, these cutoffs were closer than those determined in a similar study using deterministic tractography based on nrTMS, highlighting the promise of nrTMS-based DTI FT (26).

Consideration should also be given to other patient characteristics and variables that could contribute to the reduced predictive value of nrTMS, including pre-existing aphasia or cognitive deficits (46). Mitigation strategies and modified protocols that increase the utility of nrTMS for language mapping in these patient populations should continue to be explored. Given the complexity and variability of language function, improved nrTMS language mapping protocols are needed and will continue to be developed. Nevertheless, nrTMS for language mapping remains an exciting technology with the ability to positively impact patient care in the clinical setting. This is especially true for patients who cannot tolerate awake intraoperative language mapping, as nrTMS provides surgeons with a way to improve safety and increase eligibility for surgery in patients who might otherwise be deemed inoperable (33).

FUTURE DIRECTIONS

Despite a historical focus on motor and language mapping (47), it is also clear that additional brain functions contribute significantly to patient quality of life following surgery, ranging from vision to complex higher level cognitive functions. Indeed, a number of functions, including vision, spatial awareness, memory, attention, judgement, emotion, and calculation have been mapped intraoperatively (48). However, adding complex tasks to evaluate these cognitive functions can add a large amount of time during the awake, intraoperative mapping portion of a case which can be challenging for patients to tolerate and increase the duration of the surgical procedure, making it difficult to use these on a regular basis. Thus, the use of nTMS for the preoperative mapping of complex functions is an attractive option as this preoperative mapping occurs in a setting where more time can be taken to dissect these intricate relationships.

Visual Cortex With nTMS

For example, one of the first regions outside of language and motor mapping to be mapped using nTMS was the visual cortex (49). In 2002, Fernandez et al. demonstrated the ability for TMS to systematically map visual sensations; they consistently evoked reproducible topographically organized phosphenes (a brief flash of light) through the use of TMS, demonstrating the reliability and reproducibility of the technology. Subsequent studies have shown that a weak TMS pulse to the visual cortex will often result in the patient seeing a phosphene while stronger pulses

tend to have a more suppressive impact on the visual cortex (50). Salminen-Vaparanta et al. also demonstrated the ability to selectively stimulate the primary visual cortex when using TMS in conjunction with multifocal functional magnetic resonance imaging (mffMRI) to first identify individual retinotopic areas. However, even when using mffMRI data, the primary visual cortex was only able to be stimulated in half of the tested patients, highlighting the inaccuracies and difficulties associated TMS stimulation of the visual cortex, even when image-guided (50). Thus, while mapping of the visual cortex with TMS remains an exciting possibility, additional research is needed to refine and develop this application.

Experimental Mapping Techniques With nTMS

TMS has also been used to investigate complex functions, such as visuospatial attention and spatial orientation (51–53), facial recognition (54), and calculation (55, 56). With regards to visuospatial perception, Salatino et al. utilized a line length estimation task to capture the development of neglect when stimulating the right posterior parietal cortex (PPC) with single-pulse TMS. Interestingly, they demonstrated the development of left sided neglect when stimulating over both the right and left PPC. However, in a follow-up study, they demonstrated neglect when performing rTMS on the right PPC, but not the left, highlighting the ability of TMS to cause neglect while also suggesting that rTMS, rather than single-pulse TMS, may be a more accurate way to map visuospatial perception (52, 53). rTMS has also shown use in identifying cortical regions associated with visuospatial attention, another exciting potential future application of this technology (51).

Given the ability for brain tumor resections, especially in the frontal and parietal lobes, to cause prosopagnosia, efforts have also been made to map other complex functions, such as facial recognition. Maurer et al. sought to explore the mapping of facial recognition function in 20 volunteer patients by targeting 52 regions of the cortex with nrTMS and simultaneously testing the ability to name popular celebrities. They identified a number of locations that lead to naming dysfunction when nrTMS was applied to them; 80% of all participants demonstrated a naming error when nrTMS was utilized over the middle frontal gyrus (54). This study demonstrated the feasibility of utilizing nrTMS for mapping of facial recognition. Future investigations will likely evaluate this application of nrTMS in the setting of preoperative planning.

Finally, a number of studies have investigated the use of nrTMS to map the ability to perform mathematical calculations. Similar to how they tested the mapping of facial recognition, Maurer et al. also mapped calculation function by asking patients to perform simple arithmetic tasks while applying nrTMS to 52 predetermined cortical locations. Interestingly, an 80% error rate was observed when nrTMS was applied to the right ventral precentral gyrus, with different types of arithmetic localizing to different regions of the brain (e.g., division tasks showed the highest error rate in the left middle frontal gyrus) (55). Similar findings, with the segregation of specific types of arithmetic, were demonstrated by Montefinese, further highlighting the potential utility of nrTMS for mapping calculation ability.

While promising, the clinical utility and applicability of the aforementioned experimental mapping techniques still need to be investigated and validated. This will likely be accomplished through studies similar to what have already been performed for language and motor mapping, in which the predictive value of preoperative nTMS is assessed by comparing it to intraoperative DCS or postoperative deficits. Until then, assumptions regarding the clinical utility of these experimental mapping techniques in the setting of preoperative mapping should be considered with caution.

Postoperative Therapeutic Applications of nTMS

Finally, it is worth briefly discussing the use of TMS as a therapeutic intervention for patients with stroke, traumatic brain injury, or postoperative injuries. In the injured brain, rTMS is thought to have a beneficial effect by potentially reducing cortical hyper excitability and promoting long-term plasticity (57). Preliminary studies into the potential therapeutic benefit of TMS or transcranial direct current stimulation in patients with a stroke or brain injury have been promising, with studies highlighting the potential for these technologies to improve motor function in stoke patients (58, 59) as well as improve working memory (60, 61). While a more recent study has showed no beneficial impact of rTMS on cognition in TBI patients (62), additional investigation into the use of this technology as an adjunct to aid in recovery following an injury to the brain is warranted and holds promise for an expanded role for TMS in the management of patients afflicted by these conditions.

SAFETY

TMS is traditionally viewed as a safe technology, when the appropriate stimulation parameters are followed (63). The most common side effects associated with use of the technology are minor and include: pain (39–40%) (64, 65), headache (28–40%) (64, 65), and high frequency hearing loss (9%) (30, 66). While minor side effects are tolerable for the majority of patients, the most severe, and feared, complication of TMS is the development of a seizure. Fortunately, rates previously reported in the literature have indicated a $<1\%$ incidence of seizure related to TMS (67–70). Despite the low incidence of TMS associated seizure, the United States Food and Drug Administration requires the exclusion of patients with poorly controlled seizures (>1 seizure per week) when using TMS for preoperative mapping. However, the paucity of data surrounding TMS side effects in preoperative neurosurgical patients specifically prompted a large study by Tarapore et al. investigating the safety profile of TMS in 733 preoperative neurosurgical patients, 50% of which had preoperative seizures related to their lesions. Interestingly, while some discomfort or mild to moderate pain was reported by patients, especially those receiving rTMS, no TMS associated seizures or persistent headaches were reported; this highlighted the strong safety profile of TMS and the potential

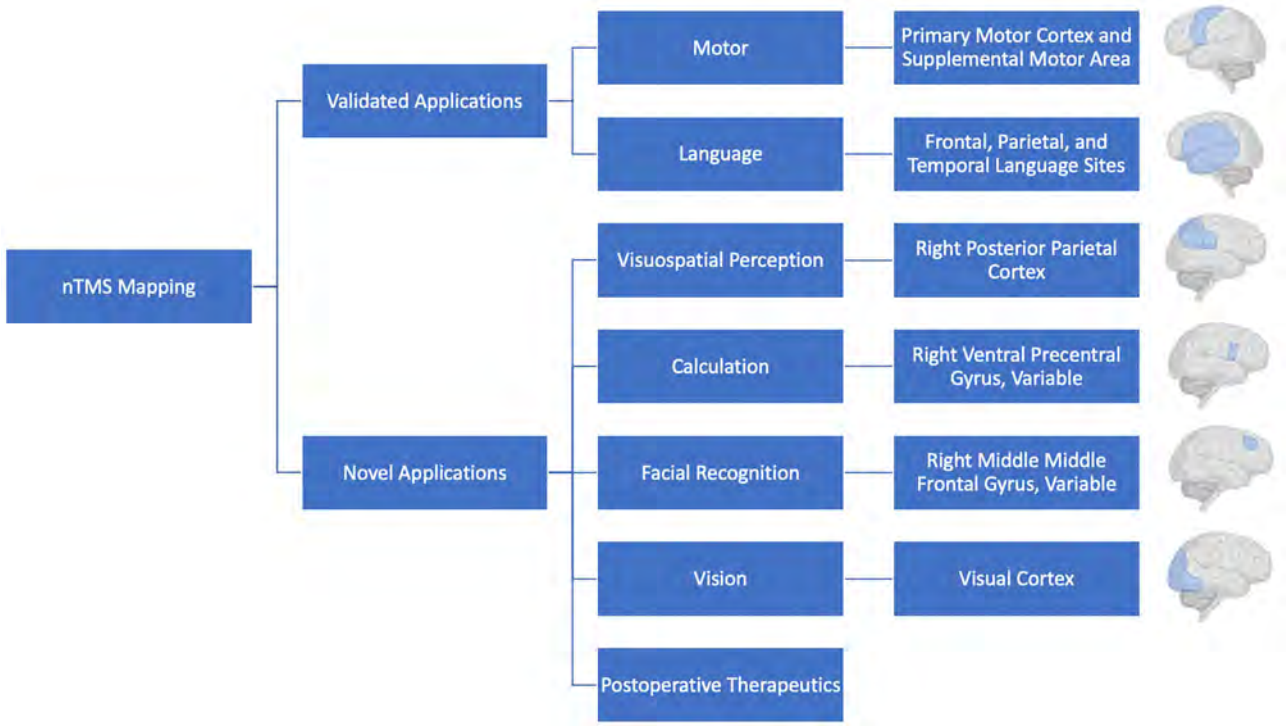

FIGURE 4 | Schematic highlighting common uses of nTMS.

of the technology to be used in all patients, including those with a history of seizures.

CONCLUSION

TMS will undoubtedly continue to see use for preoperative motor and language mapping, with additional mapping of complex functions likely to become more common as they are validated in the clinical setting (**Figure 4**). The combination of nTMS with additional mapping modalities, such as fMRI also holds great promise and should also continue to be explored. As we continue to learn more about and refresh our view on the functional topography of the brain it will be increasingly important to provide surgeons with more accurate, personalized, representations of a patient's brain. As a result, preoperative mapping using TMS has the potential to contribute to operative planning, improved patient risk-stratification, and better-informed patient counseling. It is an exciting technology that will continue to see investment and use in the neurosurgical and neuroscience communities.

AUTHOR CONTRIBUTIONS

All authors listed have made a substantial, direct and intellectual contribution to the work, and approved it for publication.

REFERENCES

1. Duffau H, Moritz-Gasser S, Mandonnet E. A re-examination of neural basis of language processing: proposal of a dynamic hodotopical model from data provided by brain stimulation mapping during picture naming. *Brain Lang.* (2014) 131:1–10. doi: 10.1016/j.bandl.2013.05.011
2. Duffau H. The error of Broca: from the traditional localizationist concept to a connectomal anatomy of human brain. *J Chem Neuroanat.* (2018) 89:73–81. doi: 10.1016/j.jchemneu.2017.04.003
3. Chang EF, Raygor KP, Berger MS. Contemporary model of language organization: an overview for neurosurgeons. *J Neurosurg.* (2015) 122:250–61. doi: 10.3171/2014.10.JNS132647
4. Chang EF, Breshears JD, Raygor KP, Lau D, Molinaro AM, Berger MS. Stereotactic probability and variability of speech arrest and anomia sites during stimulation mapping of the language dominant hemisphere. *J Neurosurg.* (2017) 126:114–21. doi: 10.3171/2015.10.JNS151087
5. Krieg SM, Lioumis P, Mäkelä JP, Wilenius J, Karhu J, Hannula H, et al. Protocol for motor and language mapping by navigated TMS in patients and healthy volunteers; workshop report. *Acta Neurochir (Wien).* (2017) 159:1187–95. doi: 10.1007/s00701-017-3187-z
6. Picht T, Schulz J, Hanna M, Schmidt S, Suess O, Vajkoczy P. Assessment of the influence of navigated transcranial magnetic stimulation on surgical planning for tumors in or near the motor cortex. *Neurosurgery.* (2012) 70:1248–56. doi: 10.1227/NEU.0b013e318243881e
7. Picht T, Schmidt S, Brandt S, Frey D, Hannula H, Neuvonen T, et al. Preoperative functional mapping for rolandic brain tumor surgery: comparison of navigated transcranial magnetic

stimulation to direct cortical stimulation. *Neurosurgery*. (2011) 69:581–8. doi: 10.1227/NEU.0b013e3182181b89
8. Raffa G, Scibilia A, Conti A, Ricciardo G, Rizzo V, Morelli A, et al. The role of navigated transcranial magnetic stimulation for surgery of motor-eloquent brain tumors: a systematic review and meta-analysis. *Clin Neurol Neurosurg.* (2019) 180:7–17. doi: 10.1016/j.clineuro.2019.03.003
9. Picht T. Current and potential utility of transcranial magnetic stimulation in the diagnostics before brain tumor surgery. *CNS Oncol*. (2014) 3:299–310. doi: 10.2217/cns.14.25
10. Tarapore PE, Tate MC, Findlay AM, Honma SM, Mizuiri D, Berger MS, et al. Preoperative multimodal motor mapping: a comparison of magnetoencephalography imaging, navigated transcranial magnetic stimulation, and direct cortical stimulation: clinical article. *J Neurosurg.* (2012) 117:354–62. doi: 10.3171/2012.5.JNS112124
11. Takahashi S, Vajkoczy P, Picht T. Navigated transcranial magnetic stimulation for mapping the motor cortex in patients with rolandic brain tumors. *Neurosurg Focus*. (2013) 34:E3. doi: 10.3171/2013.1.FOCUS133
12. Krieg SM, Shiban E, Buchmann N, Gempt J, Foerschler A, Meyer B, et al. Utility of presurgical navigated transcranial magnetic brain stimulation for the resection of tumors in eloquent motor areas: clinical article. *J Neurosurg.* (2012) 116:994–1001. doi: 10.3171/2011.12.JNS111524
13. Forster MT, Limbart M, Seifert V, Senft C. Test-retest reliability of navigated transcranial magnetic stimulation of the motor cortex. *Neurosurgery*. (1982) 10(Suppl. 1):51:5. doi: 10.1227/NEU.0000000000000075
14. Sollmann N, Hauck T, Obermüller T, Hapfelmeier A, Meyer B, Ringel F, et al. Inter- and intraobserver variability in motor mapping of the hotspot for the abductor policis brevis muscle. *BMC Neurosci*. (2013) 14:94. doi: 10.1186/1471-2202-14-94
15. Weiss C, Nettekoven C, Rehme AK, Neuschmelting V, Eisenbeis A, Goldbrunner R, et al. Mapping the hand, foot and face representations in the primary motor cortex - Retest reliability of neuronavigated TMS versus functional MRI. *Neuroimage*. (2013) 66:531–42. doi: 10.1016/j.neuroimage.2012.10.046
16. Picht T, Strack V, Schulz J, Zdunczyk A, Frey D, Schmidt S, et al. Assessing the functional status of the motor system in brain tumor patients using transcranial magnetic stimulation. *Acta Neurochir (Wien)*. (2012) 154:2075–81. doi: 10.1007/s00701-012-1494-y
17. Frey D, Schilt S, Strack V, Zdunczyk A, Sler JR, Niraula B, et al. Navigated transcranial magnetic stimulation improves the treatment outcome in patients with brain tumors in motor eloquent locations. *Neuro Oncol*. (2014) 16:1365–72. doi: 10.1093/neuonc/nou110
18. Picht T, Frey D, Thieme S, Kliesch S, Vajkoczy P. Presurgical navigated TMS motor cortex mapping improves outcome in glioblastoma surgery: a controlled observational study. *J Neurooncol*. (2016) 126:535–43. doi: 10.1007/s11060-015-1993-9
19. Weiss C, Tursunova I, Neuschmelting V, Lockau H, Nettekoven C, Oros-Peusquens AM, et al. Improved nTMS- and DTI-derived CST tractography through anatomical ROI seeding on anterior pontine level compared to internal capsule. *NeuroImage Clin*. (2015) 7:424–37. doi: 10.1016/j.nicl.2015.01.006
20. Berger MS. Lesions in functional ("eloquent") cortex and subcortical white matter. *Clin Neurosurg.* (1994) 41:444–63.
21. Skirboll SS, Ojemann GA, Berger MS, Lettich E, Winn HR. Functional cortex and subcortical white matter located within gliomas. *Neurosurgery*. (1996) 38:678–58. doi: 10.1227/00006123-199604000-00008
22. Keles GE, Lundin DA, Lamborn KR, Chang EF, Ojemann G, Berger MS. Intraoperative subcortical stimulation mapping for hemispherical perirolandic gliomas located within or adjacent to the descending motor pathways: evaluation of morbidity and assessment of functional outcome in 294 patients. *J Neurosurg*. (2004) 100:369–75. doi: 10.3171/jns.2004.100.3.0369
23. Rosenstock T, Giampiccolo D, Schneider H, Runge SJ, Bährend I, Vajkoczy P, et al. Specific DTI seeding and diffusivity-analysis improve the quality and prognostic value of TMS-based deterministic DTI of the pyramidal tract. *NeuroImage Clin*. (2017) 16:276–85. doi: 10.1016/j.nicl.2017.08.010
24. Weiss Lucas C, Tursunova I, Neuschmelting V, Nettekoven C, Oros-Peusquens AM, Stoffels G, et al. Functional MRI vs. navigated TMS to optimize M1 seed volume delineation for DTI tractography. A prospective study in patients with brain tumours adjacent to the corticospinal tract. *NeuroImage Clin*. (2017) 13:297–309. doi: 10.1016/j.nicl.2016.11.022
25. Raffa G, Conti A, Scibilia A, Cardali S, Esposito F, Angileri FF, et al. The impact of diffusion tensor imaging fiber tracking of the corticospinal tract based on navigated transcranial magnetic stimulation on surgery of motor-eloquent brain lesions. *Neurosurgery*. (2018) 83:768–82. doi: 10.1093/neuros/nyx554
26. Sollmann N, Zhang H, Fratini A, Wildschuetz N, Ille S, Schröder A, et al. Risk assessment by presurgical tractography using navigated tms maps in patients with highly motor-or language-eloquent brain tumors. *Cancers (Basel)*. (2020) 12:1264. doi: 10.3390/cancers12051264
27. Rosenstock T, Grittner U, Acker G, Schwarzer V, Kulchytska N, Vajkoczy P, et al. Risk stratification in motor area-related glioma surgery based on navigated transcranial magnetic stimulation data. *J Neurosurg.* (2017) 126:1227–37. doi: 10.3171/2016.4.JNS152896
28. Krieg SM, Sabih J, Bulubasova L, Obermueller T, Negwer C, Janssen I, et al. Preoperative motor mapping by navigated transcranial magnetic brain stimulation improves outcome for motor eloquent lesions. *Neuro Oncol*. (2014) 16:1274–82. doi: 10.1093/neuonc/nou007
29. Takakura T, Muragaki Y, Tamura M, Maruyama T, Nitta M, Niki C, et al. Navigated transcranial magnetic stimulation for glioma removal: prognostic value in motor function recovery from postsurgical neurological deficits. *J Neurosurg*. (2017) 127:877–91. doi: 10.3171/2016.8.JNS16442
30. Pascual-Leone A, Gates JR, Dhuna A. Induction of speech arrest and counting errors with rapid-rate transcranial magnetic stimulation. *Neurology.* (1991) 41:697–702. doi: 10.1212/WNL.41.5.697
31. Hoogendam JM, Ramakers GMJ, Di Lazzaro V. Physiology of repetitive transcranial magnetic stimulation of the human brain. *Brain Stimul.* (2010) 3:95–118. doi: 10.1016/j.brs.2009.10.005
32. Rösler J, Niraula B, Strack V, Zdunczyk A, Schilt S, Savolainen P, et al. Language mapping in healthy volunteers and brain tumor patients with a novel navigated TMS system: evidence of tumor-induced plasticity. *Clin Neurophysiol.* (2014) 125:526–36. doi: 10.1016/j.clinph.2013.08.015
33. Raffa G, Quattropani MC, Scibilia A, Conti A, Angileri FF, Esposito F, et al. Surgery of language-eloquent tumors in patients not eligible for awake surgery: the impact of a protocol based on navigated transcranial magnetic stimulation on presurgical planning and language outcome, with evidence of tumor-induced intra-hemispheric plasticity. *Clin Neurol Neurosurg.* (2018) 168:127–39. doi: 10.1016/j.clineuro.2018.03.009
34. Jennum P, Winkel H. Transcranial magnetic stimulation. Its role in the evaluation of patients with partial epilepsy. *Acta Neurol Scand.* (1994) 89:93–6. doi: 10.1111/j.1600-0404.1994.tb05195.x
35. Epstein CM, Woodard JL, Stringer AY, Bakay RAE, Henry TR, Pennell PB, et al. Repetitive transcranial magnetic stimulation does not replicate the Wada test. *Neurology*. (2000) 55:1025–7. doi: 10.1212/WNL.55.7.1025
36. Pelletier I, Sauerwein HC, Lepore F, Saint-Amour D, Lassonde M. Non-invasive alternatives to the Wada test in the presurgical evaluation of language and memory functions in epilepsy patients. *Epileptic Disord.* (2007) 9:111–26. doi: 10.1684/epd.2007.0109
37. Tarapore PE, Findlay AM, Honma SM, Mizuiri D, Houde JF, Berger MS, et al. Language mapping with navigated repetitive TMS: proof of technique and validation. *Neuroimage.* (2013) 82:260–72. doi: 10.1016/j.neuroimage.2013.05.018
38. Picht T, Krieg SM, Sollmann N, Rösler J, Niraula B, Neuvonen T, et al. A comparison of language mapping by preoperative navigated transcranial magnetic stimulation and direct cortical stimulation during awake surgery. *Neurosurgery.* (2013) 72:808–19. doi: 10.1227/NEU.0b013e3182889e01
39. Ille S, Sollmann N, Hauck T, Maurer S, Tanigawa N, Obermueller T, et al. Combined noninvasive language mapping by navigated transcranial magnetic stimulation and functional MRI and its comparison with direct cortical stimulation. *J Neurosurg.* (2015) 123:212–25. doi: 10.3171/2014.9.JNS14929
40. Könönen M, Tamsi N, Säisänen L, Kemppainen S, Määttä S, Julkunen P, et al. Non-invasive mapping of bilateral motor speech areas using navigated transcranial magnetic stimulation and functional magnetic resonance imaging. *J Neurosci Methods.* (2015) 248:32–40. doi: 10.1016/j.jneumeth.2015.03.030
41. Sollmann N, Negwer C, Ille S, Maurer S, Hauck T, Kirschke JS, et al. Feasibility of nTMS-based DTI fiber tracking of language pathways in neurosurgical

patients using a fractional anisotropy threshold. *J Neurosci Methods.* (2016) 267:45–54. doi: 10.1016/j.jneumeth.2016.04.002
42. Raffa G, Bährend I, Schneider H, Faust K, Germanò A, Vajkoczy P, et al. A novel technique for region and linguistic specific nTMS-based DTI fiber tracking of language pathways in brain tumor patients. *Front Neurosci.* (2016) 10:552. doi: 10.3389/fnins.2016.00552
43. Sollmann N, Zhang H, Schramm S, Ille S, Negwer C, Kreiser K, et al. Function-specific tractography of language pathways based on nTMS mapping in patients with supratentorial lesions. *Clin Neuroradiol.* (2020) 30:123–35. doi: 10.1007/s00062-018-0749-2
44. Sollmann N, Kelm A, Ille S, Schröder A, Zimmer C, Ringel F, et al. Setup presentation and clinical outcome analysis of treating highly language-eloquent gliomas via preoperative navigated transcranial magnetic stimulation and tractography. *Neurosurg Focus.* (2018) 44:E2. doi: 10.3171/2018.3.FOCUS1838
45. Sollmann N, Fratini A, Zhang H, Zimmer C, Meyer B, Krieg SM. Associations between clinical outcome and tractography based on navigated transcranial magnetic stimulation in patients with language-eloquent brain lesions. *J Neurosurg.* (2020) 132:1033–42. doi: 10.3171/2018.12.JNS182988
46. Schwarzer V, Bährend I, Rosenstock T, Dreyer FR, Vajkoczy P, Picht T. Aphasia and cognitive impairment decrease the reliability of rnTMS language mapping. *Acta Neurochir (Wien).* (2018) 160:343–56. doi: 10.1007/s00701-017-3397-4
47. Gough PM, Nobre AC, Devlin JT. Dissociating linguistic processes in the left inferior frontal cortex with transcranial magnetic stimulation. *J Neurosci.* (2005) 25:8010–6. doi: 10.1523/JNEUROSCI.2307-05.2005
48. Coello AF, Moritz-Gasser S, Martino J, Martinoni M, Matsuda R, Duffau H. Selection of intraoperative tasks for awake mapping based on relationships between tumor location and functional networks: a review. *J Neurosurg.* (2013) 119:1380–94. doi: 10.3171/2013.6.JNS122470
49. Fernandez E, Alfaro A, Tormos JM, Climent R, Martínez M, Vilanova H, et al. Mapping of the human visual cortex using image-guided transcranial magnetic stimulation. *Brain Res Protoc.* (2002) 10:115–24. doi: 10.1016/S1385-299X(02)00189-7
50. Salminen-Vaparanta N, Noreika V, Revonsuo A, Koivisto M, Vanni S. Is selective primary visual cortex stimulation achievable with TMS? *Hum Brain Mapp.* (2012) 33:652–65. doi: 10.1002/hbm.21237
51. Giglhuber K, Maurer S, Zimmer C, Meyer B, Krieg SM. Mapping visuospatial attention: the greyscales task in combination with repetitive navigated transcranial magnetic stimulation. *BMC Neurosci.* (2018) 19:40. doi: 10.1186/s12868-018-0440-1
52. Salatino A, Chillemi G, Gontero F, Poncini M, Pyasik M, Berti A, et al. Transcranial magnetic stimulation of posterior parietal cortex modulates line-length estimation but not illusory depth perception. *Front Psychol.* (2019) 10:1169. doi: 10.3389/fpsyg.2019.01169
53. Salatino A, Poncini M, George MS, Ricci R. Hunting for right and left parietal hot spots using single-pulse TMS: modulation of visuospatial perception during line bisection judgment in the healthy brain. *Front Psychol.* (2014) 5:1238. doi: 10.3389/fpsyg.2014.01238
54. Maurer S, Giglhuber K, Sollmann N, Kelm A, Ille S, Hauck T, et al. Non-invasive mapping of face processing by navigated transcranial magnetic stimulation. *Front Hum Neurosci.* (2017) 11:4. doi: 10.3389/fnhum.2017.00004
55. Maurer S, Tanigawa N, Sollmann N, Hauck T, Ille S, Boeckh-Behrens T, et al. Non-invasive mapping of calculation function by repetitive navigated transcranial magnetic stimulation. *Brain Struct Funct.* (2016) 221:3927–47. doi: 10.1007/s00429-015-1136-2
56. Montefinese M, Turco C, Piccione F, Semenza C. Causal role of the posterior parietal cortex for two-digit mental subtraction and addition: a repetitive TMS study. *Neuroimage.* (2017) 155:72–81. doi: 10.1016/j.neuroimage.2017.04.058
57. Villamar MF, Santos Portilla A, Fregni F, Zafonte R. Noninvasive brain stimulation to modulate neuroplasticity in traumatic brain injury. *Neuromodulation.* (2012) 15:326–38. doi: 10.1111/j.1525-1403.2012.00474.x
58. Boggio PS, Nunes A, Rigonatti SP, Nitsche MA, Pascual-Leone A, Fregni F. Repeated sessions of noninvasive brain DC stimulation is associated with motor function improvement in stroke patients. *Restor Neurol Neurosci.* (2007) 25:123–9.
59. Fregni F, Pascual-Leone A. Hand motor recovery after stroke: tuning the orchestra to improve hand motor function. *Cogn Behav Neurol.* (2006) 19:21–33. doi: 10.1097/00146965-200603000-00003
60. Jo JM, Kim YH, Ko MH, Ohn SH, Joen B, Lee KH. Enhancing the working memory of stroke patients using tDCS. *Am J Phys Med Rehabil.* (2009) 88:404–9. doi: 10.1097/PHM.0b013e3181a0e4cb
61. Fregni F, Boggio PS, Nitsche M, Bermpohl F, Antal A, Feredoes E, et al. Anodal transcranial direct current stimulation of prefrontal cortex enhances working memory. *Exp Brain Res.* (2005) 166:23–30. doi: 10.1007/s00221-005-2334-6
62. Neville IS, Zaninotto AL, Hayashi CY, Rodrigues PA, Galhardoni R, De Andrade DC, et al. Repetitive TMS does not improve cognition in patients with TBI: a randomized double-blind trial. *Neurology.* (2019) 93:E190–9. doi: 10.1212/WNL.0000000000007748
63. Rossi S, Hallett M, Rossini PM, Pascual-Leone A, Avanzini G, Bestmann S, et al. Safety, ethical considerations, and application guidelines for the use of transcranial magnetic stimulation in clinical practice and research. *Clin Neurophysiol.* (2009) 120:2008–39. doi: 10.1016/j.clinph.2009.08.016
64. Machii K, Cohen D, Ramos-Estebanez C, Pascual-Leone A. Safety of rTMS to non-motor cortical areas in healthy participants and patients. *Clin Neurophysiol.* (2006) 117:455–71. doi: 10.1016/j.clinph.2005.10.014
65. Loo CK, McFarquhar TF, Mitchell PB. A review of the safety of repetitive transcranial magnetic stimulation as a clinical treatment for depression. *Int J Neuropsychopharmacol.* (2008) 11:131–47. doi: 10.1017/S1461145707007717
66. Loo C, Sachdev P, Elsayed H, McDarmont B, Mitchell P, Wilkinson M, et al. Effects of a 2- to 4-week course of repetitive Transcranial Magnetic Stimulation (rTMS) on neuropsychologic functioning, electroencephalogram, and auditory threshold in depressed patients. *Biol Psychiatry.* (2001) 49:615–23. doi: 10.1016/S0006-3223(00)00996-3
67. Dhuna A, Gates J, Pascual-Leone A. Transcranial magnetic stimulation in patients with epilepsy. *Neurology.* (1991) 41:1067–71. doi: 10.1212/wnl.41.7.1067
68. Hömberg V, Netz J. GENERALISED SEIZURES INDUCED BY TRANSCRANIAL MAGNETIC STIMULATION OF MOTOR CORTEX. *Lancet.* (1989) 334:1223. doi: 10.1016/S0140-6736(89)91835-7
69. Schrader LM, Stern JM, Koski L, Nuwer MR, Engel J. Seizure incidence during single- and paired-pulse transcranial magnetic stimulation (TMS) in individuals with epilepsy. *Clin Neurophysiol.* (2004) 115:2728–37. doi: 10.1016/j.clinph.2004.06.018
70. R. K. Safety of transcranial magnetic stimulation. *Lancet*. (1990) 335:469–70.

Conflict of Interest: The authors declare that the research was conducted in the absence of any commercial or financial relationships that could be construed as a potential conflict of interest.

frontiers in Neurology

ORIGINAL RESEARCH
published: 22 January 2021
doi: 10.3389/fneur.2020.582262

Evaluation of Changes in Preoperative Cortical Excitability by Navigated Transcranial Magnetic Stimulation in Patients With Brain Tumor

Iuri Santana Neville[1,2,3], Alexandra Gomes dos Santos[2], Cesar Cimonari Almeida[2,3], Cintya Yukie Hayashi[2,3], Davi Jorge Fontoura Solla[2], Ricardo Galhardoni[2,3,4], Daniel Ciampi de Andrade[1,2,3], Andre Russowsky Brunoni[3], Manoel Jacobsen Teixeira[2] and Wellingson Silva Paiva[2,3]*

[1] Instituto do Cancer do Estado de São Paulo, Hospital das Clínicas da Faculdade de Medicina da Universidade de São Paulo, São Paulo, Brazil, [2] LIM-62/Division of Neurosurgery, Department of Neurology, Faculdade de Medicina da Universidade de São Paulo, São Paulo, Brazil, [3] Service of Interdisciplinary Neuromodulation, Instituto de Psiquiatria do Hospital das Clínicas da Faculdade de Medicina da Universidade de São Paulo, São Paulo, Brazil, [4] School of Medicine - Universidade da Cidade de São Paulo UNICID, São Paulo, Brazil

OPEN ACCESS

Edited by:
Thomas Picht, Charité – Universitätsmedizin Berlin, Germany

Reviewed by:
Yasuo Terao, Kyorin University, Japan
Petro Julkunen, Kuopio University Hospital, Finland

***Correspondence:**
Alexandra Gomes dos Santos
alexandra.gomes@fm.usp.br

Specialty section:
This article was submitted to Applied Neuroimaging, a section of the journal Frontiers in Neurology

Received: *11 July 2020*
Accepted: *14 December 2020*
Published: *22 January 2021*

Citation:
Neville IS, Gomes dos Santos A, Almeida CC, Hayashi CY, Solla DJF, Galhardoni R, de Andrade DC, Brunoni AR, Teixeira MJ and Paiva WS (2021) Evaluation of Changes in Preoperative Cortical Excitability by Navigated Transcranial Magnetic Stimulation in Patients With Brain Tumor. Front. Neurol. 11:582262. doi: 10.3389/fneur.2020.582262

Background: This prospective study aimed to evaluate the cortical excitability (CE) of patients with brain tumors surrounding or directly involving the **corticospinal tract** (CST) using navigated transcranial magnetic stimulation (nTMS).

Methods: We recruited 40 patients with a single brain tumor surrounding or directly involving the CST as well as 82 age- and sex-matched healthy controls. The patients underwent standard nTMS and CE evaluations. Single and paired pulses were applied to the primary motor area (M1) of both affected and unaffected cerebral hemispheres 1 week before surgery. The CE parameters included resting motor threshold (RMT), motor evoked potential (MEP) ratio for 140 and 120% stimulus (MEP 140/120 ratio), short-interval intracortical inhibition (SICI), and intracortical facilitation (ICF). Motor outcome was evaluated on hospital discharge and on 30-day and 90-day postoperative follow-up.

Results: In the affected hemispheres of patients, SICI and ICF were significantly higher than in the unaffected hemispheres ($p = 0.002$ and $\boldsymbol{p} = 0.009$, respectively). The 140/120 MEP ratio of patients' unaffected hemispheres was lower than that in controls ($p = 0.001$). Patients with glioblastomas (GBM) had a higher interhemispheric RMT ratio than patients with grade II and III gliomas ($\boldsymbol{p} = 0.018$). A weak correlation was observed among the RMT ratio and the preoperative motor score ($R^2 = 0.118$, $p = 0.017$) and the 90-day follow-up ($\boldsymbol{R^2} = 0.227$, $p = 0.016$).

Conclusion: Using preoperative nTMS, we found that brain hemispheres affected by tumors had abnormal CE and that patients with GBM had a distinct pattern of CE. These findings suggest that tumor biological behavior might play a role in CE changes.

Keywords: motor outcome, glioblastoma, neuromodulation, brain tumor, transcranial magnetic stimulation, cortical excitability

INTRODUCTION

Developed in 1985 by Barker and colleagues (1), transcranial magnetic stimulation (TMS) is a non-invasive, economical, accurate, and well-tolerated method of adjuvant intervention utilized in various neuropsychiatric disorders including major depression (2), Alzheimer's disease (3), diffuse axonal injury (4, 5), schizophrenia (6), and anxiety (7). In neuro-oncology, navigated TMS (nTMS) has been useful in studying electrophysiology in patients with tumors located in eloquent areas to assess motor tract integrity. Brain mapping with nTMS has been associated with a decreased risk of new postoperative neurological deficits and an increased extent of resection (EOR) (8), which are essential for achieving better progression-free survival and quality of life (9, 10).

It has been suggested that preoperative nTMS results could be used as a predictor of motor outcome in patients with lesions involving the primary motor cortex (M1) and corticospinal tract (CST). For example, an abnormal interhemispheric resting motor threshold (RMT) ratio was found to be a high-risk criterion for early poor postoperative motor outcome (7 days), but not for late outcome (3 months) (11). Recent reports also indicate the correlation of the absence of intraoperative motor evoked potential (MEP), detected by postoperative nTMS, with poor motor prognosis (12). In addition, several parameters of cortical excitability (CE), such as short-interval intracortical inhibition (SICI) and intracortical facilitation (ICF), have been described in patients with traumatic brain injury (4) and stroke (13); however, they have not been evaluated in patients with brain tumors involving the M1. Further, the association of abnormal values obtained by nTMS with motor dysfunction is not yet clear.

The aim of the current study was to characterize the CE of patients with brain tumors surrounding the rolandic area and to compare it with those of healthy controls. This would aid in the understanding of how neoplasm behavior affects the neurophysiology of the perilesional motor cortex, using preoperative nTMS.

METHODS

Setting

For this exploratory prospective study, we recruited 40 adult patients (age $\geq$18 years old), both genders, with a single brain tumor surrounding or directly involving the CST—a convenience sample—and 82 age- and gender-matched healthy controls. All participants underwent nTMS and CE evaluations at a tertiary referral hospital of São Paulo, Brazil.

Preoperative Clinical Evaluation

Muscle strength and performance scales were assessed preoperatively, at hospital discharge, and 30-day and 90-day postoperatively. Motor score was defined as upper plus lower extremity strengths of each hemibody according to the Medical Research Council (MRC) (14, 15) grade scale, with 0 indicating no muscle activation and five indicating total muscle strength. Performance status was evaluated using the Karnofsky Performance Scale (KPS) (16). Although the use of antiepileptic drugs (AED) and antidepressants had been previously associated with alterations in neuroexcitability, these drugs could not be withdrawn before nTMS sessions. Instead, we studied the interference of these drugs on CE.

Brain Tumor Management

Brain tumor diagnosis was established based on clinical history, preoperative magnetic resonance imaging (MRI) analysis, and histopathologic study of each lesion, as per the latest World Health Organization Classification of Tumors of the Central Nervous System (17). Surgical resection was aimed at achieving the best possible EOR.

We used an axial T2-weighted fluid attenuated inversion recovery (FLAIR) MRI sequence to assess the distance (mm) between cortical lesions and the posterior border of the "omega," correspondent to the area of the hand on the pre-central gyrus (M1). For subcortical lesions, we calculated the distance between the lesion and the posterior limb of the internal capsule.

nTMS Evaluation

Up to 1 week before surgery, neuronavigation was performed using a frameless stereotaxic system, combining preoperative structural MRI and a sensor-based navigation system (Brainsight TMS version 1.7, Canada) for the guidance of coil placement and visualization of the angle of impact for the magnetic impulse onto the cortical surface (18, 19). Both single- and paired-pulse TMS were applied to M1 of affected and unaffected hemispheres using a circular coil connected to an offline electromyography amplifier of a one-channel, three-surface electrode output (Magventure Tonika Elecktronic, Denmark). The MEP response curve amplitudes were recorded in microvolts (μV) for the first interosseous muscle of the contralateral hand. All evaluations were performed by the same examiner.

CE assessed RMT (%), defined as the lowest stimulus provoking a MEP of at least 50 μV in five out of 10 consecutive trials using single-pulse TMS (20). To assess the amplitude of the input/output curve, we used the MEP obtained with 120 and 140% of RMT stimulus, the most varied range of this curve, and calculated the MEP 140/120 ratio (21–24). With the conditioning stimulus set at 80% of RMT and the test stimulus set at 120% of RMT, we applied paired-pulse TMS and measured SICI by taking the ratio between the amplitude of MEP response curves at 2 and 4 ms inter-stimulus intervals (ISI), while the ICF ratio was calculated taking the ratio between the amplitudes of MEP response curves at ISI 10 ms and 15 ms, for each hemisphere (4, 21, 25). All parameters were classified as low, normal, or high, based on normative values obtained by Cueva *et al.* (25). The ratios between affected and unaffected hemispheres for each parameter were calculated, considering the normal reference range as 90–110%.

Ethical Standard

This study was approved by the Ethics and Research Committee of the University of São Paulo Medical School, and all individuals provided written informed consent, following the Declaration of Helsinki guidelines.

Statistical Analysis

Continuous variable normality was verified using the asymmetry and kurtosis values. We performed a Wilcoxon test to compare CE between the affected and unaffected hemispheres. Additionally, to compare the patients with controls, we calculated the mean scores for the controls' hemispheres and compared them with scores for both affected and unaffected hemispheres of all patients using the Mann–Whitney *U* test. Comparisons among the subgroups of patients according to brain tumor histopathology diagnosis (primary central nervous system [CNS] tumor vs. metastasis; World Health Organization [WHO] grade II and III gliomas vs. glioblastomas [GBMs]) were performed using the Mann–Whitney test. We studied the association between motor score and neurophysiological parameters using Spearman's correlation coefficients for quantitative data (absolute value) and Pearson's Chi-square test for qualitative data:

TABLE 1 | General sample characterization.

Variable, *n* (%)	Abscense of hemiparesis	Presence of hemiparesis	Total *n* (%)	*p*
Age (years)	45.08 ± 15.46	58.53 ± 11.05	50.00 ± 15.34	**0.009**
Male sex	18 (72.0)	7 (28.0)	25 (62.5)	0.154
Left hemisphere affected	13 (72.2)	5 (27.8)	18 (43.9)	0.300
Awake surgery	12 (75.0)	4 (25.0)	16 (43.2)	0.260
Preop use of dexamethasone	10 (55.6)	8 (44.4)	18 (43.9)	0.355
Preop use of antiepileptic drug	21 (65.6)	11 (34.4)	32 (80.0)	0.683
CLINICAL PRESENTATION				
Motor score (MRC)	10	8 (5–8)	10 (8–10)	-
Seizure	18 (66.7)	9 (33.3)	27 (73.0)	0.706
Preop KPS	90 ± 6.32	73.33 ± 14.96	83.90 ± 13.01	**<0.001**
HISTOLOGY				
Metastasis	3 (50.0)	3 (50.0)	6 (14.6)	0.460
Lung	2 (66.7)	1 (33.3)	3 (50.0)	
Melanoma	1 (50.0)	1 (50.0)	2 (33.3)	
GTI	0	1 (100.0)	1 (16.7)	0.422
Primary CNS Tumor	23 (65.7)	12 (34.3)	35 (85.4)	
WHO				
I	1 (100)	0	1 (2.9)	
II	9 (100)	0	9 (25.7)	
III	10 (71.4)	4 (28.6)	14 (40.0)	
IV	3 (27.3)	8 (72.7)	11 (31.4)	**0.002**
Total	26 (63.4)	15 (36.6)	41 (100)	

MRC, Medical Research Council; CNS, central nervous system; WHO, World Health Organization. Bold values are statistically significant p values (< 0.05).

TABLE 2 | Transcranial magnetic stimulation parameters in patients and controls.

Cortical excitability	Patients		*p* (e)	Controls' mean between hemispheres	*p* (f)	*p* (g)
	Unaffected hemisphere	Affected hemisphere				
RMT(a) %	52.3 ± 10.4	51.4 ± 11.7	0.501	48.7 ± 8.9	0.086	0.176
MEP(b) ratio 140/120	2.15 ± 0.86	2.33 ± 1.04	0.741	3.98 ± 3.41	**0.001**	**0.008**
SICI(c)	0.80 ± 0.59	1.12 ± 0.60	**0.002**	1.18 ± 1.27	0.070	0.191
ICF(d)	1.83 ± 1.20	2.30 ± 1.14	**0.009**	2.05 ± 1.42	0.446	**0.046**
	Ratios affected/Unaffected hemisphere				Altered (%)	
rRMT	1.0 ± 0.1				19 (51.4)	
rMEP ratio 140/120	1.11 ± 0.71				32 (88.9)	
rSIICI	1.91 (0.85–3.39)				**35 (94.6)**	
rICF	1.29 (0.86–2.27)				32 (86.5)	

RMT(a), resting motor threshold; MEP(b), motor evoked potential; SICI(c), short-interval intracortical inhibition; ICF(d), intracortical facilitation; (e), comparison between healthy and ill hemispheres; (f), comparison between patients' unaffected hemisphere and controls' mean value; (g), comparison between patients' affected hemisphere and controls' mean value. Bold values are statistically significant p values (< 0.05).

classification normal × altered (high + low). Finally, we compared pre- and postoperative muscle strength and KPS using ANOVA for repeated measures. The analyses were performed using the Statistical Package for Social Sciences, version 24.0 (IBM Statistics, Armonk, New York, USA). The data were considered significant when p was < 0.05.

RESULTS

Forty patients underwent nTMS analysis. One patient underwent a new nTMS session before undergoing an additional surgery for recurrent GBM resection a year after the first resection, totalizing 41 CE evaluations. The general characteristics of the patients are presented in **Table 1**. The mean age of the patients was 50.00 ± 15.34 years, 15 females and 25 males. Similarly, the control group had a mean age of 49.72 ± 15.37 (33 females and 50 males). The mean preoperative KPS score was 83.90 ± 13.01 (range, 50–100). The frequent clinical manifestations that were observed included seizures (27 patients, 73.0%) and hemiparesis (10 patients, 31.3%). The median motor score was 10 (8–10). Around 44% of the patients were taking dexamethasone and 80% antiepileptic drugs when submitted to nTMS session. Three patients were using antidepressants, and only one was using a neuroleptic drug at the time of nTMS session. Thirty-one patients presented cortical tumors while nine patients had subcortical lesions. Thirty-five patients had primary CNS tumors, 23 patients had WHO grade II or III gliomas, 11 had GBMs, and six had secondary brain tumors (originating from the lungs, skin, and gastrointestinal tract).

Assessing CE, we found that SICI and ICF values were significantly higher in the patients' affected hemispheres than in the unaffected hemispheres (1.12 ± 0.60 vs. 0.80 ± 0.59, $p = 0.002$; 2.30 ± 1.14 vs. 1.83 ± 1.20, $p = 0.009$, respectively; **Table 2**, **Figure 1**). RMT and MEP interhemispheric ratios exhibited normal distributions in patients, while SICI and ICF interhemispheric ratios had significant interindividual variations. We observed a high frequency of altered (outside the 90–110% range) interhemispheric ratios in the group of patients: 51% of patients had abnormal RMT ratio; 89%, MEP 140/120 ratio; 86%, ICF ratio; and 94%, SICI ratio.

When the patients were compared to the controls, it was found the MEP 140/120 ratio was lower in patients' both unaffected and affected hemispheres than in those of the controls (3.98 ± 3.41 vs. 2.15 ± 0.86, $p = 0.001$; 3.98 ± 3.41 vs. 2.33 ± 1.04, $p = 0.008$, respectively; **Table 2**, **Figure 1**).

The use of antidepressants was not associated with a different CE pattern. Preoperative use of AED seemed not to significantly influence CE in the total population. However, when we studied only the subgroup with CNS tumors, patients who used antiepileptic drugs had significant lower ratio MEP 140/120 and ICF in the affected hemisphere (2.14 vs. 3.54 for MEP ratio, $p = 0.045$, 2.21 vs. 3.42 for ICF, $p = 0.022$, respectively, **Supplementary Material 1**).

Preoperative clinical and neurophysiologic data of each patient are detailed in **Table 3**. Thirty-one patients presented abnormal RMT on the unaffected hemisphere and 33 patients presented abnormal RMT on the affected hemisphere. For the other CE parameters, altered MEP 140/120 ratio, SICI, and ICF were more frequent on unaffected hemisphere than the affected one (30 vs. 27 for MEP140/120 ratio, 31 vs. 29 for SICI, and 32 vs. 25 patients for ICF, respectively).

When we compared patients according to the presence of hemiparesis, the only difference found was a higher SICI in the unaffected hemisphere of patients with hemiparesis ($p = 0.013$). However, there was no difference in interhemispheric SICI ratio (**Table 4**). Comparing the subgroups of patients according to their histopathological diagnoses revealed no significant difference in CE between patients with primary and secondary tumors. However, comparisons of patients with GBMs with patients with WHO grade II and III gliomas indicated that

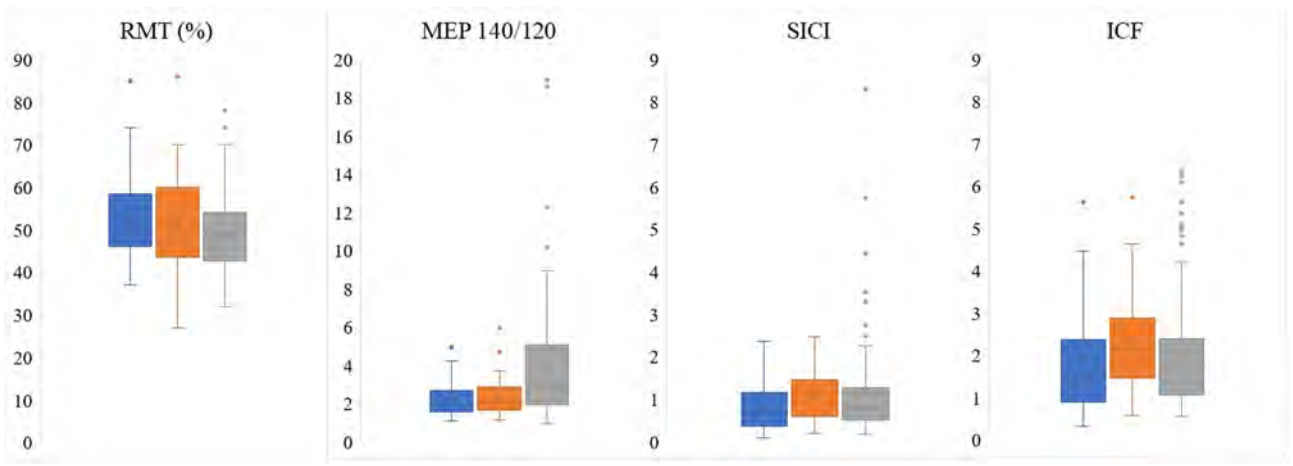

FIGURE 1 | Comparison of electrophysiological parameters obtained by preoperative TMS between unaffected (blue) and affected (orange) patients' hemispheres and the mean between controls' hemispheres (gray). RMT, resting motor threshold; MEP, motor evoked potential; SICI, short-interval intracortical inhibition; ICF, intracortical facilitation.

TABLE 3 | Preoperative clinical presentation and cortical excitability obtained by navigated transcranial magnetic stimulation of the patients.

Patient	Hemisphere affected	UL strength	Hemiparesis	KPS	Histology	Distance from motor area	Healthy hemisphere				Affected hemisphere				Ratio affected/ healthy hemisphere			
							RMT(a) %	MEP 140/120 (b)	SICI (c)	ICF (d)	RMT %	MEP 140/120	SICI	ICF	RMT %	MEP 140/120	SICI	ICF
1	Right	4	Yes	70	Anaplastic Astrocytoma	0	37	1.191	0.211	0.382	37	3.283	1.334	3.240	1.0	2.76	6.32	8.48
2	Right	4	Yes	90	Glioblastoma	0	46	2.154	1.792	1.024	55	1.156	0.544	1.094	1.2	0.53	0.30	1.07
3	Right	5	No	90	High Grade Not Otherwise Especified Glioma	0	47	1.607	0.890	2.178	48	2.910	0.921	1.369	1.0	1.81	1.03	0.62
4	Right	5	No	90	Anaplastic Oligodendroglioma	47	69	2.537	0.678	3.043	67	2.604	0.484	2.195	0.9	1.03	0.71	0.72
5	Right	0	Yes	60	Glioblastoma	0	48	1.872	2.356	1.117	64	1.385	1.229	2.651	1.3	0.73	0.52	2.37
6	Right	4	Yes	90	Metastatic Melanoma	0	72	4.230	0.684	2.549	53	4.674	1.590	5.733	0.7	1.10	2.32	2.25
7	Left	5	No	90	Metastatic Melanoma	13,4	38	1.711	0.755	0.890	42	2.013	0.462	1.265	1.1	1.18	0.61	1.42
8	Left	4	Yes	100	Anaplastic Astrocytoma	0	40	2.741	1.651	3.571	43	1.702	1.895	2.163	1.1	0.62	1.15	0.61
9	Left	4	No	80	Glioblastoma	0	48	1.809	0.393	1.937	60	1.571	1.286	1.768	1.2	0.87	3.27	0.91
10	Left	5	No	90	Anaplastic Astrocytoma	33,1	51	1.611	0.531	2.515	55	1.759	0.35	1.482	1.1	1.09	0.66	0.59
11	Left	2	Yes	60	Metastatic GTI Adenocarcinoma	0	74	1.431	0.173	1.189	86	na	1.239	0.798	1.1	na	7.16	0.67
12	Right	5	No	90	Low Grade Not Otherwise Especified Glioma	na	53	1.449	0.880	1.757	49	3.049	0.195	2.258	0.9	2.10	0.22	1.29
13	Right	4	Yes	70	Metastatic Epidermoid Carcinoma (low differentiated)	0	60	1.269	0.367	0.610	61	2.223	0.695	0.577	1.0	1.75	1.89	0.95
14	Left	5	No	90	Metastatic Lung Adenocarcinoma	10,7	40	1.911	0.426	0.597	41	1.359	1.499	1.052	1.0	0.71	3.52	1.76
15	Left	5	No	80	Metastatic Lung Adenocarcinoma	0	46	2.572	0.711	0.864	27	1.787	1.911	2.285	0.6	0.69	2.69	2.64
16	Left	2	Yes	50	Glioblastoma	0	57	1.643	2.186	4.472	na	na	na	na	na	na	na	na
17	Left	5	No	80	Glioblastoma	0	58	1.548	0.819	1.474	63	2.337	1.326	4.330	1.1	1.51	1.62	2.94
18	Left	5	No	90	Anaplastic Astrocytoma	0	63	1.647	0.270	0.545	58	3.611	1.172	4.362	0.9	2.19	4.34	8.00
19	Left	5	No	90	Diffuse Astrocytoma	29,5	57	3.526	1.469	2.233	63	2.335	1.017	2.277	1.1	0.66	0.69	1.02

(Continued)

TABLE 3 | Continued

Patient	Hemisphere affected	UL strength	Hemiparesis	KPS	Histology	Distance from motor area	Healthy hemisphere				Affected hemisphere				Ratio affected/ healthy hemisphere			
							RMT(a) %	MEP 140/120 (b)	SICI (c)	ICF (d)	RMT %	MEP 140/120	SICI	ICF	RMT %	MEP 140/120	SICI	ICF
9	Left	4	Yes	70	Glioblastoma Recurrence	0	53	1.346	0.305	1.225	70	3.474	1.204	2.540	1.3	2.58	3.95	2.07
20	Left	5	No	80	Low Grade Not Otherwise Especified Glioma	0	59	1.159	0.082	1.120	60	1.965	0.790	1.667	1.0	1.70	9.63	1.49
21	Right	5	Yes	70	Anaplastic Oligodendroglioma	0	41	2.356	1.420	3.489	45	1.960	1.050	1.457	1.1	0.83	0.74	0.42
22	Right	5	No	90	Anaplastic Astrocytoma	0	40	2.244	0.337	0.759	46	1.990	0.581	1.746	1.1	0.89	1.72	2.3
23	Right	5	No	90	Diffuse Astrocytoma	0	47	2.793	0.340	1.428	44	1.222	0.692	1.161	0.9	0.44	2.04	0.82
24	Right	5	No	90	Anaplastic Astrocytoma	0	43	3.567	0.672	1.413	33	2.088	0.436	2.155	0.7	0.59	0.65	1.52
25	Left	5	No	90	Anaplastic Astrocytoma	12,1	49	3.157	0.457	2.133	59	3.698	0.574	2.605	1.2	1.17	1.25	1.22
26	Right	5	No	100	Diffuse Astrocytoma	0	61	1.632	0.243	1.379	51	1.225	0.594	1.648	0.8	0.75	2.44	1.20
27	Right	5	No	90	Diffuse Astrocytoma	0	47	1.071	1.281	1.678	36	1.129	1.236	1.938	0.7	1.05	0.96	1.15
28	Left	5	No	90	Anaplastic Astrocytoma	15	50	2.850	0.551	3.754	41	1.757	1.146	2.708	0.8	0.62	2.08	0.72
29	Right	5	No	90	Glioblastoma	20,1	46	2.907	0.445	0.866	45	2.615	2.461	3.359	1.0	0.90	5.53	3.88
30	Right	5	No	100	Diffuse Astrocytoma	15,2	46	2.195	0.154	0.916	46	2.036	0.309	1.475	1.0	0.93	2.01	1.61
31	Right	5	No	80	Meningioma	24,3	50	1.699	0.280	0.322	51	2.573	1.908	4.643	1.0	1.51	6.81	14.42
32	Right	4	No	100	Anaplastic Oligodendroglioma	0	59	2.700	1.370	1.450	na	na	na	na	na	na	na	na
33	Right	5	Yes	90	Diffuse Astrocytoma	56	42	2.145	0.872	3.399	48	5.932	1.402	3.438	1,10	2,77	1,61	1,01
34	Right	2	Yes	80	Glioblastoma	0	65	1.243	1.319	5.631	na	na	na	na	na	na	na	na
35	Right	3	Yes	70	Glioblastoma	9	45	4.896	0.985	1.716	37	2.639	1.992	1.406	0.8	0.53	2.02	0.82
36	Left	5	No	90	Diffuse Oligodendroglioma	0	55	1.229	0.424	1.400	54	1.647	0.811	1.630	1.0	1.34	1.91	1.16
37	Left	0	Yes	50	Glioblastoma	0	85	na	2.135	3.517	na	na	na	na	na	na	na	na
38	Right	4	Yes	90	Glioblastoma	0	51	1.911	1.044	2.159	64	1.254	2.412	3.100	1.2	0.65	2.31	1.43
39	Right	5	No	100	Diffuse Oligodendroglioma	47	54	2.454	0.423	1.438	47	3.458	0.604	2.605	0.8	1.41	1.42	1.81
40	Right	5	No	100	High Grade Not Otherwise Especified Glioma	0	53	2.054	0.567	0.883	54	1.678	2.180	3.076	1.0	0.81	3.84	3.48

RMT(a), resting motor threshold (%); MEP(b), motor evoked potential; SICI(c), short-interval intracortical inhibition; ICF(d), intracortical facilitation; na, not applicable.

TABLE 4 | Ratio affected/unaffected hemisphere according to the presence of hemiparesis and histology.

Cortical excitability	Presence of hemiparesis	Absence of hemiparesis	*p*	Primary CNS tumor	Metastasis	*p*
rRMT (a)	1.1 ± 0.2	1.0 ± 0.1	0.075	1.0 ± 0.1	0.9 ± 0.2	0.635
rMEP ratio 140/120 (b)	1.21 ± 0.85	1.18 ± 0.56	0.458	1.20 ± 1.13	1.08 ± 0.43	0.909
rSICI (c)	2.02 (0.74–3.95)	1.81 (0.89–3.33)	0.842	1.72 (0.74–3.27)	2.50 (1.57–4.43)	0.303
rICF (d)	1.07 (0.67–2.25)	1.35 (0.98–2.38)	0.425	1.22 (0.82–2.30)	1.59 (0.88–2.34)	0.805
	Low-grade gliomas	**High-grade gliomas**		**WHO grade II-III glioma**	**Glioblastoma**	
rRMT (a)	0.9 ± 0.1	1.0 ± 0.1	0.078	1.0 ± 0.1	1.1 ± 0.2	**0.018**
rMEP ratio 140/120 (b)	1.41 ± 0.68	1.10 ± 0.67	0.367	1.25 ± 0.68	1.04 ± 0.69	0.270
rSICI (c)	1.61 (0.82–2.22)	1.72 (0.72–3.55)	0.860	1.52 (0.73–2.17)	2.16 (0.79–3.78)	0.482
rICF (d)	1.20 (1.08–1.55)	1.22 (0.72–2.65)	0.792	1.18 (0.72–1.66)	1.75 (0.95–2.79)	0.241

r, ratio affected/unaffected hemisphere; RMT(a), resting motor threshold; MEP(b), motor evoked potential; SICI(c), short-interval intracortical inhibition; ICF(d), intracortical facilitation. Bold values are statistically significant p values (< 0.05).

TABLE 5 | Comparison between affected and unaffected hemispheres according to the tumor diagnosis.

Cortical excitability	UH	AH	*p*	UH	AH	*p*
	Metastasis (*n*= 6)			**Primary CNS tumor (*n* = 35)**		
RMT(a) %	55.0 ± 15.9	51.7 ± 20.4	0.916	51.8 ± 9.4	51.4 ± 9.8	0.363
MEP(b) ratio 140/120	2.18 ± 1.10	2.41 ± 1.30	0.893	2.14 ± 0.83	2.32 ± 1.02	0.799
SICI (c)	0.52 ± 0.23	1.23 ± 0.55	**0.046**	0.85 ± 0.62	1.10 ± 0.62	**0.014**
ICF(d)	1.11 ± 0.73	1.95 ± 1.94	0.173	1.95 ± 1.22	2.37 ± 0.95	**0.031**
	Low-grade gliomas (*n* = 10)			**High-grade gliomas (*n* = 25)**		
RMT(a) %	52.7 ± 6.4	50.4 ± 8.0	0.292	51.6 ± 10.6	51.8 ± 10.8	0.108
MEP(b) ratio 140/120	1.87 ± 0.79	2.53 ± 1.49	0.214	2.26 ± 0.85	2.22 ± 0.81	0.476
SICI (c)	0.65 ± 0.50	0.77 ± 0.40	0.374	0.95 ± 0.65	1.20 ± 0.65	**0.039**
ICF(d)	1.70 ± 0.74	2.10 ± 0.62	**0.008**	2.10 ± 1.34	2.38 ± 0.96	0.181
	WHO grade II and III gliomas (*n* = 23)			**Glioblastomas (*n* = 11)**		
RMT(a) %	50.6 ± 8.3	49.3 ± 8.8	0.549	54.7 ± 11.8	57.2 ± 11.1	0.050
MEP(b) ratio 140/120	2.17 ± 0.74	2.41 ± 1.11	0.527	2.13 ± 1.07	2.05 ± 0.83	0.401
SICI (c)	0.68 ± 0.46	0.90 ± 0.50	0.060	1.25 ± 0.76	1.55 ± 0.67	0.327
ICF(d)	1.86 ± 1.01	2.21 ± 0.79	0.355	2.28 ± 1.57	2.53 ± 1.08	0.069

RMT(a), resting motor threshold; MEP(b), motor evoked potential; SICI(c), short-interval intracortical inhibition; ICF(d), intracortical facilitation. Bold values are statistically significant p values (< 0.05).

patients with GBMs had a higher interhemispheric RMT ratio ($p = 0.018$; **Table 4**). **Table 5** shows a detailed analysis of CE in each group of patients, according to their tumor diagnosis.

We compared the preoperative and the three postoperative motor evaluations. Patients presented the highest motor score at the preoperative moment and the lowest at the hospital discharge (**Table 6**, $p = 0.030$). A weak correlation was observed among the RMT ratio and the preoperative motor score ($R^2 = 0.118$, $p = 0.017$), and the 90-day follow-up ($R^2 = 0.227$, $p = 0.016$), and between unaffected hemisphere SICI and the pre- and postoperative motor scores ($R^2 = 0.255$, $p = 0.009$ for preoperative motor score, $R^2 = 0.271$, $p = 0.018$ for hospital discharge, $R^2 = 0.321$, $p = 0.013$ for 30-day follow-up, and $R^2 = 0.396$, $p = 0.059$ for 90-day follow-up, **Table 5**). However, preoperative RMT ratio and unaffected hemisphere SICI were not associated with motor score change ($p = 0.938$ for RMT and $p = 0.470$ for SICI, ANOVA for repeated measures, **Figure 2**).

A correlation was observed between distance (in millimeters) from motor area on MRI and the MEP 140/120 ratio of both hemispheres ($p = 0.030$, $R^2 = 0.348$ in the unaffected hemisphere and $p = 0.032$, $R^2 = 0.363$ in the affected hemisphere).

DISCUSSION

This study contributes to the knowledge about the neurophysiology of patients with tumors within M1. It evaluates

TABLE 6 | Correlation of spearman between cortical excitability and motor and performance scale outcomes.

Variables	Mean ± SD	Unaffected hemisphere				Affected hemisphere				Ratio affected/unnaffected hemisphere			
		RMT	MEP 140/120	SICI	ICF	RMT	MEP 140/120	SICI	ICF	RMT	MEP 140/120	SICI	ICF
Preoperative													
MS	10 (8–10)	0.345	0.565	**0.009**	0.161	0.206	0.764	0.099	0.296	**0.017**	0.402	0.919	0.311
KPS	83.90 ± 13.01	0.184	0.060	0.373	0.932	0.162	0.706	0.194	0.530	0.157	0.480	0.187	0.783
Hospital discharge													
MS	9 (6–10)	0.683	0.656	**0.018**	0.260	0.961	0.237	0.928	0.078	0.490	0.242	0.176	**0.220**
30-day follow-up													
MS	10 (7–10)	0.820	0.136	**0.013**	0.603	0.413	0.339	0.895	0.148	0.055	0.997	0.116	0.655
KPS	78.92 ± 18.67	0.978	0.327	0.109	0.928	0.553	0.986	0.199	0.081	0.213	0.835	0.164	0.744
90-day follow-up													
MS	10 (8–10)	0.445	0.398	0.059	0.862	0.516	0.514	0.873	0.156	**0.016**	0.718	0.232	0.717
KPS	82.73 ± 13.29	0.464	0.507	0.247	0.664	0.636	0.812	0.542	0.126	**0.039**	0.364	0.578	0.834

MS, motor score; KPS, Karnofsky Performance Scale. Bold values are statistically significant p values (< 0.05).

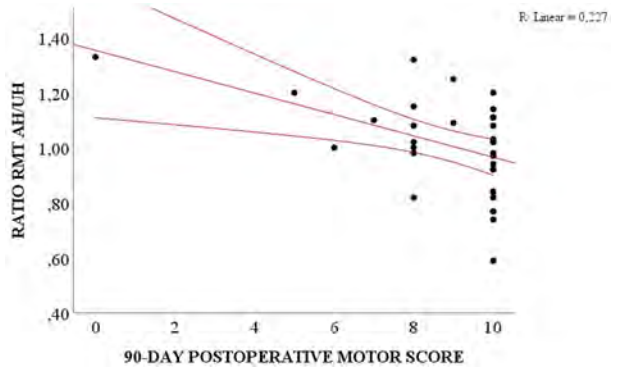

FIGURE 2 | Correlation between preoperative RMT ratio AH/UH and 90-day postoperative motor score (Spearman, $p = 0.016$).

distinct parameters that have been previously reported, RMT and MEP, as well as describes the values of SICI and ICF for the first time. The first two parameters refer to the integrity of both upper and lower motor neurons, from the cerebral cortex to the neuromuscular junction. RMT was similar between patients' hemispheres, which contradicts previous studies that reported higher RMT in the hemisphere affected by the tumor (26). SICI and ICF, the only two parameters found to be significantly higher in patients' affected hemispheres, are exclusively mediated by circuits located in the cortex (27, 28) and, therefore, have a higher specificity for cortical alterations than RMT and MEP. SICI is mediated by $GABA_A$ receptors, which are ligand-gated ion channels, while long-interval intracortical inhibition is associated with $GABA_B$. These are G-protein-coupled receptors and are, therefore, slower than $GABA_A$ (28–30). Varrasi *et al.* found abnormal intracortical inhibition in patients with partial epilepsy, which was attributed to weakness of the GABA receptors, thereby provoking an imbalance between excitatory and inhibitory circuits (31). SICI was also found to be reduced in movement disorders, such as dystonia (32) and Tourette's syndrome (33). Conversely, ICF is mediated by glutamate and is associated with excitatory cortical circuits (34). SICI was found to be lower with a concomitant increase in ICF values in patients with Parkinson's disease (35). In our study, the patients' unaffected hemisphere's excitability was lower compared to that of the controls and compared to the affected hemisphere. Since observations of significant interhemispheric differences in healthy individuals are unexpected (36), the differences found in our study might be associated with dysfunction of motor neurons in the patients' hemispheres affected by the tumor as well as an interhemispheric imbalance between excitatory and inhibitory circuits, which might be related to the greater prevalence of preoperative seizures in our study (73%). The mechanism by which the CE parameters of the contralateral hemisphere is altered as well is still unclear.

It has been reported that the use of antiepileptic, neuroleptic, and antidepressant drugs can affect neuroexcitability (37–41). Voltage-gated sodium channels blockers, such as phenytoin, carbamazepine, and lamotrigine, were previously found to increase motor threshold (41, 42), with carbamazepine associated with decreased ICF (42). In our series, the influence of AED on CE was only observed in the subgroup of patients with CNS tumors, composed of 29 patients who used AED and 6 patients who did not use it. Although the findings of lower ratio MEP 140/120 and lower ICF in the group using AED might agree with previous studies, they also might reflect a type 1 error.

It has been reported that MEP may have high interindividual variability and that the interhemispheric ratio has a more reliable value in assessing CE (26). In our sample, we found high rates of abnormal ratios (51% for RMT, 89% for MEP 140/120 ratio, 86% for ICF, and a remarkable 94% for SICI). However, only half of the patients presented with motor deficits, which led us to two main hypotheses: The first is that the alteration of these values may coexist with a normal motor function because tumor growth is not an acute process, requiring some time to progressively affect the tissue surrounding it. This conclusion applies especially to patients with low-grade gliomas, which have a relatively slower evolution, giving the unaffected brain some time to try to compensate by neuroplasticity. The second

hypothesis is that pathologic neurophysiology may predict a poor motor outcome in these patients in the future. Picht et al. speculated that patients initially without hemiparesis but with high RMT and low MEP interhemispheric ratios were at a higher risk of a decline in motor function in the future (26). These authors also suggested that patients with no previous deficits but with high MEP ratios probably have a perilesional tissue more adapted to tumor growth. Additionally, they highlighted the finding that the patients had low RMT ratios, suggesting that in these individuals, tumors might have infiltrated the inhibitory tracts of the secondary motor cortex, thereby accounting for the lack of motor deficits (26). In our study, we found six patients [patients 2, 5, 9, 19, 22, 38] with simultaneously high RMT and low MEP interhemispheric ratios, two of whom had no motor deficits prior to the resection (19, 22). Four patients had worse motor scores during the follow-up (2, 5, 22, 38), one patient remained stable (9), and one of the two patients who initially did not have any motor deficit displayed normal motor function (19). This patient is also the only one in the subgroup with a low-grade glioma, as all the others were diagnosed with high-grade gliomas. These data are consistent with Picht *et al.*'s speculation about poor outcome prediction and our second hypothesis. In our study, 10 patients (3, 7, 12, 17, 18, 20, 25, 31, 36, 39) had high MEP ratios with normal preoperative motor status, and six remained with no motor deficit (7, 18, 20, 25, 31, 39), which again is consistent with the findings of Picht *et al.* and fits our first hypothesis of adaptation of the normal tissue. The direct correlation between greater tumor's distance from motor area and higher MEP also reinforces this hypothesis.

Lastly, we observed eight patients (6, 15, 24, 26–28, 35, 39) with a low RMT ratio, and, contrary to our expectations, six of them had a high SICI ratio (6, 15, 26, 28, 35, 39). Indeed, the only difference between patients concerning hemiparesis presentation was a lower SICI in patients without this motor deficit. Concerning clinical presentation, however, the presence of preoperative motor deficit was not associated with more CE abnormalities.

The idea that preoperative TMS findings might predict motor outcome is not new. Rosenstock *et al.* studied abnormal RMT interhemispheric ratio as one criterion for high risk of poor motor outcome and found that a high RMT ratio was associated with worst motor score 7 days postoperatively, but that there was no association 3 months postoperatively (11). Therefore, more analysis is necessary to determine whether preoperative SICI and ICF are associated with presence of motor deficit at the time of CE evaluation and might predict patients' prognoses.

Tumor growth rate influences the surrounding cortex adaptation, and this could explain another finding of our study, the higher values of RMT ratio in patients with GBMs compared with patients with WHO grade II and III gliomas. It is well-known that GBM rapidly infiltrates parenchyma, hindering motor function recovery. Therefore, GBM affects CE in a way closer to the changes seen in acute/subacute brain injuries. In their meta-analysis, McDonnel *et al.* found that RMT was already higher in affected hemispheres at the early phase after stroke and continued to be altered during the chronic phase (13). As discussed previously, high RMT ratio might be a sign of a decline in motor function, even in those who do not have clinical manifestations.

This is an exploratory study whose findings contribute to the knowledge of how neuroexcitability might be affected by a tumor. However, some results require further studies to be well-understood. One of the limitations of our study is tumor heterogeneity: We included a majority of patients with gliomas (of both low and high grades and, therefore, different rates of normal tissue infiltration), a minority of patients with brain metastases (which typically provoke mass-effect alterations), and one patient with a grade I meningioma, an extra-axial tumor related to alterations due to the tumor's expansion. It is impressive that most CE parameters studied had a normal distribution considering different biological behaviors of different tumors. We had a glance on how CE in each subgroup of diagnosis is. However, focusing our attention on small subgroups increases the risk of a type 1 error. Therefore, these specific data should be considered only for descriptive purposes.

Another potential bias in the study is that the MEPs were only measured on the hands and not also on the lower extremities; more than 63% of patients presented no motor deficit or had a mild deficit preoperatively (motor score of 8–10), reflecting a possible selection bias and hindering the correlation of CE data with motor outcome. The final limitation is the lack of data on cognition and quality of life. Only minor adverse events were observed, such as light pinch on scalp and light headache during nTMS.

This study provides a detailed description of the CE of patients with tumors located in the eloquent areas of the brain. Brain hemispheres affected by tumors had abnormal CE, but further studies are needed to determine if CE is associated with loss of motor function integrity. GBMs showed a discrete pattern when compared with grade II and III gliomas, suggesting that tumor biological behavior might play a role in CE changes observed in patients with gliomas.

DATA AVAILABILITY STATEMENT

The original contributions generated for this study are included in the article/**Supplementary Material**, further inquiries can be directed to the corresponding author/s.

ETHICS STATEMENT

The studies involving human participants were reviewed and approved by Comitê de Ética e Pesquisa (Ethics and Research Committee, CEP) of University of São Paulo Medical School. The patients/participants provided their written informed consent to participate in this study.

AUTHOR CONTRIBUTIONS

IN, RG, DA, AB, MT, and WP: conception and design. IN: patients recruitment. IN, AG, CA, and CH: data collection.

IN, AG, and DS: data analysis and interpretation. IN and AG: drafting the manuscript for important intellectual content. DS, RG, CH, DA, AB, MT, and WP: text review. IN, AG, CA, CH, DS, RG, DA, AB, MT, and WP: final approval. All authors contributed to the article and approved the submitted version.

FUNDING

This work was supported by Fundação de Amparo à Pesquisa do Estado de São Paulo (São Paulo Research Foundation—FAPESP) (scholarship funding to AGS # 2019/14687-4).

ACKNOWLEDGMENTS

We would like to acknowledge the support of the secretary Sandra Falcon from the Service of Interdisciplinary Neuromodulation for organizing patient schedule.

SUPPLEMENTARY MATERIAL

The Supplementary Material for this article can be found online at: https://www.frontiersin.org/articles/10.3389/fneur.2020.582262/full#supplementary-material

REFERENCES

1. Barker AT, Jalinous R, Freeston I. Non-invasive magnetic stimulation of human motor cortex. *Lancet*. (1985) 1:1106–7. doi: 10.1016/S0140-6736(85)92413-4
2. Sonmez AI, Camsari DD, Nandakumar AL, Voort JLV, Kung S, Lewis CP, et al. Accelerated TMS for depression: a systematic review and meta-analysis. *Psychiatry Res*. (2019) 273:770–81. doi: 10.1016/j.psychres.2018.12.041
3. Dong X, Yan L, Huang L, Guan X, Dong C, Tao H, et al. Repetitive transcranial magnetic stimulation for the treatment of Alzheimer's disease: a systematic review and meta-analysis of randomized controlled trials. *PLoS ONE*. (2018) 13:1–13. doi: 10.1371/journal.pone.0205704
4. Hayashi CY, Neville IS, Rodrigues PA, Galhardoni R, Brunoni AR, Zaninotto AL, et al. Altered intracortical inhibition in chronic traumatic diffuse axonal injury. *Front Neurol*. (2018) 9:1–8. doi: 10.3389/fneur.2018.00189
5. Neville IS, Zaninotto AL, Hayashi CY, Rodrigues PA, Galhardoni R, De Andrade DC, et al. Repetitive TMS does not improve cognition in patients with TBI: a randomized double-blind trial. *Neurology*. (2019) 93:E190–9. doi: 10.1212/WNL.0000000000007748
6. Marzouk T, Winkelbeiner S, Azizi H, Malhotra AK, Homan P. Transcranial magnetic stimulation for positive symptoms in schizophrenia: a systematic review. *Neuropsychobiology*. (2020) 79:384–96.doi: 10.1159/000502148
7. Rodrigues PA, Zaninotto AL, Neville IS, Hayashi CY, Brunoni AR, Teixeira MJ, et al. Transcranial magnetic stimulation for the treatment of anxiety disorder. *Neuropsychiatr Dis Treat*. (2019) 15:2743–61. doi: 10.2147/NDT.S201407
8. Raffa G, Scibilia A, Conti A, Ricciardo G, Rizzo V, Morelli A, et al. The role of navigated transcranial magnetic stimulation for surgery of motor-eloquent brain tumors: a systematic review and meta-analysis. *Clin Neurol Neurosurg*. (2019) 180:7–17. doi: 10.1016/j.clineuro.2019.03.003
9. Frey D, Schilt S, Strack V, Zdunczyk A, Sler JR, Niraula B, et al. Navigated transcranial magnetic stimulation improves the treatment outcome in patients with brain tumors in motor eloquent locations. *Neuro Oncol*. (2014) 16:1365–72. doi: 10.1093/neuonc/nou110
10. Picht T. Current and potential utility of transcranial magnetic stimulation in the diagnostics before brain tumor surgery. *CNS Oncol*. (2014) 3:299–310. doi: 10.2217/cns.14.25
11. Rosenstock T, Grittner U, Acker G, Schwarzer V, Kulchytska N, Vajkoczy P, et al. Risk stratification in motor area-related glioma surgery based on navigated transcranial magnetic stimulation data. *J Neurosurg*. (2017) 126:1227–37. doi: 10.3171/2016.4.JNS152896
12. Seidel K, Häni L, Lutz K, Zbinden C, Redmann A, Consuegra A, et al. Postoperative navigated transcranial magnetic stimulation to predict motor recovery after surgery of tumors in motor eloquent areas. *Clin Neurophysiol*. (2019) 130:952–9. doi: 10.1016/j.clinph.2019.03.015
13. McDonnell MN, Stinear CM. TMS measures of motor cortex function after stroke: a meta-analysis. *Brain Stimul*. (2017) 10:721–34. doi: 10.1016/j.brs.2017.03.008
14. Council MR. *Aids to the Examination of Peripheral Nerves System*. London: Memo no 45 Her Majesty's Station Off (1981).
15. Paternostro-Sluga T, Grim-Stieger M, Posch M, Schuhfried O, Vacariu G, Mittermaier C, et al. Reliability and validity of the Medical Research Council (MRC) scale and a modified scale for testing muscle strength in patients with radial palsy. *J Rehabil Med*. (2008) 40:665–71. doi: 10.2340/16501977-0235
16. Karnofsky AW, Craver LBJ. The use of nitrogen mustard in the palliative treatment of cancer. *Cancer*. (1948) I:634–56.
17. Louis DN, Perry A, Reifenberger G, von Deimling A, Figarella-Branger D, Cavenee WK, et al. The 2016 World Health Organization classification of tumors of the central nervous system: a summary. *Acta Neuropathol*. (2016) 131:803–20. doi: 10.1007/s00401-016-1545-1
18. Herwig U, Schönfeldt-Lecuona C, Wunderlich AP, Von Tiesenhausen C, Thielscher A, Walter H, et al. The navigation of transcranial magnetic stimulation. *Psychiatry Res - Neuroimaging*. (2001) 108:123–31. doi: 10.1016/S0925-4927(01)00121-4
19. Lefaucheur JP. Why image-guided navigation becomes essential in the practice of transcranial magnetic stimulation. *Neurophysiol Clin*. (2010) 40:1–5. doi: 10.1016/j.neucli.2009.10.004
20. Groppa S, Oliviero A, Eisen A, Quartarone A, Cohen LG, Mall V, et al. A practical guide to diagnostic transcranial magnetic stimulation: report of an IFCN committee. *Clin Neurophysiol*. (2012) 123:858–82. doi: 10.1016/j.clinph.2012.01.010
21. Lefaucheur JP, Drouot X, Ménard-Lefaucheur I, Keravel Y, Nguyen JP. Motor cortex rTMS restores defective intracortical inhibition in chronic neuropathic pain. *Neurology*. (2006) 67:1568–74. doi: 10.1212/01.wnl.0000242731.10074.3c
22. Han TR, Kim JH, Lim JY. Optimization of facilitation related to threshold in transcranial magnetic stimulation. *Clin Neurophysiol*. (2001) 112:593–9. doi: 10.1016/S1388-2457(01)00471-0
23. Davey NJ, Smith HC, Savic G, Maskill DW, Ellaway PH, Frankel HL. Comparison of input-output patterns in the corticospinal system of normal subjects and incomplete spinal cord injured patients. *Exp Brain Res*. (1999) 127:382–90. doi: 10.1007/s002210050806
24. Rossini PM, Burke D, Chen R, Cohen LG, Daskalakis Z, Di Iorio R, et al. Non-invasive electrical and magnetic stimulation of the brain, spinal cord, roots and peripheral nerves: basic principles and procedures for routine clinical and research application: an updated report from an I.F.C.N. Committee. *Clin Neurophysiol*. (2015) 126:1071–107. doi: 10.1016/j.clinph.2015.02.001
25. Cueva AS, Galhardoni R, Cury RG, Parravano DC, Correa G, Araujo H, et al. Normative data of cortical excitability measurements obtained by transcranial magnetic stimulation in healthy subjects. *Neurophysiol Clin*. (2016) 46:43–51. doi: 10.1016/j.neucli.2015.12.003
26. Picht T, Strack V, Schulz J, Zdunczyk A, Frey D, Schmidt S, et al. Assessing the functional status of the motor system in brain tumor patients using transcranial magnetic stimulation. *Acta Neurochir (Wien)*. (2012) 154:2075–81. doi: 10.1007/s00701-012-1494-y
27. Di Lazzaro V, Restuccia D, Oliviero A, Profice P, Ferrara L, Insola A, et al. Magnetic transcranial stimulation at intensities below active motor threshold activates intracortical inhibitory circuits. *Exp Brain Res*. (1998) 119:265–8. doi: 10.1007/s002210050341

28. Nakamura H, Kitagawa H, Kawaguchi Y, Tsuji H. Intracortical facilitation and inhibition after transcranial magnetic stimulation in conscious humans. *J Physiol*. (1997) 498:817–23. doi: 10.1113/jphysiol.1997.sp021905
29. Keller A. Intrinsic synaptic organization of the motor cortex. *Cereb Cortex*. (1993) 3:430–41. doi: 10.1093/cercor/3.5.430
30. Cash RFH, Noda Y, Zomorrodi R, Radhu N, Farzan F, Rajji TK, et al. Characterization of glutamatergic and GABA A-mediated neurotransmission in motor and dorsolateral prefrontal cortex using paired-pulse TMS-EEG. *Neuropsychopharmacology*. (2017) 42:502–11. doi: 10.1038/npp.2016.133
31. Varrasi C, Civardi C, Boccagni C, Cecchin M, Vicentini R, Monaco F, et al. Cortical excitability in drug-naive patients with partial epilepsy: a cross-sectional study. *Neurology*. (2004) 63:2051–5. doi: 10.1212/01.WNL.0000145770.95990.82
32. Simonetta-Moreau M, Lourenço G, Sangla S, Mazieres L, Vidailhet M, Meunier S. Lack of inhibitory interaction between somatosensory afferent inputs and intracortical inhibitory interneurons in focal hand dystonia. *Mov Disord*. (2006) 21:824–34. doi: 10.1002/mds.20821
33. Orth M, Münchau A. Transcranial magnetic stimulation studies of sensorimotor networks in Tourette syndrome. *Behav Neurol*. (2013) 27:57–64. doi: 10.1155/2013/349137
34. Chen R. Interactions between inhibitory and excitatory circuits in the human motor cortex. *Exp Brain Res*. (2004) 154:1–10. doi: 10.1007/s00221-003-1684-1
35. Shirota Y, Ohminami S, Tsutsumi R, Terao Y, Ugawa Y, Tsuji S, et al. Increased facilitation of the primary motor cortex in *de novo* Parkinson's disease. *Park Relat Disord*. (2019) 66:125–9. doi: 10.1016/j.parkreldis.2019.07.022
36. Säisänen L, Julkunen P, Niskanen E, Danner N, Hukkanen T, Lohioja T, et al. Motor potentials evoked by navigated transcranial magnetic stimulation in healthy subjects. *J Clin Neurophysiol*. (2008) 25:367–72. doi: 10.1097/WNP.0b013e31818e7944
37. Lefaucheur JP, Aleman A, Baeken C, Benninger DH, Brunelin J, Di Lazzaro V, et al. Evidence-based guidelines on the therapeutic use of repetitive transcranial magnetic stimulation (rTMS): an update (2014–2018). *Clin Neurophysiol*. (2020) 131:474–528. doi: 10.1016/j.clinph.2019.11.002
38. Lefaucheur JP, Aleman A, Baeken C, Benninger DH, Brunelin J, Di Lazzaro V, et al. Corrigendum: "Evidence-based guidelines on the therapeutic use of repetitive transcranial magnetic stimulation (rTMS): An update (2014–2018)" (Clinical Neurophysiology. (2020) 131(2) (474–528), (S1388245719312799), (10.1016/j.clinph.2019.11.002)). *Clin Neurophysiol*. (2020) 131:1168–9. doi: 10.1016/j.clinph.2020.02.003
39. Darmani G, Bergmann TO, Zipser C, Baur D, Müller-Dahlhaus F, Ziemann U. Effects of antiepileptic drugs on cortical excitability in humans: a TMS-EMG and TMS-EEG study. *Hum Brain Mapp*. (2019) 40:1276–89. doi: 10.1002/hbm.24448
40. Ziemann U. TMS and drugs. *Clin Neurophysiol*. (2004) 115:1717–29. doi: 10.1016/j.clinph.2004.03.006
41. Ziemann U, Reis J, Schwenkreis P, Rosanova M, Strafella A, Badawy R, et al. TMS and drugs revisited 2014. *Clin Neurophysiol*. (2015) 126:1847–68. doi: 10.1016/j.clinph.2014.08.028
42. Ziemann U, Lonnecker S, Steinhoff BJ, Paulus W. Effects of antiepileptic drugs on motor cortex excitability in humans. *Ann Neurol*. (1996) 40:367–78. doi: 10.1002/ana.410400306

Conflict of Interest: The authors declare that the research was conducted in the absence of any commercial or financial relationships that could be construed as a potential conflict of interest.

frontiers in Oncology

ORIGINAL RESEARCH
published: 27 January 2021
doi: 10.3389/fonc.2020.622358

Detecting Corticospinal Tract Impairment in Tumor Patients With Fiber Density and Tensor-Based Metrics

Lucius S. Fekonja[1,2], Ziqian Wang[1], Dogu B. Aydogan[3], Timo Roine[3], Melina Engelhardt[1,4], Felix R. Dreyer[2,5], Peter Vajkoczy[1] and Thomas Picht[1,2,4]*

[1] Department of Neurosurgery, Charité-Universitätsmedizin Berlin, Berlin, Germany, [2] Cluster of Excellence: "Matters of Activity. Image Space Material", Humboldt-Universität zu Berlin, Berlin, Germany, [3] Department of Neuroscience and Biomedical Engineering, Aalto University School of Science, Espoo, Finland, [4] Einstein Center for Neurosciences Berlin, Charité-Universitätsmedizin Berlin, Berlin, Germany, [5] Brain Language Laboratory, Department of Philosophy and Humanities, Freie Universität Berlin, Berlin, Germany

OPEN ACCESS

Edited by:
David D. Eisenstat, Royal Children's Hospital, Australia

Reviewed by:
Jyrki Mäkelä, Hospital District of Helsinki and Uusimaa, Finland
Alireza Mansouri, Pennsylvania State University (PSU), United States

***Correspondence:**
Lucius S. Fekonja
lucius.fekonja@charite.de
orcid.org/0000-0003-1973-4410

Specialty section:
This article was submitted to Neuro-Oncology and Neurosurgical Oncology, a section of the journal Frontiers in Oncology

Received: *28 October 2020*
Accepted: *14 December 2020*
Published: *27 January 2021*

Citation:
Fekonja LS, Wang Z, Aydogan DB, Roine T, Engelhardt M, Dreyer FR, Vajkoczy P and Picht T (2021) Detecting Corticospinal Tract Impairment in Tumor Patients With Fiber Density and Tensor-Based Metrics. Front. Oncol. 10:622358. doi: 10.3389/fonc.2020.622358

Tumors infiltrating the motor system lead to significant disability, often caused by corticospinal tract injury. The delineation of the healthy-pathological white matter (WM) interface area, for which diffusion magnetic resonance imaging (dMRI) has shown promising potential, may improve treatment outcome. However, up to 90% of white matter (WM) voxels include multiple fiber populations, which cannot be correctly described with traditional metrics such as fractional anisotropy (FA) or apparent diffusion coefficient (ADC). Here, we used a novel fixel-based along-tract analysis consisting of constrained spherical deconvolution (CSD)-based probabilistic tractography and fixel-based apparent fiber density (FD), capable of identifying fiber orientation specific microstructural metrics. We addressed this novel methodology's capability to detect corticospinal tract impairment. We measured and compared tractogram-related FD and traditional microstructural metrics bihemispherically in 65 patients with WHO grade III and IV gliomas infiltrating the motor system. The cortical tractogram seeds were based on motor maps derived by transcranial magnetic stimulation. We extracted 100 equally distributed cross-sections along each streamline of corticospinal tract (CST) for along-tract statistical analysis. Cross-sections were then analyzed to detect differences between healthy and pathological hemispheres. All metrics showed significant differences between healthy and pathologic hemispheres over the entire tract and between peritumoral segments. Peritumoral values were lower for FA and FD, but higher for ADC within the entire cohort. FD was more specific to tumor-induced changes in CST than ADC or FA, whereas ADC and FA showed higher sensitivity. The bihemispheric along-tract analysis provides an approach to detect subject-specific structural changes in healthy and pathological WM. In the current clinical dataset, the more complex FD metrics did not outperform FA and ADC in terms of describing corticospinal tract impairment.

Keywords: tractography, corticospinal tract, diffusion magnetic resonance imaging, motor function, apparent diffusion coefficient, tumor, transcranial magnetic stimulation

INTRODUCTION

In previous studies we introduced the combination of navigated transcranial magnetic stimulation (TMS) cortical motor mapping and tractography to improve surgery of motor eloquent brain tumors (1–4). In a recent study we could also demonstrate that the segmental analysis of diffusion tensor imaging (DTI) derived metrics, such as fractional anisotropy (FA) and apparent diffusion coefficient (ADC), correlated with clinical outcomes (5). Here, we now set out to investigate whether more complex metrics derived from constrained spherical deconvolution (CSD) and probabilistic tractography, which allow for more detailed analysis of the white matter, would prove superior in terms of detecting tumor induced white matter (WM) changes (6). In this context we analyzed the structural impact of gliomas affecting the corticospinal tract (CST) in 65 patients. This was carried out without the generation of a group template because of the lateralized pathology, which allows a clear deduction of interhemispheric differences on the subject-level (7). We compared the pathological with the healthy hemisphere and focused on describing tumor-induced changes along the CST with dMRI. We used CSD-based probabilistic tractography at an individual scale within the MRtrix3 framework (8).

DTI enables quantification of the molecular diffusion rate, ADC, or the directional preference of diffusion, FA (9). ADC and FA are established metrics integrated as predictive features in neurosurgical studies (5). The two main diffusion tensor-derived parameters, ADC and FA, are based on voxel-wise eigenvalues, which represent the magnitude of the diffusion process in the principal diffusion orientation and two directions perpendicular to it. These values are influenced by different factors (10). ADC is a measure of the overall diffusivity in a single voxel, regardless of its orientation. It is higher where water diffuses more easily, *e.g.* in ventricles, lower in structures with high tissue density and consequently more diffusion barriers, such as GM (11). FA describes the directional coherence of water diffusion in tissue and is modulated by numerous biological factors, such as the microstructural and architectural organization of white matter, myelination and non-white matter partial volume effects. Further influences on FA modulation are methodological factors, such as the choice of the estimation, preprocessing methods, and subjective selection of regions of interests (ROIs) (12, 13).

In contrast to DTI, CSD can distinguish complex fiber populations in the brain. In brief, CSD estimates fiber orientation distributions (FODs) within each voxel, based on the expected signal from a single collinearly oriented fiber population (14). By leveraging the rich information in FODs, probabilistic tractography algorithms, such as the iFOD2, have been proposed to address limitations of tensor-based tractography methods (15). In up to 90% of all WM voxels, multiple fiber orientations were observed, and 30 to 40% of these WM voxels contain more than three fiber populations (16–19). Moreover, non-white matter contamination is present in more than a third of the WM voxels (12) and has been addressed by multi-tissue CSD methods (20–22).

A complete picture about the underlying white matter architecture is highly relevant with regard to adequate risk estimation and neurosurgical planning (23). To that end, in addition to the conventional DTI measures, modern CSD-based fiber density (FD) and fixel-based analysis (FBA) methods offer promising opportunities since they are related to the intra-axonal restricted compartment that is specific to a certain fiber orientation within a voxel (24). Based on its advantages for the analysis of crossing fiber regions, we expect this metric to improve the detection of tumor-induced changes along the CST and obtain more specific information about the microstructural effects of tumors in combination with traditional FA or ADC measures. Furthermore, we expect higher specificity of FD in detecting the peritumoral segments, most importantly at the tumor–white matter interface, which is surgically the most important area. However, the translation of advanced neuroimaging to clinical settings is slow both in terms of adapting modern methods and imaging protocols. While there exist tools to use the modern CSD and probabilistic tractography with conventional images, for tumor patients, little is known about how applicable they prove with existing conventional neuroimaging protocols. Nevertheless, clinical feasibility, robustness, and methodological superiority have been proven (25, 26). Until now, fixel-based studies have concentrated on group analyses without subject-specific examination of tumor patients for neurosurgical planning (24). We developed a new variant of FD for the fiber orientation specific along-tract investigation of microstructural properties in relation to infiltrating tumors.

Importantly, we used state-of-the-art TMS methods for motor mapping to find functionally critical regions of interest (ROIs) and used these as seed points to generate streamlines. This approach is shown to be highly effective for surgical planning (4); therefore it is superior to studying the whole CST, which lacks information about patient and tumor specific functional consequences of neurosurgery.

MATERIAL AND METHODS

Ethical Standard

The study proposal is in accordance with ethical standards of the Declaration of Helsinki and was approved by the Ethics Commission of the Charité University Hospital (#EA1/016/19). All patients provided written informed consent for medical evaluations and treatments within the scope of the study.

Patient Selection

We included n = 65 left- and right-handed adult patients in this study (25 females, 40 males, average age 55.6, SD = 15.2, age range 24–81). Only patients with an initial diagnosis of unilateral WHO grade III and IV gliomas (14 WHO grade III, 51 WHO

Abbreviations: ADC, apparent diffusion coefficient; CSD, constrained spherical deconvolution; CST, corticospinal tract; dMRI, diffusion magnetic resonance imaging; DTI, diffusion tensor imaging; FA, fractional anisotropy; FD, fiber density; FDI, first dorsal interosseous; FOD, fiber orientation distribution; GM, gray matter; MEP, motor evoked potentials; nTMS, navigated transcranial magnetic stimulation; WM, white matter.

grade IV) were included (**Table 1**). All tumors were infiltrating M1 and the CST or implied critical adjacency, either in the left or right hemisphere. Patients with recurrent tumors, previous radiochemotherapy, multicentric or non-glial tumors were not considered.

Image Acquisition

MRI data were acquired on a Siemens Skyra 3T scanner (Erlangen, Germany) equipped with a 32-channel receiver head coil at Charité University Hospital, Berlin, Department of Neuroradiology. These data consisted of a high-resolution T1-weighted structural (TR/TE/TI 2300/2.32/900 ms, 9° flip angle, 256 × 256 matrix, 1 mm isotropic voxels, 192 slices, acquisition time: 5 min) and a single shell dMRI acquisition (TR/TE 7500/95 ms, 2 × 2 × 2 mm^3 voxels, 128 × 128 matrix, 60 slices, 3 b 0 volumes), acquired at b = 1,000 s/mm^2 with 40 gradient orientations, for a total acquisition time of 12 min.

Preprocessing and Processing of MRI Data

All T1 images were registered to the dMRI data sets using Advanced Normalization Tools (ANTs) with the Symmetric Normalization (SyN) transformation model (27, 28). The preprocessing of dMRI data included the following and was performed within MRtrix3 (8) in order: denoising (29), removal of Gibbs ringing artefacts (30), correction of subject motion (31), eddy-currents (32) and susceptibility-induced distortions (33) in FMRIB Software Library (34), and subsequent bias field correction with ANTs N4 (35). Each dMRI data set and processing step was visually inspected for outliers and artifacts. Scans with excessive motion were initially excluded (over 10% outlier slices). We upsampled the dMRI data to a 1.3 mm isotropic voxel size before computing FODs to increase anatomical contrast and improve downstream tractography results and statistics. To obtain ADC and FA scalar maps, we first used diffusion tensor estimation using iteratively reweighted linear least squares estimator, resulting in scalar maps of tensor-derived parameters (13, 36). For voxel-wise modeling we used a robust and fully automated and unsupervised method. This method allowed to obtain three-tissue response functions representing single-fiber combined white and gray matter and cerebrospinal fluid from our data with subsequent use of multi-tissue CSD to obtain tissue specific orientation distribution functions and white matter FODs (20, 22, 37).

TABLE 1 | Patient demographics.

	Number (%)
Demographics	
Sample size	65
Age	55.6 ± 15.2
Female	25(38)
Male	40(62)
Glioma Degree	
Glioma III	14 (22)
Glioma IV	51 (78)
Tumor Location	
Frontal	33 (51)
Temporal	7 (11)
Insular	9 (14)
Parietal	16 (25)

Transcranial Magnetic Stimulation

Non-invasive functional motor mapping of both pathologic and healthy hemispheres was performed in each patient using navigated transcranial magnetic stimulation (nTMS) with Nexstim eXimia Navigated Brain Stimulation. Briefly, each patient's head was registered to the structural MRI through the use of anatomical landmarks and surface registration. The composite muscle action potentials were captured by the integrated electromyography unit (EMG) (sampling rate 3 kHz, resolution 0.3 mV; Neuroline 720, Ambu). The muscle activity (motor evoked potential, MEP amplitude ≥50 μV) was recorded by surface electrodes on the abductor pollicis brevis and first dorsal interosseous. Initially, the first dorsal interosseous hotspot, defined as the stimulation area that evoked the strongest MEP, was determined. Subsequently, the resting motor threshold, defined as the lowest stimulation intensity that repeatedly elicits MEPs, was defined using a threshold-hunting algorithm within the Nexstim eximia software. Mapping was performed at 105% resting motor threshold and 0.25 Hz. All MEP amplitudes >50 μV (peak to peak) were considered as motor positive responses and exported in the definitive mapping (38). The subject-specific positive responses of the first dorsal interosseous were exported as binary 3 × 3 × 3 mm^3 voxel masks per response in the T1 image space.

Tractography

Probabilistic tractography was performed in each hemisphere with the iFOD2 algorithm by using the above mentioned nTMS derived cortical seeding ROI. A second inclusion ROI was defined in the medulla oblongata. Tracking parameters were set to default with a FOD amplitude cutoff value of 0.1, a streamline minimum length of 5× voxel size and a maximum streamline length of 100× voxel size. For each tractogram describing the CST, we computed 5,000 streamlines per hemisphere. Each streamline of the tractograms was resampled along its length to 100 points. Peritumoral segments were defined in relation to the resampled points within the range 1–100 in all individual tractograms by visual inspection performed by one neuroscientist and one expert neurosurgeon with 4 and 20 years of experience, in that order. Subsequently, values of associated FA, ADC, and FD scalar maps were sampled along the derived 100 segments of each streamline (**Figures 1** and **2**). The code used for the tractography pipeline is archived as a shell script on Zenodo (https://zenodo.org/record/3732348) and openly accessible (39).

Computation of Along-Tract FD Values Using FBA

A fixel is considered as a specific fiber population within a voxel (7, 24). For each subject, segmentations of continuous FODs *via* the integrals of the FOD lobes were performed to produce discrete fixel maps which are developed to indicate voxel-based measures of axon diameters, weighted by their relative volumes

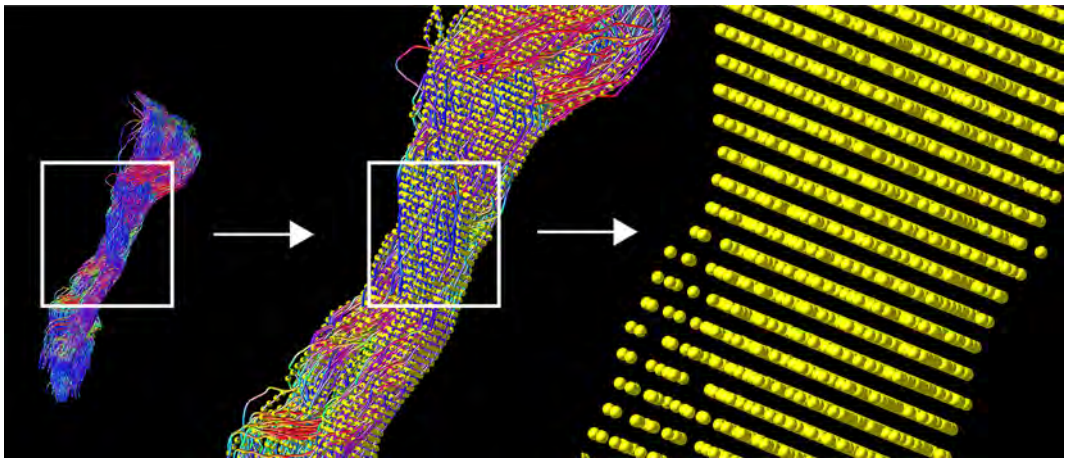

FIGURE 1 | TMS-based tractography of the CST and subsequent along-tract resampling of streamlines. The tractogram shows streamlines in relation to cortical hand representation derived by TMS-ROIs (left). The first zoom shows a combination with resampled points (yellow), overlaid on each streamline (middle). The second, larger magnification reveals the single points, derived by resampling along the streamlines (right).

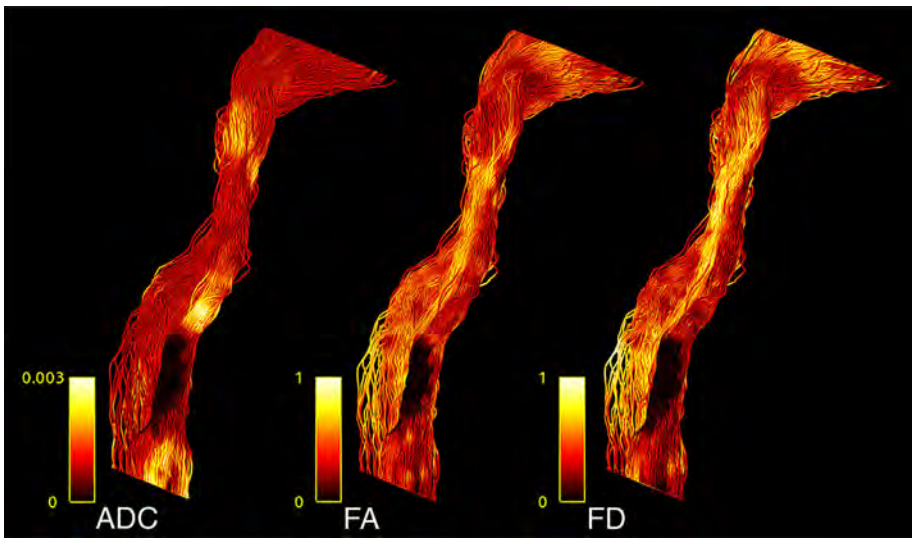

FIGURE 2 | CST tractogram with mapped ADC (left), FA (middle), and FD (right) scalar values, illustrating the methodological differences of scalar map sampling.

within voxels (24, 40). With higher-order diffusion models, such as CSD, parameters related to FD can be extracted for individual fixels (7). FBA is able to identify effects in specific fiber pathways and in crossing fiber regions, unlike voxel-based analysis (7). After obtaining the fixels for all voxels in an image, FD values along CST tractograms were computed in four steps: (i) fixels associated with CSTs were obtained using fixel tract-density imaging, (ii) fixels in the image were thresholded based on the CST fixels which eliminates the contributions of other tracts that are present in these voxels, (iii) the mean FD of the remaining fixels were exported as a scalar image, and (iv) FD values were interpolated along the 100 sampled points of each streamline present in the CST tractograms. The code used for the tract-based fixel image construction pipeline is archived as a shell script on Zenodo (https://zenodo.org/record/3732348) and openly accessible (39).

Statistical Analysis

Confirmatory statistical analysis was performed using RStudio version 1.2.5019 (https://rstudio.com) with R version 3.6.1 (https://cran.r-project.org). We compared FD with traditional tensor-derived ADC and FA to study signal changes between healthy and pathological hemispheres. To analyze the behavior of the different metrics, we used the above mentioned resampled

streamlines, comparing the median values for each of the 100 CST segments per 5,000 streamlines per hemisphere. To model the tumor-related effect on each metric, a linear mixed model (package lmerTest_3.1-0 under R version 3.6.1) was built for each metric using the metric's value as dependent variable, hemisphere (0, healthy; 1, pathological) as independent variable and a random intercept for subjects (41). Thus, each model contained 13,000 data points (65 subjects * 2 hemispheres * 100 median tract segment values per streamline). Further, we repeated this analysis for the peritumoral area according to our hypothesis to find stronger effects in these segments. Each of these models contained 4,138 data points, with each subject contributing a different number of peritumoral segments depending on tumor location and size. All effects were considered significant using a two-sided p-value of 0.05. All models were examined for patterns in the residuals (deviation from normality *via* QQ-plots, pattern fitted values *vs*. residuals). All plots were generated with the ggplot2 library within tidyverse (42, 43). Tests for sensitivity (*n* of true positive predicted segments/*n* of true positive predicted segments + *n* of false negative predicted segments) and specificity (*n* of true negative predicted segments/*n* of true negative predicted segments + *n* of false positive predicted segments) were based on classified tract segments (0 non-tumorous, 1 tumorous) in relation to the obtained significant or non-significant differences between healthy and pathological hemispheres per segment (classified as 0 and 1). These tests were performed with Bonferroni-adjusted alpha levels of 0.0005 (0.05/100) and thresholded only for large effects (≥0.474) with Cliff's delta due to the non-normal distribution. The script used to perform the statistical analysis and produce this manuscript is available on and archived in Zenodo (39).

Data Availability

Parts of the data that support the findings of this study are not publicly available due to information that could compromise the privacy of the research participants but are available from the corresponding author on reasonable request. However, code we have used is openly available under the following address (https://doi.org/10.5281/zenodo.3732348) and is cited at the corresponding passage in the article (39).

RESULTS

TMS mapping, the calculation of TMS-ROI-based streamlines and the extraction of ADC, FA and FD were feasible in each subject (cf. **Figure 3**) and showed either close tumor-tract

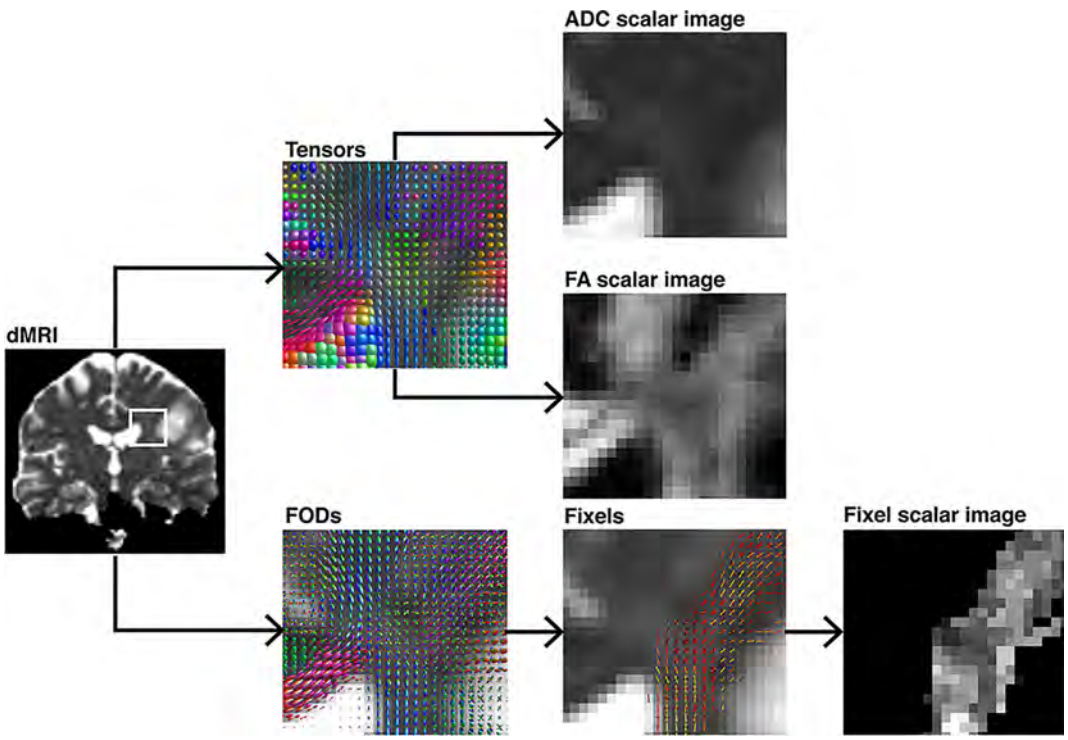

FIGURE 3 | Demonstration of different voxel-level modeling methods results and their subsequently obtained scalar maps, illustrated on a coronal section. The ROI is highlighted in a pre-processed diffusion image. Either diffusion tensor-ellipsoids as estimated by diffusion tensor imaging or FOD's estimated using CSD are shown. Further, their respective scalar maps such as ADC, FA, or fixel-based are depicted. The tensor-based scalar values do not represent any single fiber population in the voxel in comparison to the fixel-based metric.

distance (<8mm, n = 3) or adjacency or direct infiltration of the CST by the tumor (n = 62). Visual inspection of boxplots showed differences between pathological and healthy hemispheres for ADC, FA, and FD (**Figure 4A**). As expected, these differences were larger when looking at the peritumoral area only (**Figure 4B**). Further, a larger variability in ADC values could be observed in the pathological hemisphere in general and the peritumoral area specifically. When plotting values along the entire CST, distinct patterns of variation between hemispheres could be observed. ADC showed no significant differences in the non-peritumoral segments but showed significant differences in peritumoral segments, even stronger than FA and FD. In contrast, FA and FD values showed differences both in the non-peritumoral and peritumoral segments (**Figures 5**, **6**, **Table 2**). The distribution of tumors along the CST is indicated in **Figure 6**. Additionally, the tumor-induced variability in peritumoral ADC values in contrast to the entire CST becomes particularly evident here (**Figure 5**). Finally, the information shown in **Figure 2** highlights and visualizes the advantages of FOD representation in regard to multiple fiber populations. The CSD method identifies multiple appropriately oriented fiber populations in a voxel including multiple fiber populations, while the DTI-based method does not represent multiple fiber populations within each voxel and does not provide an orientation estimate corresponding to any of the existing fiber populations (25), cf. **Figure 3**.

Group Wise Analysis

The results from the mixed model analysis confirmed our hypotheses. We expected FD to improve the detection of tumor-induced changes along the tract, in combination with traditional FA or ADC measures. Furthermore, we expected stronger effects in the peritumoral segments. Our results show significant differences between healthy and pathological hemispheres for ADC, FA, and FD in the peritumoral areas (**Table 2**). As expected, these effects can be confirmed in the peritumoral segments in all tested values (**Table 3**). **Figures 4** and **5** illustrate significantly lower values in the pathological hemisphere within the entire cohort and even greater differences within the peritumoral segments for FD. Calculations for sensitivity and specificity yielded 63, 74, and 42% sensitivity and 68, 53, and 76% specificity for ADC, FA, and FD in that order, reflecting a higher sensitivity for ADC and FA to tumor induced microstructural differences, whereas FD showed higher specificity to local WM architecture complexities or orientation dispersion.

In addition to these analyses, we calculated the mean of the entire cohort of ADC, FA, and FD differences between the

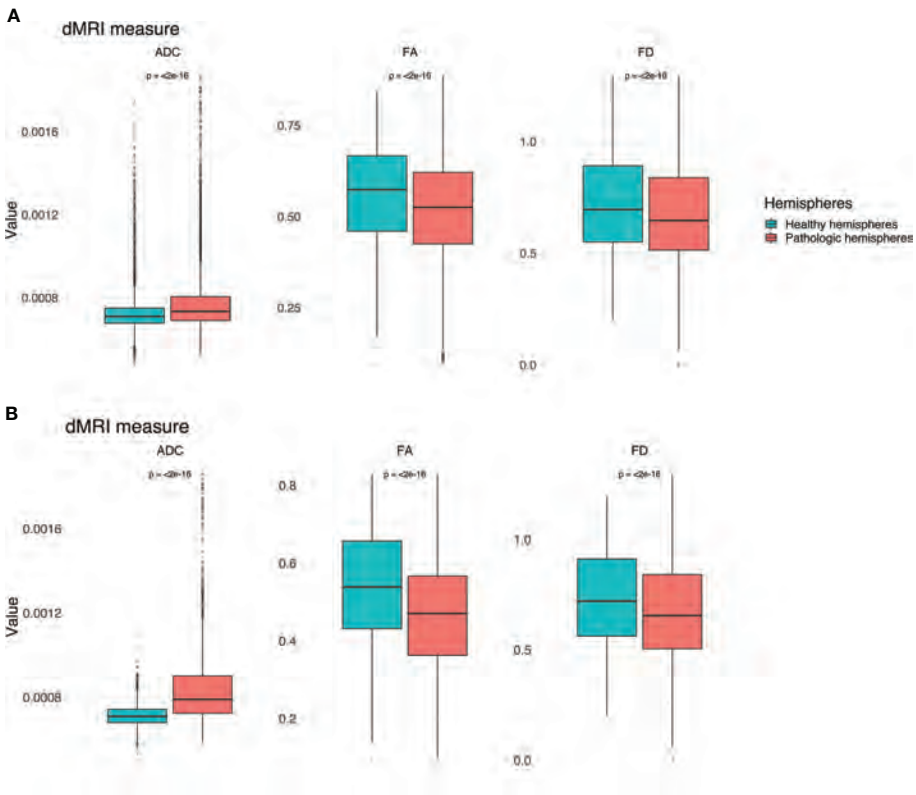

FIGURE 4 | Boxplots for ADC, FA and FD for both hemispheres. **(A)** Values for the entire CST. **(B)** Values for the peritumoral segments only. Outliers are marked by small circles.

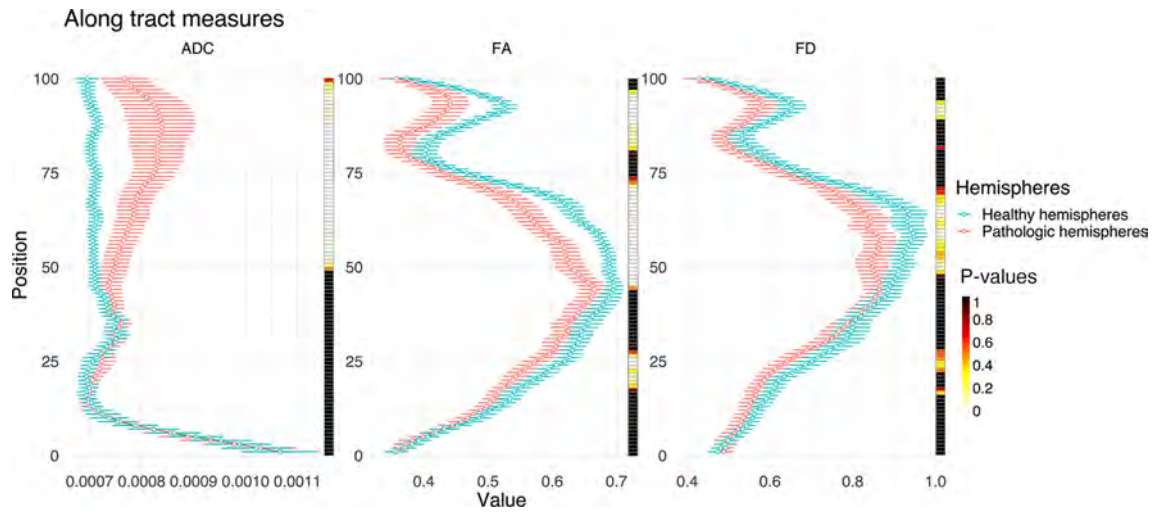

FIGURE 5 | Line plots illustrating ADC, FA, and FD along the entire CST of both hemispheres (0, medulla oblongata; 100, cortex). The points indicate median values with their respective 95% confidence intervals. The heat-maps demonstrate related Bonferroni-corrected p-values, derived by paired t-tests.

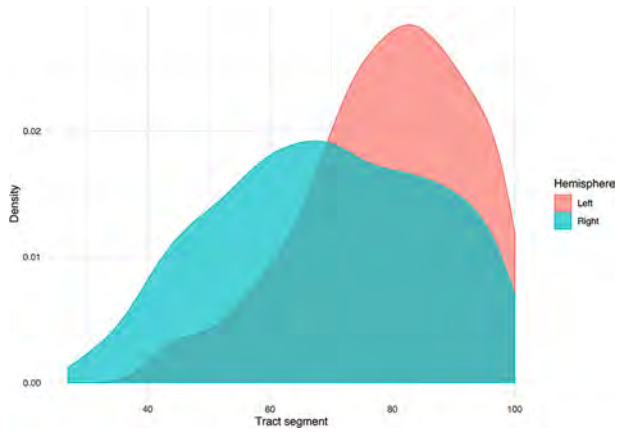

FIGURE 6 | Density plot displaying the distribution of tumors grouped by hemispheric occurrence. Additionally, the plot shows that no tumors occur below segment 25.

healthy and pathological hemispheres with respect to healthy segments only, pathological segments only, and healthy-pathological WM interface (range of three voxels) for tumor external as well as internal segments (**Figure 7**). The results indicate that ADC is strongly altered within the pathological WM area, while FA and FD show alterations along the entire CST. Furthermore, FD shows stronger differences in the healthy–pathological WM interface.

Subject-Specific Analysis

The differences are illustrated by means of two example cases (**Figure 8** and **Table 3**). Four further case-specific examples are given in the supplementary materials (**Supplementary Figures 1–4** & **Supplementary Tables 1–4**). The exemplary cases were randomly selected by a script. Case A: This patient in his 80's was brought to our emergency room with suspected stroke. A sudden weakness in the legs had occurred, causing the patient to collapse without losing consciousness. Furthermore, it was reported that the patient had been suffering from dizziness for several weeks. Conventional MRI confirmed a left parietal mass with extensive perifocal edema. The patient was diagnosed with a left postcentral WHO grade IV glioblastoma and right leg emphasized hemiparesis. The indication for resection of the mass was given.

Case B: This patient in his 60's presented with a several weeks' history of dysesthesia in his left arm and right hand with associated arm weakness. He also felt insecure when walking and suffered from a general weakness. Conventional MRI confirmed the presence of a right frontal mass. Following this, the patient was referred to our clinic. The patient was diagnosed with a complex focal seizure with right precentral WHO grade IV glioblastoma and Todd's paresis which included transient left hemiparesis. The indication for resection of the mass was given.

Our results show significant differences between healthy and pathological hemispheres in FD over the entire CST ($p < .01$ and $p < .01$) for both cases (**Table 3**). Case A shows significant differences in FA over the entire CST and in the peritumoral segments ($p < .01$ and $p < .01$). In addition, a significant difference ($p < .05$) can be seen in the peritumoral area as well with respect to ADC. However, case B shows no significant differences for ADC and FA, neither between the entire healthy and pathological hemispheres nor in the peritumoral segments.

The values of the two hemispheres overlap here in the non-peritumoral area, similar to the group-wise results described above. Case A shows less overlap for FA and FD, also in the non-peritumoral segments, while ADC shows large overlap.

TABLE 2 | Results of linear mixed model analysis.

	Dependent variable:					
	FA	**ADC**	**FD**	**FA Peritumoral**	**ADC Peritumoral**	**FD Peritumoral**
Pathologic hemispheres	–0.042	0.0001	–0.046	–0.075	0.0001	–0.067
	(–0.047, –0.038)	(0.00005, 0.0001)	(–0.052, –0.039)	(–0.082, –0.069)	(0.0001, 0.0001)	(–0.076, –0.057)
	p < 2e-16	p < 2e-16	p < 2e-16	p < 2e-16	p < 2e-16	p < 2e-16
Constant	0.560	0.001	0.718	0.540	0.001	0.729
	(0.552, 0.567)	(0.001, 0.001)	(0.704, 0.732)	(0.515, 0.564)	(0.001, 0.001)	(0.689, 0.769)
	p < 2e-16	p < 2e-16	p < 2e-16	p < 2e-16	p < 2e-16	p < 2e-16
Observations	13,000	13,000	13,000	4,138	4,138	4,138
Log Likelihood	7,926.707	97,226.680	2,486.618	3,201.497	31,060.070	1,495.331
Akaike Inf. Crit.	–15,845.410	–194,445.400	–4,965.236	–6,394.995	–62,112.150	–2,982.661
Bayesian Inf. Crit.	–15,815.520	–194,415.500	–4,935.345	–6,369.683	–62,086.840	–2,957.349

Models 1–3 show results for the entire CST for FA, ADC, and FD, models 4–6 for the peritumoral segments respectively. The table shows regression coefficients for the fixed effect of hemisphere and the intercept with their respective standard error in brackets. Further, number of observations for each model, the log likelihood ratio, Akaike information criterion, and Bayesian information criterion are stated.

TABLE 3 A, B | Subject A and B results of linear mixed model analysis.

	Dependent variable:					
	FA	**ADC**	**FD**	**FA Peritumoral**	**ADC Peritumoral**	**FD Peritumoral**
Pathologic hemispheres	0.021	0.00000	0.077	0.055	0.00004	-0.058
	(0.008, 0.034)	(-0.00002, 0.00002)	(0.038, 0.117)	(0.031, 0.080)	(0.00002, 0.0001)	(–0.138, 0.023)
	p = 0.012	p = 1	p = 0.0012	p = 0.00006	p = 0.00012	p = 0.972
Constant	0.517	0.001	0.645	0.371	0.001	0.705
	(0.488, 0.546)	(0.001, 0.001)	(0.611, 0.678)	(0.331, 0.411)	(0.001, 0.001)	(0.640, 0.771)
	p < 1.2e-15	p < 1.2e-15	p < 1.2e-15	p < 1.2e-15	p < 1.2e-15	p < 1.2e-15
Observations	200	200	200	40	40	40
Log Likelihood	172.557	1,488.435	69.184	44.545	339.211	15.904
Akaike Inf. Crit.	–337.115	–2,968.871	–130.368	–81.090	–670.423	–23.807
Bayesian Inf. Crit.	–323.921	–2,955.678	–117.175	–74.334	–663.667	–17.052
	Dependent variable:					
	FA	**ADC**	**FD**	**FA Peritumoral**	**ADC Peritumoral**	**FD Peritumoral**
Pathologic hemispheres	–0.006	0.00001	–0.033	0.013	0.00000	–0.012
	(–0.022, 0.011)	(–0.00000, 0.00003)	(–0.057, –0.010)	(–0.020, 0.045)	(–0.00002, 0.00003)	(–0.037, 0.012)
	p = 1	p = 0.606	p = 0.036	p = 1	p = 1	p = 1
Constant	0.562	0.001	0.705	0.459	0.001	0.543
	(0.539, 0.585)	(0.001, 0.001)	(0.665, 0.744)	(0.432, 0.486)	(0.001, 0.001)	(0.510, 0.577)
	p < 1.2e-15	p < 1.2e-15	p < 1.2e-15	p < 1.2e-15	p < 1.2e-15	p < 1.2e-15
Observations	200	200	200	90	90	90
Log Likelihood	176.595	1,624.744	87.184	83.431	723.449	78.396
Akaike Inf. Crit.	–345.190	–3,241.488	–166.367	–158.862	–1,438.898	–148.793
Bayesian Inf. Crit.	–331.997	–3,228.295	–153.174	–148.863	–1,428.898	–138.793

Models 1–3 show results for the entire CST for FA, ADC, and FD, models 4–6 for the peritumoral segments respectively. The table shows regression coefficients for the fixed effect of hemisphere and the intercept with their respective standard error in brackets. Further, number of observations for each model, the log likelihood ratio, Akaike information criterion, and Bayesian information criterion are stated.

DISCUSSION

Morbidity due to brain tumor growth and their surgical treatment is often caused by impairment of relevant WM. Neuroimaging-based characterization of the healthy–pathological WM interface area is therefore crucial for neurosurgical planning. DTI based tractography has seen a widespread adoption in clinical neuroscience and practice in the recent years. Especially the combination of TMS and DTI for motor function-informed tractography has shown promising

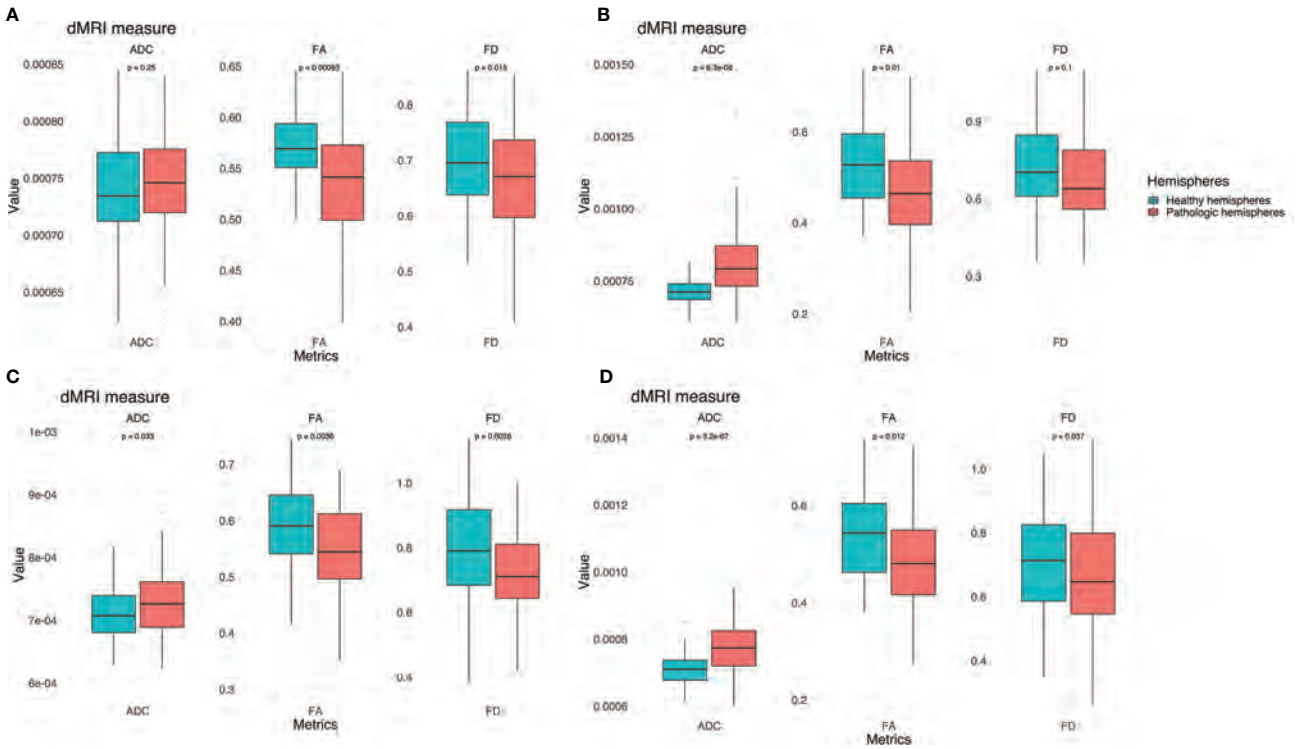

FIGURE 7 | Box plots of cohort mean of ADC, FA, and FD differences between the healthy and pathological hemispheres with respect to healthy segments only **(A)**, pathological segments only **(B)** and tumor–healthy WM interface for tumor external **(C)** as well as internal segments **(D)**.

results. Yet, the interpretation of differences as measured by tensor-based scalar values is particularly challenging in regions with crossing fibers, since tensors reflect only the main diffusion direction (16, 44). Because the tensor representation is not able to distinguish crossing fiber populations present in the majority of the WM voxels, FA offers limited opportunities to quantitatively study WM integrity (11, 16). Nevertheless, diffusion anisotropy can provide unique information about axonal anomalies (45) as it decreases as a consequence of loss of coherence in the preferred main diffusion direction (9). In this context, studies also show that ADC is generally higher in damaged tissue due to increased free diffusion. This suggests that we can compare values of above-mentioned metrics with a population average in order to determine whether they are unusually high or low, *e.g.* by comparing the subject-specific values of WM pathways of the healthy hemisphere with those of the pathological hemisphere or compare group-wise pathological populations with healthy ones (45).

It has already been confirmed that many voxels along the CST contain considerable contributions of multiple fiber populations (25, 26). Nevertheless, our results indicate more significant segment-wise differences between the healthy and pathological hemispheres for FA and ADC in comparison to FD. This result was found in the group and individual tests. While results could marginally differ with the use of other seeding strategies (*e.g.* anatomical landmarks for ROI selection), we believe when comparing different hemispheres, it is more reliable to determine seed regions based on their function using TMS. The investigation of other pathways may result in another order for the sensitivity and specificity of the metrics due to, for instance, different contributions of multiple fiber populations or extra axonal signal. Therefore, future investigations could study whether FD is more beneficial for the analysis of fiber tracts, which pass through even more complicated WM regions with highly variable fiber compositions.

FD Metrics in Clinical Settings

To better account for the complex microstructural organization of WM and its quantitative analysis, FD, which uses higher-order dMRI models such as FODs to analyze differences along WM pathways, allows to consider multiple fiber populations within a voxel. Multiple studies for group-wise statistical analysis of dMRI measures were published earlier (7, 24, 44). In contrast to these group-wise study designs, we used FD for an individual assessment of a specific tract for clinical validation. However, the presented higher sensitivity of ADC and FA indicates that these metrics are more appropriate and robust for peritumoral analysis. However, this may be due to the fact that FD has underperformed due to insufficient raw data. This finding highlights the need for better dMRI quality in clinical routine to be able to integrate advanced neuroimaging methods into clinical workflows. The discrepancy between clinical scan quality

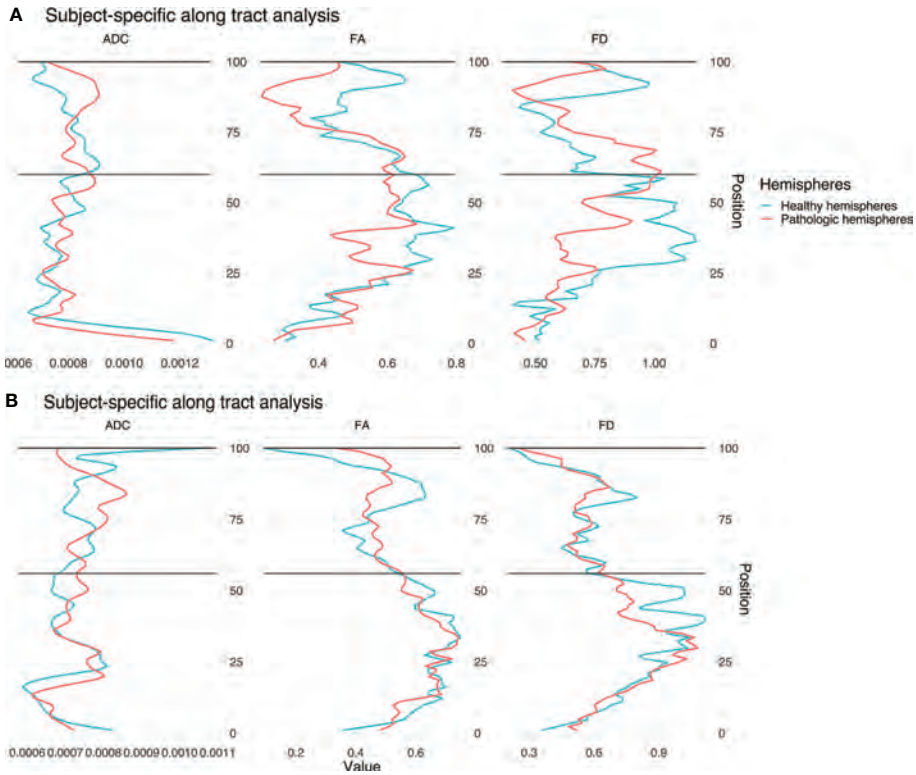

FIGURE 8 | Single subject line plots depicting ADC, FA, and FD along the CST of both hemispheres for case A **(A)** and B **(B)**. The black lines indicate the peritumoral segments.

and advanced neuroimaging highlights the need to optimize raw data acquisition in order to leverage advanced neuroimaging modalities and methods into the clinical workflow (22, 25).

Our results demonstrate the feasibility of FD along-tract analysis as a tool to describe subject-and tract-specific tumor-induced changes. Moreover, our results demonstrate the addition of further information to that obtained only *via* ADC or FA. Earlier fixel studies, designed for group wise analysis of pathology-related effects, demonstrated that fixel-analyses are sensitive to WM changes in a variety of pathologies (7, 24). In this study, we focused on subject-specific analyses, which showed higher sensitivity for ADC and FA, but higher specificity for FD. These findings are in line with other studies (23, 46). The higher specificity of FD in relation to correctly predict healthy segments is particularly relevant for presurgical analysis and intraoperative navigation in relation to risk assessment, but also for retrospective evaluation or outcome prediction models.

ADC, FA, and FD Characteristics in Brain Tumor Patients

In both cases subject-specific differences between the healthy and pathological hemispheres can be seen in the tumorous segments. Furthermore, differences between the non-pathological and pathological area can be seen as well in non-tumorous segments. This result may indicate a global effect of gliomas on the entire CST and neural connectivity, affecting diffusion and voxel-wise white matter architecture modeling, especially in regard to FD. The results are consistent with the expected behavior of the different diffusion measures: ADC was higher in the pathological hemispheres which is attributed to the damaged tissue leading to increased diffusion. This finding might reflect the tumor-related degression of WM integrity, the edema surrounding the tumor and related increase of free-water (23). FA and FD showed lower values in the pathological hemispheres compared to the corresponding segments in the healthy hemispheres. This result is consistent with the effect of the glioma-related loss of coherence in the preferred main diffusion directions (FA) and reduced fiber density (FD). This might be explained by the tumor infiltration or edema affecting the CST (23). The ADC and FD values show a higher overlap of the healthy and pathological hemispheres in the non-peritumoral area.

Limitations

Tractography suffers from a range of limitations that make its routine use problematic (47). It is well known that tractograms contain false positive (48) and false negative (49) streamlines. In addition, tractography cannot distinguish between afferent and efferent connections, and streamlines may terminate improperly (18). The dMRI data used for this study consists of a typical clinical single-shell acquisition, and is thus suboptimal for fiber

density measurement due to incomplete attenuation of apparent extra-axonal signal (44). In this study we focused on the CST. For other white matter pathways, our results might be different. Further studies could integrate a variety of fiber bundles to investigate the need for FD in along-tract statistical analysis.

CONCLUSIONS

Our results show that the direct comparison between healthy and pathological hemispheres is sensitive to glioma-induced changes in structural integrity of the CST measured by different dMRI derived metrics. In contrast to our hypothesis, according to our data and analysis, FD did not outperform FA or ADC, and all three metrics showed similar results for indicating tumor-induced changes of the CST. This finding highlights the need for better scans in clinical routine if one wants to introduce advanced neuroimaging modalities into clinical workflows.

DATA AVAILABILITY STATEMENT

The datasets presented in this study can be found in online repositories. The names of the repository/repositories and accession number(s) can be found below: https://doi.org/10.5281/zenodo.3744339.

ETHICS STATEMENT

The studies involving human participants were reviewed and approved by Ethics Commission of the Charité University Hospital. The patients/participants provided their written informed consent to participate in this study.

AUTHOR CONTRIBUTIONS

LF and TP designed the study. LF and ZW processed the data, performed all analyses, and wrote the first draft of the manuscript. BA, TR, ME, FD, PV, and TP contributed to the project management through discussions. All authors contributed to the article and approved the submitted version.

FUNDING

LF and TP acknowledge the support of the Cluster of Excellence Matters of Activity. Image Space Material funded by the Deutsche Forschungsgemeinschaft (DFG, German Research Foundation) under Germany´s Excellence Strategy–EXC 2025. TR received support from the Finnish Cultural Foundation. We acknowledge support from the German Research Foundation (DFG) and the Open Access Publication Fund of Charité–Universitätsmedizin Berlin.

ACKNOWLEDGMENTS

This work was supported by the DFG (EXC 2025). The views expressed are those of the author(s) and not necessarily those of the DFG. We thank Heike Schneider for the numerous TMS-mappings.

SUPPLEMENTARY MATERIAL

The Supplementary Material for this article can be found online at: https://www.frontiersin.org/articles/10.3389/fonc.2020.622358/full#supplementary-material

REFERENCES

1. Rosenstock T, Grittner U, Acker G, Schwarzer V, Kulchytska N, Vajkoczy P, et al. Risk stratification in motor area-related glioma surgery based on navigated transcranial magnetic stimulation data. *J Neurosurg* (2017) 126 (4):1227–37. doi: 10.3171/2016.4.JNS152896
2. Krieg SM, Picht T, Sollmann N, Bahrend I, Ringel F, Nagarajan SS, et al. Resection of Motor Eloquent Metastases Aided by Preoperative nTMS-Based Motor Maps-Comparison of Two Observational Cohorts. *Front Oncol* (2016) 6:261. doi: 10.3389/fonc.2016.00261
3. Lefaucheur JP, Picht T. The value of preoperative functional cortical mapping using navigated TMS. *Neurophysiol Clin* (2016) 46(2):125–33. doi: 10.1016/j.neucli.2016.05.001
4. Picht T, Frey D, Thieme S, Kliesch S, Vajkoczy P. Presurgical navigated TMS motor cortex mapping improves outcome in glioblastoma surgery: a controlled observational study. *J Neurooncol* (2016) 126(3):535–43. doi: 10.1007/s11060-015-1993-9
5. Rosenstock T, Giampiccolo D, Schneider H, Runge SJ, Bahrend I, Vajkoczy P, et al. Specific DTI seeding and diffusivity-analysis improve the quality and prognostic value of TMS-based deterministic DTI of the pyramidal tract. *NeuroImage Clin* (2017) 16:276–85. doi: 10.1016/j.nicl.2017.08.010
6. Dhollander T, Clemente A, Singh M, Boonstra F, Civier O, F. D. D J, et al. Fixel-based Analysis of Diffusion MRI: Methods, Applications, Challenges and Opportunities. In: *Open Science Framework*. OSF Preprints (2020). doi: 10.31219/osf.io/zu8fv
7. Raffelt DA, Smith RE, Ridgway GR, Tournier JD, Vaughan DN, Rose S, et al. Connectivity-based fixel enhancement: Whole-brain statistical analysis of diffusion MRI measures in the presence of crossing fibres. *Neuroimage* (2015) 117:40–55. doi: 10.1016/j.neuroimage.2015.05.039
8. Tournier JD, Smith R, Raffelt D, Tabbara R, Dhollander T, Pietsch M, et al. MRtrix3: A fast, flexible and open software framework for medical image processing and visualisation. *Neuroimage* (2019) 202:116137. doi: 10.1016/j.neuroimage.2019.116137
9. Soares JM, Marques P, Alves V, Sousa N. A hitchhiker's guide to diffusion tensor imaging. *Front Neurosci* (2013) 7:31. doi: 10.3389/fnins.2013.00031
10. Colby JB, Soderberg L, Lebel C, Dinov ID, Thompson PM, Sowell ER. Along-tract statistics allow for enhanced tractography analysis. *Neuroimage* (2012) 59(4):3227–42. doi: 10.1016/j.neuroimage.2011.11.004
11. Van Hecke W, Emsell L, Sunaert S. *Diffusion Tensor Imaging A Practical Handbook*. New York: Springer (2016). doi: 10.1007/978-1-4939-3118-7
12. Roine T, Jeurissen B, Perrone D, Aelterman J, Leemans A, Philips W, et al. Isotropic non-white matter partial volume effects in constrained spherical deconvolution. *Front Neuroinform* (2014) 8:28. doi: 10.3389/fninf.2014.00028
13. Veraart J, Sijbers J, Sunaert S, Leemans A, Jeurissen B. Weighted linear least squares estimation of diffusion MRI parameters: strengths, limitations, and pitfalls. *Neuroimage* (2013) 81:335–46. doi: 10.1016/j.neuroimage.2013.05.028

14. Tournier JD, Calamante F, Gadian DG, Connelly A. Direct estimation of the fiber orientation density function from diffusion-weighted MRI data using spherical deconvolution. *Neuroimage* (2004) 23(3):1176–85. doi: 10.1016/j.neuroimage.2004.07.037
15. Tournier JD, Mori S, Leemans A. Diffusion tensor imaging and beyond. *Magn Reson Med* (2011) 65(6):1532–56. doi: 10.1002/mrm.22924
16. Jeurissen B, Leemans A, Tournier JD, Jones DK, Sijbers J. Investigating the prevalence of complex fiber configurations in white matter tissue with diffusion magnetic resonance imaging. *Hum Brain Mapp* (2013) 34 (11):2747–66. doi: 10.1002/hbm.22099
17. Riffert TW, Schreiber J, Anwander A, Knösche TR. Beyond fractional anisotropy: extraction of bundle-specific structural metrics from crossing fiber models. *Neuroimage* (2014) 100:176–91. doi: 10.1016/j.neuroimage.2014.06.015
18. Tournier JD. Diffusion MRI in the brain - Theory and concepts. *Prog Nucl Magn Reson Spectrosc* (2019) 112-113:1–16. doi: 10.1016/j.pnmrs.2019.03.001
19. Vos SB, Jones DK, Jeurissen B, Viergever MA, Leemans A. The influence of complex white matter architecture on the mean diffusivity in diffusion tensor MRI of the human brain. *Neuroimage* (2012) 59(3):2208–16. doi: 10.1016/j.neuroimage.2011.09.086
20. Dhollander T, Raffelt D, Connelly A. Unsupervised 3-tissue response function estimation from single-shell or multi-shell diffusion MR data without a co-registered T1 image. In: *ISMRM Workshop on Breaking the Barriers of Diffusion MRI*. Lisbon, Portugal: Proceedings of the International Society for Magnetic Resonance in Medicine. (2016). p. 5.
21. Roine T, Jeurissen B, Perrone D, Aelterman J, Philips W, Leemans A, et al. Informed constrained spherical deconvolution (iCSD). *Med Image Anal* (2015) 24(1):269–81. doi: 10.1016/j.media.2015.01.001
22. Jeurissen B, Tournier JD, Dhollander T, Connelly A, Sijbers J. Multi-tissue constrained spherical deconvolution for improved analysis of multi-shell diffusion MRI data. *Neuroimage* (2014) 103:411–26. doi: 10.1016/j.neuroimage.2014.07.061
23. Mormina E, Longo M, Arrigo A, Alafaci C, Tomasello F, Calamuneri A, et al. MRI Tractography of Corticospinal Tract and Arcuate Fasciculus in High-Grade Gliomas Performed by Constrained Spherical Deconvolution: Qualitative and Quantitative Analysis. *AJNR Am J Neuroradiol* (2015) 36 (10):1853–8. doi: 10.3174/ajnr.A4368
24. Raffelt DA, Tournier JD, Smith RE, Vaughan DN, Jackson G, Ridgway GR, et al. Investigating white matter fibre density and morphology using fixel-based analysis. *Neuroimage* (2017) 144(Pt A):58–73. doi: 10.1016/j.neuroimage.2016.09.029
25. Farquharson S, Tournier JD, Calamante F, Fabinyi G, Schneider-Kolsky M, Jackson GD, et al. White matter fiber tractography: why we need to move beyond DTI. *J Neurosurg* (2013) 118(6):1367–77. doi: 10.3171/2013.2.JNS121294
26. Petersen MV, Lund TE, Sunde N, Frandsen J, Rosendal F, Juul N, et al. Probabilistic versus deterministic tractography for delineation of the cortico-subthalamic hyperdirect pathway in patients with Parkinson disease selected for deep brain stimulation. *J Neurosurg* (2017) 126(5):1657–68. doi: 10.3171/2016.4.JNS1624
27. Grabner G, Janke AL, Budge MM, Smith D, Pruessner J, Collins DL. Symmetric atlasing and model based segmentation: an application to the hippocampus in older adults. *Med Image Comput Comput Assist Interv* (2006) 9(Pt 2):58–66. doi: 10.1007/11866763_8
28. Avants BB, Tustison NJ, Song G, Cook PA, Klein A, Gee JC. A reproducible evaluation of ANTs similarity metric performance in brain image registration. *Neuroimage* (2011) 54(3):2033–44. doi: 10.1016/j.neuroimage.2010.09.025
29. Veraart J, Novikov DS, Christiaens D, Ades-Aron B, Sijbers J, Fieremans E. Denoising of diffusion MRI using random matrix theory. *Neuroimage* (2016) 142:394–406. doi: 10.1016/j.neuroimage.2016.08.016
30. Kellner E, Dhital B, Kiselev VG, Reisert M. Gibbs-ringing artifact removal based on local subvoxel-shifts. *Magn Reson Med* (2016) 76(5):1574–81. doi: 10.1002/mrm.26054
31. Leemans A, Jones DK. The B-matrix must be rotated when correcting for subject motion in DTI data. *Magn Reson Med* (2009) 61(6):1336–49. doi: 10.1002/mrm.21890
32. Andersson JLR, Graham MS, Drobnjak I, Zhang H, Filippini N, Bastiani M. Towards a comprehensive framework for movement and distortion correction of diffusion MR images: Within volume movement. *Neuroimage* (2017) 152:450–66. doi: 10.1016/j.neuroimage.2017.02.085
33. Andersson JL, Skare S, Ashburner J. How to correct susceptibility distortions in spin-echo echo-planar images: application to diffusion tensor imaging. *Neuroimage* (2003) 20(2):870–88. doi: 10.1016/S1053-8119(03)00336-7
34. Jenkinson M, Beckmann CF, Behrens TE, Woolrich MW, Smith SM. Fsl. *Neuroimage* (2012) 62(2):782–90. doi: 10.1016/j.neuroimage.2011.09.015
35. Tustison NJ, Avants BB, Cook PA, Zheng Y, Egan A, Yushkevich PA, et al. N4ITK: improved N3 bias correction. *IEEE Trans Med Imaging* (2010) 29 (6):1310–20. doi: 10.1109/TMI.2010.2046908
36. Basser PJ, Mattiello J, LeBihan D. MR diffusion tensor spectroscopy and imaging. *Biophys J* (1994) 66(1):259–67. doi: 10.1016/S0006-3495(94)80775-1
37. Tournier JD, Calamante F, Connelly A. Robust determination of the fibre orientation distribution in diffusion MRI: non-negativity constrained super-resolved spherical deconvolution. *Neuroimage* (2007) 35(4):1459–72. doi: 10.1016/j.neuroimage.2007.02.016
38. Picht T, Schmidt S, Brandt S, Frey D, Hannula H, Neuvonen T, et al. Preoperative functional mapping for rolandic brain tumor surgery: comparison of navigated transcranial magnetic stimulation to direct cortical stimulation. *Neurosurgery* (2011) 69(3):581–8; discussion 588. doi: 10.1227/NEU.0b013e3182181b89
39. Fekonja LS, Wang Z, Aydogan DB, Roine T, Engelhardt M, Dreyer FR, et al. Code used in article "CSD-based metric for along- tract statistical analysis in primary motor tumor patients". (2020). doi: 10.5281/zenodo.3732349
40. Smith RE, Tournier JD, Calamante F, Connelly A. SIFT: Spherical-deconvolution informed filtering of tractograms. *Neuroimage* (2013) 67:298–312. doi: 10.1016/j.neuroimage.2012.11.049
41. Kuznetsova A, Brockhoff PB, Christensen RHB. lmerTest Package: Tests in Linear Mixed Effects Models. *J Stat Softw* (2017) 82(13):26. doi: 10.18637/jss.v082.i13
42. Wickham H. *ggplot2: Elegant Graphics for Data Analysis*. Springer-Verlag New York: Springer Publishing Company, Incorporated (2009).
43. Wickham H, Averick M, Bryan J, Chang W, McGowan L, François R, et al. Welcome to the Tidyverse. *J Open Source Softw* (2019) 4(43):1686. doi: 10.21105/joss.01686
44. Raffelt D, Tournier JD, Rose S, Ridgway GR, Henderson R, Crozier S, et al. Apparent Fibre Density: a novel measure for the analysis of diffusion-weighted magnetic resonance images. *Neuroimage* (2012) 59(4):3976–94. doi: 10.1016/j.neuroimage.2011.10.045
45. Mori S, Tournier JD. Chapter 7 - New Image Contrasts from Diffusion Tensor Imaging: Theory, Meaning, and Usefulness of DTI-Based Image Contrast. In: *Introduction to Diffusion Tensor Imaging (Second Edition)*. San Diego: Academic Press (2014). doi: 10.1016/B978-0-12-398398-5.00007-2
46. Chamberland M, Raven EP, Genc S, Duffy K, Descoteaux M, Parker GD, et al. Dimensionality reduction of diffusion MRI measures for improved tractometry of the human brain. *Neuroimage* (2019) 200:89–100. doi: 10.1016/j.neuroimage.2019.06.020
47. Schilling KG, Nath V, Hansen C, Parvathaneni P, Blaber J, Gao Y, et al. Limits to anatomical accuracy of diffusion tractography using modern approaches. *Neuroimage* (2019) 185:1–11. doi: 10.1016/j.neuroimage.2018.10.029
48. Maier-Hein KH, Neher PF, Houde JC, Cote MA, Garyfallidis E, Zhong J, et al. The challenge of mapping the human connectome based on diffusion tractography. *Nat Commun* (2017) 8(1):1349. doi: 10.1038/s41467-017-01285-x
49. Aydogan DB, Jacobs R, Dulawa S, Thompson SL, Francois MC, Toga AW, et al. When tractography meets tracer injections: a systematic study of trends and variation sources of diffusion-based connectivity. *Brain Struct Funct* (2018) 223(6):2841–58. doi: 10.1007/s00429-018-1663-8

Conflict of Interest: The authors declare that the research was conducted in the absence of any commercial or financial relationships that could be construed as a potential conflict of interest.

frontiers in Neurology

ORIGINAL RESEARCH
published: 05 February 2021
doi: 10.3389/fneur.2020.633224

Time-Frequency Representation of Motor Evoked Potentials in Brain Tumor Patients

*Kathrin Machetanz[1,2], Alberto L. Gallotti[3], Maria Teresa Leao Tatagiba[1], Marina Liebsch[1], Leonidas Trakolis[1], Sophie Wang[1], Marcos Tatagiba[1], Alireza Gharabaghi[2] and Georgios Naros[1,2]**

[1] Neurosurgical Clinic, Department of Neurosurgery and Neurotechnology, Eberhard Karls University of Tuebingen, Tuebingen, Germany, [2] Department of Neurosurgery and Neurotechnology, Institute for Neuromodulation and Neurotechnology, Eberhard Karls University of Tuebingen, Tuebingen, Germany, [3] Department of Neurosurgery and Stereotactic Radiosurgery, Vita-Salute University, Milan, Italy

Background: The integrity of the motor system can be examined by applying navigated transcranial magnetic stimulation (nTMS) to the cortex. The corresponding motor-evoked potentials (MEPs) in the target muscles are mirroring the status of the human motor system, far beyond corticospinal integrity. Commonly used time domain features of MEPs (e.g., peak-to-peak amplitudes and onset latencies) exert a high inter-subject and intra-subject variability. Frequency domain analysis might help to resolve or quantify disease-related MEP changes, e.g., in brain tumor patients. The aim of the present study was to describe the time-frequency representation of MEPs in brain tumor patients, its relation to clinical and imaging findings, and the differences to healthy subject.

Methods: This prospective study compared 12 healthy subjects with 12 consecutive brain tumor patients (with and without a paresis) applying nTMS mapping. Resulting MEPs were evaluated in the time series domain (i.e., amplitudes and latencies). After transformation into the frequency domain using a Morlet wavelet approach, event-related spectral perturbation (ERSP), and inter-trial coherence (ITC) were calculated and compared to diffusion tensor imaging (DTI) results.

Results: There were no significant differences in the time series characteristics between groups. MEPs were projecting to a frequency band between 30 and 300 Hz with a local maximum around 100 Hz for both healthy subjects and patients. However, there was ERSP reduction for higher frequencies (>100 Hz) in patients in contrast to healthy subjects. This deceleration was mirrored in an increase of the inter-peak MEP latencies. Patients with a paresis showed an additional disturbance in ITC in these frequencies. There was no correlation between the CST integrity (as measured by DTI) and the MEP parameters.

Conclusion: Time-frequency analysis may provide additional information above and beyond classical MEP time domain features and the status of the corticospinal system in brain tumor patients. This first evaluation indicates that brain tumors might affect cortical physiology and the responsiveness of the cortex to TMS resulting in a temporal dispersion of the corticospinal transmission.

Keywords: transcranial magnetic stimulation, motor evoked potentials, brain tumors, time-frequency analysis, frequency domain, inter-trial coherence

OPEN ACCESS

Edited by:
Giovanni Raffa,
University of Messina, Italy

Reviewed by:
Vincenzo Rizzo,
University of Messina, Italy
Antonino Scibilia,
Institut Hospitalo-universitaire de Strasbourg, France

***Correspondence:**
Georgios Naros
georgios.naros@med.uni-tuebingen.de

Specialty section:
This article was submitted to Applied Neuroimaging, a section of the journal Frontiers in Neurology

Received: *24 November 2020*
Accepted: *21 December 2020*
Published: *05 February 2021*

Citation:
Machetanz K, Gallotti AL, Leao Tatagiba MT, Liebsch M, Trakolis L, Wang S, Tatagiba M, Gharabaghi A and Naros G (2021) Time-Frequency Representation of Motor Evoked Potentials in Brain Tumor Patients. Front. Neurol. 11:633224. doi: 10.3389/fneur.2020.633224

INTRODUCTION

The human motor system consists of several cortical, subcortical, and spinal hubs. For unobstructed voluntary movements corticospinal integrity is required. Cerebral lesions (e.g., stroke, brain tumors) can affect corticospinal transmission and impair voluntary movements (1). In the past years, there is a tremendous progress in evaluating the human motor system of these patients with electrophysiological means such as transcranial magnetic stimulation (TMS). The magnetic cortical input through TMS is suggested to activate excitatory and inhibitory neurons, transmitting their information in volleys (i.e., D- and I-waves) to the spinal cord and resulting in a synchronized activation of muscle cells, which can be measured as motor-evoked potentials (MEPs) (2–4). Cortical excitability and stimulation intensity determine the size of descending volleys and, hence, the amplitude of the MEP. The conduction time of neural impulses traveling along the cortico-spinal projections to peripheral muscles is reflected in the latency of the MEP (2–4). Thus, motor-evoked potentials are mirroring the status of the complete human motor system. In line, it has been shown that MEP characteristics are influenced by the current muscular (5, 6), spinal (7), and cortical status (6, 8).

Evoked potentials (EPs) such as MEPs are short phasic events, which are commonly evaluated in the time series domain of a single trial or after averaging over several trials. Temporal dispersion of the descending volleys changes latencies, shape, and amplitudes of the EP and impedes its interpretation (3). In fact, time domain features of MEPs are sensitive to noise and exert a high inter-subject and intra-subject variability (9–12). While an increase of the MEP latency and a decrease of the MEP amplitude are indicative of a lesion to the corticospinal network (13–15), little attention is paid to the exact shape of the MEP. However, electromagnetic signals can also be described in the frequency domain. While time-domain studies evaluate the signal fluctuation over time, frequency-domain analyses transform the signal into a sum of oscillations (i.e., sine waves) and describe the contribution of different frequencies to the complete signal (i.e., power). Despite losing some temporal information, the frequency domain perspective has several potential advantages enabling a description of EP shapes and allowing the application of further neuroscientific concepts (e.g., phase behavior or inter-trial coherence, ITC), which might help to resolve or quantify the temporal dispersion of EPs. While being ubiquitous in neuroscience (6, 16–18), frequency domain analysis techniques are infrequently found in the clinical setting. However, there is an increasing interest in the frequency representation of EPs in animals (19–24) and humans (25, 26).

The aim of the present study is to describe the time-frequency representation of MEPs in brain tumor patients, its relation to clinical and imaging findings, and the differences to healthy subjects. To the best of our knowledge, this is the first study evaluating MEPs of brain tumor patients in the frequency domain.

Abbreviations: ADC, apparent diffusion coefficient; Amp, amplitude; APB, abductor pollicis brevis muscle; AR, autoregression model; DTI, diffusion tensor imaging; EMG, electromyography; ERSP, event-related spectral perturbation; EP, evoked potentials; FA, fractional anisotropy; FDI, first dorsal interosseous muscle; ITC, inter-trial coherence; Lat, latency; MEP, motor-evoked potential; MRCS, medical research council scale; nTMS, navigated transcranial magnetic stimulation; RMT, resting motor threshold; ROI, region of interest.

METHODS

Patients

This prospective study covers 12 healthy subjects (30.2 ± 13.9 years, 10 female) and 12 consecutive patients (51.3 ± 20.3 years, nine female) with motor eloquent brain lesions who underwent an nTMS mapping in the Neurosurgical Department of the University of Tuebingen. Patients were classified into two categories by an experienced neurosurgeon based on their clinical motor status in the Medical Research Council Scale (MRCS): six patients had no motor signs (MRCS 0) and six patients showed an upper limb paresis (MRCS<5). Details of clinical and demographic characteristics of the patients are depicted in **Table 1**. The study was approved by the local ethics committee of the Eberhardt Karls University Tuebingen. All participants gave written informed consent.

Magnetic Resonance Imaging (MRI)

All healthy subjects and patients received preoperative MR imaging using a 1.5 T MR imaging unit (Skyra/Prisma-fit/Aera, Siemens Healthineers, Erlangen, Germany) with an 8-channel head coil. Patients received T1-weighted (contrast-enhanced) echo sequences and, additionally, diffusion tensor imaging (DTI). DTI was performed with a single-shot spin echo at a *b*-value of 1,000 s/mm² along 12–64 geometric directions. Following, the anatomical MRI data set was imported to our nTMS system (Nexstim Eximia, version 3.2.2, Helsinki, Finland) for further data acquisition and analysis.

Navigated Transcranial Magnetic Stimulation (nTMS)

The cortical mapping procedure was described previously and is applied here in the same way (27–30): We used a navigated TMS stimulator (eXimia®, Nexstim, Helsinki, Finland) and a biphasic figure-8 coil. Prior to the mapping, patients' anatomical T1-weighted magnetic resonance images were co-registered to the patient's head with a registration error of <2 mm. After determining the "hotspot" yielding the largest motor-evoked potential (MEP) from the contralateral abductor pollicis brevis muscle (APB), the resting motor threshold (RMT), defined as the minimum stimulus intensity to result in at least 5/10 trials a MEP > 50 μV, was obtained. The orientation of the induced current in the brain was posterior-anterior for the first phase and anterior-posterior for the second phase of the stimulus. The orientation of the electric field, calculated on the basis of the individual MRI of each subject by the eXimia software, was kept perpendicular to the central sulcus. Subsequently, the cortex was mapped with 110% RMT starting at the primary motor cortex and then extending around this spot to cover the primary motor cortex, somatosensory cortex, and premotor cortex (**Figures 1A,B**). Thus, an average of 209.2 ± 8.3 [96–394] stimuli were applied per patient and map. Stimulation sites were visualized on the surface

TABLE 1 | Patients' clinical, imaging, and electrophysiological characteristics.

	Group 1 healthy subjects	Group 2 no motor signs	Group 3 apparent paresis	*p*-value
	***n* = 12**	***n* = 6**	***n* = 6**	
Age	30.2 ± 13.9	39.2 ± 20.9	63.5 ± 10.6	**0.006**
Gender (f:m)	10:2	3:3	6:0	0.091
Diagnosis				
HGG	-	3	4	0.558
Metastasis	-	3	2	
Tumor size (cm^3)	-	8.7 ± 6.3	12.5 ± 14.9	0.873
DTI				
Mean FA	-	0.43 ± 0.06	0.46 ± 0.03	0.749
Mean ADC (10^{-4} mm^2/s)	-	8.86 ± 1.13	8.44 ± 3.44	0.522
nTMS				
RMT (%)	36 ± 6	37 ± 11	51 ± 8	**0.013**
No. of trials	226 ± 91	185 ± 85	199 ± 94	0.712
MEP + trials	90 ± 48	81 ± 57	155 ± 45	0.162
Amp (μV)	241 ± 185	160 ± 100	199 ± 132	0.827
Lat0 (ms)	23.6 ± 0.9	23.3 ± 2.5	22.8 ± 3.1	0.551
Lat1 (ms)	27.2 ± 0.8	27.3 ± 2.2	27.4 ± 3.5	0.614
Lat2 (ms)	31.4 ± 1.4	32.4 ± 1.7	32.8 ± 3.9	0.589
Lat3 (ms)	66.8 ± 16.2	59.9 ± 9.4	65.4 ± 12.2	0.906
Lat0-Lat1 (ms)	3.7 ± 0.5	4.0 ± 0.8	4.6 ± 1.0	0.103
Lat0-Lat2 (ms)	7.3 ± 0.7	9.1 ± 2.0	10.0 ± 2.8	**0.031**
Lat0-Lat3 (ms)	38.3 ± 13.3	36.6 ± 9.7	42.6 ± 12.5	0.608
Lat1-Lat2 (ms)	3.6 ± 0.5	5.1 ± 1.3	5.4 ± 2.7	**0.058**
Lat2-Lat3 (ms)	31.0 ± 13.3	27.6 ± 8.7	32.6 ± 12.8	0.898
ERSP1*	35.3 ± 6.6	31.3 ± 8.5	26.7 ± 10.1	0.158
ERSP2**	28.8 ± 7.4	28.5 ± 9.4	20.9 ± 9.8	0.221
ITC*	0.64 ± 0.15	0.74 ± 0.05	0.43 ± 0.07	**0.006**
ITC**	0.56 ± 0.16	0.73 ± 0.02	0.36 ± 0.10	**0.002**

**for 20–30 ms and 40–200 Hz.*

***for 30–40 ms and 40–200 Hz. Significant p-values are depicted in bold letters.*

at a depth of 25–30 mm. Coordinates of the stimulation sites were automatically saved by the eXimia software for later analysis (e.g., DTI-based tractographie, **Figure 1C**).

Electromyographic Recordings (EMG)

During nTMS mapping, myoelectric signals of the contralesional abductor pollicis brevis (APB) and the first dorsal interosseous muscles (FDI) were recorded with the integrated EMG device of the eXimia system (3 kHz sampling rate, band-pass filter of 10–500 Hz) using Ag/AgCl wet gel surface electrodes (AmbuNeuroline 720, Ambu GmbH, Germany).

EMG Data Analysis

Data analysis was performed using custom-written scripts in MATLAB (Mathworks Ltd, USA, R2017a), applying functions of the open source toolboxes EEGlab (31) and Fieldtrip (32). EMG data was imported into Matlab and segmented into epochs from −100 to 100 ms relative to the TMS pulse. No further data processing was performed except of linear detrending of the epochs. Generally, the APB muscle was selected for further analysis. The nTMS trials were classified in MEP+ and MEP- trials depending on a MEP amplitude ($\geq$20 μV) and latency ($\geq$15 and $\leq$ 30 ms) threshold (**Figures 1D,E**). Trials with artifacts or EMG pre-stimulus activation were automatically removed from further analysis. In case of a bad signal-to-noise ratio or a number of artifacts higher than the average, the FDI muscle was chosen for further analysis. A Matlab-based custom-written script was used to automatically detect several time series characteristics of the MEP: Amp (i.e., peak-to-peak amplitude), Lat0 (i.e., MEP onset latency), Lat1 (i.e., latency of the maximum positive deflection of the MEP), Lat2 (latency of the minimum negative deflection of the MEP), and Lat3 (i.e., ending of the MEP). The time-frequency analysis of the MEP was performed on the basis of a Morlet wavelet approach with a fixed wavelet length of 40 ms (as implemented by the *newtimef* function of the EEGlab toolbox) (31). The wavelet length was chosen considering the average length of a MEP (i.e., Lat3-Lat0) and represents a balance between power and the phase precision of the analysis (see *Discussion*). This approach resulted in a spectral resolution of 1 Hz (30–500 Hz) and temporal resolution of 0.333 ms (−79.333

to 79.333 ms relative to the TMS pulse). Event-related spectral perturbation (ERSP) was calculated (in dB) and trial-wise normalized to the baseline spectrum (−79.3 to −10 ms relative to the TMS pulse) to reduce sensitivity to noisy trials (33). The ITC measures event-related phase coherence across trials. It is obtained from the phase information in the spectral decomposition while normalizing the magnitude information. Hence, the ITC is an amplitude-independent measure for phase-locking. The ITC values represent the circular variance of phases (34) and range from 0 to 1, with a value of 1 being indicative of perfect phase-locking.

MR Imaging Analysis

After nTMS mapping, the coordinates of MEP+ trials were exported as DICOM from the Nexstim software and imported into the BrainLab iPlan 3.0 software. A cortical ROI was constructed from the summation of MEP+ and enlarged by 2 mm (35, 36). The ROI was fused to the anatomical T1-weigthed MRI and DTI dataset. In addition to the cortical ROIs, a subcortical ROI was placed in the caudal pons based on the color-coded FA map (35–41). The corticospinal tract (CST) was detected using a fiber length of 110 mm and a FA value corresponding to 75% of the individual FA threshold impeding any fiber detection (35, 36, 42). Mean FA and ADC values of the resulting CST was noted as an imaging surrogate of its integrity. Additionally, BrainLab software was used to delineate the tumor extent and to determine its volume (in cm^3).

Statistics

Statistical evaluation was performed using SPSS (IBM SPSS Statistics for Windows, Version 25.0, Armonk, NY: IBM Corp.) and custom-written Matlab scripts including the FieldTrip toolbox and Matlab statistics toolbox. Group effects on clinical (age, gender, diagnosis), imaging (FA and ADC values), as well as electrophysiological characteristics (RMT, no. of trials, MEP amplitudes and latencies, ERSP and ITC values) were evaluated by non-parametric Kruskal-Wallis, Wilcoxon, and X^2-tests when applicable. Correlation analyses between electrophysiological and clinical parameters were based on Pearson's correlations coefficients. Group differences in the time-frequency representation of the MEPs (ERSP and ITC) were assessed by an unpaired *t*-test. Multiple comparison correction was based on a non-parametric permutation test (200 permutations) as implemented in the FieldTrip toolbox. The *t*-values that exceeded an *a priori* threshold of $p < 0.05$ were subsequently clustered in connected sets based on temporal (i.e., time windows) and spectral parameters. Cluster-level statistics were then calculated by taking the sum of the *t*-values within every cluster and the resultant maximum summed *t*-values were used to compute the statistical comparisons. The significance probability was calculated using a Monte-Carlo method (43). By randomizing the data, the reference distribution of the maximum of summed cluster *t*-values was acquired to evaluate the actual data significance statistic. Clusters from the original data were considered to be significant (alpha level 5%) if <5% of the reference distribution permutations returned a maximum cluster-level statistic larger than the cluster-level value detected in the original data. This cluster-based approach was used to compare the MEP response between the different groups for ERSP and ITC. Results are shown as mean ± standard deviation (SD).

RESULTS

Patients' Characteristics

The present study includes 12 healthy subjects (*Group 1*) and 12 patients with brain tumors who underwent nTMS brain mapping prior to brain surgery. Patients were classified into two categories based on their clinical motor status (*Group 2*: six patients no motor signs, MRCS 5; *Group 3*: six patients with an apparent upper limb paresis MRCS<5). There were no significant differences in gender distribution ($p = 0.091$; X^2-test). Patients with an apparent paresis were significantly older than the other two groups ($p = 0.006$; Kruskal-Wallis); however, there were no significant age differences between the healthy subject group and the patient group without motor signs ($p = 0.471$; Wilcoxon). There were no significant differences in the distribution of tumor diagnosis or size between the patient groups ($p = 0.588$; X^2-test and $p = 0.873$; Kruskal-Wallis). nTMS results of the patients (i.e., coordinates of positive responses) were used for corticospinal fiber tracking on the individual DTI scan. There were no significant differences in the mean FA and ADC values of the detected corticospinal tract ($p = 0.749$ and $p = 0.522$; Kruskal-Wallis). All results are summarized in **Table 1**.

nTMS Time Series Results

nTMS cortical mapping was performed in all healthy subjects and patients in a similar manner (exemplary data see **Figure 1A**). Patients with an apparent paresis (*Group 3*) had a significant higher resting motor threshold than healthy subjects (*Group 1*) and patients without motor signs (*Group 2*, $p = 0.013$; Kruskal-Wallis). There were no significant group differences in the number of applied TMS pulses ($p = 0.712$; Kruskal-Wallis). Notably, there was a higher variance of the MEP shape for patients than for healthy subjects (exemplary data see **Figure 1B**). There were no significant group differences of the mean MEP amplitudes (**Table 1**, **Figure 2A**) and the different latency measures (**Table 1**). Notably, we observed a deceleration of the MEP in the patient groups as documented by the differences between Lat0, Lat1, and Lat2 (**Table 1**, **Figures 2**, **3**). There was no correlation between the time series characteristics ($p > 0.05$; Pearson's) and the age, tumor volume, ADC values, FA values, and RMT except of a significant positive correlation between the RMT and the latency Lat1-Lat2 ($r = 423$; $p = 0.049$).

nTMS Time-Frequency Results

MEP data was transferred into the frequency domain using a Morlet wavelet approach. The transformation revealed a projection of the MEPs to a frequency band between 30 and 300 Hz with a local maximum around 100 Hz. At the same time, there was a high ITC covering the same frequencies. Notably, this pattern was similar for all groups (**Figure 3**). Cluster-based significance analysis showed a significant power reduction between 100 and 200 Hz in a time period of 20–30 ms for patients without any motor signs in comparison to healthy

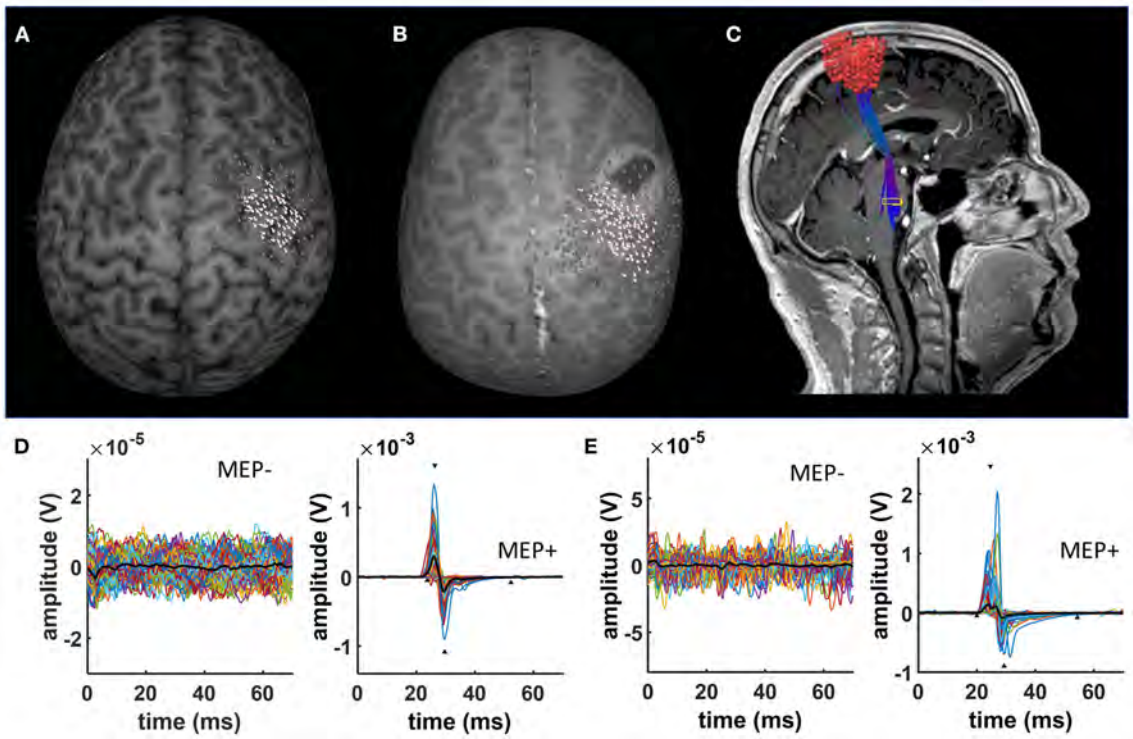

FIGURE 1 | nTMS results. Exemplary data of a characteristic nTMS map in **(A)** a healthy subject and **(B)** a patient with a brain tumor. White dots represent nTMS coordinates eliciting a MEP. In contrast, gray dots indicate spots with no MEPs. nTMS results in patients were used as a seed for deterministic DTI fiber tracking **(C)**. **(D)** Shows exemplary EMG data of a healthy subject separating trials without (MEP-) and with MEPs (MEP+). **(E)** Shows exemplary EMG data of a brain tumor patient separating trials without (MEP-) and with MEPs (MEP+).

subjects. Notably, there was no reduction of ITC in that period. In contrast, these patients showed an increased ITC during the later course of the MEP (i.e., 30–40 ms after TMS). Patients with a paresis, however, showed both a power reduction and a reduced ITC in comparison to healthy subjects during the whole MEP duration (i.e., 20–40 ms). When comparing brain tumor patients with and without paresis, we noticed no further power reduction. But there was a further disturbance of the ITC (**Figure 4**).

On the basis of these findings, we performed a secondary analysis of the mean ERSP and ITC averaging for the frequency band of 30–200 Hz and considering the time periods of 20–30 ms (ERSP1 and ITC1) and 30–40 ms (ERSP2 and ITC2), respectively. With this approach, ERSP findings were not significant anymore (**Figures 5A,B**; $p > 0.05$, Kruskal-Wallis). However, there was a significant group effect for the ITC1 and ITC2 ($p = 0.006$ and $p = 0.002$; Kruskal-Wallis). There was a significant ITC1 reduction for the patient group with paresis in comparison to the other groups (**Figure 5C**), while there was no difference between healthy subjects and patients without paresis. For ITC2, there was even an increase of the ITC in patients without paresis in comparison to healthy subjects (**Figure 5D**). There was no significant correlation of the ERSP and ITC values to age, tumor volume, ADC values, or FA values ($p > 0.05$; Pearson's).

DISCUSSION

The aim of the present study was to describe the time-frequency representation of MEPs in healthy subjects and brain tumor patients. MEPs triggered by TMS are projecting to a frequency band between 30 and 300 Hz with a local maximum around 100 Hz for both healthy subjects and patients. However, healthy subjects and patients differ in their power and ITC values, although there were no significant differences in the standard time series values of MEPs (i.e., peak-to-peak amplitudes and onset latencies). There was a significant power reduction for higher frequencies between 100 and 200 Hz in patients in contrast to healthy subjects, independent of their current motor status. This "deceleration" of the MEPs was reflected in an increase of the inter-peak latencies of the MEP time series. However, patients with an apparent paresis (MRCS<5) showed an additional disturbance in phase synchronization at these frequencies. In contrast, patients without motor signs did not experience a reduction in ITC during the MEP onset despite exerting a power reduction. Actually, there was an increased ITC during the later phase of the MEP. Since there was no correlation between the CST integrity (as measured by DTI) and the MEP representation in the frequency domain, we hypothesize that differences might have a cortical source, e.g., due to a disturbance of cortical physiology by the brain tumor.

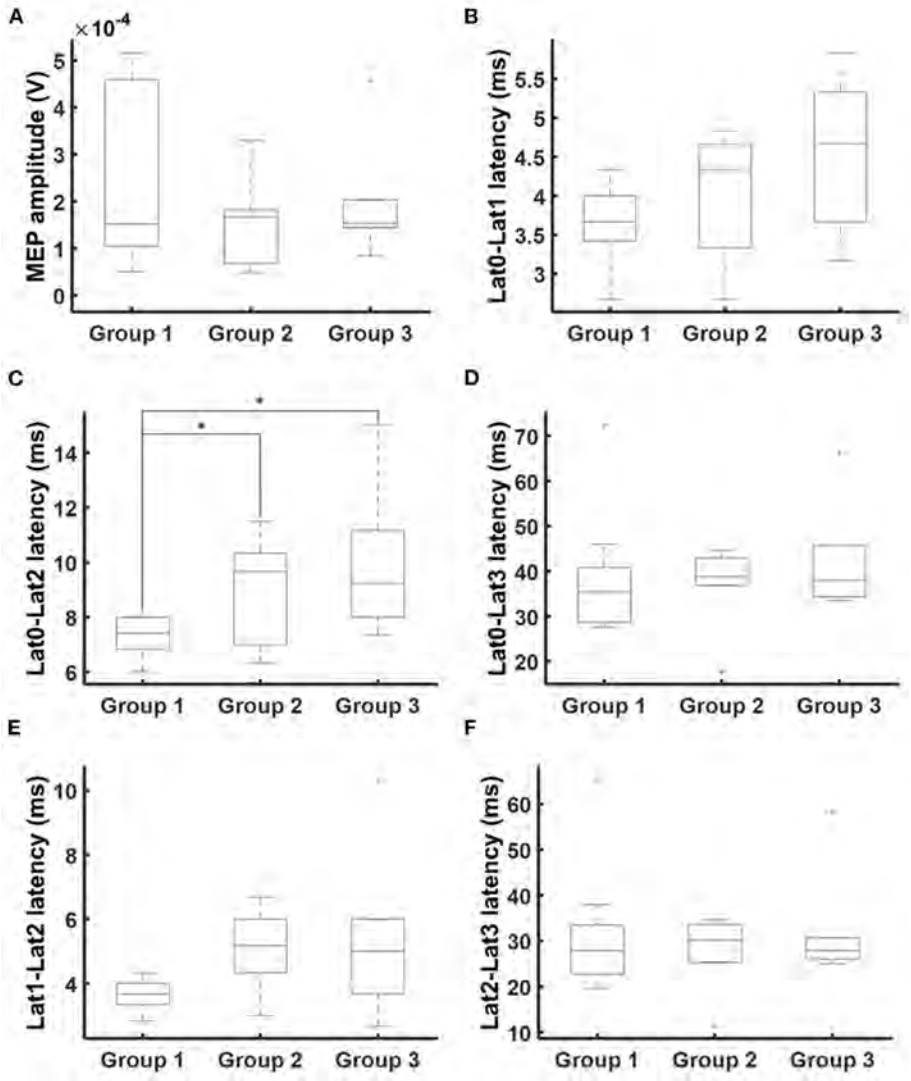

FIGURE 2 | MEP times series characteristics. Times series analysis covered MEP amplitudes **(A)** and latencies Lat0 (MEP onset), Lat1 (maximum positive deflection), Lat2 (minimum negative deflection), and Lat3 (MEP ending). Additionally, latency differences were calculated: **(B)** Lat0-Lat1, **(C)** Lat0-Lat2, **(D)** Lat0-Lat3, **(E)** Lat1-Lat2, and **(F)** Lat2-Lat3. There was a deceleration of MEP. Statistical significance is marked with an asterisk ($p < 0.05$; Wilcoxon).

An increase of MEP latency and a decrease of MEP amplitude are generally accepted to indicate a lesion to the corticospinal network (13–15). In brain tumor patients, however, MEP time domain characteristics (i.e., amplitudes and latencies) often do not differ between the lesioned and non-lesioned hemisphere and are similar to those of healthy subjects (11). Comparable to healthy subjects, MEP characteristics in brain tumor patients exert a high inter-subject and intra-subject variability, which has been related to different individual factors such as gender, body height, and antiepileptic drug intake (44). We observed no difference in MEP latencies between healthy subjects and patients. Even in patients with an apparent paresis, there was no significant increase in MEP latencies. Notably, only a significant "deceleration" of the MEP slope was detected for brain tumor patients.

For the time-frequency domain, the present study reveals a projection of MEPs to a frequency band between 30 and 200 Hz for both healthy subjects and patients. This is expected, when considering the MEP peaks (after 27 and 32 ms) as crest and trough of a sine wave with a half wavelength of 5 ms. This data is in good agreement with prior studies evaluating the time-frequency representation of MEPs in animals and humans (22, 26). In patients with brain tumors, high frequencies (>100 Hz) were reduced in comparison to healthy subjects. This represents the frequency equivalent of the MEP deceleration seen in the time series analysis. At the same time, we observed a reduction of inter-trial-coherence in brain tumor patients as a sign of

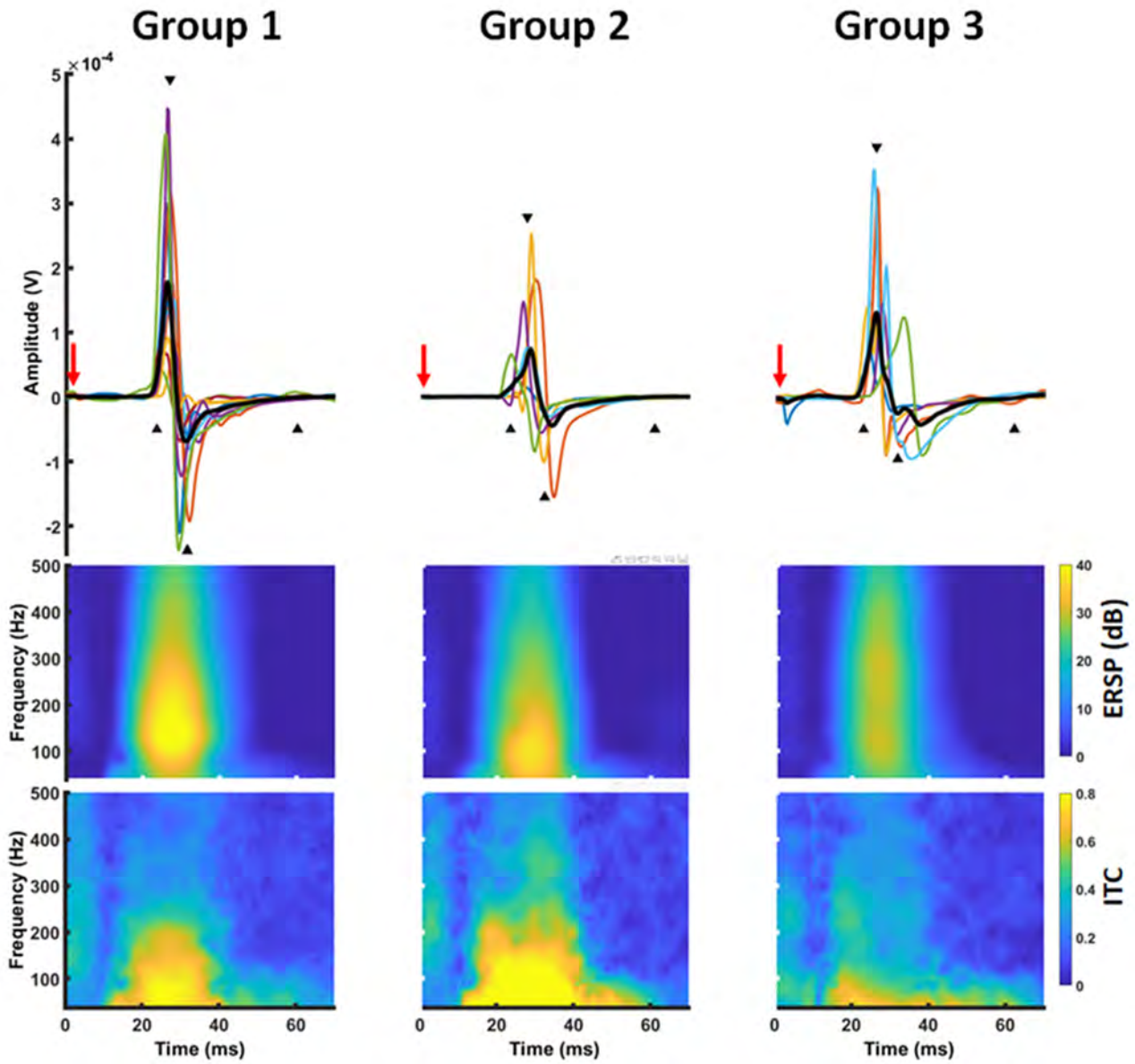

FIGURE 3 | Time-frequency representation of a MEP. MEP time series **(upper row)** were transferred into the frequency domain using a Morlet wavelet approach. The transformation revealed a power increase (ERSP) ~20–50 ms after TMS application (red arrow) in a frequency band between 30 and 300 Hz with a local maximum around 100 Hz **(middle row)**. At the same time, there was a high inter-trial-coherence covering the frequency and time range **(lower row)**.

temporal distortion of the MEPs. Notably, ITC changes were most prominent in patients with an apparent paresis. In patients without motor signs, the deceleration of MEPs (as seen in the time series characteristics and the time-frequency representation) resulted in an increase of ITC behind time.

TMS is mediating MEPs by direct (D waves) and transsynaptic activation (I waves) of pyramidal cells (3). As there was no correlation between the CST integrity (as measured by DTI parameter) and the MEP changes in these patients, we hypothesize that the observed differences in the time-frequency domain might have a cortical source, e.g., due to a disturbance of cortical physiology by the brain tumor. We hypothesize that brain tumors are usually diagnosed prior to the invasion of the CST. Thus, in contrast to spinal lesions or strokes, corticospinal transmission of D-waves might be unaffected resulting in regular MEP latencies. The activation of later I-waves produces a sequence of EPSPs that temporally summate and determine the MEP amplitudes albeit arriving at the motoneuron with a longer latency than the initial D-wave (45). Following this line of argumentation, the reduction of MEP amplitude and power in these patients could be attributed to a reduced transsynaptic recruitment of pyramidal cells in the I-wave generation. This could explain the increase of RMT, the MEP amplitude reduction, the decelerated rise of the MEP, and the temporal distortion

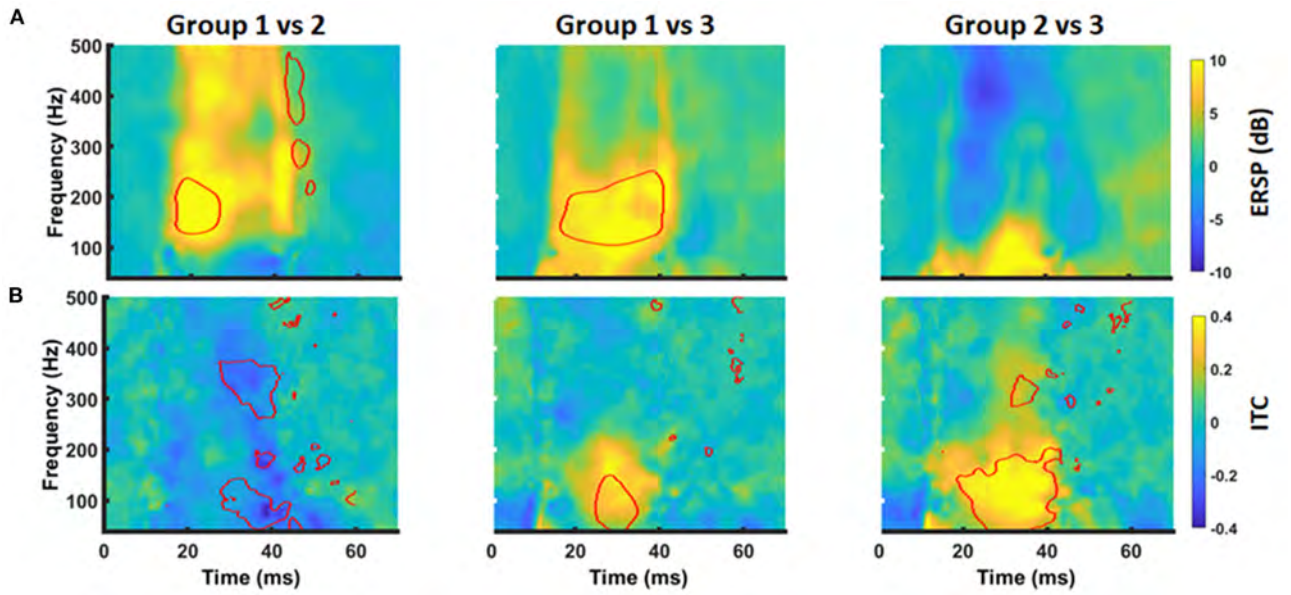

FIGURE 4 | Group differences of time-frequency MEP behavior. Group differences in ERSP **(A)** and ITC **(B)** between Group 1 and 2 (*left column*), Group1 and 3 (*middle column*), and Group 2 and 3 (*right column*) were evaluated by cluster-based permutation analysis. Significant time-frequency bins are outlined in red ($p < 0.05$, cluster corrected).

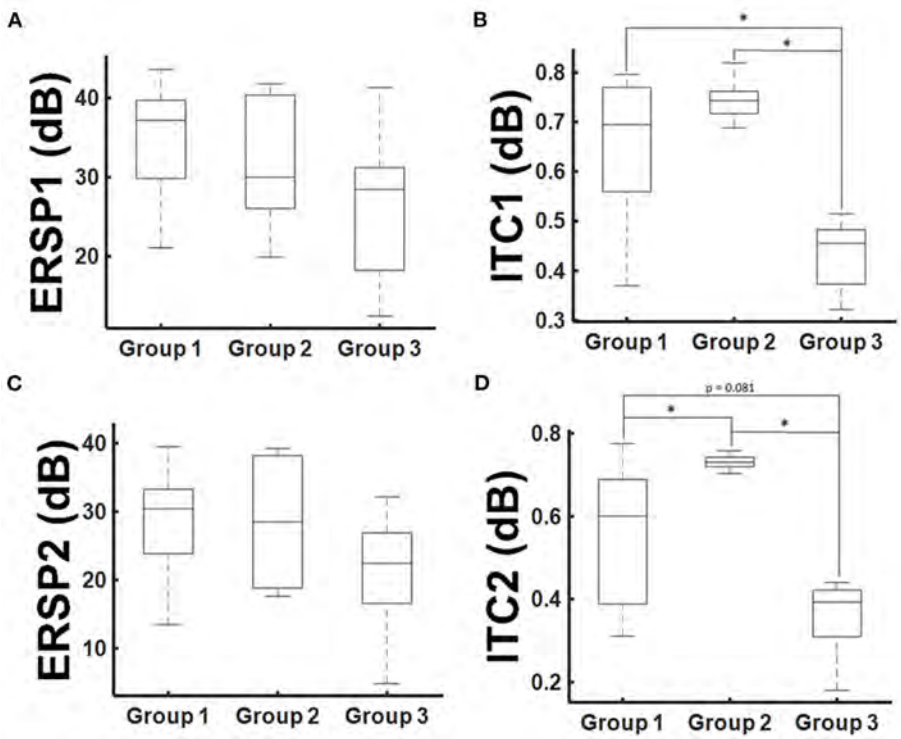

FIGURE 5 | ERSP and ITC group results. Mean ERSP and ITC values for the 30–200 Hz frequencies averaged for the time period of 20–30 ms after TMS application [ERSP1 and ITC1, **(A,B)**] and 30–40 ms [ERSP2 and ITC2, **(C,D)**]. Statistical significance is marked with an asterisk ($p < 0.05$; Wilcoxon).

of MEPs as seen in the ITC analysis. Temporal distortion can be attributed to the failure of TMS to recruit I-waves in brain tumor patients. In patients without motor signs, I-waves might be delayed but still recruitable by TMS. However, it remains unclear why TMS fail to recruit the pyramidal cells, e.g., compression effect of the tumor, oedema, or antiepileptic drug intake.

Methodological Considerations

To our knowledge, the present work is one of few studies evaluating the MEPs in the frequency domain (26). Although time-frequency methods are very common in the field of neuroscience (6, 16–18), they have not frequently been applied for the evaluation of MEPs. In addition to the need for advanced calculations, there are methodological aspects to be considered. Time-frequency analysis of fast alternating potentials (e.g., MEPs, ECG signals or ripples) are challenged by an apparent, sampling rate dependent, discontinuity of the signal in the time series. Transforming these signals into the frequency domain may cause ringing, a broad band power increase known as "leakage effect." The amount of spectral leakage depends on the amplitude of the discontinuity. As the discontinuity becomes larger, spectral leakage increases. Thus, fast rising signals like MEPs are very prone to this problem (46).

Time-frequency analysis of digitized signals is traditionally performed using the short-time Fourier transform, which computes the power spectra on successive sliding windows. Long windows provide good frequency resolution and reduce the leakage phenomenon. However, they result in a poor temporal resolution and a "smearing" of the event-related spectral perturbation beyond the actual limits of the time series event. Shortening the window will results in a degradation of frequency resolution with a strong leakage effect (46, 47). Continuous-wavelet transformations such as the Morlet wavelet were introduced to overcome this limitation. The wavelet analysis provides a better temporal resolution by compression/dilation of a mother wavelet as a function of frequency (47). Detecting oscillation packets in time, wavelet techniques seem to be more appropriate to describe MEPs. However, very short wavelets are struggling to distinguish high frequencies (47). Thus, shortening the wavelet length in high frequencies will "smear" the event-related spectral perturbation in a wide range of high frequencies. Balancing these drawbacks, we applied a Morlet wavelet analysis with fixed wavelet length, defined by the observed MEP duration in the time series (i.e., ∼40 ms). This enabled an adequate representation of the MEP in relation to the temporal and spectral resolution. However, one has to take into account that frequencies with wave lengths longer than the wavelet are not detectable (here below 25–30 Hz) and that phase detection is inaccurate in higher frequencies. Apart from these time-frequency decomposition methods, time-frequency representation can also be obtained by fitting an autoregressive (AR) model to the signal (48). This approach is very common in ECG analysis (49); however, it is strongly affected by the signal-to-noise ratio (48). Thus, it could be insufficient in situations with small MEP amplitudes such as stroke or brain tumors. Up to date, it remains unclear which method is most suitable for the time-frequency transformation of MEPs. Studies analyzing the time-frequency representation of somatosensory potentials in humans have used both a Fourier transformation (22, 25) and a Morlet wavelet approach (26).

Limitations of the Study

There are several limitations of the study that should be addressed. Although there was no statistical difference between the healthy subject group and the patient group without any motor signs, there was no good age-matched control. As age and related medical complaints (e.g., diabetes) are known to affect corticospinal conduction and MEP latencies, it cannot be completely excluded that temporal dispersion observed in Group 3 may be attributed to the higher age of the patients. Furthermore, there would be a special interest in the MEPs of the unaffected hemisphere in these patients to avoid potential biases related to a control group. Such an analysis could unravel the effect of individual but tumor-unrelated factors on MEP inter-trial-coherence (e.g., antiepileptic drug intake). Concluding, after introduction of the mentioned approach, further studies with a larger patient group and age-matched comparison cohort are necessary to confirm the described findings. Furthermore, it has to be mentioned that the current analysis includes MEPs elicited after stimulation of different brain areas (e.g., primary motor cortex and/or premotor areas) and different coil positions. Notably, it is known that slight variations in coil placement may result in different MEP responses (50).

CONCLUSION

To the best of our knowledge, this is the first study evaluating MEPs of brain tumor patients in the frequency domain. Our findings demonstrate how time-frequency analysis techniques could provide additional information about the MEP (e.g., shape) and the status of the motor system in brain tumor patients. This first evaluation indicates that brain tumors might affect cortical physiology and the responsiveness of the cortex to TMS, resulting in a temporal dispersion of the corticospinal transmission.

DATA AVAILABILITY STATEMENT

The raw data supporting the conclusions of this article will be made available by the authors, without undue reservation.

ETHICS STATEMENT

The studies involving human participants were reviewed and approved by local ethics committee of the Eberhardt Karls University Tuebingen. The patients/participants provided their written informed consent to participate in this study.

AUTHOR CONTRIBUTIONS

KM contributed to the acquisition, analysis, interpretation of data, and writing of the first draft. ALG, MTL, ML, LT, SW, and MT contributed to the data acquisition, interpretation of data, and the review and critique of the final manuscript. AG and MT contributed to the interpretation of data and the review and critique of the final manuscript. GN was responsible for the conception and design, data acquisition, analysis, and interpretation as well as the review and critique of the manuscript. All authors contributed to the article and approved the submitted version.

REFERENCES

1. Stinear CM, Barber PA, Smale PR, Coxon JP, Fleming MK, Byblow WD. Functional potential in chronic stroke patients depends on corticospinal tract integrity. *Brain.* (2007) 130:170–80. doi: 10.1093/brain/awl333
2. Chen R, Cros D, Curra A, Di Lazzaro V, Lefaucheur JP, Magistris MR, et al. The clinical diagnostic utility of transcranial magnetic stimulation: report of an IFCN committee. *Clin Neurophysiol.* (2008) 119:504–32. doi: 10.1016/j.clinph.2007.10.014
3. Rossini PM, Burke D, Chen R, Cohen LG, Daskalakis Z, Di Iorio R, et al. Non-invasive electrical and magnetic stimulation of the brain, spinal cord, roots and peripheral nerves: basic principles and procedures for routine clinical and research application: an updated report from an I.F.C.N. Committee. *Clin Neurophysiol.* (2015) 126:1071–107. doi: 10.1016/j.clinph.2015.02.001
4. Groppa S, Oliviero A, Eisen A, Quartarone A, Cohen LG, Mall V, et al. A practical guide to diagnostic transcranial magnetic stimulation: report of an IFCN committee. *Clin Neurophysiol.* (2012) 123:858–82. doi: 10.1016/j.clinph.2012.01.010
5. Darling WG, Wolf SL, Butler AJ. Variability of motor potentials evoked by transcranial magnetic stimulation depends on muscle activation. *Exp Brain Res.* (2006) 174:376–85. doi: 10.1007/s00221-006-0468-9
6. Naros G, Lehnertz T, Leão MT, Ziemann U, Gharabaghi A. Brain state-dependent gain modulation of corticospinal output in the active motor system. *Cereb Cortex.* (2019) 30:371–81. doi: 10.1093/cercor/bhz093
7. van Elswijk G, Maij F, Schoffelen J-MM, Overeem S, Stegeman DF, Fries P. Corticospinal beta-band synchronization entails rhythmic gain modulation. *J Neurosci.* (2010) 30:4481–8. doi: 10.1523/JNEUROSCI.2794-09.2010
8. Khademi F, Royter V, Gharabaghi A. Distinct beta-band oscillatory circuits underlie corticospinal gain modulation. *Cereb Cortex.* (2018) 28:1502–15. doi: 10.1093/cercor/bhy016
9. Wolf SL, Butler AJ, Campana GI, Parris TA, Struys DM, Weinstein SR, et al. Intra-subject reliability of parameters contributing to maps generated by transcranial magnetic stimulation in able-bodied adults. *Clin Neurophysiol.* (2004) 115:1740–7. doi: 10.1016/j.clinph.2004.02.027
10. Sollmann N, Wildschuetz NN, Kelm A, Conway N, Moser T, Bulubas L, et al. Associations between clinical outcome and navigated transcranial magnetic stimulation characteristics in patients with motor-eloquent brain lesions: a combined navigated transcranial magnetic stimulation–diffusion tensor imaging fiber tracking approach. *J Neurosurg.* (2017) 128:800–10. doi: 10.3171/2016.11.JNS162322
11. Picht T, Strack V, Schulz J, Zdunczyk A, Frey D, Schmidt S, et al. Assessing the functional status of the motor system in brain tumor patients using transcranial magnetic stimulation. *Acta Neurochir.* (2012) 154:2075–81. doi: 10.1007/s00701-012-1494-y
12. Butler AJ, Kahn S, Wolf SL, Weiss P. Finger extensor variability in TMS parameters among chronic stroke patients. *J Neuroeng Rehabil.* (2005) 2:10. doi: 10.1186/1743-0003-2-10
13. Cirillo J, Calabro FJ, Perez MA. Impaired organization of paired-pulse TMS-induced I-waves after human spinal cord injury. *Cereb Cortex.* (2016) 26:2167–77. doi: 10.1093/cercor/bhv048
14. Kobayashi M, Pascual-Leone A. Transcranial magnetic stimulation in neurology. *Lancet Neurol.* (2003) 2:145–56. doi: 10.1016/S1474-4422(03)00321-1
15. Hallett M. Transcranial magnetic stimulation and the human brain. *Nature.* (2000) 406:147–50. doi: 10.1038/35018000
16. Naros G, Naros I, Grimm F, Ziemann U, Gharabaghi A. Reinforcement learning of self-regulated sensorimotor β-oscillations improves motor performance. *Neuroimage.* (2016) 134:142–52. doi: 10.1016/j.neuroimage.2016.03.016
17. Naros G, Grimm F, Weiss D, Gharabaghi A. Directional communication during movement execution interferes with tremor in Parkinson's disease. *Mov Disord.* (2018) 33:251–61. doi: 10.1002/mds.27221
18. Naros G, Gharabaghi A. Physiological and behavioral effects of β-tACS on brain self-regulation in chronic stroke. *Brain Stimul.* (2017) 10:251–9. doi: 10.1016/j.brs.2016.11.003
19. Wang Y, Li G, Luk KDK, Hu Y. Component analysis of somatosensory evoked potentials for identifying spinal cord injury location. *Sci Rep.* (2017) 7:2351. doi: 10.1038/s41598-017-02555-w
20. Wang Y, Zhang Z, Li X, Cui H, Xie X, Luk KD-KK, et al. Usefulness of time-frequency patterns of somatosensory evoked potentials in identification of the location of spinal cord injury. *J Clin Neurophysiol.* (2015) 32:341–5. doi: 10.1097/WNP.0000000000000167
21. Wang Y, Cui H, Pu J, Luk KDK, Hu Y. Time-frequency patterns of somatosensory evoked potentials in predicting the location of spinal cord injury. *Neurosci Lett.* (2015) 603:37–41. doi: 10.1016/j.neulet.2015.07.002
22. Hu Y, Luk KDK, Lu WW, Holmes A, Leong JCY. Prevention of spinal cord injury with time-frequency analysis of evoked potentials: an experimental study. *J Neurol Neurosurg Psychiatry.* (2001) 71:732–40. doi: 10.1136/jnnp.71.6.732
23. Hu Y, Liu H, Luk KD. Time-frequency analysis of somatosensory evoked potentials for intraoperative spinal cord monitoring. *J Clin Neurophysiol.* (2011) 28:504–11. doi: 10.1097/WNP.0b013e318231c15c
24. Zhang ZG, Yang JL, Chan SC, Luk KDK, Hu Y. Time-frequency component analysis of somatosensory evoked potentials in rats. *Biomed Eng Online.* (2009) 8:4. doi: 10.1186/1475-925X-8-4
25. Hu Y, Luk KDK, Lu WW, Leong JCY. Application of time-frequency analysis to somatosensory evoked potential for intraoperative spinal cord monitoring. *J Neurol Neurosurg Psychiatry.* (2003) 74:82–7. doi: 10.1136/jnnp.74.1.82
26. Singh N, Saini M, Kumar N, Deepak KK, Anand S, Srivastava MVP, et al. Time-frequency analysis of motor-evoked potential in patients with stroke vs healthy subjects: a transcranial magnetic stimulation study. *SN Compr Clin Med.* (2019) 1:764–80. doi: 10.1007/s42399-019-00113-1
27. Kraus D, Naros G, Bauer R, Leão MT, Ziemann U, Gharabaghi A. Brain-robot interface driven plasticity: distributed modulation of corticospinal excitability. *Neuroimage.* (2016) 125:522–32. doi: 10.1016/j.neuroimage.2015.09.074
28. Kraus D, Gharabaghi A. Projecting navigated TMS sites on the gyral anatomy decreases inter-subject variability of cortical motor maps. *Brain Stimul.* (2015) 8:831–7. doi: 10.1016/j.brs.2015.03.006
29. Mathew J, Kübler A, Bauer R, Gharabaghi A. Probing corticospinal recruitment patterns and functional synergies with transcranial magnetic stimulation. *Front Cell Neurosci.* (2016) 10:175. doi: 10.3389/fncel.2016.00175
30. Leão MT, Naros G, Gharabaghi A. Detecting poststroke cortical motor maps with biphasic single- and monophasic paired-pulse TMS. *Brain Stimul.* (2020) 13:1102–4. doi: 10.1016/j.brs.2020.05.005
31. Delorme A, Makeig S. EEGLAB: an open source toolbox for analysis of single-trial EEG dynamics including independent component analysis. *J Neurosci Methods.* (2004) 134:9–21. doi: 10.1016/j.jneumeth.2003.10.009
32. Oostenveld R, Fries P, Maris E, Schoffelen J-MM. FieldTrip: open source software for advanced analysis of MEG, EEG, and invasive electrophysiological data. *Comput Intell Neurosci.* (2011) 2011:156869. doi: 10.1155/2011/156869
33. Grandchamp R, Delorme A. Single-trial normalization for event-related spectral decomposition reduces sensitivity to noisy trials. *Front Psychol.* (2011) 2:236. doi: 10.3389/fpsyg.2011.00236
34. Prentice MJ, Fisher NI. Statistical analysis of circular data. *J R Stat Soc Ser A.* (2006) 37:229–30. doi: 10.2307/2983422
35. Krieg SMSM, Buchmann NHNH, Gempt J, Shiban E, Meyer B, Ringel F. Diffusion tensor imaging fiber tracking using navigated brain stimulation—a feasibility study. *Acta Neurochir.* (2012) 154:555–63. doi: 10.1007/s00701-011-1255-3
36. Machetanz K, Trakolis L, Leão MT, Liebsch M, Mounts K, Bender B, et al. Neurophysiology-driven parameter selection in nTMS-based DTI tractography: a multidimensional mathematical model. *Front Neurosci.* (2019) 13:1373. doi: 10.3389/fnins.2019.01373
37. Rosenstock T, Giampiccolo D, Schneider H, Runge SJ, Bährend I, Vajkoczy P, et al. Specific DTI seeding and diffusivity-analysis improve the quality and prognostic value of TMS-based deterministic DTI of the pyramidal tract. *NeuroImage Clin.* (2017) 16:276–85. doi: 10.1016/j.nicl.2017.08.010
38. Weiss C, Tursunova I, Neuschmelting V, Lockau H, Nettekoven C, Oros-Peusquens AM, et al. Improved nTMS- and DTI-derived CST tractography through anatomical ROI seeding on anterior pontine level compared to internal capsule. *NeuroImage Clin.* (2015) 7:424–37. doi: 10.1016/j.nicl.2015.01.006
39. Raffa G, Scibilia A, Germanò A, Conti A. nTMS-based DTI fiber tracking of motor pathways. In: *Navigated Transcranial Magnetic*

Stimulation in Neurosurgery. Cham: Springer (2017). p. 97–114. doi: 10.1007/978-3-319-54918-7_6
40. Raffa G, Quattropani MC, Germanò A. When imaging meets neurophysiology: the value of navigated transcranial magnetic stimulation for preoperative neurophysiological mapping prior to brain tumor surgery. *Neurosurg Focus.* (2019) 47:9640. doi: 10.3171/2019.9.FOCUS19640
41. Weiss Lucas C, Tursunova I, Neuschmelting V, Nettekoven C, Oros-Peusquens AM, Stoffels G, et al. Functional MRI vs. navigated TMS to optimize M1 seed volume delineation for DTI tractography. A prospective study in patients with brain tumours adjacent to the corticospinal tract. *NeuroImage Clin.* (2017) 13:297–309. doi: 10.1016/j.nicl.2016.11.022
42. Frey D, Strack V, Wiener E, Jussen D, Vajkoczy P, Picht T. A new approach for corticospinal tract reconstruction based on navigated transcranial stimulation and standardized fractional anisotropy values. *Neuroimage.* (2012) 62:1600–9. doi: 10.1016/j.neuroimage.2012.05.059
43. Maris E, Oostenveld R. Non-parametric statistical testing of EEG- and MEG-data. *J Neurosci Methods.* (2007) 164:177–90. doi: 10.1016/j.jneumeth.2007.03.024
44. Sollmann N, Bulubas L, Tanigawa N, Zimmer C, Meyer B, Krieg SM. The variability of motor evoked potential latencies in neurosurgical motor mapping by preoperative navigated transcranial magnetic stimulation. *BMC Neurosci.* (2017) 18:4. doi: 10.1186/s12868-016-0321-4
45. Rossini PM, Caramia MD, Iani C, Desiato MT, Sciarretta G, Bernardi G. Magnetic transcranial stimulation in healthy humans: influence on the behavior of upper limb motor units. *Brain Res.* (1995) 676:314–24. doi: 10.1016/0006-8993(95)00113-5
46. Herrmann CS, Rach S, Vosskuhl J, Strüber D. Time-frequency analysis of event-related potentials: a brief tutorial. *Brain Topogr.* (2014) 27:438–50. doi: 10.1007/s10548-013-0327-5
47. Mallat S. *A Wavelet Tour of Signal Processing*. Burlington, MA: Academic Press (2009). doi: 10.1016/B978-0-12-374370-1.X0001-8
48. Supp GG, Schlögl A, Trujillo-Barreto N, Müller MM, Gruber T. Directed cortical information flow during human object recognition: analyzing induced EEG gamma-band responses in brain's source space. *PLoS ONE.* (2007) 2:e684. doi: 10.1371/journal.pone.0000684
49. Zhao Q, Zhang L. ECG feature extraction and classification using wavelet transform and support vector machines. In: Zhao M, Shi Z, editors. *2005 International Conference on Neural Networks and Brain, Beijing*. Piscataway, NJ: IEEE (2005). p. 1089–92. doi: 10.1109/ICNNB.2005.1614807
50. Bashir S, Perez JM, Horvath JC, Pascual-Leone A. Differentiation of motor cortical representation of hand muscles by navigated mapping of optimal TMS current directions in healthy subjects. *J Clin Neurophysiol.* (2013) 30:390–5. doi: 10.1097/WNP.0b013e31829dda6b

Conflict of Interest: The authors declare that the research was conducted in the absence of any commercial or financial relationships that could be construed as a potential conflict of interest.

frontiers in Neurology

MINI REVIEW
published: 10 February 2021
doi: 10.3389/fneur.2021.639822

Perspectives on (A)symmetry of Arcuate Fasciculus. A Short Review About Anatomy, Tractography and TMS for Arcuate Fasciculus Reconstruction in Planning Surgery for Gliomas in Language Areas

Andrea Di Cristofori[1], *Gianpaolo Basso*[1,2,3], *Camilla de Laurentis*[1,2], *Ilaria Mauri*[4], *Martina Andrea Sirtori*[5], *Carlo Ferrarese*[2,4], *Valeria Isella*[2,4] *and Carlo Giussani*[1,2*]

[1] Neurosurgery Unit, San Gerardo Hospital, ASST Monza, Monza, Italy, [2] School of Medicine and Surgery, University of Milano-Bicocca, Milan, Italy, [3] Neuroradiology Unit, San Gerardo Hospital, ASST Monza, Monza, Italy, [4] Neurology Unit, San Gerardo Hospital, ASST Monza, Monza, Italy, [5] Department of Psychology, University of Milano-Bicocca, Milan, Italy

OPEN ACCESS

Edited by:
Giovanni Raffa,
University of Messina, Italy

Reviewed by:
Tamara Ius,
University Hospital of Udine, Italy
Davide Giampiccolo,
University of Verona, Italy

***Correspondence:**
Carlo Giussani
carlo.giussani@unimib.it

Specialty section:
This article was submitted to Applied Neuroimaging, a section of the journal Frontiers in Neurology

Received: 09 December 2020
Accepted: 05 January 2021
Published: 10 February 2021

Citation:
Di Cristofori A, Basso G, de Laurentis C, Mauri I, Sirtori MA, Ferrarese C, Isella V and Giussani C (2021) Perspectives on (A)symmetry of Arcuate Fasciculus. A Short Review About Anatomy, Tractography and TMS for Arcuate Fasciculus Reconstruction in Planning Surgery for Gliomas in Language Areas. Front. Neurol. 12:639822. doi: 10.3389/fneur.2021.639822

Gliomas are brain tumors that are treated with surgical resection. Prognosis is influenced by the extent of resection and postoperative neurological status. As consequence, given the extreme interindividual and interhemispheric variability of subcortical white matter (WM) surgical planning requires to be patient's tailored. According to the "connectionist model," there is a huge variability among both cortical areas and subcortical WM in all human beings, and it is known that brain is able to reorganize itself and to adapt to WM lesions. Brain magnetic resonance imaging diffusion tensor imaging (DTI) tractography allows visualization of WM bundles. Nowadays DTI tractography is widely available in the clinical setting for presurgical planning. Arcuate fasciculus (AF) is a long WM bundle that connects the Broca's and Wernicke's regions with a complex anatomical architecture and important role in language functions. Thus, its preservation is important for the postoperative outcome, and DTI tractography is usually performed for planning surgery within the language-dominant hemisphere. High variability among individuals and an asymmetrical pattern has been reported for this WM bundle. However, the functional relevance of AF in the contralateral non-dominant hemisphere in case of tumoral or surgical lesion of the language-dominant AF is unclear. This review focuses on AF anatomy with special attention to its asymmetry in both normal and pathological conditions and how it may be explored with preoperative tools for planning surgery on gliomas in language areas. Based on the findings available in literature, we finally speculate about the potential role of preoperative evaluation of the WM contralateral to the surgical site.

Keywords: glioma, surgery, planning, arcuate fasciculus, tranancranial magnetic stimulation, diffusion tensor imaging, white matter asymmetries, white matter anatomy

INTRODUCTION

Gliomas are intra-axial infiltrating brain tumors, boundaries of which within the perilesional white matter (WM) are very difficult to define (1, 2). It is accepted that the best prognosis can be reached aiming at the most radical tumor resection possible preserving, however, a good postoperative neurological status (3, 4). In fact, The poor quality of life of patients with postoperative deficits leads to an overall survival reduction (5–8). As a consequence, the extent of resection within the possibly infiltrated but normal-appearing brain tissue must avoid damaging critical normal functioning cortical areas and their WM connections (9–11). Within the neurosurgical planning, the definition of what brain tissue must be considered "eloquent" is still mostly based on a classic localizationist model, which assumes that cortical areas are specialized for specific aspects of neurological functions. On the other hand, this localizationist model is now outdated, and cognitive neuroscience research suggests that every cognitive and motor function depends on complex neuroplastic networks connecting many cortical areas by means of long- and short-association WM fibers (12, 13). According to this connectionist model, cortical, and subcortical functional interplay may be highly variable among human beings and can reorganize in response to brain damage, such as an acute brain insult or a relatively slow-growing tumor mass (10, 14–17). These so-called neuroplastic properties might explain why, despite bearing an extensive mass located close or within brain tissue considered to be critical according to the classic localizationist model, patients with intra-axial brain tumors usually display very mild or even no neurological deficit at presentation and can maintain this status even after surgery with extensive tumoral and peritumoral tissue resection (14, 17–19). Thus, the concept of neuroplasticity should be considered for accurate presurgical planning, but full translation of this factor from basic to clinical neuroscience is still lacking because of incomplete understanding of its mechanisms. In fact, currently, it is still impossible to predict its impact on the postsurgical outcome based on an objective measure of how much the brain of the patient has already reorganized in response to the tumor and may still reorganize after surgery (20, 21). From this point of view, cortical and subcortical structures show different plastic potential. In fact, cortex seems to have a great neuroplastic potential, and it is able to reorganize effectively in case of brain tumors, while WM bundles seem to have a low plastic potential (22, 23), and extensive surgical resections might depend mainly on WM boundaries rather than on the cortical extension of the tumor (24–26). One of the most critical functions to be preserved after surgery is verbal language. Both neuropsychological studies in patient and functional studies in neurologically normal subjects have clarified that language functions are strongly lateralized to one hemisphere, defined as dominant for language (27–29). The network of areas involved comprises cortical regions that are present and overall symmetrical within the two hemispheres. However, only few individuals have a right-hemisphere dominance, which ranges from 4% in strong right-handers to 15% in ambidextrous to 27% in strong left-handers (30).

The strong well-known cortical lateralization of language functions is one of the key factors for preoperative brain tumor risk assessment in adults. A low risk is usually assigned if the lesion is located far from areas involved in this function, with the lowest risk associated with lesions located within the non-dominant hemisphere (29, 31). However, it is known that a brain lesion to the dominant hemisphere may induce a complex cortical functional reorganization of the language network that may involve a complex interplay of activity with contralateral homologous cortical areas and functional reorganization in the perilesional cortex, while it is still unclear how WM can functionally accommodate a brain damage induced by the tumor given its low neuroplastic potential (21, 22). This prevents *a priori* assumption of language lateralization in a patient with a brain tumor. Wada test was the first reliable method developed to establish the dominant hemisphere for language. Subsequently, the advances of functional magnetic resonance imaging (MRI) studies, with which an indirect measure of brain activity can be assessed based on blood oxygen level modifications [functional MRI (fMRI)], proved to be a reliable non-invasive and riskless substitute of the Wada test. Thus, fMRI is currently used to define hemispheric dominance, computing a laterality index based on the comparison of relative activation of right and left frontal and temporal areas induced by language tasks execution (32–34). Nevertheless, language functions involve activity of a vast network of areas, spanning all lobes of the dominant hemisphere. Thus, the functional properties of this network strongly depend on intrinsic efficient connections among them, and presurgical assessment must take into account also the risk of damaging critical WM bundles (31, 35, 36).

Magnetic resonance multidirectional diffusion-weighted imaging (MD-DWI) tractography allows *in vivo* indirect reconstruction of WM fibers and can be used to perform digital anatomical dissections of WM bundles (37–39). Many different MD-DWI tractography acquisition protocols, postprocessing methods, and reconstruction algorithms are currently used with different accuracy levels, and all of them are prone to false positive and false negative (40). The simplest MD-DWI tractography method is based on deterministic tracing based on voxel main diffusion direction estimated with tensor modeling [diffusion tensor imaging (DTI)]. DTI tractography (DTI-T) is currently used for preoperative surgical planning to maximize the surgical resection avoiding to damage association and projection fibers located nearby the tumor (6, 35, 41) and consistently reveals asymmetries of WM tracts between the two hemispheres (37, 42) that may be paired with cortical lateralization of cognitive and motor functions. Nevertheless, to our knowledge, very few studies explored the clinical relevance of these structural asymmetries for the functional outcome after brain surgery for gliomas. Moreover, it is still unclear if subcortical variability could have a role in postoperative outcome and if it could be of some utility for the neurosurgeon to predict the risk of neurological deficits (9, 35). In this mini-review, we focus on available evidence in the literature about one bundle considered of paramount importance for language functions, the arcuate fasciculus (AF), to better understand the meaning

of its asymmetry for preoperative risk assessment of patients undergoing surgical resection for gliomas.

ARCUATE FASCICULUS ANATOMY AND FUNCTIONAL RELEVANCE FOR LANGUAGE WITHIN THE DOMINANT HEMISPHERE

The AF has been involved in the neurobiology of language since Geschwind's (43) proposal of the "classic model," where AF was the only link between two broad anatomical regions, Broca's territory in the inferior frontal and precentral gyri and Wernicke's territory in the posterior temporal lobe, functionally specialized, respectively, for language production and language comprehension. During the last three decades, the field of language neurobiology has been slowly but steadily moving toward the definitive overcoming of the classic model (44–47). The "dual stream" model proposed by Hickok and Poeppel (48) was a major step forward both because it expanded the number of cortical regions contributing to language functions and suggested that, as previously proposed for the visuospatial system (49), some language abilities may depend more on the functional interplay among them more than on their cortical functional specialization. A critical role of AF was maintained also within this model as revealed by direct electrical stimulation of WM bundles during neurosurgery (23, 50), suggesting that the AF may be the critical anatomical connection within the dorsal functional stream devoted to speech articulation and excluding any of its role for speech comprehension that appeared to be supported by a ventral stream. Yet, even the dual-stream model does not fully explain the spectrum of aphasia symptoms resulting from ischemic brain damage and has been recently revised (46).

The work of Hickok and Poeppel, however, started a cortical delocalization conceptual shift that is leading to the new theoretical framework of a "language connectome" within which language functions would emerge from the dynamic of connections of many cortical and subcortical regions, which may have no specific language properties itself (25, 45–47). Within this view, WM bundle exploration has gained more and more importance as they provide the fundamental anatomical support for the correct functioning of the connectome. So far, many sets of intralobe, intrahemispheric, and interhemisheric association WM bundles connecting frontal, temporal, parietal, insular, and occipital areas have been identified as possibly supporting language functions (25, 45, 47). Among them, probably AF still remains the most studied WM bundle since its very first dissection description by Reil (51). Nevertheless, AF anatomy has been and is still matter of debate (39, 45, 52–54).

A simple virtual dissection method to identify AF with DTI-T has been proposed by Catani (12), and we currently use this method routinely in our glioma presurgical settings. It allows separating the bulk of fibers passing through the perisylvian lateral frontoparietal-temporal WM into three subsets. Two lateral short segments connect the inferior parietal lobule (IPL) with both the frontal operculum and the middle and superior temporal gyrus (MTG/STG), respectively, through an anterior and horizontal bundle and a posterior vertical one. The third medial segment corresponds to the proper AF, which directly connects a wide frontal cortical area made of the frontal operculum, the middle frontal gyrus, and the inferior precentral gyrus, to a wide temporal area comprising the posterior portion of MTG and STG, even if this last terminations are highly variable, probably due to intrinsic limitations of DTI-T (55). A more detailed definition of AF can be reached with high-resolution MD-DWI tractography. Using one of these methods, Fernandez-Miranda et al. (39) conducted a tractography study on 10 healthy subjects and found that STG, MTG, and ITG contributed equally to the AF with a strong left lateralization for STG and ITG, whereas MTG contributed equally in left and right AF. Concerning the frontal counterpart, AF fibers terminated in the pars opercularis in all subjects in the left part, but only in 3 subjects in the right hemisphere; the pars triangularis was a termination site in 3/10 subjects in the left and in 5/10 subjects in the right hemisphere; the ventral precentral gyrus was a site of termination of AF fibers in 8/10 subjects and in 2/10 subjects, respectively, in left and right hemispheres (39). Such distribution was similar to the one described by Martino and colleagues in 2013 on WM *postmortem* dissections (55). In 2016, Yagmurlu et al. proposed a different organization of the left-sided AF after *postmortem* WM dissections of 25 brains (54). They described the segmentation of AF as composed of a ventral and dorsal segment, in line with the model of Glasser and Rilling according to whom the AF is divided into two segments, one terminating in STG and another terminating in MTG (56). Despite detailed WM *postmortem* and WM *in vivo* dissections with several tractography techniques, cortical terminations of the AF are still a matter of debate (44, 52), with discrepancies that have been highlighted in a recent review by Bernard et al. (53).

Within the theoretical framework of the language connectome, this uncertainty poses substantial problems in terms of the functional meaning of the AF whose importance for language functions, however, has been consistently proven by intraoperative brain mapping and lesion studies (2, 31, 57, 58).

In 2012, Bizzi et al. described the importance of AF in determining preoperative aphasia. Interestingly, they showed how aphasia in patients with gliomas was related with tumoral damage to the subcortical WM more than to the infiltration of the cortex offering an indirect proof about the difference of cortical and subcortical plasticity (29). In a recent study on 54 patients undergoing surgical resection of a brain tumor, Li and colleagues showed that onset of postoperative aphasia was associated with a resection border distance to AF <5 mm as seen on postoperative DTI-T (59). In 2018, Ille et al. studied 10 patients with preoperative and postoperative DTI-T for surgical planning of left-sided glioma resection. They found that integrity of AF at DTI-T correlated with preservation of language functions, whereas patients who showed postoperative DTI-T loss of AF fibers manifested a non-fluent aphasia (60). Results by Ille et al. and Li et al. are in line with previous findings by Caverzasi et al. (61). They described preoperative and postoperative diffusion tractography of 78 patients harboring a glioma in the left hemisphere and undergoing surgical resection and found that preservation of AF was associated with a better

outcome in terms of language function also in those patients with an early postoperative speech deficit (61).

Taken together, these studies demonstrate that damage to AF within the dominant hemisphere is a crucial factor for the onset of aphasia. Moreover, a damage of AF is also suspected to hinder the reorganization of subcortical components of the entire language network that would be necessary for recovery from aphasia. Recently, in fact, it has been proposed that the dominant IFOF and AF should be considered as "non-resectable" tracts in contrast to other WM tract that can be resected without inducing deficits (50). For example, Inferior Longitudinal Fasciculus (ILF) can be considered "resectable" with a high compensatory index, whereas Inferior Fronto-Occipital Fasciculus (IFOF) can be considered with a low plastic potential when damaged in its middle and posterior part (22). AF is known to have a low compensatory index with a low plastic potential (10). AF and IFOF bear a rich bulk of connections between the temporal and frontal lobes and subserve a wide range of cognitive functions. The neuroplasticity potential of subcortical tracts might not be sufficiently efficient for a rewiring of such widespread connectivity in the presence of damage to the IFOF and AF (20). To this respect, AF representation within the non-dominant hemisphere may be of some relevance.

LATERALIZATION OF ARCUATE FASCICULUS IN RELATION TO HEMISPHERIC LANGUAGE DOMINANCE AND RECOVERY FROM APHASIA

WM interindividual variability and interhemispheric variability have been confirmed by Rademacher in 2001 and by Bürgel et al. in *postmortem* studies with microarchitectonic and MRI dissections (62, 63). In particular, WM symmetry was found on fiber tracts undergoing early myelinization like the corticospinal tract and the optic radiation, while an important asymmetry among long tracts such as AF was found, which undergo a later myelinization during the ontogeny (64). More specifically, asymmetry of the AF has been repeatedly reported in the normal brain. The direct segment, in particular, seems to be often undetected in one of the two hemispheres, usually the non-dominant one (37, 42). Such asymmetry is revealed also by DTI-T studies. Catani and colleagues found that in 62.5% of a group of healthy right-handers the AF could be reconstructed only on the left side, whereas in another 20% of subjects, it was bilateral but showed a significant leftward asymmetry (42). Such results have been confirmed by high-resolution diffusion tractography (39), but some contradicting results are reported in few WM dissection studies (37, 54, 55). Despite these discrepancies, the asymmetrical representation of AF is overall a robust finding to justify the question about its relevance for language lateralization and its possible role for aphasia recovery, as suggested by some studies that have started exploring this issue using diffusion tractography (15, 19, 65).

Forkel et al. (15) suggested that the degree of recovery from aphasia after brain ischemia may be significantly related with the volume of the right AF, suggesting a possible compensative role of AF within the non-dominant hemisphere in case of subcortical damage of the dominant one. This is particularly true in children, as demonstrated by Goradia et al. on 10 children operated on for left temporal lobe epilepsy (65). They documented an increase of the fiber density in right AF of 8 of 10 patients as a compensatory mechanism after surgery, with only one patient experiencing a decline in language performance after surgery (65). A recent study by Jiao et al. conducted on patients undergoing surgical removal of brain arteriovenous malformations in the left IPL confirmed the compensatory role of the non-dominant AF (16). In all patients of this study, surgery was associated with a damage of the left AF, which resulted in language deficit. However, DTI-T performed 6 months after surgery documented an increased number of reconstructed fibers of the right AF, and 5 of 6 patients recovered from the postoperative language deficit with a reorganization of their language areas in the right hemisphere as revealed by fMRI data (16). Similar results are reported in a case described by Chernoff (66). Taken together, these findings might suggest that the right AF may sustain functional recovery from aphasia and reorganization of the language brain network even after surgical damage.

As it may be expected, asymmetrical representation of AF is commonly found also in DTI-T performed for surgical planning of patients with gliomas. An example of AF asymmetry in one patient treated at our hospital can be seen in **Figure 1**, whereas **Table 1** reports the main studies including AF tractography for surgical planning on patients with gliomas. Only few of them took into account contralesional WM bundles (19, 69, 70). In 2018, Jehna et al. demonstrated that, at presentation, language functions were worse in patients in whom the AF was left-lateralized, whereas patients with symmetric or right-lateralized AF reconstructions showed better language performance (19). Moreover, within their cohort, patients with rapidly growing tumors showed worse performance at verbal semantic fluency test at presentation when compared with slow-growing tumor patients. Similar findings were reported by Incekara et al. (68). They found that patients in which gliomas were associated with microstructural changes of the AF had a low verbal semantic fluency, and those harboring a high-grade glioma had the worst performance (68). These few studies suggest that contralateral AF may play a role also in adults harboring a glioma within the language-dominant hemisphere.

From a functional point of view, the relevance of asymmetrical DTI-T representation of AF for lateralization of language functions has been partially questioned by studies on left-handers (71, 72). These studies stem from the assumption that the dominant hemisphere for language is also usually associated with contralateral handedness. In a particularly large study, Allendrofer et al. who performed DTI-T in 82 atypical-handers and 158 right-handers, found leftward asymmetry of AF reconstruction in both groups (72). However, in another study, Vernooij et al. (71) showed that, despite the proportion of cases with a leftward asymmetry of AF, reconstruction on DTI-T in left-handers was similar to that of right-handers; when language dominance was also taken into account as revealed by fMRI, the proportion of AF leftward asymmetry in left-handers with

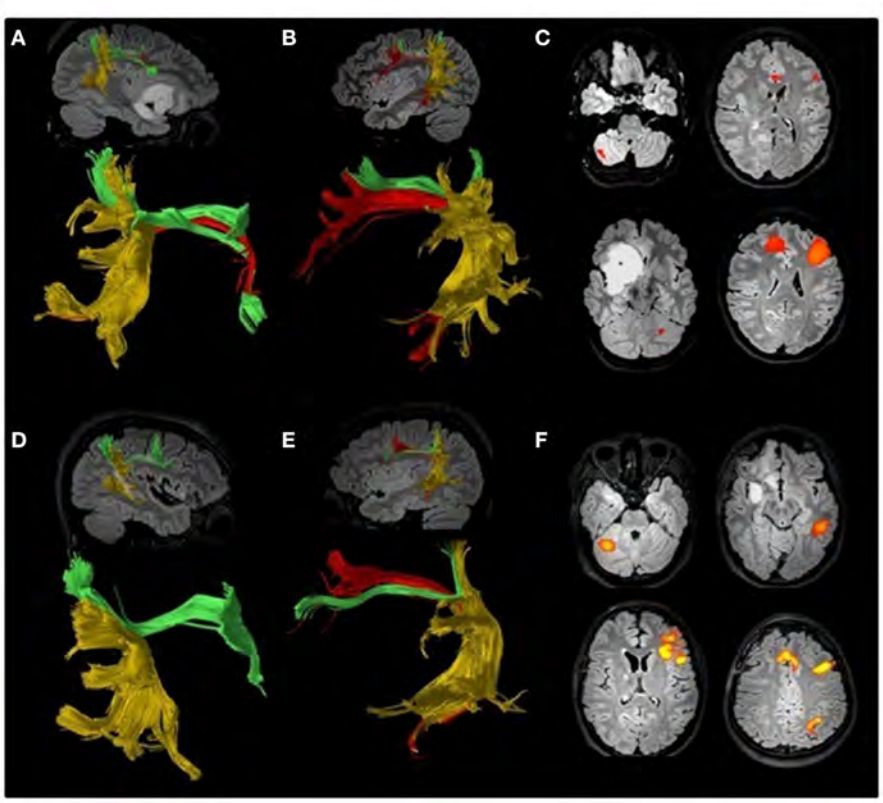

FIGURE 1 | Preoperative **(A–C)** and postoperative **(D–F)** DTI tractography and fMRI study of an 18-year-old ambidextrous woman with a right frontotemporoinsular low-grade glioma. Arcuate fasciculus (AF, red) has been reconstructed according to the method proposed by Catani (12) separating it from the anterior horizontal (green) and posterior vertical (yellow) bundles. A lower number of AF reconstructed fibers can be seen on the right hemisphere **(A)** compared to the left **(B)**. Preoperative fMRI **(C)** suggested left language lateralization. Direct cortical stimulation performed during awake surgery detected episodes of speech arrest, suggesting some degree of language lateralization to the right hemisphere. Postoperative DTI confirmed the asymmetry between the right **(D)** and left **(E)** AF, and fMRI **(F)** was consistent with a clear lateralization of language functions to the left hemisphere.

right-hemisphere language dominance increased to 100% (72). Thus, even if the degree of lateralization of DTI-T reconstruction alone may not be a good index for predicting language recovery in case of brain damage, it may add valuable information if combined with other functional measure such as fMRI. A method to directly link functional and tractography data is the use of transcranial magnetic stimulation (TMS) combined with coregistration to MRI structural and functional data by means of a neuronavigation software (14, 67). TMS allows a direct cortical and subcortical stimulation from the scalp and is able to induce a transient neurological deficit. Neuronavigated TMS (nTMS) allows to aim the neurophysiological stimulation according to the brain imaging to explore functional responses induced in specific cortical regions (41, 73). In this view, nTMS represents a very useful tool for preoperative neurophysiological mapping of the brain. Many studies show that nTMS has a good correlation with intraoperative findings obtained with direct cortical stimulation (DCS) (74, 75), although a first experience published by Picht et al. about correlation between DCS during awake craniotomy and presurgical nTMS showed a low positive predictive value of nTMS compared to DCS (76). For this reason, as suggested by some authors, nTMS for language mapping should be used with awake DCS, when possible, while nTMS alone should be only used as a rescue measure in patients not eligible for awake surgery with good results (72, 73, 77). In this view, Krieg et al. reported a standardized protocol to reduce technical limitations and increase the accuracy of nTMS language mapping (78). Recently, Sollmann et al. stratified the risk for language deficits using nTMS and described the "lesion-to-tract distance" as a predictive marker of postoperative deficit (74). Thus, combination of nTMS, fMRI, and DTI-T may shed new light on the functional importance of DTI-T asymmetries of AF for language lateralization both for assessing presurgical risk of aphasia and for understanding their roles in functional recovery in case of language deficits induced by surgery.

CONCLUSIONS

Based on our review, subcortical plasticity may play a significant role in compensating the damage to language brain networks induced by gliomas of the language-dominant hemisphere. However, further studies are needed to fully understand its role and how to take it into account for presurgical risk assessment.

TABLE 1 | The main articles cited in this mini review and focused on presurgical planning, DTI-T for AF, and postoperative outcome.

References	Type of study	No. of pts	Results
Goradia et al. (65)	Pre-operative planning and post-operative ouctome	10	Children undergoing left temporal lobectomy for epilepsy. Increase of fiber density in the right AF
Bizzi et al. (29)	Pre-operative planning	19	Aphasia in patients with gliomas is mainly due to damage of subcortical networks
Zhao et al. (58)	Pre-operative planning and post-operative ouctome	11	Adjustment of pre-operative DTI with intraoperative MRI allows preservation of AF during surgical resection
Kinoshita et al. (2)	Pre-operative planning and post-operative ouctome	12	Significant relation between preoperative increasing value of the FA of the arcuate fasciculus in the dominant hemisphere and postoperative language recovery in patients with gliomas
Caverzasi et al. (61)	Pre-operative planning and post-operative ouctome	78	Preservation of AF/SLF on post-operative tractography is related with recovery from post-operative aphasia
Ille et al. (67)	Pre-operative planning and post-operative ouctome	10	Lose of AF on post-operative MRI is related with non-fluent aphasia
Incekara et al. (68)	Pre-operative planning	77	Significant correlation between FA alterations in AF and language deficits in patients with gliomas
Jehna et al. (19)	Pre-operative planning	27	Language functions at presentation in patients with left hemisphere gliomas were worse in case the AF was left-lateralized
Li et al. (59)	Pre-operative planning and post-operative ouctome	54	Post-operative aphasia is developed when glioma resection reaches <5 mm from AF
Jiao et al. (16)	Pre-operative planning and post-operative ouctome	6	Patients undergoing resection of artero-venous malformations in the left IPL recovered from post-operative aphasia due to a compensatory increase of AF fiber density in the right hemisphere

Studying the whole WM organization, extending DTI-T reconstruction to association bundles connecting homologous language brain areas of the contralesionally hemisphere might be of help in better understanding postsurgical outcome and possible compensatory mechanisms in case of damage of associative WM bundles critical for language and located near the tumor. Moreover, a longitudinal follow-up might be of help in understanding the potential plasticity of subcortical networks after surgery. Navigated TMS could represent the future tool for studying the functional connectivity in brain tumor patients and may be able to better define if and how a right AF could supply to a language deficit induced by damage of a left-dominant AF after surgery. Along with the AF, possible compensatory roles for other long WM bundles in the non-dominant hemisphere, like the ILF or IFOF, might be matter of research with the same methodology and may prepare the path to translate brain connectionist models to the clinical practice.

AUTHOR CONTRIBUTIONS

AD, CG, and CdL: concept and writing. GB: writing and elaboration of DTI. MS, IM, CF, and VI: literature analysis and manuscript revision. All authors contributed to the article and approved the submitted version.

REFERENCES

1. Habets EJJ, Kloet A, Walchenbach R, Vecht CJ, Klein M, Taphoorn MJB. Tumour and surgery effects on cognitive functioning in high-grade glioma patients. *Acta Neurochir.* (2014) 156:1451–9. doi: 10.1007/s00701-014-2115-8
2. Kinoshita M, Nakada M, Okita H, Hamada J-I, Hayashi Y. Predictive value of fractional anisotropy of the arcuate fasciculus for the functional recovery of language after brain tumor resection: a preliminary study. *Clin Neurol Neurosurg.* (2014) 117:45–50. doi: 10.1016/j.clineuro.2013.12.002
3. Sanai N, Polley M-Y, McDermott MW, Parsa AT, Berger MS. An extent of resection threshold for newly diagnosed glioblastomas. *J Neurosurg.* (2011) 115:3–8. doi: 10.3171/2011.2.JNS10998
4. Coburger J, Scheuerle A, Pala A, Thal D, Wirtz CR, König R. Histopathological insights on imaging results of intraoperative magnetic resonance imaging, 5-aminolevulinic acid, and intraoperative ultrasound in glioblastoma surgery. *Neurosurgery.* (2017) 81:165–74. doi: 10.1093/neuros/nyw143
5. Bunevicius A, Tamasauskas S, Deltuva V, Tamasauskas A, Radziunas A, Bunevicius R. Predictors of health-related quality of life in neurosurgical brain tumor patients: focus on patient-centered perspective. *Acta Neurochirurg.* (2014) 156:367–74. doi: 10.1007/s00701-013-1930-7
6. Hervey-Jumper SL, Berger MS. Maximizing safe resection of low- and high-grade glioma. *J Neurooncol.* (2016) 130:269–82. doi: 10.1007/s11060-016-2110-4
7. DI Cristofori A, Carrabba G, Lanfranchi G, Menghetti C, Rampini P, Caroli M. Continuous tamoxifen and dose-dense temozolomide in recurrent glioblastoma. *Anticancer Res.* (2013) 33:3383–9.
8. Zarino B, Di Cristofori A, Fornara GA, Bertani GA, Locatelli M, Caroli M, et al. Long-term follow-up of neuropsychological functions in patients with high grade gliomas: can cognitive status predict patient's outcome after surgery? *Acta Neurochir.* (2020) 162:803–12. doi: 10.1007/s00701-020-04230-y
9. Bello L, Gambini A, Castellano A, Carrabba G, Acerbi F, Fava E, et al. Motor and language DTI Fiber Tracking combined with intraoperative subcortical mapping for surgical removal of gliomas. *Neuroimage.* (2008) 39:369–82. doi: 10.1016/j.neuroimage.2007.08.031
10. Ius T, Angelini E, Thiebaut de Schotten M, Mandonnet E, Duffau H. Evidence for potentials and limitations of brain plasticity using an atlas of functional resectability of WHO grade II gliomas: towards a "minimal common brain." *NeuroImage.* (2011) 56:992–1000. doi: 10.1016/j.neuroimage.2011.03.022

11. Chen X, Dai J, Jiang T. Supratentorial WHO grade II glioma invasion: a morphologic study using sequential conventional MRI. *Br J Neurosurg.* (2010) 24:196–201. doi: 10.3109/02688690903518239
12. Catani M, Jones DK, ffytche DH. Perisylvian language networks of the human brain. *Ann Neurol*. (2005) 57:8–16. doi: 10.1002/ana.20319
13. Börner K, Sanyal S, Vespignani A. Network science. *Ann Rev Info Sci Tech*. (2007) 41:537–607. doi: 10.1002/aris.2007.1440410119
14. Julkunen P, Karhu J. Brain plasticity in neurosurgery. In: Krieg SM, editor. *Navigated Transcranial Magnetic Stimulation in Neurosurgery*. Cham: Springer International Publishing. (2017). p. 267–85. doi: 10.1007/978-3-319-54918-7_16
15. Forkel SJ, Thiebaut de Schotten M, Dell'Acqua F, Kalra L, Murphy DGM, Williams SCR, et al. Anatomical predictors of aphasia recovery: a tractography study of bilateral perisylvian language networks. *Brain*. (2014) 137:2027–39. doi: 10.1093/brain/awu113
16. Jiao Y, Lin F, Wu J, Li H, Fu W, Huo R, et al. Plasticity in language cortex and white matter tracts after resection of dominant inferior parietal lobule arteriovenous malformations: a combined fMRI and DTI study. *J Neurosurg.* (2020) 20:1–8. doi: 10.3171/2019.12.JNS191987
17. Duffau H, Taillandier L, Gatignol P, Capelle L. The insular lobe and brain plasticity: lessons from tumor surgery. *Clin Neurol Neurosurg*. (2006) 108:543–8. doi: 10.1016/j.clineuro.2005.09.004
18. Duffau H. Lessons from brain mapping in surgery for low-grade glioma: insights into associations between tumour and brain plasticity. *Lancet Neurol*. (2005) 4:476–86. doi: 10.1016/S1474-4422(05)70140-X
19. Jehna M, Becker J, Zaar K, von Campe G, Mahdy Ali K, Reishofer G, et al. Symmetry of the arcuate fasciculus and its impact on language performance of patients with brain tumors in the language-dominant hemisphere. *J Neurosurg.* (2017) 127:1407–16. doi: 10.3171/2016.9.JNS161281
20. Duffau H. Does post-lesional subcortical plasticity exist in the human brain? *Neurosci Res.* (2009) 65:131–5. doi: 10.1016/j.neures.2009.07.002
21. Duffau H. Brain plasticity: from pathophysiological mechanisms to therapeutic applications. *J Clin Neurosci.* (2006) 13:885–97. doi: 10.1016/j.jocn.2005.11.045
22. Herbet G, Maheu M, Costi E, Lafargue G, Duffau H. Mapping neuroplastic potential in brain-damaged patients. *Brain*. (2016) 139:829–44. doi: 10.1093/brain/awv394
23. Duffau H. Stimulation mapping of white matter tracts to study brain functional connectivity. *Nat Rev Neurol*. (2015) 11:255–65. doi: 10.1038/nrneurol.2015.51
24. Yordanova YN, Moritz-Gasser S, Duffau H. Awake surgery for WHO Grade II gliomas within "noneloquent" areas in the left dominant hemisphere: toward a "supratotal" resection: clinical article. *JNS*. (2011) 115:232–9. doi: 10.3171/2011.3.JNS101333
25. Duffau H. The error of Broca: from the traditional localizationist concept to a connectomal anatomy of human brain. *J Chem Neuroanatomy*. (2018) 89:73–81. doi: 10.1016/j.jchemneu.2017.04.003
26. Rossi M, Conti Nibali M, Viganò L, Puglisi G, Howells H, Gay L, et al. Resection of tumors within the primary motor cortex using high-frequency stimulation: oncological and functional efficiency of this versatile approach based on clinical conditions. *J Neurosurg.* (2020) 133:642–54. doi: 10.3171/2019.5.JNS19453
27. Delgado-Fernández J, García-Pallero MÁ, Manzanares-Soler R, Martín-Plasencia P, Blasco G, Frade-Porto N, et al. Language hemispheric dominance analyzed with magnetic resonance DTI: correlation with the Wada test. *J Neurosurg*. (2020) 24:1–8. doi: 10.3171/2020.4.JNS20456
28. Matsumoto R, Okada T, Mikuni N, Mitsueda-Ono T, Taki J, Sawamoto N, et al. Hemispheric asymmetry of the arcuate fasciculus: a preliminary diffusion tensor tractography study in patients with unilateral language dominance defined by Wada test. *J Neurol*. (2008) 255:1703–11. doi: 10.1007/s00415-008-0005-9
29. Bizzi A, Nava S, Ferrè F, Castelli G, Aquino D, Ciaraffa F, et al. Aphasia induced by gliomas growing in the ventrolateral frontal region: assessment with diffusion MR tractography, functional MR imaging and neuropsychology. *Cortex*. (2012) 48:255–72. doi: 10.1016/j.cortex.2011.11.015
30. Knecht S, Dräger B, Deppe M, Bobe L, Lohmann H, Flöel A, et al. Handedness and hemispheric language dominance in healthy humans. *Brain*. (2000) 123(Pt 12):2512–8. doi: 10.1093/brain/123.12.2512
31. Kinoshita M, Miyashita K, Tsutsui T, Furuta T, Nakada M. Critical neural networks in awake surgery for gliomas. *Neurol Med Chir*. (2016) 56:674–86. doi: 10.2176/nmc.ra.2016-0069
32. Binder JR, Swanson SJ, Hammeke TA, Morris GL, Mueller WM, Fischer M, et al. Determination of language dominance using functional MRI: a comparison with the Wada test. *Neurology*. (1996) 46:978–84. doi: 10.1212/WNL.46.4.978
33. Sabbah P, Chassoux F, Leveque C, Landre E, Baudoin-Chial S, Devaux B, et al. Functional MR imaging in assessment of language dominance in epileptic patients. *NeuroImage*. (2003) 18:460–7. doi: 10.1016/S1053-8119(03)00025-9
34. Meinhold T, Hofer W, Pieper T, Kudernatsch M, Staudt M. Presurgical language fMRI in children, adolescents and young adults: a validation study. *Clin Neuroradiol*. (2020) 30:691–704. doi: 10.1007/s00062-019-00852-7
35. Raffa G, Conti A, Scibilia A, Sindorio C, Quattropani MC, Visocchi M, et al. Functional Reconstruction of Motor and Language Pathways Based on Navigated Transcranial Magnetic Stimulation and DTI Fiber Tracking for the Preoperative Planning of Low Grade Glioma Surgery: A New Tool for Preservation and Restoration of Eloquent Networks. In: M. Visocchi, H. M. Mehdorn, Y. Katayama, K. R. H. von Wild, editors. *Trends in Reconstructive Neurosurgery* Acta Neurochirurgica Supplement. Cham: Springer International Publishing (2017). p. 251–61. doi: 10.1007/978-3-319-39546-3_37
36. Soni N, Mehrotra A, Behari S, Kumar S, Gupta N. Diffusion-tensor imaging and tractography application in pre-operative planning of intra-axial brain lesions. *Cureus*. (2017) 9:e1739. doi: 10.7759/cureus.1739
37. Thiebaut de Schotten M, Ffytche DH, Bizzi A, Dell'Acqua F, Allin M, Walshe M, et al. Atlasing location, asymmetry and inter-subject variability of white matter tracts in the human brain with MR diffusion tractography. *NeuroImage*. (2011) 54:49–59. doi: 10.1016/j.neuroimage.2010.07.055
38. Sarubbo S, De Benedictis A, Merler S, Mandonnet E, Balbi S, Granieri E, et al. Towards a functional atlas of human white matter: functional atlas of white matter. *Hum Brain Mapp*. (2015) 36:3117–36. doi: 10.1002/hbm.22832
39. Fernández-Miranda JC, Wang Y, Pathak S, Stefaneau L, Verstynen T, Yeh F-C. Asymmetry, connectivity, and segmentation of the arcuate fascicle in the human brain. *Brain Struct Funct*. (2015) 220:1665–80. doi: 10.1007/s00429-014-0751-7
40. Maier-Hein KH, Neher PF, Houde J-C, Côté M-A, Garyfallidis E, Zhong J, et al. The challenge of mapping the human connectome based on diffusion tractography. *Nat Commun*. (2017) 8:1349. doi: 10.1038/s41467-017-01285-x
41. Raffa G, Quattropani MC, Germanò A. When imaging meets neurophysiology: the value of navigated transcranial magnetic stimulation for preoperative neurophysiological mapping prior to brain tumor surgery. *Neurosurg Focus*. (2019) 47:E10. doi: 10.3171/2019.9.FOCUS19640
42. Catani M, Allin MPG, Husain M, Pugliese L, Mesulam MM, Murray RM, et al. Symmetries in human brain language pathways correlate with verbal recall. *Proc Natl Acad Sci USA*. (2007) 104:17163–8. doi: 10.1073/pnas.0702116104
43. Geschwind N. The organization of language and the brain: language disorders after brain damage help in elucidating the neural basis of verbal behavior. *Science*. (1970) 170:940–4. doi: 10.1126/science.170.3961.940
44. Tremblay P, Dick AS. Broca and Wernicke are dead, or moving past the classic model of language neurobiology. *Brain Language*. (2016) 162:60–71. doi: 10.1016/j.bandl.2016.08.004
45. Dick AS, Bernal B, Tremblay P. The language connectome: new pathways, new concepts. *Neuroscientist*. (2014) 20:453–67. doi: 10.1177/1073858413513502
46. Fridriksson J, den Ouden D-B, Hillis AE, Hickok G, Rorden C, Basilakos A, et al. Anatomy of aphasia revisited. *Brain*. (2018) 141:848–62. doi: 10.1093/brain/awx363
47. Poologaindran A, Lowe SR, Sughrue ME. The cortical organization of language: distilling human connectome insights for supratentorial neurosurgery. *J Neurosurg.* (2020) 1:1–8. doi: 10.3171/2020.5.JNS191281
48. Hickok G, Poeppel D. The cortical organization of speech processing. *Nat Rev Neurosci*. (2007) 8:393–402. doi: 10.1038/nrn2113
49. Ungerleider L. "What" and "where" in the human brain. *Curr Opin Neurobiol.* (1994) 4:157–65. doi: 10.1016/0959-4388(94)90066-3
50. Duffau H, Moritz-Gasser S, Mandonnet E. A re-examination of neural basis of language processing: proposal of a dynamic hodotopical model from data provided by brain stimulation mapping during picture naming. *Brain Language*. (2014) 131:1–10. doi: 10.1016/j.bandl.2013.05.011

51. Reil J. Die sylvische Grube. *Archiv für die Physiologie.* (1809) 9:195–208.
52. Dick AS, Tremblay P. Beyond the arcuate fasciculus: consensus and controversy in the connectional anatomy of language. *Brain*. (2012) 135:3529–50. doi: 10.1093/brain/aws222
53. Bernard F, Zemmoura I, Ter Minassian A, Lemée J-M, Menei P. Anatomical variability of the arcuate fasciculus: a systematical review. *Surg Radiol Anat*. (2019) 41:889–900. doi: 10.1007/s00276-019-02244-5
54. Yagmurlu K, Middlebrooks EH, Tanriover N, Rhoton AL. Fiber tracts of the dorsal language stream in the human brain. *JNS*. (2016) 124:1396–405. doi: 10.3171/2015.5.JNS15455
55. Martino J, De Witt Hamer PC, Berger MS, Lawton MT, Arnold CM, de Lucas EM, et al. Analysis of the subcomponents and cortical terminations of the perisylvian superior longitudinal fasciculus: a fiber dissection and DTI tractography study. *Brain Struct Funct*. (2013) 218:105–21. doi: 10.1007/s00429-012-0386-5
56. Glasser MF, Rilling JK. DTI Tractography of the human Brain's language pathways. *Cereb Cortex*. (2008) 18:2471–82. doi: 10.1093/cercor/bhn011
57. Duffau H, Gatignol P, Denvil D, Lopes M, Capelle L. The articulatory loop: study of the subcortical connectivity by electrostimulation: *NeuroReport*. (2003) 14:2005–8. doi: 10.1097/00001756-200310270-00026
58. Zhao Y, Chen X, Wang F, Sun G, Wang Y, Song Z, Xu B. Integration of diffusion tensor-based arcuate fasciculus fibre navigation and intraoperative MRI into glioma surgery. *J Clin Neurosci.* (2012) 19:255–61. doi: 10.1016/j.jocn.2011.03.041
59. Li F-Y, Liu H-Y, Zhang J, Sun Z-H, Zhang J-S, Sun G-C, et al. Identification of risk factors for poor language outcome in surgical resection of glioma involving the arcuate fasciculus: an observational study. *Neural Regen Res*. (2021) 16:333. doi: 10.4103/1673-5374.290901
60. Ille S, Engel L, Kelm A, Meyer B, Krieg SM. Language-eloquent white matter pathway tractography and the course of language function in glioma patients. *Front Oncol*. (2018) 8:572. doi: 10.3389/fonc.2018.00572
61. Caverzasi E, Hervey-Jumper SL, Jordan KM, Lobach IV, Li J, Panara V, et al. Identifying preoperative language tracts and predicting postoperative functional recovery using HARDI q-ball fiber tractography in patients with gliomas. *JNS*. (2016) 125:33–45. doi: 10.3171/2015.6.JNS142203
62. Bürgel U, Amunts K, Hoemke L, Mohlberg H, Gilsbach JM, Zilles K. White matter fiber tracts of the human brain: three-dimensional mapping at microscopic resolution, topography and intersubject variability. *NeuroImage*. (2006) 29:1092–105. doi: 10.1016/j.neuroimage.2005.08.040
63. Rademacher J. Variability and asymmetry in the human precentral motor system: a cytoarchitectonic and myeloarchitectonic brain mapping study. *Brain*. (2001) 124:2232–58. doi: 10.1093/brain/124.11.2232
64. Paus T, Collins DL, Evans AC, Leonard G, Pike B, Zijdenbos A. Maturation of white matter in the human brain: a review of magnetic resonance studies. *Brain Res Bull.* (2001) 54:255–66. doi: 10.1016/S0361-9230(00)00434-2
65. Goradia D, Chugani HT, Govindan RM, Behen M, Juhász C, Sood S. Reorganization of the right arcuate fasciculus following left arcuate fasciculus resection in children with intractable epilepsy. *J Child Neurol*. (2011) 26:1246–51. doi: 10.1177/0883073811402689
66. Chernoff BL, Teghipco A, Garcea FE, Belkhir R, Sims MH, Paul DA, et al. Reorganized language network connectivity after left arcuate fasciculus resection: a case study. *Cortex*. (2020) 123:173–84. doi: 10.1016/j.cortex.2019.07.022
67. Ille S, Sollmann N, Butenschoen VM, Meyer B, Ringel F, Krieg SM. Resection of highly language-eloquent brain lesions based purely on rTMS language mapping without awake surgery. *Acta Neurochir*. (2016) 158:2265–75. doi: 10.1007/s00701-016-2968-0
68. Incekara F, Satoer D, Visch-Brink E, Vincent A, Smits M. Changes in language white matter tract microarchitecture associated with cognitive deficits in patients with presumed low-grade glioma. *J Neurosurg.* (2019) 130:1538–46. doi: 10.3171/2017.12.JNS171681
69. Liu D, Liu Y, Hu X, Hu G, Yang K, Xiao C, et al. Alterations of white matter integrity associated with cognitive deficits in patients with glioma. *Brain Behav*. (2020) 10:1–12. doi: 10.1002/brb3.1639
70. Jütten K, Mainz V, Gauggel S, Patel HJ, Binkofski F, Wiesmann M, et al. Diffusion tensor imaging reveals microstructural heterogeneity of normal-appearing white matter and related cognitive dysfunction in glioma patients. *Front Oncol*. (2019) 9:536. doi: 10.3389/fonc.2019.00536
71. Vernooij MW, Smits M, Wielopolski PA, Houston GC, Krestin GP, van der Lugt A. Fiber density asymmetry of the arcuate fasciculus in relation to functional hemispheric language lateralization in both right- and left-handed healthy subjects: a combined fMRI and DTI study. *NeuroImage*. (2007) 35:1064–76. doi: 10.1016/j.neuroimage.2006.12.041
72. Allendorfer JB, Hernando KA, Hossain S, Nenert R, Holland SK, Szaflarski JP. Arcuate fasciculus asymmetry has a hand in language function but not handedness: arcuate fasciculus in handedness and language. *Hum Brain Mapp*. (2016) 37:3297–309. doi: 10.1002/hbm.23241
73. Giampiccolo D, Howells H, Bährend I, Schneider H, Raffa G, Rosenstock T, et al. Preoperative transcranial magnetic stimulation for picture naming is reliable in mapping segments of the arcuate fasciculus. *Brain Commun.* (2020) 2:fcaa158. doi: 10.1093/braincomms/fcaa158
74. Sollmann N, Zhang H, Fratini A, Wildschuetz N, Ille S, Schröder A, et al. Risk assessment by presurgical tractography using navigated TMS maps in patients with highly motor- or language-eloquent brain tumors. *Cancers*. (2020) 12:1264. doi: 10.3390/cancers12051264
75. Bulubas L, Sardesh N, Traut T, Findlay A, Mizuiri D, Honma SM, et al. Motor cortical network plasticity in patients with recurrent brain tumors. *Front Hum Neurosci*. (2020) 14:118. doi: 10.3389/fnhum.2020.00118
76. Picht T, Krieg SM, Sollmann N, Rösler J, Niraula B, Neuvonen T, et al. A comparison of language mapping by preoperative navigated transcranial magnetic stimulation and direct cortical stimulation during awake surgery. *Neurosurgery*. (2013) 72:808–19. doi: 10.1227/NEU.0b013e3182889e01
77. Hendrix P, Senger S, Simgen A, Griessenauer CJ, Oertel J. Preoperative rTMS language mapping in speech-eloquent brain lesions resected under general anesthesia: a pair-matched cohort study. *World Neurosurg.* (2017) 100:425–33. doi: 10.1016/j.wneu.2017.01.041
78. Krieg SM, Lioumis P, Mäkelä JP, Wilenius J, Karhu J, Hannula H, et al. Protocol for motor and language mapping by navigated TMS in patients and healthy volunteers; workshop report. *Acta Neurochir*. (2017) 159:1187–95. doi: 10.1007/s00701-017-3187-z

Conflict of Interest: The authors declare that the research was conducted in the absence of any commercial or financial relationships that could be construed as a potential conflict of interest.

frontiers in Neurology

ORIGINAL RESEARCH
published: 15 February 2021
doi: 10.3389/fneur.2021.648432

Risk Assessment by Pre-surgical Tractography in Left Hemisphere Low-Grade Gliomas

Tamara Ius[1], Teresa Somma[2], Cinzia Baiano[2], Ilaria Guarracino[3], Giada Pauletto[4], Annacarmen Nilo[5], Marta Maieron[6], Francesca Palese[7], Miran Skrap[1] and Barbara Tomasino[3]*

[1] Neurosurgery Unit, Department of Neurosciences, Santa Maria della Misericordia University Hospital, Udine, Italy, [2] Division of Neurosurgery, Department of Neurosciences, Reproductive and Odontostomatological Sciences, Università degli Studi di Napoli Federico II, Naples, Italy, [3] Scientific Institute, Istituto di Ricovero e Cura a Carattere Scientifico (IRCCS) E. Medea, Pordenone, Italy, [4] Neurology Unit, Department of Neurosciences, Santa Maria della Misericordia University Hospital, Udine, Italy, [5] Clinical Neurology Unit, Department of Neurosciences, Santa Maria della Misericordia University Hospital, Udine, Italy, [6] Medical Physics, Santa Maria della Misericordia University Hospital, Udine, Italy, [7] Medical Area Department, University hospital, Udine, Italy

OPEN ACCESS

Edited by:
Giovanni Raffa, University of Messina, Italy

Reviewed by:
Antonino Scibilia, Institut hospitalo-universitaire de Strasbourg, France
Francesca Graziano, University of Palermo, Italy

****Correspondence:***
Tamara Ius
tamara.ius@gmail.com

Specialty section:
This article was submitted to Neuro-Oncology and Neurosurgical Oncology, a section of the journal Frontiers in Neurology

Received: *31 December 2020*
Accepted: *25 January 2021*
Published: *15 February 2021*

Citation:
Ius T, Somma T, Baiano C, Guarracino I, Pauletto G, Nilo A, Maieron M, Palese F, Skrap M and Tomasino B (2021) Risk Assessment by Pre-surgical Tractography in Left Hemisphere Low-Grade Gliomas. Front. Neurol. 12:648432. doi: 10.3389/fneur.2021.648432

Background: Tracking the white matter principal tracts is routinely typically included during the pre-surgery planning examinations and has revealed to limit functional resection of low-grade gliomas (LGGs) in eloquent areas.

Objective: We examined the integrity of the Superior Longitudinal Fasciculus (SLF) and Inferior Fronto-Occipital Fasciculus (IFOF), both known to be part of the language-related network in patients with LGGs involving the temporo-insular cortex. In a comparative approach, we contrasted the main quantitative fiber tracking values in the tumoral (T) and healthy (H) hemispheres to test whether or not this ratio could discriminate amongst patients with different post-operative outcomes.

Methods: Twenty-six patients with LGGs were included. We obtained quantitative fiber tracking values in the tumoral and healthy hemispheres and calculated the ratio $(H_{IFOF}–T_{IFOF})/H_{IFOF}$ and the ratio $(H_{SLF}–T_{SLF})/H_{SLF}$ on the number of streamlines. We analyzed how these values varied between patients with and without post-operative neurological outcomes and between patients with different post-operative Engel classes.

Results: The ratio for both IFOF and SLF significantly differed between patient with and without post-operative neurological language deficits. No associations were found between white matter structural changes and post-operative seizure outcomes.

Conclusions: Calculating the ratio on the number of streamlines and fractional anisotropy between the tumoral and the healthy hemispheres resulted to be a useful approach, which can prove to be useful during the pre-operative planning examination, as it gives a glimpse on the potential clinical outcomes in patients with LGGs involving the left temporo-insular cortex.

Keywords: diffusion tensor imaging analysis, intraoperative electric stimulation, low-grade gliomas, inferior fronto-occipital fasciculus, arcuate fasciculus

INTRODUCTION

Low-grade gliomas (LGGs) present a surgical challenge because of the poorly defined tumoral borders and the infiltration of white matter tracts (1, 2). Maximal safe resection is the cornerstone of LGG management, in order to provide an optimal survival benefit and preserving the quality of life (3, 4). Pre-operative risk predictions based on anatomical data are insufficient in patients with language area-related LGG, mainly considering the higher inter-individual variance of functional language anatomy (2, 5). It is thus of utmost importance to develop a reliable non-invasive pre-operative method to estimate the risk of post-operative deficits in the clinical management of these patients.

Despite the inherent limitations associated with imaging reconstruction algorithms, DTI (Diffusion Tensor Imaging) has recently been included in the presurgical glioma workup to aid in the mapping of functional pathways and to prevent extensive damage associated with radical resection (3, 6). Although DTI currently represents the only way to investigate white matter in humans *in vivo* (7), providing a non-invasive and feasible method for evaluating changes in the main language pathways, its pre-operative predictive role to estimate the risk of post-operative deficits is poorly investigated.

The aim of our study is to use pre-operative DTI data to examine changes in the main pathways of the left temporal lobe, in patients with LGG and investigating relative differences within the Superior Longitudinal Fasciculus (SLF) and Inferior Fronto-Occipital Fasciculus (IFOF).

In a previous study (8), we performed such comparison in a group of thirty-seven patients with LGGs involving the corticospinal tract. In particular, a biomarker derived from DTI differences between healthy and tumoral hemisphere was explored. The study showed that patients who had a certain pre-operative index (<0.22), calculated by comparing the healthy and the impaired hemisphere, had a significantly lower risk of developing transient post-operative deficits (8).

In this current investigation, we applied the same analytic process on the SLF and IFOF in a consecutive series of patients with LGG in the temporo-insular cortex. In a comparative approach, we contrasted the main quantitative fiber tracking values in the tumoral (T) and healthy (H) hemispheres to test whether or not this ratio could discriminate among patients with different post-operative outcomes. In addition, as secondary endpoint, we also analyzed the potential relationships between the structural white matter (WM) changes induced by LGG infiltrative growing and post-operative seizure outcomes.

Abbreviations: AF, arcuate fasciculus; AS, awake surgery; ASM, anti-seizure medication; AUC, area under the curve; DES, direct electrical stimulation; DTI, diffusion tensor imaging; EOR, extent of resection; EZ, epileptogenic zone; FA, fractional anisotropy; FACT, fiber assignment by continuous tracking; FSL, Functional Magnetic Resonance Imaging of the Brain Software Libreary; H_{SLF}, healthy SLF; H_{IFOF}, healthy IFOF; IFOF, inferior fronto-occipital fasciculus; ILAE, International League Against Epilepsy; LGG, low-grade glioma; MNI, Montreal Neurological Institute; MRI, magnetic resonance imaging; NS, number of streamlines; ROC, receiver operating characteristics; ROIs, region of interests; RTNT, real time neuropsychological testing; SLF, superior longitudinal fasciculus; T_{SLF}, tumoral SLF; T_{IFOF}, tumoral IFOF; TRE, tumor-related epilepsy; VOIs, volumes of interests; WHO, World Health Organization; WM, white matter.

MATERIALS AND METHODS

Study Population

We retrospectively reviewed a consecutive series of patients operated for LGG in the left hemisphere between 2012 and 2018.

Twenty-six patients met the strict following inclusion criteria:

- Involvement of the temporo-insular cortex.
- Age $\geq$ 18 years.
- No previous surgery.
- No pre-operative chemo- or radiotherapy.
- At least 18 months of follow-up.
- Availability of pre-operative 3-Tesla MRI including DTI.
- Objective evaluation of pre-operative tumor volume and extent of resection (EOR) on MRI images in DICOM format based on T2-weighted MRI sequences.
- Revision of histopathological specimens by using the 2016 WHO Classification of Tumors of the Central Nervous System (9).
- All patients underwent awake surgery, brain mapping, neurophysiological monitoring and intraoperative real-time neuropsychological testing (RTNT).

Needle biopsies were excluded from the study.

Medical diaries were reviewed for history of tumor- related epilepsy, seizure frequency and ictal semiology, number and type of anti-seizure medications (ASMs).

The 2017 ILAE classification was applied to classify seizures (10). For statistical analysis, seizures were dichotomized, according to ictal semeiology, in motor (tonic, atonic, clonic, myoclonic, and hypermotor) and non-motor (sensory, autonomic, emotional, and cognitive) seizures. After surgery, seizures outcome was defined following the Engel Classification of Seizures and dichotomized as Engel Class Ia (completely seizure free) vs. all the others (11). Engel Class at 1-year follow-up was used for the analysis.

The local Ethics Committee, Comitato Etico Unico Regionale del Friuli Venezia Giulia, approved this investigation (protocol N.0036567/P/GEN/EGAS, ID study 2540). Considering the retrospective nature of the study, written consent to participate in the study was not applicable. Written informed consent was obtained for surgery.

Intraoperative Surgical Protocol

The surgical procedures were conducted under cortical and subcortical white matter brain mapping, according to the intraoperative technique previously described. In addition to Direct Electrical Stimulation (DES), real-time neuropsychological testing (RTNT) was applied during Awake Surgery (AS) (1, 12).

Histological and Molecular Analysis

All histological samples were reviewed according to the 2016 World Health Organization (WHO) classification (9). Molecular markers were evaluated as previously described (13).

MRI Data

Acquisition

MRI examination, anatomical and DTI images were performed at a 3T MR system (Achieva, Philips medical system) using an SENSE eight-element phased array head coil. The images included an high-resolution T2-weighted (TR/TE, = 2500/368.328 ms; FOV = 240 mm; 190 sagittal slices; voxel size, 1 × 1 × 1 mm) and a post-gadolinium contrast T1-weighted anatomic images (TR/TE = 8.100/3.707 ms; FOV = 240 mm; 190 sagittal slices; voxel size =1 × 1 × 1 mm) both optimized for the standard pre-operative clinical protocol adopted by the Department of Neuroradiology of the Azienda Ospedaliero Universitaria S. Maria della Misericordia, Udine.

In addition, for all patients, a single-shot echo-planar DTI sequence was acquired covering the whole brain (TR/TE = 8,800/74 ms; FOV= 224 mm; 54 contiguous axial slices; voxel size, 1.8 × 1.8 × 2.2 mm, b0 and b1000 s/mm2, 64 non-coplanar images). The gradient directions were uniformly distributed on a sphere. The total acquisition time for the entire protocol was ∼20 min.

TABLE 1 | Baseline characteristics of study population.

Parameters	Value
No. of patients	**26**
Sex	
Male	15 (57.69%)
Female	11 (42.31%)
Age, (years)	
Median (years and range)	35.50 (20–64)
Onset symptoms	
Seizures	24 (92.30%)
Focal seizures	12 (46.15%)
Focal to bilateral tonic-clonic seizures	12 (46.15%)
No symptoms (incidental LGG)	2 (7.70%)
Seizure Types	
Motor	12 (46.15%)
Non-motor	12 (46.15%)
Automatism and cognitive	1 (3.85%)
Cognitive	8 (30.77%)
Sensory	2 (7.69%)
Sensory-cognitive	1 (3.85%)
Pre-operative tumor volume (T2-weighted MRI images—cm^3)	
Median	36.5
Range	6–127
EOR	95.0
Median	
Range	50–100
Molecular Class	
Oligodendroglioma	6 (23.08%)
Diffuse Astrocytoma	16 (61.54%)
Astrocytoma IDH1/2 wild-type	4 (15.38%)
Post-operative Engel class at 12 months	
Ia	17 (65.38%)
Ib–IV	9 (34.62%)
Post-operative neurological deficit 1 week after surgery	
No	15 (57.69%)
Yes	11 (42.31%)
Only language	7 (26.92%)
Language + motor	4 (15.38%)
Post-operative neurological deficit at 6 months	
No	24 (92.30%)
Yes	2 (7.70%)
Only language	2 (7.70)
Mild	1 (3.85%)
Moderate—Severe	1 (3.85%)

EOR, extent of surgical resection; IDH, isocitrate dehydrogenase.
Patients' characteristics are described using median and range for continuous variables, number of cases with relative percentages (in parentheses) for categorical variables.

MRI Structural Data

Topographic and volumetric descriptions of the tumor were obtained by retrospectively analyzing structural imaging data routinely acquired during pre-surgery investigations.

Volumes of interest (VOIs) of patients' lesions were drawn on their T2 MRI scans using MRIcron software (https://www.nitrc.org/projects/mricron). We then normalized the Region of Interests (ROIs) to the Montreal Neurological Institute (MNI) space using the "Clinical Toolbox" (https://www.nitrc.org/projects/clinicaltbx/) for SPM8 (https://www.fil.ion.ucl.ac.uk/spm/).

The MRIcron procedure was used to overlap lesion masks (VOIs) (https://www.nitrc.org/projects/mricron). The output is a percentage overlay plot showing the percentage of overlapping lesions on a color scale.

Volumetric Analysis

All pre- and post-operative tumor segmentations were performed manually across axial T2-weighted and post-contrast T1-weighted MRI slices.

EOR was evaluated by using 3D T2-weighted MRI axial images as follows: (pre-operative tumor volume—post-operative tumor volume)/pre-operative tumor volume) (14).

TABLE 2 | Montreal Neurological Institute (MNI) coordinates of the areas showing higher % lesion overlap.

Area	x	y	z	% overlap
Insula	−39	3	−13	77%
Sagittal stratum (IFOF+ILF)	−39	−9	−17	73%
Uncinate Fasciculus	−34	2	−19	77%
Temporal Pole	−41	7	19	73%
Hippocampus	−38	−10	−17	73%
Superior Temporal Gyrus	−47	−5	−1	77%
Superior Longitudinal Fasciculus	−31	−2	18	23%
Superior Fronto-Occipital Fasciculus	−21	3	19	23%

IFOF, Inferior Fronto-Occipital Fasciculus; ILF, Inferior Longitudinal Fasciculus.

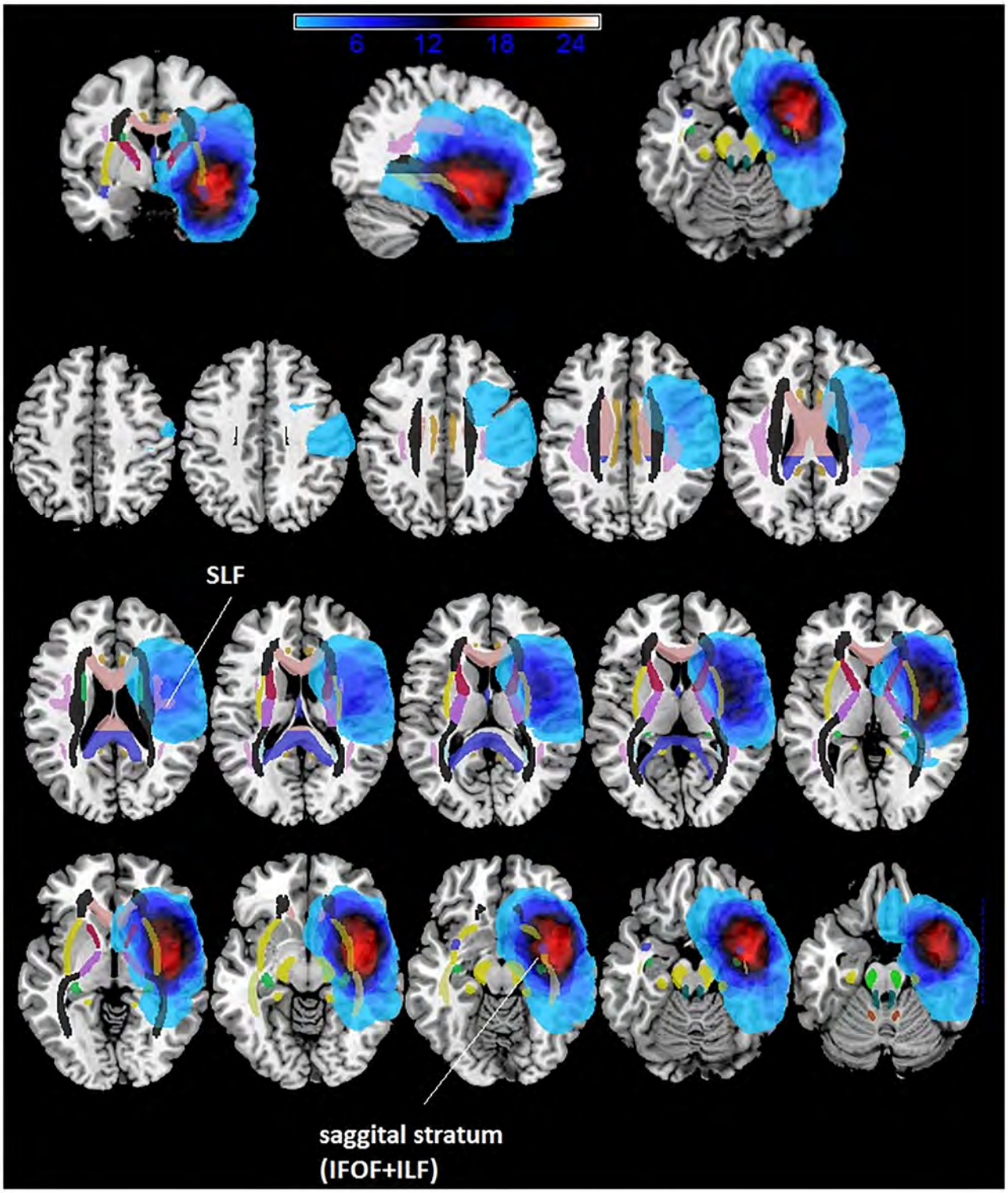

FIGURE 1 | Overlaps of lesions masks of patients with temporo-insular LGGs.

DTI: Preprocessing and Fiber Tracking Analysis

Using the FSL software (Functional Magnetic Resonance Imaging of the Brain Software Library http://www.fmrib.ox.ac.uk/fsl) DTI images were pre-processed for eddy current and head movement corrections, and a brain extraction was performed using BET tool implemented in FSL.

Those pre-processed data were later analyzed using DTI-Studio, and a three-dimensional tract reconstruction of the IFOFs was created using the FACT (Fiber Assignment by Continuous Tracking) algorithm and a multiple regions of interest (ROIs) approach. We choose a FA threshold of 0.1 and a turning angle threshold of 55° to yield biologically plausible results.

In accordance with the procedures of Wakana et al. (15), for tracking the IFOF we used two ROIs both manually drawn in a coronal plane, the first ROI included the occipital lobe, the second ROI included the entire hemisphere at the anterior part of the genu of corpus callosum. For tracking the SLF the two ROIs were located on coronal planes, the first centered at the middle of the internal capsule and the second placed at the splenium of corpus callosum. These fibers clearly don't belong to the IFOF or to the SLF and should be manually removed using "NOT."

SLF and IFOF fiber-tracking results were visually inspected to determine whether they were anatomically accurate and, if necessary, manually corrected. The number of IFOF and SLF streamlines passing through each voxel was automatically measured by the software, defined as the total NS.

The ipsilateral tumoral and healthy contralateral SLF (T_{SLF} and H_{SLF}) and IFOF (T_{IFOF} and H_{IFOF}) were both reconstructed and assessed for each patient to define potential differences between these white matter pathways induced by the presence of the brain tumor.

The number of streamlines (NS) was calculated in accordance with Ius et al. (8).

Specifically, for each patient, we calculated the ratio of the number of streamlines (NS-index) as follows:

- SLF NS-index= $(H_{SLF}-T_{SLF})/ H_{SLF}$;
- IFOF NS-index= $(H_{IFOF}-T_{IFOF})/ H_{IFOF}$.

Definition of Post-operative Neurological Outcomes

Patients were examined pre-operatively, immediately after surgery, 1-week after surgery and 6 months after surgery.

Patients' outcome examination includes the presence/absence of sensory-motor deficit and speech disorders.

Regarding language deficits, two categories were established:

- Transient aphasia or dysphasia: any new language deficit owing to surgery that resolved at 6 months follow-up;

- Permanent aphasia or dysphasia: any new language deficit owing to surgery that did not resolve at 6 months follow-up.

Statistical Analysis

Characteristics of the study population were described using the median with interquartile range of numerical variables and the percentages of categorical variables. Wilcoxon-Mann-Whitney test and non-parametric correlation were used to explore possible associations between NS-index and post-operative outcomes (expressed as dichotomous) and continuous patient characteristics, respectively.

ANOVA analysis between subjects was performed to compare patients' and healthy subjects' NS and FA for the SLF and the IFOF.

Regarding clinical parameters, post-operative language deficit was dichotomized as 0 (no deficit) and 1 (deficit: aphasia and/or dysphasia). Similarly, post-operative seizure outcome was classified as 0 (Engel Class Ia), and 1 (Engel Classes Ib-IV).

Receiver operating characteristics (ROC) analysis with estimation of 95% confidence interval (95% CI) of the area under the curve (AUC) was performed to estimate the accuracy of the NS-index in predicting post-operative outcomes, and to determine the best cut-off value to discriminate the two Engel index groups.

A bilateral $p < 0.05$ was considered significant. All statistical procedures were performed using SAS© software, version 9.4 (SAS, Cary, NC, USA).

RESULTS

Clinical Data

The baseline demographic, pre-operative clinical, and radiological characteristics of the study population are summarized in **Table 1**. Seizure was the onset symptom in 24/26 cases (92.30%). In two cases the diagnosis was incidental (7.70%). In all cases, pre-operative MRI showed hypo-intense lesions on T1-weighted sequences obtained without contrast

TABLE 3 | Baseline characteristics of FA and NS-indices both for SLF and IFOF.

DTI Parameters	Value
FA H_{IFOF}	
Median	0.50
Range	0.44–0.54
FA T_{IFOF}	
Median	0.45
Range	0.35–0.53
Number of streamlines in H_{IFOF}	
Median	299.5
Range	28–1,728
Number of streamlines in T_{IFOF}	
Median	122.0
Range	2–836
FA H_{SLF}	
Median	0.46
Range	0.40–0.50
FA T_{SLF}	
Median	0.45
Range	0.37–0.52
Number of streamlines in H_{SLF}	
Median	719
Range	199–7,521
Number of streamlines in T_{SLF}	
Median	467.0
Range	142–2,494

FA, fractional anisotropy; IFOF, Inferior Fronto-Occipital Fasciculus; SLF, Superior Longitudinal Fasciculus.
The characteristics are described using median and range.

medium and hyper-intense lesions on T2-weighted sequences. Insular lobe was involved in 17 cases, while temporal lobe in 9 cases. Immediate and 1-week post-operative language deficits were recorded in 11 cases (42.31%), while 2 patients (7.70%) developed permanent language impairment at 6 months follow-up.

MRI Structural Data

Pre-operative Tumor Volume

All the lesions were non-contrast enhancing LGGs. Pre-operative median tumor volume (cm^3) calculated on T2-weighted MRI was 36.54 ± 23.73 (range 6–127).

Maximum Lesion Overlap

The maximum overlap of the LGG lesion masks of patients mainly occurred in the left insula and superior temporal gyrus, temporal pole and the sagittal stratum (IFOF + ILF) (see **Table 2** and **Figure 1**).

Surgical Data

All patients were operated in Awake Surgery. In all cases, the resection was stopped according to DES and/or RTNT. The median EOR was 95% ± 12.24 (range 50–100).

DTI Analysis and Pre-operative Risk Factors Influencing the Outcome

Data regarding FA and NS-indices of SLF and IFOF, both in healthy and tumoral hemisphere, are reported in **Table 3** and **Figure 2**.

Correlation analysis between clinical-radiological data and NS- indices (SLF NS-index; IFOF NS-index) are displayed in **Table 4**.

In detailed, there was a significant correlation between neurological outcome and both pre-operative SLF NS-index (p = 0.009, IC 95% = 0.001–0.136) and pre-operative IFOF NS-index (p = 0.042, IC 95% = 0.001–0.854). In addition, pre-operative SLF NS-index and pre-operative IFOF NS-index appear directly correlated to each other (p = 0.028; r_s = 0.429).

We also compared patients' data with healthy controls (N = 25, all right handed, 13 F and 12 M, median age 36). The NS index was significantly different between patients and controls both for the IFOF [$F_{(1,49)} = 7.64$, $p = 0.008$] and the SLF [$F_{(1,49)} = 29.01$, $p = 0.001$]. Healthy controls data indicate that while the SLF is left lateralized (see **Figure 2**), the IFOF is almost bilateral. In addition, we found that patients had significantly lower number of streamlines for the left IFOF [$F_{(1,49)} = 4.59$, $p = 0.037$] and the left SLF [$F_{(1,49)} = 4.77$, $p = 0.034$] when compared to controls (see **Figure 2**), while for the right IFOF [$F_{(1,49)} = 1.23$, $p = 0.2$,

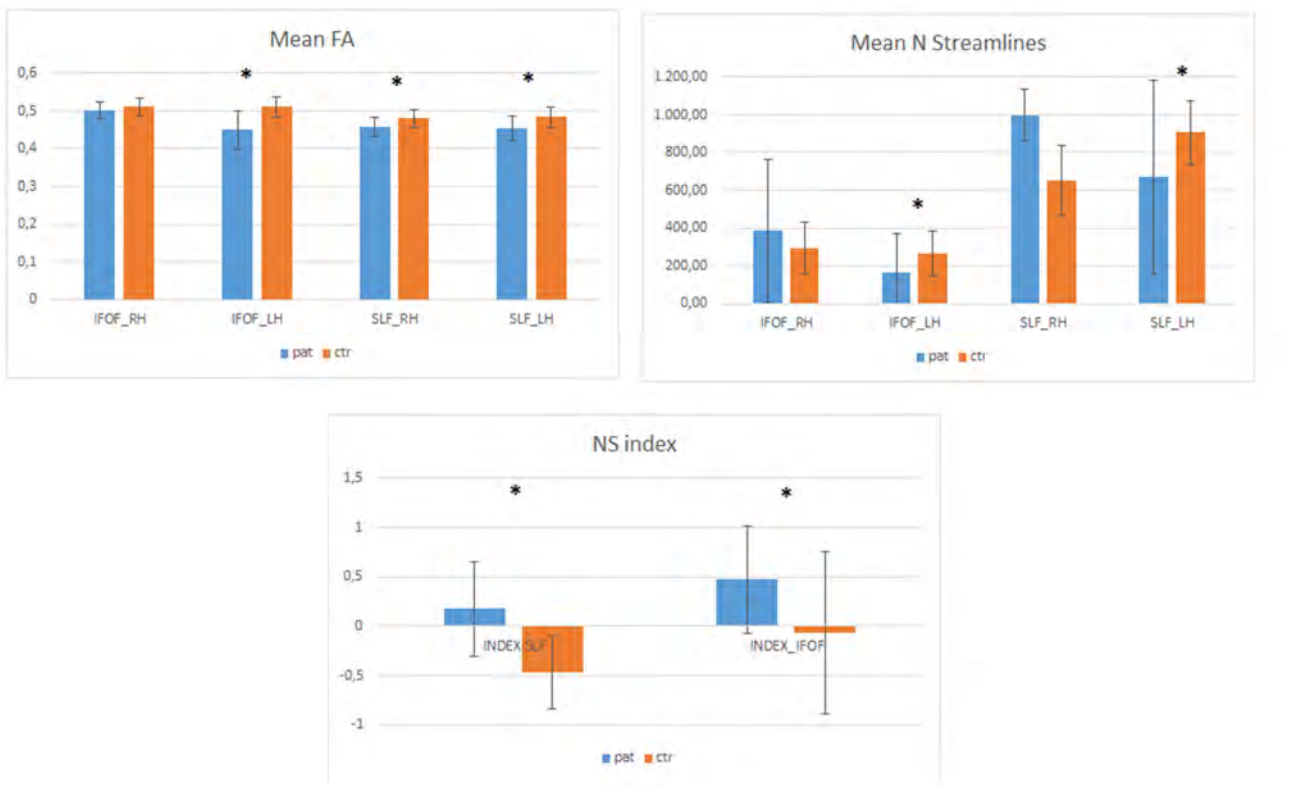

FIGURE 2 | The Plot illustrates FA (fractional anisotropy) and the number of streamlines (NS) data, expressed as mean value and standard deviations, for SLF and IFOF both in healthy (right hemisphere = RH) and tumoral (left hemisphere = LH) hemispheres for the patients (pat) and healthy controls (ctr), respectively. Asterisks denote significant differences.

TABLE 4 | Correlation analysis between clinical-radiological variables and NS-indices (Spearman's Correlation).

Spearman's correlation coefficients $N = 26$		
Variables	**IFOF NS-Index**	**SLF NS-Index**
Age		
Prob > |r|	−0.31417	0.05065
H0: Rho=0	0.1180	0.8059
Pre-operative tumor volume (T2-weighted MRI images)		
Prob > |r|	0.16393	0.17385
H0: Rho=0	0.4236	0.3957
EOR		
Prob > |r|	0.11995	−0.36204
H0: Rho=0	0.5595	0.0691
FA H_{IFOF}		
Prob > |r|	0.13472	−0.01128
H0: Rho=0	0.5117	0.9564
FA T_{IFOF}		
Prob > |r|	**−0.48632**	**−0.40253**
H0: Rho=0	**0.0118**	**0.0415**
Number of streamlines in H_{IFOF}		
Prob > |r|	0.15321	0.18947
H0: Rho=0	0.4549	0.3539
Number of streamlines in T_{IFOF}		
Prob > |r|	**−0.66644**	−0.23594
H0: Rho=0	**0.0002**	0.2459
IFOF-NS Index		
Prob > |r|	1.00000	**0.42906**
H0: Rho=0		**0.0287**
FA H_{SLF}		
Prob > |r|	−0.16345	−0.12070
H0: Rho=0	0.4250	0.5570
FA T_{SLF}		
Prob > |r|	−0.15800	−0.20725
H0: Rho=0	0.4408	0.3097
Number of streamlines in H_{SLF}		
Prob > |r|	0.36547	0.06735
H0: Rho=0	0.0664	0.7437
Number of streamlines in T_{SLF}		
Prob > |r|	−0.31966	**−0.68957**
H0: Rho=0	0.1114	**<0.0001**
SLF-NS Index		
Prob > |r|	**0.42906**	1.00000
H0: Rho=0	**0.0287**	
Post-operative neurological deficit 1 week after surgery: yes vs. no		
Prob > |r|	**−0.53457**	**−0.74217**
H0: Rho=0	**0.0049**	**<0.0001**

Bold values indicate significant results.

n.s.] and the right SLF [$F_{(1,49)} = 1.6$, $p = 0.209$, n.s.] they did not significantly differ (**Figure 3**).

In patients affected from temporo-insular LGG in dominant hemisphere, NS-index was significantly different between patients with post-operative impairment both for SLF ($p = 0.002$) and IFOF ($p = 0.008$).

In patients with post-operative deficits the median value of SLF and IFOF NS-index was 0.622 and 0.786, respectively. Otherwise in those patients with normal post-operative surgical outcome the median value of SLF and IFOF NS-index was 0.072 and 0.587, respectively.

The optimal cut-off value for the pre-operative IFOF NS-index was 0.675. It was the point with the highest sensitivity (0.727) and specificity (0.866), with a resulting area under the curve of 0.812 (CI 95% 0.635–0.988) and a predictive accuracy of 72.42%.

For the pre-operative SLF NS-index, the cut-off value of 0.248 corresponded to the point with the highest sensitivity (0.909) and specificity (0.866), with a resulting area under the curve of 0.933 (CI 95% 0.836–1) and a predictive accuracy of 86.67% (**Figure 3**).

Figures 4, **5** summarized two exemplificative conditions based on different values of SLF and IFOF NS-index.

The potential relationships between the structural white matter (WM) changes induced by LGG infiltrative growing and post-operative seizure outcome were also evaluated. No correlation has been highlighted between the FA, NS-indices and seizure outcome ($p = 0.06$ and $p = 0.91$, respectively for IFOF and SLF NS-indices).

A positive correlation between the pre-operative tumoral volume on T2 weighted MRI and both FA T_{IFOF} ($r = 0.670$; $p = 0.002$) and FA T_{SLF} ($r = 0.457$; $p = 0.018$).

In closing, we found a positive correlation between EOR and post-operatory status ($r = 0.39535$, $p = 0.0456$).

DISCUSSION

Low-grade gliomas generally affect young patients, and in almost all cases (from 70 to 90%), seizure is the onset symptom. The key point in management is based on maximal safe resection. The main technical difficulty relies on the infiltrative pattern of these tumors, especially at subcortical levels.

The cohort of patients included in this study was characterized by a relatively young age (median 35.5 years) and intermediate lesion volumes (median 36 cm^3), which were almost completely resected reaching a high EOR (median 95%). It is therefore fundamental, especially given the young age and long-life expectancy, to develop new diagnostic strategies both for surgical planning and pre-operative estimation of surgical risks.

The substantial variability of the language network organization is recognized especially in neurosurgical literature (16, 17) and represents only a superficial part of a more complex and variable networks (14, 18–21). According to the "connectionist model," there is a wide individual variability amongst both cortical areas and subcortical white matter. It is also well-documented that the brain is able to reorganize itself in pathological condition, especially in the clinical setting of slow growing tumors as LGG (20, 22–25).

In clinical practice, it would be of utmost importance to estimate the impact of surgery on the post-surgical outcomes, and to understand the potential functional recovery in response to an infiltrating slow growing tumor by means

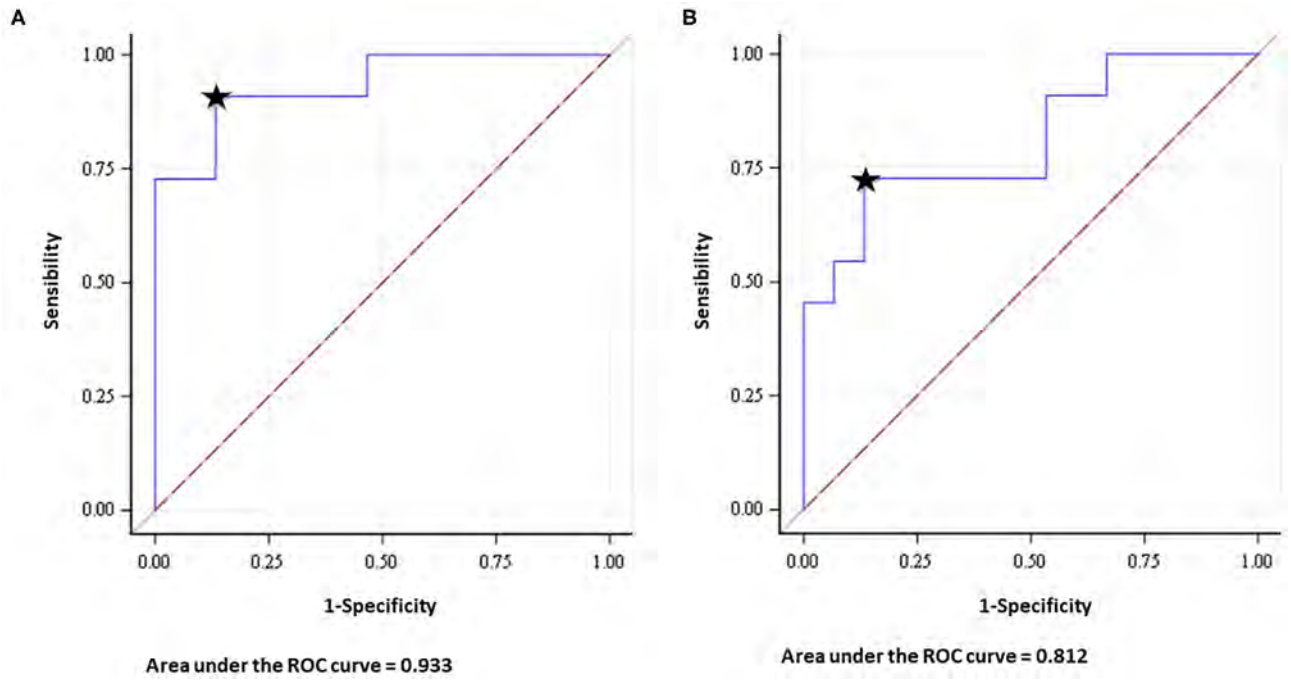

FIGURE 3 | Receiver operating characteristic (ROC) analysis showed that the area under the curve of the NS (number of streamlines) index was 0.933 (CI 95% 0.836–1) and 0.812 (CI 95% 0.635–0.988) for SLF **(A)** and IFOF **(B)**, respectively. Predictive accuracy was 86.67% for SLF and 72.42% for IFOF (It is represented by the closest point to the top left corner of the graph, indicated by the black star).

of objective measures (2, 26, 27). Given tumor-related plastic reshaping and reallocation of function, individual data are needed for patient counseling and risk assessment prior to surgery. Conventional MRI techniques provide purely anatomic information, resulting to be insufficient in patients with language area-related LGGs, mainly considering the higher inter-individual variance of functional language anatomy (2, 5, 7, 8, 21, 28–30). The DTI-based tractography has gradually become a well-established clinical tool with different applications, which include assessment of the subcortical pre-operative anatomy, characterization of epileptic networks and study of the connectomes (2, 21, 23, 28, 30–36).

The superior longitudinal fasciculus white matter complex involves transmission of speech, forming the dorsal pathway within the dual-stream model of language processing (37–39). The IFOF is mainly involved in language, specifically in lexical and semantic processing (40). With respect to naming abilities, a study involving 99 patients with glioma showed that noun naming deficits depended on damage to parts of the sagittal stratum (including the inferior fronto-occipital fasciculus and the inferior longitudinal fasciculus), in addition to cortical lesions (41). Moreover, the IFOF, together with the inferior longitudinal fasciculus, is the neuroanatomical correlate of the ventral reading route (42–45). Concerning reading, we reported that surface dyslexia could be due to impaired ventral/lexical route (as evidenced by a fractional anisotropy decrease along the inferior fronto-occipital fasciculus) in patients with glioma (46). The role of the IFOF in reading and in surface dyslexia, and of the SLF in phonological dyslexia was confirmed on a larger group study in which pre-, intra- and post-surgery reading data were presented (47).

In this investigation, we used quantitative DTI analysis in patients with LGGs involving the SLF and IFOF to estimate the potential predictive role of this technique in terms of functional post-operative outcomes. Two different white matter parameters were considered: FA and NS.

Current literature has widely documented that the FA value is lower in patients affected by glioma in comparison to FA values in healthy subjects. Our investigation confirmed these overall results. Furthermore, we found that FA values in T_{SLF} and T_{IFOF} were smaller than those in H_{SLF} and H_{IFOF}, confirming the slow infiltrative growing of LGGs (48–51).

All patients were without neurological impairment at diagnosis, despite the tumoral infiltration of white matter, supporting the brain capability to reorganize itself in pathological condition (22–24). The comparison of tumoral patient data with healthy controls highlighted that the significant effects found on the NS index, both for the IFOF and the SLF, indicate a decreased white matter representation in the pathological left hemisphere. For the right hemisphere, the differences between patients and controls were not significant, however, the mean number of streamline and standard deviations are suggestive of higher values for patients, thus implying possible plasticity related reshaping of the right hemisphere. The integrity of the IFOF and SLF, known to be part of the language-related network, were then investigated. When comparing the DTI

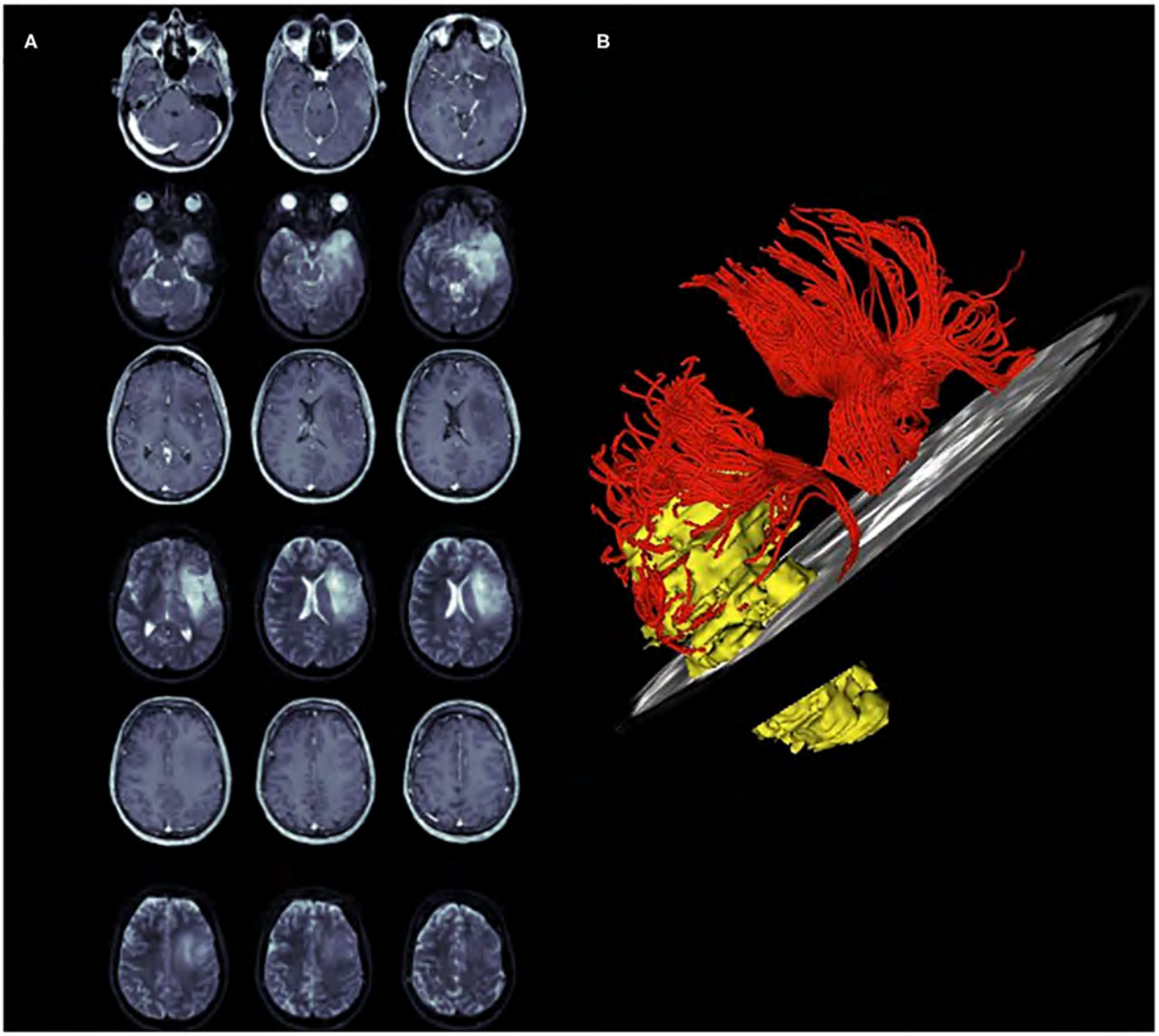

FIGURE 4 | A case of left temporo-insular low-grade glioma (LGG). The pre-operative tumor volume computed on T1-weigted MRI and on T2-weighted MRI was 36 cm^3 and 42 cm^2, respectively (axial slices **A**). **(B)** represents a 3D neurological view of the tumor, T_{SLF} and H_{SLF}. The pre-operative SLF NS-index was 0.601.

differences between the H and T hemispheres, two indices were elaborated (pre-operative SLF NS-index and pre-operative IFOF NS-index) and correlated to post-operative outcomes. Our study found that patients with pre-operative indices close to 0 (that implies a similar number of streamlines in both hemispheres) generally had less probability of developing post-operative neurological impairment. Patients with pre-operative indices close to 1 (that means a low number of streamlines in tumoral hemisphere), in contrast, were more likely to develop post-operative deficits. An SFL NS-index < 0.248, and an IFOF NS-index < 0.675 have been associated with better post-operative clinical outcomes. These results are consistent with a previous study based on DTI analysis of cortico-spinal tract in patients with premotor LGGs (8), confirming that the NS analysis of the main subcortical pathways is a valid and promising approach to pre-operatively estimate the risk of post-operative deficits.

A positive correlation was found between pre-operative SLF NS-index and pre-operative IFOF NS-index, suggesting that lesions infiltrated both, which is also consistent with the MRI structural data analyses. Lesions were shown to be mainly localized in the insula and superior temporal lobes, which are areas crossed by both the IFOF in their inferior portion and the SLF in the upper portion.

The correlations between the pre-operative tumoral volume on T2 weighted MRI and both FA T_{IFOF} and FA T_{SLF} suggest that

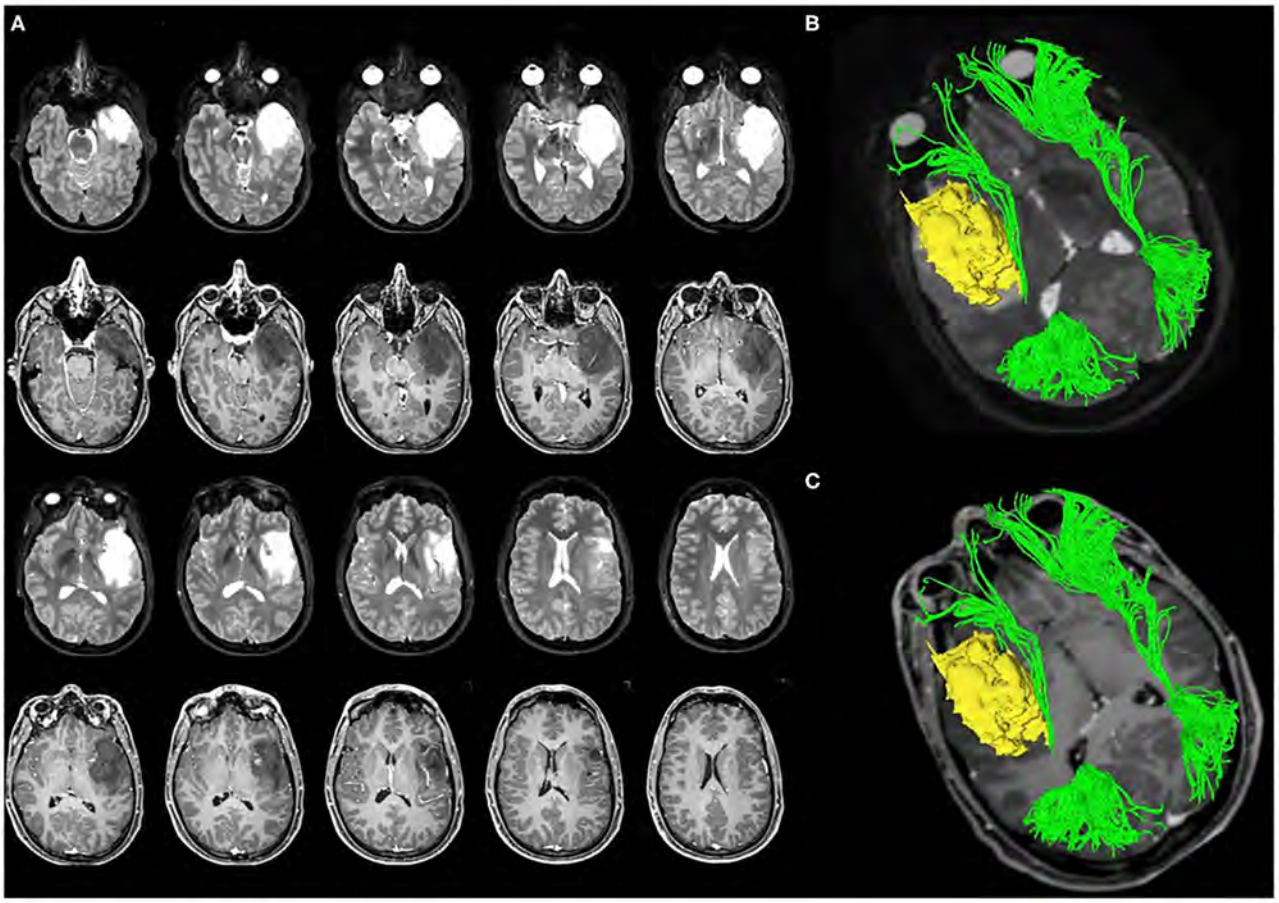

FIGURE 5 | A case of left temporo-insular low-grade glioma (LGG). The pre-operative tumor volume computed on both T1-weigted MRI and on T2-weighted MRI was 38 cm^3 (axial slices **A**). The tumor involves the Fronto-Occipital Longitudinal Fasciculus. **(B,C)** Show the 3D reconstruction of the tumor and IFOF. The pre-operative IFOF NS-index was 0.611.

higher pre-operative tumor volume may induce a higher white matter infiltration probability.

In closing, we found a positive correlation between EOR and post-operatory status, thus suggesting that maximizing the resection implies assuming the risk of observing a transient immediate post-surgery decrease. In the study, we also investigated the potential relationships between the structural changes of white matter tracts, induced by LGG infiltrative growing, and post-operative seizure outcomes. No correlation was found between the pre-operative SLF NS-index, pre-operative IFOF NS-index and post-operative seizure outcomes. These findings could be based on the possibility that the epileptogenic foci were located outside of the SLF and IFOF in our sample. It is therefore possible that concerning the cases of seizure-free patients within our cohort, the epileptogenic foci could have likely been removed with the tumor and peritumoral cortex. With regards to the patients showing poor post-operative seizure control, the failure or the impossibility of removing the epileptogenic zone, and the presence of a possible secondary epileptic focus need to be considered. In both cases, IFOF and SLF infiltration may not have been relevant. Epileptogenic processes in tumor-related epilepsy (TRE) are multifactorial and not fully understood (52). Increased evidence suggests that, in up to two-thirds of patients with glioma, seizures arise from the peritumoral cortex, due to induced changes in neurotransmitters, environment and electrical properties of these regions (53, 54). The likelihood of seizure control is thus related to the possibility of resection of the epileptogenic zone (EZ), nested in the peritumoral tissue. For this reason, the extent of resection in now recognized as one of the strongest prognostic factors for post-operative seizure control (1, 55, 56). We acknowledge that our sample is small to draw definitive considerations. Moreover, aphasic seizures were poorly represented. Regarding WM tracts, the clinical challenge, in primary brain tumor epilepsy, is represented not only by the determination of the EZ, but also by the identification of the underlying epileptic network, which requires a complex neurophysiological presurgical work-up.

There are several limitations of our study. The most important is the retrospective nature of the investigation and the small simple size. Concerning the DTI methodology, different tracking

approaches exist, although there is no consensus yet on the most suitable one. It would be interest to verify these preliminary results by using other DTI approaches.

In addition, this approach is only applicable to LGGs due to their specific biologically determined growth pattern (57). The elaboration of NS-indices based on numbers of streamlines in both hemispheres, strengthens the results, limiting the bias due to the individual variability. Moreover, an extensive neuropsychological assessment has not been included in this study, which has, however, been considered in our ongoing future studies currently underway. Despite the inherent limitation of DTI analysis, which include data acquisition, bio-mathematical models, user dependency, and software programs (58–60), it still represents the only way to investigate white matter in humans *in vivo* (7). Overall, we recognize that these preliminary results require a further validation increasing the study population and planning future prospective studies.

Future longitudinal studies, based on comparison between structural WM in healthy and tumoral hemisphere should be developed to address the strongest predictive measures of surgical risk for lesion infiltrating the functional subcortical pathways. The integration of this approach with an extensive pre- and post-operative neuropsychological assessment might provide insights into compensatory mechanisms for language deficits on the level of white matter plasticity, in patients with brain tumors. It could be of clinical importance to assess the ability of the proposed indices in identifying the risk of permanent deficits in a larger cohort of patients.

CONCLUSION

These preliminary results highlight the potential role of pre-operative DTI in assessing the risk of post-operative transient language impairment in patients undergoing surgical resection of LGGs involving the AF and IFOF in dominant hemisphere. This analytical pre-operative approach may represent a feasible predictive tool for patient counseling and risk assessment prior to surgery and pave the way to standardize approaches in glioma surgical management.

DATA AVAILABILITY STATEMENT

The raw data supporting the conclusions of this article will be made available by the authors, without undue reservation.

ETHICS STATEMENT

The studies involving human participants were reviewed and approved by the local Ethics Committee, Comitato Etico Unico Regionale del Friuli Venezia Giulia, approved this investigation (protocol N.0036567/P/GEN/EGAS, ID study 2540). Written informed consent was not provided because considering the retrospective nature of the study, written consent to participate in the study was not applicable. Written informed consent was obtained for surgery.

AUTHOR CONTRIBUTIONS

TI and BT: conception and design. IG, CB, and AN: acquisition of data. FP: formal analysis. FP and MM: software. TI, BT, TS, GP, and MS: supervision. TI, BT, and MS: validation. TI, BT, and GP: writing—original draft and review and editing. All authors have read and agreed to the published version of the manuscript. All authors had full access to all the data in the study and take responsibility for the integrity of the data and the accuracy of the data analysis.

ACKNOWLEDGMENTS

We acknowledge the support by the staff of the Medical Imaging Centre (Department of Neuroradiology of the Azienda Ospedaliero Universitaria S. Maria della Misericordia, Udine). We would like to thank Mark Zeppieri MD, Ph.D. for the English revision of the manuscript.

REFERENCES

1. Ius T, Isola M, Budai R, Pauletto G, Tomasino B, Fadiga L, et al. Low-grade glioma surgery in eloquent areas: volumetric analysis of extent of resection and its impact on overall survival. A single-institution experience in 190 patients. *J Neurosurg*. (2012) 117:1039–52. doi: 10.3171/2012.8.JNS12393
2. Mato D, Velasquez C, Gómez E, Marco de Lucas E, Martino J. Predicting the extent of resection in low-grade glioma by using intratumoral tractography to detect eloquent fascicles within the tumor. *Neurosurgery*. (2020) 88:E190–202. doi: 10.1093/neuros/nyaa463
3. Rudà R, Angileri FF, Ius T, Silvani A, Sarubbo S, Solari A, et al. SINch neuro-oncology section, AINO and SIN neuro-oncology section. Italian consensus and recommendations on diagnosis and treatment of low-grade gliomas. An intersociety (SINch/AINO/SIN) document. *J Neurosurg Sci*. (2020) 64:313–34. doi: 10.23736/S0390-5616.20.04982-6
4. Lombardi G, Barresi V, Castellano A, Tabouret E, Pasqualetti F, Salvalaggio A, et al. Clinical management of diffuse low-grade gliomas. *Cancers*. (2020) 12:3008. doi: 10.3390/cancers12103008
5. Sollmann N, Zhang H, Fratini A, Wildschuetz N, Ille S, Schröder A, et al. Risk assessment by presurgical tractography using navigated TMS maps in patients with highly motor- or language-eloquent brain tumors. *Cancers*. (2020) 12:1264. doi: 10.3390/cancers12051264
6. Mazzucchi E, La Rocca G, Ius T, Sabatino G, Della Pepa GM. Multimodality imaging techniques to assist surgery in low-grade gliomas. *World Neurosurg*. (2020) 133:423–5. doi: 10.1016/j.wneu.2019.10.120
7. Catani M, Thiebaut de Schotten M. A diffusion tensor imaging tractography atlas for virtual *in vivo* dissections. *Cortex*. (2008) 44:1105–32. doi: 10.1016/j.cortex.2008.05.004
8. Ius T, Turella L, Pauletto G, Isola M, Maieron M, Sciacca G, et al. Quantitative diffusion tensor imaging analysis of low-grade gliomas: from preclinical application to patient care. *World Neurosurg*. (2017) 97:333–43. doi: 10.1016/j.wneu.2016.10.006
9. Louis DN, Perry A, Reifenberger G, von Deimling A, Figarella-Branger D, Cavenese WK, et al. The 2016 World Health Organization classification of tumors of the central nervous system: a summary. *Acta Neuropathol*. (2016) 131:803–20. doi: 10.1007/s00401-016-1545-1
10. Fisher RS, Cross JE, French JA, Higurashi N, Hirsch E, Jansen FE, et al. Operational classification of seizure types by the International League Against Seizure: position paper of the ILAE commission for classification and terminology. *Epilepsia*. (2017) 58:522–30. doi: 10.1111/epi.13670

11. Engel J Jr, Burchfiel J, Ebersole J, Gates J, Gotman J, Homan R, et al. Long-term monitoring for epilepsy. report of an IFCN committee. *Electroencephalogr Clin Neurophysiol*. (1993) 87:437–58. doi: 10.1016/0013-4694(93)90158-R
12. Skrap M, Marin D, Ius T, Fabbro F, Tomasino B. Brain mapping: a novel intraoperative neuropsychological approach. *J Neurosurg*. (2016) 125:877–87. doi: 10.3171/2015.10.JNS15740
13. Cesselli D, Ius T, Isola M, Del Ben F, Da Col G, Bulfoni M, et al. Application of an artificial intelligence algorithm to prognostically stratify grade II gliomas. *Cancers*. (2019) 12:50. doi: 10.3390/cancers12010050
14. Ius T, Angelini E, Thiebaut de Schotten M, Mandonnet E, Duffau H. Evidence for potentials and limitations of brain plasticity using an atlas of functional resectability of WHO grade II gliomas: towards a "minimal common brain". *Neuroimage*. (2011) 56:992–1000. doi: 10.1016/j.neuroimage.2011.03.022
15. Wakana S, Caprihan A, Panzenboeck MM, Fallon JH, Perry M, Gollub RL, et al. Reproducibility of quantitative tractography methods applied to cerebral white matter. *Neuroimage*. (2007) 36:630–44. doi: 10.1016/j.neuroimage.2007.02.049
16. Chang EF, Breshears JD, Raygor KP, Lau D, Molinaro AM, Berger MS. Stereotactic probability and variability of speech arrest and anomia sites during stimulation mapping of the language dominant hemisphere. *J Neurosurg*. (2017) 126:114–21. doi: 10.3171/2015.10.JNS151087
17. Ojemann G, Ojemann J, Lettich E, Berger M. Cortical language localization in left, dominant hemisphere. An electrical stimulation mapping investigation in 117 patients. *J Neurosurg*. (1989) 71:316–26. doi: 10.3171/jns.1989.71.3.0316
18. Sanai N, Mirzadeh Z, Berger MS. Functional outcome after language mapping for glioma resection. *N Engl J Med*. (2008) 358:18–27. doi: 10.1056/NEJMoa067819
19. Conner AK, Briggs RG, Sali G, Rahimi M, Baker CM, Burks JD, et al. A connectomic atlas of the human cerebrum-chapter 13: tractographic description of the inferior fronto-occipital fasciculus. *Oper Neurosurg*. (2018) 15(Suppl. 1):S436–43. doi: 10.1093/ons/opy267
20. Brown DA, Hanalioglu S, Chaichana K, Duffau H. Transcorticosubcortical approach for left posterior mediobasal temporal region gliomas: a case series and anatomic review of relevant white matter tracts. *World Neurosurg*. (2020) 139:e737–47. doi: 10.1016/j.wneu.2020.04.147
21. Incekara F, Satoer D, Visch-Brink E, Vincent A, Smits M. Changes in language white matter tract microarchitecture associated with cognitive deficits in patients with presumed low-grade glioma. *J Neurosurg*. (2018) 8:1–9. doi: 10.3171/2017.12.JNS171681
22. Thiebaut de Schotten M, Ffytche DH, Bizzi A, Dell'Acqua F, Allin M, Walshe M, et al. Atlasing location, asymmetry and inter-subject variability of white matter tracts in the human brain with MR diffusion tractography. *Neuroimage*. (2011) 54:49–59. doi: 10.1016/j.neuroimage.2010.07.055
23. Sarubbo S, De Benedictis A, Merler S, Mandonnet E, Balbi S, Granieri E, et al. Towards a functional atlas of human white matter. *Hum Brain Mapp*. (2015) 36:3117–36. doi: 10.1002/hbm.22832
24. Cargnelutti E, Ius T, Skrap M, Tomasino B. What do we know about pre- and postoperative plasticity in patients with glioma? A review of neuroimaging and intraoperative mapping studies. *Neuroimage Clin*. (2020) 28:102435. doi: 10.1016/j.nicl.2020.102435
25. Altieri R, Melcarne A, Junemann C, Zeppa P, Zenga F, Garbossa D, et al. Inferior Fronto-Occipital fascicle anatomy in brain tumor surgeries: from anatomy lab to surgical theater. *J Clin Neurosci*. (2019) 68:290–4. doi: 10.1016/j.jocn.2019.07.039
26. Bizzi A, Nava S, Ferrè F, Castelli G, Aquino D, Ciaraffa F, et al. Aphasia induced by gliomas growing in the ventrolateral frontal region: assessment with diffusion MR tractography, functional MR imaging and neuropsychology. *Cortex*. (2012) 48:255–72. doi: 10.1016/j.cortex.2011.11.015
27. Li FY, Liu HY, Zhang J, Sun ZH, Zhang JS, Sun GC, et al. Identification of risk factors for poor language outcome in surgical resection of glioma involving the arcuate fasciculus: an observational study. *Neural Regen Res*. (2021) 16:333–7. doi: 10.4103/1673-5374.290901
28. Catani M, Howard RJ, Pajevic S, Jones DK. Virtual *in vivo* interactive dissection of white matter fasciculi in the human brain. *Neuroimage*. (2002) 17:77–94. doi: 10.1006/nimg.2002.1136
29. Vassal F, Pommier B, Sontheimer A, Lemaire JJ. Inter-individual variations and hemispheric asymmetries in structural connectivity patterns of the inferior fronto-occipital fascicle: a diffusion tensor imaging tractography study. *Surg Radiol Anat*. (2018) 40:129–37. doi: 10.1007/s00276-017-1966-0
30. Wu Y, Sun D, Wang Y, Wang Y. Subcomponents and connectivity of the inferior fronto-occipital fasciculus revealed by diffusion spectrum imaging fiber tracking. *Front Neuroanat*. (2016) 10:88. doi: 10.3389/fnana.2016.00088
31. Jellison BJ, Field AS, Medow J, Lazar M, Salamat MS, Alexander AL. Diffusion tensor imaging of cerebral white matter: a pictorial review of physics, fiber tract anatomy, and tumor imaging patterns. *AJNR Am J Neuroradiol*. (2004) 25:356–69.
32. Luat AF, Chugani HT. Molecular and diffusion tensor imaging of epileptic networks. *Epilepsia*. (2008) 49:15–22. doi: 10.1111/j.1528-1167.2008.01506.x
33. Tuncer MS, Salvati LF, Grittner U, Hardt J, Schilling R, Bährend I, et al. Towards a tractography-based risk stratification model for language area associated gliomas. *NeuroImage Clin*. (2020) 29:102541. doi: 10.1016/j.nicl.2020.102541
34. Sanvito F, Caverzasi E, Riva M, Jordan KM, Blasi V, Scifo P, et al. fMRI-targeted high-angular resolution diffusion MR tractography to identify functional language tracts in healthy controls and glioma patients. *Front Neurosci*. (2020) 14:225. doi: 10.3389/fnins.2020.00225
35. Panesar SS, Yeh FC, Deibert CP, Fernandes-Cabral D, Rowthu V, Celtikci P, et al. A diffusion spectrum imaging-based tractographic study into the anatomical subdivision and cortical connectivity of the ventral external capsule: uncinate and inferior fronto-occipital fascicles. *Neuroradiology*. (2017) 59:971–87. doi: 10.1007/s00234-017-1874-3
36. Zhao Y, Chen X, Wang F, Sun G, Wang Y, Song Z, et al. Integration of diffusion tensor-based arcuate fasciculus fibre navigation and intraoperative MRI into glioma surgery. *J Clin Neurosci*. (2012) 19:255–61. doi: 10.1016/j.jocn.2011.03.041
37. Sarubbo S, De Benedictis A, Merler S, Mandonnet E, Barbareschi M, Dallabona M, et al. Structural and functional integration between dorsal and ventral language streams as revealed by blunt dissection and direct electrical stimulation. *Hum Brain Mapp*. (2016) 37:3858–72. doi: 10.1002/hbm.23281
38. Shinoura N, Suzuki Y, Tsukada M, Yoshida M, Yamada R, Tabei Y, et al. Deficits in the left inferior longitudinal fasciculus results in impairments in object naming. *Neurocase*. (2010) 16:135–9. doi: 10.1080/13554790903329174
39. Davtian M, Ulmer JL, Mueller WM, Gaggl W, Mulane MP, Krouwer HG. The superior longitudinal fasciculus and speech arrest. *J Comput Assist Tomogr*. (2008) 32:410–4. doi: 10.1097/RCT.0b013e318157c5ff
40. Moritz-Gasser S, Herbet G, Duffau H. Mapping the connectivity underlying multimodal (verbal and non-verbal) semantic processing: a brain electrostimulation study. *Neuropsychologia*. (2013) 51:1814–22. doi: 10.1016/j.neuropsychologia.2013.06.007
41. Tomasino B, Tronchin G, Marin D, Maieron M, Fabbro F, Cubelli R, et al. Noun–verb naming dissociation in neurosurgical patients. *Aphasiology*. (2019) 33:1418–40. doi: 10.1080/02687038.2018.1542658
42. Epelbaum S, Pinel P, Gaillard R, Delmaire C, Perrin M, Dupont S, et al. Pure alexia as a disconnection syndrome: new diffusion imaging evidence for an old concept. *Cortex*. (2008) 44:962–74. doi: 10.1016/j.cortex.2008.05.003
43. Schlaggar BL, McCandliss BD. Development of neural systems for reading. *Annu Rev Neurosci*. (2007) 30:475–503. doi: 10.1146/annurev.neuro.28.061604.135645
44. Vandermosten M, Boets B, Poelmans H, Sunaert S, Wouters J, Ghesquière P. A tractography study in dyslexia: neuroanatomic correlates of ortographic, phonological and speech processing. *Brain*. (2012) 135(Pt 3):935–48. doi: 10.1093/brain/awr363
45. Maldonado IL, Moritz-Gasser S, Duffau H. Does the left superior longitudinal fascicle subserve language semantics? A brain electrostimulation study. *Brain Struct Funct*. (2011) 216:263–74. doi: 10.1007/s00429-011-0309-x
46. Tomasino B, Marin D, Maieron M, D'Agostini S, Fabbro F, Skrap M, et al. Double-letter processing in surface dyslexia and dysgraphia following a left temporal lesion: a multimodal neuroimaging study. *Cortex*. (2015) 73:112–30. doi: 10.1016/j.cortex.2015.08.010
47. Tomasino B, Ius T, Skrap M, Luzzatti C. Phonological and surface dyslexia in individuals with brain tumors: performance pre-, intra-, immediately post-surgery and at follow-up. *Hum Brain Mapp*. (2020) 41:5015–31. doi: 10.1002/hbm.25176

48. Miloushev VZ, Chow DS, Filippi CG. Meta-analysis of diffusion metrics for the prediction of tumor grade in gliomas. *AJNR Am J Neuroradiol*. (2015) 36:302–8. doi: 10.3174/ajnr.A4097
49. D'Souza S, Ormond DR, Costabile J, Thompson JA. Fiber-tract localized diffusion coefficients highlight patterns of white matter disruption induced by proximity to glioma. *PLoS ONE*. (2019) 14:e0225323. doi: 10.1371/journal.pone.0225323
50. Liu D, Liu Y, Hu X, Hu G, Yang K, Xiao C, et al. Alterations of white matter integrity associated with cognitive deficits in patients with glioma. *Brain Behav*. (2020) 10:e01639. doi: 10.1002/brb3.1639
51. Campanella M, Ius T, Skrap M, Fadiga L. Alterations in fiber pathways reveal brain tumor typology: a diffusion tractography study. *PeerJ*. (2014) 2:e497. doi: 10.7717/peerj.497
52. Ius T, Pauletto G, Tomasino B, Maieron M, Budai R, Isola M, et al. Predictors of postoperative seizure outcome in low grade glioma: from volumetric analysis to molecular stratification. *Cancer*. (2020) 12:397. doi: 10.3390/cancers12020397
53. Kohling R, Senner V, Paulus W, Speckmann EJ. Epileptiform activity preferentially arises outside tumor invasion zone in glioma xenotrasplants. *Neurobiol Dis*. (2006) 22:64–75. doi: 10.1016/j.nbd.2005.10.001
54. de Groot M, Reijneveld JC, Aronica E, Heimans JJ. Epilepsy in patients with a brain tumor: focal epilepsy requires focused treatment. *Brain*. (2012) 135(Pt 4):1002–16. doi: 10.1093/brain/awr310
55. Englot DJ, Chang EF. Rates and predictors of seizure freedom in resective epilepsy surgery: an update. *Neurosurg Rev*. (2014) 37:389–404. doi: 10.1007/s10143-014-0527-9
56. Chen DY, Chen CC, Crawford JR, Wang SG. Tumor-related epilepsy: epidemiology, pathogenesis and management. *J Neurooncol*. (2018) 139:13–21. doi: 10.1007/s11060-018-2862-0
57. Mandonnet E, Capelle L, Duffau H. Extension of paralimbic low grade gliomas: toward an anatomical classification based on white matter invasion patterns. *J Neurooncol*. (2006) 78:179–85. doi: 10.1007/s11060-005-9084-y
58. Feigl GC, Hiergeist W, Fellner C, Schebesch KM, Doenitz C, Finkenzeller T, et al. Magnetic resonance imaging diffusion tensor tractography: evaluation of anatomic accuracy of different fiber tracking software packages. *World Neurosurg*. (2014) 81:144–50. doi: 10.1016/j.wneu.2013.01.004
59. Campbell JSW, Pike GB. Potential and limitations of diffusion MRI tractography for the study of language. *Brain Lang*. (2014) 131:65–73. doi: 10.1016/j.bandl.2013.06.007
60. Ille S, Engel L, Kelm A, Meyer B, Krieg SM. Language-eloquent white matter pathway tractography and the course of language function in glioma patients. *Front Oncol*. (2018) 8:572. doi: 10.3389/fonc.2018.00572

Conflict of Interest: The authors declare that the research was conducted in the absence of any commercial or financial relationships that could be construed as a potential conflict of interest.

frontiers in Neurology

SYSTEMATIC REVIEW
published: 24 February 2021
doi: 10.3389/fneur.2021.641586

The Frontal Aslant Tract: A Systematic Review for Neurosurgical Applications

Emanuele La Corte[1†], Daniela Eldahaby[2†], Elena Greco[2†], Domenico Aquino[3], Giacomo Bertolini[1], Vincenzo Levi[1], Malte Ottenhausen[4], Greta Demichelis[3], Luigi Michele Romito[5], Francesco Acerbi[1], Morgan Broggi[1], Marco Paolo Schiariti[1], Paolo Ferroli[1‡], Maria Grazia Bruzzone[3‡] and Graziano Serrao[2,6‡]*

[1] Department of Neurosurgery, Fondazione IRCCS (Istituto di Ricovero e Cura a Carattere Scientifico) Istituto Neurologico Carlo Besta, Milan, Italy, [2] San Paolo Medical School, Department of Health Sciences, Università degli Studi di Milano, Milan, Italy, [3] Neuroradiology Department, Fondazione IRCCS (Istituto di Ricovero e Cura a Carattere Scientifico) Istituto Neurologico Carlo Besta, Milan, Italy, [4] Department of Neurological Surgery, University Medical Center Mainz, Mainz, Germany, [5] Parkinson's Disease and Movement Disorders Unit, Department of Clinical Neurosciences, Fondazione IRCCS (Istituto di Ricovero e Cura a Carattere Scientifico) Istituto Neurologico Carlo Besta, Milan, Italy, [6] Department of Health Sciences, Università degli Studi di Milano, Milan, Italy

OPEN ACCESS

Edited by:
Giovanni Raffa,
University of Messina, Italy

Reviewed by:
Tomasz Dziedzic,
Medical University of Warsaw, Poland
Patrick Schuss,
University Hospital Bonn, Germany

***Correspondence:**
Emanuele La Corte
emanuelelacorte@outlook.com
orcid.org/0000-0003-3752-8629

†These authors have contributed equally to this work and share first authorship

‡These authors have contributed equally to this work and share last authorship

Specialty section:
This article was submitted to Applied Neuroimaging, a section of the journal Frontiers in Neurology

Received: 14 December 2020
Accepted: 11 January 2021
Published: 24 February 2021

Citation:
La Corte E, Eldahaby D, Greco E, Aquino D, Bertolini G, Levi V, Ottenhausen M, Demichelis G, Romito LM, Acerbi F, Broggi M, Schiariti MP, Ferroli P, Bruzzone MG and Serrao G (2021) The Frontal Aslant Tract: A Systematic Review for Neurosurgical Applications. Front. Neurol. 12:641586. doi: 10.3389/fneur.2021.641586

The frontal aslant tract (FAT) is a recently identified white matter tract connecting the supplementary motor complex and lateral superior frontal gyrus to the inferior frontal gyrus. Advancements in neuroimaging and refinements to anatomical dissection techniques of the human brain white matter contributed to the recent description of the FAT anatomical and functional connectivity and its role in the pathogenesis of several neurological, psychiatric, and neurosurgical disorders. Through the application of diffusion tractography and intraoperative electrical brain stimulation, the FAT was shown to have a role in speech and language functions (verbal fluency, initiation and inhibition of speech, sentence production, and lexical decision), working memory, visual–motor activities, orofacial movements, social community tasks, attention, and music processing. Microstructural alterations of the FAT have also been associated with neurological disorders, such as primary progressive aphasia, post-stroke aphasia, stuttering, Foix–Chavany–Marie syndrome, social communication deficit in autism spectrum disorders, and attention–deficit hyperactivity disorder. We provide a systematic review of the current literature about the FAT anatomical connectivity and functional roles. Specifically, the aim of the present study relies on providing an overview for practical neurosurgical applications for the pre-operative, intra-operative, and post-operative assessment of patients with brain tumors located around and within the FAT. Moreover, some useful tests are suggested for the neurosurgical evaluation of FAT integrity to plan a safer surgery and to reduce post-operative deficits.

Keywords: diffusion-weighted imaging, executive function skills, frontal aslant tract, language, working memory, motor coordination, neurosurgery, tractography

INTRODUCTION

Refinements in the study of the human brain white matter by different means, such as dissection and advanced MR imaging techniques are leading to the discovery of new brain pathways. The frontal aslant tract (FAT) is a brain white matter tract connecting the superior frontal gyrus (SFG), specifically the pre-supplementary motor area (pre-SMA), supplementary motor area (SMA), and

lateral SFG to the pars opercularis and pars triangularis of the inferior frontal gyrus (IFG) and the anterior insula. The first time that connectivity between the pre-SMA and the IFG was established was in 2007 (1). Catani et al. (2) and Thiebaut de Schotten et al. (3) were the first to explicitly name the FAT because of its oblique direction within the frontal lobe. Since then, the FAT has been described using *ex vivo* fiber dissections (4–14). Although from the discovery of such white matter tract many papers described its role in different functions, such as speech and language functions (15–18), working memory (19–21), and visual–motor activities (22–25), and its possible involvement in the pathogenesis of several neurological, psychiatric, and neurosurgical disorders, the awareness of such fascicle is still not well-popularized in the neurosurgical community. For this reason, we decided to perform a systematic literature review and to focus on the neurosurgical applications of the current knowledge on the FAT. Our objective is to suggest practical indications and useful tests for the pre-operative, intra-operative, and post-operative evaluation of patients with brain tumors located around and within this tract or patients undergoing frontal lobe epilepsy surgery, providing to the neurosurgeon useful information to plan a safer surgery and to reduce post-operative deficits.

METHODS

Search Strategy

We performed a systematic review according to the Preferred Reporting Items for Systematic Reviews and Meta-analyses (PRISMA) statement guidelines (26). We used the following databases for the search: PubMed, Ovid MEDLINE, and Ovid EMBASE. We used the terms "FRONTAL," "ASLANT," and "TRACT" as individual keywords or MeSH terms in combination with the Boolean operator "AND" to maximize the identification of articles describing the FAT. Full search strategies are detailed for each database as follows: the PUBMED query was ("frontal"[All Fields] OR "frontalis"[All Fields] OR "frontalization"[All Fields] OR "frontally"[All Fields] OR "frontals"[All Fields]) AND "aslant"[All Fields] AND ("tract"[All Fields] OR "tracts"[All Fields]), and the Ovid MEDLINE and EMBASE queries were "frontal" AND "aslant" AND "tract." The search was conducted including all the articles published until 31 July 2020, and no restrictions were applied for the study design.

Data were extracted by two independent authors (DE and EG) and reviewed by a third author (ELC). The results were exported to the Mendeley citation manager, and after duplicate removal, title and abstracts were firstly screened and full text were obtained. The reference lists of the full-text papers were examined to identify additional relevant studies. Any dissension was resolved through discussion between the three independent reviewers, and an agreement was reached on all the articles included in the review.

Selection Criteria

The selection criteria applied to the systematic review were the following: studies written in English language involving human participants (only animal studies were excluded) and investigating brain white matter through post-mortem dissection or *in vivo* brain imaging techniques. Studies were excluded if they were not published as a full text in English because of insufficient data. During full-text screening, 19 articles were further excluded, including five reviews not introducing new concepts.

Data Collection

Data from the included articles were extracted, assembled, and analyzed using Microsoft Excel 2019 (Microsoft Corp, Redmond, WA). The details collected consisted of the study title, authors, first author's country, publication year, publication journal, type of research (anatomical, clinical, or surgical), subjects (patient or human cadaver), total population sample size, pathology investigated, and the main result of the study.

RESULTS

A total of 261 records were retrieved (**Figure 1**). After 166 duplicate records have been removed, the titles and abstracts of 95 records were screened. During exclusion criteria application and full-text screening, 25 records were excluded, with 70 remaining articles from 2012 to July 2020, including anatomical, clinical, and neurosurgical studies. To review the available data about the FAT, we started describing the anatomy and then we highlight its role in different brain function fields, such as language, executive functions, lexical decisions, stuttering, oro-facial movements, working memory, social community tasks, attention, and music processing.

DISCUSSION

Anatomy

Cortical Connections

The FAT is a white matter fiber tract traveling in the coronal plane connecting the SFG to the ipsilateral IFG (27) (**Figure 2**). According to the parcellation scheme developed by the Human Connectome Project (HCP), the FAT connects the SFG, in particular, two parcellations of the SMA complex (6ma and SFL) and two of the dorsolateral prefrontal cortex (8BL and S6-8) to the IFG (parcellations 44, 6r) and the frontal operculum (parcellations FOP1, FOP3, and FOP4) as well as the middle insula (MI) parcellation in the anterior insula (28, 29). In line with the parcellation scheme, the tractography of the FAT shows terminations into the SFG, including not only the pre-SMA and SMA but also the lateral SFG (30). Varriano et al. (21) defined the extended FAT, "exFAT," as the FAT projecting more anteriorly into the SFG. Catani et al. (15) reported the termination of the FAT into the anterior cingulate cortex. The major projection of the FAT in the IFG is the pars opercularis, but some fibers may also reach the pars triangularis (2, 27) and the inferior region of the pre-central gyrus (PrCG) (2). Non-homologous callosal connections have been described between the premotor areas, and some authors introduced the concept of "crossed FAT" that may have a role in the recovery from the SMA syndrome (10).

In children, the predominance of fibers that travel from the IFG-pars opercularis (IFG-Op) projects to the pre-SMA, but

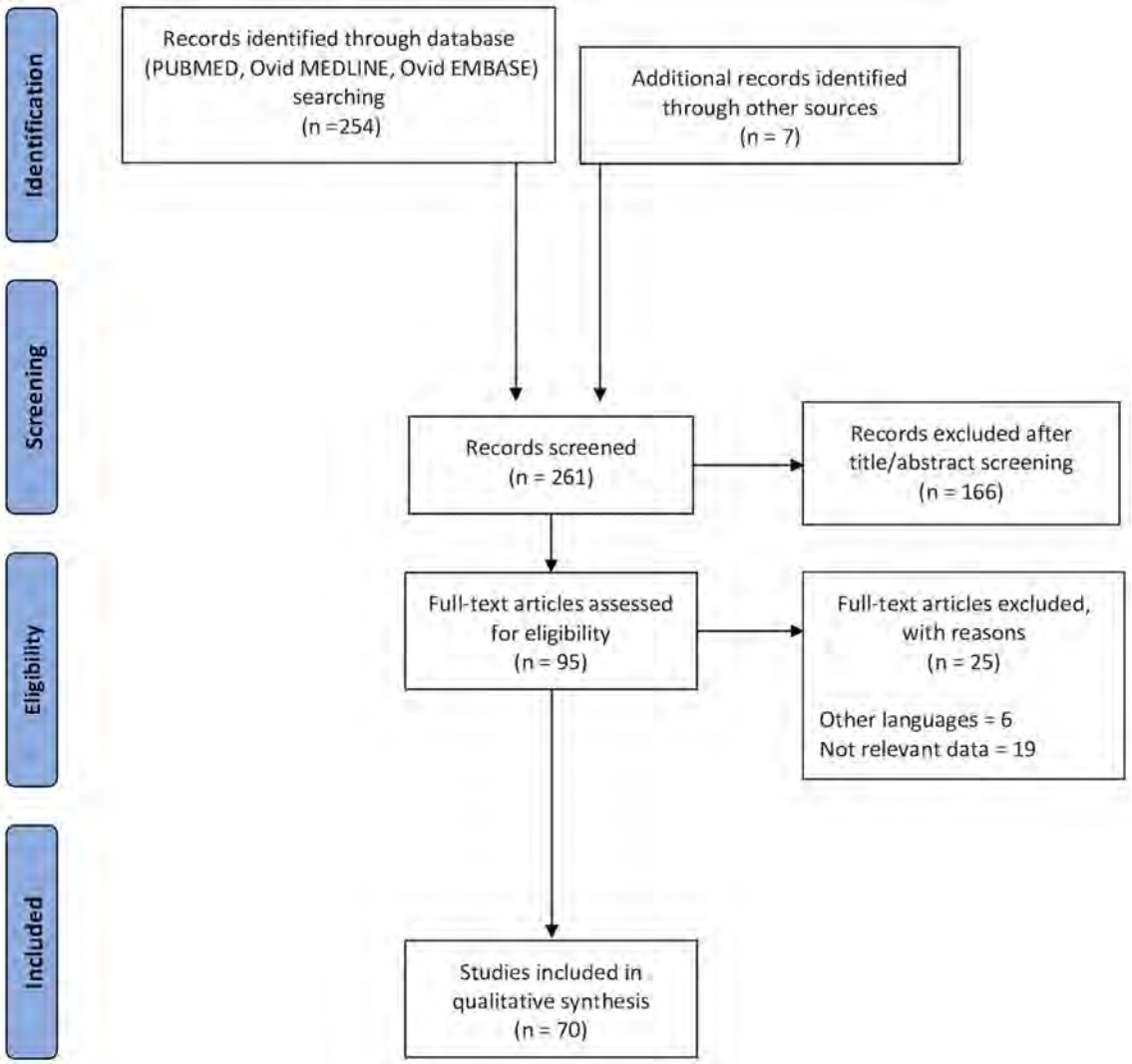

FIGURE 1 | Flow chart applied to the retrieval and selection of studies included in the systematic literature review according to PRISMA guidelines.

projections to the SMA and to the anterior cingulate are also found (31).

An anterior and posterior component of the FAT have been described, the first connecting Brodmann area (BA) 44 with the pre-SMA, and the latter connecting BA 6 with the SMA (17). Conflicting evidence about volumetric lateralization could be found in the current literature. While some papers suggested a left lateralization of the FAT in right-handed individuals (3), other studies found no trend of lateralization across 29 (32) and 10 healthy subjects (4, 33). In 19 typical 5- to 8-year-olds children, the FAT showed right laterality and a trend toward increasing left laterality with age (31). Variable age-related changes in the microstructure were noticed until early adulthood (31, 33, 34).

The presence of a bidirectional connection between the SFG to the Broca area has also been demonstrated through corticocortical evoked potentials (CCEPs). The latencies of CCEP responses were significantly shorter in the SFG from the Broca area stimulation than in the Broca area from the SFG stimulation (35). This could be explained by the presence of a direct corticocortical pathway from the Broca area to the SFG and an indirect cortico-subcortical pathway connecting the SFG to the Broca area. Another explanation is that different latencies reflect antidromic or orthodromic projection (35).

Superior Frontal Gyrus

The terminations of the FAT are still objects of study. The upper terminations are commonly identified in the SMA complex in the medial SFG, but also in the dorsolateral prefrontal cortex of the SFG (28–30). The SMA complex is subdivided into the SMA proper, the pre-SMA anteriorly and the supplementary eye field (9, 30) both in the medial surface of the SFG (30), delimitated superiorly by the superior hemispheric border, the cingulate sulcus inferomedially, and the precentral sulcus posteriorly (36) (**Figure 3**). The anterior border of the pre-SMA is an imaginary

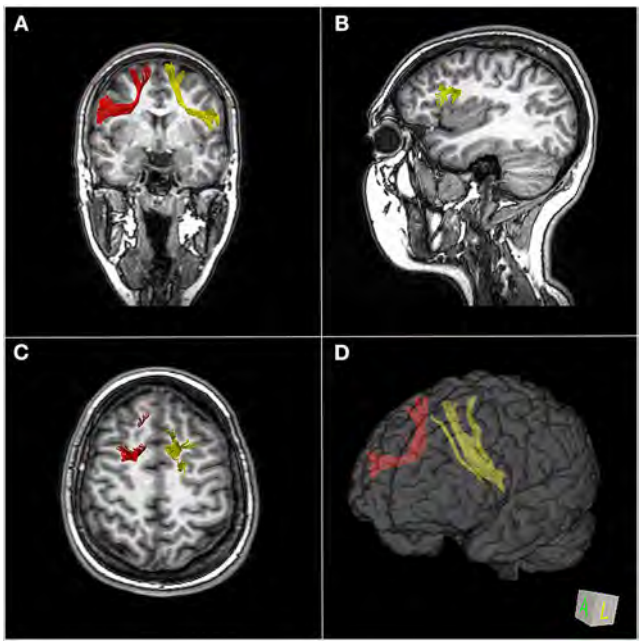

FIGURE 2 | MR-diffusion tensor imaging of the frontal aslant tract (FAT) in a 23-year-old healthy female. Right (red) and left (yellow) FAT overlaid over coronal images **(A)**, left FAT terminations in the left posterior inferior frontal gyrus overlaid over sagittal images **(B)**, superior right and left FAT terminations, respectively, in the right and left superior frontal gyrus overlaid over axial images **(C)**. 3D brain reconstruction of right and left FAT **(D)**.

line tangential to the rostral portion of the corpus callosum genu and perpendicular to the line connecting the anterior and posterior commissures (AC–PC line) (36). There are differences in histochemical and cytoarchitectonic properties between the pre-SMA and the SMA proper, but since there is no visible border between these two areas, a vertical imaginary plane passing through the anterior commissure and perpendicular to the AC–PC line is considered as the border (9, 30, 37). Instead of subdividing the SMA into the pre-SMA and SMA proper, the HCP subdivides the SMA into four parcellations: 6ma, SFL, 6mp, and SCEF; the first two parcellations are part of the terminations of the FAT. According to the HCP, from the SMA originates a medial bundle connected to the homologous contralateral SMA, a middle bundle descending to the basal ganglia and the corticospinal tract, and a lateral bundle, part of the FAT, connected to the IFG and insula (38). The HCP has also subdivided the dorsolateral prefrontal cortex into 13 areas; two of them, SFL and 8BL, are terminations of the FAT (28). The SFG is also connected to the inferior fronto-occipital fasciculus, the cingulum, and a callosal fiber bundle connecting the SFG bilaterally (5).

Inferior Frontal Gyrus

The IFG is delimitated superiorly by the inferior frontal sulcus, its posterior part inferiorly by the Sylvian fissure, and medially by the orbitofrontal gyri. The IFG is composed of three cortical regions: the pars orbitalis, the pars triangularis, and the pars opercularis, limited posteriorly by the precentral sulcus. Four major connections of the IFG have been identified and are represented by the FAT: the superior longitudinal fasciculus/arcuate fasciculus complex, the inferior fronto-occipital fasciculus, the uncinate fasciculus, and the callosal fibers connecting the IFG bilaterally (4).

Insula

The insula is hidden within the Sylvian fissure and is in continuity superiorly with the fronto-parietal opercular region and inferiorly with the temporal lobe. The central insular sulcus divides the anterior three short gyri from the posterior long gyri. The MI area lies in the posterior superior part of the short insular gyrus (39). The Human Connectome Project divided the insula in numerous parcellations (39) and found connections of the MI area with three SFG parcellations (6ma, 8BL, and SFL) through the FAT (29). The termination of the FAT in the insula has not been extensively studied, but Baker et al. (39) noted that a previously known network, the salience network (SN), has as nodes both FAT terminations and the anterior insula. The SN connects the fronto-insular cortex, composed of the ventrolateral prefrontal cortex and the anterior insula, to the anterior cingulate cortex (ACC) (40). This network, which also includes the amygdala, hypothalamus, ventral striatum, thalamus, and specific brainstem nuclei, is not only part of a functional network (41) but is also the only localization in the brain, jointly with BA 9 in the prefrontal human cortex, of the von Economo neurons (42). The fronto-insular cortex plays a role in interoceptive awareness of changes in homeostatic states, whereas the ACC generates relevant visceral, autonomic, behavioral, and cognitive responses. Through mutual interactions, these regions could respond to homeostatically relevant internal or external stimuli and enrich them with emotional weight (41). The salience network could mediate the switching between the processing streams of the default mode network and the central executive network during cognitively demanding tasks (40). This interconnection of the FAT with the anterior insula is also suggested by the similar spectrum of disorders that lesions to those regions cause. As the FAT, the anterior insula has been associated with progressive non-fluent aphasia PNFA, showing hypometabolism, atrophy (43), and gray matter damage (17) atrophy progression in large areas. This connection is also supported by the evidence that neurodegeneration in non-fluent variant (nfv) primary progressive aphasia (PPA) starts in a syndrome-specific epicenter and in the opercular region of the left IFG and then spreads to the most connected regions such as the SMA, insula, striatum, and inferior parietal regions (44).

Subcortical Connections

The SMA complex is connected to the limbic system *via* the cingulum and to the striatum (caudate nucleus and putamen) *via* short "U" association fibers and the superior longitudinal fasciculus I, cingulum, claustrocortical fibers, callosal fibers, corticospinal tract, frontal aslant tract, and frontostriatal tract (9). About 10% of the corticospinal fibers arise in the SMA proper, but no corticospinal fibers originate from the pre-SMA (45). The FAT is medial to the superior longitudinal fasciculus II (SLF II),

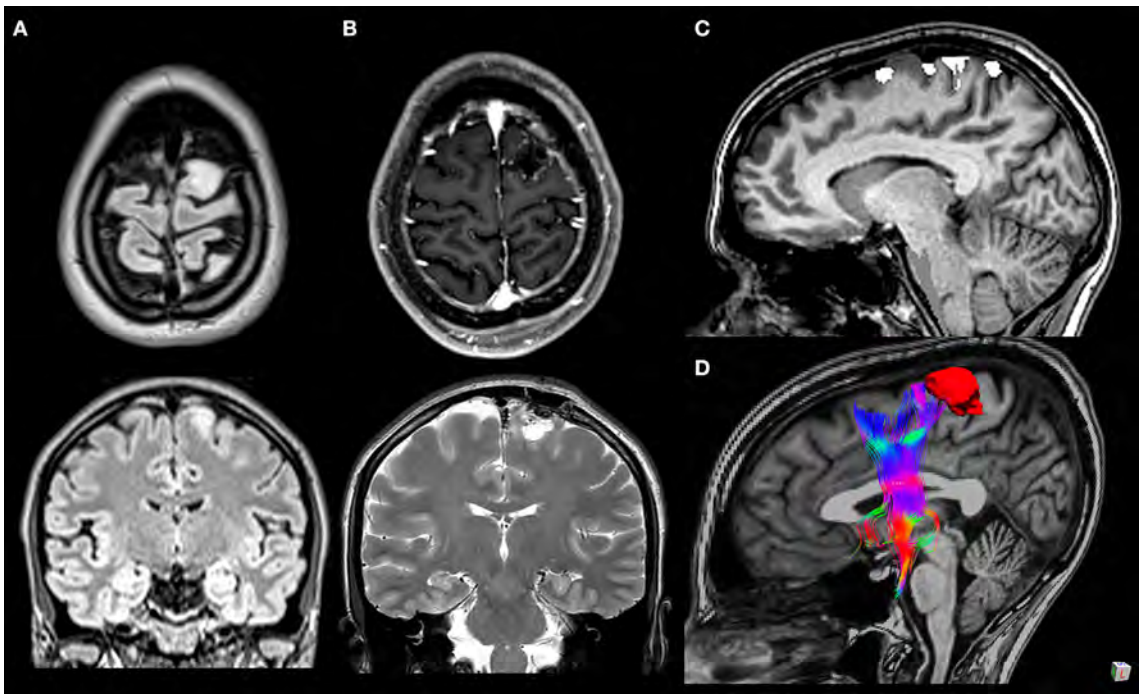

FIGURE 3 | A 33-year-old woman with a WHO grade II astrocytoma located in the left cortico-subcortical region of the superior frontal gyrus. Surgical resection was performed through fluorescein-guided microsurgical technique guided by intraoperative neurophysiological monitoring and by functional MRI (fMRI)/tractography-integrated neuro-navigation system. Pre-operative symptoms included motor partial seizure affecting the right leg, followed by a generalized seizure. The patient post-operatively developed a transient mild weakness in the right leg. Preoperative axial and coronal T2-weighted MR images **(A)**, post-operative axial T1-weighted post-gadolinium and coronal T2-weighted MR images **(B)**, fMRI with blood oxygen level-dependent response in the left paracentral lobule evoked during voluntary movement of the right foot overlaid on sagittal T1-weighted MR images **(C)**, and 3D relationship between the tumor and frontal aslant tract tractography reconstruction **(D)**.

which is orthogonal to the FAT, and lateral to the frontostriatal tract (FST) and claustrocortical fibers (CCF) (9, 13).

Regions of Interest for FAT Tracking

The FAT tracking is usually delineated by an axial "AND" region of interest (ROI) on the white matter of the SFG and a sagittal "AND" ROI on the white matter of the IFG (including the pars opercularis and triangularis) (22). The SMA ROI's anterior border is the anterior tip of the cingulate gyrus, while the posterior border is the precentral sulcus (34).

Surgery-Related Deficits

Acute deficits reported immediately after surgery involving the FAT were aphasia, impairment of speech, self-initiated speech disorders, speech hesitancy, numerous pauses and delays during conversation, anomia, delays in naming and word finding difficulties, errors in verb generation tasks, perseverations, need for phonological cues, errors with reading, delay in counting, and simple calculations (35, 46–49).

Lesion of the FAT during tumor resection can result in peculiar deficits. In six patients with lesion close or inside the left FATs, only the last ones experienced transient impairment of speech. All patients recovered language function within 8 weeks (35). Young et al. (47) reported a case of a patient operated for a lower-grade diffuse glioma invading the dominant FAT, which was significantly disrupted in the post-operative diffusion tensor image (DTI). After transient symptoms, from post-operative day 4 to follow-up at 9 months after surgery, the patient still experienced fluent speech and intact naming/counting/sentence repetition. In one patient with brain tumor at the level of the left FAT, noun-based verb generation task and inverse task (i.e., verb-based noun generation) impairment, noted during intra-operatory stimulation of pre-SMA and left FAT, partially persisted 1 month after surgery, while performance on other language tasks remained acceptable. DTI confirmed left FAT damage and corona radiata partial damage, but left Broca's area was intact and the SMA/preSMA region was the only cortical region damaged (49). On five patients with left insular or frontal language-eloquent glioma, no one had a permanent surgery-related aphasia (46). A total of 19 patients with frontal glioma (14 left and five right) underwent awake surgery. Persistent speech initiation disturbances 3 months after the resection of a SMA glioma were noted only in one patient with left FAT disappearance. No post-operative speech disorders were observed after right-side surgeries (48).

Surgical access to frontal subcortical pathology has primarily been fulfilled *via* either transcortical or transcallosal routes. In order to reduce surgical injury to the white matter tracts and cortex, a tailored trans-sulcal para-fascicular corridor surgery to the frontal horn, third ventricle, and subcortical

frontal lobe has been developed (13). Kocher's point (KP) represents the most used entry point to access the frontal horn of the lateral ventricle, and it relies exclusively on craniometric landmarks, not considering brain matter tracts, such as FAT, CCF, and SLF-II which are directly on KP trajectory. Kassam et al. purposely built and designed an optimized corridor to diminish subcortical surgical damage (50).

The role of the FAT in speech initiation was investigated through studies of electrical stimulation. Vassal et al. were the first to observe arrest of speech induced by stimulation of the left FAT during an awake resection of a left frontal lobe glioma in a right-handed patient without language deficits. The speech normalized again when the stimulation stopped (51). In another study by Fuji et al., FAT stimulation, on five right-handed patients, induced speech arrest in four patients and speech initiation delay in the other patient (52). Similar results were obtained by Kinoshita et al., who performed intra-operative electrical stimulation in 19 patients with frontal lobe tumors. Sixteen of these patients had speech arrest during the stimulation (48). The frontal aslant tract has been considered as part of the "negative motor network"; in fact, direct electrical stimulation over this tract causes movement arrest defined as negative motor response (53, 54).

During awake surgery of frontal tumors, direct cortical and subcortical electrostimulation (52, 55) combined with navigated tractography (51, 52) permitted to map and respect the FAT as a functional boundary.

Bizzi et al. observed that low-grade glioma (LGG) infiltration into the frontal intralobar tracts, including the FAT, may not always cause language deficits. In fact, LGGs tend to spare pars opercularis, the most eloquent area in the IFG, since infiltration of pars orbitalis and triangularis did not cause any language impairment (56). This could be explained by the adaptive plasticity of the frontal operculum and the presence of natural macroscopic (i.e., sulci) and microscopic barriers (i.e., cortical cyto-architecture) that may prevent the diffusion of the tumor into the pars opercularis (56).

The preservation of the FAT, despite acute post-surgical transient speech and motor disorders, permitted complete functional recovery within a few weeks after resection (51, 52, 55). Despite the preservation of the FAT, two patients out of 50, had permanent motor deficit, one due to injury to the supplementary motor area proper and one due to a partial injury of the corticospinal tract, but none of the patients experienced permanent speech disturbance after tumor removal (55).

Roles in Verbal Fluency

Verbal fluency is a cognitive function that helps information retrieval from memory. Semantic fluency is tested by asking to generate words belonging to given categories (e.g., names of animals), while phonemic fluency is tested by asking for words beginning with a given letter, usually F, A, and S (57).

Microstructural abnormalities of the FAT were significantly associated with verbal fluency deficits measured by mean length of utterance and words-per-minute tasks in patients with primary progressive aphasia. Catani et al. found no correlations between the FAT and measures of overall language impairment, grammar deficit, repetition or single word comprehension (measured, respectively by Western Aphasia Battery Aphasia Quotient, Northwestern Anagram Test Western Aphasia Battery—Repetition and Peabody Picture Vocabulary Test) (15). Alteration of the left FAT is correlated only with nfv in PPA (15, 16). This suggests a dissociation between verbal fluency and semantic processing functions, which relay, respectively on the FAT and on the uncinate fasciculus (15, 17). Mandelli et al. results strongly suggest that neurodegeneration in nfv-PPA starts in a syndrome-specific epicenter in the dorsal portion of the opercular region of the left IFG and then spreads most significantly to the SMA through the FAT (44).

In chronic post-stroke aphasia speech, fluency was uniquely correlated with left motor cortex and underlying white matter (including the anterior section of the arcuate fasciculus and the frontal aslant tract) (18, 58, 59). Damage to FAT in chronic aphasia due to left-hemisphere ischemic stroke correlated with both semantic and phonological fluencies (60).

In a patient with crossed aphasia, cholinergic potentiation and audiovisual repetition–imitation therapy improved language deficit through modifications in the right FAT and the right direct segment of the arcuate fasciculus (61).

In multiple sclerosis patients, verbal fluency is significantly correlated with mean fractional anisotropy (FA) in bilateral frontal aslant tract (62, 63).

In adults with a history of very preterm birth worse verbal fluency than controls is correlated to FAT properties and laterality (64). No association between the frontal aslant tract and verbal fluency was found in 29 right-handed, healthy university students; however, lexical decision was correlated with FAT laterality (32).

Single-photon emission computed tomography and functional near-infrared spectroscopy suggested that FAT may play a crucial role in word retrieval difficulty in acute thalamic stroke survivors; furthermore, SMA may contribute to improve word retrieval difficulty (65). No correlation between FAT and apraxia of speech (66) or syntax (67) has been noticed. Naming recovery in patients with aphasia after a left hemispheric stroke also showed no correlation with FAT (68). In subthalamic nucleus deep brain stimulation, the most reported adverse effect is verbal fluency impairment, but it could be not associated with the damage of fiber pathways along the electrode trajectories, including the FAT (69).

Speech fluency can be measured by different tests, such as the Western Aphasia Battery-Revised (WAB-R) fluency subtest and words per minutes (WPM) test. The WPM and WAB fluency are related, but not redundant, measures of fluency. The WPM and WAB fluency scores highlight the role of the FAT in verbal fluency (15, 58). Patients with FAT disconnection showed significantly worse phonemic fluency test scores (70). Low scores in Brief Language Assessment for Surgical Tumours patients' articulatory agility task, which requires reciting utterances as rapidly as possible (e.g., 50, 50, 50…), are associated with pathologies overlapping with the territory of the FAT (71). In nfvPPA, the FAT microstructural properties were associated with the number of distortion errors per hundred words that patients

made in spontaneous speech during the WAB spoken picture description task (17).

Roles in Lexical Decision

Sierpowska et al. firstly suggested a relationship between a FAT damage and lexical retrieval deficits. The authors performed awake surgery to resect a left frontal tumor and observed, at the time of tumor resection and at the left FAT intraoperative electrical stimulation, that the patient, while performing a noun-based verb generation task, applied a morphological derivation rule to the given nouns to form new inexistent verbs instead of retrieving proper existing verbs (49). Pre-operative and post-operative fMRI analyses revealed that Broca's area and preSMA were both activated during the verb generation task. Indeed several studies have established the role of Broca's area in language production, lexical retrieval, and/or selection of semantic knowledge and grammatical/morphological processing (49, 72–77), the role of the SMA in speech initiation, coordination and monitoring, and articulatory abilities (78–81), and the role of the pre-SMA in linguistic production (15). All of these regions are cortical terminals of the FAT which, in the post-operative tractography DTI, was confirmed to be damaged. After surgery, the patient had good abilities in semantic decisions, past and present tense forms, and phonological production; verbal fluency and working memory were instead considerably affected along with the performance in the noun-based verb generation task and also in the inverse task of verb-based noun generation. In another case study, Chernoff et al. considered two patients, one underwent surgical resection of a left frontal glioma and the other one underwent left anterior temporal and hippocampal resection (82). In the first patient, the post-operative DTI evaluation revealed microstructural impairment of the left FAT and clinically dysfluent speech in complex sentences without impairment in lexical access. On the contrary, the second patient presented impairment of the left inferior longitudinal fasciculus and word finding difficulties without dysfluent speech. Other language functions were not affected in any patient. To further investigate the role of the FAT in the mediation process from sentence planning to lexical access, the authors performed a second case study of a patient undertaking awake surgery to remove a left frontal brain tumor. During the surgery, the patient was given a task consisting of generating a sentence to describe the spatial relation of a target marked shape (the grammatical subject of the sentence) with the shape above or below it. In the course of the intra-operative task execution, stimulation of the left FAT generated a prolonged inter-word time at the beginning of syntactic phrases, but inter-word duration within phrases was either not affected by stimulation or reduced, along with the sentence's total extent and intra-word duration. Given this result, the authors suggested a potential role of the left FAT in integrating grammatical information with the sentence structure, thus introducing the "Syntagmatic Constraints On Positional Elements" hypothesis (83). These evidences lead Corrivetti et al. to retrospectively analyze functional language maps of both white and gray matter regions obtained in 17 patients undergoing awake surgery for left frontal lobe glioma resection. The conclusion of this study was that motor–speech responses and lexico-semantic responses are both functions conveyed by the FAT; specifically, the lexico-semantic role belongs to the anterior FAT, while the motor–speech function is attributable to the posterior FAT (84). In contrast with these findings, a recent study considering 20 patients with a left-hemisphere stroke located in the frontal lobe did not show any association between a lower FAT volume and lower conceptual or lexical selection abilities. The behavioral assessment was measured using the sentence completion task to evaluate conceptual and lexical selection and the picture–word interference task to specifically evaluate the lexical selection. The authors tried to explain this variance from previous findings, confirming the idea of the FAT involvement in these functions but assuming a possible reorganization of the FAT during the post-stroke recovery period (85). Finally, Vallesi et al. investigated, in a group of 29 healthy university students, the correlation between macrostructural and microstructural properties of the FAT, evaluated though the utilization of DTI indices and the lexical decision processes. The latter were evaluated through a lexical decision task, in which the students had to estimate if the letter strings provided were real Italian terms or invented ones, and the color and shape discrimination task, in which they had to specify the color and the shape of the presented stimulus. The result of this study was the evidence, for the first time, of a positive association between left lateralization of the FAT and faster lexical decision latency. However, no correlation was observed between the lateralization indices of the FAT and verbal fluency (32).

Roles in Stuttering

Stuttering is a childhood-onset speech fluency disorder that sometimes persists into adulthood, consisting in sound prolongations and repetitions along with interrupted words regardless of articulatory features (86). Recently, persistent developmental stuttering has been associated with anatomical abnormalities and lower activation of the IFG and the ventral premotor cortex (PMv) (87, 88). This theory is aligned with the results obtained by Chesters et al. who, after applying direct current stimulation on the left IFG/PMv, observed an improvement of speech fluency in people with stuttering (89). Starting from these evidences, recent studies have investigated the role of the FAT in speech fluency in people with stuttering. Among these, Kronfeld-Duenias et al. grouped 15 adults with persistent developmental stuttering and nine healthy controls and then analyzed through tractography the volume and diffusion properties of the FAT. As a result, increased mean diffusivity in the left FAT was observed in the group with stuttering compared with controls. Moreover, a negative association was found between diffusivity values and speech rate and fluency in the individuals with stuttering. To evaluate the occurrence of stuttering, the authors used an interview about a neutral topic and a reading task, and the severity was instead assessed with the Stuttering Severity Instrument-III (90, 91). In another study considering eight patients with no pre-operative stuttering, Kemerdere et al. showed that direct electrical stimulation of the left FAT, conducted throughout awake surgical resection of a left frontal glioma, induced intra-operative transient stuttering. No patient experienced

post-operative stuttering though during tumor resection, and the FAT was preserved in all cases. In two patients, minor speech initiation disorders persisted after surgery (92). Based on these results and on the studies observed above, the authors identify the disconnection of the cortico-subcortical circuit, including the FAT that supports the speech motor control, as a potential etiopathogenesis of stuttering. Recently, Neef et al. recruited a group of 31 adults with stuttering and a second group of 34 healthy controls (93) and found impaired white matter integrity of the right FAT in the group with stuttering. Moreover, a stronger connectivity of the right FAT was positively associated with stuttering severity, suggesting an enhanced speech–motor suppression mechanism in stuttering.

Roles in Executive Functions

Taking the premise that the FAT is a white matter bundle connecting secondary motor areas, in particular, the Broca's area with the SMA and the pre-SMA regions were shown to be involved, respectively in the online control and in the planning of simple reaching and grasping actions (94).

The SMA syndrome is a well-known neurosurgical disturbance that may appear after surgery has been performed in the unilateral SMA region. This syndrome is defined by a transient inability to initiate contralateral voluntary movements which typically spontaneously disappear within 3 months, except for the incapability to alternate bimanual gestures that is often irreversibly affected (95). In six patients operated through surgical excision of low-grade glioma located in the SMA region, no statistically significant association was found between recovery time and damage of white matter tracts contiguous to the SMA, including the FAT, FST, and pyramidal tract, except for the cingulum (96). The mechanism of functioning restoration after surgical damage of the FAT is undiscovered, but it likely involves plasticity of the cortical language network and recruitment of the contralateral hemisphere, possibly through transcallosal fibers (47). In fact, right FAT has also a role in recovery after left FAT lesion-associated speech deficit as suggested by the evidence that cholinergic enhancing, alone or integrated with a model-based aphasia therapy, promotes improvements in aphasia by inducing structural plastic changes in right FAT. Baker et al. hypothesize that a possible mechanism involved in the recovery from SMA syndrome may be represented by not equivalent bonds between contralateral motor areas by supporting interhemispheric connectivity (10). For this reason, commissural fibers from the contralateral SMA region should be preserved in order to facilitate the resolution of transcortical motor aphasia that typically occurs after resection of SMA lesions (52).

Budisavljevic et al. suggested, for the first time, a potential role of the FAT in the visuo-motor process that supports movement planning and feedback control during hand movement vs. a target object. To support this idea, the authors used DTI to analyze the microstructural organization of the bilateral FATs in 32 right-handed, healthy participants who were asked to perform a reach to grasp task and a reach task vs. a target object. As a result, a higher anisotropy of the bilateral FAT resulted to be associated with a more efficient visuo-motor processing and more stable paths, in particular, with lower acceleration and deceleration amplitude ranges of reach and reach-to-grasp movements (22).

Afterwards, the hypothesis of a potential FAT involvement in the neurological mechanisms underlying visuo-motor integration was supported by two other studies. In the first one, Serra et al. enrolled 23 patients with Alzheimer's disease (AD) and conducted a probabilistic tractography analysis and examination of the bilateral FATs FA. Not only the mean FA resulted to be significantly lower bilaterally in patients with AD compared to healthy subjects (HS) but also the FA in the right FAT resulted to be positively associated with patients' performance at copy of drawings and copy of drawings with landmarks tests (that evaluate constructional praxis) and Raven's colored matrices (that evaluates visuo-spatial logical reasoning) (23). In the other study, Tsai et al. considered 10 adults with amblyopia and showed a lower mean FA in in the left FAT compared to HS (97). Considering that both apraxia and amblyopia are associated to visuo-motor integration deficits—in fact, constructional apraxia is defined as the inability to reproduce spatial patterns due to an impairment of visuo-spatial analysis and integration with motor planning and skills (25), while amblyopia was reported to be associated with visuo-motor defective abilities in tasks demanding precision and speed (98, 99)—these results support the idea that the FAT may have a role in these processes. Moreover, Budisavljevic et al., relying on the observed association between movement deceleration and the bilateral FATs and supported by previous subcortical stimulation studies of the white matter corresponding to the nowadays FAT producing a deceleration (100) or complete interruption (101) of both hands movements, also suggested for the first time a potential involvement of the FAT in the inhibitory control of motor pathway (22). This idea is supported by studies of fMRI, DWI, TMS, direct cortical/subcortical stimulation, and electrocorticography showing that the right IFG and the right SMA and pre-SMA, both interconnected by the FAT, play a role in the neural motor network in conducting inhibitory regulation processes (24). In particular, these regions have been described by Aron et al. as parts of a cortico–basal ganglia–thalamic–cerebellar circuit (102) where, more specifically, both the right IFG and the pre-SMA connect to the subthalamic nucleus and play a role, respectively, in suppressing cortical output and resolving conflicting behaviors (103, 104). Motor inhibition has been evaluated through go/no-go and stop signal experimental models, where a powerful response is launched at first (go trial), and then it must be supplanted when a stop signal appears (stop trial) (105–108).

Based on these evidences, Dick et al. assumed that the FAT is a component of the cortico–basal ganglia–thalamic–cerebellar anatomical–functional circuit described above and plays a role in executive functions, especially in the programming and coordination of sequential motor movements through a selection among motor plans that compete for the same motor resources. The authors, in accordance with computational models of inhibitory regulation for speech and for manual actions, assume that this function is present bilaterally but is differently specialized between the two hemispheres: the left

FAT is specialized for speech programming and controls the articulatory apparatus, while the right FAT is specialized for general action and for visuo-motor integration, regulating the manual/limb and the oculomotor systems (24).

Roles in Oro-Facial Movements

Foix–Chavany–Marie syndrome (FCMS) is a rare syndrome, usually caused by bilateral lesions of the anterior operculum, for this reason it is also known as opercular syndrome. FCMS is a form of pseudobulbar palsy, clinical manifestations range from severe articulatory disorders to mutism (109), limb weakness and bowel and bladder incontinence, but with preservation of involuntary reflex motor movements of the affected muscles, such as smiling or crying (110). Symptoms usually recover over a matter of days or over a timespan of months (111). Surgical damage of connections between FAT and arcuate fasciculus, and the right pars opercularis caused post-operative FCMS. For this reason a trans-opercular approach to insulo-opercular gliomas can generate FCMS (112). In a patient with opercular syndrome, a volume reduction was noticed in the primary motor cortex, SMA, posterior portion (BA6) of the operculum and white matter of the frontal lobe, with a left prevalence, including the CC, AF, SLF, FAT, and CST (109, 113).

Signs of spastic and atrophic bulbar palsy are also present in amyotrophic lateral sclerosis. Disease duration in amyotrophic lateral sclerosis patients is associated with atrophy in the cortical terminations of left FAT and the right precentral gyrus (114).

Roles in Working Memory

Working memory comprises a complex brain system that maintains information for periods of time going from seconds to minutes and allows processing of information for future goal-directed behavior and complex cognitive tasks (115). Recent studies showed that the FAT can also have implications in working memory performances. Rizio et al. performed neuropsychological tasks and DTI in two groups of adults, one group under 35 years old and the other over 59 years old, with the aim to evaluate age-related changes in speed, language, working memory, episodic memory, and inhibitory control. Working memory evaluation included spatial working memory and both backward and forward digit span. In both groups, age was a predictor of working memory, but only in the older group the integrity of bilateral FAT and left SLF/AF, evaluated through FA, was a marginal predictor of working memory ability (19). This result paved the way to other studies that investigated the FAT functional implication in working memory. Varriano et al. proposed an extended definition of the FAT ("exFAT") that ends further anteriorly into the SFG. The authors evaluated its volume and laterality in four groups of participants selected from a total of 900 subjects according to their performance in language and working memory tasks. The authors observed that the exFAT was not lateralized in any group; there were statistically significant differences instead in the volume of the left exFAT between the groups of best performers and worst performers in the language task and of the right exFAT between top performers and bottom performers for 2-back working memory task, but not for the 0-back working memory task (21). In these *n*-back tasks, a series of visual stimuli appears, and the subjects were asked for each stimulus as to whether it corresponds a stimulus *n* trials ahead (20). The FA of the right FAT was also found to be associated with better visual memory performance in the delayed matching to sample task in a study considering 39 healthy brothers of autism spectrum disorder (ASD)-affected boys (116). This task consists on presenting a stimulus to the subject to make them memorize it, and after a delay, the stimulus is presented again but with other stimuli, and the subject has to choose the right one (117). These evidences suggest that the FAT is another tract to be considered during tasks performed in awake surgical resection of tumors located in the right frontal lobe in order to preserve the working memory function. The working memory was particularly examined in individuals with right non-dominant frontal tumors so far, using intraoperative tests, such as

TABLE 1 | Summary of putative frontal aslant tract functions and useful assessment tests.

Roles	Specific functions	Evaluation tests
Language	Verbal fluency	Phonemic fluency tests (FAS) Mean length of utterance Western Aphasia Battery-Revised (WAB-R) fluency subtest Words per minutes (WPM) test
	Control of the articulatory apparatus	Interview about a neutral topic Reading task Stuttering Severity Instrument (SSI)
	Lexical and semantic word selection	Noun-based verb generation task Verb-based noun generation task Sentence completion task Picture-word interference task Lexical decision task
	Grammatical processing	Sentence generation task
Motor and executive functions	Visuo-motor integration	Reach to grasp task Reach task vs. a target object
	Constructional praxis	Copy of drawings test Copy of drawings with landmarks test Raven's Colored Matrices
	Inhibitory regulation of speech and motor actions	Go/No Go trial Stop-Signal trial
	Executive function abilities	Behavior Rating Inventory of Executive Function (BRIEF)
Working memory	Verbal, spatial and visual working memory	Backward and forward digit span test n-back working memory task Delayed Matching to Sample (DMS) task
Social community and attention tasks	Identification and expression of communicative purposes and ability to concentrate	Autism Diagnostic Interview-Revised (ADI-R) Social Responsiveness Scale (SRS) Social Communication Questionnaire (SCQ) Child Behavior Checklist (CBCL)
Music processing	Online correlation and differentiation of subsequent sounds	Montreal Battery of Evaluation of Amusia (MBEA)

the digit span test for verbal working memory and the 2-back test for spatial working memory (55, 118).

Finally, in a study conducted by Chen et al., mean diffusivity of the bilateral FAT, along with the bilateral superior longitudinal fasciculus, was observed to be significantly associated to fluid intelligence (119). Fluid intelligence is defined as an innate capability, independent from experience and education, that allows one to make logical reasons and decisions to solve problems and respond to complex and unpredictable situations. Since this ability is also linked with working memory, executive functions, and attention, this result is aligned with the studies mentioned above (120).

Roles in Social Community Tasks

In 2014, Catani and Bambini have proposed a five-levels model for social communication based on results of functional and anatomical neuroimaging studies in humans. For each level, including informative actions, communicative intentions, lexical and semantic processing, syntactic analysis, and pragmatic integration, they identified the correlated white matter tracts. On the bases of the regions and relative functions connected by the FAT, the authors associated this tract to the communicative intentions level (level 2), suggesting a role in identification and expression of communicative purposes (121). Recently, a relationship has been described between social communication deficits in ASD and FAT integrity, evaluated through FA. ASD is a neurological and developmental disorder with social communication deficits and social reciprocal interaction impairment as core symptoms, and the diagnosis is clinical according to the Diagnostic and Statistical Manual of Mental Disorders (DSM–5) diagnostic criteria (122, 123). These problems may be seen with various grades of severity using different scales, of which the most important are the Autism Diagnostic Interview—Revised and the Social Responsiveness

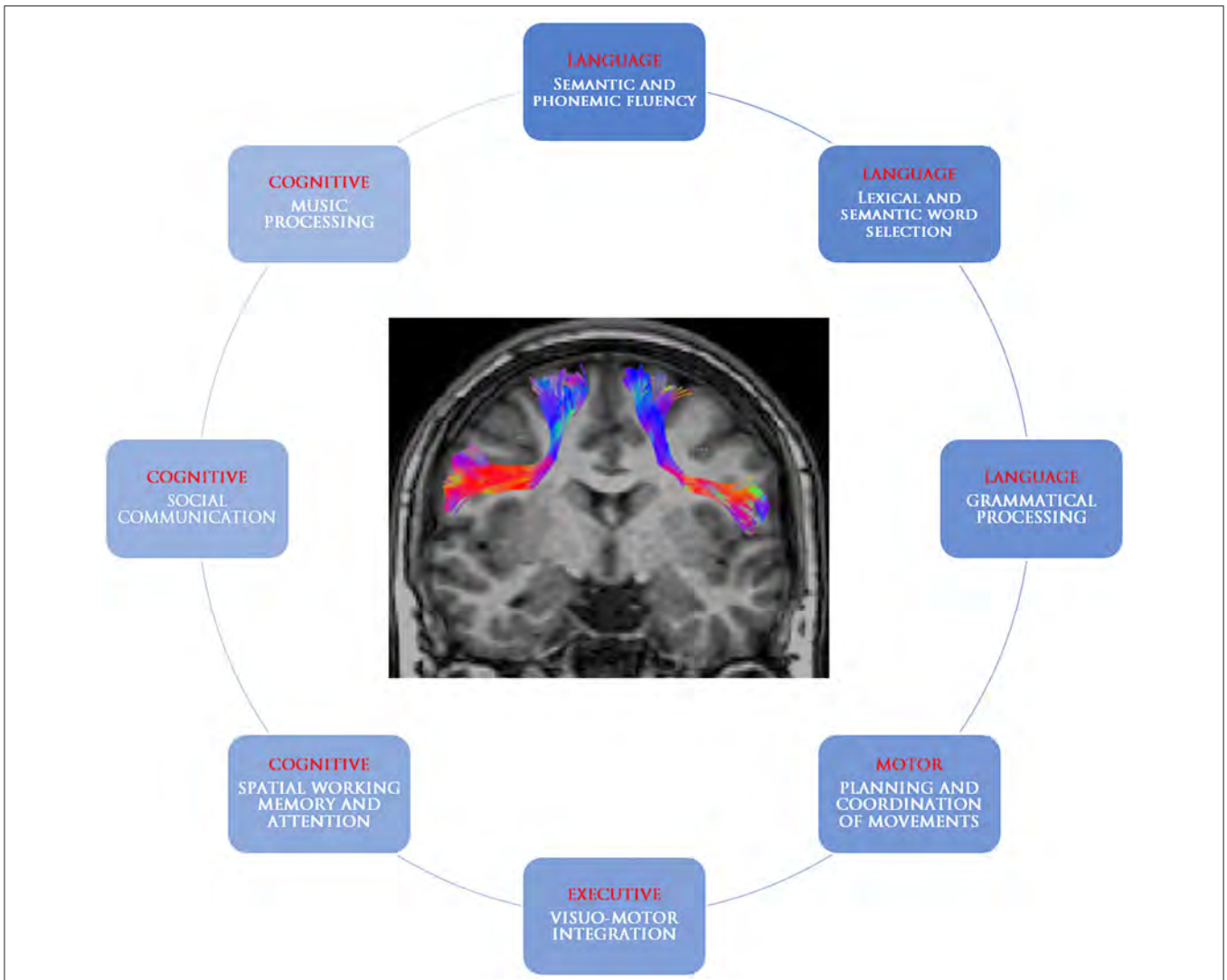

FIGURE 4 | Graphical representation of the frontal aslant tract and its putative roles.

Scale for subjects above 18 months, the Social Communication Questionnaire, and the Child Behavior Checklist (CBCL) for individuals above 4 years old (124). Lo et al. firstly identified that the microstructural integrity of the bilateral FAT was decreased in a group of 62 right-handed boys with ASD compared to a group of 55 normally developing boys. Moreover, the FA values resulted to be significantly associated with the severity of socially related communication and interaction deficits in the ASD group (125). The same results were obtained later in another study that had also shown a reduction of the bilateral FAT integrity in unaffected siblings of subjects with ASD (116). Based on these results, Lo et al. tried to identify intermediate phenotypes of social communication deficits in ASD, taking into consideration three different groups: 30 boys with ASD, 27 healthy brothers of individuals with ASD, and 30 normally developing boys. According to previous results, the FAT integrity was reduced both in ASD subjects and in the unaffected siblings. Moreover, the reduction was also associated with the social communication scores (126). These findings suggest that the FAT may potentially contribute to the neural processes involved in social communication deficits in ASD.

Roles in Attention

Attention-Deficit Hyperactivity Disorder (ADHD) is a complex and heterogeneous brain developmental condition associated with excesses levels of hyperactivity and inability to concentrate (127). The clinical diagnosis is made according to the DSM-5 criteria (123), but ADHD tendency can be assessed through the Conner's Comprehensive Behavior Rating Scale in children and the Conner's Adult ADHD Rating Scales in adults (128). Garic et al. observed, for the first time, a relationship between left laterality of the FAT and attention problems in children (34). In a group of 70 subjects younger than 19 years old, the left laterality of the FAT predicted greater attention problems (measured *via* CBCL) and lower executive function abilities (measured *via* the Behavior Rating Inventory of Executive Function). This result is aligned with the previous structural and functional neuroimaging studies showing that right IFG and pre-SMA alterations are also associated with impaired executive function and ADHD (129–131).

Roles in Music Processing

Since the IFG and the motor cortical areas have been shown to contribute to music–syntactic and rhythm processing, the FAT, connecting these areas, may also be involved in music processing (132). The first evidence comes from a study conducted in a group of 42 right-handed stroke patients. Structural impairment of different white matter tracts, including the FAT, resulted to be associated with post-stroke non-recovered amusia. To evaluate the music perception of the patients, the authors used the Montreal Battery of Evaluation of Amusia (133). According to the other FAT functions mentioned above, the role of the FAT in music processing and perception may be, in particular, related to its role in attention and working memory, both of which are useful to allow online correlation and differentiation of subsequent sounds.

CONCLUSION

The frontal aslant tract is a recently identified white matter tract connecting the supplementary motor area complex and the lateral superior frontal gyrus to the ipsilateral inferior frontal gyrus and the anterior insula. The present review retrieved studies suggesting its involvement in speech and language functions (verbal fluency, initiation and inhibition of speech, sentence production, and lexical decision) as well as executive functions, visual–motor activities, orofacial movements, inhibitory control, working memory, social community tasks, attention, and music processing (**Table 1**, **Figure 4**). The acquired knowledge on the FAT anatomical connectivity and its functional roles may raise awareness in the neurosurgical community to set up their practical applications in routine surgical activities and to pose future foundation for intraoperative stimulation research studies.

DATA AVAILABILITY STATEMENT

The original contributions presented in the study are included in the article/**Supplementary Material**, further inquiries can be directed to the corresponding author/s.

AUTHOR CONTRIBUTIONS

ELC, DE, and EG: conception and design, and drafting the article. ELC: approved the final version of the manuscript on behalf of all authors. PF, MB, and GS: administrative/technical/material support and study supervision. All authors: acquisition of data, critically revising the article, and reviewed submitted version of manuscript.

SUPPLEMENTARY MATERIAL

The Supplementary Material for this article can be found online at: https://www.frontiersin.org/articles/10.3389/fneur.2021.641586/full#supplementary-material

Supplementary Table 1 | Studies included in the qualitative synthesis of the systematic literature review according to PRISMA guidelines.

REFERENCES

1. Aron AR, Behrens TE, Smith S, Frank MJ, Poldrack RA. Triangulating a cognitive control network using diffusion-weighted magnetic resonance imaging (MRI) and functional MRI. *J Neurosci.* (2007) 27:3743–52. doi: 10.1523/JNEUROSCI.0519-07.2007
2. Catani M, Dell'Acqua F, Vergani F, Malik F, Hodge H, Roy P, et al. Short frontal lobe connections of the human brain. *Cortex.* (2012) 48:273–91. doi: 10.1016/j.cortex.2011.12.001
3. Thiebaut de Schotten M, Dell'Acqua F, Valabregue R, Catani M. Monkey to human comparative anatomy of the frontal lobe association tracts. *Cortex.* (2012) 48:82–96. doi: 10.1016/j.cortex.2011.10.001

4. Briggs RG, Chakraborty AR, Anderson CD, Abraham CJ, Palejwala AH, Conner AK, et al. Anatomy and white matter connections of the inferior frontal gyrus. *Clin Anat.* (2019) 32:546–56. doi: 10.1002/ca.23349
5. Briggs RG, Khan AB, Chakraborty AR, Abraham CJ, Anderson CD, Karas PJ, et al. Anatomy and white matter connections of the superior frontal gyrus. *Clin Anat.* (2020) 33:823–32. doi: 10.1002/ca.23523
6. Liu X, Kinoshita M, Shinohara H, Hori O, Ozaki N, Hatta T, et al. Direct evidence of the relationship between brain metastatic adenocarcinoma and white matter fibers: a fiber dissection and diffusion tensor imaging tractography study. *J Clin Neurosci.* (2020) 77:55–61. doi: 10.1016/j.jocn.2020.05.043
7. Bozkurt B, Yagmurlu K, Middlebrooks EH, Cayci Z, Cevik OM, Karadag A, et al. Fiber connections of the supplementary motor area revisited: methodology of fiber dissection, DTI, and three dimensional documentation. *J Vis Exp.* (2017) 55681. doi: 10.3791/55681
8. Goryaynov SA, Kondrashov A V., Gol'Dberg MF, Batalov AI, Sufianov RA, Zakharova NE, et al. Long association tracts of the human white matter: an analysis of 18 hemisphere dissections and *in vivo* HARDI-CSD tractography. *Zhurnal Vopr Nejrokhirurgii Im NN Burdenko.* (2017) 81:13–25. doi: 10.17116/neiro201780713-25
9. Bozkurt B, Yagmurlu K, Middlebrooks EH, Karadag A, Ovalioglu TC, Jagadeesan B, et al. Microsurgical and tractographic anatomy of the supplementary motor area complex in humans. *World Neurosurg.* (2016) 95:99–107. doi: 10.1016/j.wneu.2016.07.072
10. Baker CM, Burks JD, Briggs RG, Smitherman AD, Glenn CA, Conner AK, et al. The crossed frontal aslant tract: a possible pathway involved in the recovery of supplementary motor area syndrome. *Brain Behav.* (2018) 8:e55681. doi: 10.1002/brb3.926
11. Komaitis S, Kalyvas A V., Skandalakis GP, Drosos E, Lani E, Liouta E, et al. The frontal longitudinal system as revealed through the fiber microdissection technique: Structural evidence underpinning the direct connectivity of the prefrontal-premotor circuitry. *J Neurosurg.* (2020) 133:1503–15. doi: 10.3171/2019.6.JNS191224
12. Koutsarnakis C, Liakos F, Kalyvas AV, Skandalakis GP, Komaitis S, Christidi F, et al. The superior frontal transsulcal approach to the anterior ventricular system: exploring the sulcal and subcortical anatomy using anatomic dissections and diffusion tensor imaging tractography. *World Neurosurg.* (2017) 106:339–54. doi: 10.1016/j.wneu.2017.06.161
13. Monroy-Sosa A, Chakravarthi SS, Fukui MB, Kura B, Jennings JE, Celix JM, et al. White matter-governed superior frontal sulcus surgical paradigm: a radioanatomic microsurgical study—part I. *Oper Neurosurg.* (2020) 19:E343–56. doi: 10.1093/ons/opaa065
14. Bertolini G, La Corte E, Aquino D, Greco E, Rossini Z, Cardia A, et al. Real-time *ex-vivo* magnetic resonance image—guided dissection of human brain white matter: a proof-of-principle study. *World Neurosurg.* (2019) 125:198–206. doi: 10.1016/j.wneu.2019.01.196
15. Catani M, Mesulam MM, Jakobsen E, Malik F, Martersteck A, Wieneke C, et al. A novel frontal pathway underlies verbal fluency in primary progressive aphasia. *Brain.* (2013) 136:2619–28. doi: 10.1093/brain/awt163
16. Canu E, Agosta F, Imperiale F, Fontana A, Caso F, Spinelli EG, et al. Added value of multimodal MRI to the clinical diagnosis of primary progressive aphasia variants. *Cortex.* (2019) 113:58–66. doi: 10.1016/j.cortex.2018.11.025
17. Mandelli ML, Caverzasi E, Binney RJ, Henry ML, Lobach I, Block N, et al. Frontal white matter tracts sustaining speech production in primary progressive aphasia. *J Neurosci.* (2014) 34:9754–67. doi: 10.1523/JNEUROSCI.3464-13.2014
18. Halai AD, Woollams AM, Lambon Ralph MA. Using principal component analysis to capture individual differences within a unified neuropsychological model of chronic post-stroke aphasia: revealing the unique neural correlates of speech fluency, phonology and semantics. *Cortex.* (2017) 86:275–89. doi: 10.1016/j.cortex.2016.04.016
19. Rizio AA, Diaz MT. Language, aging, and cognition: frontal aslant tract and superior longitudinal fasciculus contribute toward working memory performance in older adults. *Neuroreport.* (2016) 27:689–93. doi: 10.1097/WNR.0000000000000597
20. Gajewski PD, Hanisch E, Falkenstein M, Thönes S, Wascher E. What does the n-Back task measure as we get older? Relations between working-memory measures and other cognitive functions across the lifespan. *Front Psychol.* (2018) 9:2208. doi: 10.3389/fpsyg.2018.02208
21. Varriano F, Pascual-Diaz S, Prats-Galino A. When the FAT goes wide: right extended frontal aslant tract volume predicts performance on working memory tasks in healthy humans. *PLoS ONE.* (2018) 13:e0200786. doi: 10.1371/journal.pone.0200786
22. Budisavljevic S, Dell'Acqua F, Djordjilovic V, Miotto D, Motta R, Castiello U. The role of the frontal aslant tract and premotor connections in visually guided hand movements. *Neuroimage.* (2017) 146:419–28. doi: 10.1016/j.neuroimage.2016.10.051
23. Serra L, Gabrielli GB, Tuzzi E, Spanò B, Giulietti G, Failoni V, et al. Damage to the frontal aslant tract accounts for visuo-constructive deficits in Alzheimer's disease. *J Alzheimers Dis.* (2017) 60:1015–24. doi: 10.3233/JAD-1706388
24. Dick AS, Garic D, Graziano P, Tremblay P. The frontal aslant tract (FAT) and its role in speech, language and executive function. *Cortex.* (2019) 111:148–63. doi: 10.1016/j.cortex.2018.10.015
25. Ruffolo JS. Visual-motor function. In: Kreutzer JS, DeLuca J, Caplan B, editors. *Encyclopedia of Clinical Neuropsychology*. Cham: Springer (2018). p. 3644–50. doi: 10.1007/978-3-319-57111-9_1417
26. Moher D, Shamseer L, Clarke M, Ghersi D, Liberati A, Petticrew M, et al. Preferred reporting items for systematic review and meta-analysis protocols (PRISMA-P) 2015 statement. *Rev Esp Nutr Humana y Diet.* (2016) 20:148–60. doi: 10.1186/2046-4053-4-1
27. Szmuda T, Rogowska M, Słoniewski P, Abuhaimed A, Szmuda M, Springer J, et al. Frontal aslant tract projections to the inferior frontal gyrus. *Folia Morphol.* (2017) 76:574–81. doi: 10.5603/FM.a2017.0039
28. Glasser MF, Coalson TS, Robinson EC, Hacker CD, Harwell J, Yacoub E, et al. A multi-modal parcellation of human cerebral cortex. *Nature.* (2016) 536:171–8. doi: 10.1038/nature18933
29. Briggs RG, Conner AK, Rahimi M, Sali G, Baker CM, Burks JD, et al. A connectomic atlas of the human cerebrum-chapter 14: tractographic description of the frontal aslant tract. *Oper Neurosurg.* (2018) 15:S444–9. doi: 10.1093/ons/opy268
30. Ruan J, Bludau S, Palomero-Gallagher N, Caspers S, Mohlberg H, Eickhoff SB, et al. Cytoarchitecture, probability maps, and functions of the human supplementary and pre-supplementary motor areas. *Brain Struct Funct.* (2018) 223:4169–86. doi: 10.1007/s00429-018-1738-6
31. Broce I, Bernal B, Altman N, Tremblay P, Dick AS. Fiber tracking of the frontal aslant tract and subcomponents of the arcuate fasciculus in 5-8-year-olds: relation to speech and language function. *Brain Lang.* (2015) 149:66–76. doi: 10.1016/j.bandl.2015.06.006
32. Vallesi A, Babcock L. Asymmetry of the frontal aslant tract is associated with lexical decision. *Brain Struct Funct.* (2020) 225:1009–17. doi: 10.1007/s00429-020-02054-1
33. Siless V, Davidow JY, Nielsen J, Fan Q, Hedden T, Hollinshead M, et al. Registration-free analysis of diffusion MRI tractography data across subjects through the human lifespan. *Neuroimage.* (2020) 214:116703. doi: 10.1016/j.neuroimage.2020.116703
34. Garic D, Broce I, Graziano P, Mattfeld A, Dick AS. Laterality of the frontal aslant tract (FAT) explains externalizing behaviors through its association with executive function. *Dev Sci.* (2019) 22:e12744. doi: 10.1111/desc.12744
35. Ookawa S, Enatsu R, Kanno A, Ochi S, Akiyama Y, Kobayashi T, et al. Frontal fibers connecting the superior frontal gyrus to broca area: a corticocortical evoked potential study. *World Neurosurg.* (2017) 107:239–48. doi: 10.1016/j.wneu.2017.07.166
36. Hiroshima S, Anei R, Murakami N, Kamada K. Functional localization of the supplementary motor area. *Neurol Med Chir (Tokyo).* (2014) 54:511–20. doi: 10.2176/nmc.oa2012-0321
37. Lehéricy S, Ducros M, Krainik A, Francois C, Van De Moortele PF, Ugurbil K, et al. 3-D diffusion tensor axonal tracking shows distinct SMA and pre-SMA projections to the human striatum. *Cereb Cortex.* (2004) 14:1302–9. doi: 10.1093/cercor/bhh091
38. Baker CM, Burks JD, Briggs RG, Sheets JR, Conner AK, Glenn CA, et al. A connectomic atlas of the human cerebrum-chapter 3: the motor, premotor, and sensory cortices. *Oper Neurosurg.* (2018) 15:S75–121. doi: 10.1093/ons/opy256
39. Baker CM, Burks JD, Briggs RG, Conner AK, Glenn CA, Robbins JM, et al. A connectomic atlas of the human cerebrum-chapter 5:

the insula and opercular cortex. *Oper Neurosurg.* (2018) 15:S175–244. doi: 10.1093/ons/opy259
40. Sridharan D, Levitin DJ, Menon V. A critical role for the right fronto-insular cortex in switching between central-executive and default-mode networks. *Proc Natl Acad Sci USA.* (2008) 105:12569–74. doi: 10.1073/pnas.0800005105
41. Seeley WW. The salience network: a neural system for perceiving and responding to homeostatic demands. *J Neurosci.* (2019) 39:9878–82. doi: 10.1523/JNEUROSCI.1138-17.2019
42. Fajardo C, Escobar MI, Buriticá E, Arteaga G, Umbarila J, Casanova MF, et al. Von Economo neurons are present in the dorsolateral (dysgranular) prefrontal cortex of humans. *Neurosci Lett.* (2008) 435:215–8. doi: 10.1016/j.neulet.2008.02.048
43. Nestor PJ, Graham NL, Fryer TD, Williams GB, Patterson K, Hodges JR. Progressive non-fluent aphasia is associated with hypometabolism centred on the left anterior insula. *Brain.* (2003) 126:2406–18. doi: 10.1093/brain/awg240
44. Mandelli ML, Vilaplana E, Brown JA, Hubbard HI, Binney RJ, Attygalle S, et al. Healthy brain connectivity predicts atrophy progression in non-fluent variant of primary progressive aphasia. *Brain.* (2016) 139:2778–91. doi: 10.1093/brain/aww195
45. Maier MA, Armand J, Kirkwood PA, Yang HW, Davis JN, Lemon RN. Differences in the corticospinal projection from primary motor cortex and supplementary motor area to macaque upper limb motoneurons: an anatomical and electrophysiological study. *Cereb Cortex.* (2002) 12:281–96. doi: 10.1093/cercor/12.3.281
46. Ille S, Engel L, Kelm A, Meyer B, Krieg SM. Language-eloquent white matter pathway tractography and the course of language function in glioma patients. *Front Oncol.* (2018) 8:572. doi: 10.3389/fonc.2018.00572
47. Young JS, Morshed RA, Mansoori Z, Cha S, Berger MS. Disruption of the frontal aslant tract is not associated with long-term postoperative language deficits: a case report. *World Neurosurg.* (2020) 133:192–5. doi: 10.1016/j.wneu.2019.09.128
48. Kinoshita M, de Champfleur NM, Deverdun J, Moritz-Gasser S, Herbet G, Duffau H. Role of fronto-striatal tract and frontal aslant tract in movement and speech: an axonal mapping study. *Brain Struct Funct.* (2015) 220:3399–412. doi: 10.1007/s00429-014-0863-0
49. Sierpowska J, Gabarrós A, Fernandez-Coello A, Camins A, Castañer S, Juncadella M, et al. Morphological derivation overflow as a result of disruption of the left frontal aslant white matter tract. *Brain Lang.* (2015) 142:54–64. doi: 10.1016/j.bandl.2015.01.005
50. Kassam AB, Monroy-Sosa A, Fukui MB, Kura B, Jennings JE, Celix JM, et al. White matter governed superior frontal sulcus surgical paradigm: a radioanatomic microsurgical study—part II. *Oper Neurosurg.* (2020) 19:E357–69. doi: 10.1093/ons/opaa066
51. Vassal F, Boutet C, Lemaire JJ, Nuti C. New insights into the functional significance of the frontal aslant tract: an anatomo-functional study using intraoperative electrical stimulations combined with diffusion tensor imaging-based fiber tracking. *Br J Neurosurg.* (2014) 28:685–7. doi: 10.3109/02688697.2014.889810
52. Fujii M, Maesawa S, Motomura K, Futamura M, Hayashi Y, Koba I, et al. Intraoperative subcortical mapping of a language-associated deep frontal tract connecting the superior frontal gyrus to Broca's area in the dominant hemisphere of patients with glioma. *J Neurosurg.* (2015) 122:1390–6. doi: 10.3171/2014.10.JNS14945
53. Rech F, Herbet G, Gaudeau Y, Mézières S, Moureau JM, Moritz-Gasser S, et al. A probabilistic map of negative motor areas of the upper limb and face: a brain stimulation study. *Brain.* (2019) 142:952–65. doi: 10.1093/brain/awz021
54. Yokoyama R, Enatsu R, Kanno A, Suzuki H, Suzuki Y, Sasagawa A, et al. Negative motor networks: electric cortical stimulation and diffusion tensor imaging. *Rev Neurol.* (2020) 176:592–600. doi: 10.1016/j.neurol.2019.12.005
55. Motomura K, Chalise L, Ohka F, Aoki K, Tanahashi K, Hirano M, et al. Neurocognitive and functional outcomes in patients with diffuse frontal lower-grade gliomas undergoing intraoperative awake brain mapping. *J Neurosurg.* (2020) 132:1683–91. doi: 10.3171/2019.3.JNS19211
56. Bizzi A, Nava S, Ferrè F, Castelli G, Aquino D, Ciaraffa F, et al. Aphasia induced by gliomas growing in the ventrolateral frontal region: assessment with diffusion MR tractography, functional MR imaging and neuropsychology. *Cortex.* (2012) 48:255–72. doi: 10.1016/j.cortex.2011.11.015
57. Patterson J. Verbal fluency. In: Kreutzer JS, DeLuca J, Caplan B, editors. *Encyclopedia of Clinical Neuropsychology*. New York, NY: Springer (2011). p. 2603–6. doi: 10.1007/978-0-387-79948-3_1423
58. Basilakos A, Fillmore PT, Rorden C, Guo D, Bonilha L, Fridriksson J. Regional white matter damage predicts speech fluency in chronic post-stroke aphasia. *Front Hum Neurosci.* (2014) 8:845. doi: 10.3389/fnhum.2014.00845
59. Alyahya RSW, Halai AD, Conroy P, Lambon MA. A unified model of post-stroke language deficits including discourse production and their neural correlates. *Brain.* (2020) 143:1541–54. doi: 10.1093/brain/awaa074
60. Li M, Zhang Y, Song L, Huang R, Ding J, Fang Y, et al. Structural connectivity subserving verbal fluency revealed by lesion-behavior mapping in stroke patients. *Neuropsychologia.* (2017) 101:85–96. doi: 10.1016/j.neuropsychologia.2017.05.008
61. Berthier ML, De-Torres I, Paredes-Pacheco J, Roé-Vellvé N, Thurnhofer-Hemsi K, Torres-Prioris MJ, et al. Cholinergic potentiation and audiovisual repetition-imitation therapy improve speech production and communication deficits in a person with crossed aphasia by inducing structural plasticity in white matter tracts. *Front Hum Neurosci.* (2017) 11:304. doi: 10.3389/fnhum.2017.00304
62. Blecher T, Miron S, Schneider GG, Achiron A, Ben-Shachar M. Association between white matter microstructure and verbal fluency in patients with multiple sclerosis. *Front Psychol.* (2019) 10:1607. doi: 10.3389/fpsyg.2019.01607
63. Keser Z, Hillis AE, Schulz PE, Hasan KM, Nelson FM. Frontal aslant tracts as correlates of lexical retrieval in MS. *Neurol Res.* (2020) 42:805–10. doi: 10.1080/01616412.2020.1781454
64. Tseng CEJ, Froudist-Walsh S, Kroll J, Karolis V, Brittain PJ, Palamin N, et al. Verbal fluency is affected by altered brain lateralization in adults who were born very preterm. *eNeuro.* (2019) 6:ENEURO.0274-18.2018. doi: 10.1523/ENEURO.0274-18.2018
65. Obayashi S. The supplementary motor area responsible for word retrieval decline after acute thalamic stroke revealed by coupled spect and near-infrared spectroscopy. *Brain Sci.* (2020) 10:247. doi: 10.3390/brainsci100402477
66. Chenausky K, Paquette S, Norton A, Schlaug G. Apraxia of speech involves lesions of dorsal arcuate fasciculus and insula in patients with aphasia. *Neurol Clin Pract.* (2020) 10:162–9. doi: 10.1212/CPJ.0000000000000699
67. Teichmann M, Rosso C, Martini JB, Bloch I, Brugières P, Duffau H, et al. A cortical-subcortical syntax pathway linking Broca's area and the striatum. *Hum Brain Mapp.* (2015) 36:2270–83. doi: 10.1002/hbm.22769
68. Keser Z, Sebastian R, Hasan KM, Hillis AE. Right hemispheric homologous language pathways negatively predicts poststroke naming recovery. *Stroke.* (2020) 51:1002–5. doi: 10.1161/STROKEAHA.119.028293
69. Costentin G, Derrey S, Gérardin E, Cruypeninck Y, Pressat-Laffouilhere T, Anouar Y, et al. White matter tracts lesions and decline of verbal fluency after deep brain stimulation in Parkinson's disease. *Hum Brain Mapp.* (2019) 40:2561–70. doi: 10.1002/hbm.24544
70. Cipolotti L, Molenberghs P, Dominguez J, Smith N, Smirni D, Xu T, et al. Fluency and rule breaking behaviour in the frontal cortex. *Neuropsychologia.* (2020) 137:107308. doi: 10.1016/j.neuropsychologia.2019.107308
71. Faulkner JW, Wilshire CE. Mapping eloquent cortex: a voxel-based lesion-symptom mapping study of core speech production capacities in brain tumour patients. *Brain Lang.* (2020) 200:104710. doi: 10.1016/j.bandl.2019.104710
72. Novick JM, Trueswell JC, Thompson-Schill SL. Cognitive control and parsing: reexamining the role of Broca's area in sentence comprehension. *Cogn Affect Behav Neurosci.* (2005) 5:263–81. doi: 10.3758/CABN.5.3.263
73. Grodzinsky Y, Santi A. The battle for Broca's region. *Trends Cogn Sci.* (2008) 12:474–80. doi: 10.1016/j.tics.2008.09.001
74. Schnur TT, Schwartz MF, Kimberg DY, Hirshorn E, Coslett HB, Thompson-Schill SL. Localizing interference during naming: convergent neuroimaging and neuropsychological evidence for the function of Broca's area. *Proc Natl Acad Sci USA.* (2009) 106:322–7. doi: 10.1073/pnas.0805874106
75. Bozic M, Szlachta Z, Marslen-Wilson WD. Cross-linguistic parallels in processing derivational morphology: evidence from Polish. *Brain Lang.* (2013) 127:533–8. doi: 10.1016/j.bandl.2013.09.0011

76. Bozic M, Tyler LK, Ives DT, Randall B, Marslen-Wilson WD. Bihemispheric foundations for human speech comprehension. *Proc Natl Acad Sci USA.* (2010) 107:17439–44. doi: 10.1073/pnas.1000531107
77. Shapiro K, Caramazza A. Grammatical processing of nouns and verbs in left frontal cortex? *Neuropsychologia.* (2003) 41:1189–98. doi: 10.1016/S0028-3932(03)00037-X
78. Alario FX, Chainay H, Lehericy S, Cohen L. The role of the supplementary motor area (SMA) in word production. *Brain Res.* (2006) 1076:129–43. doi: 10.1016/j.brainres.2005.11.104
79. Gabarrós A, Martino J, Juncadella M, Plans G, Pujol R, Deus J, et al. Identificación intraoperatoria del área motora suplementaria en cirugía neurooncológica. *Neurocirugia.* (2011) 22:123–32. doi: 10.1016/S1130-1473(11)70010-0
80. Indefrey P. The spatial and temporal signatures of word production components: a critical update. *Front Psychol.* (2011) 2:255. doi: 10.3389/fpsyg.2011.00255
81. Indefrey P, Levelt WJM. The spatial and temporal signatures of word production components. *Cognition.* (2004) 92:101–44. doi: 10.1016/j.cognition.2002.06.001
82. Chernoff BL, Teghipco A, Garcea FE, Sims MH, Paul DA, Tivarus ME, et al. A role for the frontal aslant tract in speech planning: a neurosurgical case study. *J Cogn Neurosci.* (2018) 30:752–69. doi: 10.1162/jocn_a_01244
83. Chernoff BL, Sims MH, Smith SO, Pilcher WH, Mahon BZ. Direct electrical stimulation of the left frontal aslant tract disrupts sentence planning without affecting articulation. *Cogn Neuropsychol.* (2019) 36:178–92. doi: 10.1080/02643294.2019.1619544
84. Corrivetti F, de Schotten MT, Poisson I, Froelich S, Descoteaux M, Rheault F, et al. Dissociating motor–speech from lexico-semantic systems in the left frontal lobe: insight from a series of 17 awake intraoperative mappings in glioma patients. *Brain Struct Funct.* (2019) 224:1151–65. doi: 10.1007/s00429-019-01827-7
85. Zyryanov A, Malyutina S, Dragoy O. Left frontal aslant tract and lexical selection: evidence from frontal lobe lesions. *Neuropsychologia.* (2020) 147:107385. doi: 10.1016/j.neuropsychologia.2020.107385
86. Perez HR, Stoeckle JH. Stuttering. *Can Fam Physician.* (2016) 62:479–84. Available online at: http://www.cfp.ca/content/62/6/479.abstract
87. Budde KS, Barron DS, Fox PT. Stuttering, induced fluency, and natural fluency: a hierarchical series of activation likelihood estimation meta-analyses. *Brain Lang.* (2014) 139:99–107. doi: 10.1016/j.bandl.2014.10.002
88. Neef NE, Bütfering C, Anwander A, Friederici AD, Paulus W, Sommer M. Left posterior-dorsal area 44 couples with parietal areas to promote speech fluency, while right area 44 activity promotes the stopping of motor responses. *Neuroimage.* (2016) 142:628–44. doi: 10.1016/j.neuroimage.2016.08.030
89. Chesters J, Möttönen R, Watkins KE. Transcranial direct current stimulation over left inferior frontal cortex improves speech fluency in adults who stutter. *Brain.* (2018) 141:1161–71. doi: 10.1093/brain/awy011
90. Riley G. *The Stuttering Severity Instrument for Adults and Children (SSI-3).* 3rd ed. Austin, TX: PRO-ED (1994).
91. Kronfeld-Duenias V, Amir O, Ezrati-Vinacour R, Civier O, Ben-Shachar M. The frontal aslant tract underlies speech fluency in persistent developmental stuttering. *Brain Struct Funct.* (2016) 221:365–81. doi: 10.1007/s00429-014-0912-8
92. Kemerdere R, de Champfleur NM, Deverdun J, Cochereau J, Moritz-Gasser S, Herbet G, et al. Role of the left frontal aslant tract in stuttering: a brain stimulation and tractographic study. *J Neurol.* (2016) 263:157–67. doi: 10.1007/s00415-015-7949-3
93. Neef NE, Anwander A, Bütfering C, Schmidt-Samoa C, Friederici AD, Paulus W, et al. Structural connectivity of right frontal hyperactive areas scales with stuttering severity. *Brain.* (2018) 141:191–204. doi: 10.1093/brain/awx316
94. Glover S, Wall MB, Smith AT. Distinct cortical networks support the planning and online control of reaching-to-grasp in humans. *Eur J Neurosci.* (2012) 35:909–15. doi: 10.1111/j.1460-9568.2012.08018.x
95. Laplane D, Talairach J, Meininger V, Bancaud J, Orgogozo JM. Clinical consequences of corticectomies involving the supplementary motor area in man. *J Neurol Sci.* (1977) 34:301–14. doi: 10.1016/0022-510X(77)90148-4
96. Nakajima R, Kinoshita M, Yahata T, Nakada M. Recovery time from supplementary motor area syndrome: relationship to postoperative day 7 paralysis and damage of the cingulum. *J Neurosurg.* (2020) 132:865–74. doi: 10.3171/2018.10.JNS182391
97. Tsai TH, Su H Te, Hsu YC, Shih YC, Chen CC, Hu FR, et al. White matter microstructural alterations in amblyopic adults revealed by diffusion spectrum imaging with systematic tract-based automatic analysis. *Br J Ophthalmol.* (2019) 103:511–6. doi: 10.1136/bjophthalmol-2017-311733
98. Webber AL, Black A, Hoang S, English E, Wood J. *Amblyopia Affects Visual Attention, Visual Search and Scanning in Children.* Anaheim, CA: American Academy of Optometry (2016).
99. Suttle CM, Melmoth DR, Finlay AL, Sloper JJ, Grant S. Eye-hand coordination skills in children with and without amblyopia. *Investig Ophthalmol Vis Sci.* (2011) 52:1851–64. doi: 10.1167/iovs.10-6341
100. Rutten GJ. Speech hastening during electrical stimulation of left premotor cortex. *Brain Lang.* (2015) 141:77–9. doi: 10.1016/j.bandl.2014.11.014
101. Rech F, Herbet G, Moritz-Gasser S, Duffau H. Disruption of bimanual movement by unilateral subcortical electrostimulation. *Hum Brain Mapp.* (2014) 35:3439–45. doi: 10.1002/hbm.22413
102. Aron AR, Robbins TW, Poldrack RA. Inhibition and the right inferior frontal cortex: one decade on. *Trends Cogn Sci.* (2014) 18:177–85. doi: 10.1016/j.tics.2013.12.00
103. Wessel JR, Aron AR. On the globality of motor suppression: unexpected events and their influence on behavior and cognition. *Neuron.* (2017) 93:259–80. doi: 10.1016/j.neuron.2016.12.013
104. Aron AR, Herz DM, Brown P, Forstmann BU, Zaghloul K. Frontosubthalamic circuits for control of action and cognition. *J Neurosci.* (2016) 36: 11489–95. doi: 10.1523/JNEUROSCI.2348-16.2016
105. Rubia K, Russell T, Overmeyer S, Brammer MJ, Bullmore ET, Sharma T, et al. Mapping motor inhibition: conjunctive brain activations across different versions of go/no-go and stop tasks. *Neuroimage.* (2001) 13:250–61. doi: 10.1006/nimg.2000.0685
106. Aron AR, Monsell S, Sahakian BJ, Robbins TW. A componential analysis of task-switching deficits associated with lesions of left and right frontal cortex. *Brain.* (2004) 127:1561–73. doi: 10.1093/brain/awh169
107. Aron AR, Fletcher PC, Bullmore ET, Sahakian BJ, Robbins TW. Stop-signal inhibition disrupted by damage to right inferior frontal gyrus in humans. *Nat Neurosci.* (2003) 6:115–6. doi: 10.1038/nn1003
108. Aron AR. The neural basis of inhibition in cognitive control. *Neuroscientist.* (2007) 13:214–28. doi: 10.1177/1073858407299288
109. Silveri MC, Incordino F, Lo Monaco R, Bizzarro A, Masullo C, Piludu F, et al. Neural substrates of the 'low-level' system for speech articulation: evidence from primary opercular syndrome. *J Neuropsychol.* (2017) 11:450–7. doi: 10.1111/jnp.12099
110. Turgut A, Tubbs RS, Turgut M. French neurologists Charles Foix and Jean Alfred Émile Chavany and French pediatrician Julien Marie and the Foix-Chavany-Marie syndrome. *Childs Nerv Syst.* (2020) 36:2597–8. doi: 10.1007/s00381-019-04290-1
111. Digby R, Wells A, Menon D, Helmy A. Foix-Chavany-Marie syndrome secondary to bilateral traumatic operculum injury. *Acta Neurochir (Wien).* (2018) 160:2303–5. doi: 10.1007/s00701-018-3702-x
112. Martino J, De Lucas EM, Ibáñez-Plágaro FJ, Valle-Folgueral JM, Vázquez-Barquero A. Foix-Chavany-Marie syndrome caused by a disconnection between the right pars opercularis of the inferior frontal gyrus and the supplementary motor area. *J Neurosurg.* (2012) 117:844–50. doi: 10.3171/2012.7.JNS12404
113. Ohtomo R, Iwata A, Tsuji S. Unilateral opercular infarction presenting with foix-chavany-marie syndrome. *J Stroke Cerebrovasc Dis.* (2014) 23:179–81. doi: 10.1016/j.jstrokecerebrovasdis.2012.08.015
114. Shen D, Cui L, Fang J, Cui B, Li D, Tai H. Voxel-wise meta-analysis of gray matter changes in amyotrophic lateral sclerosis. *Front Aging Neurosci.* (2016) 8:64. doi: 10.3389/fnagi.2016.00064
115. D'Esposito M, Postle BR. The cognitive neuroscience of working memory. *Annu Rev Psychol.* (2015) 66:115–42. doi: 10.1146/annurev-psych-010814-015031
116. Chien YL, Chen YJ, Hsu YC, Tseng WYI, Gau SSF. Altered white-matter integrity in unaffected siblings of probands with autism spectrum disorders. *Hum Brain Mapp.* (2017) 38:6053–67. doi: 10.1002/hbm.23810

117. Daniel TA, Katz JS, Robinson JL. Delayed match-to-sample in working memory: a BrainMap meta-analysis. *Biol Psychol.* (2016) 120:10–20. doi: 10.1016/j.biopsycho.2016.07.015
118. Motomura K, Chalise L, Ohka F, Aoki K, Tanahashi K, Hirano M, et al. Supratotal resection of diffuse frontal lower grade gliomas with awake brain mapping, preserving motor, language, and neurocognitive functions. *World Neurosurg.* (2018) 119:30–9. doi: 10.1016/j.wneu.2018.07.193
119. Chen PY, Chen C Le, Hsu YC, Tseng WYI. Fluid intelligence is associated with cortical volume and white matter tract integrity within multiple-demand system across adult lifespan. *Neuroimage.* (2020) 212:116576. doi: 10.1016/j.neuroimage.2020.116576
120. Gray JR, Chabris CF, Braver TS. Neural mechanisms of general fluid intelligence. *Nat Neurosci.* (2003) 6:316–22. doi: 10.1038/nn1014
121. Catani M, Bambini V. A model for social communication and language evolution and development (SCALED). *Curr Opin Neurobiol.* (2014) 28:165–71. doi: 10.1016/j.conb.2014.07.018
122. Faras H, Al Ateeqi N, Tidmarsh L. Autism spectrum disorders. *Ann Saudi Med.* (2010) 30:295–300. doi: 10.4103/0256-4947.65261
123. American Psychiatric Association. *Diagnostic and Statistical Manual of Mental Disorders: Diagnostic and Statistical Manual of Mental Disorders*. 5th ed. Arlington, VA: American Psychiatric Association (2013). doi: 10.1176/appi.books.9780890425596
124. Moody EJ, Reyes N, Ledbetter C, Wiggins L, DiGuiseppi C, Alexander A, et al. Screening for autism with the SRS and SCQ: variations across demographic, developmental and behavioral factors in preschool children. *J Autism Dev Disord.* (2017) 47:3550–61. doi: 10.1007/s10803-017-3255-5
125. Lo YC, Chen YJ, Hsu YC, Tseng WYI, Gau SSF. Reduced tract integrity of the model for social communication is a neural substrate of social communication deficits in autism spectrum disorder. *J Child Psychol Psychiatry Allied Discip.* (2017) 58:576–85. doi: 10.1111/jcpp.12641
126. Lo YC, Chen YJ, Hsu YC, Chien YL, Gau SSF, Tseng WYI. Altered frontal aslant tracts as a heritable neural basis of social communication deficits in autism spectrum disorder: a sibling study using tract-based automatic analysis. *Autism Res.* (2019) 12:225–38. doi: 10.1002/aur.2044
127. Tarver J, Daley D, Sayal K. Attention-deficit hyperactivity disorder (ADHD): an updated review of the essential facts. *Child Care Health Dev.* (2014) 40:762–74. doi: 10.1111/cch.12139
128. DuPaul GJ, Power TJ, Anastopoulos AD, Reid R. *ADHD Rating Scale—IV: Checklists, Norms, and Clinical Interpretation*. New York: Guilford (1998).
129. Mostofsky SH, Cooper KL, Kates WR, Denckla MB, Kaufmann WE. Smaller prefrontal and premotor volumes in boys with attention-deficit/hyperactivity disorder. *Biol Psychiatry.* (2002) 52:785–94. doi: 10.1016/S0006-3223(02)01412-9
130. Suskauer SJ, Simmonds DJ, Caffo BS, Denckla MB, Pekar JJ, Mostofsky SH. fMRI of intrasubject variability in ADHD: anomalous premotor activity with prefrontal compensation. *J Am Acad Child Adolesc Psychiatry.* (2008) 47:1141–50. doi: 10.1097/CHI.0b013e3181825b1f
131. Suskauer SJ, Simmonds DJ, Fotedar S, Blankner JG, Pekar JJ, Denckla MB, et al. Functional magnetic resonance imaging evidence for abnormalities in response selection in attention deficit hyperactivity disorder: differences in activation associated with response inhibition but not habitual motor response. *J Cogn Neurosci.* (2008) 20:478–93. doi: 10.1162/jocn.2008.20032
132. Hyde KL, Zatorre RJ, Peretz I. Functional MRI evidence of an abnormal neural network for pitch processing in congenital amusia. *Cereb Cortex.* (2011) 21:292–9. doi: 10.1093/cercor/bhq094
133. Sihvonen AJ, Ripollés P, Särkämö T, Leo V, Rodríguez-Fornells A, Saunavaara J, et al. Tracting the neural basis of music: deficient structural connectivity underlying acquired amusia. *Cortex.* (2017) 97:255–73. doi: 10.1016/j.cortex.2017.09.028

Conflict of Interest: The authors declare that the research was conducted in the absence of any commercial or financial relationships that could be construed as a potential conflict of interest.

frontiers in Oncology

ORIGINAL RESEARCH
published: 24 February 2021
doi: 10.3389/fonc.2020.631255

High Grade Glioma Treatment in Elderly People: Is It Different Than in Younger Patients? Analysis of Surgical Management Guided by an Intraoperative Multimodal Approach and Its Impact on Clinical Outcome

Giuseppe Maria Vincenzo Barbagallo[1,2], *Roberto Altieri*[1,2,3*], *Marco Garozzo*[1], *Massimiliano Maione*[1], *Stefania Di Gregorio*[1], *Massimiliano Visocchi*[4], *Simone Peschillo*[1], *Pasquale Dolce*[5] *and Francesco Certo*[1,2]

[1] Department of Neurological Surgery, Policlinico "G. Rodolico" University Hospital, Catania, Italy, [2] Interdisciplinary Research Center on Brain Tumors Diagnosis and Treatment, University of Catania, Catania, Italy, [3] Department of Neuroscience, University of Turin, Turin, Italy, [4] Neurosurgical Unit, Catholic University, Rome, Italy, [5] Department of Public Health, University of Naples Federico II, Naples, Italy

OPEN ACCESS

Edited by:
Giovanni Raffa,
University of Messina, Italy

Reviewed by:
Federico Pessina,
Humanitas University, Italy
Güliz Acker,
Charité Medical University of Berlin, Germany
Antonino Scibilia,
Universitaire de Strasbourg, France

***Correspondence:**
Roberto Altieri
roberto.altieri.87@gmail.com

Specialty section:
This article was submitted to Neuro-Oncology and Neurosurgical Oncology, a section of the journal Frontiers in Oncology

Received: 19 November 2020
Accepted: 30 December 2020
Published: 24 February 2021

Citation:
Barbagallo GMV, Altieri R, Garozzo M, Maione M, Di Gregorio S, Visocchi M, Peschillo S, Dolce P and Certo F (2021) High Grade Glioma Treatment in Elderly People: Is It Different Than in Younger Patients? Analysis of Surgical Management Guided by an Intraoperative Multimodal Approach and Its Impact on Clinical Outcome. Front. Oncol. 10:631255. doi: 10.3389/fonc.2020.631255

Objective: Age is considered a negative prognostic factor for High Grade Gliomas (HGGs) and many neurosurgeons remain skeptical about the benefits of aggressive treatment. New surgical and technological improvements may allow extended safe resection, with lower level of post-operative complications. This opportunity opens the unsolved question about the most appropriate HGG treatment in elderly patients. The aim of this study is to analyze if HGG maximal safe resection guided by an intraoperative multimodal imaging protocol coupled with neuromonitoring is associated with differences in outcome in elderly patients versus younger ones.

Methods: We reviewed 100 patients, 53 (53%) males and 47 (47%) females, with median (IQR) age of 64 (57; 72) years. Eight patients were diagnosed with Anaplastic Astrocytoma (AA), 92 with Glioblastoma (GBM). Surgery was aimed to achieve safe maximal resection. An intraoperative multimodal imaging protocol, including neuronavigation, neurophysiological monitoring, 5-ALA fluorescence, ^{11}C MET-PET, navigated i-US system and i-CT, was used, and its impact on EOTR and clinical outcome in elderly patients was analyzed. We divided patients in two groups according to their age: <65 and >65 years, and surgical and clinical results (EOTR, post-operative KPS, OS and PFS) were compared. Yet, to better understand age-related differences, the same patient cohort was also divided into <70 and >70 years and all the above data reanalyzed.

Results: In the first cohort division, we did not found KPS difference over time and survival analysis did not show significant difference between the two groups ($p = 0.36$ for OS and $p = 0.49$ for PFS). Same results were obtained increasing the age cut-off for age up to 70 years ($p = 0.52$ for OS and $p = 0.92$ for PFS).

Conclusions: Our data demonstrate that there is not statistically significant difference in post-operative EOTR, KPS, OS, and PFS between younger and elderly patients treated with extensive tumor resection aided by a intraoperative multimodal protocol.

Keywords: elderly, glioblastoma, glioma, 5ALA, geriatric population, brain tumor, ICT, IOUS

INTRODUCTION

Elderly population was defined by the United Nations as people aged >60 years However, the World Health Organization (WHO) set the limit at 65 years; improvement of wellness, health and lifestyle conditions suggests that this limit could be moved up to 70 years, although this is still debated (1). Geriatric population increases rapidly, at a projected 2.9%/year increment by year 2050 (2). Glioblastoma (GBM), the third most frequent tumor of the Central Nervous System (CNS) (14.9%) and the first among malignant ones (47.1%), is usually diagnosed at a median age of 64 years (3). The estimated incidence of GBM in the elderly patients in the United States is 6000/year (4), with rising incidence in patients >70 years in the last decade (5). Predictably, this rate should further increase within few years as life expectancy is continuously growing up. Age is a negative prognostic factor and HGG in elderly patients seem to have a most aggressive behavior because of clinical and genetic features (6–8). Although the population in such age range is constantly increasing, because of the frailty of elderly and the well-known aggressivity of HGG, many neurosurgeons and neuro-oncologists remain skeptical about the benefits of aggressive resective surgery in the geriatric population and brain biopsy or limited cytoreductive surgery are commonly used to obtain histological diagnosis. As a consequence, >65 years HGG patients were not even involved in clinical trials for new treatments (9); indeed, they represent a small group also in the Stupp study on the use of RT combined with temozolomide (TMZ) (10). Innovations in surgical planning and peri-operative medical and anesthesiological support as well as technological advancements provide the opportunity to be more aggressive in the management of CNS tumors, with less post-operative complications (11). And such opportunity opens the unsolved question about the most appropriate treatment in elderly patients.

The aim of this study is to analyze if HGG maximal safe resection guided by an intraoperative multimodal imaging protocol coupled with neuromonitoring is associated with differences in outcome in elderly patients versus younger ones, with regard to post-operative Karnofsky Performance Score (KPS), Overall Survival (OS), the Progression Free Survival (PFS) and Extent of Tumor Resection (EOTR). Specifically our primary outcome is to check if there are difference between the OS of young and elderly population. The secondary outcomes are to check if there are difference between the EOTR, post-operative KPS and PFS of the two groups.

MATERIALS AND METHODS

We have retrospectively analyzed all patients surgically treated at University Hospital of Catania from January 2014 to May 2020 and followed up until now. Inclusion criteria were: histopathological diagnosis of HGG; KPS > 60; feasible GTR of enhancing nodule (EN) according to preoperative MRI; age >18 years old; positive 11C-methionine-positron emission tomography (11C-MET-PET).

Exclusion criteria were: low KPS (≤ 60) and poor general conditions; unfeasible GTR due to tumor location (i.e. eloquency) or multifocality, recurrences, adjuvant treatment not performed at our institution, patients loss at follow-up.

In the time period before indicated 117 patients affected by gliomas were admitted at our Neurosurgical Unit. One hundred patients, 53 (53%) males and 47 (47%) females, with median (IQR) age of 64 (57; 72) years meet the inclusion criteria. In all cases postoperative adjuvant therapies included radiotherapy and TMZ (Stupp regimen).

Eight patients were diagnosed with Anaplastic Astrocytoma (AA), 92 with Glioblastoma (GBM) (WHO 2016).

The KPS was used for clinical evaluation and the mean (± standard deviation) preoperative KPS was 75.1 (±13.1). The immediate post-op KPS, as well as KPS at 5 months after surgery, was recorded.

Before and after (within 48 h) surgery all patients underwent MRI with the following sequences: pre- and post-gadolinium T1, T2, T2-FLAIR, DWI, DTI and spectroscopy. Tumor volumes were calculated by neurosurgeons with experience in neuro-oncology and by neuroradiologists (12). The Horos software for MacOs was used for manual segmentation of T1 3D volumetric images. The enhancing nodule (EN) was calculated on pre and post-operative MRI. Necrotic and cystic areas present in the EN were also considered in EN volume. Preoperatively, mean (± standard deviation) maximal tumor diameter was 43.3 (±16.9).

Surgery was always performed aiming to safely remove as much enhancing tumor as possible.

A multimodal intraoperative protocol, including 5-ALA fluorescence, neuronavigation (Medtronic StealthStation™ S7 or S8), neurophysiological monitoring with MEPs, SEPs and cortical-subcortical DES, i-CT (CereTom or BodyTom, Neurologica, US), and navigated bi-dimensional US system (MyLab Twice™ Esaote), was used in all cases to guide safe resection of the tumor. Surgery was stopped in proximity of eloquent areas to avoid post-operative deficits (motor responses at 10 mA stimulation with subcortical DES).

Extent Of Tumor Resection (EOTR) was calculated as preopVol − postopVol/preopVol × 100. We considered as Gross Total Resection (GTR) the complete removal of the EN, as Subtotal Resection (STR) an EOR >75% but less than 99% and as biopsy EOR <75%.

OS was calculated from the date of surgery to date of death, while PFS from date of surgery to date of radiological progression disease (PD) according to the RANO criteria.

Follow-up cut-off for the survival analysis was 2 years after surgery. We divided the entire cohort in two groups according to patients' age: <65 and >65 years. Clinical (age, sex, and KPS), neuroradiological and histological data were recorded and analyzed. We then compared surgical and clinical results (EOTR, early post-operative and follow-up KPS, OS and PFS) of the above groups.

In order to further investigate possible changes in surgical and clinical outcomes related to age difference, we also divided the same patient cohort into <70 and >70 years and all the above variables were reanalyzed accordingly.

A literature search was performed using the PubMed MEDLINE database. The search term "glioma" was combined with the following: "elderly," "extent of resection," "extent of tumor resection," "neuronavigation," "intraoperative CT," "intraoperative ultrasound," "5-ALA," "neuromonitoring."

Statistical Analysis

Assuming a median OS of 8.6 months in the group of patients with age >65 years old (13) and a median OS of 16 months in the group of patients with age <65 years old (14), a two-sided log-rank test with an overall sample size of 100 subjects (50 in each group) achieved 80% power, at a significance level of $\alpha = 5\%$, to detect a difference between the two groups. Power analysis was performed considering that the study lasted 78 months, from January 2014 to May 2020, of which subject accrual (the entry) occurred uniformly in the first 70 months.

Data were reported as mean (± standard deviation) for continuous variables and as frequencies and percentages (%) for categorical data. To determine demographics and clinic-pathological features differences between the groups created according to the age, x^2 tests or Student's t-tests were performed, as appropriate. Kaplan-Meier analysis and log-rank test were used to compare OS and PFS between groups.

We used lme4 to perform a longitudinal linear mixed effects analysis, to test for statistical differences between the groups of patients in terms of the variations from early to delayed post-operative of KPS. As fixed effects, we considered the groups of patients and time. As random effects, we had intercepts for subjects to take into account the non-independence that stems from having three measurements, preoperative KPS, immediate postoperative KPS and KPS 5 months after surgery, by the same subject.

The statistical software R version 3.2.5 (R Core Team, 2018) was used for all statistical analyses. A p-value <0.05 was taken as significance level.

RESULTS

We divided the entire cohort in two groups according to the age: Group A: patients ≥ 65 and Group B: patients < 65.

In Group A, there were 48 patients, 24 (50%) males and 24 (50%) female, 3 (6.2%) patients were diagnosed with AA and 45 (93.8%) with GBM. In Group B there were 52 patients, 29 (55.8%) males and 23 (44.2%) females, 5 (9.6%) patients with AA and 47 (90.4%) with GBM. GTR was performed in 45 Group A patients (93.8%), and 3 (6.2%) underwent STR; in Group B, we performed 48 (92.3%) GTRs and 4 (7.7%) STRs. The two groups were homogeneous for clinical, surgical and pathological features (**Table 1**).

Figure 1 shows the KPS partial means over time, estimated by mixed effects model. As shown in the figure, differences between the two groups were not significant at each time point.

Survival analysis showed that the two groups did not significantly differed in terms of OS (p = 0.36) and PFS (p = 0.49) (**Figure 2**).

We then divided the same patient's cohort in two other groups, using 70 years as new cut-off: Group C patients aged ≥ 70 and Group D patients < 70. In Group C there were 32 patients, 16 (50%) males and 16 (50%) females, 2 (6.2%) patients were diagnosed with AA and 30(93.8%) with GBM. Group D included 68 patients, 37 (54.4%) males and 31 (45.6%) females, 6 (8.8%) patients with AA and 62 (91.2%) with GBM. In Group C, 30 (93.8%) patients had tumor GTR and 2 (6.2%) STR; in Group D, 63 (92.6%) patients underwent GTR, and 5 (7.4%) STR.

The two groups were homogeneous for clinical, surgical and pathological data (**Table 2**).

Figure 3 shows the KPS partial means over time, estimated by mixed effects model. Differences between the two groups were not significant at each time point. Survival analysis showed that the two did not significantly differed in terms of OS (p = 0.52) and PFS (p = 0.92) (**Figure 4**).

DISCUSSION

"Conservative" Versus "More Aggressive" Treatment

In the past decades, treatment of elderly patients with HGG was usually based on either conservative measures or limited surgery, like biopsy, followed by RT and/or chemotherapy (15).

The main reason for such "minimalist" strategy in over 65 years HGG patients relies on the high rate of comorbidities and on the significant risk of postoperative complications. Moreover, HGGs in elderly population have a larger volume than in

TABLE 1 | Clinical and pathological features of patients stratified for age (<65 years old vs. ≥65 years old).

	Total n = 100	<65 years old n = 52	≥65 years old n = 48	p value
Sex	47(47)	23(44.2)	24(50)	0.706
Female	53(53)	29(55.8)	24(50)	
Male				
Max tumor diameter	43.3(±16.9)	40.9(± 14.7)	45.8(±18.8)	0.206
Tumor type	8(8)	5(9.6)	3(6.2)	0.717
AA	82(92)	40(90.4)	45(93.8)	
GBM				
Type of operation	7(7)	4(7.7)	3(6.2)	0.999
0	93(93)	48(92.3)	45(93.8)	
1				
Preoperative KPS	75.1(±13.1)	76.5(±14)	73.3(±11.9)	0.231

Data are reported as number of patients (%), mean (± standard deviation), as appropriate. p-values are based on χ^2 test or Student's t-test, as appropriate. Note that frequencies over classes do not always sum to the total number of patients, because of some missing values.

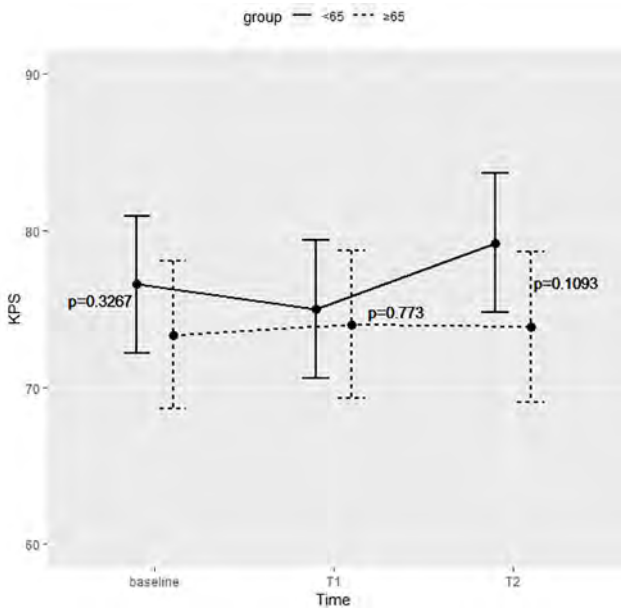

FIGURE 1 | Differences between the two groups were not significant at preoperative time (baseline), immediate postoperative (T1), and 5 months after surgery (T2).

younger people (probably due to concurrent brain atrophy causing late symptoms onset) (16), are more aggressive and present more chemo-resistance because of the higher number of genetic mutations (17, 18).

Indeed, Iwamoto et al. published a study based on SEER (Surveillance, Epidemiology and End Results) cancer registry cases treated between 1994 and 2002, and reported that older

TABLE 2 | Clinical and pathological features of patients stratified for age (<70 years old vs. ≥70 years old).

	Total n = 100	<70 years old n = 68	≥70 years old n = 32	p value
Sex	47(47)	31(45.6)	16(50)	0.843
Female	53(53)	37(54.4)	16(50)	
Male				
Max tumor diameter	43.3(±16.9)	43.5(± 16.4)	42.9(±18.1)	0.887
Tumor type	7(7)	7(7.4)	2(6.2)	0.999
AA	93(92.6)	63(92.6)	30(93.8)	
GBM				
Type of operation	7(7)	5(7.4)	2(6.2)	0.999
0	93(92.6)	63(92.6)	30(93.8)	
1				
Preoperative KPS	75.1(±13.1)	76(±13.4)	72.8(±12.2)	0.262

Data are reported as number of patients (%) or mean (± standard deviation), as appropriate. p-values are based on χ^2 test or Student's t-test, as appropriate. Note that frequencies over classes do not always sum to the total number of patients, because of some missing values.

GBM patients (more than 65 years) constantly received a less aggressive treatment than younger ones, and their OS was reduced from 14.6 months to only 4 months (19).

In 2012, Oszvald et al. compared EOTR in GBM patients, dividing their overall study population in two groups using 65 years as cutoff: no difference in survival rate was found in patients with similar EOTR despite different age groups. The mean PFS in elderly patients improved in the resection group (7.9 months) versus the biopsy one (3.9 months); mean OS increased from biopsy (4 months) to partial (11.4 months) and complete (17.7 months) resection (20). Since Oszvald's et al. report, other studies supported the concept of as much extended as possible resection (21–24).

However, not every patient over 65 years can be treated with more aggressive (i.e. extensive) surgical management. Trying to

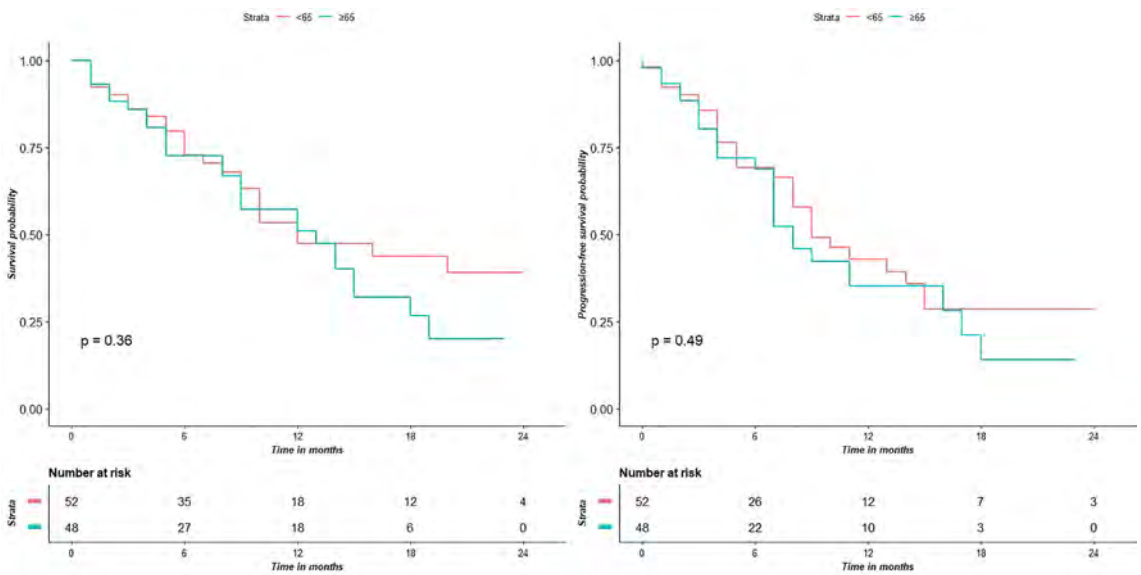

FIGURE 2 | Survival analyses show that the two groups don't have significantly different for OS (p = 0.36) and PFS (p = 0.49) values.

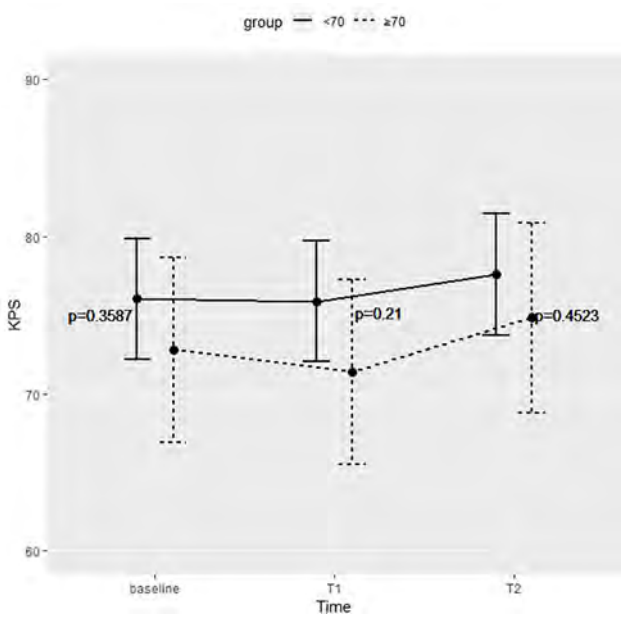

FIGURE 3 | Differences between the two groups were not significant at preoperative time (baseline), immediate postoperative (T1), and 5 months after surgery (T2).

evaluate the likely surgical outcome preoperatively, Chaichana et al. identified a panel of preoperative prognostic factors, which are associated with a worse clinical outcome: KPS < 80, Chronic Obstructive Pulmonary Disease (COPD), pre-existing neurological impairment (motor, language and cognitive deficits) and tumor size > 4 cm (25). However, such prognostic factors were reported as negative by different studies (26–30). Oszvald et al. reported worst prognosis in patients with KPS < 80, brain edema, seizures, venous thromboembolism and cognitive dysfunction (20), and Bauchet et al. proposed to use the Charlson Comorbidity Index (CCI), the Mini-Mental State Examination (MMSE) and the comprehensive geriatric assessment (CGA) as decision-making elements to choose the appropriate management in patients >70 years old (31). So far, only KPS (with 80 as cut off) remains the main prognostic factor in multivariate analysis and age does not represents an univocal prognostic value in all studies including over-70 years patients (32–35) .

Despite the above data and concerns, it is currently accepted that clinical outcome may also be influenced by EOTR and, consequently, by different techniques used intraoperatively to increase the extent of a safe surgery.

Our study reports that in elderly patients it is possible to achieve a similar clinical outcome to younger patients, also by applying a multimodal intraoperative imaging protocol, including neuronavigation, 5-ALA fluorescence, i-CT and navigated i-US, coupled with brain mapping, to reach maximal and safe tumor resection.

Surgical Outcome

The prognostic role of EOTR in HGG is well demonstrated (14, 36, 37). Lacroix et al. showed that 98% resection of the enhancing nodule (EN) in patients suffering from GBM was associated with survival advantage (38). Sanai and Berger, in a retrospective study on 500 patients, challenged the doctrine of all or none, demonstrating that EOTR >78% of EN is related to OS improvement. Moreover, they showed that this applies also to cases in which an even greater resection of the EN is performed (39). Following the constant

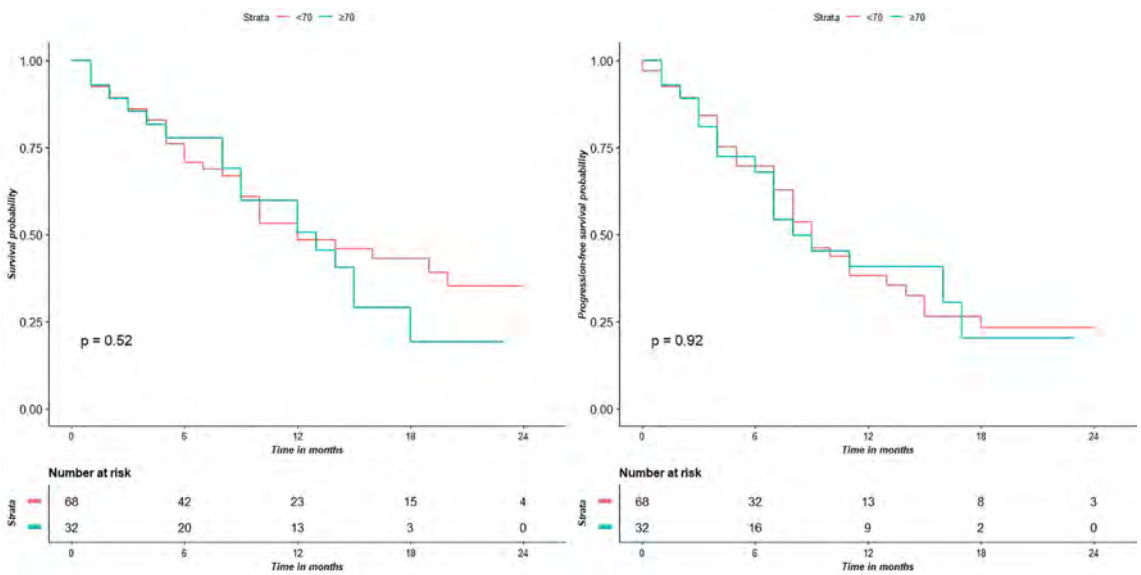

FIGURE 4 | Survival analyses show that the two groups do not have significantly different OS (p = 0.52) and PFS (p = 0.92) values.

literature increase supporting the relationship between resection rate of EN and OS, some authors investigated the possibility to obtain a further clinical gain (i.e. survival improvement) with a supratotal resection targeting the FLAIR hyperintense area around the EN; however, results are still controversial (36, 37, 40–44).

The aforementioned studies show the prognostic role of surgery in the general population but in the elderly the potential gain of a more extensive tumor resection should be weighed against its risks. In the Glioma Outcome Project the complication rate after craniotomy is 24.2% (8.1% permanent neurological worsening, 10% regional complications, 9.2% systemic complications, and 1.5% mortality). A retrospective study on 81 patients by De Eulate-Beramendi et al. reports a 17.28% complication rate after surgery (77.8% of patients underwent gross or subtotal resection, 22.2% biopsy only); a higher rate is reported after GTR (22).

The Mayo Clinic retrospective analysis on patients who underwent neuronavigation-assisted GBM resection or biopsy reported complications in 24.8% of patients; in the group who received resection (53/105), 11.3%, 7.6 %, 3.8% had neurological, regional and systemic complications, respectively (45). Moreover, the Mayo Clinic study reports a higher incidence of complications following biopsy rather than tumor resection. The authors' explanation for such findings focuses on lesion site (eloquent areas or deep locations, thus with a higher effect of even little edematous or hemorrhagic alterations).

In a recent meta-analysis, Almenawer et al. did not found higher rates of morbidity and mortality in older patients undergoing extended tumor resection. Indeed, GTR is reported to relieve neurological deficits and reduce morbidity (21).

Role of 5-ALA Fluorescence in Guiding Resection

Improvement in achieving GTR comes from 5-ALA fluorescence guidance. 5-ALA helps in distinguishing between tumor and normal brain parenchyma or radiotherapy-induced necrosis; strong 5-ALA fluorescence usually correlates with tumor seen on T1-weighted, gadolinium-enhanced, MRI images; it can also help to recognize tumor tissue in recurrent cases. Moreover, recent studies investigated the correlation between different intensities of 5-ALA and tumor cellularity, highlighting the importance of an extended resection of all fluorescent tissue, when safely feasible, aiming to the so-called "supramarginal resection" [32-34]. The use of 5-ALA is gaining credit also in elderly patients' surgery. Ewelt et al. reported a series of elderly patients treated with 5-ALA fluorescence: these authors achieved partial and complete resection in 29% and 22% of patients, respectively. Considering the group treated with surgery plus adjuvant chemo- and radiotherapy, the reported OS was 8.6, 13.6, and 7.3 months in total resection vs partial vs biopsy, respectively (13). Yet, Young et al. reported a phase III randomized trial in which 5-ALA fluorescence improved quality and extension of resection in elderly patients in comparison to white light surgery (46).

Role of Neuromonitoring and Awake Surgery in EOTR

Chaichana et al. reported a 20% rate of new postoperative neurological deficits in series of 129 elderly patients (23% had GBM in eloquent areas) operated using neuronavigation and intraoperative neurophysiological monitoring. The information provided by these tools were useful to detect cortical and subcortical motor functional margins of the resection area, thus reducing the rate of postoperative motor deficits. By applying such strategy, GTR (>99%), NTR (>95%) and STR (80-95%) were reached in 30%, 42%, 28% of patients, respectively (25). Unfortunately, despite neuronavigated tractography and intraoperative neurophysiological monitoring, it is impossible to predict language and neuropsycological outcome with asleep craniotomy (47–49).

Grossman et al. reported their experience on awake craniotomy for brain tumors (gliomas and metastases) in the elderly population. Comparing the results of two patient groups, under and over 65 years of age, respectively, no differences in post-surgical outcome were noted. In particular, in HGG surgery GTR was achieved for young and older patients in 70% and 76% of cases, respectively. Moreover, GTR as opposite to STR showed a gain in survival of 3 months (10.8 vs. 7.8) (50).

Role of Intraoperative Imaging in Tumor Resection

More recently, the use of advanced intraoperative imaging techniques has been spreading among neurosurgeons; i-CT and i-US represent feasible, fast and reproducible technical tools helping surgeons to accurately perform real-time navigation during brain tumor surgery, to analyze anatomical resection margins and identify query tumor remnants, and to obtain early diagnosis of intra- or perioperative complications (i.e. hemorrhage) (51–53). i-US also helps surgeons to correct for brain shift and to suspect, with high sensibility, the presence of tumor remnants. Yet, the use of specific contrast medium improves vascular and margins visualization, particularly in HGGs (52, 54–57). i-CT is useful in evaluating early complications and specifically identify tumor remnants in the surgical field (49, 51, 58). Yet, i-CT images, which also include brain shift-related changes, can be uploaded into the navigation system and used for a *real-time* navigation, providing more accurate data, which are very useful to pursue extended tumor resection. As already reported in recent papers both i-US and i-CT have limitations related to image interpretation. I-US images are frequently altered by the presence of artifacts and detection and localization of tumor remnants is often limited in presence of large surgical cavity or after hemostatic agents application. Combination of i-US with i-CT may overcome the intrinsic limitations of i-US, as the navigated i-CT may be useful to localize small remnants in hidden portions of surgical field, not clearly identified by ultrasounds [58].

Role of Multimodal Approach in EOTR

Brain tumor surgery is routinely supported by several intraoperative techniques, such as neuronavigation, i-US, i-CT, i-MRI, fluorescence, and neuromonitoring, which are often used

independently. Efficacy of preoperative MRI-based navigation is limited by the brain-shift phenomenon, particularly in cases of large or deep-sited tumors. Intraoperative imaging was introduced also to update neuronavigation data, to reduce brain-shift phenomenon-related pitfalls and to increase overall surgical safety. Nevertheless, each intraoperative imaging modality has intrinsic limitations and technical shortcomings. The possibility to combine them in a multimodal intraoperative imaging protocol could overcome some of these limitations. Combining different intraoperative imaging modalities may increase surgical safety and extent of tumor resection. In particular, i-US seems to be highly sensitive to detect residual tumors, but it may generate false positives due to artifacts. Conversely, i-CT is more specific to localize remnants, as it allows a reliable and more timely (i.e. *real time*) updating of navigation data (59, 60). Finally, neuromonitoring and brain mapping improve the chance to identify brain functional edges in order to achieve a maximal safe resection (61). Such strategy can make a more extensive surgical resection feasible, with lower neurological damage, also in elderly population.

Role of Age in HGG Surgery

Whenever treating HGG in elderly patients, Neurosurgeons should always consider some factors to choose the most appropriate treatment, including clinical presentation, tumor size and shape as well as overall patient health condition. Indeed, in this specific patient population, all of the above factors may have significant impact on the risk-benefit ratio of surgical management, as these patients often have less physiological reserve, and are predisposed to higher surgical complications rate and delays in recovery (11).

We have shown that the intraoperative multimodal approach is useful to achieve >90% GTR rate in all patient groups and there is no significant OS and PFS difference between younger and elderly patients (both 65 and 70 years as cut off).

LIMITATIONS

This is a retrospective, single center, study with patient enrolled from 2014. The new era of molecular classification start from 2016 and there are not data on tumor molecular markers before that time. Anyway the aim of this paper is to underline the safety and efficacy of a multimodal intraoperative approach demonstrating that an aggressive surgery is technically feasible also in elderly patients.

CONCLUSION

Our data show that a more extensive surgery is feasible even in the elderly population. We have demonstrated that there is no statistically significant difference in EOTR, OS, PFS, early post-operative and delayed KPS between younger and elderly patients treated with multimodal intraoperative imaging approach. Although our findings should be confirmed by larger studies, they open the way for further investigations.

DATA AVAILABILITY STATEMENT

The original contributions presented in the study are included in the article/**Supplementary Material**. Further inquiries can be directed to the corresponding author.

ETHICS STATEMENT

Ethical review and approval was not required for the study on human participants in accordance with the local legislation and institutional requirements. The patients/participants provided their written informed consent to participate in this study.

AUTHOR CONTRIBUTIONS

RA with FC has written the paper. GB has supervised and reviewed the manuscript. MG, MM, SD, MV, and SP searched the data. PD has performed the statistical analyses. All authors contributed to the article and approved the submitted version.

REFERENCES

1. Cohen-Inbar O. Geriatric brain tumor management part II: Glioblastoma multiforme. *J Clin Neurosci* (2019) 67:1–4.
2. Gondim JA, Almeida JP, de Albuquerque LAF, Gomes E, Schops M, Mota JI. Endoscopic endonasal transsphenoidal surgery in elderly patients with pituitary adenomas. *J Neurosurg* (2015) 123:31–8.
3. Ostrom QT, Gittleman H, Liao P, Vecchione-Koval T, Wolinsky Y, Kruchko C, et al. CBTRUS Statistical Report: Primary brain and other central nervous system tumors diagnosed in the United States in 2010–2014. *Neuro-Oncology* (2017) 19:v1–v88.
4. (2019). https://www-ncbi-nlm-nih-gov.bibliopass.unito.it/pubmed/25304271. CBTRUS statistical report: primary brain and central nervous system tumors diagnosed in the United States in 2007-2011. - PubMed - NCBI: Available. Accessed 27 October.
5. Ostrom QT, Gittleman H, Farah P, Ondracek A, Chen Y, Wolinsky Y, et al. CBTRUS statistical report: Primary brain and central nervous system tumors diagnosed in the United States in 2006-2010. *Neuro-oncology* (2013) 15 (Suppl 2):ii1–56.
6. Altieri R, Zenga F, Ducati A, Melcarne A, Cofano F, Mammi M, et al. Tumor location and patient age predict biological signatures of high-grade gliomas. *Neurosurg Rev* (2018) 41(2):599–604. doi: 10.1007/s10143-017-0899-8
7. Ferguson M, Rodrigues G, Cao J, Bauman G. Management of high-grade gliomas in the elderly. *Semin Radiat Oncol* (2014) 24:279–88.
8. Monticelli M, Zeppa P, Zenga F, Altieri R, Mammi M, Bertero L, et al. The post-surgical era of GBM: How molecular biology has impacted on our clinical management. A review. *Clin Neurol Neurosurg* (2018) 170:120–6.
9. Siu LL. Clinical Trials in the Elderly — A Concept Comes of Age. *New Engl J Med* (2007) 356:1575–6.

10. Stupp R, Mason WP, van den Bent MJ, Weller M, Fisher B, Taphoorn MJB, et al. Radiotherapy plus Concomitant and Adjuvant Temozolomide for Glioblastoma. *New Engl J Med* (2005) 352:987–96.
11. Tardivo V, Penner F, Garbossa D, Di Perna G, Pacca P, Salvati L, et al. Surgical management of pituitary adenomas: does age matter? *Pituitary* (2020) 23 (2):92–102:. doi: 10.1007/s11102-019-01014-1
12. Zeppa P, Neitzert L, Mammi M, Monticelli M, Altieri R, Castaldo M, et al. How Reliable Are Volumetric Techniques for High-Grade Gliomas? A Comparison Study of Different Available Tools. *Neurosurgery* (2020) nyaa282. doi: 10.1093/neuros/nyaa282
13. Ewelt C, Goeppert M, Rapp M, Steiner H-J, Stummer W, Sabel M. Glioblastoma multiforme of the elderly : the prognostic effect of resection on survival. *J Neuro-Oncol* (2011) 103:611–8.
14. Sanai N, Berger MS. Extent of resection influences outcomes for patients with gliomas. *Rev Neurol* (2011) 167:648–54.
15. Barnholtz-Sloan JS, Williams VL, Maldonado JL, Shahani D, Stockwell HG, Chamberlain M, et al. Patterns of care and outcomes among elderly individuals with primary malignant astrocytoma. *J Neurosurg* (2008) 108:642–8.
16. Brandes A, Monfardini S. The treatment of elderly patients with high-grade gliomas. *Semin Oncol* (2003) 30:58–62.
17. Rickert CH, Stäter R, Kaatsch P, Wassmann H, Jürgens H, Dockhorn-Dworniczak B, et al. Pediatric high-grade astrocytomas show chromosomal imbalances distinct from adult cases. *Am J Pathol* (2001) 158:1525–32.
18. Sung T, Miller DC, Hayes RL, Alonso M, Yee H, Newcomb EW. Preferential inactivation of the p53 tumor suppressor pathway and lack of EGFR amplification distinguish de novo high grade pediatric astrocytomas from de novo adult astrocytomas. *Brain Pathol* (2000) 10:249–59.
19. Iwamoto FM, Reiner AS, Panageas KS, Elkin EB, Abrey LE. Patterns of care in elderly glioblastoma patients. *Ann Neurol* (2008) 64:628–34.
20. Oszvald A, Güresir E, Setzer M, Vatter H, Senft C, Seifert V, et al. Glioblastoma therapy in the elderly and the importance of the extent of resection regardless of age. *J Neurosurg* (2012) 116:357–64.
21. Almenawer SA, Badhiwala JH, Alhazzani W, Greenspoon J, Farrokhyar F, Yarascavitch B, et al. Biopsy versus partial versus gross total resection in older patients with high-grade glioma: A systematic review and meta-analysis. *Neuro-Oncology* (2015) 17:868–81.
22. Álvarez de Eulate-Beramendi S, Álvarez-Vega MA, Balbin M, Sanchez-Pitiot A, Vallina-Alvarez A, Martino-González J. Prognostic factors and survival study in high-grade glioma in the elderly. *Br J Neurosurg* (2016) 30:330–6.
23. Babu R, Komisarow JM, Agarwal VJ, Rahimpour S, Iyer A, Britt D, et al. Glioblastoma in the elderly: the effect of aggressive and modern therapies on survival. *J Neurosurg* (2016) 124:998–1007.
24. Ostrom QT, Gittleman H, Xu J, Kromer C, Wolinsky Y, Kruchko C, et al. CBTRUS statistical report: Primary brain and other central nervous system tumors diagnosed in the United States in 2009-2013. *Neuro-Oncology* (2016) 18:v1–v75.
25. Chaichana KL, Chaichana KK, Olivi A, Weingart JD, Bennett R, Brem H, et al. Surgical outcomes for older patients with glioblastoma multiforme: preoperative factors associated with decreased survival. *J Neurosurg* (2011) 114:587–94.
26. Chaichana KL, McGirt MJ, Laterra J, Olivi A, Quiñones-Hinojosa A. Recurrence and malignant degeneration after resection of adult hemispheric low-grade gliomasfile:///C:/Users/raffaele/Desktop/Ricerca/GBM elderly/Almenawer2015.pdf. *J Neurosurg* (2010) 112:10–7.
27. Kreth FW, Faist M, Rossner R, Volk B, Ostertag CB. Supratentorial World Health Organization grade 2 astrocytomas and oligoastrocytomas. *Cancer* (1997) 79:370–9.
28. Krex D, Klink B, Hartmann C, Von Deimling A, Pietsch T, Simon M, et al. Long-term survival with glioblastoma multiforme. *Brain* (2007) 130:2596–606.
29. Lamborn KR, Chang SM, Prados MD. Prognostic factors for survival of patients with glioblastoma: Recursive partitioning analysis. *Neuro-Oncology* (2004) 6:227–35.
30. Laws ER, Parney IF, Huang W, Anderson F, Morris AM, Asher A, et al. Survival following surgery and prognostic factors for recently diagnosed malignant glioma: data from the Glioma Outcomes Project. *J Neurosurg* (2003) 99:467–73.
31. Bauchet L, Zouaoui S, Darlix A, De Champfleur NM, Ferreira E, Fabbro M, et al. Assessment and treatment relevance in elderly glioblastoma patients. *Neuro-Oncology* (2014) 16:1459–68.
32. Bauchet L, Mathieu-Daude H, Fabbro-Peray P, Rigau V, Fabbro M, Chinot O, et al. Oncological patterns of care and outcome for 952 patients with newly diagnosed glioblastoma in 2004. *Neuro-oncology* (2010) 12:725–35.
33. Hoffermann M, Bruckmann L, Mahdy Ali K, Asslaber M, Payer F, Von Campe G. Treatment results and outcome in elderly patients with glioblastoma multiforme - A retrospective single institution analysis. *Clin Neurol Neurosurg* (2015) 128:60–9.
34. Scott JG, Bauchet L, Fraum TJ, Nayak L, Cooper AR, Chao ST, et al. Recursive partitioning analysis of prognostic factors for glioblastoma patients aged 70 years or older. *Cancer* (2012) 118:5595–600.
35. Zouaoui S, Darlix A, Fabbro-Peray P, Mathieu-Daudé H, Rigau V, Fabbro M, et al. Oncological patterns of care and outcomes for 265 elderly patients with newly diagnosed glioblastoma in France. *Neurosurg Rev* (2014) 37:415–23.
36. Altieri R, Melcarne A, Soffietti R, Rudá R, Franchino F, Pellerino A, et al. Supratotal Resection of Glioblastoma: Is Less More? *Surg Technol Int* (2019) 35:432–44.
37. Certo F, Stummer W, Farah JO, Freyschlag C, Visocchi M, Morrone A, et al. Supramarginal resection of glioblastoma: 5-ALA fluorescence, combined intraoperative strategies and correlation with survival. *J Neurosurg Sci* (2019) 63(6):625–32. doi: 10.23736/S0390-5616.19.04787-8
38. Lacroix M, Abi-Said D, Fourney DR, Gokaslan ZL, Shi W, DeMonte F, et al. A multivariate analysis of 416 patients with glioblastoma multiforme: prognosis, extent of resection, and survival. *J Neurosurg* (2001) 95:190–8.
39. Sanai N, Polley M-Y, McDermott MW, Parsa AT, Berger MS. An extent of resection threshold for newly diagnosed glioblastomas. *J Neurosurg* (2011) 115:3–8.
40. Mampre D, Ehresman J, Pinilla-Monsalve G, Osorio MAG, Olivi A, Quinones-Hinojosa A, et al. Extending the resection beyond the contrast-enhancement for glioblastoma: feasibility, efficacy, and outcomes. *Br J Neurosurg* (2018) 32:528–35.
41. Pessina F, Navarria P, Cozzi L, Ascolese AM, Simonelli M, Santoro A, et al. Maximize surgical resection beyond contrast-enhancing boundaries in newly diagnosed glioblastoma multiforme: is it useful and safe? A single institution retrospective experience. *J Neuro-Oncol* (2017) 135:129–39.
42. Altieri R, Zenga F, Fontanella MM, Cofano F, Agnoletti A, Spena G, et al. Glioma Surgery: Technological Advances to Achieve a Maximal Safe Resection. *Surg Technol Int* (2015) 27:297–302.
43. Certo F, Altieri R, Maione M, Schonauer C, Sortino G, Fiumanò G, et al. FLAIRectomy in Supramarginal Resection of Glioblastoma Correlates With Clinical Outcome and Survival Analysis: A Prospective, Single Institution, Case Series. *Oper Neurosurg (Hagerstown)* (2021) 20(2):151–63. doi: 10.1093/ons/opaa293
44. Chang SM, Parney IF, Mcdermott M, Barker FG, Schmidt MH, Huang W, et al. Perioperative complications and neurological outcomes of first and second craniotomies among patients enrolled in the Glioma Outcome Project. *J Neurosurg* (2003) 98:1175–81.
45. Tanaka S, Meyer FB, Buckner JC, Uhm JH, Yan ES, Parney IF. Presentation, management, and outcome of newly diagnosed glioblastoma in elderly patients. *J Neurosurg* (2013) 118:786–98.
46. Young JS, Chmura SJ, Wainwright DA, Yamini B, Peters KB, Lukas RV. Management of glioblastoma in elderly patients. *J Neurol Sci* (2017) 380:250–5.
47. Altieri R, Melcarne A, Junemann C, Zeppa P, Zenga F, Garbossa D, et al. Inferior Fronto-Occipital fascicle anatomy in brain tumor surgeries: From anatomy lab to surgical theater. *J Clin Neurosci* (2019) 68:290–4. doi: 10.1016/j.jocn.2019.07.039
48. Altieri R, Raimondo S, Tiddia C, Sammarco D, Cofano F, Zeppa P, et al. Glioma surgery: From preservation of motor skills to conservation of cognitive functions. *J Clin Neurosci* (2019) 70:55–60. doi: 10.1016/j.jocn.2019.08.091
49. Barbagallo GMV, Morrone A, Certo F. Intraoperative CT and awake craniotomy: a useful and safe combination in brain surgery. *World Neurosurg* (2018) 119:e159–66. doi: 10.1016/j.wneu.2018.07.078
50. Grossman R, Nossek E, Sitt R, Hayat D, Shahar T, Barzilai O, et al. Outcome of elderly patients undergoing awake-craniotomy for tumor resection. *Ann Surg Oncol* (2013) 20:1722–8.

51. Barbagallo GMV, Palmucci S, Visocchi M, Paratore S, Attinà G, Sortino G, et al. Portable intraoperative computed tomography scan in image-guided surgery for brain highgrade gliomas: Analysis of technical feasibility and impact on extent of tumor resection. *Oper Neurosurg* (2015) 12:19–30.
52. Prada F, Del Bene M, Fornaro R, Vetrano IG, Martegani A, Aiani L, et al. Identification of residual tumor with intraoperative contrast-enhanced ultrasound during glioblastoma resection. *Neurosurg Focus* (2016) 40:E7.
53. Riva M, Hennersperger C, Milletari F, Katouzian A, Pessina F, Gutierrez-Becker B, et al. 3D intra-operative ultrasound and MR image guidance: pursuing an ultrasound-based management of brainshift to enhance neuronavigation. *Int J Comput Assist Radiol Surg* (2017) 12:1711–25.
54. Altieri R, Melcarne A, Di Perna G, Specchia FMC, Fronda C, La Rocca G, et al. Intra-Operative Ultrasound: Tips and Tricks for Making the Most in Neurosurgery. *Surg Technol Int* (2018) 33:353–60.
55. Altieri R, Meneghini S, Agnoletti A, Tardivo V, Vincitorio F, Prino E, et al. Intraoperative ultrasound and 5-ALA: the two faces of the same medal? *J Neurosurg Sci* (2019) 63(3):258–64. doi: 10.23736/S0390-5616.16.03641-9
56. Arlt F, Chalopin C, Müns A, Meixensberger J, Lindner D. Intraoperative 3D contrast-enhanced ultrasound (CEUS): a prospective study of 50 patients with brain tumours. *Acta Neurochir* (2016) 158:685–94.
57. Moiyadi AV, Kannan S, Shetty P. Navigated intraoperative ultrasound for resection of gliomas: Predictive value, influence on resection and survival. *Neurol India* (2015) 63:727.
58. Hosoda T, Takeuchi H, Hashimoto N, Kitai R, Arishima H, Kodera T, et al. Usefulness of Intraoperative Computed Tomography in Surgery for Low-Grade Gliomas: a Comparative Study Between Two Series Without and With Intraoperative Computed Tomography. *Neurol Med-chirurgica* (2011) 51:490–5.
59. Della Pepa GM, Marchese E, Pedicelli A, Olivi A, Ricciardi L, Rapisarda A, et al. CEUS and Color Doppler - guided intraoperative embolization of intracranial highly vascularized tumors. *World Neurosurg* (2019) 128:547–55. doi: 10.1016/j.wneu.2019.05.142
60. Della Pepa GM, Sabatino G, la Rocca G. "Enhancing Vision" in High Grade Glioma Surgery: A Feasible Integrated 5-ALA + CEUS Protocol to Improve Radicality. *World Neurosurg* (2019) 129:401–3.
61. Barbagallo G, Maione M, Peschillo S, Signorelli F, Visocchi M, Sortino G, et al. Intraoperative Computed Tomography, navigated ultrasound, 5-Amino-Levulinic Acid fluorescence and neuromonitoring in brain tumor surgery: overtreatment or useful tool combination? *J Neurosurg Sci* (201911. doi: 10.23736/S0390-5616.19.04735-0

Conflict of Interest: The authors declare that the research was conducted in the absence of any commercial or financial relationships that could be construed as a potential conflict of interest.

frontiers in Neurology

ORIGINAL RESEARCH
published: 26 February 2021
doi: 10.3389/fneur.2021.633209

From Neurosurgical Planning to Histopathological Brain Tumor Characterization: Potentialities of Arcuate Fasciculus Along-Tract Diffusion Tensor Imaging Tractography Measures

Matteo Zoli[1,2†], Lia Talozzi[2†], Matteo Martinoni[3], David N. Manners[2], Filippo Badaloni[3], Claudia Testa[4], Sofia Asioli[2,5], Micaela Mitolo[6], Fiorina Bartiromo[6], Magali Jane Rochat[6], Viscardo Paolo Fabbri[2], Carmelo Sturiale[3], Alfredo Conti[2,3], Raffaele Lodi[2,6], Diego Mazzatenta[1,2‡] and Caterina Tonon[2,6‡]*

[1] Pituitary Unit, IRCCS Istituto delle Scienze Neurologiche di Bologna, Bologna, Italy, [2] Department of Biomedical and Neuromotor Sciences, University of Bologna, Bologna, Italy, [3] Neurosurgery Unit, IRCCS Istituto delle Scienze Neurologiche di Bologna, Bologna, Italy, [4] Department of Physics and Astronomy, University of Bologna, Bologna, Italy, [5] Anatomic Pathology Unit, Azienda USL di Bologna, Bologna, Italy, [6] Functional and Molecular Neuroimaging Unit, IRCCS Istituto delle Scienze Neurologiche di Bologna, Bologna, Italy

OPEN ACCESS

Edited by:
Giovanni Raffa, University of Messina, Italy

Reviewed by:
Enricomaria Mormina, University of Messina, Italy
Gabor Perlaki, University of Pécs, Hungary

***Correspondence:**
Diego Mazzatenta
diego.mazzatenta@unibo.it

[†] These authors have contributed equally to this work and share first authorship

[‡] These authors have contributed equally to this work and share last authorship

Specialty section:
This article was submitted to Applied Neuroimaging, a section of the journal Frontiers in Neurology

Received: *24 November 2020*
Accepted: *26 January 2021*
Published: *26 February 2021*

Citation:
Zoli M, Talozzi L, Martinoni M, Manners DN, Badaloni F, Testa C, Asioli S, Mitolo M, Bartiromo F, Rochat MJ, Fabbri VP, Sturiale C, Conti A, Lodi R, Mazzatenta D and Tonon C (2021) From Neurosurgical Planning to Histopathological Brain Tumor Characterization: Potentialities of Arcuate Fasciculus Along-Tract Diffusion Tensor Imaging Tractography Measures. Front. Neurol. 12:633209. doi: 10.3389/fneur.2021.633209

Background: Tractography has been widely adopted to improve brain gliomas' surgical planning and guide their resection. This study aimed to evaluate state-of-the-art of arcuate fasciculus (AF) tractography for surgical planning and explore the role of along-tract analyses *in vivo* for characterizing tumor histopathology.

Methods: High angular resolution diffusion imaging (HARDI) images were acquired for nine patients with tumors located in or near language areas (age: 41 ± 14 years, mean ± standard deviation; five males) and 32 healthy volunteers (age: 39 ± 16 years; 16 males). Phonemic fluency task fMRI was acquired preoperatively for patients. AF tractography was performed using constrained spherical deconvolution diffusivity modeling and probabilistic fiber tracking. Along-tract analyses were performed, dividing the AF into 15 segments along the length of the tract defined using the Laplacian operator. For each AF segment, diffusion tensor imaging (DTI) measures were compared with those obtained in healthy controls (HCs). The hemispheric laterality index (LI) was calculated from language task fMRI activations in the frontal, parietal, and temporal lobe parcellations. Tumors were grouped into low/high grade (LG/HG).

Results: Four tumors were LG gliomas (one dysembryoplastic neuroepithelial tumor and three glioma grade II) and five HG gliomas (two grade III and three grade IV). For LG tumors, gross total removal was achieved in all but one case, for HG in two patients. Tractography identified the AF trajectory in all cases. Four along-tract DTI measures potentially discriminated LG and HG tumor patients (false discovery rate < 0.1): the number of abnormal MD and RD segments, median AD, and MD measures. Both a higher number of abnormal AF segments and a higher AD and MD measures were

associated with HG tumor patients. Moreover, correlations (unadjusted $p < 0.05$) were found between the parietal lobe LI and the DTI measures, which discriminated between LG and HG tumor patients. In particular, a more rightward parietal lobe activation (LI < 0) correlated with a higher number of abnormal MD segments ($R = -0.732$) and RD segments ($R = -0.724$).

Conclusions: AF tractography allows to detect the course of the tract, favoring the safer-as-possible tumor resection. Our preliminary study shows that along-tract DTI metrics can provide useful information for differentiating LG and HG tumors during pre-surgical tumor characterization.

Keywords: neurosurgery, tractography, arcuate fasciculus, along-tract, gliomas grading, language network, fMRI laterality index, pre-surgical planning

INTRODUCTION

In 2014, it was argued that brain diffusion-weighted MRI tractography was not yet ready as a clinical tool (1), but recently, the synergistic collaboration of neurosurgeons, neuroradiologists, scientists, and vendors has rendered the technique suitable for clinical practice (2–8). Indeed, MRI tractography has gained a role in neuro-oncology and brain tumor surgery in both adult and pediatric patients (2–8).

Many technical limitations such as the inability of deterministic tractography to resolve kissing and crossing fibers have been overcome by the use of high angular resolution diffusion imaging (HARDI) acquisitions and innovative high-order crossing fiber models, such as constrained spherical deconvolution (9). Tractography can currently provide an accurate visualization of the spatial relationship between the intra-axial tumors, such as gliomas, and the subcortical tracts, contributing to more precise surgical planning and to guiding tumor resection intraoperatively (2–8).

Several studies have demonstrated that tractography can reliably image many white matter (WM) tracts, including the cortico-spinal tract (CST), optic radiations, and, among those involved in the language functions, the arcuate fasciculus (AF) (10–13). This latter tract is one of the most clinically relevant structures, connecting Wernicke's and Broca's areas and represents a significant portion of the superior longitudinal fasciculus (SLF), belonging to the dorsal stream, which is involved in language production and comprehension (14). The critical role of the AF is demonstrated by the interruption of speech production typically observed when the tract is electrically stimulated intraoperatively. When injured, it has been found to disrupt phonological processing and reduce speech fluency (15–18).

AF reconstruction is particularly useful for the surgery of gliomas located in the proximity of the language areas, when performed in combination with language fMRI tasks, permitting the identification of the language-eloquent cortical regions near frontal, insular, and temporal tumors in the dominant hemisphere (2–8). Indeed, it has recently been demonstrated that the adoption of this neuroimaging approach can improve surgical outcomes by reducing the risk of permanent language deficits (16).

Nevertheless, although the effectiveness of the AF tractography for guiding pre-and intraoperative resection of tumors in eloquent language areas has already been demonstrated, its ability to determine the biological nature of the tumor or assess its aggressiveness has not been thoroughly investigated (19–24). Previous studies have highlighted microstructural abnormalities in fascicles localized in proximity to a glioma in or near language or motor cortex (25). However, the absence of a reliable healthy control (HC) population for patient-specificity microstructural comparisons has led to discrepant results (19–24). Furthermore, to date, the potential role of along-tract analysis has not been tested for language eloquent area gliomas. No studies have explored the relationship between along-tract microstructural measures and the reorganization of brain activity in the presence of tumors, as determined by language task fMRI.

Our study investigates the correlation between language area tumor histopathology and AF integrity by using an along-tract analysis, as a more accurate alternative to whole-tract tractography analysis. This study aimed to demonstrate that AF tractography contributed to the safe resection of gliomas in language areas and secondarily to investigate how along-tract analyses can shed light on tumor histopathology and, in combination with fMRI, functional neuroplasticity.

MATERIALS AND METHODS

Subjects

From August 2019 to June 2020, we recruited consecutive adult patients referred to the Functional and Molecular Neuroimaging Unit, IRCCS Istituto delle Scienze Neurologiche di Bologna (Italy), according to the following criteria: ≥18 years of age and the presence of a single primary tumor lesion in a language-related area. All patients recruited underwent a standardized MRI acquisition protocol on a 3-T scanner, and histopathological and molecular testing.

As controls, a cohort of healthy volunteers was also recruited for this study. HCs were selected from the database of the

Neuroimaging Laboratory, designed to collect normative values of quantitative MR parameters for clinical and research purposes.

The study was approved by the local Ethical Committee (183/2019/OSS/AUSLBO-19027 (20/03/19), and written informed consent was obtained from all participants.

Pre-surgery Protocol

The medical history of all patients was considered, particularly if they had already undergone surgical or adjuvant treatment for the brain tumor. Each patient underwent a complete neurological examination with a specific focus on possible language impairments, such as aphasia, anomia, paraphasia, or grammatical or syntactic mistakes, thanks to a semi-structured interview performed by a neuropsychologist. All patients and HCs were assessed for years of education and handedness dominance using the Edinburgh Handedness Inventory (EHI) (26). EHI scores between −1 and −0.5 were considered indices of left-handedness, right-handedness was defined by scores between 0.5 and 1, and scores between −0.5 and 0.5 indicated ambidextrousness. In order to ensure that patients understood and were able to execute required tasks during fMRI acquisition, they each undertook a training session for the functional paradigms.

A complete neurophysiological assessment, including somatosensorial, motor, and brainstem auditory evoked responses, was performed 24 h before surgery.

Brain MRI Acquisition Protocol

The MRI protocol was performed using a high-field Siemens MAGNETOM Skyra 3-T MRI scanner equipped with a high-density array coil, with 64 channels and full head–neck coverage.

The MRI protocol included volumetric T1-weighted imaging based on 3D MPRAGE [176 continuous sagittal slices, 1-mm isotropic voxel, no slice gap, echo time (TE) = 2.98 ms, repetition time (TR) = 2,300 ms, Inversion Time (IT) = 900 ms, flip angle = 9°, acquisition matrix = 256 × 256, pixel bandwidth = 240 Hz, in-plane acceleration factor = 2, duration ∼5 min] and volumetric fluid-attenuated inversion recovery (FLAIR) T2-weighted imaging (3D SPACE, 176 sagittal acquisition slices, 1-mm isotropic voxel, no slice gap, TE = 428 ms, TR = 5,000 ms, IT = 1,800 ms, flip angle = 120°, acquisition matrix = 256 × 256, pixel bandwidth = 780 Hz, in-plane acceleration factor = 2, duration ∼5 min). In patients, volumetric T1-weighted images were also acquired after the injection of gadolinium contrast agent (0.1 mmol/kg).

For tractography analyses, a HARDI diffusion-weighted protocol was acquired with b-value = 2,000 s/mm^2 along 64 diffusion gradient directions, and five volumes without diffusion weighting, based on a 2D single-shot echo planar imaging (EPI) sequence [87 continuous axial slices, 2-mm isotropic voxel, no slice gap, TE = 98 ms, TR = 4,300 ms, flip angle = 90°, acquisition matrix = 110 × 110, pixel bandwidth = 1,820 Hz, in-plane acceleration factor = 2, multiband acceleration factor = 3, phase encoding anterior–posterior (AP), duration ∼8 min]. An additional sequence of three null b-value volumes was acquired immediately prior to the full diffusion data set, with the same acquisition geometry and timing parameters but inverted phase encoding [posterior–anterior (PA)]. The information from this sequence was used to correct EPI distortion artifacts in the diffusion-weighted scan.

In order to assess hemispheric language laterality, the neural correlates of verbal fluency were elicited via a phonemic fluency task performed during block-design functional MRI based on a 2D single-shot EPI sequence (56 continuous axial slices, 2.5-mm isotropic voxel, no slice gap, TE = 37 ms, TR = 735 ms, flip angle = 53°, acquisition matrix = 94 × 94, pixel bandwidth = 2,130 Hz, no in-plane acceleration, multiband acceleration factor = 3, phase encoding AP, duration ∼5 min). The block design consisted of alternated resting and active blocks, each lasting 30 s, starting and ending with the resting condition (five resting blocks and four active task blocks in total). The active task blocks were composed of acoustic cues delivered at 5-s intervals. During resting blocks, continuous white noise was delivered. The acoustic cues were administered through MR-compatible earphones that isolated the background MRI noise. During active cycles of phonemic fluency, the acoustic cue stimulus was a letter of the alphabet, delivered every 5 s. After the presentation of the cue, subjects were prompted to covertly generate (i.e., think about) a noun starting with the given letter. Subjects were instructed to generate as many nouns as possible within the time lapse between stimuli but not to generate proper names or names of places (cities/lands/continents). During rest cycles, patients were instructed to lie quietly in the scanner without active thinking (27).

Tumor Segmentation

The patient's tumor volume was manually segmented by LT and by an experienced neuroradiologist with more than 10 years of experience (FB) using the itk-SNAP software (http://www.itksnap.org) (28).

A multiparametric segmentation approach was used: all the voxels presenting signal intensity alterations in either the FLAIR T2-weighted or T1-weighted (with/without 0.1 mmol/kg of gadolinium contrast agent administration) images were included.

Tractography

Imaging Preprocessing

Diffusion-weighted images were skull-stripped using the FSL-bet function (https://fsl.fmrib.ox.ac.uk/fsl/fslwiki). Image denoising was performed with the MRtrix3-dwidenoise function (https://www.mrtrix.org), using a principal component analysis approach. Susceptibility-related distortions in the EPI acquisition were estimated using the FSL-topup function; subsequently, a combined correction for susceptibility, eddy-current effects, and signal dropout, most commonly induced by subject movement, was performed for the FSL-topup estimates.

The FSL-dtifit function was used to model diffusivity along the spatial eigenvectors using the tensor model, obtaining the following diffusion tensor imaging (DTI) maps: fractional anisotropy (FA), mean diffusivity (MD), axial diffusivity (AD), and radial diffusivity (RD). These maps were used to assess changes in diffusivity parameters in the presence of tumor edema or infiltration.

Arcuate Fasciculus Tractography Pipeline

The tractography pipeline was fully automatized. High-order fiber modeling was used to evaluate crossing fibers, and a probabilistic streamline propagation approach was adopted. Regions of interest (ROIs) defined in the Montreal Neurological Institute (MNI)-152 space were non-linearly registered (FSL-fnirt function) for subject T1-weighted images. The T1-weighted images were then registered to the diffusion-weighted images using the FSL-epi_reg function, which aligns images, simultaneously correcting for distortions using gray–white intensity contrast.

To reconstruct the AF bilaterally, a previously validated seed-target approach was used, described in detail in Talozzi et al. (29). Briefly, adapting the procedure by Giorgio et al. (30), the tractography seed was defined in the MNI-152 space, located in the WM underlying the angular gyrus, anteriorly to the point where the AF begins to arch toward the temporal terminations. Symmetrical bilateral seed ROIs had a rectangular shape extending from $|X| = 42$ to 30, $Y = -38$ to -37, and $Z = 20$ to 34 in MNI-152 coordinate space. Tractography target ROIs were placed in both the frontal and temporal lobes, including ROIs defined by the Harvard–Oxford probabilistic atlas, thresholded at 25% of subject probability. The frontal target ROI was defined as comprising all the frontal Harvard–Oxford regions, inclusive of the precentral gyrus and precentral operculum, while the temporal target ROI comprised all the temporal Harvard–Oxford regions. Moreover, a dilatation kernel (flsmaths–dilM) was applied to include the tractography streamlines stopping just before the gray matter. A midsagittal exclusion ROI was defined at MNI-152 space $X = 0$.

Constrained spherical deconvolution diffusion modeling and probabilistic tractography were performed (tckgen ifod2-Mrtrix3) in native diffusion space, into which the tractography ROIs defined in MNI-152 space were non-linearly registered. Tractography results were thresholded at 10% of the maximum of connectivity within each voxel, to reduce false-positive artifactual reconstructions.

Subsequently, along-tract mapping and statistical calculations were performed in MNI-152 space. AF tractographic reconstructions and DTI maps were linearly aligned to the MNI = 152 space (FSL-flirt, allowing 12 degrees of freedom). A linear registration approach was preferred to preserve the native tract bundle geometry, allowing comparisons of patients and HCs in a common space.

Along-Tract Analyses

For accurate quantification of DTI maps along with the AF, a previously developed along-tract approach was applied (29). This method parameterizes the tract volume evaluating its three-dimensional mesh. In the mesh connectivity matrix, the Laplacian operator was computed; and the first Laplacian eigenvalue, which described the three-dimensional geodetic trajectory, was evaluated.

To standardize along-tract subdivision of the AF, the tract was parameterized after registration to the MNI-152 space and restricted to the compact WM core prior to its branching toward cortical areas, where intersubject variability was elevated.

MNI-152 coordinate limits were set anteriorly at y_max = 65 mm for frontal AF projections and inferiorly at z_min = 40 mm for temporal AF projections. After WM core restriction, the AF was divided into 15 equally spaced segments (29). This AF subdivision was adopted to extract along-tract DTI maps profiles within each AF segment. Along-tract analyses were performed using locally developed software written in Matlab 2019R (https://matlab.mathworks.com).

Functional MRI Analyses

The fMRI processing pipeline was created using only FSL software. Images were skull-stripped using the FSL-bet function.

During preprocessing, motion correction was performed with the tool "motion correction of functional images using the linear image registration" (FSL-MCFLIRT) (31). Spatial smoothing was performed using a full width at half maximum (FWHM) Gaussian kernel of 5 mm.

FSL-epi_reg permitted registration between structural and functional images. High-pass filtering of task-based fMRI time series was performed with a threshold of 60 s.

Language-based fMRI data were processed using the FSL-FEAT GUI (FMRI Expert Analysis Tool) (32). Task and rest cycles in block conditions were convolved with the hemodynamic response function to generate the general linear model (GLM). For each subject, fixed-effect GLM was performed using a threshold of $z \geq 3.1$, and then a cluster-extent-based thresholding was used, setting $p < 0.05$.

In order to evaluate a hemispheric laterality index (LI), the fMRI activation regions obtained were masked with bilateral ROIs to evaluate activations in selected language areas. Frontal, parietal, and temporal ROIs were extracted from the cortical Harvard–Oxford atlas:

- Frontal ROIs included the inferior frontal gyrus pars triangularis, pars opercularis, and the frontal operculum.
- Parietal ROIs included the angular gyrus and the posterior supramarginal gyrus.
- Temporal ROIs included the posterior portion of both superior and medial temporal gyri.

fMRI activations were non-linearly registered to the MNI-152 space, using the warp field defined by FSL-FEAT. fMRI activation maps registered to the MNI-152 space were thresholded at $Z > 3.1$ and then masked for each subject using the previously defined bilateral frontal, parietal, and temporal areas (fslmaths–mas). The number of activated fMRI voxels was evaluated within each area.

The LI was calculated according to the following formula (33):

$LI = (\text{Left} - \text{Right})/(\text{Left} + \text{Right})$,

where "Left" and "Right" indicate the number of voxels activated within the left and right homologous areas, respectively.

These ROIs were investigated on the basis of a previous study that investigated the correlation between WM pathways and cortical areas related to language functions (34). While this analysis undoubtedly over-simplifies the fMRI neural activations correlating with language, it aims to robustly extract a laterality activation index in each lobe and quantify the reorganization of brain activity in the presence of tumors.

The SurfIce software (https://www.nitrc.org/plugins/mwiki/index.php/surfice:MainPage) was used for the projection of

voxel-wise data onto a surface mesh and to display fMRI results in three dimensions.

Brain Tumor Surgery

Surgery was performed in all cases with a resective aim. Intraoperative neurophysiological monitoring was used in all cases, and, when indicated, an awake setting was adopted (we opted for the sleeping–awake–sleeping technique). Anesthesia was performed consequently, avoiding the use of myorelaxant.

All surgeries were performed with neuronavigational guidance (StealthStation S8 Surgical Navigation System, MEDTRONIC, Louisville, CO, USA) provided by the co-registered data sets of morphological MRI, tractography reconstructions, and phonemic task activations.

Post-operative Course and Follow-Up

All patients underwent an MRI with and without gadolinium contrast agent administration (0.1 mmol/kg) within 72 h since surgery to assess the extension of tumor removal. For purposes of assessment, "gross total resection" (GTR) refers to the absence of residual tumor detected by early post-operative MRI scans compared with preoperative MRI scans (i.e., with respect to any residual enhancement); "subtotal resection" refers to possible residual tumor $< 10\%$; "partial resection" refers to possible residual tumor more than 10% (35).

Neurological and neuropsychological examination, with particular regard to language deficits, was performed at awakening at then daily for the first 5–7 days until discharge from hospital.

Surgical and medical complications were analyzed using electronic medical records. After case-by-case discussion at the tumor board multidisciplinary meeting, adjuvant treatments (radio- and chemotherapies) were started 1 month after surgery. Follow-up consisted of morphological MRI scan and neurological examination performed every 3–6 months.

Tumor Histopathological and Molecular Characterization

Surgical specimens were formalin-fixed and paraffin-embedded (FFPE) according to routine procedures. Diagnosis was assessed by two neuropathologists (SA and VPF) according to the 2016 WHO classification of tumors of the central nervous system.

Immunohistochemistry was performed in an automated stainer (Ventana, Tucson, AZ, using Ventana purchased pre-diluted antibodies): antibodies anti-GFAP (clone EP672Y, Cell-Marquez), anti-Olig2 (clone EP112, Cell-Marquez), anti-synaptophysin (clone MRQ-40, Cell-Marquez), anti-BRAF V600E (clone VE1, Roche), anti-CD34 (clone QBEnd/10, Roche), anti-IDH1 R132H (clone H09, Dianova), anti-ATRX (polyclonal, Sigma), and anti-p53 (clone DO-7, Roche) were used. Ki67 labeling index (clone 30–9, Ventana Medical Systems Inc., Tucson, AZ, USA) was evaluated by counting at least 1,000 neoplastic cells.

Molecular analyses for IDH1 (exon 4), IDH2 (exon 4), and TERT (promoter) were performed by next-generation sequencing (NGS). Briefly, representative tissue was identified from FFPE specimens and extracted with the Quick Extract FFPE DNA Extraction Kit (Epicentre, Madison, WI, USA). Sequencing was performed using the 454 GS-Junior NGS (Roche Diagnostic, Mannheim, Germany).

The methylation status of the MGMT promoter region was assessed by MS-qLNAPCR (rapid methylation sensitive quantitative PCR assay using Locked Nucleic Acid) (36). Identification of the 1p/19q allelic status was obtained using a dual-color fluorescence *in situ* hybridization (FISH) analysis and an Olympus BX61 epifluorescence microscope: for each case, at least 100 neoplastic nuclei were counted, and the copy numbers of 1p36/1q25 and 19q13/19p25 were recorded for each nucleus (37).

Patients were stratified into two groups according to the tumor grading: low grade (LG) including dysembryoplastic neuroepithelial tumor (DNT) and gliomas grade II, and high grade (HG) including gliomas grades III and IV.

STATISTICAL ANALYSES

Tractography

Normative ranges for along-tract AF microstructural DTI measures (FA, MD, RD, and AD) were defined, adopting the following criteria. For each of the 15 AF segments within the HC population, the median DTI value of each parameter was subtracted from the raw measure to obtain de-medianed measures, and segment outliers lying beyond three times the mean absolute deviation were removed. The normative range for each parameter was then defined by the interval bracketed by the 2.5th to 97.5th percentiles of all such segment measures, estimated from the standard deviation of distribution excluding outliers. This calculation was performed separately for the right and left AF.

For patients, within each AF segment, median DTI measures were calculated for each parameter (FA, MD, RD, and AD). AF DTI measures were considered abnormal if they laid outside the HC normative range for each DTI parameter, more precisely, when the segment median measure was less than the 2.5th percentile or greater the 97.5th percentile of the HC distribution. The total number of abnormal AF segments was counted. Additionally, the median across all segments was calculated for each parameter. For patients, outlier detection was not applied since out-of-range DTI measures are potentially a marker of pathological conditions.

Group Comparison and Correlation Analyses

The Mann–Whitney test was used to compare LG and HG tumor patients for measures including tumor volume, along-tract DTI measures, and fMRI LI evaluated in the frontal, parietal, and temporal ROIs. The DTI-derived measures considered included the number of AF segments with decreased FA and AD, the number of AF segments with increased MD and RD, and median measures of FA, AD, MD, and RD along the AF.

An adaptive significance threshold was applied using the Benjamini–Hochberg false discovery rate (FDR) procedure to account for multiple comparisons (38). Matlab 2020 statistical

TABLE 1 | Demographic information is reported for tumor patients [low-grade tumors (LG) and high-grade tumors HG)] including education and Edinburgh Handedness Inventory (EHI) scores.

	Age (years)	Sex	Education (years)	EHI	Location	Tumor volume (cm^3)	Tumor grade	Histopathology	Molecular analysis
LG									
T_L_I	21	M	13	−0.3	Left MTG	4.2	I	DNT	NA
F_L_II	30	F	13	1	Left IFG, MFG, SFG	22.8	II	Diffuse astrocytoma	IDH mutant, MGMT methylated, 1p/19q non-codelated
I_L_II	40	M	18	0.89	Left insula	122.0	II	Astrocytoma	IDH mutant, MGMT methylated
I_R_II	38	F	11	1	Right insula	43.0	II	Oligodendroglioma	IDH mutant, MGMT methylated, 1p/19q codelated
HG									
P_L_III	63	F	11	0.94	Left ANG	26.4	III	Anaplastic diffuse astrocytoma	IDH mutant, MGMT methylated, 1p/19q non-codelated
F_L_III	58	M	13	0.68	Left IFG, MFG, SFG	17.5	III	Anaplastic oligodendroglioma	IDH mutant, MGMT methylated, 1p/19q codelated
P_L_IV	51	M	18	0.89	Left ANG	13.1	IV	Glioblastoma	DH wild type, TERT promoter mutated, MGMT wild type
F_L_IV	41	M	19	0.78	Left IFG, MFG, SFG	57.9	IV	Glioblastoma	IDH mutant, MGMT methylated, 1p/19q non-codelated
T_L_IV	31	F	17	−0.4	Left MTG	115.7	IV	Glioblastoma	IDH mutant, MGMT methylated, 1p/19q non-codelated

Tumor volume, grade, histopathology, and molecular analyses are also reported.
In the first table column, patients are labeled according to the tumor's (lobe)_(hemisphere)_(grade): frontal (F), temporal (T), parietal (P), and insular (I) lobe; right (R) and left (L) hemisphere. NA, not available; MTG, middle temporal gyrus; IFG, inferior frontal gyrus; MFG, middle frontal gyrus; SFG, superior frontal gyrus; ANG, angular gyrus.

and bioinformatics toolbox functions were used for these statistical analyses.

Subsequently, correlations between different DTI measures (FDR < 0.1) and fMRI LIs were calculated using the non-parametric Spearman rank, in order to evaluate the strength and significance of the structural–functional correlations (SPSS v27), again accounting for multiple comparisons using the Benjamini–Hochberg procedure (38), setting the FDR to 0.1 since in our study the number of subjects was < 20 (39).

TABLE 2 | Demographic information is reported for the healthy control (HC) population.

HC	Age (years)	Sex	Education (years)	EHI
$N = 32$	39 ± 16 (18–72)	$N = 16$ male	20 ± 4 (13–30)	$N = 3$ left-handedness
		$N = 16$ female		$N = 5$ ambidextrousness
				$N = 24$ right-handedness

Mean ± standard deviation (range) is shown. Edinburgh Handedness Inventory (EHI) scores between −1 and −0.5 were considered indices of left-handedness; right-handedness was defined by scores between 0.5 and 1; and scores between −0.5 and 0.5 indicated ambidextrousness.

RESULTS

Nine patients were recruited (age: 41 ± 14 years, mean ± standard deviation; 5 males). Tumors were located in the left hemisphere in eight cases and in the right in one. They were mainly involving the middle temporal gyrus in two cases; the inferior, middle, and superior frontal gyri in three; the insula in two; and the angular gyrus in two.

At histological examination, one was DNT, three tumors were gliomas grade II, and five were HG tumors (two grade III and three grade IV). One patient (F, 63 years old) with an anaplastic astrocytoma had been operated 13 years before for a grade II astrocytoma (**Table 1**).

Thirty-two healthy volunteers (age: 39 ± 16 years, 16 males) were also recruited (**Table 2**). Diffusion MRI tractography identified the AF in all cases, demonstrating its spatial relationship with the tumor (**Figure 1**). Patients' main demographic and clinical data, and tumor characterization (location, volume, histopathology, and molecular status), are reported in **Table 1**, dividing patients into two subgroups corresponding to the LG and HG tumors.

Low-Grade Tumors

Three LG gliomas presented with epileptic seizures, and the DNT was an incidental finding. At hospital admission, all patients were neurologically intact, with no language impairments. The patient with DNT presented a history of dyslexia, and he referred no recent alteration in his language function.

Surgery was performed in an awake setting in two cases, and GTR was achieved in all but one case.

One patient developed a post-operative transient mild aphasia, which regressed completely in 7 days. All patients with

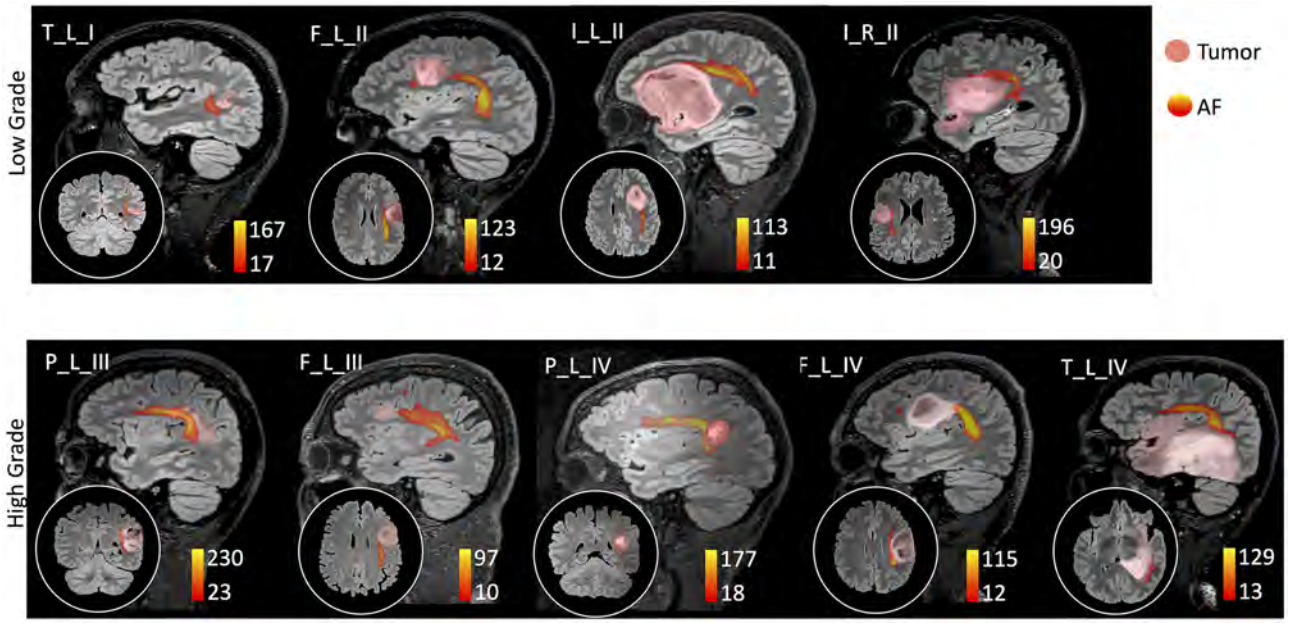

FIGURE 1 | Sagittal view on the tumor side and coronal or axial focus of the spatial relationship between the tumor (pink colormap) and the arcuate fasciculus (AF) tractography (colormap red to yellow indicating increasing fiber reconstruction probability). Patients were divided according to low-grade (top panel) and high-grade (bottom panel) tumors. Patients are labeled according to the tumor's (lobe)_(hemisphere)_(grade): frontal (F), temporal (T), parietal (P), and insular (I) lobe; and right (R) and left (L) hemisphere. For patient P_L_IV, a secondary tumor component (light green) is shown within the AF course.

LG tumors underwent radio- and chemotherapy. At follow-up (13 ± 1.3 months), they were alive without disease in three cases, and with a stable remnant in the other case.

High-Grade Tumors

Seizures were the manifesting symptom in four patients with HG tumors, while in the fifth case, an asymptomatic progression was detected at scheduled MRI follow-up for LG tumor treated by surgery 13 years previously. At hospital admission, no patient presented neurological deficits.

Tumor removal was performed in awake in four of the five cases. GTR was obtained in two patients and subtotal resection in the other three. Post-operative complications consisted of one case of epileptic seizures, controlled by antiepileptic drugs. One patient presented a post-operative transient aphasia and one some semantic paraphasia, which recovered completely after 30 and 2 days, respectively.

All patients underwent radio- and chemotherapies. At follow-up (mean 13 ± 5.7 months), all patients were alive, and one locally recurred, requiring a second surgery followed by chemotherapy.

Along-Tract Analyses

In HCs, the profiles of DTI along-tract measures differed between the right and left hemispheres (**Figures 2**, **3**). Outlier detection within the distribution of each HC DTI measure was used to define a normative range. The number of values identified as outliers was between 10 (MD of left AF) and 20 (MD of right AF) out of 480 (15 segments and 32 HCs). No specific AF segment localization or control subject was more prone to producing outliers. There was no systematic bias of outliers in the upper or lower tail.

Comparing the patients' along-tract measures with HCs', no abnormal or a maximum of four abnormal segments were detected in the LG tumor group, whereas within each HG tumor patient, more than four AF abnormal segments were measured with a maximum of 14 abnormal segments (**Table 3**).

In particular, considering the FA measure, there was no clear stratification of LG and HG tumors, as both groups presented some abnormalities compared with HCs (**Figure 2A**): for LG tumors, a maximum of four abnormal segments, and for HG tumors, a maximum of eight. A similar unclear stratification was also detected for the AD measure (**Figure 2B**), for which only two HG tumors presented more than four abnormal segments.

Considering the MD and RD measures, LG and HG tumor stratifications were clearer. MD measures were normal in all segments of the left LG tumor, whereas two segments showed increased MD in the right LG, while in the AF of the HG tumors, between two and 14 abnormal segments were detected. For RD, up to three abnormal segments were found only in the right hemisphere of LG tumors, whereas a minimum of four and a maximum of 10 abnormal segments were detected in the HG patients.

Functional MRI

Phonemic fluency activations during fMRI were evaluated both by visual inspection and by calculation of LI to assess

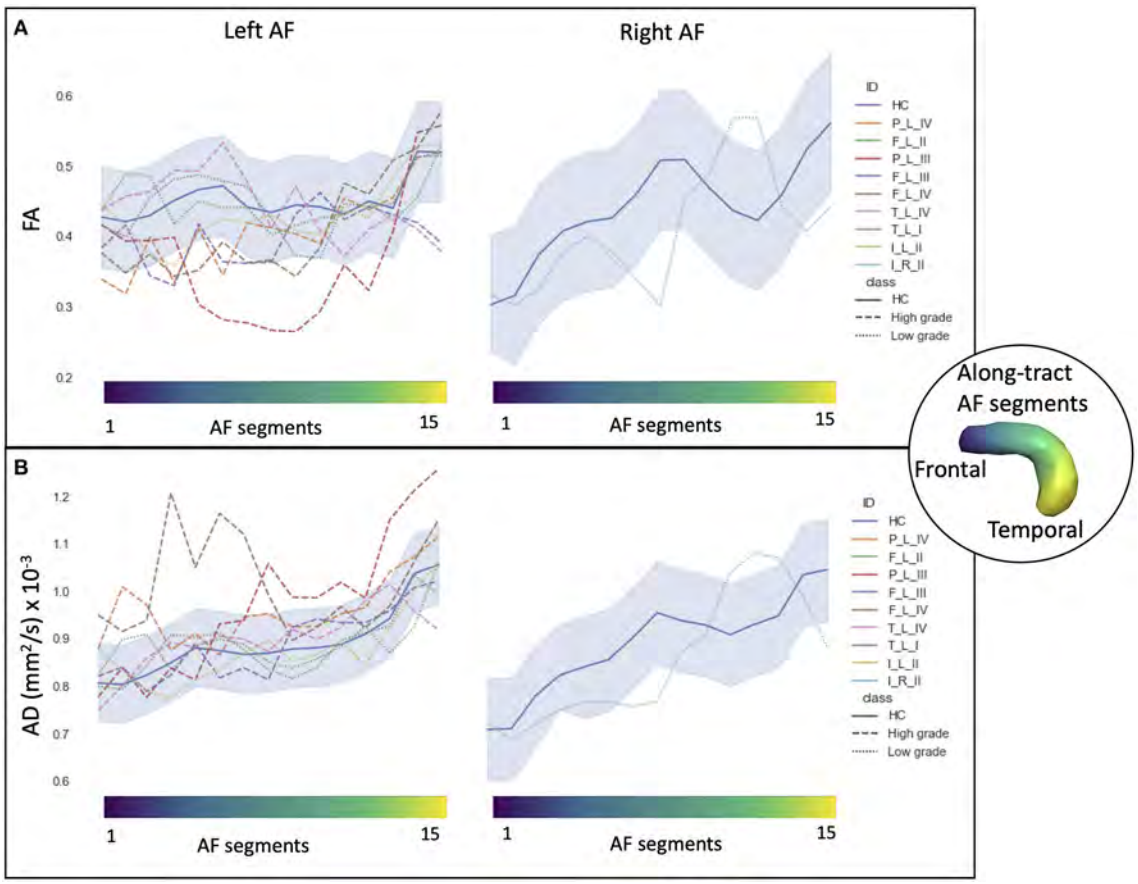

FIGURE 2 | Along-tract diffusion tensor imaging (DTI) measures [**A**: fractional anisotropy (FA); **B**: axial diffusivity (AD)] of the left and right arcuate fasciculi (AFs) are shown for both the patient group and the healthy control (HC) population. The AF was divided into 15 segments, ranging from frontal (blue) to temporal (yellow) divisions. Along-tract plots were colored to identify HC normative range and patient ID. Patients are labeled according to the tumor's (lobe)_(hemisphere)_(grade): frontal (F), temporal (T), parietal (P), and insular (I) lobe; and right (R) and left (L) hemisphere. Different line styles were used for HC, high-grade, and low-grade tumor patients. The blue-shaded areas indicate the normative HC range (2.5th–97.5th percentile).

language hemispheric dominance and agreement with the EHI handedness score.

The visual inspection of the overall task fMRI activations revealed five patients with left hemispheric dominance and four patients with a bilateral fMRI activation pattern in homologous language network regions. For six patients out of nine, fMRI activations' visual inspection was congruent with the EHI handedness scores, with a predominant activation in the left hemisphere if the patient was right-handed. The exceptions were as follows: one ambidextrous patient who presented a predominant activation on the left, and three right-handed patients showed a similar bilateral activation pattern.

The visual examination of fMRI activation patterns was in agreement with the LI measures, presenting predominant activations in the left hemisphere in all the LG tumor patients (LI $>$ 0), with the exception of the right hemisphere tumor patient, whereas for the HG tumors, mixed lateralization patterns were present. In particular, within the HG tumor patients, four presented right-lateralized language parietal activations, one patient presented only frontal right-lateralized activation, and one patient presented all three lobes activations right-lateralized (**Figure 4**).

Low Grade vs. High Grade Group Comparisons

In the comparison of DTI metrics across LG and HG tumor patient groups, differences were detected (at FDR = 0.1, 12 comparisons) in the number of abnormal MD and RD segments, median AD measure, and MD measures (**Table 3**). In particular, the number of increased MD and RD segments was higher in the HG tumor group than in the LG tumor group, and the median AD and MD measures were increased.

No differences were detected considering the tumor volume or fMRI LIs in the frontal, parietal, and temporal ROIs.

Along-Tract Diffusion Tensor Imaging and Functional MRI Laterality Correlations

The four DTI metrics, which differed in the LG vs. HG tumor comparison, were correlated to the fMRI LIs in the frontal, parietal, and temporal ROIs.

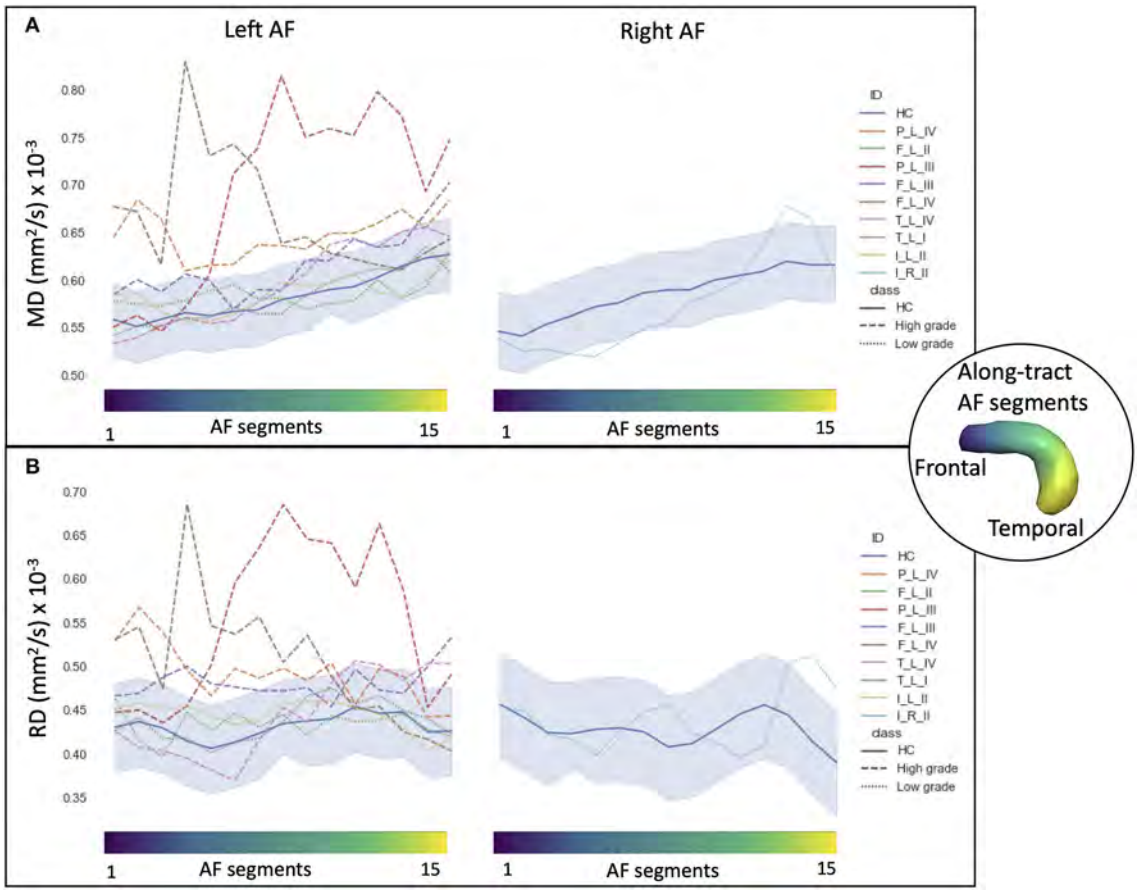

FIGURE 3 | Along-tract diffusion tensor imaging (DTI) measures (**A**: mean diffusivity (MD); **B**: radial diffusivity (RD)] of the left and right arcuate fasciculi (AFs) are shown for both the patient group and the healthy control (HC) population. The AF was divided into 15 segments ranging from frontal (blue) to temporal (yellow) divisions. Along-tract plots were colored to identify HC normative range and patient ID. Patients are labeled according to the tumor's (lobe)_(hemisphere)_(grade): frontal (F), temporal (T), parietal (P), and insular (I) lobe; and right (R) and left (L) hemisphere. Different line styles were used for HC, high-grade, and low-grade tumor patients. The blue-shaded areas indicate the normative HC range (2.5th–97.5th percentile).

TABLE 3 | Non-parametric comparison of low-grade (LG) and high-grade (HG) tumor patients using Mann–Whitney test, considering tumor volume, along-tract DTI measures [fractional anisotropy (FA), axial diffusivity (AD), mean diffusivity (MD), and radial diffusivity (RD)] median value and number of abnormal AF segments (#) compared with the healthy control (HC) normative distribution, and fMRI laterality index (LI).

Measures	LG tumors Median (min-max)	HG tumors Median (min-max)	LG vs. HG *p*-value	FDR
Tumor volume	32.9 (4.2–122)	26.4 (13–115.8)	1	1
FA # decreased segments	1.5 (0–4)	6 (2–8)	0.047*	0.11
Median FA	0.43 (0.40–0.45)	0.41 (0.36–0.44)	0.142	0.21
AD # decreased segments	1 (1–3)	4 (0–9)	0.306	0.37
Median AD	0.88 (0.77–0.90) mm^2/s	0.95 (0.89–0.99) mm^2/s	0.027*	**0.08**
MD # increased segments	0 (0–2)	10 (2–14)	0.017*	**0.07**
Median MD	0.58 (0.56–0.59) mm^2/s	0.64 (0.59–0.74) mm^2/s	0.014*	**0.07**
RD # increased segments	0 (0–3)	8 (4–10)	0.012*	**0.07**
Median RD	0.44 (0.43–0.45) mm^2/s	0.50 (0.44–0.59) mm^2/s	0.086	0.17
LI fMRI frontal	0.30 (0.02–0.86)	0.02 (−0.26 to 0.56)	0.221	0.29
LI fMRI parietal	0.37 (−0.20 to 1)	−0.18 (−0.62 to 0.18)	0.142	0.21
LI fMRI temporal	0.36 (−0.62 to 0.57)	0.33 (−0.06 to 0.75)	0.806	0.88

**uncorrected $p < 0.05$. In bold are comparisons at false discovery rate (FDR) < 0.1.*

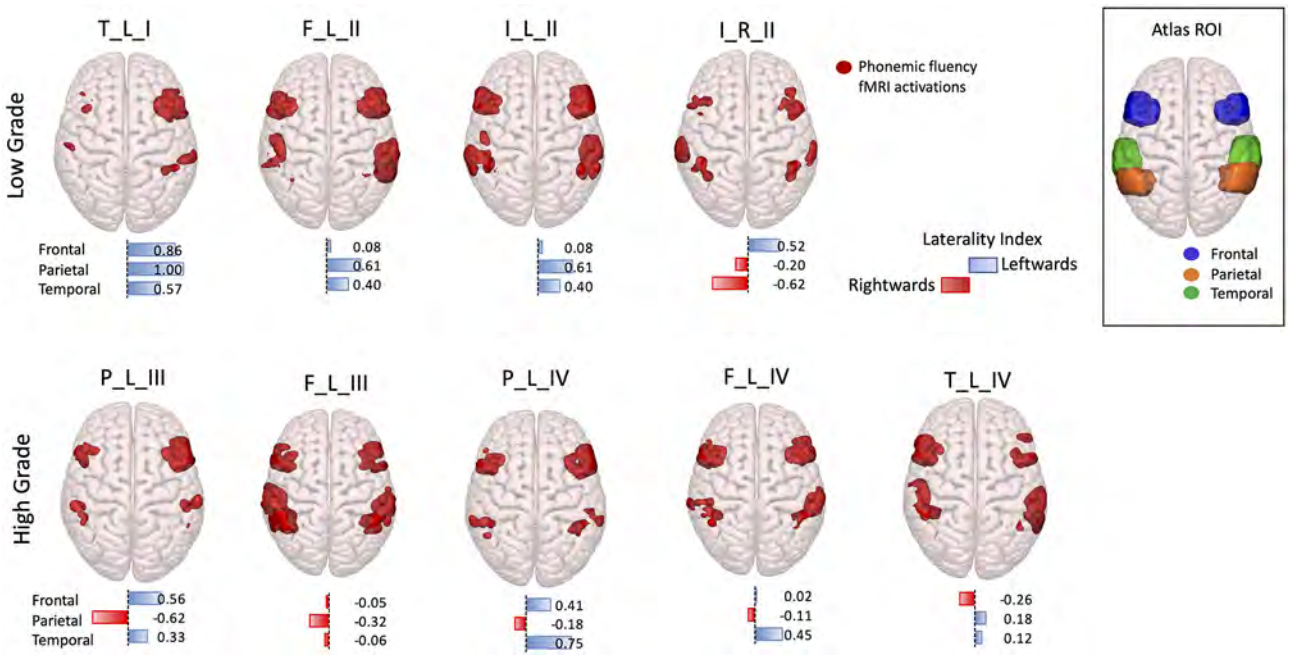

FIGURE 4 | 3D rendering with a superior prospective of fMRI phonemic fluency activations in the Montreal Neurological Institute (MNI)-152 brain. Activations were restricted to the frontal, parietal, and temporal regions according to regions of interest selected in the Harvard–Oxford Atlas, shown in the top right corner box. Patients were divided according to low-grade (top panel) and high-grade (bottom panel) tumors. Under each 3D-rendered brain, a horizontal laterality index bar is shown for each lobe, where the color, and orientation encode the hemisphere lateralization (red rightward and blue leftward), and the bar length gives the laterality index value. Patients are labeled according to the tumor's (lobe)_(hemisphere)_(grade): frontal (F), temporal (T), parietal (P), and insular (I) lobe; and right (R) and left (L) hemisphere.

During the phonemic fluency task, a more rightward-lateralized fMRI pattern (LI < 0) in the parietal ROIs only correlated with a higher number of abnormal MD segments (-0.732, unadjusted $p < 0.05$) and RD segments (-0.724, unadjusted $p < 0.05$) (**Table 4**).

None of the correlations survived after correcting for 12 multiple comparisons at FDR = 0.1.

TABLE 4 | Spearman rank non-parametric correlations (R) between fMRI laterality index (LI) and along-tract diffusion tensor imaging (DTI) measures, which differed (FDR < 0.1) between LG and HG tumor patients [axial diffusivity (AD), mean diffusivity (MD), and radial diffusivity (RD)], are reported.

Along-tract measures	LI fMRI frontal	LI fMRI parietal	LI fMRI temporal
Median AD	0.033	−0.233	0.533
MD # increased segments	−0.034	**−0.732* ($p = 0.025$, FDR = 0.14)**	0.187
Median MD	−0.183	−0.55	0.317
RD # increased segments	−0.068	**−0.724* ($p = 0.028$, FDR = 0.14)**	0.17

Number of abnormal AF segments (#), compared with the HC normative distribution, and median along-tract DTI measures were evaluated.
**uncorrected $p < 0.05$.*
FDR, false discovery rate.
In bold are correlations at false discovery rate (FDR) < 0.1.

Longitudinal Case Presentation

Low Grade Tumor (LGC) Case 1

A 30-year-old woman came to our attention in July 2019 after she had a generalized seizure, anticipated by an episode of dysphasia. Medical history was unremarkable. Brain MRI scan demonstrated a left frontal intra-axial tumor, showing hypointensity in T1-weighted and hyperintensity in T2- and FLAIR T2-weighted images and not enhancing after gadolinium administration (**Figure 5A**).

The AF tractography showed the close proximity of the tumor to the AF (**Figure 1**, case F_L_II). Along-tract AF DTI measures are shown in **Figure 6**, for both the pre-surgery and 8-month follow-up MRI scans. The fMRI activations demonstrated left hemispheric dominance (**Figure 4**, case F_L_II), corresponding to the right-handed dominance showed by the EHI score of 1.

Despite start of pharmacological treatment with levetiracetam 1,000 mg/day, a further seizure, with comparable semiology, re-occurred 3 months later. After an increase of the antiepileptic drug dosage, a surgical procedure was performed with awake technique. Cortical and subcortical mapping of the frontal region adjacent to the tumor was performed with direct electrical stimulation (DES), and afterwards, central debulking was performed with a Cavitron Ultrasonic Surgical Aspirator (CUSA, Integra LifeSciences, Princeton, NJ, USA).

The AF was located by the neuronavigation system, and after direct stimulation during reading, counting, and denomination of objects tasks, the portion of the tumor in its close proximity

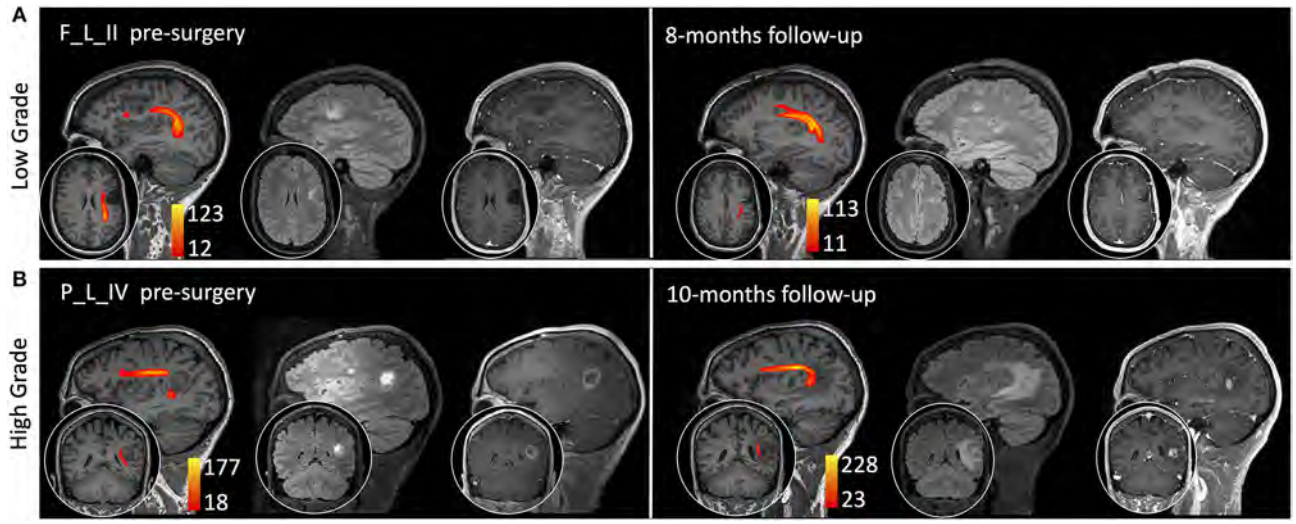

FIGURE 5 | Sagittal view on the tumor side and coronal or axial focus of T1-weighted, fluid-attenuated inversion recovery (FLAIR) T2-weighted, and T1-weighted images after gadolinium administration (0.1 mm/kg). The arcuate fasciculus tractography is superimposed on T1-weighted images (colormap red to yellow indicating increasing fiber reconstruction probability). **(A)** A low-grade glioma patient pre-surgery (left side) and 8 months post-surgery (right side). **(B)** A high-grade glioma patient pre-surgery (left side) and 10 months post-surgery (right side). Patients are labeled according to the tumor's (lobe)_(hemisphere)_(grade) classification: parietal (P) and frontal (F) lobe; and left (L) hemisphere.

was also resected without provoking any language disturbances, achieving a gross tumor resection. The histopathological analysis confirmed the diagnosis of diffuse astrocytoma grade II, isocitrate dehydrogenase (IDH) mutant, MGMT methylated, and 1p/19q non-codelated.

Post-operative course was uneventful, and the patient was discharged home after 3 days. Three months' MRI scan confirmed the radical resection of the tumor, and at 12 months' follow-up, the patient was neurologically intact, with no recurrence of the glioma.

High Grade Tumor HGC Case 2

A 51-year-old man came to our attention in October 2019 for a partial epileptic seizure, consisting of an episode of aphasia with speech arrest lasting a few minutes. Medical history was unremarkable. Treatment with levetiracetam 1,000 mg/day was started, and brain MRI showed a left fronto-temporal intra-axial tumor, hypointense in T1-weighted, and hyperintense in T2- and FLAIR T2-weighted images, with peripheral enhancement after gadolinium administration (**Figure 5B**).

AF tractography demonstrated the close proximity of the tumor to the AF (**Figure 1**, case P_L_IV). Along-tract AF DTI measures are shown in **Figure 6**, for both the pre-surgery and 8-month follow-up MRI scans. The diagnostic suspicion was of HG. Functional MRI demonstrated a left-hemispheric dominance (**Figure 4**, case P_L_IV), confirmed at EHI evaluation (score 0.89), showing a right-handed dominance. LI presented a rightward activation in the parietal lobe only.

Surgery was performed with awake technique. After cortical mapping of the supramarginal and angular gyri, the tumor was initially centrally debulked. With the neuronavigation system, the location of the AF was identified, and the tumor resection in its proximity was performed until the onset of reproducible phonemic and semantic paraphasia, induced by subcortical DES. The histopathological diagnosis confirmed the nature of glioblastoma grade IV, IDH wild type, TERT promoter mutated, and MGMT wild type.

The post-operative course was characterized by semantic paraphasia, regressing in 2 days, and the patient was discharged home after 4 days. Post-operative MRI demonstrated the presence of a small remnant, and radio- and chemo-therapies with temozolomide were performed.

After 11 months, the patient presented a further epileptic seizure with dysphasia. The subsequent MRI showed progression of the remnant. Because of the excellent general conditions, a further surgery was performed in September 2020 with awake technique and 5-alanine administration. A cortical and subcortical mapping of the peritumoral region was again conducted, followed by central debulking of the tumor with CUSA. Both the AF and inferior fronto-occipital fasciculus (IFOF) was identified by the onset of phonemic and semantic paraphasia, and their location was confirmed by the neuronavigation system. WM fascicles were extensively infiltrated by the tumor (with observation of 5-alanine captation), while they appeared to be functionally intact. For this reason, resection was arrested at that level. Histopathological examination confirmed the previous diagnosis.

Post-operative course was characterized by occasional semantic and phonemic paraphasia, which progressively regressed in 2 days. The patient was discharged home after 5 days. Post-operative MRI demonstrated contrast agent enhancement at the level of the remnant. At 1-month follow-up, no language impairments were present, and further chemotherapies were planned.

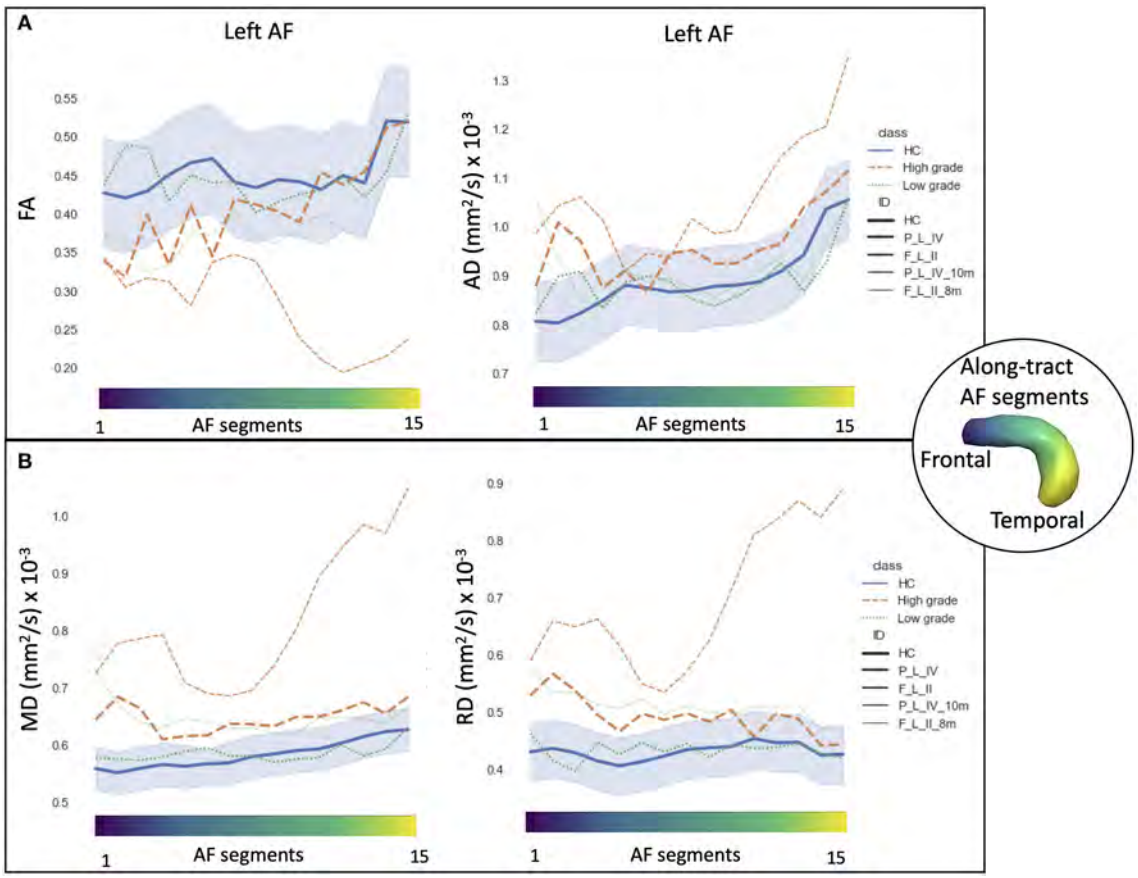

FIGURE 6 | Along-tract diffusion tensor imaging (DTI) measures [**A**: fractional anisotropy (FA) and axial diffusivity (AD); **B**: mean diffusivity (MD) and radial diffusivity (RD)] of the left arcuate fasciculus (AF) are shown for the longitudinal trajectories of two patients: one high-grade tumor with a 10-month follow-up after surgery (orange dashed line) and a low-grade tumor patient with an 8-month follow-up (green dashed line). Normative healthy control (HC) DTI measures were reported: median values (blue continuous line) and normative range, from the 2.5th to 97.5th percentiles (blue-shaded area). The AF was divided into 15 segments ranging from frontal (blue) to temporal (yellow) divisions. Patients are labeled according to the tumor's (lobe)_(hemisphere)_(grade) classification: parietal (P), frontal (F), and left (L) hemispheres.

DISCUSSION

In this pilot study, we have demonstrated that diffusion-weighted tractography of AF may be useful not only to provide accurate anatomical details for preoperative surgical planning and intraoperative cortical/subcortical brain mapping in combination with DES but also to characterize the histological grade of the tumor. Previous studies have demonstrated that decreased MD values and increased FA values show a positive correlation with the tumor cellularity (40, 41). Based on these findings, multiple studies have used DTI metrics in along-tract and perilesional regions to define brain tumor grade (42–53). Holly et al. (20, 21) described that FA and MD values were, respectively, higher and lower in perilesional regions of gliomas than in metastases. On the other hand, other studies suggest that FA increases intratumorally in gliomas (20, 21, 47, 49–51).

The possibility of differentiating between LG and HG gliomas using quantitative DTI measures is still under investigation, given the conflicting results available so far (19). As stated by Costabile et al. (4) the lack of homogeneous findings may be due to differences in diffusion-weighted acquisition protocols, pre- or post-processing methods, ROI selection, or the characteristics or size of the sample studied. Recently, Leroy et al. (19) have demonstrated that for tract fibers studied by histopathological examination after "en-bloc" resection, evaluation based on FA maps permits tract disruption to be predicted with sensitivity 89% and specificity 90%, reporting results similar to those obtained in rats (54).

Regarding AF tractography, we observed that four measures were able to discriminate (FDR = 0.1) LG and HG tumor patients: (1) median AD value, (2) number of abnormal MD segments, (3) median MD value, and (4) the number of abnormal RD segments. These results indicate the potential utility of the number of abnormal segments as a novel along-tract index, independent of tumor localization and related only to tract microstructure preservation. A future increase in the study cohort would allow us to make stronger statistical inferences. These results suggest that complementary to the role of AF tractography in the preoperative surgical planning and intraoperative brain tumor resection, the along-tract DTI

measures are suitable as *in vivo* biomarkers for tract integrity. Indeed, as demonstrated by several studies, fiber tracking obtained with diffusion-weighted tractography has a high concordance rate with intraoperative findings, achieved with DES, for a large number of tracts, such as the pyramidal tract (10, 11). Remarkably, the sensitivity and specificity of diffusion-weighted tractography for SLF, IFOF, and uncinate fasciculus have been assessed at around 97–100% by Bello et al. (10). Unlike some previous studies, our tractography protocol uses constrained spherical deconvolution modeling to parameterize crossing fibers and probabilistic tracking to estimate the uncertainty in fiber propagation. These methodological steps were chosen to provide the most reliable tractographic AF reconstruction possible. Moreover, the full automated AF tractography pipeline employed allowed fiber tracking reconstruction to be standardized across subjects and allowed comparison with normative parameters derived from an HC data set.

We used the topographical information describing the spatial relationship between the glioma and the AF course to determine the surgical flap design and the operative strategy for tumor removal and to predict the risk of post-operative language disturbances. It has been demonstrated that AF preservation is correlated with a low rate of long-term language dysfunction (16). Intraoperatively, the tractography provides an optimal tool for integrate DES information in order to refine the localization of the AF during the tumor removal (55). Indeed, the current standard paradigm in brain glioma surgery involves pursuing the maximal safe resection, which means the most extensive tumor removal without affecting neurological function. Castellano et al. (56) demonstrated in their series of 73 gliomas that the most relevant parameters to achieve the maximal safe resection were the tumor volume and involvement of CST and IFOF tracts, evaluated at preoperative tractography.

Regarding functional investigations, we recorded phonemic fluency activations using fMRI to investigate tumor-related cortical plasticity by evaluating the LI in the perisylvian network. None of the frontal, parietal, temporal lobe fMRI LIs resulted significantly different in LG vs. HG tumor patients. However, when comparing the DTI measures able to discriminate LG vs. HG tumor patients and fMRI LIs, a negative correlation (uncorrected $p < 0.05$) was found between the parietal lobe LI and the number of AF abnormal MD segments ($R = -0.732$) RD segments ($R = -0.724$). Thus, these results hint at a compensatory activation of the right parietal lobe ($LI < 0$) and angular and supramarginal gyri, in the presence of left HG tumors characterized by a higher number of abnormal AF segments compared with the HC population.

The cortical plasticity of language functions in response to different injuries remains an open question due to the methodological difficulties and lack of sizeable patient cohorts (57). Moreover, a correspondence of structural and functional lateralization has also been reported in normal conditions (58, 59). Interestingly, Powell et al. (58) reported the most significant correlation between voxel-wise fMRI activity for verbal fluency and mean arcuate FA in the left supramarginal gyrus. However, in our study, we found a correspondence with a rightward parietal lobe activation, and MD and RD pathological tractography measures, using a newly described index, the number of abnormal AF segments compared with an HC population. This result suggests that the difference in microstructural organization compared with HCs may reflect tumor malignancy and compensatory activation in the contralateral hemisphere (60).

However, a control population for fMRI activations, equivalent to that employed for evaluating DTI measures, is needed to assess the specificity of this result to the cortical plasticity mechanism. Further limitations of the proposed fMRI analyses are the dependency of fMRI LIs to the applied threshold ($Z = 3.1$) as shown by Suarez et al. (61) and the mainly frontal activations obtained by administrating the phonemic fluency task (27).

We report two cases longitudinally in greater depth, from the perspective of personalized precision medicine. The along-tract DTI trajectories of an LG and HG tumors highlight the different progression rates and microstructural alterations compared with HC (**Figure 6**).

In the last few years, neuronavigator-integrated TMS (nTMS) has been used to identify seeding regions for DTI tractography for multiple tracts, including CTS and AF, thus improving the reliability of the DTI fiber reconstruction results (62–68). The association of these neurophysiological and neuroimaging techniques has notable advantages for reconstruction of subcortical language tracts such as the AF, which is affected by elevated intersubject anatomical variability in cortical projections (14), which can be accurately identified by nTMS, as recently shown by Giampiccolo et al. (69).

We note that the encouraging results presented in this paper are preliminary, as they were obtained in a relatively small group of patients and need to be confirmed in larger studies.

Moreover, the presence of outlier values even within the HC population suggests that there is scope for further improvement of the method of calculating along-segment DTI measures.

CONCLUSION

Our pilot study suggests that the AF tractography could be considered a valid tool in the surgical planning phase and intraoperatively, guiding the subcortical eloquent regions identification. In addition, analysis of fMRI activations provides a way to delineate eloquent cortical regions. Moreover, along-tract tractography analyses can potentially characterize the histological grade of the tumor *in vivo*, as demonstrated by the higher median AD and MD values, and greater number of segments with abnormal RD or MD measures, in HG gliomas. We also found that in patients with an HG glioma, a higher number of segments with abnormal RD and MD were associated with increased compensatory language

fMRI activation in the right parietal lobe contralateral to the lesion.

Our findings suggest that along-tract analysis is a useful tool in evaluating AF tractography, providing information on tumor grade and, in combination with fMRI, related cortical reorganization, thus contributing to preoperative surgical planning and longitudinal patient monitoring after surgery.

DATA AVAILABILITY STATEMENT

The raw data supporting the conclusions of this article will be made available by the authors, without undue reservation.

ETHICS STATEMENT

The studies involving human participants were reviewed and approved by CE-AVEC. The patients/participants provided their written informed consent to participate in this study.

AUTHOR CONTRIBUTIONS

AC, RL, DMaz, and CTo: study design. MZ, LT, MMa, DMan, FBad, SA, MMi, FBar, MR, and VF: data collection and paper preparation. CTo, AC, RL, DMaz, and CTe: study supervision. All authors contributed to the article and approved the submitted version.

REFERENCES

1. Duffau H. Diffusion tensor imaging is a research and educational tool, but not yet a clinical tool. *World Neurosurg.* (2013) 82:e43–5. doi: 10.1016/j.wneu.2013.08.054
2. Vanderweyen DC, Theaud G, Sidhu J, Rheault F, Sarubbo S, Descoteaux M, et al. The role of diffusion tractography in refining glial tumor resection. *Brain Struct Funct.* (2020) 225:1413–36. doi: 10.1007/s00429-020-02056-z
3. Conti Nibali M, Rossi M, Sciortino T, Riva M, Gay LG, Pessina F, et al. Preoperative surgical planning of glioma: limitations and reliability of fMRI and DTI tractography. *J Neurosurg Sci.* (2018) 63:127–34. doi: 10.23736/S0390-5616.18.04597-6
4. Costabile JD, Alaswad E, D'Souza S, Thompson JA, Ormond DR. Current applications of diffusion tensor imaging and tractography in intracranial tumor resection. *Front Oncol.* (2019) 9:426. doi: 10.3389/fonc.2019.00426
5. Tunç B, Ingalhalikar M, Parker D, Lecoeur J, Singh N, Wolf RL, et al. Individualized map of white matter pathways: connectivity-based paradigm for neurosurgical planning. *Neurosurgery.* (2016) 79:568–77. doi: 10.1227/NEU.0000000000001183
6. Ostrý S, Belšan T, Otáhal J, Beneš V, Netuka D. Is intraoperative diffusion tensor imaging at 3.0T comparable to subcortical corticospinal tract mapping? *Neurosurgery.* (2013) 73:797–807; discussion 806–7. doi: 10.1227/NEU.0000000000000087
7. Lorenzen A, Groeschel S, Ernemann U, Wilke M, Schuhmann MU. Role of presurgical functional MRI and diffusion MR tractography in pediatric low-grade brain tumor surgery: a single-center study. *Childs Nerv Syst.* (2018) 34:2241–8. doi: 10.1007/s00381-018-3828-4
8. Shukla G, Alexander GS, Bakas S, Nikam R, Talekar K, Palmer JD, et al. Advanced magnetic resonance imaging in glioblastoma: a review. *Chin Clin Oncol.* (2017) 6:40. doi: 10.21037/cco.2017.06.28
9. Henderson F, Abdullah KG, Verma R, Brem S. Tractography and the connectome in neurosurgical treatment of gliomas: the premise, the progress, and the potential. *Neurosurg Focus.* (2020) 48:E6. doi: 10.3171/2019.11.FOCUS19785
10. Bello L, Gambini A, Castellano A, Carrabba G, Acerbi F, Fava E, et al. Motor and language DTI fiber tracking combined with intraoperative subcortical mapping for surgical removal of gliomas. *Neuroimage.* (2008) 39:369–82. doi: 10.1016/j.neuroimage.2007.08.031
11. Zhu FP, Wu JS, Song YY, Yao CJ, Zhuang DX, Xu G, et al. Clinical application of motor pathway mapping using diffusion tensor imaging tractography and intraoperative direct subcortical stimulation in cerebral glioma surgery: a prospective cohort study. *Neurosurgery.* (2012) 71:1170–83. doi: 10.1227/NEU.0b013e318271bc61
12. Mormina E, Longo M, Arrigo A, Alafaci C, Tomasello F, Calamuneri A, et al. MRI tractography of corticospinal tract and arcuate fasciculus in high-grade gliomas performed by constrained spherical deconvolution: qualitative and quantitative analysis. *AJNR Am J Neuroradiol.* (2015) 36:1853–8. doi: 10.3174/ajnr.A4368
13. Mormina E, Arrigo A, Calamuneri A, Alafaci C, Tomasello F, Morabito R et al. Optic radiations evaluation in patients affected by high-grade gliomas: a side-by-side constrained spherical deconvolution and diffusion tensor imaging study. *Neuroradiology.* (2016) 58:1067–75. doi: 10.1007/s00234-016-1732-8
14. Thiebaut de Schotten M, Ffytche DH, Bizzi A, Dell'Acqua F, Allin M, Walshe M, et al. Atlasing location, asymmetry and inter-subject variability of white matter tracts in the human brain with MR diffusion tractography. *Neuroimage.* (2011) 54:49–59. doi: 10.1016/j.neuroimage.2010.07.055
15. Voets NL, Bartsch A, Plaha P. Brain white matter fibre tracts: a review of functional neuro-oncological relevance. *J Neurol Neurosurg Psychiatry.* (2017) 88:1017–25. doi: 10.1136/jnnp-2017-316170
16. Caverzasi E, Hervey-Jumper SL, Jordan KM, Lobach IV, Li J, Panara V, et al. Identifying preoperative language tracts and predicting postoperative functional recovery using HARDI q-ball fiber tractography in patients with gliomas. *J Neurosurg.* (2016) 125:33–45. doi: 10.3171/2015.6.JNS142203
17. Marchina S, Zhu LL, Norton A, Zipse L, Wan CY, Schlaug G. Impairment of speech production predicted by lesion load of the left arcuate fasciculus. *Stroke.* (2011) 42:2251–6. doi: 10.1161/STROKEAHA.110.606103
18. Rolheiser T, Stamatakis EA, Tyler LK. Dynamic processing in the human language system: synergy between the arcuate fascicle and extreme capsule. *J Neurosci.* (2011) 31:16949–57. doi: 10.1523/JNEUROSCI.2725-11.2011
19. Leroy HA, Lacoste M, Maurage CA, Derré B, Baroncini M, Reyns N, et al. Anatomo-radiological correlation between diffusion tensor imaging and histologic analyses of glial tumors: a preliminary study. *Acta Neurochir.* (2020) 162:1663–72. doi: 10.1007/s00701-020-04323-8
20. Holly KS, Barker BJ, Murcia D, Bennett R, Kalakoti P, Ledbetter C, et al. High-grade gliomas exhibit higher peritumoral fractional anisotropy and lower mean diffusivity than intracranial metastases. *Front Surg.* (2017) 4:18. doi: 10.3389/fsurg.2017.00018
21. Holly KS, Fitz-Gerald JS, Barker BJ, Murcia D, Daggett R, Ledbetter C, et al. Differentiation of high-grade glioma and intracranial metastasis using volumetric diffusion tensor imaging tractography. *World Neurosurg.* (2018) 120:e131–41. doi: 10.1016/j.wneu.2018.07.230
22. Celtikci P, Fernandes-Cabral DT, Yeh FC, Panesar SS, Fernandez-Miranda JC. Generalized q-sampling imaging fiber tractography reveals displacement and infiltration of fiber tracts in low-grade gliomas. *Neuroradiology.* (2018) 60:267–80. doi: 10.1007/s00234-018-1985-5
23. Nilsson D, Rutka JT, Snead OC III, Raybaud CR, Widjaja E. Preserved structural integrity of white matter adjacent to low-grade tumors. *Childs Nerv Syst.* (2008) 24:313–20. doi: 10.1007/s00381-007-0466-7. [Epub ahead of print].
24. Seow P, Hernowo AT, Narayanan V, Wong JHD, Bahuri NFA, Cham CY, et al. Neural fiber integrity in high- versus low-grade glioma using probabilistic fiber tracking. *Acad Radiol.* (2020). doi: 10.1016/j.acra.2020.09.007
25. D'Souza S, Ormond DR, Costabile J, Thompson JA. Fiber-tract localized diffusion coefficients highlight patterns of white matter disruption induced by proximity to glioma. *PLoS ONE.* (2019) 14:e0225323. doi: 10.1371/journal.pone.0225323

26. Oldfield RC. The assessment and analysis of handedness: the Edinburgh inventory. *Neuropsychologia.* (1971) 9:97–113. doi: 10.1016/0028-3932(71)90067-4
27. Black DF, Vachha B, Mian A, Faro SH, Maheshwari M, Sair HI, et al. American society of functional neuroradiology-recommended fMRI paradigm algorithms for presurgical language assessment. *AJNR Am J Neuroradiol.* (2017) 38:E65–73. doi: 10.3174/ajnr.A5345
28. Yushkevich PA, Piven J, Hazlett HC, Smith RG, Ho S, Gee JC, et al. User-guided 3D active contour segmentation of anatomical structures: significantly improved efficiency and reliability. *Neuroimage.* (2006) 31:1116–28. doi: 10.1016/j.neuroimage.2006.01.015
29. Talozzi L, Testa C, Evangelisti S, Cirignotta L, Bianchini C, Ratti S, et al. Along-tract analysis of the arcuate fasciculus using the Laplacian operator to evaluate different tractography methods. *Magn Reson Imaging.* (2018) 54:183–93. doi: 10.1016/j.mri.2018.08.013
30. Giorgio A, Watkins KE, Chadwick M, James S, Winmill L, Douaud G et al. Longitudinal changes in grey and white matter during adolescence. *Neuroimage.* (2010) 49:94–103. doi: 10.1016/j.neuroimage.2009.08.003
31. Jenkinson M, Bannister P, Brady M, Smith S. Improved optimization for the robust and accurate linear registration and motion correction of brain images. *Neuroimage.* (2002) 17:825–84. doi: 10.1006/nimg.2002.1132
32. Smith SM, Jenkinson M, Woolrich MW, Beckmann CF, Behrens TEJ, Johansen-Berg H, et al. Advances in functional and structural MR image analysis and implementation as FSL. *Neuroimage.* (2004) 23:S208–19. doi: 10.1016/j.neuroimage.2004.07.051
33. Seghier ML. Laterality index in functional MRI: methodological issues. *Magn Reson Imaging.* (2008) 26:594–601. doi: 10.1016/j.mri.2007.10.010
34. Forkel SJ, Rogalski E, Drossinos Sancho N, D'Anna L, Luque Laguna P, Sridhar J, et al. Anatomical evidence of an indirect pathway for word repetition. *Neurology.* (2020) 94:e594–606. doi: 10.1212/WNL.0000000000008746
35. Wu JS, Zhou LF, Tang WJ, Mao Y, Hu J, Song YY, et al. Clinical evaluation and follow-up outcome of diffusion tensor imaging-based functional neuronavigation: a prospective, controlled study in patients with gliomas involving pyramidal tracts. *Neurosurgery.* (2007) 61:935–48; discussion 948–9. doi: 10.1227/01.neu.0000303189.80049.ab
36. Morandi L, de Biase D, Visani M, Cesari V, De Maglio G, Pizzolito S, et al. Allele specific locked nucleic acid quantitative PCR (ASLNAqPCR): an accurate and cost-effective assay to diagnose and quantify KRAS and BRAF mutation. *PLoS ONE.* (2012) 7:e36084. doi: 10.1371/journal.pone.0036084
37. Smith JS, Perry A, Borell TJ, Lee HK, O'Fallon J, Hosek SM, et al. Alterations of chromosome arms 1p and 19q as predictors of survival in oligodendrogliomas, astrocytomas, and mixed oligoastrocytomas. *J Clin Oncol.* (2000) 18:636–45. doi: 10.1200/JCO.2000.18.3.636
38. Benjamini Y, Hochberg, Y. Controlling the false discovery rate: a practical and powerful approach to multiple testing. *J R Stat Soc.* (1995) 57:289–300. doi: 10.1111/j.2517-6161.1995.tb02031.x
39. Frommlet F, Bogdan, M. Some optimality properties of FDR controlling rules under sparsity. *Electron J Stat.* (2013) 7:1328–68. doi: 10.1214/13-EJS808
40. Sugahara T, Korogi Y, Kochi M, Ikushima I, Shigematu Y, Hirai T, et al. Usefulness of diffusion-weighted MRI with echo-planar technique in the evaluation of cellularity in gliomas. *J Magn Reson Imaging.* (1999) 9:53–60. doi: 10.1002/(SICI)1522-2586(199901)9:1<53::AID-JMRI7>3.0.CO;2-2
41. Beppu T, Inoue T, Shibata Y, Yamada N, Kurose A, Ogasawara K, et al. Fractional anisotropy value by diffusion tensor magnetic resonance imaging as a predictor of cell density and proliferation activity of glioblastomas. *Surg Neurol.* (2005) 63:56–61; discussion 61. doi: 10.1016/j.surneu.2004.02.034
42. Lu S, Ahn D, Johnson G, Cha S. Peritumoral diffusion tensor imaging of high-grade gliomas and metastatic brain tumors. *AJNR Am J Neuroradiol.* (2003) 24:937–41.
43. El-Serougy L, Abdel Razek AA, Ezzat A, Eldawoody H, El-Morsy A. Assessment of diffusion tensor imaging metrics in differentiating low-grade from high-grade gliomas. *Neuroradiol J.* (2016) 29:400–7. doi: 10.1177/1971400916665382
44. Tan Y, Wang XC, Zhang H, Wang J, Qin JB, Wu XF, et al. Differentiation of high-grade-astrocytomas from solitary-brain-metastases: comparing diffusion kurtosis imaging and diffusion tensor imaging. *Eur J Radiol.* (2015) 84:2618–24. doi: 10.1016/j.ejrad.2015.10.007
45. Bette S, Huber T, Wiestler B, Boeckh-Behrens T, Gempt J, Ringel F, et al. Analysis of fractional anisotropy facilitates differentiation of glioblastoma and brain metastases in a clinical setting. *Eur J Radiol.* (2016) 85:2182–7. doi: 10.1016/j.ejrad.2016.10.002
46. Byrnes TJ, Barrick TR, Bell BA, Clark CA. Diffusion tensor imaging discriminates between glioblastoma and cerebral metastases *in vivo*. *NMR Biomed.* (2011) 24:54–60. doi: 10.1002/nbm.1555
47. Bauer AH, Erly W, Moser FG, Maya M, Nael K. Differentiation of solitary brain metastasis from glioblastoma multiforme: a predictive multiparametric approach using combined MR diffusion and perfusion. *Neuroradiology.* (2015) 57:697–703. doi: 10.1007/s00234-015-1524-6
48. Toh CH, Wei KC, Chang CN, Ng SH, Wong HF, Lin CP. Differentiation of brain abscesses from glioblastomas and metastatic brain tumors: comparisons of diagnostic performance of dynamic susceptibility contrast-enhanced perfusion MR imaging before and after mathematic contrast leakage correction. *PLoS ONE.* (2014) 9:e109172. doi: 10.1371/journal.pone.0109172
49. Wang S, Kim S, Chawla S, Wolf RL, Knipp DE, Vossough A, et al. Differentiation between glioblastomas, solitary brain metastases, and primary cerebral lymphomas using diffusion tensor and dynamic susceptibility contrast-enhanced MR imaging. *AJNR.* (2011) 32:507–14. doi: 10.3174/ajnr.A2333
50. Wang S, Kim S, Chawla S, Wolf RL, Zhang WG, O'Rourke DM, et al. Differentiation between glioblastomas and solitary brain metastases using diffusion tensor imaging. *Neuroimage.* (2009) 44:653–60. doi: 10.1016/j.neuroimage.2008.09.027
51. Wang S, Kim SJ, Poptani H, Woo JH, Mohan S, Jin R, et al. Diagnostic utility of diffusion tensor imaging in differentiating glioblastomas from brain metastases. *AJNR.* (2014) 35:928–34. doi: 10.3174/ajnr.A3871
52. Papageorgiou TS, Chourmouzi D, Drevelengas A, Kouskouras K, Siountas A. Diffusion tensor imaging in brain tumors: a study on gliomas and metastases. *Phys Med.* (2015) 31:767–73. doi: 10.1016/j.ejmp.2015.03.010
53. Svolos P, Tsolaki E, Kapsalaki E, Theodorou K, Fountas K, Fezoulidis I, et al. Investigating brain tumor differentiation with diffusion and perfusion metrics at 3T MRI using pattern recognition techniques. *Magn Reson Imaging.* (2013) 31:1567–77. doi: 10.1016/j.mri.2013.06.010
54. Jia X, Su Z, Hu J, Xia H, Ma H, Wang X, et al. The value of diffusion tensor tractography delineating corticospinal tract in glioma in rat: validation via correlation histology. *PeerJ.* (2019) 7:e6453. doi: 10.7717/peerj.6453
55. Yamao Y, Suzuki K, Kunieda T, Matsumoto R, Arakawa Y, Nakae T, et al. Clinical impact of intraoperative CCEP monitoring in evaluating the dorsal language white matter pathway. *Hum Brain Mapp.* (2017) 38:1977–91. doi: 10.1002/hbm.23498
56. Castellano A, Bello L, Michelozzi C, Gallucci M, Fava E, Iadanza A, et al. Role of diffusion tensor magnetic resonance tractography in predicting the extent of resection in glioma surgery. *Neuro Oncol.* (2012) 14:192–202. doi: 10.1093/neuonc/nor188
57. Cirillo S, Caulo M, Pieri V, Falini A, Castellano A. Role of functional imaging techniques to assess motor and language cortical plasticity in glioma patients: a systematic review. *Neural Plast.* (2019) 2019:4056436. doi: 10.1155/2019/4056436
58. Powell HW, Parker GJ, Alexander DC, Symms MR, Boulby PA, Wheeler-Kingshott CA, et al. Hemispheric asymmetries in language-related pathways: a combined functional MRI and tractography study. *Neuroimage.* (2006) 32:388–99. doi: 10.1016/j.neuroimage.2006.03.011
59. Perlaki G, Horvath R, Orsi G, Aradi M, Auer T, Varga E, et al. White-matter microstructure and language lateralization in left-handers: a whole-brain MRI analysis. *Brain Cogn.* (2013) 82:319–28. doi: 10.1016/j.bandc.2013.05.005
60. Forkel SJ, Thiebaut de Schotten M, Dell'Acqua F, Kalra L, Murphy DG, Williams SC, et al. Anatomical predictors of aphasia recovery: a tractography study of bilateral perisylvian language networks. *Brain.* (2014) 137(Pt 7):2027–39. doi: 10.1093/brain/awu113
61. Suarez OR, Whalen S, O'Shea JP, Golby AJ. A surgical planning method for functional mri assessment of language dominance: influences from threshold, region-of-interest, and stimulus mode. *Brain Imaging Behav.* (2008) 2:59–73. doi: 10.1007/s11682-007-9018-8
62. Raffa G, Bährend I, Schneider H, Faust K, Germanò A, Vajkoczy P, et al. A novel technique for region and linguistic specific nTMS-based DTI fiber

tracking of language pathways in brain tumor patients. *Front Neurosci.* (2016) 10:552. doi: 10.3389/fnins.2016.00552

63. Raffa G, Conti A, Scibilia A, Cardali SM, Esposito F, Angileri FF, et al. The impact of diffusion tensor imaging fiber tracking of the corticospinal tract based on navigated transcranial magnetic stimulation on surgery of motor-eloquent brain lesions. *Neurosurgery.* (2018) 83:768–82. doi: 10.1093/neuros/nyx554
64. Raffa G, Conti A, Scibilia A, Sindorio C, Quattropani MC, Visocchi M, et al. Functional reconstruction of motor and language pathways based on navigated transcranial magnetic stimulation and DTI fiber tracking for the preoperative planning of low grade glioma surgery: a new tool for preservation and restoration of eloquent networks. *Acta Neurochir Suppl.* (2017) 124:251–61. doi: 10.1007/978-3-319-39546-3_37
65. Raffa G, Picht T, Scibilia A, Rösler J, Rein J, Conti A, et al. Surgical treatment of meningiomas located in the rolandic area: the role of navigated transcranial magnetic stimulation for preoperative planning, surgical strategy, and prediction of arachnoidal cleavage and motor outcome. *J Neurosurg.* (2019) 14:1–12. doi: 10.3171/2019.3.JNS183411
66. Raffa G, Quattropani MC, Scibilia A, Conti A, Angileri FF, Esposito F, et al. Surgery of language-eloquent tumors in patients not eligible for awake surgery: the impact of a protocol based on navigated transcranial magnetic stimulation on presurgical planning and language outcome, with evidence of tumor-induced intra-hemispheric plasticity. *Clin Neurol Neurosurg.* (2018) 168:127–39. doi: 10.1016/j.clineuro.2018.03.009
67. Negwer C, Ille S, Hauck T, Sollmann N, Maurer S, Kirschke JS, et al. Visualization of subcortical language pathways by diffusion tensor imaging fiber tracking based on rTMS language mapping. *Brain Imaging Behav.* (2017) 11:899–914. doi: 10.1007/s11682-016-9563-0
68. Vassal F, Schneider F, Nuti C. Intraoperative use of diffusion tensor imaging-based tractography for resection of gliomas located near the pyramidal tract: comparison with subcortical stimulation mapping and contribution to surgical outcomes. *Br J Neurosurg.* (2013) 27:668–75. doi: 10.3109/02688697.2013.771730
69. Giampiccolo D, Howells H, Bährend I, Schneider H, Raffa G, Rosenstock T, et al. Preoperative transcranial magnetic stimulation for picture naming is reliable in mapping segments of the arcuate fasciculus. *Brain Commun.* (2020) 2:fcaa158. doi: 10.1093/braincomms/fcaa158

Conflict of Interest: The authors declare that the research was conducted in the absence of any commercial or financial relationships that could be construed as a potential conflict of interest.

frontiers in Oncology

ORIGINAL RESEARCH
published: 26 February 2021
doi: 10.3389/fonc.2021.628007

Optimizing Adjuvant Stereotactic Radiotherapy of Motor-Eloquent Brain Metastases: Sparing the nTMS-Defined Motor Cortex and the Hippocampus

Yvonne Dzierma[1†], Michaela Schuermann[1†], Patrick Melchior[1], Frank Nuesken[1], Joachim Oertel[2], Christian Rübe[1] and Philipp Hendrix[2]*

[1] Department of Radiotherapy and Radiation Oncology, Saarland University Medical Centre, Homburg, Germany, [2] Department of Neurosurgery, Saarland University Medical Centre and Saarland University Faculty of Medicine, Homburg, Germany

OPEN ACCESS

Edited by:
Thomas Picht,
Charité – Universitätsmedizin Berlin, Germany

Reviewed by:
Tizian Rosenstock,
Charité – Universitätsmedizin Berlin, Germany
Sandro M. Krieg,
Technical University of Munich, Germany
Ina Bährend,
Charité-Klinik für Neurochirurgie, Germany

***Correspondence:**
Yvonne Dzierma
Yvonne.dzierma@uks.eu

†These authors share first authorship

Specialty section:
This article was submitted to Neuro-Oncology and Neurosurgical Oncology, a section of the journal Frontiers in Oncology

Received: 10 November 2020
Accepted: 06 January 2021
Published: 26 February 2021

Citation:
Dzierma Y, Schuermann M, Melchior P, Nuesken F, Oertel J, Rübe C and Hendrix P (2021) Optimizing Adjuvant Stereotactic Radiotherapy of Motor-Eloquent Brain Metastases: Sparing the nTMS-Defined Motor Cortex and the Hippocampus. Front. Oncol. 11:628007. doi: 10.3389/fonc.2021.628007

Brain metastases can effectively be treated with surgical resection and adjuvant stereotactic radiotherapy (SRT). Navigated transcranial magnetic stimulation (nTMS) has been used to non-invasively map the motor cortex prior to surgery of motor eloquent brain lesions. To date, few studies have reported the integration of such motor maps into radiotherapy planning. The hippocampus has been identified as an additional critical structure of radiation-induced deficits. The aim of this study is to assess the feasibility of selective dose reduction to both the nTMS-based motor cortex and the hippocampi in SRT of motor-eloquent brain metastases. Patients with motor-eloquent brain metastases undergoing surgical resection and adjuvant SRT between 07/2014 and 12/2018 were retrospectively analyzed. The radiotherapy treatment plans were retrieved from the treatment planning system ("original" plan). For each case, two intensity-modulated treatment plans were created: the "motor" plan aimed to reduce the dose to the motor cortex, the "motor & hipp" plan additionally reduce the dose to the hippocampus. The optimized plans were compared with the "original" plan regarding plan quality, planning target volume (PTV) coverage, and sparing of organs at risk (OAR). 69 plans were analyzed, all of which were clinically acceptable with no significant differences for PTV coverage. All OAR were protected according to standard protocols. Sparing of the nTMS motor map was feasible: mean dose 9.66 ± 5.97 Gy (original) to 6.32 ± 3.60 Gy (motor) and 6.49 ± 3.78 Gy (motor & hipp), $p<0.001$. In the "motor & hipp" plan, dose to the ipsilateral hippocampi could be significantly reduced (max 1.78 ± 1.44 Gy vs 2.49 ± 1.87 Gy in "original", $p = 0.003$; mean 1.01 ± 0.92 Gy vs. 1.32 ± 1.07 Gy in "original", $p = 0.007$). The study confirms the results from previous studies that inclusion of nTMS motor information into radiotherapy treatment planning is possible with a relatively straightforward workflow and can achieve reduced doses to the nTMS-defined motor area without compromising PTV coverage. Furthermore, we demonstrate the feasibility of selective dose reduction to the hippocampus at the same time. The clinical significance of

these optimized plans yet remains to be determined. However, with no apparent disadvantages these optimized plans call for further and broader exploration.

Keywords: nTMS mapping, motor cortex, hippocampus sparing, treatment planning, functional optimization, IMRT, stereotactic radiation, brain metastases

INTRODUCTION

Brain metastases can effectively be treated with surgical resection and/or stereotactic radiotherapy (SRT). Lesions located within or adjacent to critical motor areas pose a challenge to both the neuro- and radiosurgeon. Increasing survival from effective interdisciplinary treatment regimens shifts attention to ameliorated secondary outcome rates such as improved motor function, cognitive function and quality of life. Preoperative neurosurgical planning and surgical resection itself predominantly aim to identify and preserve critical motor areas. In the past decade, navigated transcranial magnetic stimulation (nTMS) has been used to non-invasively map the motor cortex prior to surgery of motor eloquent brain lesions. Here, these preoperative motor maps appear to facilitate better resection rates while maintaining neurological function (1–5).

Whereas planning of SRT focusses on sparing distinct structures at risks, motor-eloquent areas have not routinely been integrated. Motor deficits have been observed to occur after high-dose Gamma Knife SRS to sites close to the motor cortex (6). Beyond direct motor-deficits, Pfeiffer et al. (7) have postulated a relationship between higher dose to the precentral gyrus and impaired verbal and working memory, attention and executive functions. To date, a small number of studies have reported the integration of motor maps into radiotherapy planning for dose reduction to motor areas, primarily in CyberKnife and GammaKnife treatment (8–11). Two studies (12, 13) have been carried out for linear accelerator (linac)-based radiotherapy, one of which considered patients with brain metastases. All studies showed that the inclusion of nTMS information into the radiotherapeutic planning workflow was possible and allowed for improved dose sparing of the motor-eloquent areas. However, additional confirmation from different medical centers and using different planning systems is still warranted. Furthermore, the hippocampus has been identified as an additional critical structure of radiation-induced cognitive deficits, which has not been considered in previous studies on nTMS in radiotherapy. In addition to the observed negative impact of whole-brain radiotherapy on cognitive outcome (14, 15), several studies have focussed on the hippocampus itself as one of the most critical structures for radiation injury owing to the ongoing neurogenesis in the subgranular zone of its dentate gyrus (16–25). Higher dose to the hippocampus has particularly been associated with impaired verbal memory and higher executive functions (20, 25). Thus, hippocampal sparing in brain radiotherapy planning has also recently gained significant attention.

The aim of this study is hence to confirm the implementation of nTMS motor information into treatment planning of linac-based stereotactic radiotherapy of motor-eloquent brain metastases, and to assess the feasibility of selective dose reduction to both the nTMS-based motor cortex and the hippocampi at the same time.

MATERIALS AND METHODS

Patients with motor-eloquent brain metastases undergoing nTMS-based surgical resection and adjuvant SRT between 07/2014 and 12/2018 were retrospectively analyzed. Metastases were regarded as motor-eloquent when infiltration of the precentral gyrus and/or pyramidal tract was presumed, or if the precentral gyrus and adjacent sulci could not be distinguished due to neuroanatomical distortion.

nTMS Mapping and Import Into the Radiotherapy Treatment Planning System

Patients received pre-operative magnetic resonance imaging (MRI) on a 1.5 T or 3 T scanner (Magnetom Symphony-TIM 1.5 T, Magnetom Skyra 3.0 T, Siemens, Erlangen, Germany) with contrast-enhanced T1-weighted MPRage in the axial direction (repetition time TR = 0.9 ms, echo time TE = 3.52 ms, flip-angle 15°, slice thickness 1 mm), on which dataset navigated transcranial magnetic stimulation was performed. The nTMS motor mapping was carried out using the Nexstim NBS system 4.3 (Nexstim Oy, Helsinki, Finlany) as previously described (5, 26, 27). In brief, the patients were sitting reclining in a chair with open eyes with surface electromyography electrodes attached to the muscles used for mapping (m. first dorsal interosseus, abductor pollicis brevis, abductor digiti minimi). The presumed location of the hand knob was used as a starting point, then varying the coil location and orientation to determine the resting motor threshold (RMT), defined as the lowest stimulus intensity which will elicit a 50 μV peak-to-peak amplitude motor evoked potential in five out of ten stimulations. The hand area was then mapped using 110% of the RMT and 0.25 Hz, holding the coil perpendicular to the precentral gyrus. Where possible, the lower extremity was mapped as delineated by the anterior tibial and plantar muscles, using 130% RMT intensity and a coil orientation perpendicular to the midline/falx. However, since lower extremity mapping was not available for all patients in this study collective, we only included patients who suffered from a motor-eloquent lesion where imaging predominantly appeared to demonstrate jeopardy of the upper extremity/hand area. Consequently, retrospective dose planning was carried out only for sparing of the upper extremity motor area.

In all cases the nTMS motor maps for the upper limb (i.e. hand area) were exported as an additional secondary dataset into the original radiotherapy treatment plan in the Philips Pinnacle treatment planning system (TPS) V16.2 for each patient. The secondary image was rigidly co-registered to the primary data set

(planning computed tomography (CT)) and planning MRI (acquired post-operatively in both T1 MPRage and T2 flair weighting) based on a mutual information algorithm and then manually shifted until optimal correspondence was achieved. Correspondence was verified independently by two radiation physicists and/or radiation oncologists. The original clinical target volume (CTV), planning target volume (PTV) and organs at risk (OAR: lenses, bulbi, optic nerves, chiasm, cochleae, brainstem) for brain irradiation as defined on the planning-CT and planning-MRI were re-checked and the additional organs at risk (OAR's) were contoured (i.e. nTMS-based motor cortex, basal ganglia, thalamus, hippocampus) based on the T1 weighted planning MRI sequences according to (28, 29). Each hippocampus was expanded by 5 mm into all directions to create the "hippocampus avoidance zone" for plan optimization.

Treatment Planning

For the original plans, different radiotherapy techniques were used: static beams with 3D-conformal radiotherapy (3D-CRT), intensity-modulated radiotherapy (IMRT) or non-coplanar arcs (30); 6 MV or flattening-filter-free 7 MV photons were used (31, 32).

For each metastasis, two re-optimized treatment plans were created in addition to the original clinically treated plan ("original"). The "motor" plan spared the hand motor areas delineated by nTMS. The "motor & hipp" plan aimed to reduce the dose to the nTMS-based motor cortex and the hippocampi. If the plan was originally planned by IMRT or by 3D-CRT, the same beam arrangements were used for the re-optimization; if the original plan used conformal non-coplanar arcs, a new plan was established by IMRT planning with between 8 and 13 beams. The maximum number of segments allowed was 35. The optimization objective for the motor cortex was to lower the maximum as well as the mean dose as much as possible without reducing the coverage of the PTV. Regarding the hippocampi, the optimization objectives were iteratively reduced to lower the maximum and the mean dose as much as possible without reducing the coverage of the PTV or burden the motor cortex again.

Optimization was performed using direct machine parameter optimization (DMPO) on a 0.2 cm dose grid; the final dose distributions were calculated using a collapsed cone (CC) convolution algorithm. All plans were revised by an experienced radiation oncologist and were in agreement with the general guidelines of the DEGRO Working Group on SRS for clinical stereotactic treatment (33) and the dose limits for sensitive brain structures based on the criteria of the Quantitative Analysis of Normal Tissue Effects in the Clinic (QUANTEC, 34).

Plan Evaluation

To evaluate plan differences, several measures of quality are considered.

The Paddick conformity index (CI) (34–36)

$$CI = OR \cdot UR = \frac{TV_{PIV}^2}{PIV \cdot TV}$$

is the product of the Paddick overdose ratio (OR) and underdose ratio (UR).

The overdose ratio

$$OR = \frac{TV_{PIV}}{PIV}$$

estimates the ratio of the PTV volume inside the prescribed 80 % isodose (TV_{PIV}) to the total volume encompassing the 80% isodose (PIV = $V_{80\ \%}$). This relates the covered PTV volume to the total volume irradiated with the prescribed encompassing dose.

The underdose ratio

$$UR = \frac{TV_{PIV}}{TV}$$

estimates the ratio of the PTV volume inside the 80 % isodose (TV_{PIV}) to the PTV volume (TV). This relates the covered PTV volume to the total PTV volume.

The homogeneity index (HI) (34–36)

$$HI = \frac{PTV_{1\,\%} - PTV_{99\,\%}}{PTV_{mean}}$$

measures the PTV homogeneity by considering $PTV_{1\%}$ as a measure of the maximum and $PTV_{99\%}$ as a measure of the minimum dose in the PTV.

The gradient index (GI)

$$GI = \frac{V_{40\,\%}}{PIV}$$

indicates the steepness of dose fall-off by comparing the volume of the prescription encompassing isodose to the volume (80%) of half this dose ($V_{40\%}$).

Two important values are $V_{12\ Gy}$ and $V_{10\ Gy}$ as well as their relative value to the total brain volume, as they correlate with the risk for necrosis in the case of stereotactic radiosurgery (37).

Besides these plan quality parameters, the doses in the critical sensitive brain structures based on the QUANTEC recommendations (38) as well as the PTV are determined. For the PTV, $D_{01\ \%}$ is given as a measure of the relative maximum; it is considered relative to the prescription dose in target point to estimate the amount of overdosage. $D_{99\%}$ of the PTV is considered as a measure of the relative mimimum PTV dose, it is considered relative to the prescribed encompassing dose of 80% to estimate the amount of underdosage.

For the motor cortex, the intersections with the PTV, 90 %, 80 %, 70 %, 50 % and 20 % isodose are determined. Furthermore, $D_{01\%}$ as a measure for the maximum dose and the mean dose are evaluated for the motor cortex and hippocampus as well as the other OARs.

Statistical Analyses

Dose-volume histogram (DVH) values were exported by an in-house Pinnacle script. Each OAR as well as the motor cortex and the PTV were saved in a CSV (comma separated variables) table. The reorganization into one table for each OAR and all calculations were performed with MATLAB R2019b. A normal

distribution could not be presumed, so Wilcoxon's signed-rank test for paired data was used. A 5 % level of significance was applied. For multiple comparisons (three scenarios), a Bonferroni correction was applied, in which p values below 0.0167 were considered statistically significant.

RESULTS

A total of 52 patients were identified. Of these, 24 patients received stereotactic radiation therapy at this department. The remaining patients either received a different radiotherapy regimen or received radiotherapy elsewhere. For all but one patient, the 80% isodose of the prescribed maximum dose in the isocentre was required to encompass the PTV. One patient received a different fractionation with the 95% isodose level surrounding the target volume and was therefore excluded from the analysis. Another patient received irradiation for three neighboring target volumes which were jointly optimized – this patient was also excluded, since re-optimization would have involved all three target volumes with different prescriptions and isocenters. Treatment details for the remaining 22 patients included in the analysis are given in **Table 1**.

For all 22 patients, the "motor" and "motor & hipp" treatment plans were considered acceptable for treatment. An example of the resulting isodose distributions is shown in **Figure 1**. Metrics for plan quality and dose to organs at risk are given in **Table 2**.

TABLE 1 | Patient characteristics.

Number of patients/cases	22/23
Age (average, range) [years]	65.1 (45–86)
Sex (female/male)	11/11 (50.0/50.0%)
Location (pre-/postcentral)	15/8 (65.2%/34.7%)
Paresis preoperatively	15 (68.2%)
Ø BMRC rank preoperatively	4.2 ± 0.7 (3–5)
Paresis post-operative day 7	12 (54.5%)
Resolved	3 (20.0% of 15)
Improved (but not resolved)	8 (53.3% of 15)
Unchanged	12 (54.5% of 22)
Deteriorate (new or worse)	0 (0%)
BMRC rank post-operative day 7	4.4 ± 0.6 (3–5)
Paresis post-operative day 60	4 (18.2%)
Resolved	11 (73.3% of 15)
Improved (but not resolved)	2 (13.3% of 15)
Unchanged	10 (45.5% of 22)
Deteriorate (new or worse)	0 (0%)
BMRC rank post-operative day 60	4.8 (4–5)
CTV/GTV volume (mean, range) [cm³]	9.5 ± 10.3 (0.6–36.5)
PTV volume (mean, range) [cm³]	16.4 ± 16.0 (2.1–56.7)
Prescription to the isocenter	
1 x 2,500 cGy	2 (8.7%)
1 x 2,250 cGy	3 (13.0%)
1 x 1,800 cGy	1 (4.3%)
3 x 1,125 cGy	6 (26.1%)
5 x 625 cGy	11 (47.8%)
Radiotherapy technique	
IMRT (7–21 beams)	11 (47.8%)
Conformal arcs (7–9 arcs)	6 (26.1%)
static beams 3D-CRT (7-20)	6 (26.1%)
Motor cortex inside PTV	9 (39.1%)
If yes, percent of motor cortex outside PTV	90.1 ± 6.6 (76.9–98.6)
If no, minimum distance (mm)	8.3 ± 8.5 (0–31.5)

CTV, clinical target volume; GTV, gross tumor volume; GTV were used in case of single-fraction treatment (stereotactic radiosurgery, SRS), whereas CTV were used for fractionated stereotactic radiation therapy SRT; in both cases, expansion was performed to create the PTV, planning target volume; IMRT, intensity-modulated radiation therapy; 3D-CRT, 3 dimensional conformal radiotherapy; BMRC, British Medical Research Council.

PTV and Organs at Risk in the Re-Optimized Plans

No significant differences between the "original", "motor" and "motor & hipp" plans were observed for the coverage of the planning target volume as assessed by the conformity index, PTV minimum and maximum, and overdose ratio (**Figure 2**). There was a small, but statistically significant improvement in the underdose ratios of the "motor" and "motor & hipp" plans when compared with the original plans (but not with each other). The gradient index assessing dose fall-off outside the PTV was slightly worse in the newly-optimized plans, however, this did not affect the clinical acceptability of the plans.

All organs at risk could be well protected in both the "motor" and "motor & hipp" plans. The volume of the brain receiving a dose of 10 Gy or 12 Gy was slightly increased in the "motor & hipp" plans relative to the original and "motor" plans by ca. 3–4 cm³. However, this parameter is only relevant for stereotactic radiosurgery, i.e. very high single dose fractionation regimes. If we consider only patients receiving stereotactic radiosurgery (five cases), the three planning scenarios do not exhibit a significant difference in the volume of the 12 Gy isodose inside healthy brain, although there appears to be a trend toward somewhat increased volume (9.2 ± 2.8 cm³ and 9.5 ± 2.4 cm³ in the "motor" and "motor & hipp" plans, respectively, compared with 5.9 ± 1.9 cm³ in the original plan, p = 0.0625 and p = 0.3125, respectively). Simultaneously, sparing of the hippocampus resulted in reduced dose to the brainstem, thalami and basal ganglia. Some variations in OAR sparing were observed between the planning scenarios, however, all these organs received very little dose as compared with the planning objectives remained far below the clinically acceptable limits.

Sparing of the Motor Cortex

Sparing of the motor cortex could significantly be improved by both scenarios with nTMS information included, with mean dose to the motor cortex reduced from 9.66 ± 5.97 Gy (original) to 6.32 ± 3.60 Gy (motor) and 6.49 ± 3.78 Gy (motor & hipp), respectively ($p<0.001$ for both re-optimized plans vs. "original"). Regarding the spatial relationship of the motor cortex with the isodose levels (**Figure 3**), a reduction of overlap with all isodoses from 20 to 90% of the prescribed dose was observed relative to the original plans; however, this difference only reached statistical significance for the 70% isodose, becoming more pronounced for the lower isodose levels. The volume of the nTMS-derived motor map covered inside the 70% isodose could hence be reduced from an average of 7.4% (max 30.5%) to 4.8% (max 21.9%) (p = 0.015). A larger reduction was observed for the

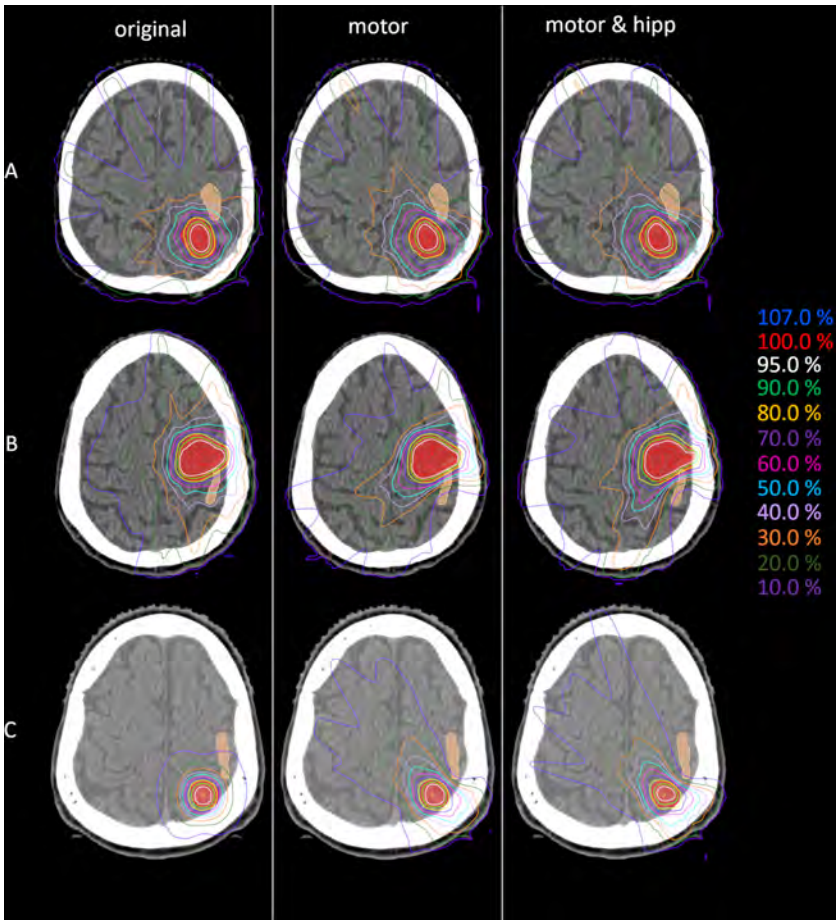

FIGURE 1 | Example dose distributions for the original (left), motor (middle) and motor&hipp (right) plans for three different patients and planning scenarios. **(A)** patient treated originally by static beams, **(B)** patient treated originally with intensity-modulated radiotherapy (IMRT), **(C)** patient treated originally with non-coplanar arcs. The planning target volume (PTV) is delineated by the red filled contour, the nTMS-based motor cortex in skin color.

volume contained within the 50% isodose (22.3% vs. 10.1%, $p = 0.003$) and 20% isodose (61.8% vs. 34.7%, $p < 0.001$).

Since the patients in the collective received the original radiation treatment using three different technical approaches (3D-CRT, IMRT, non-coplanar arcs), a separate analysis of the dose to the motor cortex is performed for planning techniques relying on static beams with the original geometry ("beams" plans including 3D-CRT and IMRT) and non-coplanar "arcs" plans. Dose to the motor cortex in the "motor" and "motor & hipp" plans is compared with the original plans separately for the "beams" and "arcs" techniques in **Figure 4**. A considerably greater improvement could be attained by re-optimizing the "beams" plans than the "arcs" plans. This can also been visually confirmed in the isodose distribution (**Figure 1**). In all cases, the re-optimized plans show a more asymmetric behavior than the original plans since the isodoses are deformed so as to avoid the nTMS volume. While the prescription isodoses still encompass the PTV at least as well as in the original plan, the intermediate isodoses show a relatively strong asymmetry, where the gradient toward the motor cortex is much steeper than in all other directions. In particular, the original "arcs" plans already had a very steep gradient from the combination of many non-coplanar arcs, which cannot be achieved by a relatively simple co-planar IMRT beam configuration. Therefore, this planning scenario suffers from a relatively strong change in gradient (also reflected in GI), while achieving relatively little additional sparing of the motor cortex.

For the "beams" plans, a strong positive correlation (Pearson correlation coefficient $r = 0.903$, $p < 0.001$) is observed between the distance PTV to nTMS-derived motor map and the relative change in nTMS mean dose, i.e., a greater improvement in nTMS mean dose is obtained the closer the motor cortex is located to the PTV.

Both the absolute dose reduction to the nTMS and its clinical relevance depend on the fractionation scheme. **Figure 5** therefore shows the absolute difference in nTMS mean dose achieved for different fractionation regimes (one, three, or five fractions as detailed in **Table 1**). The amount of sparing

TABLE 2 | Plan evaluation using metrics for plan quality, planning target volume (PTV) coverage, and dose to organs at risk.

	Original	Motor	Motor & hipp	p 1-2	p 1-3	p 2-3
CI	0.767 ± 0.106 (0.524–0.907)	0.789 ± 0.087 (0.609–0.932)	0.784 ± 0.089 (0.586–0.908)	0.287	0.523	0.503
OR	0.801 ± 0.115 (0.524–0.932)	0.797 ± 0.095 (0.610–0.946)	0.792 ± 0.095 (0.587–0.938)	0.761	0.484	0.523
UR	0.959 ± 0.047 (0.843–1.000)	0.991 ± 0.021 (0.901–1.000)	0.991 ± 0.020 (0.903–1.000)	**0.001**	**0.001**	0.689
HI	1.276 ± 1.894 (0.198–8.381)	1.512 ± 1.517 (0.171–4.306)	1.439 ± 1.450 (0.178–4.024)	0.465	0.465	0.055
GI	3.775 ± 0.897 (2.555–6.700)	4.129 ± 1.046 (2.990–7.314)	4.357 ± 1.122 (3.044–7.252)	0.024	**0.003**	**0.003**
PTV						
$D_{01\%,rel\ [\%]}$	102.43 ± 5.84 (99.81–128.64)	102.57 ± 1.65 (99.76–104.70)	102.59 ± 1.55 (99.76–104.80)	**0.014**	0.030	0.858
$D_{99\%,rel\ [\%]}$	97.61 ± 5.92 (83.72–109.72)	103.20 ± 4.57 (86.16–108.60)	102.72 ± 4.53 (85.48–108.64)	**0.001**	**0.001**	0.273
nTMS motor map						
$D_{01\%}$ [Gy]	18.762 ± 9.734 (1.82–33.24)	16.895 ± 10.198 (1.68–34.23)	16.895 ± 10.148 (1.11–33.33)	**0.002**	**0.002**	0.661
D_{mean} [Gy]	9.659 ± 5.972 (0.906–19.559)	6.319 ± 3.596 (0.348–15.008)	6.493 ± 3.784 (0.294–15.800)	**<0.001**	**<0.001**	0.162
Hippocampus ipsilateral						
$D_{01\%}$ [Gy]	2.493 ± 1.870 (0.08–7.36)	3.426 ± 2.468 (0.09–9.67)	1.775 ± 1.440 (0.09–4.99)	**0.003**	**0.003**	**<0.001**
D_{mean} [Gy]	1.320 ± 1.074 (0.039–3.458)	1.818 ± 1.718 (0.051–6.595)	1.005 ± 0.918 (0.051–2.747)	**0.002**	**0.006**	**<0.001**
Hippocampus contralateral						
$D_{01\%}$ [Gy]	0.723 ± 1.106 (0.05–4.84)	0.736 ± 1.148 (0.04–4.63)	0.562 ± 0.801 (0.04–3.04)	0.402	0.554	0.302
D_{mean} [Gy]	0.323 ± 0.396 (0.021–1.439)	0.238 ± 0.314 (0.022–1.462)	0.204 ± 0.207 (0.023–0.744)	0.648	0.648	0.951
Hippocampus avoidance zone ipsilateral						
$D_{01\%}$ [Gy]	3.027 ± 2.775 (0.10–13.15)	4.316 ± 3.186 (0.11–14.21)	2.433 ± 2.191 (0.11–10.06)	**<0.001**	0.019	**<0.001**
D_{mean} [Gy]	1.338 ± 1.078 (0.042–3.665)	1.794 ± 1.597 (0.053–5.700)	1.044 ± 0.944 (0.053–3.183)	**0.002**	**0.006**	**<0.001**
Brain without PTV						
D_{12Gy} [cm^3]	41.37 ± 34.88 (3.72–110.91)	40.15 ± 29.21 (6.52–111.55)	44.28 ± 34.02 (7.05–120.41)	0.378	**0.011**	**<0.001**
D_{10Gy} [cm^3]	57.04 ± 47.08 (6.06–157.31)	56.04 ± 39.32 (9.71–141.69)	61.95 ± 46.57 (10.76–177.80)	0.394	**0.008**	**<0.001**
$D_{01\%}$ [Gy]	15.920 ± 7.148 (1.11–25.31)	16.472 ± 5.867 (3.46–24.24)	16.806 ± 5.928 (3.60– 24.35)	0.191	0.026	**0.004**
D_{mean} [Gy]	2.000 ± 1.176 (0.543–4.130)	2.140 ± 1.093 (0.749–4.395)	2.173 ± 1.112 (0.750–4.327)	0.024	**0.004**	0.447
Brainstem						
$D_{01\%}$ [Gy]	1.489 ± 1.300 (0.06–5.20)	2.088 ± 1.843 (0.08–5.99)	1.254 ± 1.120 (0.06–4.67)	0.029	0.191	**0.001**
D_{mean} [Gy]	0.483 ± 0.480 (0.029–1.782)	0.543 ± 0.644 (0.035–2.604)	0.366 ± 0.350 (0.030–1.442)	0.078	0.378	**<0.001**
Thalamus ipsilateral						
$D_{01\%}$ [Gy]	3.482 ± 3.271 (0.14–14.07)	4.472 ± 3.565 (0.16–11.43)	3.234 ± 2.825 (0.12–10.02)	**0.010**	0.280	**0.001**
D_{mean} [Gy]	1.730 ± 1.628 (0.079–6.643)	2.185 ± 2.130 (0.086–7.771)	1.610 ± 1.593 (0.077–6.296)	0.033	0.033	**0.001**
Basal ganglia ipsilateral						
$D_{01\%}$ [Gy]	6.073 ± 7.368 (0.17–26.79)	6.813 ± 7.374 (0.17–27.00)	6.733 ± 7.481 (0.15–27.01)	0.128	0.161	0.733
D_{mean} [Gy]	1.963 ± 2.131 (0.064–8.024)	2.413 ± 2.795 (0.077–9.065)	2.315 ± 2.683 (0.066–8.587)	0.144	0.201	0.236

Average ± standard deviation (min-max). After Bonferroni correction, p values below 0.017 were considered statistically significant and are marked in bold. Lenses, cochleae, bulbi, optic nerves, chiasma, contralateral hippocampus avoidance zone, contralateral thalamus and basal ganglia are not listed. For these organs, the dose was far below the clinical acceptable limits, most comparisons did not show statistically significant differences and no clear tendencies in improved sparing could be observed. CI, conformity index; OR, overdose ratio; UR, underdose ratio; HI, homogeneity index; GI, gradient index.

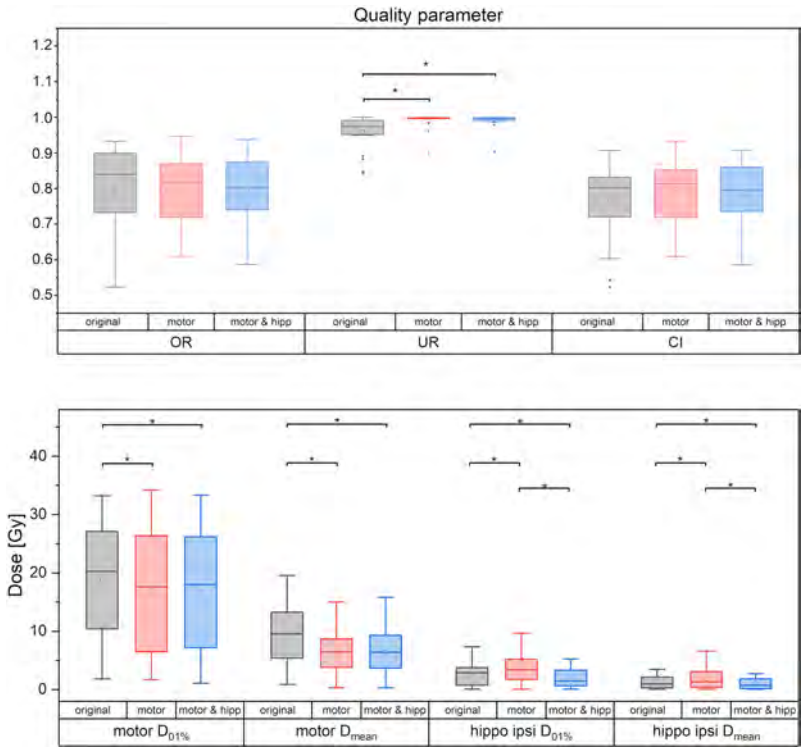

FIGURE 2 | Quality measures of planning target volume (PTV) coverage (upper panel) and dose to motor cortex and ipsilateral hippocampus. Statistically significant differences are denoted by asterisk.

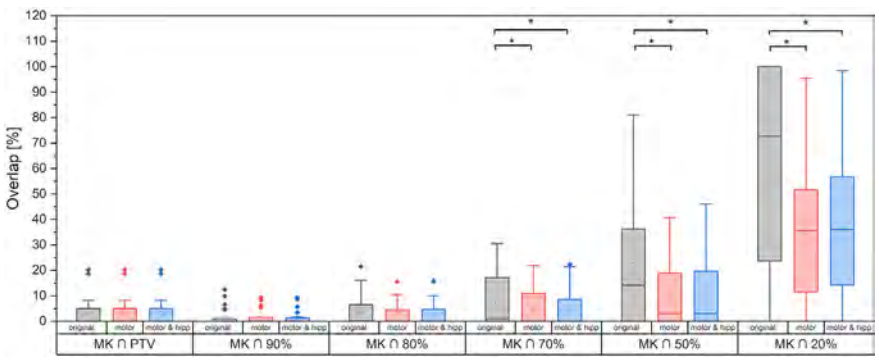

FIGURE 3 | Motor cortex volume included inside planning target volume (PTV) and different relative isodose lines. Statistically significant differences are denoted by asterisk.

achievable was higher in absolute dose for the more fractionated schedules. The single-fraction regimes included in our collective comprised three "arcs" plans. We have already seen that the "arcs" plans provided least improvement in nTMS dose by reoptimization, which will also influence the relatively low sparing achieved by the single-fraction regimes. Still, an average dose reduction (nTMS mean dose) of 0.88 Gy (both for "motor" and "motor & hipp") plans could be achieved for this sub-collective, and for two patients around 2 Gy decrease were reached.

Sparing of the Hippocampus

In the "motor" plans without hippocampus sparing, the dose to the ipsilateral hippocampus was increased over the original plan (in which also no attempt at hippocampus sparing was made): maximum dose 3.43 ± 2.47 Gy vs. 2.49 ± 1.87 Gy, $p = 0.003$; mean dose 1.82 ± 1.72 Gy vs. 1.32 ± 1.07 Gy, $p = 0.002$. After reoptimization in the "motor & hipp" plans, hippocampus ipsilateral mean and maximum dose (**Figure 2**) were significantly lower, even when compared with the original plan (maximum dose 1.78 ± 1.44 Gy in "motor & hipp" vs. 2.49 ± 1.87 Gy in "original",

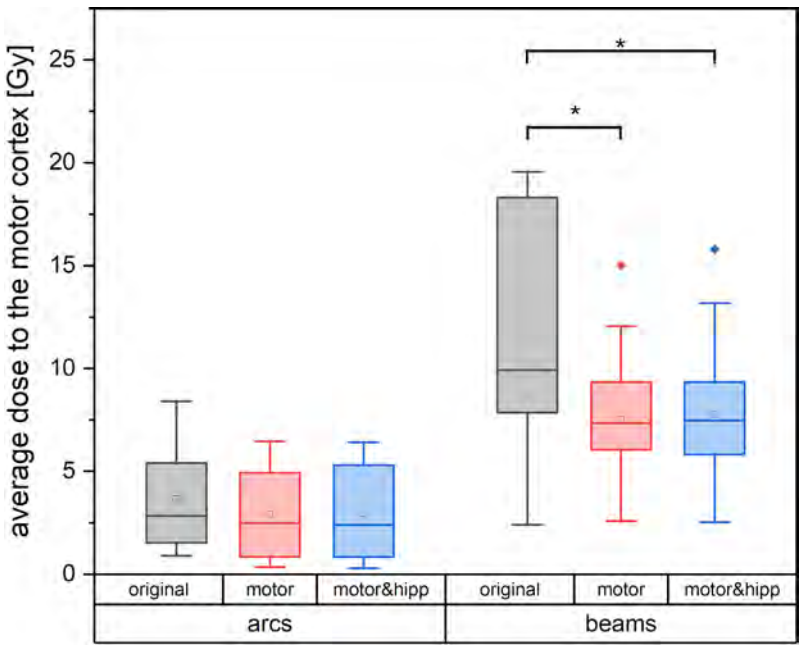

FIGURE 4 | Average dose to the motor cortex for plans using non-coplanar conformal arcs vs. plans with static beams or intensity-modulated radiotherapy (IMRT). Statistically significant differences are denoted by asterisk.

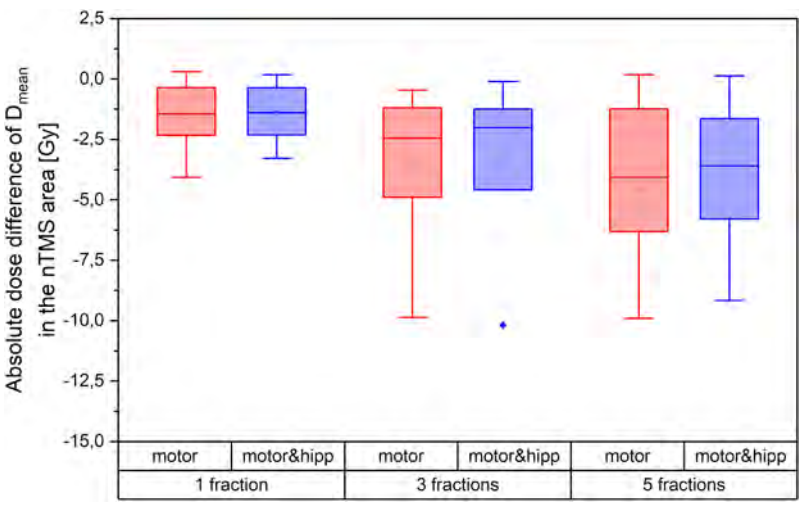

FIGURE 5 | Absolute dose sparing in the navigated transcranial magnetic stimulation (nTMS) area (mean dose) achieved by the reoptimized plans as a function of fractionation regime.

p = 0.003; mean dose 1.01 ± 0.92 Gy in "motor & hipp" vs. 1.32 ± 1.07 Gy in "original", p = 0.006). Also, hippocampus contralateral mean and maximum dose could be reduced by re-optimization, though not reaching statistical significance (max dose 0.56 ± 0.80 Gy in "motor & hipp" vs. 0.72 ± 1.11 Gy in "original"; mean dose 0.20 ± 0.21 Gy in "motor & hipp" vs. 0.32 ± 0.40 Gy in "original").

DISCUSSION

The study demonstrates the feasibility of selective dose reduction to both the nTMS-identified motor area and hippocampus for a comparison of treatment 69 plans, including three different planning approaches (static 3D-CRT, IMRT, non-coplanar

conformal arcs). Even though this introduces some heterogeneity in the study collective, this wide selection of planning methods is representative of routine radiotherapy practice and differences could actually be identified in the amount of sparing achieved depending on the original planning technique.

The presented study cohort adds to hitherto only two reports investigating the implementation of nTMS into linac-based radiotherapy planning (12, 13), whereas the remaining studies investigated nTMS maps for CyberKnife (8, 9) or GammaKnife (10, 11) stereotactic radiosurgery. Linac-based radiotherapy, CyberKnife and GamaKnife differ in technical implementation, planning and dosimetry. As CyberKnife and GammaKnife availability is restricted to a small selection of specialized centers, whereas linear accelerators with stereotactic capability are much more wide-spread, an evaluation of motor cortex and hippocampus sparing achievable with linac stereotactic radiotherapy will be useful for a wider range of patients and treatment centers.

Diehl et al. (12) presented a planning study for 30 patients with high-grade gliomas treated by volumetric modulated arc therapy (VMAT) in a simultaneously integrated boost (SiB) concept. By including dose constraints to the nTMS motor maps (only areas outside the planning target volume), they could achieve a dose reduction of 12.8% (4.6 Gy), without compromising PTV coverage. In a collective more similar to the herein presented cohort, Schwendner et al. (13) presented a re-optimization of VMAT plans for a collective of 30 patients with supratentorial brain metastases. Again, the nTMS motor map not included in the PTV was spared in the re-optimized plans, resulting in a dose reduction of ca. 4.1 Gy (18.1%). Our study presents a similar collective of patients with brain metastases, but with a wider variation in original planning techniques, and with a larger range of distances of the motor cortex from the PTV. In line with those previous reports motor cortex sparing by about 3 Gy in mean dose (ca. 30%), with best results obtained for the static 3D-CRT and IMRT treatment plans was observed. Additionally, a correlation of dose reduction with proximity to the motor cortex was recognized.

A considerably greater improvement could be attained by re-optimizing the static 3D-CRT and IMRT plans than the plans using non-conformal arcs. However, this does not imply that non-conformal arcs should generally be the preferred planning scenario, since this is only applicable to relatively spherical and small target volumes. The dose to the motor cortex in the "beams" plans might be higher than in the "arcs" plans not primarily because of a presumably inferior planning technique, but possibly because a more complex PTV shape or volume, which might have been associated with a higher motor cortex dose and precluded the use of arcs. Yet, in the "arcs" plans, a small improvement could still be achieved by re-planning.

For the first time, the hippocampus is included as an additional organ at risk in the attempt to spare the motor map. Reducing radiation dose to the hippocampus and nTMS based motor map was feasible simultaneously without compromising the PTV or other organs at risk. Despite the inherent low dose to the ipsilateral hippocampi in the original plans ($D_{01\%}$ 2.49 ± 1.87 Gy, mean dose 1.32 ± 1.07 Gy), a further dose reduction by 23%–28% could be achieved ($D_{01\%}$ 1.78 ± 1.44 Gy, mean dose 1.01 ± 0.92 Gy). In particular, in the plans re-optimized for motorcortex sparing without hippocampus inclusion, the dose to the ipsilateral hippocampus was increased, so that the optimization of hippocampus dose reduced the dose from the "motor" plans by over 40%. Singular optimization of the motor cortex resulted in increased doses to the ipsilateral hippocampus avoidance zone and thalamus. A similar trend (without reaching statistical significance) could be found for the brainstem and ipsilateral basal ganglia. Although these changes would not have resulted in clinical rejection of the plans – partly because these structures are not routinely contoured and dosimetrically evaluated in clinical plans and partly because no clinically evaluated dose limits are yet available for these structures – the inclusion of hippocampus protection at the optimization stage could totally reverse this effect without loss of motor cortex sparing.

The external validity of the study is limited since nTMS mappings were not uniformly performed for the entire primary cortex. In a subset of included patients, lesion-specific mapping was performed to outline peri-lesional and critical motor areas to facilitate surgery. To increase internal validity, we included only nTMS-motor areas of the upper extremity into the optimization assessment. The omission of these structures means that for some patients at least the anatomic leg or face areas of the motor cortex may have received higher doses, since functional leg or face areas were not optimized in the plans. For future studies, comprehensive nTMS mapping of bilateral primary motor cortices including nTMS-based tractography is required to allow evaluation to which extent specific motor areas can be spared and whether sparing causes increased doses to other critical areas. Few authors have hitherto presented treatment plans with dose optimization for white-matter tracts (8, 9), and the clinical significance of this improvement is yet unclear.

Clinical Significance of the Dosimetric Improvements

The clinical significance of these dose-optimized plans for motor function, cognitive function and quality of life yet remains to be elucidated. The risk of brain radionecrosis in single-session radiosurgery is correlated with the volume receiving doses of 10 Gy and 12 Gy, and motor deficits are among the complications observed (39). However, a dose threshold has not yet been definitely established for functional impairment of the motor cortex. For SRS of the corticospinal tract, Maruyama et al. (40) proposed a 5% risk of motor complication when the volume receiving 20 and 25 Gy exceeded 58 mm^3 and 21 mm^2, respectively. Based on a neuroanatomical target theory for a patient collective treated by whole-brain radiotherapy with boost in conventional fractionation (1.8–2Gy/fraction), Pfeiffer et al. (41) proposed that cognitive outcomes were affected by the volume of the left hippocampus receiving 10 Gy and by the volume of the left precentral gyrus receiving 40 Gy, among a range of other regions.

For the hippocampus, recent radiotherapy optimization studies have aimed at reducing maximum dose to 16–17 Gy and minimum dose to 9 Gy in hippocampus-sparing whole-

brain radiotherapy (14, 25). However, while a significant correlation was observed between mean dose to the left hippocampus and cognitive deterioration (25) as well as hippocampal volume reduction (41), no dose cut-off was defined in these studies. Hippocampus volume loss was observed to be significant one year after high-dose radiotherapy (> 40 Gy), but not after low-dose radiotherapy (< 10 Gy) by Seibert et al. (42). The normal-tissue complication probability (NTCP) model proposed for the hippocampus by Gondi et al. (17) suggests that an EQD_2 dose (dose equivalent to 2 Gy fractions) of greater than 7.3 Gy to 40% of the bilateral hippocampi may be associated with memory impairment as assessed by list-learning delayed verbal recall; however, this model could not be confirmed for low-grade glioma patients in the EORTC 22033 clinical trial (21). In the Hopkins Verbal Learning Test-Revised Delayed Recall, Ma et al. (19) reported 20% probability of decline for $D_{100\%}$ hippocampus doses above 10.9 Gy and 50% probability for 59.3 Gy. Taken together, a relatively steep gradient appears to exist in this dose range, making any attempts of hippocampus sparing potentially relevant for cognitive performance.

In the present patient collective, doses to the hippocampus were already low in the original plans due to the location of the brain metastases near motor-eloquent cortical areas. However, even low doses to the hippocampus may influence neurogenesis and differentiation of the dendritic arbor, as has been shown in animal studies for single-fractions of 1 Gy (16) and fractionated low dose irradiation [5 to 20 fractions of 0.1 Gy (43)]. Although a reduction in hippocampus dose as attained in our study has not yet been proven to result in an observable change in clinical outcome, with no apparent disadvantages these optimized plans call for further and broader exploration. Prospective studies are required to assess whether dose sparing to the motor cortex and hippocampus can contribute to improved motor and/or cognitive outcomes and higher health-related quality of life.

In contrast to radiotherapy, surgical treatment of motor-eloquent lesions does not take brain areas into account that are deemed uncritical for the procedure or even contralateral. For radiotherapy, however, this information is essential due to the larger expansion of intermediate- and low-dose areas. From the neurosurgical perspective, uncritical areas may not be mapped or tractography not be performed unless explicitly requested for. The quality of the localization would be improved if post-operative mapping was performed at the same time with the planning MRI, so that a more precise fusion of the images unbiased by changes in tumor or edema distribution would become possible. On this basis, a clinical evaluation of the motor and cognitive performance could be correlated with the dose to the motor cortex and corticospinal tract, which will be a prerequisite for exploring dose-effect relationships. Furthermore, the distance of these structures from the high-dose volume may serve for risk stratification of radiation-induced effects. Rosenstock et al. (44). and Sollmann et al. (45). proposed nTMS-based risk-stratification models for neurosurgery. They correlated the proximity of motor-eloquent brain lesions to the motor cortex and corticospinal tract with the risk of motor deterioration due to treatment. Furthermore, the RMT was also reported as a marker of increased hazard for post-operative deficit. Possibly, a similar observation can be established for radiotherapy.

While exploring these possibilities, we would like to emphasize the importance of including in the considerations a critical structure such as the hippocampus, which might even be less well protected when a new optimization objective such as motor cortex sparing is added to the planning process without adequate hippocampus constraints. On-going neurogenesis in this structure renders it particularly sensitive to radiation-induced damage, so care should be taken to reduce hippocampus dose if this is possible. As we could show, sparing of the motor cortex and hippocampus is not mutually exclusive. Rather, adequate coverage of the PTV can be reconciled with combined dose reduction to the nTMS-defined hand area and hippocampus at no detriment in plan quality.

CONCLUSIONS

Selective dose reduction to the motor cortex and hippocampus is feasible without compromising PTV coverage or other organs at risk. The inclusion of the nTMS-based information on the motor cortex into plan optimization allowed for about 30% dose reduction (approximately 3 Gy in mean dose). However, singular optimization of the motor cortex causes an increase in dose to the hippocampus, thalamus and brain stem, which can be prevented by including hippocampus dose as an additional planning objective. In these plans, a further dose reduction to the hippocampus along with the motor cortex can be achieved, resulting in increased overall protection of these functional cortical areas.

DATA AVAILABILITY STATEMENT

The raw data supporting the conclusions of this article will be made available by the authors, without undue reservation.

AUTHOR CONTRIBUTIONS

YD and PH designed the study concept. PH and JO recruited the patient. JO was responsible for the surgical treatment of the patients and CR for the radiotherapy. nTMS mapping was performed by PH. Patient datasets were retrieved from the data base and retrospectively revised by YD. Import into the planning system and rigid registration with the planning CT was performed by YD and MS. PM and YD contoured the organs at risk. MS created the re-optimized radiotherapy treatment plans and performed the plan evaluation and statistical analysis. PM and FN evaluated the treatment plans. YD wrote the manuscript. MS prepared the figures and tables. All authors were involved in the interpretation of the results. All authors contributed to the article and approved the submitted version.

REFERENCES

1. Frey D, Schilt S, Strack V, Zdunczyk A, Rösler J, Niraula B, et al. Navigated transcranial magnetic stimulation improves the treatment outcome in patients with brain tumors in motor eloquent locations. *Neuro Oncol* (2014) 16(10):1365–72. doi: 10.1093/neuonc/nou110
2. Krieg SM, Sabih J, Bulubasova L, Obermueller T, Negwer C, Janssen I, et al. Preoperative motor mapping by navigated transcranial magnetic brain stimulation improves outcome for motor eloquent lesions. *Neuro-Oncol* (2014) 16(9):1274–82. doi: 10.1093/neuonc/nou007
3. Krieg SM, Picht T, Sollmann N, Bährend I, Ringel F, Nagarajan SS, et al. Resection of Motor Eloquent Metastases Aided by Preoperative nTMS-Based Motor Maps – Comparison of Two Observational Cohorts. *Front Oncol* (2016) 6:261. doi: 10.3389/fonc.2016.00261
4. Raffa G, Scibilia A, Conti A, Ricciardo G, Rizzo V, Morelli A, et al. The role of navigated transcranial magnetic stimulation for surgery of motor-eloquent brain tumors: a systematic review and meta-analysis. *Clin Neurol Neurosurg* (2019) 180:7–17. doi: 10.1016/j.clineuro.2019.03.003
5. Hendrix P, Dzierma Y, Burkhardt BW, Simgen A, Wagenpfeil G, Griessenauer CJ, et al. Preoperative navigated transcranial magnetic stimulation improves gross total resection rates in patients with motor eloquent high-grade gliomas: A matched cohort study. *Neurosurgery* (2020) 0:1–10. doi: 10.1093/neuros/nyaa486
6. Park C-Z, Choi H-Y, Lee S-R, Roh TH, Seo M-R, Kim S-H. Neurological Change after Gamma Knife Radiosurgery for Brain Metastases Involving the Motor Cortex. *Brain Tum Res Treat* (2016) 4(2):111–5. doi: 10.14791/btrt.2016.4.2.111
7. Pfeiffer AM, Leyrer CM, Greene-Schloesser DM, Shing E, Kearns WT, Hinson WH, et al. Neuroanatomical target theory as a predictive model for radiation-induced cognitive decline. *Neurology* (2013) 80:747–53. doi: 10.1212/WNL.0b013e318283bb0a
8. Picht T, Schilt S, Frey D, Vajkoczy P, Kufeld M. Integration of navigated brain stimulation data into radiosurgical planning: potential benefits and dangers. *Acta Neurochir* (2014) 156:1125–33. doi: 10.1007/s00701-014-2079-8
9. Conti A, Pontoriero A, Ricciardi GK, Granata F, Vinci S, Angileri FF, et al. Integration of functional neuroimaging in CyberKnife radiosurgery: feasibility and dosimetric results. *Neurosurg Focus* (2013) 34(4):E5. doi: 10.3171/2013.2.FOCUS12414
10. Islam M, Cooray G, Benmakhlouf H, Hatiboglu M, Sinclair G. Integrating navigated transcranial magnetic stimulation motor mapping in hypofractionated and single-dose gamma knife radiosurgery: A two-patient case series and a review of literature. *Surg Neurol Int* (2020) 11(29):1–11. doi: 10.25259/SNI_406_2019
11. Tokarev AS, Rak VA, Sinkin MV, Evdokimova EL, Stepanov VN, Koynash GV, et al. Appliance of Navigated Transcranial Magnetic Stimulation in Radiosurgery of Brain Metastases. *J Clin Neurophysiol* (2020) 37(1):50–5. doi: 10.1097/WNP.0000000000000621
12. Diehl CD, Schwendner MJ, Sollmann N, Oechsner M, Meyer B, Combs SE, et al. Application of presurgical navigated transcranial magnetic stimulation motor mapping for adjuvant radiotherapy planning in patients with high-grade gliomas. *Radiother Oncol* (2019) 138:30–7. doi: 10.1016/j.radonc.2019.04.029
13. Schwendner MJ, Sollmann N, Diehl CD, Oechsner M, Meyer B, Krieg SM, et al. The Role of Navigated Transcranial Magnetic Stimulation Motor Mapping in Adjuvant Radiotherapy Planning in Patients With Supratentorial Brain Metastases. *Front Oncol* (2018) 8:424. doi: 10.3389/fonc.2018.00424
14. Brown PD, Jaeckle K, Ballmann KV, Farace E, Cerhan JH, Anderson K, et al. Effect of Radiosurgery Alone vs Radiosurgery with Whole Brain Radiation Therapy on Cognitive Function in Patients with 1 to 3 Brain Metastases – A Randomized Clinical Trial. *JAMA* (2016) 316(4):401–9. doi: 10.1001/jama.2016.9839
15. Chang EL, Wegel JS, Hess KR, Allen PK, Lang FF, Kornguth DG, et al. Neurocognition in patients with brain metastases treated with radiosurgery or radiosurgery plus whole-brain irradiation: a randomies controlled trial. *Lancet* (2009) 10:1037–44. doi: 10.1016/S1470-2045(09)70263-3
16. Parihar VK, Limoli CL. Cranial irradiation compromises neuronal architecture in the hippocampus. *PNAS* (2013) 110(31):12822–7. doi: 10.1073/pnas.1307301110
17. Gondi V, Hermann BP, Mehta MP, Tomé WA. Hippocampal Dosimetry Predicts Neurocognitive Function Impairment After Fractionated Stereotactic Radiotherapy for Benign or Low-Grade Adult Brain Tumors. *Int J Radiat Oncol Biol Phys* (2013) 85(2):348–54. doi: 10.1016/j.ijrobp.2012.11.031
18. Gondi V, Pugh SL, Tome WA, Caine C, Corn B, Kanner A, et al. Preservation of Memory With Conformal Avoidance of the Hippocampal neural Stem-Cell Compartment During Whole-Brain Radiotherapy for Brain Metastases (RTOG 0933): A Phase II Multi-Institutional Trial. *J Clin Onc* (2014) 32 (34):3810–6. doi: 10.1200/JCO.2014.57.2909
19. Ma TM, Grimm J, McIntyre R, Anderson-Keightly H, Kleinberg LR, Hales RK, et al. A prospective evaluation of hippocampal radiation dose volume effects and memory deficits following cranial irradiation. *Radiother Oncol* (2017) 125:234–40. doi: 10.1016/j.radonc.2017.09.035
20. Tsai P-F, Yang C-C, Chuang C-C, Huang T-Y, Wu Y-M, Pai P-C, et al. Hippocampal dosimetry correlates with the change in neurocognitive function after hippocampal sparing during whole brain radiotherapy: a prospective study. *Radiat Oncol* (2015) 10:253. doi: 10.1186/s13014-015-0562-x
21. Jaspers J, Mèndez Romero A, Hoogeman MS, van den Bent M, Wiggenraad RGJ, Taphoorn MJB, et al. Evaluation of the Hippocampal Normal Tissue Complication Model in a Prospective Cohort of Low Grade Glioma Patients – An Analysis Within the EORTC 22033 Clinical Trial. *Font Oncol* (2019) 9:991. doi: 10.3389/fonc.2019.00991
22. Birer SR, Olson AC, Adamson J, Hood R, Susen M, Kim G, et al. Hippocampal dose from stereotactic radiosurgery for 4 to 10 brain metastases: Risk factors, feasibility of dose reduction via re-optimization, and patient outcomes. *Med Dosim* (2017) 42(4):310–6. doi: 10.1016/j.meddos.2017.06.007
23. Okoukoni C, McTyre ER, Ayala Peacock DN, Pfeiffer AM, Strowd R, Cramer C, et al. Hippocampal dose volume histogram predicts Hopkins Verbal Learning Test scores after brain irradiation. *Adv Radiat Oncol* (2017) 2:624–9. doi: 10.1016/j.adro.2017.08.013
24. Brown PD, Gondy V, Pugh S, Tome WA, Wefel JS, Armstrong TS, et al. Hippocampal Avoidance During Whole-Brain Radiotherapy Plus Memantine for Patients With Brain Metastases: Phase III Trial NRG Oncology CC001. *J Clin Oncol* (2020) 38(10):1019. doi: 10.1200/JCO.19.02767
25. Kim KS, Wee CW, Seok J-Y, Hong JW, Chung J-B, Eom K-Y, et al. Hippocampus-sparing radiotherapy using volumetric modulated arc therapy (VMAT) to the primary brain tumor: the result of dosimetric study and neurocognitive function assessment. *Radiat Oncol* (2018) 13:29. doi: 10.1186/s13014-018-0975-4
26. Hendrix P, Senger S, Griessenauer CJ, Simgen A, Schwerdtfeger K, Oertel J. Preoperative Navigated Transcranial Magnetic Stimulation in Patients with Motor Eloquent Lesions with Emphasis on Metastasis. *Clin Anat* (2016) 29:925–31. doi: 10.1002/ca.22765
27. Hendrix P, Senger S, Griessenauer CJ, Simgen A, Linsler S, Oertel J. Preoperative navigated transcranial magnetic stimulation and tractography in transparietal approach to the trigone of the lateral ventricle. *J Clin Neurosci* (2017) 41:154–61. doi: 10.1016/j.jocn.2017.02.029
28. Eekers DBP, Ven L, Roelofs E, Postma A, Alapetite C, NG B, et al. The EPTN consensus-based atlas for CT- and MR-based contouring in neuro-oncology, 2018. *Radiother Oncol* 128:37–43. doi: 10.1016/j.radonc.2017.12.013
29. Scoccianti S, Detti B, Gadda D, Greto D, Furfaro I, Fiammetta M, et al. Organs at risk in the brain and their dose-constraints in adults and in children: A radiation oncologist's guide for delineation in everyday practice. *Radiother Oncol* (2015) 2015:114:230–238. doi: 10.1016/j.radonc.2015.01.016
30. Dzierma Y, Nuesken FG, Palm J, Licht NP, Ruebe C. Planning study and dose measurements of intracranial stereotactic radiation surgery with a flattening filter-free linac. *Pract Radiat Oncol* (2014) 4(2):e109–116. doi: 10.1016/j.prro.2013.04.004
31. Dzierma Y, Licht N, Nuesken F, Ruebe C. Beam properties and stability of a flattening-filter free 7 MV beam – an overview. *Med Phys* (2012) 39(5):2595–602. doi: 10.1118/1.3703835
32. Sadrollahi A, Nuesken F, Licht N, Rübe C, Dzierma Y. Monte-Carlo simulation of the Siemens Artiste linear accelerator flat 6 MV and flattening-filter-free 7 MV beam line. *PloS One* (2019) 14(1):e0210069. doi: 10.1371/journal.pone.0210069
33. Kocher M, Wittig A, Piroth MD, Treuer H, Seegenschmiedt H, Ruge M, et al. Stereotactic radiosurgery for brain metastases. A report of the DEGRO Working Group on Stereotactic Radiotherapy. *Strahlenther onkol* (2014) 190(6):521–32. doi: 10.1007/s00066-014-0648-7

34. Shaw E, Kline R, Gillin M, Souhami L, Hirschfeld A, Dinapoli R, et al. Radiation Therapy Oncology Group: radiosurgery quality assurance guidelines. *Int J Radiat Oncol Biol Phys* (1993) 27:1231–9. doi: 10.1016/0360-3016(93)90548-A
35. Paddick I. A simple scoring ratio to index the conformity of radiosurgical treatment plans. Technical note. *J Neurosurg* (2000) 93(Suppl 3):219–22. doi: 10.3171/jns.2000.93.supplement_3.0219
36. Paddick I, Lippitz B. A simple dose gradient measurement tool to complement the conformity index. *J Neurosurg* (2006) 105(Suppl):194–201. doi: 10.3171/sup.2006.105.7.194
37. Lawrence YR, Allen Li X, el Naqa I, Hahn CA, Marks LB, Merchant TE, et al. Radiation dose-volume effects in the brain. *Int J Radiat Oncol Biol Phys* (2010) 76(3):20–7. doi: 10.1016/j.ijrobp.2009.02.091
38. Marks LB, Yorke ED, Jackson A, Ten Haken RK, Constine LS, Eisbruch A, et al. Use of normal tissue complication probability models in the clinic. *Int J Radiat Oncol Biol Phys* (2010) 76(3):S10–9. doi: 10.1016/j.ijrobp.2009.07.1754
39. Minniti G, Clarke E, Lanzetta G, Osti MF, Trasimeni G, Bozzao A, et al. Stereotactic radiosurgery for brain metastases: analysis of outcome and risk of brain radionecrosis. *Radiat Oncol* (2011) 6:48. doi: 10.1186/1748-717X-6-48
40. Maruyama K, Kamada K, Ota T, Koga T, Itoh D, Ino K, et al. Tolerance of pyramidal tract to gamma knife radiosurgery based on diffusion-tensor tractography. *Int J Radiat Oncol Biol Phys* (2008) 70(5):1330–5. doi: 10.1016/j.ijrobp.2007.08.010
41. Takeshita Y, Watanabe K, Kakeda S, Hamamura T, Sugimoto K, Masaki H, et al. Early volume reduction of the hippocampus after whole-brain radiation therapy: an automated brain structure segmentation study. *Jap J Radiol* (2020) 38:118–25. doi: 10.1007/s11604-019-00895-3
42. Seibert TM, Karunamuni R, Bartsch H, Kaifi S, Krishnan AP, Dalia Y, et al. Radiation Dose-Dependent Hippocampal Atrophy Detected With Longitudinal Volumetric Magnetic Resonance Imaging. *Int J Radiat Oncol Biol Physis* (2017) 97(2):263–9. doi: 10.1016/j.ijrobp.2016.10.035
43. Schmal Z, Isermann A, Hladik D, von Toerne C, Tapio S, Rübe CE. DNA damage accumulation during fractionated low-dose radiation compromises hippocampal neurogenesis. *Radiother Oncol* (2019) 137:45–54. doi: 10.1016/j.radonc.2019.04.021
44. Rosenstock T, Grittner U, Acker G, Schwarzer V, Kulchytska N, Vajkoczy P, et al. Risk stratification in motor area-related glioma surgery based on navigated transcranial magnetic stimulation data. *J Neurosurg* (2017) 126:1227–37. doi: 10.3171/2016.4.JNS152896
45. Sollmann N, Wildschuetz N, Kelm A, Conway N, Moser T, Bulubas L, et al. Associations between clinical outcome and navigated transcranial magnetic stimulation characteristics in patients with motor-eloquent brain lesions: a combined navigated transcranial magnetic stimulation-diffusion tensor imaging fiber tracking approach. *J Neurosurg* (2018) 128:800–10. doi: 10.3171/2016.11.JNS162322

Conflict of Interest: The authors declare that the research was conducted in the absence of any commercial or financial relationships that could be construed as a potential conflict of interest.

frontiers in Oncology

MINI REVIEW
published: 02 March 2021
doi: 10.3389/fonc.2021.645854

Brain Mapping-Aided SupraTotal Resection (SpTR) of Brain Tumors: The Role of Brain Connectivity

*Giuseppe Roberto Giammalva[1], Lara Brunasso[1], Roberta Costanzo[1], Federica Paolini[1], Giuseppe Emmanuele Umana[2], Gianluca Scalia[3], Cesare Gagliardo[4], Rosa Maria Gerardi[1], Luigi Basile[1], Francesca Graziano[3], Carlo Gulì[1], Domenico Messina[1], Maria Angela Pino[1], Paola Feraco[5], Silvana Tumbiolo[6], Massimo Midiri[1], Domenico Gerardo Iacopino[1] and Rosario Maugeri[1]**

[1] Unit of Neurosurgery, Department of Biomedicine, Neuroscience and Advanced Diagnostics, Post Graduate Residency Program in Neurosurgery, University of Palermo, Palermo, Italy, [2] Department of Neurosurgery, Cannizzaro Hospital, Catania, Italy, [3] Department of Neurosurgery, ARNAS Garibaldi, Catania, Italy, [4] Section of Radiological Sciences, Department of Biomedicine, Neuroscience and Advanced Diagnostics, University of Palermo, Palermo, Italy, [5] Neuroradiology Unit, S. Chiara Hospital, Trento, Italy, [6] Department of Neurosurgery, Villa Sofia Hospital, Palermo, Italy

OPEN ACCESS

Edited by:
Giovanni Raffa,
University of Messina, Italy

Reviewed by:
Matteo Zoli,
IRCCS Institute of Neurological Sciences of Bologna (ISNB), Italy
Gianluca Trevisi,
Azienda USL di Pescara, Italy

***Correspondence:**
Rosario Maugeri
rosario.maugeri1977@gmail.com

Specialty section:
This article was submitted to Neuro-Oncology and Neurosurgical Oncology, a section of the journal Frontiers in Oncology

Received: 24 December 2020
Accepted: 18 January 2021
Published: 02 March 2021

Citation:
Giammalva GR, Brunasso L, Costanzo R, Paolini F, Umana GE, Scalia G, Gagliardo C, Gerardi RM, Basile L, Graziano F, Gulì C, Messina D, Pino MA, Feraco P, Tumbiolo S, Midiri M, Iacopino DG and Maugeri R (2021) Brain Mapping-Aided SupraTotal Resection (SpTR) of Brain Tumors: The Role of Brain Connectivity. Front. Oncol. 11:645854. doi: 10.3389/fonc.2021.645854

Brain gliomas require a deep knowledge of their effects on brain connectivity. Understanding the complex relationship between tumor and functional brain is the preliminary and fundamental step for the subsequent surgery. The extent of resection (EOR) is an independent variable of surgical effectiveness and it correlates with the overall survival. Until now, great efforts have been made to achieve gross total resection (GTR) as the standard of care of brain tumor patients. However, high and low-grade gliomas have an infiltrative behavior and peritumoral white matter is often infiltrated by tumoral cells. According to these evidences, many efforts have been made to push the boundary of the resection beyond the contrast-enhanced lesion core on T1w MRI, in the so called supratotal resection (SpTR). SpTR is aimed to maximize the extent of resection and thus the overall survival. SpTR of primary brain tumors is a feasible technique and its safety is improved by intraoperative neuromonitoring and advanced neuroimaging. Only transient cognitive impairments have been reported in SpTR patients compared to GTR patients. Moreover, SpTR is related to a longer overall and progression-free survival along with preserving neuro-cognitive functions and quality of life.

Keywords: supratotal resection, brain mapping, connectomics, brain connectome, high-grade gliomas, low-grade gliomas, brain tumor, extent of resection

INTRODUCTION

Gliomas constitute a common type of primary brain tumor. Malignant histological subtypes (high-grade gliomas, HGGs), are classified by the World Health Organization (WHO) as either grade III or IV tumors. Glioblastoma (GBM) is the most common and aggressive malignant primary brain tumor (1–7). It carries an unfavorable prognosis with a median overall survival of 12–18 months and early death after diagnosis in case of no intervention (8–10). Currently, surgical intervention

represents the first stage of GBM therapy and it is well documented that the extent of surgery has the key role in affecting the patient overall survival (OS) (8, 10, 11).

Contrast-enhancement on brain MRI is commonly considered a consequence of the blood-brain barrier (BBB) permeabilization because of the tumor infiltrative behaviour; consequently, the boundaries of contrast-enhancement on brain MRI are considered to reflect the margins of the tumoral lesion (10). In support of this assumption, the extent of resection (EOR) of the tumoral lesion is independently correlated to survival time. In facts, it has been reported that the resection of more than 95% of the contrast-enhancement mass, or residual tumor volume lower than 2 cm^3 are independently associated with improved OS and delayed recurrence (12). According to these evidences, EOR has been assumed as a metric to judge the success of tumor resection and to predict improved long-term outcomes, such as progression-free survival (PFS) and OS (13): in particular, lesser residual tumor volume is directly correlated to longer OS (10).

Low grade gliomas (LGGs - WHO grade II) are less frequent than HGGs; they are usually diagnosed in young adults with no or mild neurological and neuropsychological impairments and they are characterized by a better prognosis (12). Their growth is characterized by gradual and slow infiltrating behaviour through the adjacent brain tissue; The slow-growing pattern of LGGs induces brain plasticity phenomena which may result in functional compensation and may explain the lack of detectable neurological impairments in LGGs (14).

A significant correlation between the EOR and the OS in LGGs has been demonstrated by MRI-based volumetric studies (12). Even if with lesser extent than HGGs, LGGs infiltrate the adjacent normal-appearing brain parenchyma and tumor cells have been found up to 20 mm beyond the area of MRI pathological boundaries. According to this evidence, LGGs are considered potential malignant tumors since the diagnosis, thus early and aggressive surgical treatment is advised (12, 15). Currently, the main purpose of LGGs treatment is to delay the malignant transformation by reaching the supratotal resection of normal-appearing but infiltrated brain parenchyma, in order to increase patient OS and to preserve quality of life (QoL) (12, 16). It has been clearly demonstrated that supratotal resection positively influences the natural history of LGGs compared to the only GTR which has been associated more frequently to malignant transformation (12). Considering the easier access to brain imaging and consequent earlier diagnosis, more patients are discovered with incidentally and asymptomatic LGGs. In these cases, preventive surgery may be considered legitimate for the lower morbidity related to surgery, the higher rate of successful supratotal resection and the strong impact on the OS (12, 15, 17–21).

Nowadays, GBM is considered not only a highly proliferative tumor with high rate of recurrence even after radical surgery (8), but it should be also considered as a "diffuse disease of the brain" migrating along the white matter tracts (18). In fact, it was histologically demonstrated that tumoral cells may be found far from the primary lesion, beyond the enhanced boundaries on T1-weighted brain MRI (22, 23). According to these evidences, MRI imaging may underestimate the real extent of the tumor (24); thus, a Gross Total Resection (GTR, defined as the removal of the T1-weighted contrast-enhanced zone on brain MRI) of the tumor may not be enough (13). Despite EOR up to 100% of the contrast-enhanced tumor volume (10), it has been shown that tumoral infiltration may be found within 2 to 3 cm from the border of the original lesion (8), making tumor recurrences inevitable and mostly located near the resection cavity (10). Consequently, the infiltrative nature of GBM cells makes it difficult to eliminate microscopic disease and macroscopic GTR should not be considered a complete resection (8). In this setting, research has gone so far to broaden the contribution of gliomas surgery extending the concept of just a "tumorectomy" (18). The concept of supramarginal resection has been developed to describe the resection of the peritumoral tissue beyond the distinctive enhanced tumor mass on T1-wheighet brain MRI, with the aim to remove the microscopically infiltrated surrounding brain parenchyma (10, 11).

MATERIALS AND METHODS

An extensive systematic literature review was performed according to PRISMA guidelines on PubMed, MEDLINE and Scopus databases using the following keywords: "supratotal resection", "supramarginal resection" "supratotal resection AND GTR" "supratotal resection AND connectomics", "supratotal resection AND brain mapping", "supratotal resection AND brain connectivity", "supratotal resection AND glioma", "brain mapping AND glioma". Meta-analyses, review, clinical series and case reports were included. Non-English works and studies lacking of full text were excluded. After the initial identification, each article was screened according to the topic of this review and only articles discussing the feasibility and application of SpTR in brain gliomas were selected. Moreover, pre- and intra-operative brain mapping techniques were enlightened in order to clarify their application in case of SpTR and their relationship with brain connectomics. Among the selected articles, we included those concerning the concept of connetome and brain connectomics, the role of SpTR for the treatment of brain gliomas and the pre-operative and intra-operative tools and techniques aimed to perform SpTR.

RESULTS

Through a careful analysis of the literature, we obtained an insightful review of the current applications of brain mapping-aided SpTR for brain gliomas. From the first queries, 1924 unique records were identified. These records were screened according to our above mentioned inclusion criteria; thus, 223 articles were identified and 137 articles were later excluded due to the lack of full text or relevance according to the topic of this review and our inclusion criteria. From the 86 full-text articles assessed for eligibility, 16 more articles were excluded because of

the lack of relevance about brain mapping and connectomics in SpTR. Finally, after a careful revision, we included in this systematic review 70 articles (**Figure 1**).

DISCUSSION

Brain Connectomics and SupraTotal Resection (SpTR) of Brain Gliomas

During the last decade, the principle of locationism and the distinction of eloquent areas have been replaced by the emerging concept of brain "connectomics" (25). Connectomics is a novel multidisciplinary paradigm in which the brain is seen as a complex network of individual components interacting through continuous communication (26). This paradigm overcomes the former existence of eloquent areas and it relies on the concept of "connectome", which represents the interconnection of every part of the brain through white matter fibers (27).

According to this concept, focal and slow growth tumors determine an upsetting of normal functional relations within the brain, leading to an anatomical reshaping and functional reconfiguration of both cortical and subcortical networks even far beyond the tumor borders (26). Thus, the functional sequelae of brain tumors should be considered also at a global level since these functional changes influence whole-brain functional complexity and network architecture (26, 28). Moreover, the effects of tumor removal are related to the individual network robustness since the removal of the surrounding peritumoral brain might be functionally counterbalanced and might not result in significant additional functional impairment (26). This opens up the doors to the concept of onco-functional balance. According to this, surgical resection is guided by pre-operative assessment and intraoperative functional mapping and it takes account of the considerable structural-functional variability and the individual neural dynamics across glioma patients, in order to significantly increase patient's OS and to decrease the rate of neurological impairments and the consequent disability (17, 29). This rising concept paves the way even for the treatment of tumors within brain structures previously considered inoperable (17).

The adoption of supratotal resection (SpTR) is a further step toward the treatment of brain gliomas. SpTR was firstly adopted for the treatment of diffuse LGGs, taking advantage from the reshaping of brain networks induced by neuroplasticity and related to LGGs slower growth rate; then, SpTR has been also adopted for the treatment of HGGs (12, 30).

It has been shown that the complete resection of T1w contrast enhanced tumoral tissue together with the resection of more than 53,21% of the surrounding T2-weighted fluid-attenuated inversion recovery (FLAIR) abnormalities is associated whit a longer OS, than in case of less extensive resection (12, 31). The

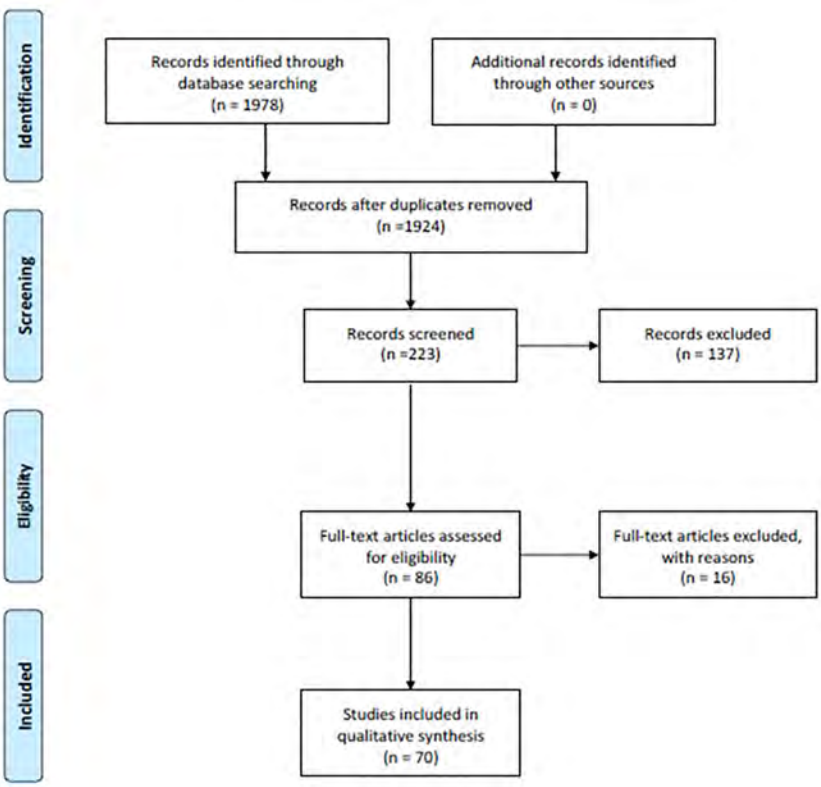

FIGURE 1 | Flow-diagram of the results of this systematic review according to PRISMA statement.

concept of SpTR is not limited to the T1-w contrast enhanced volume as boundaries of tumor resection but it tends toward a maximal resection of the T2/FLAIR signal abnormalities (18). Obviously, an extensive tumor resection could dramatically increase the risk of neurological deterioration and negative influence on patient OS (10). Thus, actual preservation of neurological function and maintenance of QoL are being actively pursued as a fundamental aspect of treating patients with gliomas, and improvement in QoL is considered to be an integral part for determining OS (1). This reveal a fundamental change from the idea of a surgery related to anatomical boundaries to the idea of a surgery guided by functional boundaries (18). The aim of this new surgical concept is to safely push the boundaries of surgical resection through FLAIR abnormalities under the guidance of functional brain-mapping until eloquent structures have been encountered. This type of functional guidance relies on an accurate study of the individual brain functional anatomy, intraoperative mapping through cortical and sub-cortical electrical stimulation, neurophysiological monitoring, and intraoperative imaging guidance (32, 33). This underlines the importance of safest surgical resection possible according not only to anatomical but also to functional boundaries. Since the OS is directly related to the EOR, SpTR may be taken into account not only in case of involvement of non-eloquent structures but also when a mild neurological impairment with few consequences on daily life is an acceptable price to pay for the patient in order to prolong OS while attending a neurological recover (18).

Pre-Operative Evaluation, Functional Imaging, and Cognitive Assessment

A careful preoperative selection of patients who can benefit from surgery is mandatory in order to meet the most favorable onco-functional balance (17).

Pre-operative imaging technique is accomplished MRI using different and specific sequences (34). Functional MRI (fMRI) plays a key role for the identification of motor cortex and language dominance through the evaluation of regional blood flow (BOLD or blood-oxygen-level dependent) changes, thus contributing to the analysis of connectome (35). Two different types of fMRI could be performed: task-based fMRI and task-free resting state fMRI. Since the execution of repetitive tasks could create artifacts in the evaluation of BOLD signals, resting-state fMRI is considered a more reliable mapping technique in pre-operative surgical planning (36). However, fMRI reliability is influenced by perfusion changes induced by different gliomas (37), in particular in HGGs (38).

Diffusion Tensor Imaging (DTI) and Diffusion Tensor Tractography (DTT) represent two MRI techniques which are capable to depict subcortical white matter tracts. DTI relies on evaluation of diffusion tensor basing on diffusion indexes of water molecules. Starting from DTI, DTT is employed to depict subcortical neural networks basing on the orientation of axonal bundles according to their anisotropy; this technique shows the capability to depict white matter tracts through the direction of water molecules, to identify signal anomalies and axonal integrity (39). Unfortunately, DTI is prone to distortions during computation of fiber-tracking algorithm (40). However, DTT is a useful preoperative tool for tridimensional representation of the fiber tracts capable to influence the surgical strategy; moreover, more complex DTI processing and the corroboration of intraoperative monitoring such ash Direct Electrical Stimulation (DES) may overcome DTI limitations thus allowing a precise functional evaluation and estimation of EOR in glioma patients (39, 40).

Recently, functional neuroimaging (fMRI, DTI, DTT) has been being supported by navigated transcranial magnetic stimulation (nTMS). Through nTMS it is possible to accurately map eloquent and motor areas using magnetic stimulation. nTMS can significantly reduce surgical time and guarantee a better functional outcome if coupled intraoperatively with DES (41). fMRI, nTMS, and DES guarantee a continuous control of motor, sensory or language domains on awake patients, thus ensuring a more radical excision according to functional boundaries (42).

Besides functional imaging, neuropsychological assessment plays a key-role in the pre-operative functional evaluation. Through the administration of several different tasks it is possible to gather information about patients' cognitive pre-operative status and to diagnose functional impairments about information processing speed, attention, working memory, verbal memory, visual memory, executive and phasic functions (43, 44). In order to perform a standardized neuropsychological assessment several tests have been developed and validated to explore several neurological domains; some of them can also be run on a friendly and common device such an iPad (45–50).

Intraoperative Monitoring and Surgical Technique During Brain Mapping-Guided SpTR

Onco-functional balance represents the crucial node of SpTR in order to obtain the maximal feasible resection without unrecoverable functional impairments (12). For this purpose, a novel surgical perspective which relies on integrated preoperative and intraoperative functional evaluation is demanded (12, 30, 51).

Feasibility of SpTR is related to some functional and technical issues. Firstly, surgical resection extended beyond contrast-enhanced tumoral margins on T1-w MRI could interfere with the functionality of neighbouring eloquent areas. Secondly, infiltrated brain tissue with low density of tumoral cells could not be correctly discriminated by normal brain tissue, leading to partial or non-complete resection (10, 52, 53). In order to achieve SpTR while preserving neurological functions, image-guided surgery must be overtaken and replaced by a functional-guided surgery (12).

The most reliable intraoperative method to directly identify functional neural networks is intraoperative DES during awake surgery. DES uses a biphasic electrical current to generate direct transient stimulation or interference within cortical or subcortical networks (54). DES could be associated by intraoperative sensorimotor localization, which relies on phase

reversal technique (PRT) and it is capable to localize the transition between sensitive and motor cortex through the registration of somatosensory evoked potential (SSEP) electrical phase (54).

Usually, intraoperative functional mapping through electrostimulation is performed during staged "asleep-awake-asleep" surgery (55). In the first stage, cortical areas are exposed and local markers are placed along the tumor borders before surgical manipulation. Functional areas are detected through neuronavigation on former functional brain imaging and through DES. During the second stage, the patient is awakened. Basing on preoperative functional assessment, patient undergoes selective tasks related to the tumor localization; during tasks execution, surgeon simultaneously apply DES on peritumoral areas in order to evoke incorrect or inappropriate neurological response if functional network is stimulated (25, 45). During this stage, DES is alternated to tumor excision in order to identify functional boundaries which will limit the resection; then, the patient is asleep in order to perform haemostasis and closure (55, 56). During the whole procedure, somatosensory and motor evoked potentials are recorded and continuous electrocorticograms is performed to detect discharge phenomena during direct brain stimulation and tumor resection (45).

This surgical technique allows surgeon to remove non-functional areas within a functional "security boundary" and to obtain greater EOR without an increased risk of permanent neurological impairments (12, 55). According to this evidence, tumor resection may be extended even to eloquent networks in order to optimize the "onco-functional" balance (57).

Brain mapping techniques have demonstrated increased rates of SpTR and a subsequent increased OS, especially in LGGs (22, 25, 32, 54, 55, 58). Intraoperative DES in awake patients allows a dramatic decrease in permanent neurological impairment, while increasing transient ones which are mostly recoverable (54, 55). On the other hand, surgical strategy for resection of HGGs should be more tailored on an accurate balance between EOR and preservation of cognitive functions since the short time for neurological recovery before the mandatory postoperative treatments (radio- and chemo-therapy) (16, 59).

Anatomical boundaries of gliomas during surgical resection may be enlightened by the use of fluorophores such as 5-aminolevulinic acid (5-ALA) and sodium fluorescein, intraoperative MRI (iMRI) and intraoperative ultrasound (IOUS) in order to verify the extent of resection (10, 30, 51, 60–66). iMRI with integrated functional neuronavigation is commonly used to achieve better visualization of residual tumor volume and to reassess neuronavigation during surgical manipulation to overcome brain shift (60, 67). As an adjunct, IOUS with our without contrast enhancement (CEUS) is a valuable tools to distinguish tumoral tissue from normal brain parenchyma; notably, IOUS is more accessible than iMRI and it immediately allows a real-time visualization of tumoral tissue during surgical manipulation (68). As regards fluorescent dyes, 5-ALA is specifically accumulated by glioma cells and it is enlightened by intraoperative source of blue-light (10, 52, 53, 69). The use of fluorescent dyes with neuronavigation guarantees greater EOR than the only neuronavigation. The maximum rate of resection could be achieved by combining fluorescent dyes and neuronavigation into the "dual intraoperative visualization approach" (DiVA), which permits further improvement in EOR and a consequent prolonged OS (10, 30, 51, 61, 62, 70).

CONCLUSIONS

Despite extended surgical resection, LGGs and HGGs are still burdened by the possibility of tumor recurrence. Specific selection criteria are needed before surgery in order to achieve the best possible result in removing safely the maximum of infiltrated brain tissue beyond tumoral margins. SpTR represents a novel concept of glioma surgery which relies on the evaluation of brain connectomics. SpTR reflects the effort to reach the best oncological outcome while preventing any permanent neurological and/or cognitive postoperative impairment, thus preserving patient's QoL and accordingly increasing OS.

AUTHOR CONTRIBUTIONS

Conceptualization: RM, GG, LaB, RC, and FP. Methodology: RM, MP, and GS. Validation: LuB, GU, and PF. Formal analysis: FG and CeG. Investigation: LaB and RC. Data curation: GG, PF, and CaG. Writing—original draft preparation: GG, LaB, RC, and FP. Writing—review and editing: RG and DM. Supervision: RM and DI. Project administration: ST, MM, and DI. All authors contributed to the article and approved the submitted version.

REFERENCES

1. Bush NAO, Chang SM, Berger MS. Current and future strategies for treatment of glioma. *Neurosurg Rev* (2017) 40(1):1–14. doi: 10.1007/s10143-016-0709-8
2. Maugeri R, Schiera G, di Liegro CM, Fricano A, Iacopino DG, Di Liegro I. Aquaporins and brain tumors. *Int J Mol Sci* (2016) 17(7):1029. doi: 10.3390/ijms17071029
3. La Torre D, Maugeri R, Angileri FF, Pezzino G, Conti A, Cardali SM, et al. Human leukocyte antigen frequency in human high-grade gliomas: a case-control study in Sicily. *Neurosurgery* (2009) 64(6):1082–8; discussion 1088–9. doi: 10.1227/01.NEU.0000345946.35786.92
4. Graziano F, Bavisotto CC, Gammazza AM, Rappa F, de Macario EC, Macario AJL, et al. Chaperonology: The Third Eye on Brain Gliomas. *Brain Sci* (2018) 8(6):110. doi: 10.3390/brainsci8060110
5. Bavisotto CC, Graziano F, Rappa F, Gammazza AM, Logozzi M, Fais S, et al. Exosomal chaperones and miRNAs in gliomagenesis: State-of-art and theranostics perspectives. *Int J Mol Sci* (2018) 19(9):2626. doi: 10.3390/ijms19092626
6. Mangogna A, Belmonte B, Agostinis C, Zacchi P, Iacopino DG, Martorana A, et al. Prognostic Implications of the Complement Protein C1q in Gliomas. *Front Immunol* (2019) 10:2366. doi: 10.3389/fimmu.2019.02366
7. Umana GE, Alberio N, Amico P, Lavecchia A, Fagone S, Fricia M, et al. Giant cystic brain metastasis from ovarian papillary serous adenocarcinoma: Case

report and review of the literature. *Interdiscip Neurosurg Adv Tech Case Manage* (2020) 20:100668. doi: 10.1016/j.inat.2020.100668
8. Hou LC, Veeravagu A, Hsu AR, Tse VCK. Recurrent glioblastoma multiforme: a review of natural history and management options. *Neurosurg Focus* (2006) 20(4):E5. doi: 10.3171/foc.2006.20.4.2
9. Brown TJ, Brennan MC, Li M, Church EW, Brandmeir NJ, Rakszawski KL, et al. Association of the extent of resection with survival in glioblastoma a systematic review and meta-Analysis. *JAMA Oncol* (2016) 2(11):1460–9. doi: 10.1001/jamaoncol.2016.1373
10. Eyüpoglu IY, Hore N, Merkel A, Buslei R, Buchfelder M, Savaskan N. Supra-complete surgery via dual intraoperative visualization approach (DiVA) prolongs patient survival in glioblastoma. *Oncotarget* (2016) 7(18):25755–68. doi: 10.18632/oncotarget.8367
11. Incekara F, Koene S, Vincent AJPE, van den Bent MJ, Smits M. Association Between Supratotal Glioblastoma Resection and Patient Survival: A Systematic Review and Meta-Analysis. *World Neurosurg* (2019) 127:617–24.e2. doi: 10.1016/j.wneu.2019.04.092
12. Yordanova YN, Duffau H. Supratotal resection of diffuse gliomas – an overview of its multifaceted implications. *Neurochirurgie* (2017) 63(3):243–9. doi: 10.1016/j.neuchi.2016.09.006
13. De Leeuw CN, Vogelbaum MA. Supratotal resection in glioma: A systematic review. *Neuro Oncol* (2019) 21(2):179–88. doi: 10.1093/neuonc/noy166
14. Duffau H. Lessons from brain mapping in surgery for low-grade glioma: Insights into associations between tumour and brain plasticity. *Lancet Neurol Lancet Neurol* (2005) 4:476–86. doi: 10.1016/S1474-4422(05)70140-X
15. Lima GLO, Dezamis E, Corns R, Rigaux-Viode O, Moritz-Gasser S, Roux A, et al. Surgical resection of incidental diffuse gliomas involving eloquent brain areas. Rationale, functional, epileptological and oncological outcomes. *Neurochirurgie* (2017) 63(3):250–8. doi: 10.1016/j.neuchi.2016.08.007
16. Giammalva GR, Iacopino DG, Azzarello G, Gaggiotti C, Graziano F, Gulì C, et al. End-of-Life Care in High-Grade Glioma Patients. *Palliative Support Perspect Brain Sci* (2018) 8(7):125. doi: 10.3390/brainsci8070125
17. Duffau H. Functional mapping before and after low-grade glioma surgery: A new way to decipher various spatiotemporal patterns of individual neuroplastic potential in brain tumor patients. *Cancers* (2020) 12:1–21. doi: 10.3390/cancers12092611
18. Duffau H. Is supratotal resection of glioblastoma in noneloquent areas possible? *World Neurosurg* (2014) 82(1–2):1–3. doi: 10.1016/j.wneu.2014.02.015
19. Lacroix M, Abi-Said D, Fourney DR, Gokaslan ZL, Shi W, DeMonte F, et al. A multivariate analysis of 416 patients with glioblastoma multiforme: prognosis, extent of resection, and survival. *J Neurosurg* (2001) 95(2):190–8. doi: 10.3171/jns.2001.95.2.0190
20. McGirt MJ, Chaichana KL, Gathinji M, Attenello FJ, Than K, Olivi A, et al. Independent association of extent of resection with survival in patients with malignant brain astrocytoma: Clinical article. *J Neurosurg* (2009) 110(1):156–62. doi: 10.3171/2008.4.17536
21. Sanai N, Polley MY, McDermott MW, Parsa AT, Berger MS. An extent of resection threshold for newly diagnosed glioblastomas: Clinical article. *J Neurosurg* (2011) 115(1):3–8. doi: 10.3171/2011.2.JNS10998
22. Yordanova YN, Moritz-Gasser S, Duffau H. Awake surgery for WHO Grade II gliomas within "noneloquent" areas in the left dominant hemisphere: toward a "supratotal" resection. *J Neurosurg* (2011) 115(2):232–9. doi: 10.3171/2011.3.JNS101333
23. Kelly PJ, Daumas-Duport C, Kispert DB, Kall BA, Scheithauer BW, Illig JJ. Imaging-based stereotaxic serial biopsies in untreated intracranial glial neoplasms. *J Neurosurg* (1987) 66(6):865–74. doi: 10.3171/jns.1987.66.6.0865
24. Esquenazi Y, Friedman E, Liu Z, Zhu JJ, Hsu S, Tandon N. The Survival Advantage of "supratotal" Resection of Glioblastoma Using Selective Cortical Mapping and the Subpial Technique. *Neurosurgery* (2017) 81(2):275–88. doi: 10.1093/neuros/nyw174
25. Duffau H. Stimulation mapping of white matter tracts to study brain functional connectivity. *Nat Rev Neurol* (2015) 11(5):255–65. doi: 10.1038/nrneurol.2015.51
26. Hart MG, Romero-Garcia R, Price SJ, Suckling J. Global Effects of Focal Brain Tumors on Functional Complexity and Network Robustness: A Prospective Cohort Study. *Clin Neurosurg* (2019) 84:1201–13. doi: 10.1093/neuros/nyy378
27. Altieri R, Raimondo S, Tiddia C, Sammarco D, Cofano F, Zeppa P, et al. Glioma surgery: From preservation of motor skills to conservation of cognitive functions. *J Clin Neurosci* (2019) 70:55–60. doi: 10.1016/j.jocn.2019.08.091
28. Brennum J, Engelmann CM, Thomsen JA, Skjøth-Rasmussen J. Glioma surgery with intraoperative mapping—balancing the onco-functional choice. *Acta Neurochir (Wien)* (2018) 160(5):1043–50. doi: 10.1007/s00701-018-3521-0
29. Umana GE, Raudino G, Alberio N, Inserra F, Giovinazzo G, Fricia M, et al. Slit-like hypertensive hydrocephalus: Report of a late, complex, and multifactorial complication in an oncologic patient. *Surg Neurol Int* (2020) 11:219. doi: 10.25259/SNI_145_2020
30. Dimou J, Beland B, Kelly J. Supramaximal resection: A systematic review of its safety, efficacy and feasibility in glioblastoma. *J Clin Neurosci* (2020) 72 (xxxx):328–34. doi: 10.1016/j.jocn.2019.12.021
31. Li YM, Suki D, Hess K, Sawaya R. The influence of maximum safe resection of glioblastoma on survival in 1229 patients: Can we do better than gross-total resection? *J Neurosurg* (2016) 124(4):977–88. doi: 10.3171/2015.5.JNS142087
32. Duffau H. Long-term outcomes after supratotal resection of diffuse low-grade gliomas: a consecutive series with 11-year follow-up. *Acta Neurochir (Wien)* (2016) 158(1):51–8. doi: 10.1007/s00701-015-2621-3
33. Barone F, Alberio N, Iacopino D, Giammalva G, D'Arrigo C, Tagnese W, et al. Brain Mapping as Helpful Tool in Brain Glioma Surgical Treatment—Toward the "Perfect Surgery"? *Brain Sci* (2018) 8(11):192. doi: 10.3390/brainsci8110192
34. Hendriks EJ, Idema S, Hervey-Jumper SL, Bernat AL, Zwinderman AH, Barkhof F, et al. Preoperative Resectability Estimates of Nonenhancing Glioma by Neurosurgeons and a Resection Probability Map. *Neurosurgery* (2019) 85(2):E304–13. doi: 10.1093/neuros/nyy487
35. Hart MG, Price SJ, Suckling J. Connectome analysis for pre-operative brain mapping in neurosurgery. *Br J Neurosurg* (2016) 30(5):506–17. doi: 10.1080/02688697.2016.1208809
36. Zhang S, Li X, Lv J, Jiang X, Guo L, Liu T. Characterizing and differentiating task-based and resting state fMRI signals via two-stage sparse representations. *Brain Imaging Behav* (2016) 10(1):21–32. doi: 10.1007/s11682-015-9359-7
37. Kuchcinski G, Mellerio C, Pallud J, Dezamis E, Turc G, Rigaux-Viodé O, et al. Three-tesla functional MR language mapping : Comparison with direct cortical stimulation in gliomas. *Neurology* (2015) 84(6):560–8. doi: 10.1212/WNL.0000000000001226
38. Morrison MA, Churchill NW, Cusimano MD, Schweizer TA, Das S, Graham SJ. Reliability of Task-Based fMRI for Preoperative Planning: A Test-Retest Study in Brain Tumor Patients and Healthy Controls. Hayasaka S, editor. *PloS One* (2016) 11(2):e0149547. doi: 10.1371/journal.pone.0149547
39. Mellerio C, Charron S, Lion S, Roca P, Kuchcinski G, Legrand L, et al. Perioperative functional neuroimaging of gliomas in eloquent brain areas. *Neurochirurgie* (2017) 63(3):129–34. doi: 10.1016/j.neuchi.2016.10.012
40. Freyschlag CF, Kerschbaumer J, Pinggera D, Bodner T, Grams AE, Thomé C. Preoperative prediction of language function by diffusion tensor imaging. *Brain Inf* (2017) 4:201–5. doi: 10.1007/s40708-017-0064-8
41. Jung J, Lavrador JP, Patel S, Giamouriadis A, Lam J, Bhangoo R, et al. First United Kingdom Experience of Navigated Transcranial Magnetic Stimulation in Preoperative Mapping of Brain Tumors. *World Neurosurg* (2019) 122: e1578–87. doi: 10.1016/j.wneu.2018.11.114
42. Chacko AG, Thomas SG, Babu KS, Daniel RT, Chacko G, Prabhu K, et al. Awake craniotomy and electrophysiological mapping for eloquent area tumours. *Clin Neurol Neurosurg* (2013) 115(3):329–34. doi: 10.1016/j.clineuro.2012.10.022
43. Habets EJJ, Hendriks EJ, Taphoorn MJB, Douw L, Zwinderman AH, Vandertop WP, et al. Association between tumor location and neurocognitive functioning using tumor localization maps. *J Neurooncol* (2019) 144(3):573–82. doi: 10.1007/s11060-019-03259-z
44. Kelm A, Sollmann N, Ille S, Meyer B, Ringel F, Krieg SM. Resection of gliomas with and without neuropsychological support during awake Craniotomy-Effects on surgery and clinical outcome. *Front Oncol* (2017) 7:176. doi: 10.3389/fonc.2017.00176
45. Motomura K, Chalise L, Ohka F, Aoki K, Tanahashi K, Hirano M, et al. Supratotal Resection of Diffuse Frontal Lower Grade Gliomas with Awake

Brain Mapping, Preserving Motor, Language, and Neurocognitive Functions. *World Neurosurg* (2018) 119:30–9. doi: 10.1016/j.wneu.2018.07.193
46. Lang S, Cadeaux M, Opoku-Darko M, Gaxiola-Valdez I, Partlo LA, Goodyear BG, et al. Assessment of Cognitive, Emotional, and Motor Domains in Patients with Diffuse Gliomas Using the National Institutes of Health Toolbox Battery. *World Neurosurg* (2017) 99:448. doi: 10.1016/j.wneu.2016.12.061
47. Maugeri R, Giammalva RG, Iacopino DG. On the Shoulders of Giants, with a Smartphone: Periscope in Neurosurgery. *World Neurosurg* (2016) 92:569–70. doi: 10.1016/j.wneu.2016.03.019
48. Graziano F, Maugeri R, Iacopino DG. Telemedicine versus WhatsApp: From tradition to evolution. *NeuroReport* (2015) 26(10):602–3. doi: 10.1097/WNR.0000000000000393
49. Graziano F, Maugeri R, Giugno A, Iacopino DG. WhatsAPP in neurosurgery: the best practice is in our hands. *Acta Neurochirurgica* (2016) 159(4):601. doi: 10.1007/s00701-016-2853-x
50. Tymowski M, Kaspera W, Metta-Pieszka J, Zarudzki Ł, Ładziński P. Neuropsychological assessment of patients undergoing surgery due to low-grade glioma involving the supplementary motor area. *Clin Neurol Neurosurg* (2018) 175:1–8. doi: 10.1016/j.clineuro.2018.09.036
51. Delgado-López PD, Corrales-García EM, Martino J, Lastra-Aras E, Dueñas-Polo MT. Diffuse low-grade glioma: a review on the new molecular classification, natural history and current management strategies. *Clin Transl Oncol* (2017) 19(8):931–44. doi: 10.1007/s12094-017-1631-4
52. Stummer W, Pichlmeier U, Meinel T, Wiestler OD, Zanella F, Reulen HJ. Fluorescence-guided surgery with 5-aminolevulinic acid for resection of malignant glioma: a randomised controlled multicentre phase III trial. *Lancet Oncol* (2006) 7(5):392–401. doi: 10.1016/S1470-2045(06)70665-9
53. Kreth FW, Thon N, Simon M, Westphal M, Schackert G, Nikkhah G, et al. Gross total but not incomplete resection of glioblastoma prolongs survival in the era of radiochemotherapy. *Ann Oncol* (2013) 24(12):3117–23. doi: 10.1093/annonc/mdt388
54. Silverstein JW, Rosenthal A, Patel NV, Boockvar JA. Electrophysiological Mapping and Monitoring during an Awake Craniotomy for Low-Grade Glioma: Case Report. *Neurodiagn J* (2019) 59(3):133–41. doi: 10.1080/21646821.2019.1627148
55. Duffau H. Awake surgery for incidental WHO grade II gliomas involving eloquent areas. *Acta Neurochir (Wien)* (2012) 154(4):575–84. doi: 10.1007/s00701-011-1216-x
56. Umana GE, Scalia G, Spitaleri A, Alberio N, Fricia M, Tomasi SO, et al. Use of gelatin-thrombin hemostatic matrix for control of ruptured cerebral aneurysm. *J Neurol Surg A* (2020) 1–5. doi: 10.1080/02688697.2020.1836324
57. Duffau H. Is non-awake surgery for supratentorial adult low-grade glioma treatment still feasible? *Neurosurg Rev* (2018) 41(1):133–9. doi: 10.1007/s10143-017-0918-9
58. Saito T, Muragaki Y, Maruyama T, Tamura M, Nitta M, Okada Y. Intraoperative Functional Mapping and Monitoring during Glioma Surgery. *Neurol Med Chir (Tokyo)* (2015) 55(1):1–13. doi: 10.2176/nmc.ra.2014-0215
59. Zigiotto L, Annicchiarico L, Corsini F, Vitali L, Falchi R, Dalpiaz C, et al. Effects of supra-total resection in neurocognitive and oncological outcome of high-grade gliomas comparing asleep and awake surgery. *J Neurooncol* (2020) 148(1):97–108. doi: 10.1007/s11060-020-03494-9
60. Senft C, Bink A, Franz K, Vatter H, Gasser T, Seifert V. Intraoperative MRI guidance and extent of resection in glioma surgery: A randomised, controlled trial. *Lancet Oncol* (2011) 12(11):997–1003. doi: 10.1016/S1470-2045(11)70196-6
61. Coburger J, Hagel V, Wirtz CR, König R. Surgery for glioblastoma: Impact of the combined use of 5-aminolevulinic acid and intraoperative MRI on extent of resection and survival. *PloS One* (2015) 10(6):e0131872. doi: 10.1371/journal.pone.0131872
62. Quick-Weller J, Lescher S, Forster M-T, Konczalla J, Seifert V, Senft C. Combination of 5-ALA and iMRI in re-resection of recurrent glioblastoma. *Br J Neurosurg* (2016) 30(3):313–7. doi: 10.3109/02688697.2015.1119242
63. Díez Valle R, Tejada Solis S, Idoate Gastearena MA, García De Eulate R, Domínguez Echávarri P, Aristu Mendiroz J. Surgery guided by 5-aminolevulinic fluorescence in glioblastoma: Volumetric analysis of extent of resection in single-center experience. *J Neurooncol* (2011) 102(1):105–13. doi: 10.1007/s11060-010-0296-4
64. Stummer W, Tonn JC, Mehdorn HM, Nestler U, Franz K, Goetz C, et al. Counterbalancing risks and gains from extended resections in malignant glioma surgery: A supplemental analysis from the randomized 5-aminolevulinic acid glioma resection study: Clinical article. *J Neurosurg* (2011) 114(3):613–23. doi: 10.3171/2010.3.JNS097
65. Maugeri R, Villa A, Pino M, Imperato A, Giammalva GR, Costantino G, et al. With a little help from my friends: The role of intraoperative fluorescent dyes in the surgical management of high-grade gliomas. *Brain Sci* (2018) 8(2):31. doi: 10.3390/brainsci8020031
66. Francaviglia N, Iacopino DG, Costantino G, Villa A, Impallaria P, Meli F, et al. Fluorescein for resection of high-grade gliomas: A safety study control in a single center and review of the literature. *Surg Neurol Int* (2017) 8:145. doi: 10.4103/sni.sni_89_17
67. Tomasi SO, Umana GE, Scalia G, Rubio-Rodriguez RL, Cappai PF, Capone C, et al. Importance of veins for neurosurgery as landmarks against brain shifting phenomenon: an anatomical and 3D-MPRAGE MR reconstrution of superficial cortical veins. *Front Neuroanat* 14:596167. doi: 10.3389/fnana.2020.596167
68. Pino MA, Imperato A, Musca I, Maugeri R, Giammalva GR, Costantino G, et al. New hope in brain glioma surgery: The role of intraoperative ultrasound. A review. *Brain Sci* (2018) 8(11):202. doi: 10.3390/brainsci8110202
69. Roder C, Bisdas S, Ebner FH, Honegger J, Naegele T, Ernemann U, et al. Maximizing the extent of resection and survival benefit of patients in glioblastoma surgery: High-field iMRI versus conventional and 5-ALA-assisted surgery. *Eur J Surg Oncol* (2014) 40(3):297–304. doi: 10.1016/j.ejso.2013.11.022
70. Eyüpoglu IY, Hore N, Savaskan NE, Grummich P, Roessler K, Buchfelder M, et al. Improving the Extent of Malignant Glioma Resection by Dual Intraoperative Visualization Approach. *PloS One* (2012) 7(9):1–10. doi: 10.1371/journal.pone.0044885

Conflict of Interest: The authors declare that the research was conducted in the absence of any commercial or financial relationships that could be construed as a potential conflict of interest.

frontiers in Neurology

ORIGINAL RESEARCH
published: 03 March 2021
doi: 10.3389/fneur.2021.633068

The Cologne Picture Naming Test for Language Mapping and Monitoring (CoNaT): An Open Set of 100 Black and White Object Drawings

Carolin Weiss Lucas[1*†], *Julia Pieczewski*[1†], *Sophia Kochs*[1], *Charlotte Nettekoven*[1], *Christian Grefkes*[2], *Roland Goldbrunner*[1] *and Kristina Jonas*[3†]

[1] Center for Neurosurgery, Faculty of Medicine and University Hospital, University of Cologne, Cologne, Germany,
[2] Department of Neurology, Faculty of Medicine and University Hospital, University of Cologne, Cologne, Germany,
[3] Department of Special Education and Rehabilitation, Faculty of Human Sciences, University of Cologne, Cologne, Germany

OPEN ACCESS

Edited by:
Thomas Picht,
Charité – Universitätsmedizin Berlin, Germany

Reviewed by:
Pantelis Lioumis,
Aalto University, Finland
Shalini Narayana,
University of Tennessee Health Science Center, United States

***Correspondence:**
Carolin Weiss Lucas
carolin.weiss-lucas@uk-koeln.de

[†]These authors have contributed equally to this work

Specialty section:
This article was submitted to Neuro-Oncology and Neurosurgical Oncology, a section of the journal Frontiers in Neurology

Received: 24 November 2020
Accepted: 12 January 2021
Published: 03 March 2021

Citation:
Weiss Lucas C, Pieczewski J, Kochs S, Nettekoven C, Grefkes C, Goldbrunner R and Jonas K (2021) The Cologne Picture Naming Test for Language Mapping and Monitoring (CoNaT): An Open Set of 100 Black and White Object Drawings. Front. Neurol. 12:633068. doi: 10.3389/fneur.2021.633068

Language assessment using a picture naming task crucially relies on the interpretation of the given verbal response by the rater. To avoid misinterpretations, a language-specific and linguistically controlled set of unambiguous, clearly identifiable and common object–word pairs is mandatory. We, here, set out to provide an open-source set of black and white object drawings, particularly suited for language mapping and monitoring, e.g., during awake brain tumour surgery or transcranial magnetic stimulation, in German language. A refined set of 100 black and white drawings was tested in two consecutive runs of randomised picture order and was analysed in respect of correct, prompt, and reliable object recognition and naming in a series of 132 healthy subjects between 18 and 84 years (median 25 years, 64% females) and a clinical pilot cohort of 10 brain tumour patients (median age 47 years, 80% males). The influence of important word- and subject-related factors on task performance and reliability was investigated. Overall, across both healthy subjects and patients, excellent correct object naming rates (97 vs. 96%) as well as high reliability coefficients (Goodman–Kruskal's gamma = 0.95 vs. 0.86) were found. However, the analysis of variance revealed a significant, overall negative effect of low word frequency ($p < 0.05$) and high age ($p < 0.0001$) on task performance whereas the effect of a low educational level was only evident for the subgroup of 72 or more years of age ($p < 0.05$). Moreover, a small learning effect was observed across the two runs of the test ($p < 0.001$). In summary, this study provides an overall robust and reliable picture naming tool, optimised for the clinical use to map and monitor language functions in patients. However, individual familiarisation before the clinical use remains advisable, especially for subjects that are comparatively prone to spontaneous picture naming errors such as older subjects of low educational level and patients with clinically apparent word finding difficulties.

Keywords: picture naming, neuromonitoring, intraoperative, TMS, language, brain tumour, assessment, German

INTRODUCTION

The correct identification and semantic retrieval of object names in a behavioural task is the basis of investigating conceptual knowledge of objects in the human brain (1). When using an overt object naming task, also expressive speech motor functions (i.e., articulation) are involved. This task, therefore, combines important language domains, which might have led to its wide use in the assessment and monitoring of language functions, e.g., for language mapping and monitoring in the context of awake neurosurgery (2). Controlling the correctness of the verbal answer is essential to assess either object identification, lexical/semantic retrieval, or word articulation. Different linguistic factors are known that affect the ease of the retrieval process and task performance in general. Three of these important factors are addressed in this work:

First, the uniqueness of the object drawing to be named and the disambiguity of the corresponding word to be retrieved are crucial pre-requisites of reliable testing and calls for objects that can be easily depicted graphically as well as for the non-existence of alternative expressions (i.e., synonyms) to name the respective object [see (3) for review]. Second, word frequency, i.e., how often a certain word is typically used in a certain language, is described as an objective and highly relevant factor influencing lexical access in naming tasks [e.g., (4) for review, (5, 6)], given the association of higher frequency words with a lower error rate as well as with faster retrieval process (6). A third relevant factor is the word length, here expressed by the number of syllables, since longer words are associated with a higher error rate (7). All factors vary, however, with respect to age or educational level as well as cultural background and language so that existing stimuli and procedures cannot be directly transferred from one language to another (8, 9).

Although overt object naming tasks are widely used in both neurocognitive science and clinical practise, linguistically controlled and validated open-source assessment tools are scarce. As a result, to date, there is no consensus tool for intraoperative monitoring of language functions during awake surgery of cerebral lesions or related pre-surgical investigations, especially for the German language. Providing a linguistically controlled and validated stimulus set for use in German language might be of great value, e.g., to allow for data comparison in multicentre studies and to assure a state-of-the-art testing procedure, robust to possibly erroneous interpretations due to low reliability of the test protocol itself.

In the context of neurosurgery, the precise delineation of the boundaries of eloquent brain areas by intraoperative direct cortical stimulation (DCS) is extremely important not only to achieve maximum tumour control and improve survival but also to avoid permanent neurological deficits (10). For language, this is particularly relevant since the anatomical correlates of function underlie a much higher variability as compared to, e.g., primary motor functions, in both healthy (11) and, even more, in diseased brain (12–15).

Since its introduction by Penfield and Roberts (16), visual object naming has become the most common task for intraoperative language mapping and monitoring (17). Apart from its inclusion in neuropsychological and language-related assessment batteries and its use for non-invasive functional imaging [e.g., magnetoencephalography, functional magnetic resonance imaging and positron emission tomography; (18–20)], the object naming task has also been used for neuronavigated, repetitive, task-locked transcranial magnetic stimulation (TMS). This technique simulates the intraoperative situation during awake surgery where task execution is temporarily hampered by local electrical stimulation (i.e., DCS) of a cortex site, also referred to as "virtual lesion" (21–23).

Like neurocognitive and language assessment for diagnostic purposes, the results of both TMS and DCS rely crucially on the *ad hoc* (intraoperative) or *post-hoc* (post-operative) interpretation of the given verbal response by the rater. Here, a language-specific and linguistically controlled set of unambiguous, clearly identifiable and common object–word pairs is particularly important.

Existing stimulus sets are of limited usability for German-speaking subjects due to language specificity of the normative data and/or the stimuli, mostly designed for English native speakers [e.g., (24–26)], and/or due to copyright protection [e.g., (27, 28)]. We, therefore, set out to validate and provide an open-source set of black and white object drawings, specifically for German-speaking subjects, intended for both research and clinical use: The Cologne Picture Naming Test for Language Mapping and Monitoring (CoNaT). We expected high correct object naming rates and a strong correlation between the given answers and hypothesised that both word-related linguistic characteristics, i.e., higher number of syllables and lower word frequency, have a significant negative impact on object naming performance. Moreover, we expected better task performance from subjects of young age and high educational level. Apart from investigating the robustness of the task and the influence of these word- and subject-related factors on the object naming performance in a representative cohort of healthy adults of all age groups, we also assessed the suitability of the CoNaT as a reliable language monitoring instrument in a pilot cohort of brain tumour patients.

MATERIALS AND METHODS

General Study Design

A set of 112 black and white drawings was tested in respect of correct object identification as well as correct, prompt and reliable object naming in a representative series of 132 healthy subjects and a clinical pilot cohort of 10 brain tumour patients.

For the development of the picture set, we generally included concrete monomorphematic simple nouns (no compound nouns) for which a clear and unambiguous pictorial illustration was feasible (29). In addition, two linguistic factors (i.e., word frequency, number of syllables) were considered to build four equally large subgroups of object–word pairs (see Stimuli Set section).

We set out to assess (i) the feasibility as expressed by the overall rate of correctly identified items and (ii) the test–retest reliability of the object naming performance, both of which

are important to qualify the CoNaT e.g. for intraoperative monitoring, as well as (iii) the influence of stimulus- and subject-related characteristics on correct object recognition and naming reliability. Moreover, we investigated whether or not a correlation between object naming performance and the test result of a standard assessment of word finding difficulties (i.e., Bielefeld Screening for word finding difficulties for mild aphasia [BIWOS]; (29)) could be found in the pilot cohort of patients with utmost mild to moderate clinical signs of aphasia. Both groups, healthy subjects and brain tumour patients, performed the naming task twice, in two consecutive runs.

The study was carried out according to the declaration of Helsinki [(30), last revision 2013] and was approved by the local ethics committee.

Subjects

Healthy Subjects

A total of 132 healthy subjects between 18 and 84 years of age were prospectively enrolled between 2016 and 2019. Subjects were characterised by age (group 1: 18–35 years; group 2: 36–53 years; group 3: 54–71 years; group 4: 72 years or older), gender, handedness, and general educational level (i.e., holding vs. missing university entrance diploma, generally corresponding to $\geq$/$<$12 years of general school education). Here, technical college entrance qualification was considered as equivalent to a university entrance diploma. Inclusion criteria were as follows: age of at least 18 years; German language skills on native speaker level; no intake of alcohol, drugs or psychoactive agents prior to the experiment with risk of reduced attention and/or alertness levels; and sufficient vision (i.e., $\geq$0.7 corrected visual acuity). Subjects with neurological or psychiatric diseases (including brain lesions and seizures) in medical history were excluded.

Patients

In addition, 10 adult patients with clinical signs of mild to moderate aphasia were included in this study in order to test the protocol under clinical conditions. All patients were newly diagnosed with a focal brain tumour of the left hemisphere.

The additional inclusion criteria were identical for both healthy subjects and patients. In contrast, specific exclusion criteria for patients were as follows: (i) neurological/psychiatric diseases unrelated to the brain tumour, (ii) clinical signs of moderate to severe cognitive dysfunction as indicated by a Mini Mental State Examination [MMSE; (31)] score of $<$20/30, and (iii) severe word finding difficulties according to a screening of object naming competence using 10 pictures (which were not included in the protocol). Here, correct naming of at least 7 out of the 10 objects was required to qualify for study inclusion.

The severity of word finding difficulties of all participating patients was characterised using the BIWOS assessment. Of note, the BIWOS was chosen since it tests for a comprehensive set of semantic and lexical language skills for diagnosing word finding difficulties by a series of well-standardised tasks (i.e., antonyms, rhymes [free, category specific], hyperonyms, verbal fluency [lexical, semantic], word composition, semantic feature analysis, naming by definition) but does not include visual object naming so that a low level of interference was expected. The BIWOS was analysed according to the standard procedure given in the manual, resulting in separate scores for lexical and semantic word finding skills as well as a total score and corresponding severity levels to describe the word finding difficulties.

Of note, all complementary examinations (i.e., MMSE, screening of object naming competence, BIWOS) were administered prior to the beginning of the object naming tests.

Stimuli Set

The entire picture set ($N = 112$) consisted of four different categories (A–D as defined by number of syllables and high vs. low word frequency) and included a total of 12 back-up illustrations to allow for a posteriori selection of the 100 best suited pictures (**Table 1**). All object–word pairs were chosen based on the pilot data by a clinical neuroscientist together with an experienced linguist (i.e., authors CWL and KJ) and were controlled regarding the following criteria: (i) (gender neutral) word frequency [cf. (33, 34)], (ii) number of syllables, and (iii) unambiguity of both the object illustration and the expected verbal response (i.e., good recognizability of the illustrated object, expected non-existence of synonyms for the object name in German language as well as the absence of semantically related attributes, which could lead to compound nouns and over-specified verbal responses such as "egg cup" instead of "egg").

Illustrations were black and white drawings (presented on a white screen), drawn by author CWL and were either (i) freely designed ($n = 53$) or inspired (ii) by the Snodgrass & Vanderwart picture set [$n = 25$; (24)] or (iii) by the pictures included in the commercial software Nexspeech (Nexstim Oy, Helsinki, Finland; $n = 22$). A total of $n = 12$ drawings (i.e., three drawings per class A–D) were omitted due to poor performance in respect of either correctness or unambiguity of the naming responses (mean correct naming rate: 87 $\pm$ 7%; mean Goodman and Kruskal's gamma [referred to as "GK-gamma" throughout the manuscript]: 0.94 $\pm$ 0.05) and were, thus, not considered for further statistical analysis (see **Supplementary Table 1** for details). The remaining selection of $n = 100$ objects is provided in **Table 2** (see **Supplementary Material** for stimuli, i.e., drawings). Example drawings are shown in **Figure 1**.

Test Protocol and Scoring

Pictures were presented in a pseudorandomised sequence on a white screen. The display time for each stimulus was 500 ms, interleaved by a time interval of 3 s for healthy subjects and 5 s for patients. No feedback was provided regarding the task performance (i.e., correctness of picture naming) during the experiment. Between the two consecutive sessions, a break of up to 10 min was allowed if required by the test subject, e.g., in case of tiring.

For each run, the verbal responses were audio-taped for additional *post-hoc* assessment of promptness, accuracy, and reliability of object recognition and naming (**Table 3**) to account for both the uniqueness of the illustration and the unambiguity/simplicity of the semantic word retrieval and its articulation. Here, more specific object names compared to the expected verbal response like "sparrow" instead of "bird" as well as compound nouns instead of simple nouns such as "church

bell" for "bell" were rated as over-specification and thus fell into the category of unexpected naming variants (i.e., category III, cf. **Table 3**). In contrast, generalisations like "animal" instead of "bird" were categorised as wrong naming response (i.e., category V; cf. **Table 3**). Response delays were assessed by acoustic evaluation, a common procedure in clinical practise (e.g., for pre-surgical and intraoperative language mapping using TMS/DCS), hereby considering the individual baseline response latency. For further analyses, correct responses were assigned to the types (A) "correct object naming," including only correctly recognised and expectedly named objects (i.e., categories I–II), and (B) "correct object recognition," including also correctly recognised but unexpectedly named objects (i.e., categories I–III; **Table 3**).

TABLE 1 | Stimulus set characteristics.

Class	Number of syllables	Word frequency		Number of stimuli	
		Category	Median [range]	Tested	Selected
A	1	High	53 [14–729]	28	25
B	2	High	24 [11–170]	28	25
C	1	Low	5 [1–10]	28	25
D	2	Low	4 [0–9]	28	25
Total	1–2		11 [0–729]	112	100

Word frequencies are given according to the CELEX database (http://celex.mpi.nl) (32) of word frequencies in German language. Word frequencies > 10/1,000,000 words were defined as high.

Statistics

Normality of data distributions was tested according to Shapiro–Wilk. The reliability of naming performance (categorical data; five levels; see above) between the first and the second run was assessed using GK-gamma for each stimulus item.

An analysis of variance (ANOVA) was performed to test for the influence of stimulus- and subject-related factors on the results, i.e., on the average rate of correct object recognition as well as correct object naming (two levels: right vs. wrong; see above) in percent of total trials and the reliability of the naming responses (five levels i–v; **Table 3**) as expressed by GK-gamma. GK-gamma is a symmetric measure of association, based on a sorted list of paired observations, which ranges from

TABLE 2 | Word lists.

A (One syllable, high WF)		B (Two syllables, high WF)		C (One syllable, low WF)		D (Two syllables, low WF)	
Object name	**WF**	**Object name**	**WF**	**Object name**	**WF**	**Object name**	**WF**
Arm [arm]	57	Auge [eye]	56	Blitz [lightning]	8	Apfel [apple]	6
Bank [bank]	85	Auto [car]	78	Bus [bus]	7	Birne [pear]	0
Baum [tree]	24	Brille [glasses]	17	Ei [egg]	9	Blume [flower]	3
Bett [bed]	80	Engel [angel]	27	Fass [barrel]	3	Bürste [brush]	2
Brot [bread]	28	Feder [feather]	11	Frosch [frog]	1	Drache [dragon]	2
Buch [book]	99	Fenster [window]	75	Kamm [comb]	5	Eimer [bucket]	5
Fisch [fish]	17	Finger [finger]	42	Knopf [button]	6	Gabel [fork]	4
Fuß [foot]	49	Hose [trousers/pants]	11	Kran [crane]	5	Glocke [bell]	0
Glas [glass]	60	Insel [island]	29	Maus [mouse]	5	Harfe [harp]	1
Hand [hand]	316	Kette [chain]	17	Pfeil [arrow]	7	Hase [rabbit]	7
Haus [house]	104	Kirche [church]	170	Pilz [mushroom]	1	Igel [hedgehog]	5
Herz [heart]	79	Koffer [suitcase]	18	Rock [skirt]	10	Käse [cheese]	6
Hund [dog]	35	König [king]	84	Schal [scarf]	1	Katze [cat]	9
Hut [hat]	14	Krone [crown]	18	Schuh [shoe]	5	Kerze [candle]	3
Kleid [dress]	29	Leiter [ladder]	56	Schwamm [sponge]	2	Löffel [spoon]	6
Kuh [cow]	23	Löwe [lion]	11	Schwein [pig]	5	Messer [knife]	7
Mund [mouth]	53	Mauer [wall]	35	Schwert [sword]	7	Muschel [mussel]	1
Pferd [horse]	29	Schlange [snake]	11	Ski [ski]	10	Puppe [doll]	5
Rad [wheel]	25	Schlüssel [key]	23	Storch [stork]	4	Säge [saw]	2
Schloss [padlock]	64	Sonne [sun]	90	Topf [pot]	7	Schaukel [swing]	0
Stern [star]	34	Teppich [carpet]	24	Wurst [sausage]	9	Schere [scissor]	4
Stuhl [chair]	26	Teufel [devil]	24	Zahn [tooth]	2	Schleife [bow]	6
Tisch [table]	89	Trommel [drum]	24	Zaun [fence]	10	Spritze [syringe]	5
Tür [door]	113	Vogel [bird]	24	Zelt [tent]	6	Wecker [alarm clock]	0
Uhr [clock]	729	Zeitung [newspaper]	24	Zwerg [dwarf]	2	Würfel [dice]	3

Object names are given in German [English translation]. WF, word frequency in German.

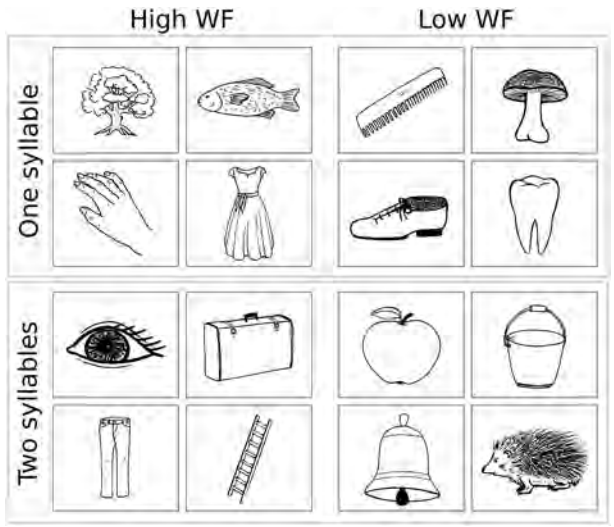

FIGURE 1 | Example stimuli. Four example drawings are given for class A (upper left) to D (lower right). WF, Word frequency.

TABLE 3 | Verbal response rating.

Verbal response		Correct performance type	
Category	**Description**	**"Naming"**	**"Recognition"**
I	Prompt and correct as expected	x	x
II	Correct as expected but response delayed	x	x
III	Unexpected naming variant, e.g., dialect or cultural synonym, over-specification, diminutive or plural		x
IV	Wrong but self-correction		
V	Wrong or non-response		

Overt naming responses were categorised as follows: (i) prompt and correct, (ii) correct but delayed, (iii) unexpected naming variants like dialectal, cultural, or other previously unexpected synonyms (e.g., "Beelzebub" instead of "devil"), over-specification, diminutive, or plural, (iv) wrong but self-correction, and (v) wrong or non-response, with (i–ii) being considered as correct object recognition expressed by a correct and expected naming response (referred to as "correct naming response") and (i–iii) being considered as correct object recognition, including both expected and unexpected naming responses (referred to as "correct objection recognition" throughout the manuscript).

-1.0 to $+1.0$, with $+1.0$ indicating perfect correlation. Please note that, for the ANOVA and for calculation of correlations, GK-gamma $= 1$ was assumed if GK-gamma could not be calculated due to perfect naming rates (i.e., 100% correct naming in both sessions). For ANOVA with GK-gamma as dependent (outcome) variable, outliers (i.e., >2 SD deviation from average) were omitted. Of note, this outlier removal had to be applied only for subjects/stimuli where the confidence interval was zero due to very low incidence of errors. In total, this procedure removed 10% (subjects)/13% (stimuli) of the total data. Levels of significance according to ANOVA are indicated without leading zeros (e.g., "$p < 0.01$") throughout the manuscript to allow for better distinction from results of group mean comparisons and correlations.

Post-hoc comparison of means between paired data (e.g., correct naming rates of session 1 vs. session 2) were calculated using paired *t*-tests or Wicoxon's signed rank test, depending on the normality of the data distribution (as assessed by the Shapiro–Wilk test). Accordingly, for comparison between independent groups, Wicoxon's rank test was applied in case of not normally distributed data.

Pearson's correlation was calculated to test for significant relationships between metric variables (i.e., behavioural scores).

In cases of comparisons between more than two groups (e.g., between different word groups: A–D), the levels of significance were adjusted using the false discovery rate (FDR) correction (35).

The statistical analysis was performed using R (R Studio, Version 0.98.507, Boston, MA, USA; packages: {psych}, {vcdExtra}, {ggplot2}).

RESULTS

Subject Characteristics

Healthy Subjects

Of the 132 subjects included in the study, 64% ($n = 84$) were female. With a median age of 35 years (range: 18–84 years), most healthy participants were of relatively young age (group 1 [18–35 years]: 50%; group 2 [36–53 years]: 20%; group 3 [54–71 years]: 19%; group 4 [72–89 years]: 11%), right-handed (86%) and had a high educational level (71%).

Patients

Ten patients (two females, median age 47 years, range 24–76 years) with normal to moderate word finding skills according to the BIWOS results were included in the clinical pilot part of the study. Most patients were right-handed (80%) and had a high educational level (78%; **Table 4**).

Correctness and Reliability of Object Recognition and Naming

Healthy Subjects

Overall, mean correct object recognition and picture naming rates were in the range of 98 ± 4 and 97 ± 4% and were significantly higher in the second as compared to the first run (object recognition: 98.3 ± 3.6 vs. 97.9 ± 4.0%, $p < 0.001$; object naming: 97.7 ± 3.9 vs. 97.2 ± 4.3%, $p < 0.0001$; **Table 5**). Of note, the rate of delays decreased from the first to the second run ($p = 0.001$), whereas no significant differences between runs were observed for the other error categories (**Table 6**). However, the overall reproducibility of object naming in-between both runs was excellent, as expressed by an overall Goodman and Kruskal's GK-gamma correlation coefficient of 0.95 ± 0.004 [confidence interval: 0.95; 0.96] (**Table 5**). The two most common error categories were wrong item naming (43% of all errors) and delay (25%; **Table 6**).

TABLE 4 | Patient characteristics.

No	Gender	Age	Handedness	Education	BIWOS [raw score (percentile)]			Word finding difficulties
					Semantic	Lexical	Overall	
1	Male	27	Right	UED	63 (69)	31 (16)	47 (42)	Moderate
2	Male	53	Right	UED	95 (>97)	89 (>97)	93 (>97)	Normal
3	Male	27	Left	UED	95 (>97)	97 (>97)	96 (>97)	Normal
4	Male	63	Right	UED equivalent	56 (62)	71 (90)	65 (84)	Slight
5	Male	74	Right	Not reported	63 (69)	59 (73)	61 (69)	Slight
6	Female	34	Right	UED equivalent	83 (96)	64 (82)	73 (88)	Normal
7	Female	76	Left	UED	76 (90)	83 (>97)	79 (96)	Normal
8	Male	40	Right	UED	93 (>97)	91 (>97)	92 (>97)	Normal
9	Male	53	Right	UED	83 (96)	66 (84)	75 (93)	Slight
10	Male	24	Right	UED	81 (95)	73 (92)	77 (95)	Slight

BIWOS, Bielefeld Screening for word finding difficulties for mild aphasia (29); UED, university entrance diploma.

Influence of Word Characteristics on Object Naming Correctness and Reliability

A two-factorial ANOVA including the factors SYLLABLES (two levels: one, two) and FREQUENCY (two levels: high, low) revealed no influence of both factors on the GK-gamma coefficients as a measure of reproducibility or an interaction between them (**Table 7**). In contrast, a significant main effect was found for the factor FREQUENCY on the correct object recognition rates ($F_{1,96} = 6.471$; $p < 0.05$) as well as on the correct picture naming rates ($F_{1,96} = 4.166$; $p < 0.05$) whereas there was no main or interaction effect on the correct object recognition or naming rates of the factor SYLLABLES (**Table 7**). Accordingly, *post-hoc* tests revealed significantly higher correct object recognition rates for the high vs. low word frequency (98 ± 3 vs. 99 ± 2%; $p < 0.05$) and a concordant statistical trend regarding the correct object naming rates (98 ± 2 vs. 97 ± 3%, $p = 0.06$; **Figure 2**).

Post-hoc comparisons revealed the lowest rates of delays for word class A (high WF, one syllable) as compared to all other classes ($p < 0.0001$, FDR-corrected, **Table 6**). In contrast, category III responses (e.g., dialect-related variants; see **Table 3** and **Supplementary Table 2**) were more frequent when naming one-syllable words and were highest in word class C (C-B: $p < 0.01$; C-D: $p < 0.001$; A-D: $p < 0.01$, FDR-corrected; **Table 6**). Self-corrections were equally distributed across the stimulus classes. Of note, all unexpected correct naming alternatives (e.g., dialect variants) encountered in the study are provided in the supplement (**Supplementary Table 2**). According to our hypothesis, the rate of wrong object namings increased with the difficulty level and was particularly more frequent in the stimulus classes of low WF (A-B: $p < 0.01$; A-CD: $p < 0.0001$; B-C: $p < 0.001$; B-D: $p < 0.05$, FDR-corrected; **Table 6**).

Influence of Subject Characteristics on Object Naming Correctness

To analyze the influence of subject characteristics on correct object recognition and naming rates (sum of both runs), we performed a three-factorial ANOVA with the factors GENDER (two levels), EDUCATION (two levels) and AGE GROUP (four levels). We, here, found a significant main effect of the factors AGE GROUP and EDUCATION on both correct object recognition and naming rates as well as a significant interaction between those two factors (**Table 8**). In contrast, the factor GENDER had no significant main effect on either object recognition or naming correctness and showed no interactions regarding the dependent variable object naming correctness. However, we observed an interaction with the factor AGE GROUP when analysing the effects on object recognition correctness (**Table 8**).

Second-level one-factorial ANOVA confirmed a significant main effect of the factor AGE in both the subgroups of lower and high education levels on the correct object recognition rates (low: $F_{1,35} = 12.3$, $p < 0.01$; high: $F_{1,90} = 12.2$, $p < 0.001$) as well as on the correct object naming rates (low: $F_{1,35} = 12.3$, $p < 0.01$; high: $F_{1,90} = 17.0$, $p < 0.0001$), thus suggesting the strongest influence of age on object naming in highly educated subjects. Of interest, *post-hoc* tests revealed a significantly lower rate of correct recognition as well as object naming for elderly subjects (age group 4) compared to all other age groups ($p < 0.01$, FDR-corrected; **Figure 3**). In addition, subjects of slightly advanced age, i.e., between the age of 54 and 71 years showed similar object recognition performance ($p > 0.1$) but worse object naming rates compared to younger individuals (age group 3 vs. 1 [2]: $p < 0.05$ [$p = 0.07$], FDR-corrected; **Figure 3**). These findings go along with a larger variance and less skewed data distribution in the elderly—particularly when less educated—as compared to young age (**Supplementary Figures 1, 2**).

In contrast, analysed by age categories, a one-factorial ANOVA showed a significant main effect of the factor EDUCATION on the picture naming performance only for young subjects that represented the largest age group (object recognition: $F_{1,64} = 4.0$, $p < 0.05$; object naming: $F_{1,64} = 5.0$, $p < 0.05$). No noteworthy effect of this factor was found in the other groups, apart from the elderly group, which showed a statistical trend (object naming: $F_{1,11} = 3.4$, $p = 0.09$). *Post-hoc* tests confirmed a statistical trend towards better picture recognition

TABLE 5 | Object recognition rates and naming reliability by stimulus.

A (one syllable, high WF)				B (two syllables, high WF)				C (one syllable, low WF)				D (two syllables, low WF)			
Object	Correct object recognition (naming) in %		γ [CI]	Object	Correct object recognition (naming) in %		γ [CI]	Object	Correct object recognition (naming) in %		γ [CI]	Object	Correct object recognition (naming) in %		γ [CI]
	Run 1	Run 2			Run 1	Run 2			Run 1	Run 2			Run 1	Run 2	
Arm	97 (96)	93 (92)	0.94 [0.85;1]	Eye	100	100		Lightning	98 (96)	98 (96)	1.0 [1;1]	Apple	100	100	
Bank	95	100		Car	99 (98)	100		Bus	99 (96)	99 (98)	0.99 [0.98;1]	Pear	100	98	
Tree	100	100		Glasses	100	100		Egg	98	100		Flower	100	100	
Bed	100	99		Angel	99 (98)	99 (98)	0.93 [0.83;1]	Barrel	95 (92)	97 (96)	0.91 [0.80;1]	Brush	96	97	0.72 [0.30;1]
Bread	98 (95)	99 (98)	0.91 [0.67;1]	Feather	97	99	1.0 [1;1]	Frog	98	99	0.94 [0.78;1]	Dragon	92 (91)	93 (92)	0.95 [0.89;1]
Book	99	100		Window	92	98		Comb	100	100		Bucket	100	100	
Fish	100	100		Finger	92 (88)	97 (95)	0.96 [0.91;1]	Button	94 (93)	96	0.98 [0.94;1]	Fork	98	100	
Foot	100	99 (98)		Trousers	100	100		Crane	98	98	0.83 [0.43;1]	Bell	99	100	
Glass	97 (95)	100 (99)	0.94 [0.88;1]	Island	93 (92)	95	0.98 [0.95;1]	Mouse	98	100		Harp	92	93	1.0 [1;1]
Hand	100	100		Chain	98 (97)	97 (96)	0.76 [0.5;1]	Arrow	98 (97)	97 (95)	0.94 [0.85;1]	Rabbit	95	95	0.96 [0.90;1]
House	99	99		Church	98 (97)	99 (98)	0.99 [0.97;1]	Mushroom	100 (99)	100		Hedgehog	100	100	
Heart	100	99		Suitcase	100	100		Skirt	94	95	0.92 [0.82;1]	Cheese	99 (96)	99 (97)	1.0 [1;1]
Dog	99	100	1.0 [1;1]	King	97	98	1.0 [0.98;1]	Scarf	97	99	0.95 [0.85;1]	Cat	100	100	
Hat	100	100		Crown	100	98		Shoe	100	98		Candle	100	100	
Dress	99	99	1.0 [1;1]	Ladder	100	100		Sponge	92	93	0.95 [0.87;1]	Spoon	100	100	
Cow	97	95 (94)	0.94 [0.85;1]	Lion	98	100		Pig	98 (95)	99	0.97 [0.92;1]	Knife	100 (98)	100 (98)	0.94 [0.78;1]
Mouth	99 (89)	100 (90)	0.87 [0.72;1]	Wall	98 (97)	98	0.98 [0.92;1]	Sword	90 (89)	87 (87)	0.91 [0.81;1]	Mussel	95	95	0.93 [0.83;1]
Horse	100	100		Snake	99	100		Ski	97 (95)	97 (95)	0.91 [0.81;1]	Doll	88	93	0.92 [0.82;1]
Wheel	98 (96)	98 (95)	0.83 [0.56;1]	Key	100	98		Stork	97 (96)	96	0.93 [0.84;1]	Saw	98 (96)	99 (98)	0.83 [0.57;1]
Padlock	100 (98)	100 (98)	0.91 [0.67;1]	Sun	99	100		Pot	99	99	0.98 [0.94;1]	Swing	99	99	0.96 [0.83;1]
Star	100	98		Carpet	100 (98)	100 (99)	0.97 [0.88;1]	Sausage	98	99 (98)	0.99 [0.97;1]	Scissor	100	99	
Chair	99	98		Devil	95	95 (94)	0.92 [0.82;1]	Tooth	99	100		Bow	94 (93)	95	0.98 [0.93;1]
Table	100	99		Drum	100	100		Fence	98 (95)	98 (96)	0.88 [0.73;1]	Syringe	98	98 (97)	0.95 [0.85;1]
Door	99	99		Bird	100 (98)	100 (95)	0.89 [0.68;1]	Tent	99	99	1.0 [1;1]	Alarm clock	86 (84)	92 (91)	0.89 [0.79;099]

(Continued)

TABLE 5 | Continued

A (one syllable, high WF)				B (two syllables, high WF)				C (one syllable, low WF)				D (two syllables, low WF)			
Object	**Correct object recognition (naming) in %**		**γ [CI]**	**Object**	**Correct object recognition (naming) in %**		**γ [CI]**	**Object**	**Correct object recognition (naming) in %**		**γ [CI]**	**Object**	**Correct object recognition (naming) in %**		**γ [CI]**
	Run 1	**Run 2**			**Run 1**	**Run 2**			**Run 1**	**Run 2**			**Run 1**	**Run 2**	
Clock	100 (99)	100 (99)	1.0 [1;1]	Newspaper	94 (93)	93	0.99 [0.97;1]	Dwarf	95 (91)	94 (88)	0.95 [0.89;1]	Dice	100	100	
Overall	**99 ± 1 (98±3)**	**99 ± 2 (98±3)**	**0.94 [0.91;0.97]**	**Overall**	**98 ± 3 (97±3)**	**99 ± 2 (98±2)**	**0.95 [0.93;0.97]**	**Overall**	**97 ± 3 (96±3)**	**97 ± 3**	**0.95 [0.94;0.97]**	**Overall**	**97 ± 4**	**98 ± 3 (97±3)**	**0.96 [0.94;0.97]**

*Object names are given in English (for original German words, please see **Table 2**). Correct object naming rates are provided in brackets following the correct object recognition rates if differing from those. The percentage of delayed (however correct) object namings was maximum 5.3% and is indicated by colour-encoding for each run: white = no delay; light yellow = <1% delays; yellow = 1–3% delays; orange = >3% delays. Reliability measures (GK-gamma) are provided for each word and overall, including the confidence interval. Light grey: GK-gamma could not be calculated due to perfect object naming in at least one run. Dark grey: Confidence interval was zero due to very low number of errors in at least one run; thus, the respective GK-gamma values were not considered for further analysis. γ, GK-gamma; CI, confidence interval.*

TABLE 6 | Error frequencies by category and stimulus class.

Error		Run	Stimulus class				Overall
Category	**Description**		**A (1 syllable, high WF)**	**B (2 syllables, high WF)**	**C (1 syllable, low WF)**	**D (2 syllables, low WF)**	
2	Delay	1	12.3% (0.2%)	32.3% (1.2%)	25.7% (1.4%)	31.2% (1.5%)	27.2% (1.1%)
		2	12.5% (0.2%)	26.8% (0.7%)	23.1% (1.0%)	27.4% (0.9%)	23.4% (0.7%)
		Pooled	12.4% (0.2%)	30.1% (0.9%)	24.5% (1.2%)	29.6% (1.2%)	25.5% (0.9%)
3	Alternative naming, e.g., dialect-related variant	1	41.5% (0.8%)	16.1% (0.6%)	21.7% (1.2%)	8.4% (0.4%)	18.9% (0.7%)
		2	39.1% (0.8%)	19.5% (0.5%)	21.0% (0.9%)	9.7% (0.3%)	20.4% (0.6%)
		Pooled	40.3% (0.8%)	17.5% (0.5%)	21.4% (1.0%)	9.0% (0.4%)	19.6% (0.7%)
4	Self-corrected	1	16.9% (0.3%)	13.7% (0.5%)	8.0% (0.4%)	10.4% (0.5%)	11.2% (0.4%)
		2	14.1% (0.3%)	18.3% (0.5%)	6.3% (0.3%)	12.4% (0.4%)	11.7% (0.4%)
		Pooled	15.5% (0.3%)	15.5% (0.5%)	7.2% (0.3%)	11.2% (0.5%)	11.4% (0.4%)
5	Wrong	1	29.2% (0.6%)	37.9% (1.4%)	44.6% (2.4%)	50.0% (2.3%)	42.7% (1.7%)
		2	34.4% (0.7%)	35.4% (0.9%)	49.7% (2.2%)	50.4% (1.7%)	44.5% (1.4%)
		Pooled	31.8% (0.6%)	36.5% (1.2%)	46.9% (2.3%)	50.2% (2.0%)	43.5% (1.5%)

*Percentages of error rates are shown relative to the total amount or errors and relative to all stimuli (in brackets). For a more comprehensive description of the error types, please consider **Table 3**. For a descriptive overview of the delay rates by stimulus/word, cf. **Table 5** (colour-encoding). WF, word frequency.*

and naming for the subgroups of young and elderly subjects ($p = 0.09$, FDR-corrected; **Figure 3**). In summary, the effect of the subject's age—and particularly the affiliation to the age group of 72 or more years—seems to overweigh clearly the effect of the educational level on correct object identification and naming.

Influence of Subject Characteristics on Object Naming Reliability

In accordance with the factors on naming performance, we here analysed the influence of subject characteristics on the retest reliability of the object naming, i.e., on GK-gamma coefficients using a three-factorial ANOVA that included the factors GENDER (two levels), EDUCATION (two levels) and AGE GROUP (four levels).

In line with our results regarding object recognition and naming correctness, the factor AGE GROUP had a significant main effect on naming reliability ($F_{1,93} = 5.3, p < 0.05$). However, no main effect was found for the factors EDUCATION and GENDER. Although no two-way interactions were observed, the ANOVA revealed a significant interaction between the factors AGE GROUP × EDUCATION × GENDER ($F_{1,93} = 6.0, p < 0.05$).

Post-hoc tests showed that higher age was associated with worse test–retest reliability of the naming responses. Accordingly, lower GK-gamma coefficients were found in the age group of 72 years or older as compared to subjects younger than 54 years (i.e., groups 1 and 2; $p < 0.05$, FDR-corrected; **Figure 4**).

Patients

In the pilot cohort of patients, showing evidence for impaired lexicosemantic word finding skills according to the BIWOS score in at least half of the cases, results for correct object recognition

and naming (**Table 9**) were not significantly different from those of an age-matched cohort of $n = 30$ healthy subjects (median age [range] = 46 [24;79] years; 40% male; pooled object naming [recognition] rate: 96.4 ± 4.9 [97.4 ± 4.2]%; $p > 0.1$). Overall, the test–retest reliability of the response category (five levels; see **Table 3**) was high, as expressed by a GK-gamma coefficient ranging from 0.74 (A) to 0.94 (D; **Table 9**). In line with our results from the healthy population indicating high age (above 72 years) as the major factor influencing task performance, we here observed the least correct object recognition and naming rates in the two older patients (patient 5: 91/88%; patient 7: 94/91%). In contrast to the healthy subjects, the better object recognition performance in run 2 could not be reproduced in the patients (run 1: 97 ± 2/97 ± 3% vs. run 2: 97 ± 4/95 ± 5%; $p > 0.1$). However, we found a significantly lower frequency of delayed responses in the second run (run 1: 5.4 ± 7.7 vs. run 2: 2.7 ± 5.7%; $p < 0.001$; **Table 9**). There was no significant correlation of correctness, delay or reliability of object identification or naming with the clinical aphasia score (BIWOS).

TABLE 7 | Influence of word-specific factors on object recognition and naming.

Factor	Object recognition		Object naming		Df, residuals
	F	*p/p* level	*F*	*p/p* level	
Main effects					
Syllables	0.503	0.480	0.020	0.888	1,96
Word frequency	6.471	0.013	4.166	0.044	
Interactions					
Syllables:word frequency	0.920	0.340	0.971	0.327	1,96

F statistics and p-values are provided for the two dependent variables object recognition and object naming.

DISCUSSION

This work provides the first freely available data set of pictures, developed for experimental and clinical use (e.g., in the context of pre-surgical and intraoperative functional language mapping), specifically for German-speaking subjects. The CoNaT was especially designed for the context of language mapping using picture naming, where highly reliable naming performance is a pre-requisite of successful testing. The picture set, consisting

TABLE 8 | Influence of subject-specific factors on object recognition and naming.

Factor	Object recognition		Object naming		Df, residuals
	F	*p/p* level	*F*	*p/p* level	
Main effects					
Age group	39.8	<0.0001	43.5	<0.0001	1,121
Education	4.4	0.039	4.2	0.044	
Gender	1.7	0.193	0.6	0.424	
Interactions					
Age group:education	11.1	0.001	9.1	0.003	1,121
Age group:gender	4.4	0.037	2.7	0.105	
Education:gender	0.05	0.830	0.0	0.981	
Age group:education:gender	4.0	0.048	1.7	0.189	

F statistics and p-values are provided for the two dependent variables object recognition and object naming.

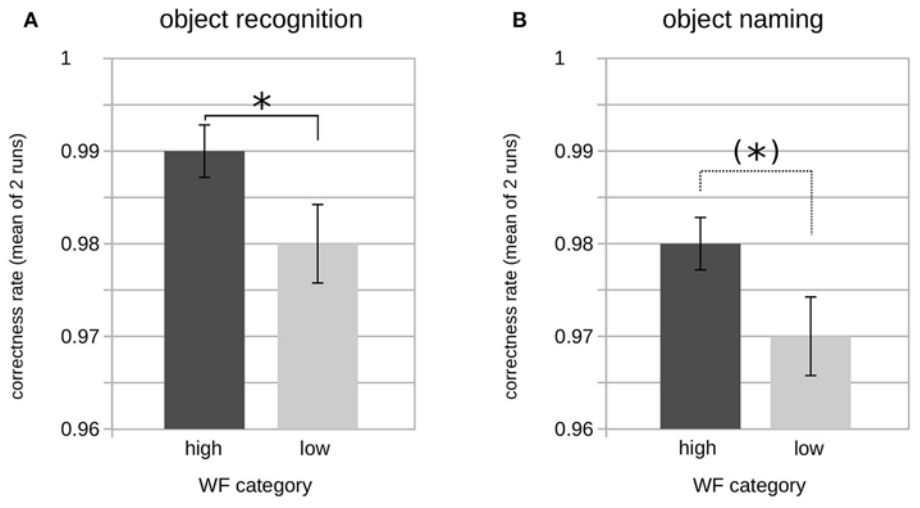

FIGURE 2 | Rates of correct object recognition and naming by word frequency category. Bar plot showing the average correct object recognition **(A)** and object naming **(B)** rates of both runs (pooled) by word frequency (WF). Significant differences according to groupwise *post-hoc* comparison of means are indicated by asterisks [(*)$p < 0.1$; *$p < 0.05$]. Please note the limited ranges of the *y*-axis, for better readability.

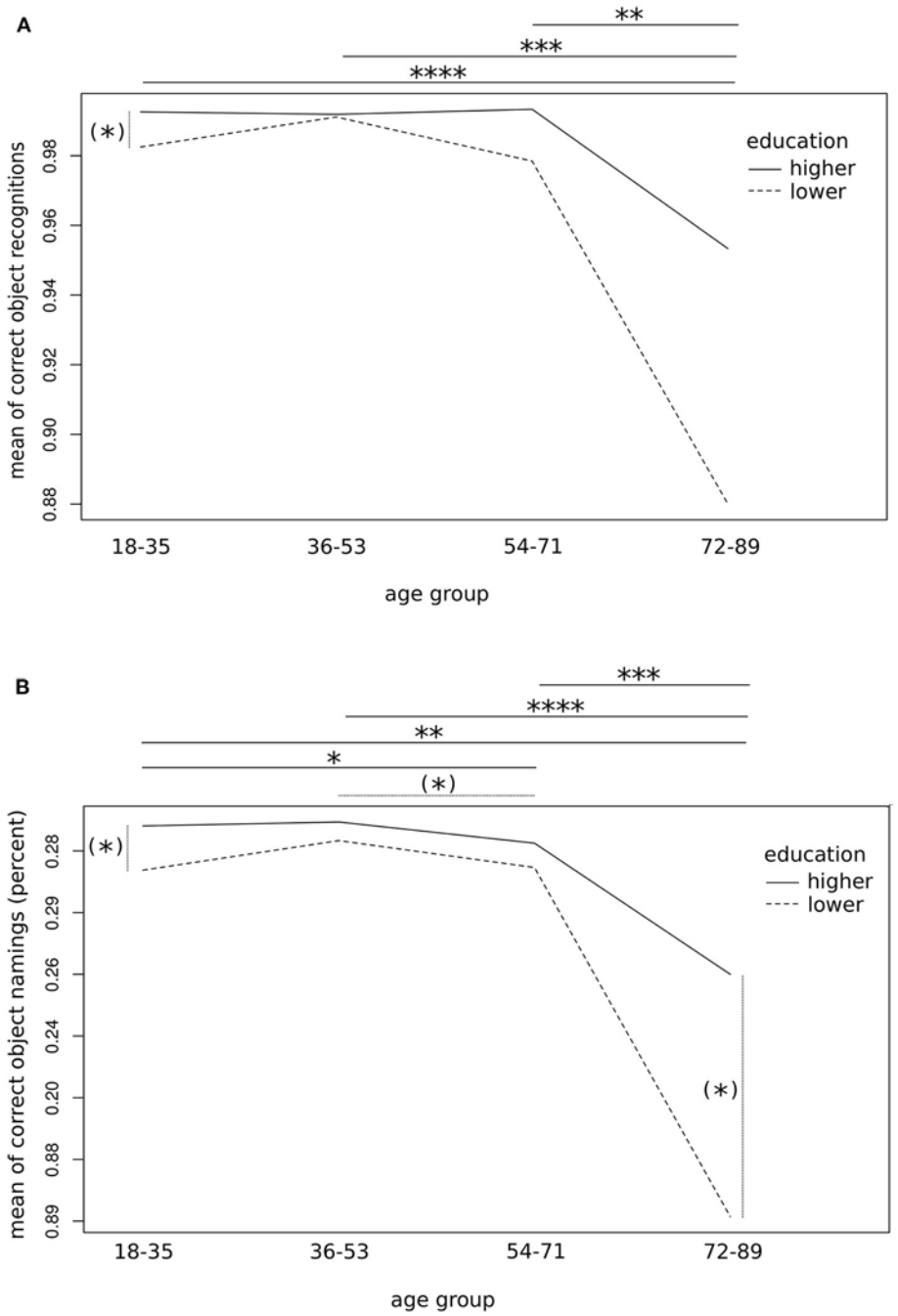

FIGURE 3 | Influence of age group on object naming performance. Interaction plots showing average correctness of object recognition **(A)** and naming **(B)** by age groups and education level (i.e., with/without university admission diploma or equivalent). Pooled data of both runs per 100 trials are provided. Significant differences according to groupwise *post-hoc* comparison of means followed by FDR correction are indicated by asterisks [(*)$p < 0.1$; *$p < 0.05$; **$p < 0.01$, ***$p < 0.001$, ****$p < 0.0001$]. Please note the limited ranges of the *y*-axis, for better readability.

of 100 black and white drawings, stratified by word length (number of syllables) and word frequency, showed excellent correct object recognition and naming rates as well as high reliability coefficients across all item categories and subjects. However, a small learning effect was observed across the two runs of the test. Moreover, we found a significant negative effect of low word frequency and high age (older than 72 years) on the task performance.

Influence of Subject Characteristics

Amongst subject-related factors, age had the strongest effect on both the picture naming correctness and the test–retest

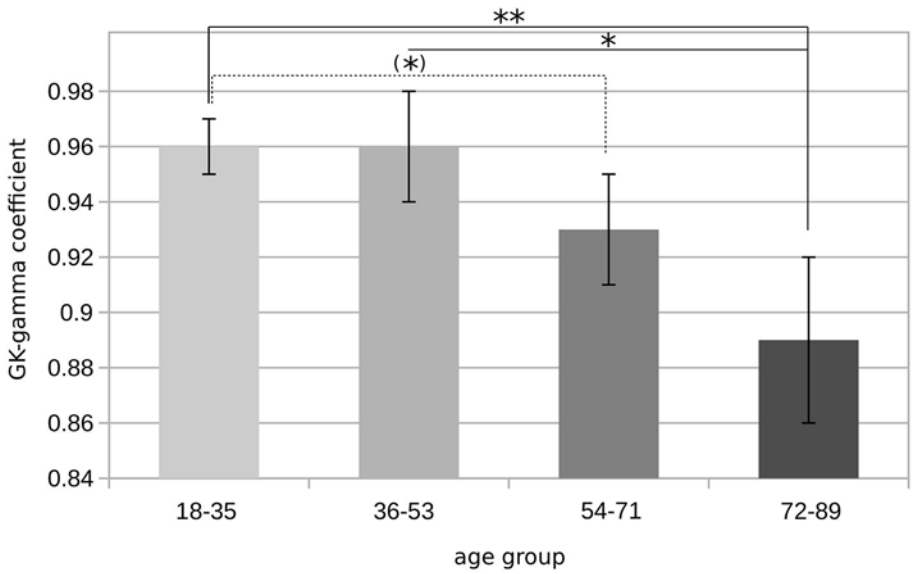

FIGURE 4 | Object naming reliability by age groups. Bar plot showing mean GK-gamma coefficients (*y*-axis), grouped by age categories; error bars represent SEM; significance levels are indicated by asterisks [(*)$p < 0.1$; *$p < 0.05$; **$p < 0.01$].

TABLE 9 | Object naming performance of patients by stimulus class and run.

	Run	Stimulus class				Overall
		A	B	C	D	
Correct object recognition (/naming) rates	1	98 ± 2% (97 ± 3%)	97 ± 4% (96 ± 5%)	98 ± 3% (97 ± 4%)	96 ± 4%	97 ± 3% (96 ± 4%)
	2	96 ± 4% (95 ± 6%)	98 ± 4% (97 ± 5%)	97 ± 4% (95 ± 8%)	95 ± 5%	97 ± 4% (95 ± 6%)
	Pooled	97 ± 3% (96 ± 4%)	98 ± 4% (97 ± 5%)	97 ± 3% (96 ± 6%)	95 ± 5%	97 ± 4% (96 ± 5%)
Reliability (GK-gamma [CI])		0.74 ± 0.10 [0.54; 0.95]	0.83 ± 0.08 [0.67; 0.99]	0.87 ± 0.06 [0.76; 0.97]	0.94 ± 0.03 [0.88; 1.00]	0.86 ± 0.03 [0.80; 0.92]

Correct object recognition and naming rates as well as GK-gamma coefficients are indicated by stimulus class, run and overall. Please note that correct object naming rates are indicated in brackets following the corresponding object recognition rates if different from those. The average percentage of delayed (however correct) object namings per word class was maximum 7.2% and is indicated by colour-encoding for each run: yellow = <3% delays; orange = 3–5% delays; light red = >5% delays.

reliability of the naming responses. Its negative effect on the task performance increased with age and was most evident in elderly subjects who are 72 years or older. The high effect size of the factor AGE was also reflected by its significant correlation with the object naming performance in the patient cohort, despite the small sample size of $n = 10$.

This finding is widely in line with previous research that also found an effect of age on language skills in general and picture naming in particular (36–38). Furthermore, multiple subject-related factors including vision impairment, general cognitive decline, reduced attention span, slowed perceptual analysis (37, 39, 40), as well as linguistic factors such as weakening of semantic connections within the language system (36, 41) have been discussed to affect language performance.

In line with previous publications of other groups (42, 43), a high general educational level (i.e., qualification for admission to university or equivalent) was associated with higher rates of correct picture recognition and naming in our data set. This effect was most prominent in the subgroups of elderly participants (i.e., 54 years or older) for which the factor education was more balanced as opposed to the mostly highly educated younger participants (cf. Limitations). The finding, however, that educational level did not correlate with the test–retest reliability of the responses, might reflect the robustness of the factorial influence on naming correctness, independent of supposable learning effects between both runs.

From the clinical point of view, the clearly impaired and less reliable task performance of elderly healthy subjects, especially when their level of education is low, points out that language

mapping and monitoring results should be interpreted with particular caution to avoid false-positive results. In such cases, a more rigorous selection of the items to be included in the picture set prior to the clinical use might be advisable to reduce the risk of misinterpretations, e.g., by omitting items with generally suboptimal correct naming rates and delayed responses (cf. **Table 5**). Moreover, increasing the usual number of individual test runs may be helpful to make sure that potentially problematic items are excluded.

As opposed to age and educational level, we found no significant influence of the factor GENDER on picture naming correctness, indicating that the selected items can be considered gender neutral and appropriate for testing procedures with both male and female participants. This finding could explain the disagreement, e.g., with the previous work of (42) who reported a gender effect with mostly better performance of male subjects in a picture naming task, which they explained by specific components of their picture set [e.g., items like "tripod," "compass," and "dart"; cf. **Table 3** in (42)]. In this regard, the result of "gender neutrality" met with our expectations, given that we excluded words with assumed gender effect, e.g., "screw-driver" from our picture set a priori in order to establish a robust, gender-independent picture set for clinical use.

The robustness of the picture set is also reflected by the overall excellent and highly reliable picture naming performance of the patient cohort, showing no significant difference in naming correctness rates compared to a matched group of healthy subjects. At least for the tested cohort of patients with utmost mild aphasic symptoms, we also found no significant correlation between picture naming correctness and lexicosemantic performance according to the formal testing using the BIWOS. This finding underlines the intention of the picture set, which was not designed to be used as a sensitive screening instrument for (even mild) aphasia but rather as reliable and robust monitoring tool, also suited for patients with mild aphasic symptoms.

Influence of Word Characteristics

Response Correctness

In this study, we investigated the influence of two important word characteristics, i.e., the word frequency and the number of syllables, on the correctness of picture recognition and verbal naming responses. Here, we used the factor lexical word frequency as the most common and standardised measure of frequency of (word) use in everyday life. We found a significantly better performance, i.e., higher correct object recognition and naming rates, when the subjects were asked to name high-frequency words. In addition, there were fewer delays when naming high-frequency words, at least in the subset of monosyllables. These results agree well with previous research that also showed an effect of word frequency on naming accuracy [e.g., (44–46)].

In contrast to the word frequency, there was no significant influence of the factor word length, expressed by the number of syllables (mono- vs. bisyllabic), on neither the correctness of picture recognition or naming nor the retest reliability of the naming responses between the two runs. This finding is in line with the results of Santiago et al. (47) who also did not find a significant influence of the number of syllables (also comparing mono- vs. bisyllabic words) on the occurrence of errors in a standard picture naming task.

Delay

We observed significantly less delays (as a measure of response latency) for class A words (i.e., monosyllabic, high WF) as compared to all other word categories.

This finding indicates an influence of word frequency on response latency only for monosyllabic words and, vice versa, an influence of the number of syllables only for high-frequency words, thereby reflecting the heterogeneous results of previous studies regarding the effect of word length and word frequency on response latency. In line with others (46, 48), Alario et al. (49) identified word frequency but not the number of syllables as significant contributors for the prediction of response latency. Other research groups, in contrast, could not confirm an effect of word length on response latency (50–52).

The divergent study results could be explained by methodological differences across studies such as the distinct characteristics of the applied picture sets. For instance, we here used comparatively high median word frequencies and a small range of word lengths (number of syllables), due to the primary objective of our study to develop a robust language monitoring tool rather than a very sensitive screening instrument. Further possible influencing factors include (i) the different age ranges of the study participants (usually university students younger than 30 year-old compared to a wide age range of 18–89 years in our study), (ii) interactions with other item- or word-related characteristics [e.g., lexical/conceptual characteristics such as age of acquisition, animacy, relevance to everyday life, frequency of syllables or word form characteristics such as phonological or morphological complexity; cf. (49, 53, 54)], and (iii) priming processes (55, 56) inherent to the respective picture sets, which were not controlled in this study (see also Limitations).

Taken together, due to the influence of word characteristics on both naming correctness and response latency, it might be advisable to start the clinical testing routine for patients with relatively advanced aphasic symptoms using the components of the stimulus classes A–D consecutively in alphabetic order. Items might even be omitted class-wise in severe cases.

Alternative Naming Variants and Clinical Implications

In addition to different response delay rates between mono- vs. bisyllabic high-frequency words, the word-class-wise analysis also showed a higher rate of unexpected, alternative responses like over-specifications, dialectal or cultural variants for monosyllabic words. In accordance with our hypothesis that rather short, monosyllabic words are generally more prone to over-specification (e.g., "water glass" for "glass"), this was the reason for two thirds of the unexpected alternative responses in word class A in our study.

In clinical practise, e.g., for monitoring during awake surgery using DCS or for preoperative language mapping

using TMS, where robustness of the test is of particular importance to assure correct identification of transient language impairments, it might be advisable to reduce the pictures by avoiding items with relatively high alternative naming rates (cf. **Supplementary Table 2**). However, given the overall excellent reliability of the naming responses as expressed by high GK-gamma coefficients (cf. **Table 5**), alternative naming responses should usually be identifiable in the preparatory test run, i.e., the baseline investigation, which allows to tailor the picture set on an individual basis (cf. Influence of Subject Characteristics section). In general, a baseline investigation of naming performance is highly recommended, especially regarding the clinical application in patients using TMS and/or DCS for language mapping, in order to identify speech language difficulties such as increased response latencies (delayed naming) related to distinct stimuli/words.

Learning Effect

Although the overall reproducibility of the object naming in-between both runs was excellent (GK-gamma = 0.95), the mean correct object recognition and naming rates improved slightly from the first to the second run in the healthy volunteers. In line with this finding, we found a concordant decrease in the rate of delayed namings. These findings might result from a repetition priming effect, which is considered an implicit learning phenomenon of non-hippocampal origin described for repeated picture naming, correlating to reduced neural activity in repeated conditions [e.g., (57)], which lasts for at least several weeks [cf. (58) for review]. In this regard, the observation of a learning effect further supports the evidence that high word frequency (as a measure of repetition) correlates with better picture naming performance.

In contrast to healthy subjects, the second run was not associated with a higher overall rate of correct object naming or recognition in patients, which could be attributed to the much smaller sample size as well as to the comparatively stronger effects of reduced attention, lower cognitive resilience or exertion fatigue in this cohort [cf. (59–61)]. However, repetition had a significant and—compared to the healthy subjects—relatively strong facilitating effect on the rate of delayed namings in this cohort. This finding indicates that naming delays are particularly prone to repetition priming effects in patients. Accordingly, our data support the assumption that the risk of spontaneous naming errors, unrelated to TMS/DCS stimulation, decreases with the number of repetitions. On the other hand, it seems likely that the susceptibility to TMS interference expressed by naming errors in general and by prolonged naming latencies in particular decreases along with the repetition of stimuli during a TMS/DCS mapping. Therefore, it seems mandatory to define an optimal trade-off regarding the size of the stimuli/word set to be used during language mapping, as well as to take the number of stimuli/word repetitions into account when analysing the mapping results. A more detailed investigation of this topic, however, lies beyond the scope of this study and deserves to be further addressed in the future.

Limitations

As the intended use of the picture set is to serve, i.a., for clinical mapping and monitoring of patients with brain tumours, which mostly occur in advanced age, our study cohort comprises a broad age range—in contrast to the vast majority of previous, similar studies. However, due to several constraints regarding the recruitment of older subjects (i.e., reduced access to the population via existing databases and media, morbidity/reduced mobility impeding on-site participation, non-matching of in- and exclusion criteria), the cohort of older subjects remains underrepresented in our study collective. Moreover, the factorial analysis regarding the influence of age and educational level suffers from an unavoidable interaction between both factors, which we attribute mostly to a considerably increased access to high education over the past decades.

Although we analysed two major word-related factors on picture naming performance and response delay, i.e., word frequency and the number of syllables, other possible factors such as alternative measures of word familiarity [e.g., frequency of syllables and age of acquisition; (53)] and word length as well as picture-related factors like the visual complexity of the drawing, image agreement and imageability [e.g., (49)] were not controlled in this study.

The CoNaT has been specifically designed for German native speakers although the stimuli might be well-suited to be used also in other languages. Please note that the suitability of individual items should be checked prior to the test administration to ensure their fit with respect to relevant linguistic criteria.

CONCLUSION

In summary, the CoNaT provides an overall robust and reliable picture naming tool, optimised for the clinical use to map and monitor language functions in patients. We here provide normative data along with practical, clinical suggestions for the administration of the picture set, hereby taking important word- and subject-related factors of object recognition and naming into account. Based on the results, we are convinced that the entire picture set can be readily used in healthy subjects and patients, even with mild to moderate aphasic symptoms but should always be tested and—if necessary—reduced on an individual basis, particularly in elderly subjects of low educational level and patients. Here, starting to test with the most robust stimulus class A (high WF, monosyllables) over B (high WF, bisyllables) to C and D (low WF) and paying particular attention to items that are comparatively prone to alternative naming variants seem to be advisable.

DATA AVAILABILITY STATEMENT

The raw data supporting the conclusions of this article will be made available by the authors, without undue reservation.

ETHICS STATEMENT

The studies involving human participants were reviewed and approved by local ethics committee (Ethikkommission der Medizinischen Fakultät der Universität zu Köln). Written informed consent for participation was not required for this study in accordance with the national legislation and the institutional requirements.

AUTHOR CONTRIBUTIONS

CWL: conceptualisation, methodology, formal analysis, investigation, writing – original draught, visualisation, and supervision. JP: formal analysis, investigation, and writing – original draught. SK: investigation and data curation. CN: investigation and writing – review and editing. CG: conceptualisation and writing – review and editing. RG: funding acquisition and writing – review and editing. KJ: conceptualisation, methodology, writing – original draught, and supervision. All authors contributed to the article and approved the submitted version.

FUNDING

This work was supported by institutional fundings of the Department of Neurosurgery of the University Hospital of Cologne. CWL received further funding from the Faculty of Medicine of the University of Cologne (Gerok 16/8).

ACKNOWLEDGMENTS

We thank the authors Aichert, Marquardt, and Ziegler for their permission to use the computer-based speech analysis (Computergestützte Generierung und Analyse von Sprachmaterial nach Struktur- und Frequenzmerkmalen; Munich, Germany: EKN; unpublished).

SUPPLEMENTARY MATERIAL

The Supplementary Material for this article can be found online at: https://www.frontiersin.org/articles/10.3389/fneur.2021.633068/full#supplementary-material

REFERENCES

1. Mahon BZ, Caramazza C. Organization of conceptual knowledge of objects in the human brain. In: Ochsner KN, Kosslyn S, editors. *The Oxford Handbook of Cognitive Neuroscience. Vol 1*. New York, NY: Oxford University Press (2014). p. 554–77. doi: 10.1093/oxfordhb/9780199988693.013.0027
2. Freyschlag CF, Duffau H. Awake brain mapping of cortex and subcortical pathways in brain tumor surgery. *J Neurosurg Sci*. (2014) 58:199–213.
3. Eddington CM, Tokowicz N. How meaning similariy influences ambiguous word processing: the current state of the literature. *Psychon Bull Rev*. (2014) 22:13–37. doi: 10.3758/s13423-014-0665-7
4. Levelt WJM. Accessing words in speech production: stages, processes and representations. *Cognition*. (1992) 42:1–22. doi: 10.1016/0010-0277(92)90038-J
5. Newman RS, German DJ. Life span effects of lexical factors on oral naming. *Lang Speech*. (2005) 48:123–56. doi: 10.1177/00238309050480020101
6. Kittredge AK, Dell GS, Verkuilen J, Schwartz MF. Where is the effect of frequency in word production? Insights from aphasic picture-naming errors. *Cogn Neuropsychol*. (2008) 25:463–92. doi: 10.1080/02643290701674851
7. Nickels L, Howard D. Aphasic naming: what matters? *Neuropsychologia*. (1995) 33:1281–303. doi: 10.1016/0028-3932(95)00102-9
8. Brodeur MB, Kehayia E, Dion-Lessard G, Chauret M, Montreuil T, Dionne-Dostie E, et al. The bank of standardized stimuli (BOSS): comparison between French and English norms. *Behav Res Methods*. (2012) 44:961–70. doi: 10.3758/s13428-011-0184-7
9. Kremin H, Akhutina T, Basso A, Davidoff J, De Wilde M, Kitzing P, et al. A cross-linguistic data bank for oral picture naming in Dutch, English, German, French, Italian, Russian, Spanish, and Swedish (PEDOI). *Brain Cogn*. (2003) 53:243–6. doi: 10.1016/S0278-2626(03)00119-2
10. Hervey-Jumper SL, Berger MS. Technical nuances of awake brain tumor surgery and the role of maximum safe resection. *J Neurosurg Sci*. (2015) 59:351–60.
11. Seghier ML, Price CJ. Interpreting and utilising intersubject variability in brain function. *Trends Cogn Sci*. (2018) 22:517–30. doi: 10.1016/j.tics.2018.03.003
12. Ojemann GA. Individual variability in cortical localization of language. *J Neurosurg*. (1979) 50:164–9. doi: 10.3171/jns.1979.50.2.0164
13. Siegel JS, Ramsey LE, Snyder AZ, Metcalf NV, Chacko RV, Weinberger K, et al. Disruptions of network connectivity predict impairment in multiple behavioral domains after stroke. *PNAS*. (2016) 113:4367–87. doi: 10.1073/pnas.1521083113
14. Vilasboas T, Herbet G, Duffau H. Challenging the myth of right "non-dominant" hemisphere: lessons from cortico-subcortical stimulation mapping in awake surgery and surgical implications. *World Neurosurg*. (2017) 103:449–56. doi: 10.1016/j.wneu.2017.04.021
15. Duffau H. Mapping the connectome in awake surgery for gliomas: an update. *J Neurosurg Sci*. (2017) 61:612–30. doi: 10.23736/S0390-5616.17.04017-6
16. Penfield W, Roberts L. *Speech and Brain Mechanisms*. Princeton, NJ: Princeton University Press (1959). doi: 10.1515/9781400854677
17. Mandonnet E, Sarubbo S, Duffau H. Proposal of an optimized strategy for intraoperative testing of speech and language during awake mapping. *Neurosurg Rev*. (2016) 40:29–35. doi: 10.1007/s10143-016-0723-x
18. Levelt WJM, Praamstra P, Meyer AS, Helenius P, Salmelin R. An MEG study of picture naming. *J Cogn Neurosci*. (1998) 10:5. doi: 10.1162/089892998562960
19. Liljeström M, Hultén A, Parkkonen L, Salmelin R. Comparing MEG and fMRI views to naming actions and objects. *Hum Brain Mapp*. (2009) 30:6. doi: 10.1002/hbm.20785
20. Emmorey K, Mehta S, Grabowski TJ. The neural correlates of sign versus word production. *NeuroImage*. (2007) 36:202–8. doi: 10.1016/j.neuroimage.2007.02.040
21. Pascual-Leone A, Bartrés-Faz D, Keenan JP. Transcranial magnetic stimulation: studying the brain-behaviour relationship by induction of 'virtual lesions'. *Philos T R Soc B*. (1999) 354:1229–38. doi: 10.1098/rstb.1999.0476
22. Lioumis P, Zhdanov A, Mäkelä N, Lehtinen H, Wilenius J, Neuvonen T, et al. A novel approach for documenting naming errors induced by navigated transcranial magnetic stimulation. *J Neurosci Methods*. (2012) 204:349–54. doi: 10.1016/j.jneumeth.2011.11.003
23. Hernandez-Pavon JC, Mäkelä N, Lehtinen H, Lioumis P, Mäkelä J. Effects of navigated TMS on object and action naming. *Front Hum Neurosci*. (2014) 8:660. doi: 10.3389/fnhum.2014.00660
24. Snodgrass JG, Vanderwart M. A standardized set of 260 pictures: norms for name agreement, image agreement, familiarity, and visual complexity. *J Human Learn Memory*. (1980) 6:174–215. doi: 10.1037/0278-7393.6.2.174
25. Brodeur MB, Dionne-Dostie E, Montreuil T, Lepage M. The bank of standardized stimuli (BOSS), a new set of 480 normative photos of objects to be used as visual stimuli in cognitive research. *PLoS ONE*. (2010) 5:e10773. doi: 10.1371/journal.pone.0010773

26. Brodeur MB, Guérard K, BourasM. Bank of standardized stimuli (BOSS) phase II: 930 new normative photos. *PLoS ONE*. (2014) 9:e106953. doi: 10.1371/journal.pone.0106953
27. Huber W, Poeck K, Weniger D, Willmes K. *Aachener Aphasie Test (AAT)*. Göttingen: Hogrefe - Verlag für Psychologie (1983).
28. Deloche G, Hannequin D, Dordain M, Perrier D, Pichard B, Quint S, et al. Picture confrontation oral naming: performance differences between aphasics and normals. *Brain Lang*. (1996) 53:105–20. doi: 10.1006/brln.1996.0039
29. Benassi A, Gödde V, Richter K. *BIWOS: Bielefelder Wortfindungsscreening für leichte Aphasien*. Hofheim: natverlag (2012).
30. World Medical Association. World Medical Association Declaration of Helsinki: ethical principles for medical research involving human subjects. *JAMA*. (2013) 310:2191–4. doi: 10.1001/jama.2013.281053
31. Folstein MF, Folstein SE, McHugh PR. "Mini-mental state". A practical method for grading the cognitive state of patients for the clinician. *J Psychiatr Res*. (1975) 12:189–98. doi: 10.1016/0022-3956(75)90026-6
32. Baayen R, Piepenbrock R, Gulikers L. *Data From: The CELEX Lexical Database*. Philadelphia, PA: Liguistic Data Consortium (1995).
33. Barbarotto R, Laiacona M, Macchi V, Capitani E. Picture reality decision, semantic categories and gender: a new set of pictures, with norms and an experimental study. *Neuropsychologia*. (2002) 40:1637–55. doi: 10.1016/S0028-3932(02)00029-5
34. Laiacona M, Barbarotto R, Capitani E. Human evolution and the brain representation of semantic knowledge: is there a role for sex differences? *Evol Hum Behav*. (2006) 27:158–68. doi: 10.1016/j.evolhumbehav.2005.08.002
35. Benjamini Y, Hochberg Y. Controlling the false discovery rate – a practical and powerful approach to multiple testing. *J Royal Stat Soc Ser B*. (1995) 57:289–300. doi: 10.1111/j.2517-6161.1995.tb02031.x
36. Verhaegen C, Poncelet M. Changes in naming and semantic abilities with aging from 50 to 90 years. *J Int Neuropsychol Soc*. (2012) 19:119–26. doi: 10.1017/S1355617712001178
37. Tsang HL, Lee TM. The effect of ageing on confrontational naming ability. *Arch Clin Neuropsychol*. (2003) 18:81–9.
38. Zec RF, Markwell SJ, Burkett NR, Larsen DL. A longitudinal study of confrontation naming in the "normal" elderly. *J Int Neuropsychol Soc*. (2005) 11:716–26. doi: 10.1017/S1355617705050897
39. Albert MS, Heller HS, Milberg W. Changes in naming ability with age. *Psychol Aging*. (1988) 3:173–8. doi: 10.1037/0882-7974.3.2.173
40. Goulet P, Ska B, Kahn HJ. Is there a decline in picture naming with advancing age? *J Speech Hear Res*. (1994) 37:629–44. doi: 10.1044/jshr.3703.629
41. Valente A, Laganaro M. Ageing effects on word production processes: an ERP topographic analysis. *Lang Cogn Neurosci*. (2015) 30:1259–72. doi: 10.1080/23273798.2015.1059950
42. Randolph C, Lansing AE, Ivnik RJ, Cullum CM, Hermann BP. Determinants of confrontation naming performance. *Arch Clin Neuropsych*. (1999) 14:489–96. doi: 10.1093/arclin/14.6.489
43. Reis AID, Guerreiro M, Castro-Caldas A. Influence of educational level of non brain-damaged subjects on visual naming capacities. *J Clin Exp Neuropsychol*. (1995) 16:6. doi: 10.1080/01688639408402705
44. Dell GS. The retrieval of phonological forms in production: tests of predictions from a connectionist model. *J Mem Lang*. (1988) 27:124–42. doi: 10.1016/0749-596X(88)90070-8
45. Vitevitch MS. The neighborhood characteristics of malapropisms. *Lang Speech*. (1997) 40:211–28. doi: 10.1177/002383099704000301
46. Newman RS, Ratner N. The role of selected lexical factors on confrontation naming accuracy, speed, and fluency in adults who do and do not stutter. *J Speech Lang Hear Res*. (2007) 50:196–213. doi: 10.1044/1092-4388 (2007/016)
47. Santiago J, Mackay DG, Palma A. Length effects turn out to be syllable structure effects: response to Roelofs. *Lang Cognit Process*. (2002) 17:15–29. doi: 10.1080/01690960042000148
48. Oldfield RC, Wingfield A. Response latencies in naming objects. *Q J Exp Psychol*. (1965) 17:273–81. doi: 10.1080/17470216508416445
49. Alario FX, Ferrand L, Laganaro M, New B, Frauenfelder UH, Segui J. Predictors of picture naming speed. *Behav Res Meth Instrum Comput*. (2004) 36:140–55. doi: 10.3758/BF03195559
50. Snodgrass JG, Yuditsky T. Naming times for the Snodgrass and Vanderwart pictures. *Behav Res Meth Instrum Comput*. (1996) 28:516–36. doi: 10.3758/BF03200540
51. Barry C, Morrison CM, Ellis AW. Naming the Snodgrass and Vanderwart pictures: effects of age of acquisition, frequency and name agreement. *Q J Exp Psychol*. (1997) 50:560–85. doi: 10.1080/783663595
52. Dell'Acqua R, Lotto L, Job R. Naming times and standardized norms for the Italian PDIDPSS set of 266 pictures: direct comparisons with American, English, French, and Spanish published databases. *Behav Res Meth Instrum Comput*. (2000) 32:588–615. doi: 10.3758/BF03200832
53. Cholin J, Levelt WJM, Schiller NO. Effects of syllable frequency in speech production. *Cognition*. (2006) 99:205–35. doi: 10.1016/j.cognition.2005.01.009
54. Richter K, Wittler M, Hielscher-Fastabend M. *Bielefelder Aphasie Screening (BiAS) – Zur Diagnostik akuter Aphasien*. Hofheim: NAT-Verlag (2006).
55. Dell'Acqua R, Grainger J. Unconscious semantic priming from pictures. *Cognition*. (1999) 73:1–15. doi: 10.1016/S0010-0277(99)00049-9
56. Salles J, Holderbaum C, Parente MAMP, Mansur L, Ansaldo AI. Lexical-semantic processing in the semantic priming paradigm in aphasic patients. *Arq Neuro Psiquiatr*. (2012) 70:718–26. doi: 10.1590/S0004-282X2012000900014
57. Nettekoven C, Reck N, Goldbrunner R, Grefkes C, Weiß Lucas C. Short- and long-term reliability of language fMRI. *NeuroImage*. (2018) 176:215–25. doi: 10.1016/j.neuroimage.2018.04.050
58. Francis WS. Repetition priming in picture naming: sustained learning through the speeding of multiple processes. *Psychon Bull Rev*. (2014) 21:1301–8. doi: 10.3758/s13423-014-0610-9
59. Bullier B, Cassoudesalle H, Villain M, Cogné M, Mollo C, De Gabory I, et al. New factors that affect quality of life in patients with aphasia. *Ann Phys Rehabil Med*. (2020) 63:33–7. doi: 10.1016/j.rehab.2019.06.015
60. Riley EA, Owora A. Relationship between physiologically measured attention and behavioral task engagement in persons with chronic aphasia. *J Speech Lang Hear Res*. (2020) 63:1430–45. doi: 10.1044/2020_JSLHR-19-00016
61. Riley EA, Owora AH, McCleary JA, Anderson A. Sleepiness, exertion fatigue, arousal, and vigilant attention in persons with chronic aphasia. *Am J Speech-Lang Pat*. (2019) 28:1491–508. doi: 10.1044/2019_AJSLP-18-0301

Conflict of Interest: The authors declare that the research was conducted in the absence of any commercial or financial relationships that could be construed as a potential conflict of interest.

frontiers in Neurology

SYSTEMATIC REVIEW
published: 04 March 2021
doi: 10.3389/fneur.2021.644198

Navigated Transcranial Magnetic Stimulation Motor Mapping Usefulness in the Surgical Management of Patients Affected by Brain Tumors in Eloquent Areas: A Systematic Review and Meta-Analysis

Giuseppe Emmanuele Umana[1], Gianluca Scalia[2], Francesca Graziano[2,3], Rosario Maugeri[3], Nicola Alberio[1], Fabio Barone[1], Antonio Crea[1,4], Saverio Fagone[1], Giuseppe Roberto Giammalva[3], Lara Brunasso[3], Roberta Costanzo[3], Federica Paolini[3], Rosa Maria Gerardi[3], Silvana Tumbiolo[5], Salvatore Cicero[1], Giovanni Federico Nicoletti[2] and Domenico Gerardo Iacopino[3]*

[1] Department of Neurosurgery, Cannizzaro Hospital, Trauma Center, Gamma Knife Center, Catania, Italy, [2] Department of Neurosurgery, Highly Specialized Hospital and of National Importance "Garibaldi", Catania, Italy, [3] Department of Experimental Biomedicine and Clinical Neurosciences, School of Medicine, Postgraduate Residency Program in Neurological Surgery, Neurosurgical Clinic, AOUP "Paolo Giaccone," Palermo, Italy, [4] Neurosurgery Unit, Department of Clinical-Surgical, Diagnostic and Pediatric Sciences, University of Pavia, Pavia, Italy, [5] Division of Neurosurgery, Villa Sofia Hospital, Palermo, Italy

OPEN ACCESS

Edited by:
Giovanni Raffa,
University of Messina, Italy

Reviewed by:
Antonino Scibilia,
Universitaire de Strasbourg, France
Vincenzo Rizzo,
University of Messina, Italy

***Correspondence:**
Giuseppe Emmanuele Umana
umana.nch@gmail.com

Specialty section:
This article was submitted to Applied Neuroimaging, a section of the journal Frontiers in Neurology

Received: 20 December 2020
Accepted: 08 February 2021
Published: 04 March 2021

Citation:
Umana GE, Scalia G, Graziano F, Maugeri R, Alberio N, Barone F, Crea A, Fagone S, Giammalva GR, Brunasso L, Costanzo R, Paolini F, Gerardi RM, Tumbiolo S, Cicero S, Federico Nicoletti G and Iacopino DG (2021) Navigated Transcranial Magnetic Stimulation Motor Mapping Usefulness in the Surgical Management of Patients Affected by Brain Tumors in Eloquent Areas: A Systematic Review and Meta-Analysis. Front. Neurol. 12:644198. doi: 10.3389/fneur.2021.644198

Background: The surgical strategy for brain glioma has changed, shifting from tumor debulking to a more careful tumor dissection with the aim of a gross-total resection, extended beyond the contrast-enhancement MRI, including the hyperintensity on FLAIR MR images and defined as supratotal resection. It is possible to pursue this goal thanks to the refinement of several technological tools for pre and intraoperative planning including intraoperative neurophysiological monitoring (IONM), cortico-subcortical mapping, functional MRI (fMRI), navigated transcranial magnetic stimulation (nTMS), intraoperative CT or MRI (iCT, iMR), and intraoperative contrast-enhanced ultrasound. This systematic review provides an overview of the state of the art techniques in the application of nTMS and nTMS-based DTI-FT during brain tumor surgery.

Materials and Methods: A systematic literature review was performed according to the PRISMA statement. The authors searched the PubMed and Scopus databases until July 2020 for published articles with the following Mesh terms: *(Brain surgery OR surgery OR craniotomy) AND (brain mapping OR functional planning) AND (TMS OR transcranial magnetic stimulation OR rTMS OR repetitive transcranial stimulation)*. We only included studies regarding motor mapping in craniotomy for brain tumors, which reported data about CTS sparing.

Results: A total of 335 published studies were identified through the PubMed and Scopus databases. After a detailed examination of these studies, 325 were excluded from our review because of a lack of data object in this search. TMS reported an accuracy range of 0.4–14.8 mm between the APB hotspot (n1/4 8) in nTMS and DES from the DES spot; nTMS influenced the surgical indications in 34.3–68.5%.

Conclusion: We found that nTMS can be defined as a safe and non-invasive technique and in association with DES, fMRI, and IONM, improves brain mapping and the extent of resection favoring a better postoperative outcome.

Keywords: NTMs, motor mapping, surgical planning, glioma, craniotomy, tractography

INTRODUCTION

The surgical strategy for brain glioma has changed dramatically throughout the years, shifting from tumor debunking with subtotal resection to a more careful tumor dissection with the aim of a gross-total resection (GTR) while sparing neurologic functions. This more aggressive strategy was demonstrated to increase survival, the actual goal of glioma surgery, and has been extended beyond the contrast-enhancement MRI, including the hyperintensity on FLAIR MR images and defined as supratotal resection (SpTR). It is possible to pursue this goal thanks to the refinement of several technological tools for pre and intraoperative planning including intraoperative neurophysiological monitoring (IONM), cortico-subcortical mapping, functional MRI (fMRI), navigated transcranial magnetic stimulation (nTMS), intraoperative CT or MRI (iCT, iMR), and intraoperative contrast-enhanced ultrasound (CEUS) (1–6). These methods not only allow more detailed preoperative planning but are effective in the evaluation of motor pathways integrity and are a valuable tool to guide tumor resection. It has been reported that, cortically, the closer the distance between the tumor and motor cortex, the greater the risk of new motor deficit, as demonstrated by lesion to activation distance (LAD) assessment in fMRI (1, 7–9). Similarly, at the subcortical stage, usually the proximity of the tumor to the corticospinal tract (CST) is related to a higher risk of motor deficits, but a great variability has also been reported (10–12). Moreover, repeated subcortical stimulation and its intensity modulation present a positive correlation for the detection of the CST (13, 14). The reliability of preoperative tractography is well-demonstrated to be consistent with subcortical stimulation for the CST location, in about 95% of cases (15), providing a marked improvement in the tractography data, which is not surgeon-dependent and has a strong clinical correlation allowing for reliable subcortical mapping associated with diffusion tensor imaging fiber-tracking (DTI FT) (16–19). This association has only been reported twice in literature, stating that it offers patient-specific analysis of the risk of deficit for lesions sited in eloquent areas, which can be avoided when keeping 8 mm from the CTS (15, 19). This systematic review provides an overview of the state of the art techniques in the application of nTMS and nTMS-based DTI-FT during brain tumor surgery.

Abbreviations: fMRI, Functional MRI; nTMS, Navigated transcranial magnetic stimulation; IONM, Intraoperative monitoring; SpTR, Supratotal resection; GTR, Gross-total resection; CST, Corticospinal tract; EOR, Extent of resection; CEUS, Contrast-enhanced ultrasound; DES, Direct electrical stimulation.

MATERIALS AND METHODS

A systematic literature review was performed according to the PRISMA statement and related checklists. The authors searched the PubMed and Scopus databases until July 2020 for published articles with the following Mesh terms: *(Brain surgery OR surgery OR craniotomy) AND (brain mapping OR functional planning) AND (TMS OR transcranial magnetic stimulation OR rTMS OR repetitive transcranial stimulation)*; a language restriction to English only papers was also applied. All included studies were meticulously reviewed and scrutinized for their study design, methodology, and patient characteristics. We only included 10 studies regarding motor mapping in craniotomy for brain tumors, which reported data about CTS sparing (**Figure 1**). Data for all patients were recorded when available, including accuracy, GTR, STR, permanent deficits, change of strategy, and intraoperative tools used (**Table 1**).

A linear regression analysis was performed using Excel software. R2 is the coefficient of determination. We compared estimated and actual y-values, and ranges in value from 0 to 1. If it was 1, there was perfect correlation in the sample—there was no difference between the estimated y-value and the actual y-value. At the other extreme, if the coefficient of determination was 0, the regression equation was not helpful in predicting a y-value. f is the F statistic, or the F-observed value. We used the F statistic to determine whether the observed relationship between the dependent and independent variables occurred by chance (slope +− fault slope, intercepts +− fault intercepts, r2, f).

RESULTS

A total of 335 published studies were identified through the PubMed and Scopus databases. After a detailed examination of these studies, 325 were excluded from our review because of a lack of data object in this search, or did not report accurate data.

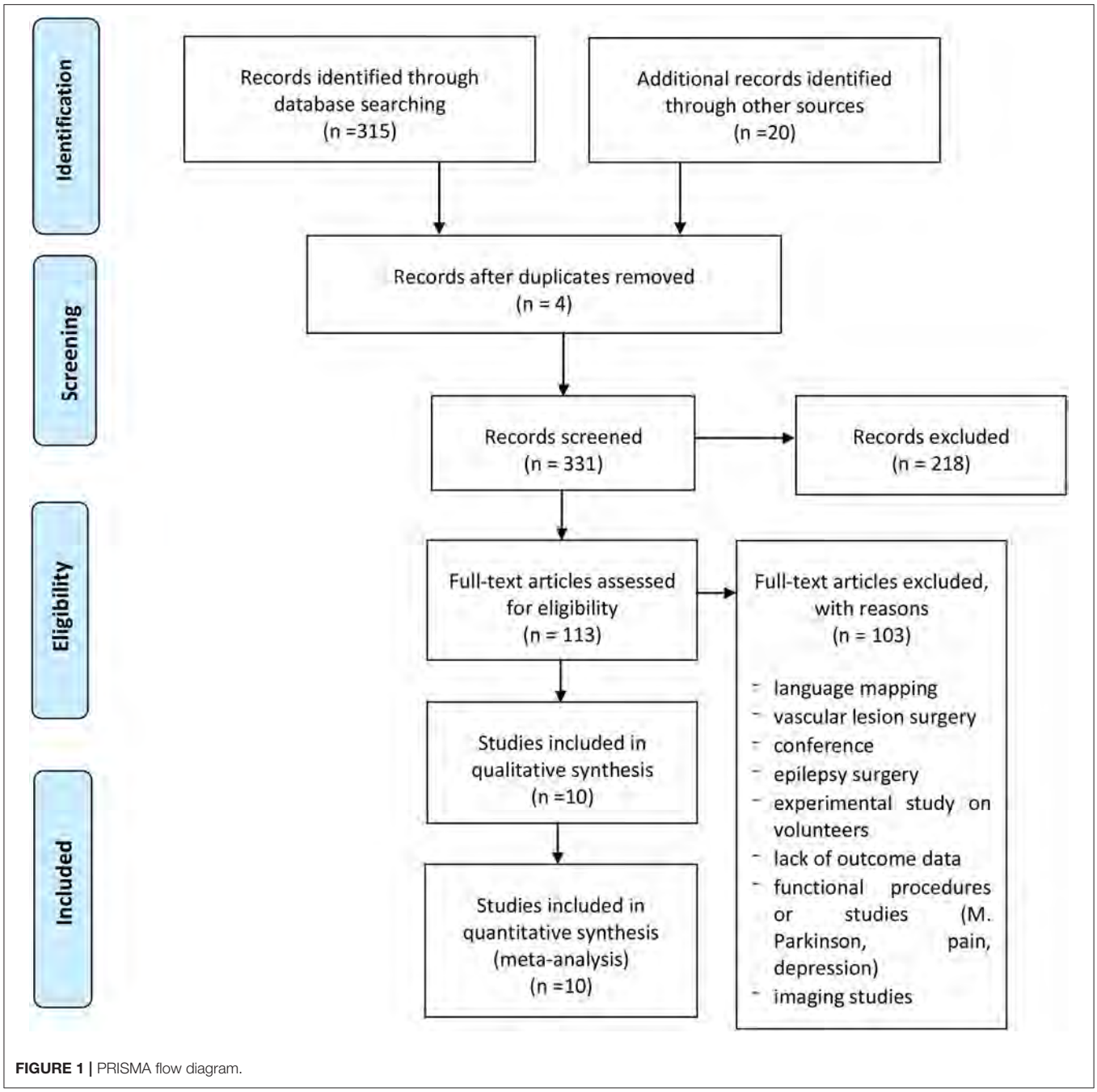

FIGURE 1 | PRISMA flow diagram.

All the fits showed a low r2 value, while F was high. Linear multiple regression analysis showed that there was no correlation from the extracted data among the variables plotted in the graphs (**Figure 2**). Accuracy reported rate ranged from 0.4 to 14.8 mm; GTR range was 33–98%, and STR range 9.4–66.6%. The associated nTMS tools used included DTI fiber tracking, fMRI, MPRAGE MRI, IONM, and sodium-fluorescein. IONM was used in 8 out of 10 studies suggesting that this was considered the most reliable tool, followed by DTI fiber tracking (6 out of 10), fMRI (4 out of 10), and sodium fluorescence as the emerging tool (1 out of 10).

DISCUSSION

Multimodal Functional Surgical Planning

The gold standard for functional assessment and surgical planning is represented by DES associated with IONM (29–32). With the aim to improve risk stratification of motor eloquent area detection in the preoperative phase, other techniques have been introduced. Function MRI is a valuable tool, which helps to obtain visuo-spatial data of motor and language functions, which can be merged with the anatomic multiplanar MRI study in navigation planning (22, 33–35). fMRI offers

TABLE 1 | Summary of the systematic review including authors, motor mapping accuracy, extent of resection nTMS related, associated nTMS tools, eventual change of surgical strategy and outcome.

Authors	Motor mapping accuracy	Extent of resection nTMS related	Associated nTMS tools	Change of surgical strategy	Outcome
Paiva et al. (20)	4.1 +−1.2 mm	GTR in 33.34%; STR in 66.66%	IONM, MPRAGE MRI	Not reported	Not reported
Coburger et al. (21)	2.33 ± 0.97 mm	GTR in 85.2%; STR in 14.8%	DTI fiber tracking, fMRI, MPRAGE MRI	26.6%	Not reported
Rosenstock et al. (19)	2 mm	GTR in 50%; STR in 33%	DTI fiber tracking, IONM	Not reported	Permanent deficits in 22%
Raffa et al. (22)	<11 mm	GTR in 61.3%	DTI fiber tracking, IONM	20%	Permanent deficits in 11.4%
Jung et al. (23)	3.50 ± 0.66 mm	GTR in 75%; STR in 25%	IONM	31.5%	Permanent deficits in 5.7%
Raffa et al. (24)	1.1 + −14-8 mm	GTR in 67.6%; STR in 24.1%;	DTI fiber tracking	Not reported	Permanent deficits in 7.5%
Raffa et al. (25)	<11 mm	GTR in 73.13%; STR in 41.46%	DTI fiber tracking, IONM, sodium-fluorescein	Not reported	Permanent deficit in 9.75%
Frey et al. (26)	0.4 + −14.8 mm	GTR in 58.6%; STR in 9.4%	DTI fiber tracking, IONM	35.2%	Permanent deficits in 6.1%
Krieg et al. (27)	6.2 + −6 mm	GTR in 50%; STR in 50%	IONM, fMRI	Not reported	Permanent deficits in 12.5%
Sollmann et al. (28)	8.2 + −9.4 mm	GTR 98%	fMRI, IONM	Not reported	Permanent deficits 22%

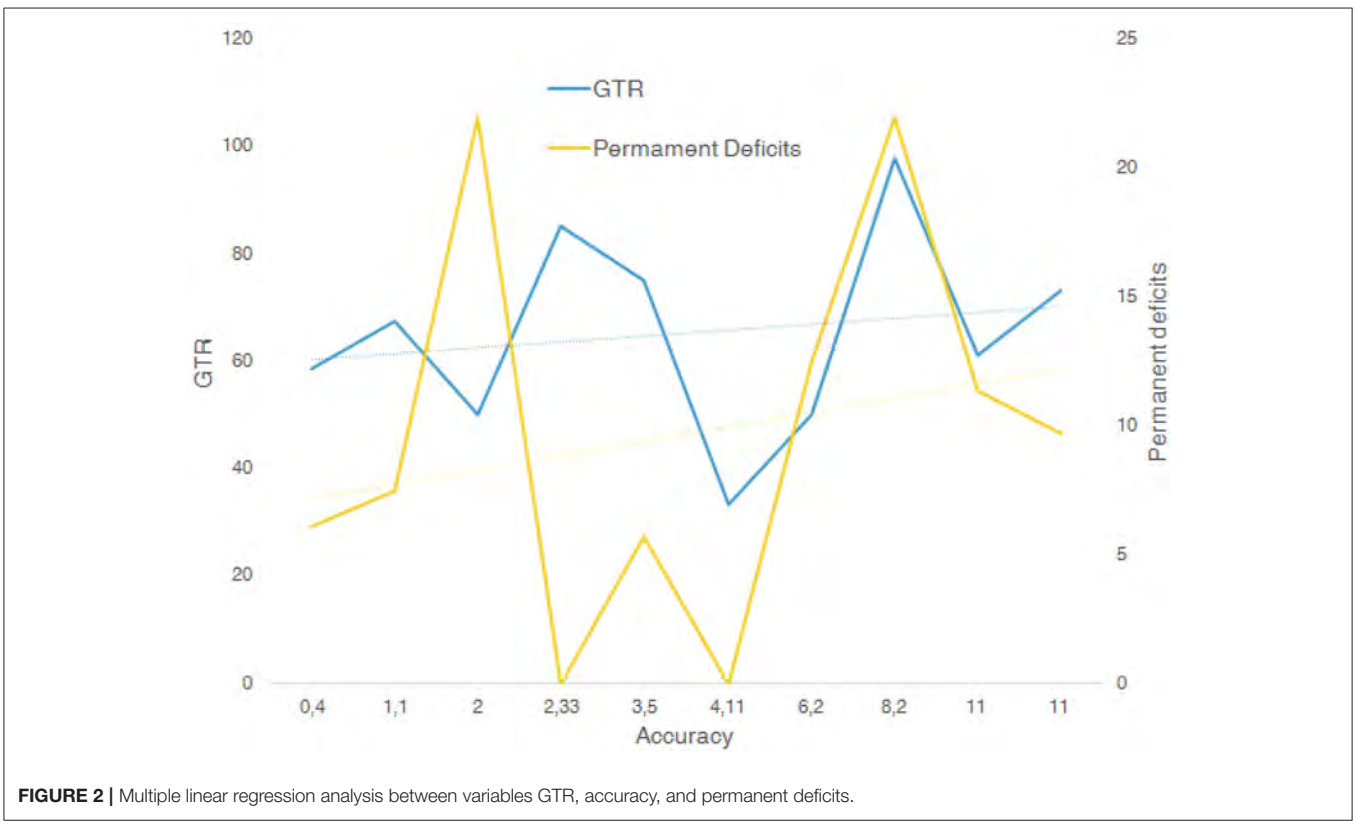

FIGURE 2 | Multiple linear regression analysis between variables GTR, accuracy, and permanent deficits.

59–100% sensitivity, with 0–97% specificity, which although a drawback offers a great variability operator dependent of language mapping, while tractography representation does not offer functional data (36–39). TMS mapping is not a novelty by itself, introduced in 1985 (40), it has been reported to be a valuable tool in risk stratification and the mapping of

motor and language areas for surgical planning (41–50). Of notice, nTMS is used directly by neurosurgeons, in the context of the neurosurgical department and it is independent of neuroradiological availability, helping its routine use in the setting of surgical planning.

Motor Mapping Accuracy

An important TMS parameter is stimulation focality, which corresponds to the cortical area where the TMS' electric field strength reaches half the maximum value (51, 52). The smaller this area is, the better the focally and accuracy. Thielscher and Kammer (52) reported that the variability map size documented among patients can related to different coil–cortex distances and cortex radii. The focally of a coil can be quantitatively estimated by the electric field on a hemisphere representing the brain cortex radius $r = 8$ cm. Furthermore, Thielscher and Kammer reported that the variability in map dimension among different patients is related to two parameters: coil–cortex distances and cortex radii. Thus, the variability documented in our research can be related mainly to operator-dependent variables, rather than technical TMS characteristics, confirming the reliability and the utility of nTMS in a multimodal motor mapping setting. In literature, it has been reported that TMS displayed an accuracy range of 0.4–14.8 mm between the APB hotspot (n1/4 8) in nTMS and DES from the DES spot (19, 23–28, 48, 52–57). These data endorse the reliability of nTMS in motor mapping, representing a useful tool in multimodal brain mapping. An important point is the reduction of the surgical time: nTMS plays an important role in the guidance of the intraoperative stimulation, saving time during cortical mapping. Moreover, the preoperative cortical mapping related to nTMS reduces the need of large cortical exposure, thus reducing the craniotomy size and again the surgical time related to the craniotomy opening/closing step.

Surgical Strategy and Clinical Outcomes

nTMS reliability has been proven to be very strong and can influence the surgical indication to change from no surgery/biopsy to craniotomy removal in 34.3–68.5% of cases (23, 24, 26, 58–60). As already reported in the previous paragraph, the size of the craniotomy is reduced and thus the surgical strategy is modified according to the nTMS mapping, which allows professionals to plan for the location of the motor cortex, guiding the "no-look" positioning of the strip electrode, without direct visualization of the cortical motor cortex. Moreover, if brain mapping shows the absence of an eloquent area at the level of the anatomic cortical landmark, it allows surgeons to conduct the surgical removal through the cortex in otherwise considered functional areas. Jung et al. (23) reported a transopercular approach guided by the negative correspondence between the anatomic area and the language mapping of the nTMS, likewise another patient in which nTMS documented the absence of motor function at the level of the premised primary motor cortex in a patient affected by cavernoma, modifying the clinical management from no survey to indication of craniotomy.

In literature, several authors documented the positive influence of nTMS on surgical planning and postoperative outcome, with a significant role in risk stratification (26, 27, 31, 45, 61, 62). Interestingly, and apparently in contrast to these data, some authors reported more postoperative neurological deficits, with delayed recovery. An interpretation of this finding could be that more deficits are relative to a more aggressive surgical strategy encouraged by the combined use of DES and nTMS in eloquent areas (26). Even if in the literature there are several reports about sodium fluorescence (63, 64), it is not possible to provide statistically significant data as it is an emerging tool, reported only in 1 out of 10 of the selected paper in this review.

Extent of Surgical Resection

About the role of nTMS and its effect on the extent of surgical resection (ESR), there are no univocal reports. Despite the fact that some authors (23) did not find a direct relation between nTMS and ESR, others documented a greater ESR in surgical series in which nTMS was associated with DES and IONM, and a longer progression-free survival (26, 27, 45, 65–67). These different findings could be related to the novelty of this technique and thus to the learning curve. Of course, a better understanding and a systematic analysis of data is required through randomized multicentric studies.

CONCLUSIONS

From the analysis of the present systematic review, we found that nTMS can be defined as a safe and non-invasive technique, which when associated with DES, fMRI, and IONM improves brain mapping and the extent of resection with a better postoperative outcome. Of notice, the reliability of nTMS has been documented to modify the surgical strategy for oncologic patients.

DATA AVAILABILITY STATEMENT

The original contributions generated for this study are included in the article/supplementary material, further inquiries can be directed to the corresponding author/s.

AUTHOR CONTRIBUTIONS

GU, GS, FG, and RM: conception and design of study and analysis and/or interpretation of data. GU and GS: acquisition of data. GU, GS, FG, RM, NA, FB, AC, SF, GG, LB, RC, FP, and RG: drafting the manuscript. ST, SC, GN, and DI: revising the manuscript critically for important intellectual content. GU, GS, FG, RM, NA, FB, AC, SF, GG, LB, RC, FP, RG, ST, SC, GN, and DI: approval of the version of the manuscript to be published. All authors contributed to the article and approved the submitted version.

REFERENCES

1. Almenawer SA, Badhiwala JH, Alhazzani W, Greenspoon J, Farrokhyar F, Yarascavitch B, et al. Biopsy versus partial versus gross total resection in older patients with high-grade glioma: a systematic review and meta-analysis. *Neuro Oncol*. (2015) 17:868–81. doi: 10.1093/neuonc/nou349
2. Brown TJ, Brennan MC, Li M, Church EW, Brandmeir NJ, Rakszawski KL, et al. Association of the extent of resection with survival in glioblastoma: a systematic review and meta- analysis. *JAMA Oncol*. (2016) 2:1460–9. doi: 10.1001/jamaoncol.2016.1373
3. Duffau H, Mandonnet E. The "onco-functional balance" in surgery for diffuse low-grade glioma: integrating the extent of resection with quality of life. *Acta Neurochir (Wien)*. (2013) 155:951–7. doi: 10.1007/978-1-4471-2213-5
4. Lee CH, Kim DG, Kim JW, Han JH, Kim YH, Park CK, et al. The role of surgical resection in the management of brain metastasis: a 17-year longitudinal study. *Acta Neurochir (Wien)*. (2013) 155:389–97. doi: 10.1007/s00701-013-1619-y
5. McGirt MJ, Mukherjee D, Chaichana KL, Than KD, We- ingart JD, Quinones-Hinojosa A. Association of surgically acquired motor and language deficits on overall survival after resection of glioblastoma multiforme. *Neurosurgery*. (2009) 65:463–70. doi: 10.1227/01.NEU.0000349763.42238.E9
6. Sanai N, Berger MS. Glioma extent of resection and its impact on patient outcome. *Neurosurgery*. (2008) 62:753–64. doi: 10.1227/01.neu.0000318159.21731.cf
7. Håberg A, Kvistad KA, Unsgård G, Haraldseth O. Preoperative blood oxygen level-dependent functional magnetic resonance imaging in patients with primary brain tumors: clinical application and outcome. *Neurosurgery*. (2004) 54:902–15. doi: 10.1227/01.NEU.0000114510.05922.F8
8. Krishnan R, Raabe A, Hattingen E, Szelenyi A, Yahya H, Hermann E, et al. Functional magnetic resonance imagingintegrated neuronavigation: correlation between lesion-to- motor cortex distance and outcome. *Neurosurgery*. (2004) 55:904–15. doi: 10.1227/01.NEU.0000137331.35014.5C
9. Wood JM, Kundu B, Utter A, Gallagher TA, Voss J, Nair VA, et al. Impact of brain tumor location on morbidity and mortality: a retrospective functional MR imaging study. *AJNR Am J Neuroradiol*. (2011) 32:1420–5. doi: 10.3174/ajnr.A2679
10. Bailey PD, Zacà D, Basha MM, Agarwal S, Gujar SK, Sair HI, et al. Presurgical fMRI and DTI for the prediction of perioperative motor and language deficits in primary or metastatic brain lesions. *J Neuroimaging*. (2015) 25:776–84. doi: 10.1111/jon.12273
11. Nimsky C, Ganslandt O, Merhof D, Sorensen AG, Fahlbusch R. Intraoperative visualization of the pyramidal tract by diffusion-tensor-imaging-based fiber tracking. *Neuroimage*. (2006) 30:1219–29. doi: 10.1016/j.neuroimage.2005.11.001
12. Ulmer JL, Salvan CV, Mueller WM, Krouwer HG, Stroe GO, Aralasmak A, et al. The role of diffusion tensor imaging in establishing the proximity of tumor borders to functional brain systems: implications for preoperative risk assessments and postoperative outcomes. *Technol Cancer Res Treat*. (2004) 3:567–76. doi: 10.1177/153303460400300606
13. Raabe A, Beck J, Schucht P, Seidel K. Continuous dynamic mapping of the corticospinal tract during surgery of motor eloquent brain tumors: evaluation of a new method. *J Neuro Surg*. (2014) 120:1015–24. doi: 10.3171/2014.1.JNS13909
14. Seidel K, Beck J, Stieglitz L, Schucht P, Raabe A. The warning-sign hierarchy between quantitative subcortical motor mapping and continuous motor evoked potential monitoring during resection of supratentorial brain tumors. *J Neurosurg*. (2013) 118:287–96. doi: 10.3171/2012.10.JNS12895
15. Sollmann N, Wildschuetz N, Kelm A, Conway N, Moser T, Bulubas L, et al. Associations between clinical outcome and navigated transcranial magnetic stimulation characteristics in patients with motor-eloquent brain lesions: a combined navigated transcranial magnetic stimulation-diffusion tensor imaging fiber tracking approach. *J Neurosurg*. (2018) 128:800–10. doi: 10.3171/2016.11.JNS162322
16. Conti A, Raffa G, Granata F, Rizzo V, Germanò A, Tomasello F. Navigated transcranial magnetic stimulation for "somatotopic" tractography of the corticospinal tract. *Neurosurgery*. (2014) 10:542–54. doi: 10.1227/NEU.0000000000000502
17. Frey D, Strack V, Wiener E, Jussen D, Vajkoczy P, Picht T. A new approach for corticospinal tract reconstruction based on navigated transcranial stimulation and standardized frac- tional anisotropy values. *Neuroimage*. (2012) 62:1600–9. doi: 10.1016/j.neuroimage.2012.05.059
18. Krieg SM, Buchmann NH, Gempt J, Shiban E, Meyer B, Ringel F. Diffusion tensor imaging fiber tracking using navi- gated brain stimulation—a feasibility study. *Acta Neurochir (Wien)*. (2012) 154:555–63. doi: 10.1007/s00701-011-1255-3
19. Rosenstock T, Grittner U, Acker G, Schwarzer V, Kulchytska N, Vajkoczy P, et al. Risk stratification in motor area-related glioma surgery based on navigated transcranial magnetic stimulation data. *J Neurosurg*. (2017) 126:1227–37. doi: 10.3171/2016.4.JNS152896
20. Paiva WS, Fonoff ET, Marcolin MA, Cabrera HN, Teixeira MJ. Cortical mapping with navigated transcranial magnetic stimulation in low-grade glioma surgery. *Neuropsychiatr Dis Treat*. (2012) 8:197–201. doi: 10.2147/NDT.S30151
21. Coburger J, Musahl C, Henkes H, Horvath-Rizea D, Bittl M, Weissbach C, et al. Comparison of navigated transcranial magnetic stimulation and functional magnetic resonance imaging for preoperative mapping in rolandic tumor surgery. *Neurosurg Rev*. (2013) 36:65–75. doi: 10.1007/s10143-012-0413-2
22. Raffa G, Conti A, Scibilia A, Sindorio C, Quattropani MC, Visocchi M, et al. Functional reconstruction of motor and language pathways based on navigated transcranial magnetic stimulation and DTI fiber tracking for the preoperative planning of low grade glioma surgery: a new tool for preservation and restoration of eloquent networks. *Acta Neurochir Suppl*. (2017) 124:251–61. doi: 10.1007/978-3-319-39546-3_37
23. Jung J, Lavrador JP, Patel S, Giamouriadis A, Lam J, Bhangoo R, et al. First United Kingdom experience of navigated transcranial magnetic stimulation in preoperative mapping of brain tumors. *World Neurosurg*. (2019) 122:e1578–87. doi: 10.1016/j.wneu.2018.11.114
24. Raffa G, Quattropani MC, Germanò A. When imaging meets neurophysiology: the value of navigated transcranial magnetic stimulation for preoperative neurophysiological mapping prior to brain tumor surgery. *Neurosurg Focus*. (2019) 47:E10. doi: 10.3171/2019.9.FOCUS19640
25. Raffa G, Scibilia A, Conti A, Cardali SM, Rizzo V, Terranova C, et al. Multimodal surgical treatment of high-grade gliomas in the motor area: the impact of the combination of navigated transcranial magnetic stimulation and fluorescein-guided resection. *World Neurosurg*. (2019) 128:e378–90. doi: 10.1016/j.wneu.2019.04.158
26. Frey D, Schilt S, Strack V, Zdunczyk A, Rösler J, Niraula B, et al. Navigated transcranial magnetic stimulation improves the treatment outcome in patients with brain tumors in motor eloquent locations. *Neuro Oncol*. (2014) 16:1365–72. doi: 10.1093/neuonc/nou110
27. Krieg SM, Sabih J, Bulubasova L, Obermueller T, Negwer C, Janssen I, et al. Preoperative motor mapping by navigated transcranial magnetic brain stimulation improves outcome for motor eloquent lesions. *Neuro Oncol*. (2014) 16:1274–82. doi: 10.1093/neuonc/nou007
28. Sollmann N, Zhang H, Fratini A, Wildschuetz N, Ille S, Schröder A, et al. Risk assessment by presurgical tractography using navigated TMS maps in patients with highly motor- or language-eloquent brain tumors. *Cancers (Basel)*. (2020) 12:1264. doi: 10.3390/cancers12051264
29. Ojemann G, Ojemann J, Lettich E, Berger M. Cortical language localization in left, dominant hemisphere: an electrical stimulation mapping investigation in 117 patients. *J Neurosurg*. (1989) 71:316–26. doi: 10.3171/jns.1989.71.3.0316
30. Sollmann N, Kelm A, Ille S, Schröder A, Zimmer C, Ringel F, et al. Setup presentation and clinical outcome analysis of treating highly language-eloquent gliomas via preoperative navigated transcranial magnetic stimulation and tractography. *Neurosurg Focus*. (2018) 44:E2. doi: 10.3171/2018.3.FOCUS1838
31. Raffa G, Picht T, Scibilia A, Rösler J, Rein J, Conti A, et al. Surgical treatment of meningiomas located in the rolandic area: the role of navigated transcranial magnetic stimulation for preoperative planning, surgical strategy, and prediction of arachnoidal cleavage and motor outcome. *J Neurosurg*. (2019) 14:1–12. doi: 10.3171/2019.3.JNS183411
32. Rizzo V, Terranova C, Conti A, Germanò A, Alafaci C, Raffa G, et al. Preoperative functional mapping for rolandic brain tumor

surgery. *Neurosci Lett*. (2014) 583:136–41. doi: 10.1016/j.neulet.2014.09.017
33. Tie Y, Rigolo L, Norton IH, Huang RY, Wu W, Orringer D, et al. Defining language networks from resting-state fMRI for surgical planning—a feasibility study. *Hum Brain Mapp*. (2014) 35:1018–30. doi: 10.1002/hbm.22231
34. Kallioniemi E, Pitkänen M, Könönen M, Vanninen R, Julkunen P. Localization of cortical primary motor area of the hand using navigated transcranial magnetic stimulation, BOLD and arterial spin labeling fMRI. *J Neurosci Methods*. (2016) 273:138–48. doi: 10.1016/j.jneumeth.2016.09.002
35. Umana GE, Raudino G, Alberio N, Inserra F, Giovinazzo G, Fricia M, et al. Slit-like hypertensive hydrocephalus: report of a late, complex, and multifactorial complication in an oncologic patient. *Surg Neurol Int*. (2020) 11:219. doi: 10.25259/SNI_145_2020
36. Giussani C, Roux FE, Ojemann J, Sganzerla EP, Pirillo D, Papagno C. Is preoperative functional magnetic resonance imaging reliable for language areas mapping in brain tumor surgery? Review of language functional magnetic resonance imaging and direct cortical stimulation correlation studies. *Neurosurgery*. (2010) 66:113–20. doi: 10.1227/01.NEU.0000360392.15450.C9
37. Jbabdi S, Johansen-Berg H. Tractography: where do we go from here? *Brain Connect*. (2011) 1:169–83. doi: 10.1089/brain.2011.0033
38. Dell'Acqua F, Catani M. Structural human brain networks: hot topics in diffusion tractography. *Curr Opin Neurol*. (2012) 25:375–83. doi: 10.1097/WCO.0b013e328355d544
39. Tomasi SO, Umana GE, Scalia G, Rubio-Rodriguez RL, Cappai PF, Capone C, et al. Importance of veins for neurosurgery as landmarks against brain shifting phenomenon: an anatomical and 3D-MPRAGE MR reconstruction of superficial cortical veins. *Front Neuroanat*. (2020) 14:596167. doi: 10.3389/fnana.2020.596167
40. Barker AT, Jalinous R, Freeston IL. Non-invasive magnetic stimulation of human motor cortex. *Lancet*. (1985) 1:1106–7. doi: 10.1016/S0140-6736(85)92413-4
41. Tarapore PE, Tate MC, Findlay AM, Honma SM, Mizuiri D, Berger MS, et al. Preoperative multimodal motor mapping: a comparison of magnetoencephalography imaging, navigated transcranial magnetic stimulation, and direct cortical stimulation. *J Neurosurg*. (2012) 117:354–62. doi: 10.3171/2012.5.JNS112124
42. Tarapore PE, Findlay AM, Honma SM, Mizuiri D, Houde JF, Berger MS, et al. Language mapping with navigated repetitive TMS: proof of technique and validation. *Neuroimage*. (2013) 82:260–72. doi: 10.1016/j.neuroimage.2013.05.018
43. Sollmann N, Hauck T, Obermüller T, Hapfelmeier A, Meyer B, Ringel F, et al. Inter- and intraobserver variability in motor mapping of the hotspot for the abductor policis brevis muscle. *BMC Neurosci*. (2013) 14:94. doi: 10.1186/1471-2202-14-94
44. Lefaucheur JP, Picht T. The value of preoperative functional cortical mapping using navigated TMS. *Neurophysiol Clin*. (2016) 46:125–33. doi: 10.1016/j.neucli.2016.05.001
45. Picht T, Schulz J, Hanna M, Schmidt S, Suess O, Vajkoczy P. Assessment of the influence of navigated transcranial magnetic stimulation on surgical planning for tumors in or near the motor cortex. *Neurosurgery*. (2012) 70:1248–56. doi: 10.1227/NEU.0b013e318243881e
46. Picht T, Frey D, Thieme S, Kliesch S, Vajkoczy P. Presurgical navigated TMS motor cortex mapping improves outcome in glioblastoma surgery: a controlled observational study. *J Neurooncol*. (2016) 126:535–43. doi: 10.1007/s11060-015-1993-9
47. Raffa G, Picht T, Angileri FF, Youssef M, Conti A, Esposito F, et al. Surgery of malignant motor-eloquent gliomas guided by sodium-fluorescein and navigated transcranial magnetic stimulation: a novel technique to increase the maximal safe resection. *J Neurosurg Sci*. (2019) 63:670–8. doi: 10.23736/S0390-5616.19.04710-6
48. Raffa G, Conti A, Scibilia A, Cardali SM, Esposito F, Angileri FF, et al. The impact of diffusion tensor imaging fiber tracking of the corticospinal tract based on navigated transcranial magnetic stimulation on surgery of motor-eloquent brain lesions. *Neurosurgery*. (2018) 83:768–82. doi: 10.1093/neuros/nyx554
49. Umana GE, Alberio N, Amico P, Lavecchia AM, Fagone S, Fricia M, et al. Giant cystic brain metastasis from ovarian papillary serous adenocarcinoma: case report and review of the literature. *Interdiscip Neurosurg*. (2020) 20:100668. doi: 10.1016/j.inat.2020.100668
50. Umana GE, Scalia G, Spitaleri A, Alberio N, Fricia M, Tomasi SO, et al. Use of gelatin-thrombin hemostatic matrix for control of ruptured cerebral aneurysm. *Cent Eur Neurosurg*. (2020). doi: 10.1055/s-0040-1720986
51. Roth BJ, Saypol JM, Hallett M, Cohen LG. A theoretical calculation of the electric field induced in the cortex during magnetic stimulation. *Muscle Nerve*. (1990) 13:734–41. doi: 10.1002/mus.880130812
52. Thielscher A, Kammer T. Electric field properties of two commercial figure-8 coils in TMS: calculation of focality and efficiency. *Clin Neurophysiol*. (2004) 115:1697–708. doi: 10.1016/j.clinph.2004.02.019
53. Picht T, Schmidt S, Brandt S, Frey D, Hannula H, Neuvonen T, et al. Preoperative functional mapping for rolandic brain tumor surgery: comparison of navigated transcranial magnetic stimulation to direct cortical stimulation. *Neurosurgery*. (2011) 69:581–8. doi: 10.1227/NEU.0b013e3182181b89
54. Takahashi S, Vajkoczy P, Picht T. Navigated transcranial magnetic stimulation for mapping the motor cortex in patients with rolandic brain tumors. *Neurosurg Focus*. (2013) 34:E3. doi: 10.3171/2013.1.FOCUS133
55. Raffa G, Scibilia A, Germanò A, Conti A. "nTMS-Based DTI Fiber Tracking of Motor Pathways. In: Krieg SM, editor. *Navigated Transcranial Magnetic Stimulation in Neurosurgery*. Cham: Springer International Publishing (2017). p. 97–114. doi: 10.1007/978-3-319-54918-7_6
56. La Torre D, Maugeri R, Angileri FF, Pezzino G, Conti A, Cardali SM, et al. Human leukocyte antigen frequency in human high-grade gliomas: a case-control study in Sicily. *Neurosurgery*. (2009) 64:1082–8. doi: 10.1227/01.NEU.0000345946.35786.92
57. Maugeri R, Schiera G, Liegro Di CM, Fricano A, Iacopino DG, Di Liegro I. Aquaporins and Brain Tumors. *Int J Mol Sci*. (2016) 17:1029. doi: 10.3390/ijms17071029
58. Raffa G, Scibilia A, Conti A, Ricciardo G, Rizzo V, Morelli A, et al. The role of navigated transcranial magnetic stimulation for surgery of motor-eloquent brain tumors: a systematic review and meta-analysis. *Clin Neurol Neurosurg*. (2019) 180:7–17. doi: 10.1016/j.clineuro.2019.03.003
59. Giammalva GR, Iacopino DG, Azzarello G, Gaggiotti C, Graziano F, Gulì C, et al. End-of-life care in high-grade glioma patients. The palliative and supportive perspective. *Brain Sci*. (2018) 8:125. doi: 10.3390/brainsci8070125
60. Pino MA, Imperato A, Musca I, Maugeri R, Giammalva GR, Costantino G, et al. New hope in brain glioma surgery: the role of intraoperative ultrasound. A review. *Brain Sci*. (2018) 8:202. doi: 10.3390/brainsci8110202
61. Barone F, Alberio N, Iacopino DG, Giammalva GR, D'Arrigo C, Tagnese W, et al. Brain mapping as helpful tool in brain glioma surgical treatment-toward the "perfect surgery"? *Brain Sci*. (2018) 8:192. doi: 10.3390/brainsci8110192
62. Graziano F, Bavisotto CC, Gammazza AM, Rappa F, de Macario EC, Macario AJL, et al. Chaperonology: the third eye on brain gliomas. *Brain Sci*. (2018) 8:110. doi: 10.3390/brainsci8060110
63. Maugeri R, Villa A, Pino M, Imperato A, Giammalva GR, Costantino G, et al. With a little help from my friends: the role of intraoperative fluorescent dyes in the surgical management of high-grade gliomas. *Brain Sci*. (2018) 8:31. doi: 10.3390/brainsci8020031
64. Francaviglia N, Iacopino DG, Costantino G, Villa A, Impallaria P, Meli F, et al. Fluorescein for resection of high-grade gliomas: a safety study control in a single center and review of the literature. *Surg Neurol Int*. (2017) 8:145. doi: 10.4103/sni.sni_89_17
65. Caruso Bavisotto C, Graziano F, Rappa F, Marino Gammazza A, Logozzi M, Fais S, et al. Exosomal chaperones and miRNAs in gliomagenesis: state-of-art and theranostics perspectives. *Int J Mol Sci*. (2018) 19:2626. doi: 10.3390/ijms19092626
66. Iacopino DG, Gagliardo C, Giugno A, Giammalva GR, Napoli A, Maugeri R, et al. Preliminary experience with a transcranial magnetic resonance-guided focused ultrasound surgery system integrated with a 1.5-T MRI unit in a series of patients with essential tremor and Parkinson's disease. *Neurosurg Focus*. (2018) 44:E7. doi: 10.3171/2017.11.FOCUS17614
67. Francaviglia N, Maugeri R, Odierna Contino A, Meli F, Fiorenza V, Costantino G, et al. Skull bone defects reconstruction with custom-made titanium graft shaped with electron beam melting technology:

preliminary experience in a series of ten patients. *Acta Neurochirurgica Supplementum*. (2017) 124:137–41. doi: 10.1007/978-3-319-39546-3_21

Conflict of Interest: The authors declare that the research was conducted in the absence of any commercial or financial relationships that could be construed as a potential conflict of interest.

frontiers in Neurology

ORIGINAL RESEARCH
published: 10 March 2021
doi: 10.3389/fneur.2021.646075

Middle Frontal Gyrus and Area 55b: Perioperative Mapping and Language Outcomes

Sally Rosario Hazem[1,2†], Mariam Awan[1,2*†], Jose Pedro Lavrador[1,2†], Sabina Patel[1,2], Hilary Margaret Wren[1], Oeslle Lucena[3], Carla Semedo[3,4], Hassna Irzan[3,4], Andrew Melbourne[3,4], Sebastien Ourselin[3], Jonathan Shapey[1,2,3], Ahilan Kailaya-Vasan[1,2], Richard Gullan[1], Keyoumars Ashkan[1,2], Ranjeev Bhangoo[1,2] and Francesco Vergani[1,2]*

[1] Department of Neurosurgery, King's College Hospital National Health Service Foundation Trust, London, United Kingdom, [2] King's Neuro Lab, Department of Neurosurgery, King's College Hospital National Health Service Foundation Trust, London, United Kingdom, [3] School of Biomedical Engineering and Imaging Sciences, King's College London, London, United Kingdom, [4] Department of Medical Physics and Biomedical Engineering, University College London, London, United Kingdom

OPEN ACCESS

Edited by:
Giovanni Raffa,
University of Messina, Italy

Reviewed by:
Cesare Zoia,
Fondazione IRCCS Policlinico San Matteo, Italy
Philipp Hendrix,
Geisinger Health System, United States

***Correspondence:**
Sally Rosario Hazem
sally.hazem@nhs.net
Mariam Awan
m.awan1@nhs.net

[†]These authors have contributed equally to this work

Specialty section:
This article was submitted to Neuro-Oncology and Neurosurgical Oncology, a section of the journal Frontiers in Neurology

Received: 24 December 2020
Accepted: 29 January 2021
Published: 10 March 2021

Citation:
Hazem SR, Awan M, Lavrador JP, Patel S, Wren HM, Lucena O, Semedo C, Irzan H, Melbourne A, Ourselin S, Shapey J, Kailaya-Vasan A, Gullan R, Ashkan K, Bhangoo R and Vergani F (2021) Middle Frontal Gyrus and Area 55b: Perioperative Mapping and Language Outcomes. Front. Neurol. 12:646075. doi: 10.3389/fneur.2021.646075

Background: The simplistic approaches to language circuits are continuously challenged by new findings in brain structure and connectivity. The posterior middle frontal gyrus and area 55b (pFMG/area55b), in particular, has gained a renewed interest in the overall language network.

Methods: This is a retrospective single-center cohort study of patients who have undergone awake craniotomy for tumor resection. Navigated transcranial magnetic simulation (nTMS), tractography, and intraoperative findings were correlated with language outcomes.

Results: Sixty-five awake craniotomies were performed between 2012 and 2020, and 24 patients were included. nTMS elicited 42 positive responses, 76.2% in the inferior frontal gyrus (IFG), and hesitation was the most common error (71.4%). In the pMFG/area55b, there were seven positive errors (five hesitations and two phonemic errors). This area had the highest positive predictive value (43.0%), negative predictive value (98.3%), sensitivity (50.0%), and specificity (99.0%) among all the frontal gyri. Intraoperatively, there were 33 cortical positive responses—two (6.0%) in the superior frontal gyrus (SFG), 15 (45.5%) in the MFG, and 16 (48.5%) in the IFG. A total of 29 subcortical positive responses were elicited—21 in the deep IFG–MFG gyri and eight in the deep SFG–MFG gyri. The most common errors identified were speech arrest at the cortical level (20 responses—13 in the IFG and seven in the MFG) and anomia at the subcortical level (nine patients—eight in the deep IFG–MFG and one in the deep MFG–SFG). Moreover, 83.3% of patients had a transitory deterioration of language after surgery, mainly in the expressive component ($p = 0.03$). An increased number of gyri with intraoperative positive responses were related with better preoperative ($p = 0.037$) and worse postoperative ($p = 0.029$) outcomes. The involvement of the SFG–MFG subcortical area was related with worse language outcomes

($p = 0.037$). Positive nTMS mapping in the IFG was associated with a better preoperative language outcome ($p = 0.017$), relating to a better performance in the expressive component, while positive mapping in the MFG was related to a worse preoperative receptive component of language ($p = 0.031$).

Conclusion: This case series suggests that the posterior middle frontal gyrus, including area 55b, is an important integration cortical hub for both dorsal and ventral streams of language.

Keywords: area 55b, language mapping, speech arrest, perioperative mapping, DTI, TMS, language network, nTMS

INTRODUCTION

Previous models of parcellation of the cerebral cortex have been proposed based on cytoarchitectonic (1, 2), myeloarchitectonic (3, 4), or functional characteristics of the different cerebral cortical areas (5, 6).

More recently, a new mapping of the human cortex has been described, using a multi-modal gradient-based parcellation approach (7). One of the novelties of this approach has been the identification of new cortical areas with a distinctive myelo/cytoarchitectonic and functional profile. A particularly interesting region is the frontal area 55b. Initially noted by Hopf in 1956 (4), this area is located at the posterior aspect of the middle frontal gyrus (MFG) and is delimited by the frontal eye field (FEF) superiorly, the premotor eye field (PEF) inferiorly, the primary motor cortex and the ventral motor cortex posteriorly, and by the prefrontal areas anteriorly (7, 8). Area 55b appears to be lightly myelinated and lies between moderately myelinated areas (i.e., FEF above and PEF below) and anteriorly to heavily myelinated areas (i.e., primary motor cortex). It has been described to be involved in various language production tasks and fluency of speech (7, 9, 10). These findings are responsible for the renewed interest in the contribution of the posterior MFG to the overall language network.

Techniques of brain mapping that have evolved to increase the extent and safety of tumor resection in eloquent areas of the brain (11) have the unique advantage of testing different functions of specific cortical areas and networks at the individual level (12). Direct electrical stimulation (DES) at the cortical and subcortical levels is the gold standard for intraoperative mapping, defining the functional borders of resection in glioma surgery (13–15). In addition, navigated transcranial magnetic stimulation (nTMS) has emerged over the past decade as a useful adjunct for the preoperative mapping of motor (16–21) and language (22–27) areas of the brain.

In the present paper, we reviewed the results obtained by combining DES and nTMS in the functional assessment of the middle frontal gyrus and area 55b in a series of patients undergoing awake surgery for brain tumors. In addition, we evaluated the potential relationship between preoperative and intraoperative language mapping and between the assessment of language performed prior to and following surgery, with a view to assess the relative contribution of the MFG on the language outcome. The preoperative and intraoperative findings are reviewed, and the potential role of these areas as part of the language network is discussed.

MATERIALS AND METHODS

This is a retrospective single-center cohort study of non-consecutive patients admitted with language eloquent tumors for surgical treatment from January 2012 to January 2020. The inclusion criteria for the current study were age above 18 years old, awake craniotomy with DES for language mapping, and a tumor located in the dominant frontal lobe. Hemispheric dominance was assessed with the Edinburgh Handedness Inventory scale. The exclusion criteria included failed awake craniotomy and awake craniotomy for non-language mapping purposes.

Language Assessment

The preoperative and postoperative assessments were performed using the Sheffield Aphasia Screening Test for Acquired Language Disorder (SST) (28). This test was applied by the same speech and language therapist responsible for the intraoperative language testing. The patients were interviewed pre- and postoperatively to assess their communication abilities in conversational speech. Subtle subjective changes pertaining to comprehension, speech, reading, or writing abilities affecting daily living were evaluated. Where relevant, additional subtests were administered from the Mount Wilga Higher Level Language Test (29). The language errors were divided into speech arrest, hesitation, fluency disturbance, repetition disturbance, semantic paraphasia, and anomia.

Intraoperative Mapping

An asleep–awake–asleep craniotomy was performed in all the included patients. Low-frequency intraoperative stimulation according to the Penfield technique (30) was performed. Then, 50-Hz biphasic square wave pulses of 1-ms duration were applied using a constant current stimulator (ISIS Neurostimulator; Inomed Medizintechnik GmbH). The current threshold used for brain mapping was the minimal current responsible for speech arrest during the counting task (two out of three attempts) or the highest current non-responsible for after-discharges. The exposed cortical area was mapped with one stimulation area every 2–3 cm at least three times per language task. The selection of the intraoperative tasks were performed according to the

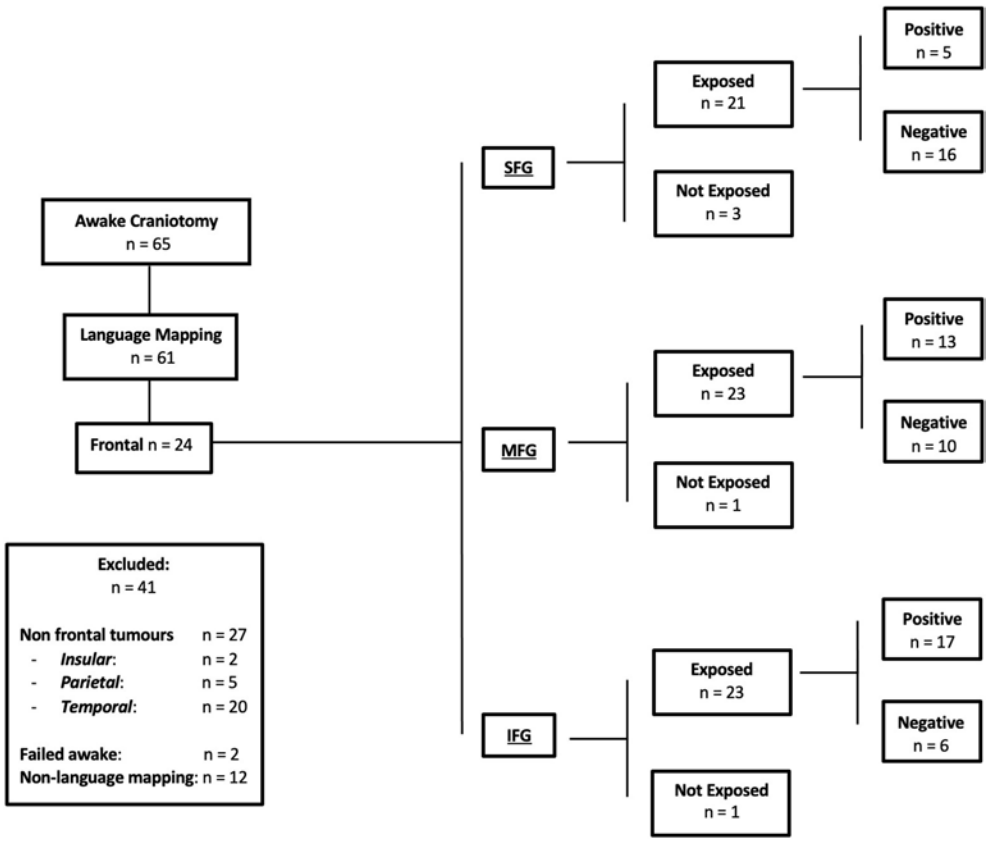

FIGURE 1 | Flow chart of the present study, detailing the inclusion and exclusion criteria. Positive responses indicate language errors elicited by direct electric stimulation. Negative responses indicate no language errors elicited by direct electric stimulation. Exposure indicates the specific frontal gyrus exposed during craniotomy.

Dutch Linguistic Intra-operative Protocol (31) and the Verb and Noun Test for Peri-Operative Testing (32).

Positive and negative responses were recorded, indicating the presence and absence of language errors elicited by DES respectively. After a speech arrest was identified and the threshold was established, the entire exposed cortical area of the frontal lobe was mapped with object naming and action naming in both present and past tenses. At the subcortical level, repetition tasks were used for mapping the arcuate fasciculus (AF), sentence completion for the fronto-aslant tract (FAT), and semantic odd-one-out and object naming for the inferior fronto-occipital fasciculus (IFOF). The positive responses—two out of three attempts—with induced speech deficit in the absence of after-discharges on electrocorticography were documented with intraoperative pictures.

Navigated Transcranial Magnetic Stimulation

Preoperative mapping with nTMS has been used at our center since 2016 as an adjunct to intraoperative DES mapping. Whenever available, data from nTMS were included in the analysis.

Language mapping was performed following resting motor threshold determination (33). A set series of pre-designed images were presented to the patient for baseline assessment in two consecutive rounds: object naming, action naming in the present tense, and action naming in the past tense (32). The inter-picture interval was set to 2,500 ms, and the display time (DT) varied between 500 and 1,000 ms, which was dependent on a patient's ability. Images that were incorrectly described or with hesitation were excluded from the final exam. An offline analysis was performed, comparing the stimulation assessment to the baseline assessment and identifying any changes in language function during the exam. Language errors were classified into distinct categories (hesitation, expressive, semantic, anomia, arrest, other, and no errors).

The intraoperative pictures of positive stimulation sites collected during intraoperative mapping were included in the preoperative MRI studies (T1-weighted images after gadolinium injection) by comparing the anatomical landmarks (i.e., sulci and gyri) of the single pictures with the axial brain volumetric images and reformatted sagittal/coronal images (33). It was therefore possible to correlate the positive intraoperative sites with nTMS mapping, allowing for the calculation of TMS

specificity, sensitivity, and positive and negative predictive values (PPV and NPV, respectively).

Statistical Analysis

STATA 13.0 software was used for statistical analysis. Regression techniques were performed to compare the language outcomes—screening test for acquired language disorder (SST) and its receptive and expressive subdivisions—with the number of gyri and the main subcortical areas infiltrated by the tumor. A p-value < 0.05 was considered as significant.

RESULTS

Sixty-five awake craniotomies were performed between 2012 and 2020. There were 24 (36.9%) frontal tumors that constitute the object of the current study. The demographics showed an even distribution between males and females, with a mean age of 47 ± 13.8 years old (standard deviation). The majority of the included patients had left-sided tumors (22, 91.6%). Meanwhile, 19 (79.1%) patients presented with a new-onset seizure; two (8.3%) had a motor deficit, and two (8.3%) presented with a language deficit. The vast majority of patients (20, 83.4%) presented with a performance status of 0. High-grade gliomas were prevalent in this series [71% World Health Organization (WHO) grade III and IV]. Isocitrate dehydrogenase was positive in 10 (41.6%) tumors, whereas 1p/19q co-deletion was present in nine (37.5%) oligodendrogliomas. **Figure 1** and **Table 1** summarize the patients' characteristics.

TABLE 1 | Demographics of the included subjects along with the classification of tumors based on histology, grade, and biomarkers.

Subject demographics and tumor classification	
Sex	
Female	12 (50%)
Male	12 (50%)
Age group	
18–24	1 (4.1%)
25–34	5 (20.8%)
35–44	5 (20.8%)
45–54	5 (20.8%)
55–64	6 (25%)
65–74	2 (8.3%)
Presentation	
Motor deficit	2 (8.3%)
Language deficit	2 (8.3%)
Cognitive deficit	1 (4.2%)
Seizure	19 (79.2%)
Tumor laterality	
Right	2 (8.3%)
Left	22 (91.6%)
Histology	
Anaplastic Astrocytoma	3 (12.5%)
Anaplastic Oligodendroglioma	6 (25%)
Diffuse Astrocytoma	4 (16.7%)
Glioblastoma Multiforme	5 (21%)
Glioneuronal Tumor	1 (4%)
High Grade Glioma	2 (8.3%)
Low Grade Glioma	3 (12.5%)
Oligodendroglioma	3 (12.5%)
WHO grading	
I	0 (0%)
II	3 (12.5%)
II	4 (16.7%)
III	12 (50%)
IV	5 (21%)
Tumor marker	
IDH	
Positive	10 (41.6%)
Negative	7 (29.1%)
Mutant	6 (25%)
Wildtype	1 (4.2%)
1p/19q	
Co deletion	9 (37.5%)
No deletion	2 (8.3%)
19q deletion	1 (4.2%)
N/A	12 (50%)

Preoperative Language Assessment

The average preoperative SST was 18.9/20. The average receptive language skill score was 8.1/9, and the average expressive language skill score was 10.7/11 (seven patients were excluded due to incomplete assessments). From the SST, the most frequent receptive errors were auditory semantic differentiation and the ability to fully comprehend a paragraph-level narrative. Expressive errors were rare, but when present, the most frequent error was the ability to provide word definitions. The SST does not measure phonemic ability, but no patient displayed any marked phonemic errors in conversation preoperatively (**Table 2**).

Preoperative nTMS Assessment

nTMS was performed in 14 (58.3%) patients with frontal tumors (1,844 stimulations distributed across the gyri as follows: SFG−172, MFG−428, IFG−1,244), and positive responses were elicited in 12 patients (85.7%), with a total of 42 positive responses: three responses in the SFG (one hesitation and two anomic errors); seven responses in the MFG (five hesitations and two phonemic errors); 32 responses in the IFG (24 hesitations, six phonemic, and two semantic errors). This shows a preferential distribution of the stimulations in the IFG, particularly given the likelihood of positive responses in the area of the frontal operculum.

Overall, the nTMS had a PPV of 31.0%, a NPV of 97.8%, sensitivity of 45.7%, and specificity of 98.3%. When the gyri were compared, the MFG had the highest PPV (43.0% vs. IFG−31.25% and SFG−0%), NPV (98.3% vs. IFG−97.8% and SFG−95.9%), sensitivity (50.0% vs. IFG−47.1%, and SFG−30.0%), and specificity (99.0% vs. IFG−98.2% and SFG−98.1%) (**Table 2**, **Figure 2**, and **Supplementary Video 1**).

TABLE 2 | A comprehensive table detailing the navigated transcranial magnetic simulation language errors, intraoperative stimulation positive responses, a comparison of language pathway error, Sheffield Aphasia Screening Test (SST) for Acquired Language Disorder assessments pre- and postoperatively, changes in SST score, and a comprehensive speech and language therapy pre-, intra-, and postoperative assessment.

ID	nTMS Language Error	Intra-operative mapping response	Sheffield screening test (SST)			Speech and language therapist (SLT) assessment		
			Preoperative	Postoperative	Difference in scores	Preoperative	Intraoperative	Postoperative
1	*SFG:* None *MFG*: Stutter (1) *IFG:* Hesitation (3)	SFG-MFG	Total: Spanish: 18/20 *English*: 13/20	None *2 years post op:* 12/20	Total: −6	Mild receptive and expressive dysphasia Semantic errors in Spanish Action and object naming difficulties	No language errors in English or Spanish	Mild receptive and expressive dysphasia Increase in word finding difficulties compared to pre op (in both languages)
2	*SFG:* None *MFG*: Word finding difficulty (1) *IFG:* None	SFG-MFG	Total: 15/20 Receptive 6/9 Expressive 9/11	Total: 9/20 Receptive 4/9 Expressive 5/11	Total: −6 Receptive −2 Expressive −4	No obvious dysphasia Difficulties more likely to be due to English as additional Action and object naming difficulties	Semantic errors, hesitation in Farsi for object naming. End of awake period: difficulty with object naming in both languages More difficulty in first language (Farsi) than in English	Moderate dysphasia in English Word finding difficulties (semantic errors) and perseveration in English (5 days post op)
3	*SFG:* None *MFG*: None *IFG:* Hesitation, Apraxia, Semantic Anomia (13)	IFG-MFG	Total: 20/20	*2 days post op:* unable to participate *5 days post op:* Total: 14/20 Receptive 8/9 Expressive 6/11	Total: −6 Receptive −1 Expressive −5	No overt dysphasia in conversation	Hesitation and semantic error (object naming, action naming) with 2 perseveration errors in object naming	Mild/moderate dysphasia Difficulty with complex reading tasks Hesitancy Word finding difficulty
4	*SFG:* None *MFG*: None *IFG:* None	SFG-MFG	Total: 19/20 Receptive 8/9 Expressive 11/11	Total: 2/20 Receptive 2/9, test abandoned as too difficult	Total: −17 Receptive −6	No communication and language dysfunction	Semantic, phonemic, reading, and fluency errors	Moderate expressive and receptive dysphasia Fluency errors and difficulties with semantic tasks Spontaneous speech notably easier than when asked direct questions
5	*SFG:* None *MFG*: None *IFG:* Not performed	SFG-MFG	Total: 19/20 Receptive 8/9 Expressive 11/11	Unable to complete SST *7 days post op:* Total: 13/20 Receptive 8/9 Expressive 5/11	Total: −6 Receptive 0 Expressive −6	Semantic errors	Semantic errors SMA-like syndrome No automatic speech, counting errors	Semantic and phonemic errors Moderate expressive aphasia
6	Not performed	SFG-MFG	Total: 20/20	Total: 18/20	Total: −2	Difficulty following complex commands Phonemic errors in conversation reported by family but not seen in clinic	No difficulties with repetition, object or verb naming	*5 days post op*: mild receptive and severe expressive dysphasia with likely overlay of verbal dyspraxia *1 month post op:* mild expressive dysphasia Semantic word finding difficulties in conversation and/or difficulties with grammatical structure

(Continued)

TABLE 2 | Continued

ID	nTMS Language Error	Intra-operative mapping response	Sheffield screening test (SST)			Speech and language therapist (SLT) assessment		
			Preoperative	Postoperative	Difference in scores	Preoperative	Intraoperative	Postoperative
7	*SFG:* Hesitation (1) *MFG*: Hesitation (1) *IFG:* Word formation (1)	SFG-MFG	Total: 19/20 Receptive 8/9 Expressive 11/11	*5 days post op* unable to complete: severe expressive dysphasia, SMA initiation difficulties. *7 days post op:* Total: 13/20 Receptive 7/9 Expressive 6/11	Total: −6 Receptive −1 Expressive −5	No overt dysphasia in conversation.	Speech arrest 2 semantic errors 1 hesitation error (all in verb naming) 2 sentence completion errors	Mild receptive with moderate expressive dysphasia Semantic difficulties with additional difficulties initiating speech
8	*SFG:* None *MFG*: None *IFG:* Hesitation (6)	IFG-MFG	Total: 18/20 Receptive 8/9 Expressive 10/11	Total: 18/20 Receptive 8/9 Expressive 10/11	Total: 0 Receptive 0 Expressive 0	No overt dysphasia in conversation but semantic difficulties in testing.	Semantic, hesitation, fluency errors.	Mild dysphasia - mild word finding difficulties in conversation - using circumlocution to good effect
9	*SFG:* Anomia (2) *MFG*: Hesitation (2) *IFG:* None	SFG-MFG	Total: 18/20 Receptive 7/9 Expressive 11/11	Total: 9/20 Receptive 2/9 Expressive 7/11 (cognitive overlay)	Total: −9 Receptive −5 Expressive −4	No overt difficulties, occasional hesitations Semantic errors	Word finding difficulties in conversation and object naming	Mild dysarthria, moderate dysphasia with phonemic errors in conversation Cognitive communication difficulties
10	*SFG:* None *MFG*: None *IFG:* Hesitation (6)	IFG-MFG	Total: 20/20	Total: 14/20 Receptive 9/9 Expressive 5/11	Total: −6 Receptive 0 Expressive −6	No overt dysphasia	2 phonemic errors in mapping	Mild to moderate expressive dysphasia Motor planning difficulties
11	*SFG:* None *MFG*: Hesitation (1) *IFG:* None	IFG-MFG	Total: 17/20 Receptive 6/9 Expressive 11/11	Total: 20/20	Total: +3 Receptive +3 Expressive 0	No communication difficulties in conversation	Imprecise articulation/dysarthric errors in mapping (2) and in cortical resection	No obvious dysphasia
12	Not performed	None	Not performed	Not performed	Unable to determine	No obvious dysphasia in first language (Polish)	Perseveration and word finding difficulties during resection	No data available
13	Not performed	IFG-MFG	Total: 19/20 Receptive 8/9 Expressive 11/11	Total: 14/20 Receptive 6/9 Expressive 8/11	Total: −5 Receptive −2 Expressive −3	Higher level word finding difficulties	4 phonemic errors in mapping, 1x phonemic error and 1x hesitation in resection	Mild receptive and expressive dysphasia Word finding difficulties more evident in testing than in conversation
14	*SFG:* None *MFG*: Hesitation (1) *IFG:* Hesitation, Anomia (2)	IFG-MFG	Total: 20/20 Receptive 9/9 Expressive 11/11	Total: 15/20 Receptive 7/9 Expressive 8/11	Total: −5 Receptive −2 Expressive −3	Initial difficulty in recalling details	Phonemic errors noted in mapping (2 separate areas) Self-correcting phonemic errors in conversation during resection 1 phonemic error at final testing at the end of resection	Mild receptive and expressive dysphasia Improvements noted in verbal sequencing compared to immediately after previous surgery
15	*SFG:* None *MFG*: None *IFG:* Hesitation, Dysarthria, Semantic (4)	IFG-MFG	Total: 20/20	Total: 18/20 Receptive 8/9 Expressive 10/11 (phonemic errors not significant to impact on score)	Total: −2 Receptive −1 Expressive−1	No communication difficulties	Action naming, 1 clear speech arrest in lead up phrase Object naming, phonemic difficulty during mapping, resection of arcuate fasciculus Slurred speech at the end of resection	Mild word finding difficulties with lower frequency nouns Mildly reduced associated naming Mild-moderate verbal apraxia, mild dysarthria and mild expressive dysphasia

(Continued)

TABLE 2 | Continued

ID	nTMS Language Error	Intra-operative mapping response	Sheffield screening test (SST)			Speech and language therapist (SLT) assessment		
			Preoperative	**Postoperative**	**Difference in scores**	**Preoperative**	**Intraoperative**	**Postoperative**
16	Not performed	None	Not performed	Not performed	Unable to determine	No communication difficulties reported	No data available	Mild receptive and moderate-severe expressive dysphasia Unable to speak in phrases or sentences, occasional word, using Yes/No
17	Not performed	None	Not performed	Not performed	Unable to determine	All normal except planning (constructing sentences from given words) Mildly impaired in efficiency, auditory memory, auditory comprehension and numeracy	Prompting for biological information, one-word answers, Counting: perseveration at number 7 Visual and semantic errors on picture naming Speech arrest	*2 days post op*: moderate receptive and expressive dysphasia Semantic and phonemic errors Speech slow and effortful *5 days post op:* Mild/moderate dysphasia but still with phonemic and semantic errors
18	Not performed	None	Not performed	Not performed	Unable to determine	No overt dysphasia Mild difficulties with planning for sentence construction and in planning for sequencing on Mount Wilga higher level language tasks Some word finding difficulties previous to taking steroids	Minor visual and semantic errors Speech arrest very obvious during stimulation when counting 1–10 during first half of testing No obvious dysphasia in intra-operative testing. At end of testing, able to name single object pictures, describe pictures, repeat words and participate in conversation	No obvious dysphasia in conversation or Brisbane Language screen
19	Not performed	None	Not performed	Not performed	Unable to determine	No difficulties communicating in conversation Mild higher-level language difficulties in Mount Wilga tests (7/10 in auditory comprehension and recall questions, difficulty with jumbled sentences task) No difficulty with planning tasks.	No communication errors	Mild dysphasia Word finding difficulties in conversation (phonemic and semantic) and difficulties organizing sentences within a narrative
20	*SFG:* None *MFG*: None *IFG:* None	SFG-MFG	Total: 20/20	*Post op*: Total: 0/20 *Post op week 1*: Total: 8/20 *Post op week 2*: Total: 14/20 Receptive 9/9 Expressive 5/11	Total: −6 Receptive 0 Expressive −6	No difficulties in communication	No issues with naming objects and actions Possible hesitation with lower frequency items Later stages of resection, able to name intermittently, preservation and mild semantic errors noted At the end of resection, unable to name or repeat or count to 10	Severe expressive and receptive dysphasia Non-verbal post-op Overlay of difficulties initiating speech - at times these severely impact on patient's ability to make self understood

(Continued)

TABLE 2 | Continued

ID	nTMS Language Error	Intra-operative mapping response	Sheffield screening test (SST)			Speech and language therapist (SLT) assessment		
			Preoperative	Postoperative	Difference in scores	Preoperative	Intraoperative	Postoperative
21	Not performed	SFG-MFG	Total: 19/20 Receptive 8/9 Expressive 11/11	Total: 20/20 Receptive 9/9 Expressive 11/11	Total: +1 Receptive +1 Expressive 0	No communication difficulties	No communication errors but drowsy	No obvious dysphasia or difficulties in short conversation
22	Not performed	None	Not performed	Not performed	Unable to determine	Mild difficulty with written calculation and planning sentence construction	Periods of motor speech and naming deficits during mapping and surgery. At end of SLT assessment: -Decreased spontaneous verbal output -Producing automatics and single words/short phrases to sentence closure tasks	*2 days post op*: severe expressive dysphasia *5 days post op:* mild receptive with moderate expressive dysphasia Dyspraxia of speech, comprehending complex info during conversations.
23	*SFG:* None *MFG*: None *IFG:* Hesitation, Anomia (2)	IFG-MFG	Total: 18/20 Receptive 8/9 Expressive 10/11	Total: 16/20 Receptive 7/9 Expressive 9/11	Total: −2 Receptive −1 Expressive−1	Some higher-level language difficulties apparent	Minor difficulty with repetition during subcortical mapping Intermittent repetition, naming, and spontaneous speech during resection No difficulties with spontaneous speech at the end of surgery; able to answer direct questions, name high frequency objects and 9/10 on repetition tasks but fatigued	Mild dysphasia and higher level language difficulties likely linked to ability to retain and organize information
24	*SFG:* None *MFG*: None *IFG:* Language reversion to French (1)	SFG-MFG IFG-MFG	Total: 20/20	Total: 13/20 Receptive 6/9 Expressive 7/11	Total: −7 Receptive −3 Expressive −4	Mild to moderate impairment in verbal explanation. Moderate impairment in sentence construction and understanding inferential information, this is likely akin to mild dysphasia though EAL (English as an Additional Language)	Semantic errors in initial mapping, too drowsy to comment on phonemic errors	Mild/moderate receptive and expressive dysphasia Able to answer basic questions in conversation but difficulty with longer explanations: likely combination of cognitive communication difficulty and dysphasia

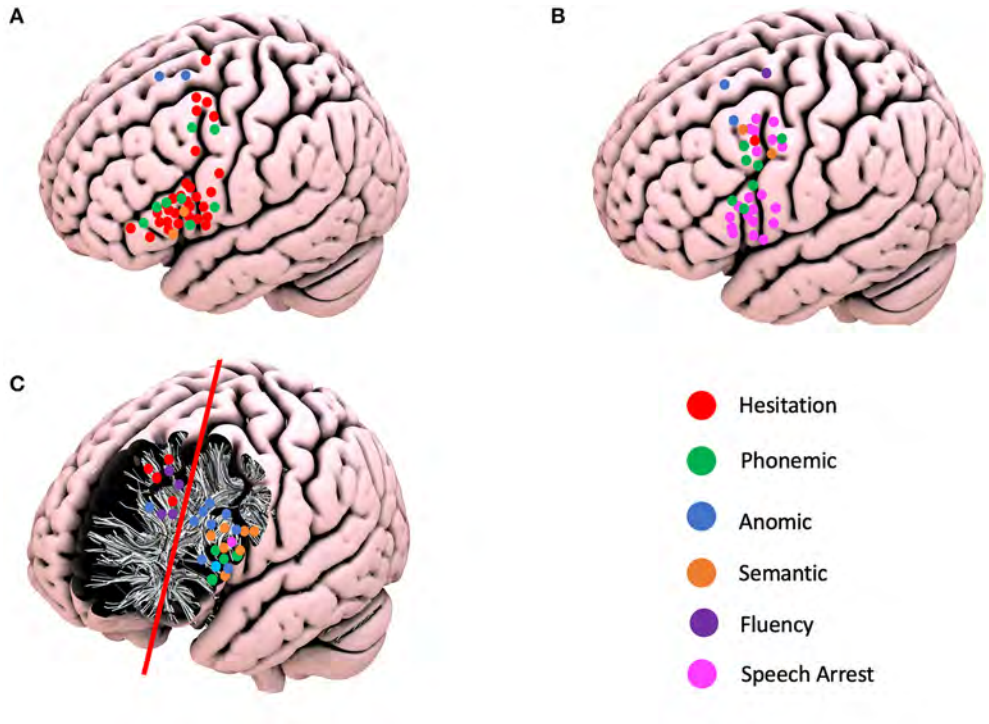

FIGURE 2 | Schematic representation of the positive navigated transcranial magnetic simulation responses, intraoperative cortical responses, and positive subcortical responses according to the different language errors. **(A)** Positive TMS responses. **(B)** Positive cortical intraoperative responses. **(C)** Positive subcortical intraoperative responses.

A preoperative structural connectome analysis performed in three patients with positive responses in the area 55b showed the strongest connectivity of this area not only with the primary motor cortex but as well as with the supplementary motor area, inferior frontal gyrus, and anterior aspect of the MFG (**Figure 3**). Positive nTMS mapping in the inferior frontal gyrus was related with a better preoperative overall SST score ($p = 0.017$) due to a better receptive component ($p = 0.001$). Positive nTMS mapping for the posterior MFG/area 55b was related with a worse receptive preoperative component of the SST ($p = 0.031$), but with no expression in the overall score ($p = 0.059$) (**Table 3**).

Intraoperative Speech Errors

The superior frontal gyrus (SFG) was exposed in 21 (87.5%), the middle frontal gyrus (MFG) in 23 (95.8%), and the inferior frontal gyrus (IFG) in 23 (95.8%) craniotomies. A total of 33 cortical positive responses for language were recorded. Two (6.0%) responses were recorded in the SFG, 15 (45.5%) in the MFG, and 16 (48.5%) in the IFG. Of relevance is the fact that all positive responses recorded in the MFG were demonstrated in area 55b. The following responses were identified: speech arrest in 20 patients (13 in IFG; seven in area 55b), hesitation in one patient (area 55b), decreased fluency in one patient (SFG), phonemic errors in seven patients (four in area 55b and three in IFG), semantic paraphasias in two patients (area 55b), and anomia in two patients (one in MFG and one in SFG). At the subcortical level, 29 positive responses were identified and divided into two main areas: 21 patients in the deep IFG–MFG area and eight patients in the deep MFG–SFG area. These positive responses were divided as follows: repetition disturbance in one patient (deep IFG), speech arrest in one patient (deep IFG), hesitation in four patients (deep MFG–SFG), decreased fluency in three patients (deep SFG), phonemic errors in four patients (deep IFG–MFG), semantic paraphasias in seven patients (deep IFG–MFG), and nine anomias (eight in deep IFG–MFG and one in deep MFG–SFG) (**Figure 2**).

Postoperative Language Assessment

Twenty (83.3%) patients had a transient deterioration of their language function after surgery (mean postoperative SST = 14.67 ± 0.76). Both the expressive (−2.875 ± 0.55) and the receptive (−1.36 ± 0.37) components of the SST deteriorated, with a statistically significant greater deterioration of the expressive component ($p = 0.03$). The single involvement of a particular gyrus (including area 55b) was not related *per se* with significant changes in language outcomes. The number of gyri with documented intraoperative positive language mapping was correlated with language outcomes: an increased number of gyri involvement was related with a better preoperative assessment ($p = 0.037$) and worse immediate language outcome ($p = 0.029$). This is mainly due to the changes in the expressive component of language (SST expressive preoperatively—$p = 0.045$) and SST expressive postoperatively−0.030). No significant changes were identified at the level of the receptive component of language. At the subcortical level, the involvement of the deep white matter of the SFG–MFG was related with worse expressive

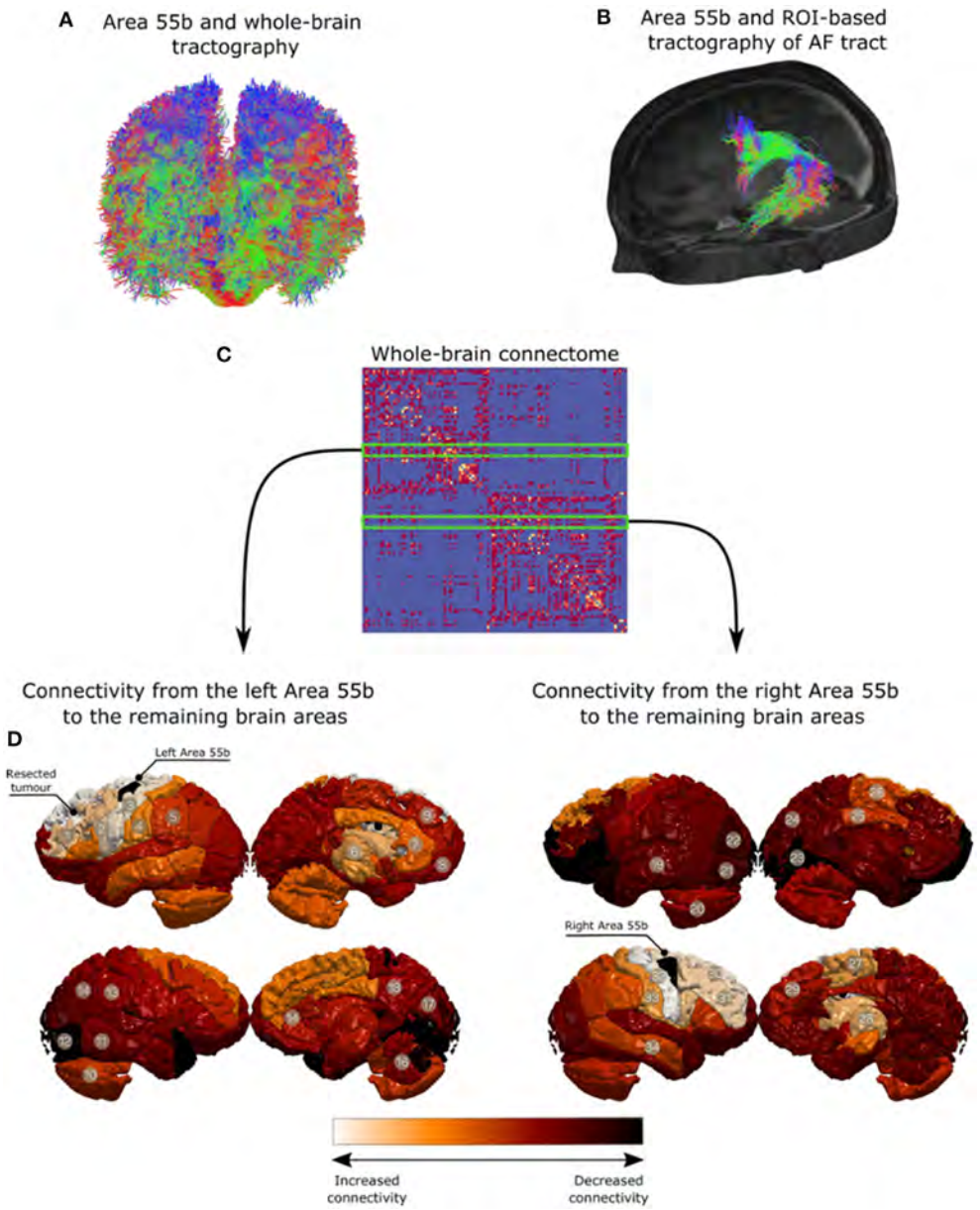

FIGURE 3 | Qualitative analysis for region of interest-based tractography of the arcuate fasciculus (AF). The middle frontal gyrus region is in red, where the streamlines from the AF terminate. **(A)** Area 55b and whole-brain tractography. **(B)** Area 55b and ROI-based tractography of AF tract. **(C)** Whole-brain connectome. **(D)** Connectivity from the left Area 55b to the remaining brain areas. **(E)** Connectivity from the right Area 55b to the remaining brain areas.

outcome postoperatively ($p = 0.037$), but no correlation was identified with the preoperative assessment ($p = 0.780$), and no overall impact was reflected in the overall SST assessment (SST preoperatively—$p = 0.895$; SST postoperatively−0.109). The preoperative nTMS mapping was not related with the language outcome (**Table 4**).

DISCUSSION

The inferior frontal gyrus and the "classical" Broca's area have been traditionally considered as the main language hub in the dominant frontal lobe. However, the findings from multiple intraoperative reports showed that the functional organization of the frontal lobe is more complex, with positive language sites described both at the level of the MFG and, to a lesser extent, in the SFG (34–39).

In recent years, there has been a renewed interest in the role of the MFG as part of the language network. This is particularly the case after the description of area 55b, located at the posterior aspect of the MFG (7). Previous studies have implicated the role of posterior MFG and area 55b in language (7, 9, 10). In the present series, we report a high rate of positive speech responses at the level of the MFG (45% of intraoperative errors).

TABLE 3 | Correlation of navigated transcranial magnetic simulation responses per gyrus and the preoperative language assessment (Sheffield aphasia screening test for acquired language disorder).

	Coef.	95%CI	*p*-value
nTMS IFG			
SST	0.21 ± 0.7	(0.05–0.38)	0.017
Receptive	0.35 ± 0.08	(0.18–0.53)	0.001
Expressive	0.22 ± 0.25	(−0.35–0.78)	0.407
nTMS MFG			
SST	−0.19 ± 0.09	(−0.38–0.01)	0.059
Receptive	−0.29 ± 0.11	(−0.54 to −0.03)	0.031
Expressive	−0.15 ± 0.26	(−0.75–0.45)	0.579
nTMS SFG			
SST	−0.01 ± 0.8	(−0.19–0.16)	0.877
Receptive	−0.07 ± 0.11	(−0.32–0.18)	0.538
Expressive	0.13 ± 0.20	(−0.33–0.59)	0.538

TABLE 4 | Cortical and subcortical intraoperative involvement and pre- and postoperative language outcomes.

	Coef.	95%CI	*p*-value
Number of gyri involved			
SST preoperative	1.35 ± 0.65	(0.08–2.62)	0.037
SST postoperative	−0.66 ± 0.30	(−1.26 to −0.69)	0.029
SST receptive preoperative	0.25 ± 0.21	(−0.20–0.69)	0.250
SST receptive postoperative	−0.11 ± 0.11	(−0.34–0.12)	0.316
SST expressive preoperative	0.59 ± 0.26	(0.01–1.16)	0.045
SST expressive postoperative	−0.17 ± 0.07	(−0.32 to −0.02)	0.030
Subcortical involvement – SFG-MFG			
SST preoperative	−0.06 ± 0.48	(−1.00–0.88)	0.895
SST postoperative	−0.31 ± 0.19	(−0.69–0.07)	0.109
SST receptive preoperative	−0.18 ± 0.61	(−1.36–1.01)	0.770
SST receptive postoperative	−0.41 ± 0.37	(−1.14–0.32)	0.276
SST expressive preoperative	0.32 ± 1.14	(−1.91–2.55)	0.780
SST expressive postoperative	−0.72 ± 0.34	(−1.40 to −0.04)	0.037
Subcortical involvement – IFG-MFG			
SST preoperative	0.29 ± 0.48	(−0.64–1.22)	0.544
SST postoperative	0.24 ± 0.18	(−0.12–0.60)	0.193
SST receptive preoperative	0.57 ± 0.62	(−0.64–1.78)	0.357
SST receptive postoperative	0.20 ± 0.33	(−0.46–0.85)	0.557
SST expressive preoperative	−0.01 ± 1.13	(−2.23–2.21)	0.992
SST expressive postoperative	0.66 ± 0.34	(−0.01–1.33)	0.055

Two points require further discussion: First, the high incidence of positive responses in the MFG were replicated with the use of preoperative nTMS in addition to intraoperative DES. In addition, the majority of positive language sites in the MFG were confined to the posterior aspect of the gyrus, covering the anatomical location of area 55b. We hypothesize that these results can be explained due to the involvement of area 55b when stimulating the posterior aspect of the MFG. This is consistent with previous descriptions of the intraoperative responses obtained at area 55b (9).

Second, the responses recorded in the MFG with the combined nTMS and DES were both phonological (hesitations and phonemic errors) and semantic (semantic paraphasias and anomias). The involvement of this area in both semantic processing (12) and speech articulation (40) has been well recognized. The results therefore show that the posterior MFG is likely implicated in both the "dorsal phonological" and the "ventral semantic" streams of language (36). The involvement of the posterior MFG area in both streams of language was also supported at the subcortical level, where again both phonological (speech arrest, hesitation, and fluency disturbance) and semantic disturbances (semantic paraphasia and anomia) were elicited while stimulating the white matter deep to the MFG.

The subcortical areas were divided into two main areas (IFG–MFG and MFG–SFG) as the included tumors all involved more than one subcortical area. The majority of the recorded errors at the subcortical level occurred in the IFG–MFG area (72.4%). Both the arcuate fasciculus (AF) and the inferior fronto-occipital fasciculus (IFOF) are known to cross deep to the IFG–MFG area, with terminations at the level of the posterior MFG. AF, the main dorsal stream fasciculus, has terminations in the MFG documented by anatomical cadaveric, diffusion imaging, and resting-state fMRI studies. It is reported that up to 56% of patients can have terminations of the AF in the MFG, particularly the long segment (41–44). From a ventral stream perspective, multiple components of the IFOF were proposed based on anatomical studies (45), DES (46), and diffusion imaging (47). These methods concur that this tract has a termination in the posterior aspect of the MFG and therefore may serve as a substrate for the semantic errors identified in this area (45). The errors detected at the level of the MFG–SFG could be related to the stimulation of the fronto-aslant tract (hesitation and decreased fluency). This tract has been recently involved in the dorsal stream functions of language, particularly the fluency and initiation of speech (48–50).

In addition, the original structural connectivity data presented also support a strong connectivity of the MFG with the adjacent cortical gyri (IFG and SFG), likely mediated *via* U-fiber short association fibers. These findings are similar to those of other connectivity studies reported in the literature (7, 8). In this context, the interaction with the FEF in the anterior/middle frontal gyrus raises the possibility of a potential integration of visual recognition processes with speech production (51).

Therefore, two hypotheses can be formulated to support the interaction of posterior MFG and area 55b with both streams of language: a direct connectivity *via* relay of some subcomponents of both AF and IFOF and an indirect connectivity *via* the stimulation of U-fibers to the adjacent gyri (IFG and SMA). In addition to previous imaging and dissection data, recent nTMS data support a strong connectivity of language positive sites *via* the U-fiber system, supporting the indirect connectivity theory (52). The strong connectivity

to the primary motor cortex further supports the potential role for hand movement integration in language (43) and the involvement of this area in the articulation and praxis of speech (9).

The impact of positive responses in the area 55b on clinical outcomes is difficult to establish, as these are usually associated with positive responses in either the IFG or SFG. Generally, the overall SST score and each of its components deteriorated temporarily after resection. Thus, the direct involvement of the posterior middle frontal gyrus and area 55b was not related with language outcome. However, the involvement of an increased number of gyri was related with better preoperative SST but with worse postoperative SST scores, particularly due to the receptive component. We believe that neuroplasticity within the language network can be partially responsible for these findings. A higher number of involved gyri may imply the involvement of preoperative adaptive mechanisms to maintain a high level of language function. However, at the same time, they may represent an overall stretched network that has a limited ability to recover from the hit provided by surgical resection and therefore linked to worse language outcomes. This natural process of adaptation has been seen in other systems of the human brain, such as the motor system (53), and further studies are required to ascertain if a similar process may be involved in the language connectivity and network.

There is evidence for language network plasticity in patients, given the intrinsic changes in the intra- and interhemispheric inhibition mechanisms altered by pathological conditions (54). Furthermore, multiple preoperative and intraoperative studies have documented the presence of language network plasticity, particularly in tumors with a long course and natural history, such as low-grade gliomas (55–59).

Despite it being acknowledged that there are different degrees of plasticity potential for different functions of language (60), we hypothesize that an increased number of frontal lobe gyri involved in language may act as a surrogate for the degree of plasticity and adaptation of the language network already present before surgery.

To this regard, preoperative speech mapping with nTMS can play an important role in detecting the extent of involvement of the different frontal gyri in language function, thus providing a useful tool for preoperative counseling. It is crucial to take a patient-centred approach in neuro-oncology in order to meet patient expectations with surgical and oncological treatment (61).

This study has the general limitations of a retrospective cohort study. The most significant one is the incomplete preoperative data for some of the patients included, where the posterior middle frontal gyrus and the area 55b were mapped intraoperatively. However, it provides evidence for the added value of the integration of preoperative advanced mapping and intraoperative language mapping of area 55b and further establishes this area within the MFG as a potential relay for both ventral and dorsal streams of language.

CONCLUSION

This case series suggests that the posterior MFG, including area 55b, is an important integration cortical hub for both dorsal and ventral streams of language. It demonstrates this area as a cluster of positive responses in the MFG for both preoperative nTMS and intraoperative DES language mapping with a potential impact on language outcomes in dominant frontal lobe surgery.

DATA AVAILABILITY STATEMENT

The original contributions presented in the study are included in the article/**Supplementary Material**, further inquiries can be directed to the corresponding author/s.

ETHICS STATEMENT

Written informed consent was obtained from the individual(s) for the publication of any potentially identifiable images or data included in this article.

AUTHOR CONTRIBUTIONS

SH and MA: data collection, data analysis, literature review, and manuscript writing. JL: data collection, data analysis, literature review, manuscript writing, and statistical analysis. SP: data collection (nTMS, demographics), and written part of methodology. HW: reviewed speech and language data, written part of methodology. OL, CS, HI, AM, and SO: area 55b seed, connectivity data. JL, AK-V, RG, KA, and RB: reviewed manuscript. FV: principal manuscript reviewer, innovative concepts and ideas. All authors contributed to the article and approved the submitted version.

FUNDING

OL was funded by the EPSRC Research Council (EPSRC DTP EP/R513064/1). HI and CS were supported by the EPSRC-funded UCL Centre for Doctoral Training in Medical Imaging (EP/L016478/1).

SUPPLEMENTARY MATERIAL

The Supplementary Material for this article can be found online at: https://www.frontiersin.org/articles/10.3389/fneur.2021.646075/full#supplementary-material

Supplementary Material 1 | Tractography. Diffusion and T1-weighted data were pre-processed using the framework described by Mancini et al. (62). Multi-fiber orientations were estimated using single-shell two-tissue constrained spherical deconvolution using order $l_{max} = 8$ (63). Probabilistic tractography was done using Second-order integration over Fiber Orientation Distributions (iFOD2) (63) and seeding randomly from the white-matter/grey-matter interface, both to reconstruct whole-brain (FOD amplitude cut-off = 0.05 and total_streamlines = 10 million) and region-of-interest (ROI) based tractography (FOD amplitude cut-off = 0.05 and total_streamlines = 1,000). ROI-based tractography relied on reconstructing the

arcuate fasciculus (AF) tract from the left side of the brain based on similar pipeline introduced in (62). The posterior MFG was used to filter the reconstructed AF and its connectivity analysis. Additionally, qualitative results are shown in **Figure 3**. For surgical planning purposes, region of interest based tractography using subcortical anatomical areas was performed as described by Fekonja et al., in (64). The nTMS responses were overlayed over the dissected tracts considered for language network.

Supplementary Video 1 | Preoperative language mapping (nTMS assessment) demonstrating language errors.

REFERENCES

1. Brodmann K. *Vergleichende Lokalisationslehre der Grosshirnrinde in ihren Prinzipien dargestellt auf Grund des Zellenbaues (English Translation by Garey, L.J.: Brodmann's Localization in the Cerebral Cortex; Smith Gordon, London, 1994), Barth* (1909).
2. von Economo CF, Koskinas GN. *Die cytoarchitektonik der hirnrinde des erwachsenen menschen*. London: Springer (1925).
3. Vogt C, Vogt O. Allgemeinere Ergebnisse unserer Hirnforschung. *J Psychol Neurol*. (1919) 25:279–462.
4. Hopf A. Distribution of myeloarchitectonic marks in the frontal cerebral cortex in man. *J Hirnforschung*. (1956) 2:311–33.
5. Nieuwenhuys R. The myeloarchitectonic studies on the human cerebral cortex of the Vogt-Vogt school, and their significance for the interpretation of functional neuroimaging data. *Brain Struct Func*. (2013) 218:303–52. doi: 10.1007/s00429-012-0460-z
6. Van Essen DC, Glasser MF, Dierker DL, Harwell J, Coalson T. Parcellations and hemispheric asymmetries of human cerebral cortex analyzed on surface-based atlases. *Cerebral Cortex*. (2012) 22:2241–62. doi: 10.1093/cercor/bhr291
7. Glasser MF, Coalson TS, Robinson EC, Hacker CD, Harwell J, Yacoub E, et al. A multi-modal parcellation of human cerebral cortex. *Nature*. (2016) 536:171–8. doi: 10.1038/nature18933
8. Baker CM, Burks JD, Briggs RG, Sheets JR, Conner AK, Glenn CA, et al. A connectomic Atlas of the human cerebrum-chapter 3: the motor, premotor, and sensory cortices. *Operat Neurosurg*. (2018) 15 (suppl_1), S75–S121. doi: 10.1093/ons/opy256
9. Chang EF, Kurteff G, Andrews JP, Briggs RG, Conner AK, Battiste JD, et al. Pure apraxia of speech after resection based in the posterior middle frontal gyrus. *Neurosurgery*. (2020) 87:E383–9. doi: 10.1093/neuros/nyaa002
10. Donahue CJ, Glasser MF, Preuss TM, Rilling JK, Van Essen DC. Quantitative assessment of prefrontal cortex in humans relative to nonhuman primates. *Proc Natl Acad Sci*. (2018) 115:E5183–92. doi: 10.1073/pnas.1721653115
11. De Witt Hamer PC, Robles SG, Zwinderman AH, Duffau H, Berger MS. Impact of intraoperative stimulation brain mapping on glioma surgery outcome: a meta-analysis. *J Clin Oncol*. (2012) 30:2559–65. doi: 10.1200/JCO.2011.38.4818
12. Sarubbo S, Tate M, De Benedictis A, Merler S, Moritz-Gasser S, Herbet G, et al. Mapping critical cortical hubs and white matter pathways by direct electrical stimulation: an original functional atlas of the human brain. *Neuroimage*. (2020) 205:116237. doi: 10.1016/j.neuroimage.2019.116237
13. Mandonnet E, Winkler PA, Duffau H. Direct electrical stimulation as an input gate into brain functional networks: principles, advantages and limitations. *Acta Neurochirurgica*. (2010) 152:185–93. doi: 10.1007/s00701-009-0469-0
14. Borchers S, Himmelbach M, Logothetis N, Karnath HO. Direct electrical stimulation of human cortex - the gold standard for mapping brain functions? *Nat Rev Neurosci*. (2011) 13:63–70. doi: 10.1038/nrn3140
15. Pallud J, Zanello M, Kuchcinski G, Roux A, Muto J, Mellerio C, et al. Individual variability of the human cerebral cortex identified using intraoperative mapping. *World Neurosurg*. (2018) 109:e313–7. doi: 10.1016/j.wneu.2017.09.170
16. Forster M-T, Hattingen E, Senft C, Gasser T, Seifert V, Szelényi A. Navigated transcranial magnetic stimulation and functional magnetic resonance imaging: advanced adjuncts in preoperative planning for central region tumors. *Neurosurgery*. (2011) 68:1317–25. doi: 10.1227/NEU.0b013e31820b528c
17. Picht T, Schmidt S, Brandt S, Frey D, Hannula H, Neuvonen T, et al. Preoperative functional mapping for rolandic brain tumour surgery: comparison of navigated transcranial magnetic stimulation to direct cortical stimulation. *Neurosurgery*. (2011) 69:581–8. Discussion 588. doi: 10.1227/NEU.0b013e3182181b89
18. Picht T, Frey D, Thieme S, Kliesch S, Vajkoczy P. Presurgical navigated TMS motor cortex mapping improves outcome in glioblastoma surgery: a controlled observational study. *J Neurooncol*. (2016) 126:535–43. doi: 10.1007/s11060-015-1993-9
19. Krieg SM, Sabih J, Bulubasova L, Obermueller T, Negwer C, Janssen I, et al. Preoperative motor mapping by navigated transcranial magnetic brain stimulation improves outcome for motor eloquent lesions. *Neurooncology*. (2014) 16:1274–82. doi: 10.1093/neuonc/nou007
20. Raffa G, Scibilia A, Conti A, Ricciardo G, Rizzo V, Morelli A, et al. The role of navigated transcranial magnetic stimulation for surgery of motor-eloquent brain tumors: a systematic review and metaanalysis. *Clin Neurol Neurosurg*. (2019) 180:7–17. doi: 10.1016/j.clineuro.2019.03.003
21. Raffa G, Picht T, Scibilia A, Rösler J, Rein J, Conti A, et al. Surgical treatment of meningiomas located in the rolandic area: the role of navigated transcranial magnetic stimulation for preoperative planning, surgical strategy, and prediction of arachnoidal cleavage and motor outcome. *J Neurosurg*. (2019) 14:1–12. doi: 10.3171/2019.3.JNS183411
22. Sollmann N, Picht T, Mäkelä JP, Meyer B, Ringel F, Krieg SM. Navigated transcranial magnetic stimulation for preoperative language mapping in a patient with a left frontoopercular glioblastoma. *J Neurosurg*. (2013) 118:175–9. doi: 10.3171/2012.9.JNS121053
23. Krieg SM, Lioumis P, Mäkelä JP, Wilenius J, Karhu J, Hannula H, et al. Protocol for motor and language mapping by navigated TMS in patients and healthy volunteers; workshop report. *Acta Neurochirurgica*. (2017) 159:1187–95. doi: 10.1007/s00701-017-3187-z
24. Jeltema HR, Ohlerth AK, de Wit A, Wagemakers M, Rofes A, Bastiaanse R, et al. Comparing navigated transcranial magnetic stimulation mapping and "gold standard" direct cortical stimulation mapping in neurosurgery: a systematic review. *Neurosurg Rev*. (2020). doi: 10.1007/s10143-020-01397-x
25. Bährend I, Muench MR, Schneider H, Moshourab R, Dreyer FR, Vajkoczy P, et al. Incidence and linguistic quality of speech errors: a comparison of preoperative transcranial magnetic stimulation and intraoperative direct cortex stimulation. *J Neurosurg*. (2020) 29:1–10. doi: 10.3171/2020.3.JNS193085
26. Krieg SM, Tarapore PE, Picht T, Tanigawa N, Houde J, Sollmann N, et al. Optimal timing of pulse onset for language mapping with navigated repetitive transcranial magnetic stimulation. *Neuroimage*. (2014) 100:219–36. doi: 10.1016/j.neuroimage.2014.06.016
27. Raffa G, Quattropani MC, Germanò A. When imaging meets neurophysiology: the value of navigated transcranial magnetic stimulation for preoperative neurophysiological mapping prior to brain tumor surgery. *Neurosurg Focus*. (2019) 47:E10. doi: 10.3171/2019.9.FOCUS19640
28. Syder D, Body R, Parker M, Boddy M. *Sheffield Screening Test for Acquired Language Disorders*. Windsor: NFER-NELSON (1993).
29. Simpson F, Christie J, Mortensen L, Clark W. *Mount Wilga High Level Language Test: Administration & Scoring Manual Plus Test Form with UK Adaptations and Large Print Additions*. (2006). Available online at: http://nebula.wsimg.com/5dc06d53fe8a246679ba15f02e226ed0?AccessKeyId=5861B1733117182DC99B&disposition=0&alloworigin=1
30. Penfield W, Boldrey E. Somatic motor and sensory representation in the cerebral cortex of man as studied by electrical stimulation. *Brain*. (1937) 60:389–443. doi: 10.1093/brain/60.4.389
31. De Witte E, Satoer D, Robert E, Colle H, Verheyen S, Visch-Brink E, et al. The Dutch linguistic intraoperative protocol: a valid linguistic approach to awake brain surgery. *Brain Lang*. (2015) 140:35–48. doi: 10.1016/j.bandl.2014.10.011
32. Ohlerth AK, Valentin A, Vergani F, Ashkan K, Bastiaanse R. The verb and noun test for peri-operative testing (VAN-POP): standardized language tests for navigated transcranial magnetic stimulation and direct electrical stimulation. *Acta Neurochirurgica*. (2020) 162:397–406. doi: 10.1007/s00701-019-04159-x

33. Jung J, Lavrador JP, Patel S, Giamouriadis A, Lam J, Bhangoo R, et al. First United Kingdom experience of navigated transcranial magnetic stimulation in preoperative mapping of brain tumors. *World Neurosurg*. (2019) 122:e1578–87. doi: 10.1016/j.wneu.2018.11.114
34. Sanai N, Mirzadeh Z, Berger MS. Functional outcome after language mapping for glioma resection. *N Engl J Med*. (2008) 358:18–27. doi: 10.1056/NEJMoa067819
35. Sarubbo S, De Benedictis A, Merler S, Mandonnet E, Balbi S, Granieri E, et al. Towards a functional atlas of human white matter. *Hum Brain Map*. (2015) 36:3117–36. doi: 10.1002/hbm.22832
36. Sarubbo S, De Benedictis A, Merler S, Mandonnet E, Barbareschi M, Dallabona M, et al. Structural and functional integration between dorsal and ventral language streams as revealed by blunt dissection and direct electrical stimulation. *Hum Brain Map*. (2016) 37:3858–72. doi: 10.1002/hbm.23281
37. Gonen T, Gazit T, Korn A, Kirschner A, Perry D, Hendler T, et al. Intra-operative multi-site stimulation: Expanding methodology for cortical brain mapping of language functions. *PLoS ONE*. (2017) 12:e0f180740. doi: 10.1371/journal.pone.0180740
38. Duffau H. The error of Broca: from the traditional localizationist concept to a connectomal anatomy of human brain. *J Chem Neuroanat*. (2017) 89:73–81. doi: 10.1016/j.jchemneu.2017.04.003
39. Rahimpour S, Haglund MM, Friedman AH, Duffau H. History of awake mapping and speech and language localization: from modules to networks. *Neurosurg Focus*. (2019) 47:E4. doi: 10.3171/2019.7.FOCUS19347
40. Duffau H, Gatignol P, Mandonnet E, Peruzzi P, Tzourio-Mazoyer N, Capelle L. New insights into the anatomo-functional connectivity of the semantic system: a study using cortico-subcortical electrostimulations. *Brain J Neurol*. (2005) 128 (Pt 4):797–810. doi: 10.1093/brain/awh423
41. Catani M, Jones DK, Ffytche DH. Perisylvian language networks of the human brain. *Ann Neurol*. (2005) 57:8–16. doi: 10.1002/ana.20319
42. Martino J, De Witt Hamer PC, Berger MS, Lawton MT, Arnold CM, de Lucas EM, et al. Analysis of the subcomponents and cortical terminations of the perisylvian superior longitudinal fasciculus: a fiber dissection and DTI tractography study. *Brain Struct Funct*. (2013) 218:105–21. doi: 10.1007/s00429-012-0386-5
43. Barbeau EB, Descoteaux M, Petrides M. Dissociating the white matter tracts connecting the temporo-parietal cortical region with frontal cortex using diffusion tractography. *Sci Rep*. (2020) 10:8186. doi: 10.1038/s41598-020-64124-y
44. Yagmurlu K, Middlebrooks EH, Tanriover N, Rhoton, ALJr. Fiber tracts of the dorsal language stream in the human brain. *J Neurosurg*. (2016) 124:1396–405. doi: 10.3171/2015.5.JNS15455
45. Sarubbo S, De Benedictis A, Maldonado IL, Basso G, Duffau H. Frontal terminations for the inferior fronto-occipital fascicle: anatomical dissection, DTI study and functional considerations on a multi-component bundle. *Brain Struct Funct*. (2013) 218:21–37. doi: 10.1007/s00429-011-0372-3
46. Martino J, Brogna C, Robles SG, Vergani F, Duffau H. Anatomic dissection of the inferior fronto-occipital fasciculus revisited in the lights of brain stimulation data. *Cortex*. (2010) 46:691–9. doi: 10.1016/j.cortex.2009.07.015
47. Wu Y, Sun D, Wang Y, Wang Y. Subcomponents and connectivity of the inferior fronto-occipital fasciculus revealed by diffusion spectrum imaging fiber tracking. *Front Neuroanat*. (2016) 10:88. doi: 10.3389/fnana.2016.00088
48. Catani M, Mesulam MM, Jakobsen E, Malik F, Martersteck A, Wieneke C, et al. A novel frontal pathway underlies verbal fluency in primary progressive aphasia. *Brain J Neurol*. (2013). 136 (Pt 8):2619–28. doi: 10.1093/brain/awt163
49. Vergani F, Lacerda L, Martino J, Attems J, Morris C, Mitchell P, et al. White matter connections of the supplementary motor area in humans. *J Neurol Neurosurg Psychiatry*. (2014) 85:1377–85. doi: 10.1136/jnnp-2013-307492
50. Kinoshita M, de Champfleur NM, Deverdun J, Moritz-Gasser S, Herbet G, Duffau H. Role of fronto-striatal tract and frontal aslant tract in movement and speech: an axonal mapping study. *Brain Struct Funct*. (2015) 220:3399–412. doi: 10.1007/s00429-014-0863-0
51. Genon S, Reid A, Li H, Fan L, Müller VI, Cieslik EC, et al. Preoperative transcranial magnetic stimulation for picture naming is reliable in mapping segments of the arcuate fasciculus. *Brain Commun*. (2020) 2:fcaa158. doi: 10.1093/braincomms/fcaa158
52. Zhang H, Schramm S, Schröder A, Zimmer C, Meyer B, Krieg SM, et al. Function-based tractography of the language network correlates with aphasia in patients with language-eloquent glioblastoma. *Brain Sci*. (2020) 10:412. doi: 10.3390/brainsci10070412
53. Zdunczyk A, Schwarzer V, Mikhailov M, Bagley B, Rosenstock T, Picht T, et al. The corticospinal reserve capacity: reorganization of motor area and excitability as a novel pathophysiological concept in cervical myelopathy. *Neurosurgery*. (2018) 83:810–8. doi: 10.1093/neuros/nyx437
54. Tzourio-Mazoyer N, Perrone-Bertolotti M, Jobard G, Mazoyer B, Baciu M. Multi-factorial modulation of hemispheric specialization and plasticity for language in healthy and pathological conditions: a review. *Cortex*. (2017) 86:314–39. doi: 10.1016/j.cortex.2016.05.013
55. Raffa G, Quattropani MC, Scibilia A, Conti A, Angileri FF, Esposito F, et al. Surgery of language-eloquent tumors in patients not eligible for awake surgery: the impact of a protocol based on navigated transcranial magnetic stimulation on presurgical planning and language outcome, with evidence of tumor-induced intra-hemispheric plasticity. *Clin. Neurol. Neurosurg*. (2018) 168:127–39. doi: 10.1016/j.clineuro.2018.03.009
56. Zheng G, Chen X, Xu B, Zhang J, Lv X, Li J, et al. Plasticity of language pathways in patients with low-grade glioma: a diffusion tensor imaging study. *Neural Regen Res*. (2013) 8:647–54. doi: 10.3969/j.issn.1673-5374.2013.07.009
57. Cirillo S, Caulo M, Pieri V, Falini A, Castellano A. Role of functional imaging techniques to assess motor and language cortical plasticity in glioma patients: a systematic review. *Neural Plast*. (2019) 2019:4056436. doi: 10.1155/2019/4056436
58. Southwell DG, Hervey-Jumper SL, Perry DW, Berger MS. Intraoperative mapping during repeat awake craniotomy reveals the functional plasticity of adult cortex. *J Neurosurg*. (2016) 124:1460–9. doi: 10.3171/2015.5.JNS142833
59. Duffau H. Mapping the connectome in awake surgery for gliomas: an update. *J Neurosurg Sci*. (2017) 61:612–30.
60. van Geemen K, Herbet G, Moritz-Gasser S, Duffau H. Limited plastic potential of the left ventral premotor cortex in speech articulation: evidence from intraoperative awake mapping in glioma patients. *Hum Brain Map*. (2014) 35:1587–96. doi: 10.1002/hbm.22275
61. Lavrador JP, Ghimire P, Brogna C, Furlanetti L, Patel S, Gullan R, et al. Pre- and intraoperative mapping for tumors in the primary motor cortex: decision-making process in surgical resection. *J Neurol Surg A Cent Eur Neurosurg*. (2020). doi: 10.1055/s-0040-1709729
62. Mancini M, Casamitjana A, Peter L, Robinson E, Crampsie S, Thomas DL, et al. A multimodal computational pipeline for 3D histology of the human brain. *Sci. Rep*. (2020) 10:13839. doi: 10.1038/s41598-020-69163-z
63. Tournier JD, Smith R, Raffelt D, Tabbara R, Dhollander T, Pietsch M, et al. MRtrix3: A fast, flexible and open software framework for medical image processing and visualisation. *Neuroimage*. (2019) 202:116137. doi: 10.1016/j.neuroimage.2019.116137
64. Fekonja L, Wang Z, Bährend I, Rosenstock T, Rösler J, Wallmeroth L, et al. Manual for clinical language tractography. *Acta Neurochirurgica*. (2019) 161:1125–37. doi: 10.1007/s00701-019-03899-0

Conflict of Interest: The authors declare that the research was conducted in the absence of any commercial or financial relationships that could be construed as a potential conflict of interest.

frontiers in Neurology

OPINION
published: 12 April 2021
doi: 10.3389/fneur.2021.635439

Should Complex Cognitive Functions Be Mapped With Direct Electrostimulation in Wide-Awake Surgery? A Network Perspective

Guillaume Herbet [1,2]*

[1] Institute of Functional Genomics, INSERM, CNRS, University of Montpellier, Montpellier, France, [2] Gui de Chauliac Hospital, Montpellier University Medical Center, Montpellier, France

Keywords: intraoperative cognitive mapping, electrostimulation, glioma, awake surgery, network architecture

OPEN ACCESS

Edited by:
András Büki,
University of Pécs, Hungary

Reviewed by:
Alireza Mansouri,
Pennsylvania State University (PSU), United States

***Correspondence:**
Guillaume Herbet
Guillaume.herbet@umontpellier.fr

Specialty section:
This article was submitted to Neuro-Oncology and Neurosurgical Oncology, a section of the journal Frontiers in Neurology

Received: *01 December 2020*
Accepted: *17 March 2021*
Published: *12 April 2021*

Citation:
Herbet G (2021) Should Complex Cognitive Functions Be Mapped With Direct Electrostimulation in Wide-Awake Surgery? A Network Perspective. Front. Neurol. 12:635439. doi: 10.3389/fneur.2021.635439

INTRODUCTIVE REMARKS

It is now well-established that wide-awake neurosurgery with electrostimulation mapping is a safe technique for removing cerebral tumors drastically (1, 2), whilst sparing central, lowly compensable pieces of the anatomo-functional architecture (3, 4). In the last 10-year period, significant efforts have been made to implement new behavioral paradigms in the operating theater with the aim of giving patients the best opportunities to quickly recover after surgery and to resume a normal socio-professional life. Without being fully exhaustive, this includes tasks probing semantic (5, 6) and social cognition (7–9), motor (10, 11), and spatial cognition (12, 13), reading (14), and working memory (15). In turn, neuroscientic knowledge gained from multifunctional electrostimulation mapping procedures has been accumulating over the years in at least three directions: (i) the neuroplasticity potential of neurocognitive networks, (ii) the interindividual variability in the neural implementation of functional systems and (iii), the role of the main white matter tracts in different forms of cognition [for a review, see Herbet and Duffau (16)]. Overall, this growing knowledge is vital not only to help neurosurgeons better anticipate the surgery's functional outcomes (and thus better improve patient care), but also to continuously refine the way patients are operated on based upon valid neuroscientific foundations. In this respect, the virtuous circle that constitute the reciprocal interactions between neurosurgery and cognitive neuroscience (17) should be considered as the cornerstone on which to orient our decision-making regarding the ongoing debate on what kind of functions should be monitored *on-line* during awake procedures (18). This reflection is fully justified as wide-awake neurosurgery is now proposed much earlier for oncological purpose, and patients' survival is considerately longer than a couple of years ago. In this context, we have to set higher expectations with respect to preserving functions and to maintaining quality of life. But where to place the cursor for cognitive mapping without losing touch with the onco-functional balance (i.e. the best trade-off between extent of resection vs. preservation of functions) (19)? In this opinion article, I give some balanced perspectives on this debate, especially on the issue whether complex or flexible cognitions and behaviors (e.g., adaptive, multidetermined cognitions such as contextual decision-making or fast learning) can be reliably mapped given the network architecture on which they rest.

CAN HIGHLY DISTRIBUTED VS. MODULAR NEURAL SYSTEMS BE ACTUALLY MAPPED WITH DIRECT ELECTROSTIMULATION?

It is certainly not new to say that the main functional systems of the human brain are physically rooted in a web of interconnected neurons, which are structured in the form of

well-organized neural networks (20). These networks, however, differ significantly in terms of modularity, as a function of the wide range of more or less complex cognitions and behaviors they are supposed to underlay (21). It is indeed known that basic sensorimotor processes are supported by highly modular and local networks, whereas higher-order but still modality-specific or domain-specific cognitive functions are rather supported by distributed networks of cortical areas within which neural information needs to be integrated locally in each cortical node forming the network as well as globally between each node of the network. On a third level, goal-directed and flexible cognitions (resulting in complex behaviors) rest on the instantiation of transient and context-sensitive functional meta-systems that reflect specific patterns of between-network coordination, the functional integration of which is permitted by cortical hubs with a high degree of centrality (such as for e.g., the posterior part of the dorsolateral prefrontal cortex or the posterior dorsal cingulate cortex) (16, 22). Such highly integrative functioning is probably essential in the human ability to form new and creative behaviors, to efficiently perform cognitive-demanding activities, and to learn complex abilities. For example, learning a simple motor task necessitates the engagement of the sensorimotor, the attention, the visual and the executive networks, the sensori-motor system becoming sufficient to perform the task when automaticity is reached after several sessions of training (23). Different behavioral parameters seems to constrain the recruitment of this kind of highly distributed processing, in particular the complexity of the behavior task to be performed (complex materials necessitates intervention of domain-general networks, such as of the attention, executive, and working memory networks), the goal-directed vs. effortless nature of the task and the recruitment of conscious vs. unconscious processing (24).

Within the hierarchical anatomo-functional architecture described above (from highly modular to highly distributed processing) (see **Figure 1**), I argue that electrostimulation mapping performs very efficiently to identify and spare neural systems associated with sensorimotor or modality-specific/domain-specific functions (e.g., language and semantic processes, visuo-spatial attention among many others). As a matter of fact, the rate of lasting and debilitating deficits has been considerably reduced, leading almost all patients to quickly resume a normal professional activity even in the event of incidental discovery (97%) (25). However, electrostimulation is somewhat limited in its ability to identify higher-order, complex and flexible cognitions. In my view, this limitation is mainly due to three reasons. First, flexible cognitions heavily rely on the resources of multiple large-scale networks working in synchrony. It thus remains to see the extent to which short electrostimulations with low intensity might disturb brain-wide processing and lead to complex behavioral impairments. We currently know from works combining electrostimulation mapping and functional connectivity analyses that positive stimulation sites can be considered as veritable gateways to domain-specific networks (26, 27), but the behavioral impact of disrupting cortical areas that interface with multiple networks is unknown. Some studies indicate that electrostimulation is able to transiently abolish aspects of self-awareness or external awareness (5, 28, 29), but it is unclear whether the physiological basis of these behavioral impairments is the brain inability to form transient metasystems. It is possible that the disruption of highly integrative white matter tracts (i.e., that project in several lobes such as the inferior fronto-occipital fasciculus) is more capable of disorganizing the way networks communicate. Alternatively, as multiple hubs are likely to synchronize during normal behavior, multi-focal electrostimulations (i.e., stimulations performed on two or several cortical hubs at the same time) might be a way to map more accurately complex functions. While this approach needs to be explored, it may be quite difficult to set up in the constraining context of neurosurgery. Moreover, its potential oncological benefit must be evaluated.

Second, with the exception of multitasking-like paradigms (typically, motor execution plus semantic association, or picture naming) or *n*-back-like task (strong cognitive load) the neuropsychological tasks employed in the operating theater are well-controlled but might be considered as reductionist because not necessitating strong cognitive requirements. Yet recent meta-analytic studies indicate that ecological, realistic (vs. highly controlled, reductionist) behavioral paradigms are associated with recurrent patterns of functional activations that overlap with numerous functional networks (sensorimotor, modality-specific, and domain-general), suggesting that flexible and complex behaviors triggered by lifelike situations result from the integration of distinct but cooperating networks (30). This is not without interest considering that, what we want ultimately for patients, is to maintain the best level of interactions with the everyday (including social) environment after surgery. However, the intraoperative cognitive mapping does not really accommodate with complex behavioral stimuli due to the constraints inherent to the surgical procedure (e.g., stimulation time, positioning constrain, and so one). Some adaptations are nevertheless possible, in particular varying the complexity of the materials used. In this situation, the neurocognitive system under scrutiny is necessarily up-regulated by domain-general networks (i.e., attention and cognitive control), increasing sensitivity. More broadly, this raises the question as to how more ecological but still controlled tasks can be constructed without losing interpretability (i.e., what is the precise impact of stimulation on the function probed by the task). This is of course central to maintaining the validity of cognitive monitoring.

Third, some studies have shown that the efficiency with which the brain is able to reconfigure its networks as a function of current cognitive demands is strongly predictive of behavioral output (31). This important interindividual variability implies that complex behaviors are likely to be more difficult to map with electrostimulation.

That said, it remains an open question whether the cognitive mapping should be pushed forward, keeping in mind the onco-functional balance. However, it may be not necessary given the possible high resilience of the distributed systems that flexible cognitions engage, especially in the context of conditions known to stimulate neuroplasticity such as slow-growing tumors (32).

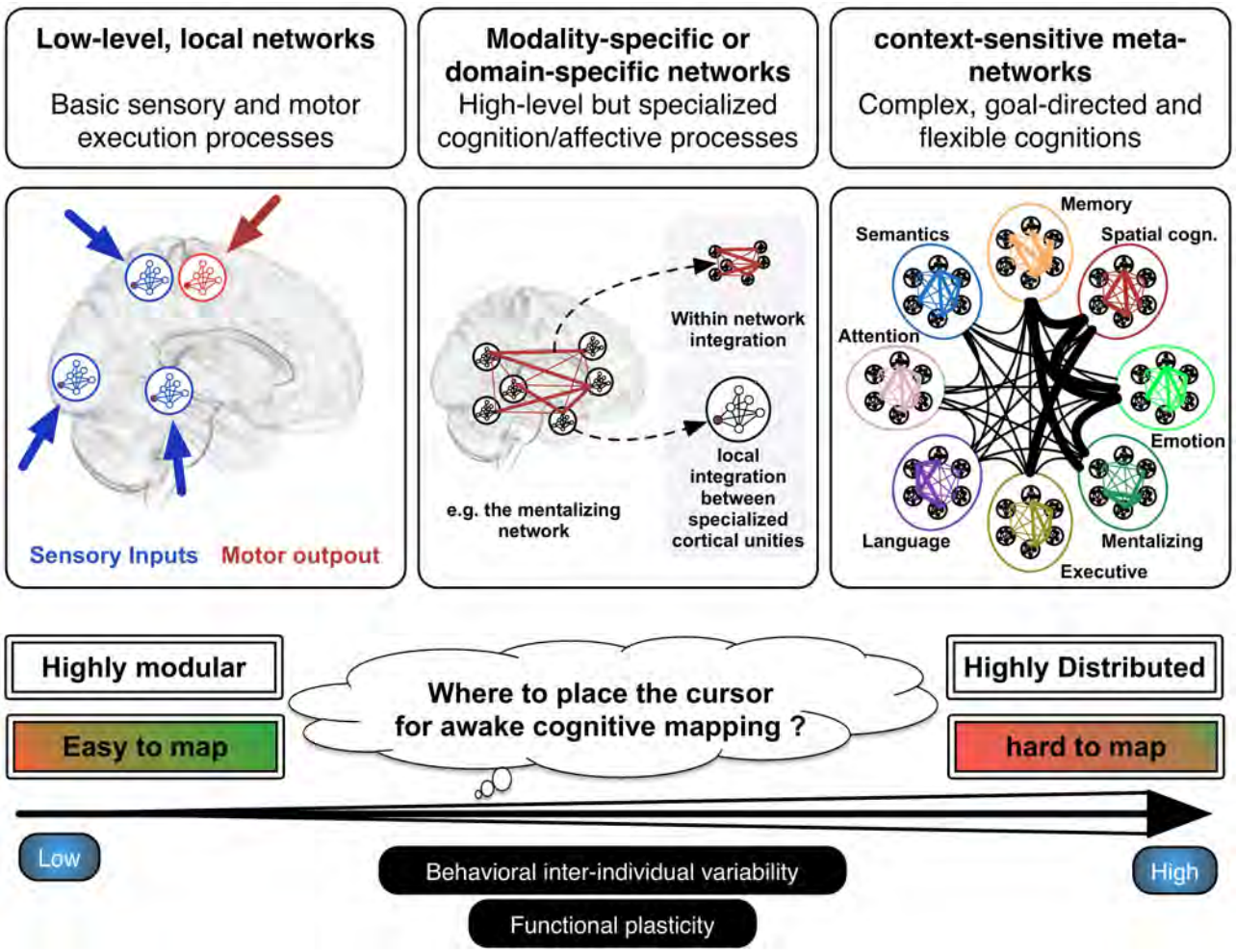

FIGURE 1 | Hierarchical functioning of the anatomo-functional architecture. Basic sensorimotor processes are performed by low-level, local and highly modular networks, whereas modality-specific or domain-specific functions are rather underlain by distributed networks. The latter are composed of different cortical epicenters, the functional integration of which is permitted by anatomical connectivity. At a higher level, complex or flexible cognitions or behavior result from the instantiation of meta-networks, which consist in specific and unique patterns of cross-network integration transiently generated to reach the task demands. Adapted from Herbet and Duffau (16) with permission.

ON THE RESILIENCE AND FLEXIBILITY OF COMPLEX FUNCTIONAL SYSTEMS

Although it is established that the brain reorganizes over time in response to glioma infiltration (32, 33), the mechanistic aspects of this reactional plasticity remains poorly understood. Several patterns of functional remodeling has been described, including loco-regional, intra-hemispheric and inter-hemispheric/homotopic reorganization patterns [e.g., (34, 35)]. However, the different factors constraining these dynamic modulations are clearly not understood, even if several advances have been recently made thanks to serial stimulation mappings performed in patients with recurrent tumors (36). In particular, bulky (weakly diffusive) gliomas may favor peritumoral plasticity whereas widely diffuse tumors may cause brain-wide reorganization. On the other hand, it is likely that the more integrated the function is, the more resilient the dedicated network is, especially when the function is underlain by a neural system that is distributed in both cerebral hemispheres. For example, despite the central role of the anterior temporal structures within the semantic memory network, unilateral damage of this region in various pathophysiological conditions (including glioma) does not result in the severe impairments of semantic representations it might be expected. The current interpretation is that the absence of strict lateralization increases the robustness of this functional system, with a central role of homotopic areas (37). Beyond, it has been shown that neurocognitive networks resting on associative areas are especially prone to be functionally compensated (4).

In the context of dynamic metasystems, it is somewhat expected that damage to cortical hubs established to participate to between-system coordination may have widespread

neuropsychological consequences because of their central position in the anatomo-functional architecture. This is the case, especially in patients with sudden lesion such as stroke or traumatic injury. In these patient populations, it is indeed shown that focal disruption of connector or highly participating hubs has dramatic effects on both global network dynamics (38) and the brain's ability to coordinate its networks (39), leading to multidomain cognitive impairments (40, 41). In patients with diffuse low-grade glioma, to the best of my knowledge there are no well-conducted studies specifically assessing the impact of the tumor on the brain's ability to generate meta-networks and the extent to which this may cause neuropsychological deficits. However, some works seem to indicate that this is not the case. For example, in the study by Herbet et al. (42) the surgical excision of the ventral precuneus/posterior cingulate, a cortical hub with highly connective properties (43, 44), was not associated with severe and multidomain impairments, suggesting that activities of such hubs can be redeployed. Admittedly, however, longitudinally designed and well powered studies are needed to confirm it.

CONCLUSION

In this opinion article, my attempt was to fuel the debate on whether higher-order and complex cognitions can be appropriately mapped during awake surgery in view of the flexible and highly distributed neural architecture from which they emerge. From a network perspective, such functions are probably difficult (but not impossible) to map with a good reliability because they necessitate coordination of multiple networks and are associated with a high-level of inter-individual behavioral variability. Furthermore, they are more likely to be easily compensable compared to basic or domain-specific functions. From a neuro-oncological standpoint, however, no works have currently assessed in a longitudinal manner if complex and flexible cognitions/behaviors are impaired following neurosurgical procedures (knowing that they are not probed with routine neuropsychological tasks) and if these possible impairments are disabling in daily life. This is an important point to assess before we go any further.

Some of the challenges described in this article might be potentially mitigated by the combined use of other tools that allow to manipulate more complex materials, outside the operating theater. From this perspective, navigated transcranial magnetic stimulation (TMS) may offer good opportunities to identify the critical cortical structures [and perhaps the interconnected white matter pathways if diffusion tractography is combined; e.g., (45)] involved in high-level cognitive or social processes before the surgery is performed. It may also help evaluate the functional impact of stimulation (and possibly of surgical resections) on neural hubs that interface with multiple networks. To my knowledge, *n*TMS is to date only used with (most of the time language) stimuli which are classically employed during the intraoperative cognitive monitoring. On the other hand, task-based functional connectivity MRI may provide critical information on how efficiently complex networks reorganize in response to tumor invasion or on how the different networks engaged in a complex function up-modulate their activities to compensate the neural loss (46). Determining the physiological markers of resilient networks is of major importance in adjusting the surgical procedure.

AUTHOR CONTRIBUTIONS

GH wrote the manuscript.

REFERENCES

1. Sanai N, Berger MS. Glioma extent of resection and its impact on patient outcome. *Neurosurgery.* (2008) 62:753–66. doi: 10.1227/01.neu.0000318159.21731.cf
2. Hamer PDW, Robles SG, Zwinderman AH, Duffau H, Berger MS. Impact of intraoperative stimulation brain mapping on glioma surgery outcome: a meta-analysis. *J Clin Oncol.* (2012) 30:2559–65. doi: 10.1200/JCO.2011.38.4818
3. Duffau H, Gatignol P, Mandonnet E, Peruzzi P, Tzourio-Mazoyer N, Capelle L. New insights into the anatomo-functional connectivity of the semantic system: a study using cortico-subcortical electrostimulations. *Brain.* (2005) 128:797–810. doi: 10.1093/brain/awh423
4. Herbet G, Maheu M, Costi E, Lafargue G, Duffau H. Mapping neuroplastic potential in brain-damaged patients. *Brain.* (2016) 139:829–44. doi: 10.1093/brain/awv394
5. Moritz-Gasser S, Herbet G, Duffau H. Mapping the connectivity underlying multimodal (verbal and non-verbal) semantic processing: a brain electrostimulation study. *Neuropsychologia.* (2013) 51:1814–22. doi: 10.1016/j.neuropsychologia.2013.06.007
6. Herbet G, Moritz-Gasser S, Duffau H. Direct evidence for the contributive role of the right inferior fronto-occipital fasciculus in non-verbal semantic cognition. *Brain Struct Funct.* (2017) 222:1597–610. doi: 10.1007/s00429-016-1294-x
7. Herbet G, Lafargue G, Moritz-Gasser S, Bonnetblanc F, Duffau H. Interfering with the neural activity of mirror-related frontal areas impairs mentalistic inferences. *Brain Struct Funct.* (2015) 220:2159–69. doi: 10.1007/s00429-014-0777-x
8. Nakajima R, Yordanova YN, Duffau H, Herbet G. Neuropsychological evidence for the crucial role of the right arcuate fasciculus in the face-based mentalizing network: a disconnection analysis. *Neuropsychologia.* (2018) 115:179–87. doi: 10.1016/j.neuropsychologia.2018.01.024
9. Yordanova YN, Duffau H, Herbet G. Neural pathways subserving face-based mentalizing. *Brain Struct Funct.* (2017) 222:3087–105. doi: 10.1007/s00429-017-1388-0
10. Rossi M, Fornia L, Puglisi G, Leonetti A, Zuccon G, Fava E, et al. Assessment of the praxis circuit in glioma surgery to reduce the incidence of postoperative and long-term apraxia: a new intraoperative test. *J Neurosurg.* (2018) 130:17–27. doi: 10.3171/2017.7.JNS17357
11. Rech F, Herbet G, Gaudeau Y, Mézières S, Moureau J-M, Moritz-Gasser S, et al. A probabilistic map of negative motor areas of the upper limb and face: a brain stimulation study. *Brain.* (2019) 142:952–65. doi: 10.1093/brain/awz021
12. Thiebaut de. Schotten MT, Urbanski M, Duffau H, Volle E, Lévy R, Dubois B, et al. Direct evidence for a parietal-frontal pathway subserving spatial awareness in humans. *Science.* (2005) 309:2226–8. doi: 10.1126/science.1116251
13. Vallar G, Bello L, Bricolo E, Castellano A, Casarotti A, Falini A, et al. Cerebral correlates of visuospatial neglect: a direct cerebral stimulation study. *Hum Brain Mapp.* (2014) 35:1334–50. doi: 10.1002/hbm.22257
14. Zemmoura I, Herbet G, Moritz-Gasser S, Duffau H. New insights into the neural network mediating reading processes provided by

cortico-subcortical electrical mapping. *Hum Brain Mapp.* (2015) 36:2215–30. doi: 10.1002/hbm.22766
15. Papagno C, Comi A, Riva M, Bizzi A, Vernice M, Casarotti A, et al. Mapping the brain network of the phonological loop. *Hum Brain Mapp..* (2017) 38:3011–24. doi: 10.1002/hbm.23569
16. Herbet G, Duffau H. Revisiting the functional anatomy of the human brain: toward a meta-networking theory of cerebral functions. *Physiological Reviews.* (2020) 100:1181–228. doi: 10.1152/physrev.00033.2019
17. Duffau H. Stimulation mapping of white matter tracts to study brain functional connectivity. *Nat Rev Neurol.* (2015) 11:255. doi: 10.1038/nrneurol.2015.51
18. Mandonnet E, Herbet G, Duffau H. Introducing new tasks for intraoperative mapping in awake glioma surgery: clearing the line between patient care and scientific research. *Neurosurgery.* (2020) 86:E256–7. doi: 10.1093/neuros/nyz447
19. Duffau H, Mandonnet E. The "onco-functional balance" in surgery for diffuse low-grade glioma: integrating the extent of resection with quality of life. *Acta Neurochirurgica.* (2013) 155:951–7. doi: 10.1007/978-1-4471-2213-5
20. Mesulam M-M. From sensation to cognition. *Brain.* (1998) 121:1013–52. doi: 10.1093/brain/121.6.1013
21. Park HJ, Friston K. Structural and functional brain networks: from connections to cognition. *Science.* (2013) 342:1238411. doi: 10.1126/science.1238411
22. Cocchi L, Zalesky A, Fornito A, Mattingley JB. Dynamic cooperation and competition between brain systems during cognitive control. *Trends Cogn Sci.* (2013) 17:493–501. doi: 10.1016/j.tics.2013.08.006
23. Bassett DS, Yang M, Wymbs NF, Grafton ST. Learning-induced autonomy of sensorimotor systems. *Nat Neurosci.* (2015) 18:744–51. doi: 10.1038/nn.3993
24. Shine JM, Poldrack RA. Principles of dynamic network reconfiguration across diverse brain states. *NeuroImage.* (2018) 180:396–405. doi: 10.1016/j.neuroimage.2017.08.010
25. Ng S, Herbet G, Moritz-Gasser S, Duffau H. Return to work following surgery for incidental diffuse low-grade glioma: a prospective series with 74 patients. *Neurosurgery.* (2020) 87:720–9. doi: 10.1093/neuros/nyz513
26. Cochereau J, Deverdun J, Herbet G, Charroud C, Boyer A, Moritz-Gasser S, et al. Comparison between resting state fMRI networks and responsive cortical stimulations in glioma patients. *Hum Brain Mapp.* (2016) 37:3721–32. doi: 10.1002/hbm.23270
27. Yordanova YN, Cochereau J, Duffau H, Herbet G. Combining resting state functional MRI with intraoperative cortical stimulation to map the mentalizing network. *Neuroimage.* (2019) 186:628–36. doi: 10.1016/j.neuroimage.2018.11.046
28. Herbet G, Lafargue G, De Champfleur NM, Moritz-Gasser S, Le Bars E, Bonnetblanc F, et al. Disrupting posterior cingulate connectivity disconnects consciousness from the external environment. *Neuropsychologia.* (2014) 56:239–44. doi: 10.1016/j.neuropsychologia.2014.01.020
29. Herbet G, Lafargue G, Duffau H. The dorsal cingulate cortex as a critical gateway in the network supporting conscious awareness. *Brain.* (2016) 139:e23. doi: 10.1093/brain/awv381
30. Bottenhorn KL, Flannery JS, Boeving ER, Riedel MC, Eickhoff SB, Sutherland MT, et al. Cooperating yet distinct brain networks engaged during naturalistic paradigms: a meta-analysis of functional MRI results. *Netw Neurosci.* (2018) 3:27–48. doi: 10.1162/netn_a_00050
31. Kelly AC, Uddin LQ, Biswal BB, Castellanos FX, Milham MP. Competition between functional brain networks mediates behavioral variability. *Neuroimage.* (2008) 39:527–37. doi: 10.1016/j.neuroimage.2007.08.008
32. Desmurget M, Bonnetblanc F, Duffau H. Contrasting acute and slow-growing lesions: a new door to brain plasticity. *Brain.* (2007) 130:898–914. doi: 10.1093/brain/awl300
33. Duffau H. Lessons from brain mapping in surgery for low-grade glioma: insights into associations between tumour and brain plasticity. *Lancet Neurol.* (2005) 4:476–86. doi: 10.1016/S1474-4422(05)70140-X
34. Almairac F, Herbet G, Moritz-Gasser S, de Champfleur NM, Duffau H. The left inferior fronto-occipital fasciculus subserves language semantics: a multilevel lesion study. *Brain Struct Funct.* (2015) 220:1983–95. doi: 10.1007/s00429-014-0773-1
35. De Baene W, Rutten G-JM, Sitskoorn MM. Cognitive functioning in glioma patients is related to functional connectivity measures of the non-tumoural hemisphere. *Euro J Neurosci.* (2019) 50:3921–33. doi: 10.1111/ejn.14535
36. Picart T, Herbet G, Moritz-Gasser S, Duffau H. Iterative surgical resections of diffuse glioma with awake mapping: how to deal with cortical plasticity and connectomal constraints? *Neurosurgery.* (2019) 85:105–16. doi: 10.1093/neuros/nyy218
37. Lambon Ralph MA. Neurocognitive insights on conceptual knowledge and its breakdown. *Philos Trans R Soc B Biol Sci.* (2014) 369:20120392. doi: 10.1098/rstb.2012.0392
38. Gratton C, Nomura EM, Pérez F, D'Esposito M. Focal brain lesions to critical locations cause widespread disruption of the modular organization of the brain. *J Cogn Neurosci.* (2012) 24:1275–85. doi: 10.1162/jocn_a_00222
39. Eldaief MC, McMains S, Hutchison RM, Halko MA, Pascual-Leone A. Reconfiguration of intrinsic functional coupling patterns following circumscribed network lesions. *Cereb Cortex.* (2017) 27:2894–910. doi: 10.1093/cercor/bhw139
40. Warren DE, Power JD, Bruss J, Denburg NL, Waldron EJ, Sun H, et al. Network measures predict neuropsychological outcome after brain injury. *Proc Natl Acad Sci USA.* (2014) 111:14247–52. doi: 10.1073/pnas.1322173111
41. Siegel JS, Ramsey LE, Snyder AZ, Metcalf NV, Chacko RV, Weinberger K, et al. Disruptions of network connectivity predict impairment in multiple behavioral domains after stroke. *Proc Natl Acad Sci USA.* (2016) 113:E4367–76. doi: 10.1073/pnas.1521083113
42. Herbet G, Lemaitre A-L, Moritz-Gasser S, Cochereau J, Duffau H. The antero-dorsal precuneal cortex supports specific aspects of bodily awareness. *Brain.* (2019) 142:2207–14. doi: 10.1093/brain/awz179
43. van den Heuvel MP, Sporns O. Network hubs in the human brain. *Trends Cogn Sci.* (2013) 17:683–96. doi: 10.1016/j.tics.2013.09.012
44. Gordon EM, Lynch CJ, Gratton C, Laumann TO, Gilmore AW, Greene DJ, et al. Three distinct sets of connector hubs integrate human brain function. *Cell Rep.* (2018) 24:1687–95.e4. doi: 10.1016/j.celrep.2018.07.050
45. Negwer C, Sollman N, Ille S, Hauck T, Maurer S, Kirschke JS, et al. Language pathway tracking: comparing nTMS-Based DTI fiber tracking with a cubic ROIs-based protocol. *J Neurosurg.* (2016) 126:1006–14. doi: 10.3171/2016.2.JNS152382
46. Stefaniak JD, Halai AD, Lambon Ralph MA. The neural and neurocomputational bases of recovery from post-stroke aphasia. *Nat Rev Neurol.* (2020) 16:43–55. doi: 10.1038/s41582-019-0282-1

Conflict of Interest: The author declares that the research was conducted in the absence of any commercial or financial relationships that could be construed as a potential conflict of interest.

frontiers in Neurology

ORIGINAL RESEARCH
published: 12 April 2021
doi: 10.3389/fneur.2021.646014

Repetitive Transcranial Magnetic Stimulation for Tinnitus Treatment in Vestibular Schwannoma: A Pilot Study

*Maria Teresa Leao[1,2], Kathrin Machetanz[1], Joey Sandritter[1], Marina Liebsch[1], Andreas Stengel[2,3,4], Marcos Tatagiba[1] and Georgios Naros[1]**

[1] Department of Neurosurgery and Neurotechnology, Eberhard Karls University, Tuebingen, Germany, [2] Section Psychooncology, Comprehensive Cancer Center Tuebingen-Stuttgart, University Hospital Tuebingen, Tuebingen, Germany, [3] Department of Psychosomatic Medicine and Psychotherapy, University Hospital Tuebingen, Tuebingen, Germany, [4] Charité Center for Internal Medicine and Dermatology, Department for Psychosomatic Medicine, Charité-Universitätsmedizin Berlin, Corporate Member of Freie Universität Berlin, Humboldt-Universität zu Berlin and Berlin Institute of Health, Berlin, Germany

OPEN ACCESS

Edited by:
Giovanni Raffa,
University of Messina, Italy

Reviewed by:
Jose Pedro Lavrador,
King's College Hospital NHS Foundation Trust, United Kingdom
Antonino Scibilia,
Universitaire de Strasbourg, France

***Correspondence:**
Georgios Naros
georgios.naros@med.uni-tuebingen.de

Specialty section:
This article was submitted to Applied Neuroimaging, a section of the journal Frontiers in Neurology

Received: 24 December 2020
Accepted: 23 February 2021
Published: 12 April 2021

Citation:
Leao MT, Machetanz K, Sandritter J, Liebsch M, Stengel A, Tatagiba M and Naros G (2021) Repetitive Transcranial Magnetic Stimulation for Tinnitus Treatment in Vestibular Schwannoma: A Pilot Study.
Front. Neurol. 12:646014.
doi: 10.3389/fneur.2021.646014

Background: Vestibular schwannomas (VS) are brain tumors affecting the vestibulocochlear nerve. Thus, VS patients suffer from tinnitus (TN). While the pathophysiology is mainly unclear, there is an increasing interest in repetitive transcranial magnetic stimulation (rTMS) for TN treatment. However, the results have been divergent. In addition to the methodological aspects, the heterogeneity of the patients might affect the outcome. Yet, there is no study evaluating rTMS exclusively in VS-associated tinnitus. Thus, the present pilot study evaluates low-frequency rTMS to the right dorsolateral pre-frontal cortex (DLPFC) in a VS-associated tinnitus.

Methods: This prospective pilot study enrolled nine patients with a monoaural VS-associated tinnitus ipsilateral to the tumor. Patients were treated with a 10-day rTMS regime (1 Hz, 100% RMT, 1,200 pulses, right DLPFC). The primary endpoint of the study was the reduction of TN distress (according to the Tinnitus Handicap Inventory, THI). The secondary endpoint was a reduction of TN intensity (according to the Tinnitus Matching Test, TMT) and the evaluation of factors predicting tinnitus outcome (i.e., hearing impairment, TN duration, type of tinnitus).

Results: No complications or side effects occurred. There was one drop-out due to a non-responsiveness of the complaint. There was a significant acute effect of rTMS on the THI and TMT. However, there was no significant long-term effect after 4 weeks. While the THI failed to detect any clinically relevant acute effect of rTMS in 56% of the patients, TMT revealed a reduction of TN intensity for more than 20 in 89% and for more than 50 in 56% of the patients. Notably, the acute effect of rTMS was influenced by the TN type and duration. In general, patients with a tonal TN and shorter TN duration showed a better response to the rTMS therapy.

Conclusion: The present pilot study is the first one to exclusively evaluate the effect of low-frequency rTMS to the right DLPFC in a VS-associated tinnitus. Our results prove the

feasibility and the efficacy of rTMS in this patient cohort. There is a significant acute but a limited long-term effect. In addition, there is evidence that patients with a tonal tinnitus and shorter tinnitus duration might have the strongest benefit. A larger, randomized controlled study is necessary to prove these initial findings.

Keywords: repetitive transcranial magnetic simulation, tinnitus, vestibular schwannoma, neurosurgery, neuromodulation

INTRODUCTION

Brain tumors affect functions related to the affected neuronal structure. Hence, patients with a vestibular schwannoma (VS), a benign tumor of the vestibulocochlear nerve, suffer from audiovestibular symptoms (i.e., hearing loss, tinnitus, or dizziness) (1–4). Tinnitus (TN) is affecting 63–75% of the VS patients (3, 5–7) and significantly impairing patients' quality of life (2, 8, 9). Notably, VS-associated tinnitus, however, is one of the few TN conditions accessible to causal therapy (10, 11). Thus, TN ceases in one third of the patients after a surgical removal of the tumor (4, 12, 13). The pathophysiology of the VS-associated TN has not yet been fully clarified (3, 4, 10). However, it is generally assumed that the pathophysiology might be similar to that of idiopathic TN (3). The current concept hypothesizes spurious auditory signals after partial sensory deafferentation, e.g., after damage to the cochlea (e.g., bang trauma) or cochlear nerve (e.g., vestibular schwannoma), to cause TN onset (1, 14–17). After chronification, however, TN perpetuation is theorized to depend on central maladaptive neuroplasticity because of the disturbed signal-to-noise ratio. These neuroplastic changes are thought to cause a neuronal hyperexcitability for the residual auditory input resulting in the subjective misperception (10, 11, 18, 19). Having a central origin, TN is hardly accessible to therapy (20). In the last years, there is a growing interest in using repetitive transcranial magnetic stimulation (rTMS) in TN therapy (20–24). rTMS is suggested to modify the excitability of relevant neurons and neurotransmitter systems in TN (25). However, the results have been divergent and even contradictory (21, 24, 26–29). First, there are still unsolved methodological issues, e.g., uncertainties concerning appropriate stimulation sites and stimulation intensities (20, 23). Second, there has been a large heterogeneity in the treated patient cohorts (20, 26). Most studies have evaluated the rTMS effects in patients with an idiopathic TN which are characterized by a large variability or ambiguity of the underlying cause. Additionally, the amount of hearing loss, tinnitus duration, and quality of the tinnitus seem to play important roles for the treatment outcome (26, 30, 31). In contrast, patients with anatomical causes of TN, such as VS, are usually excluded from rTMS studies. To our opinion, however, these patients represent a relatively homogenous cohort with a definite TN origin (3, 4). As these patients are presumably seeking medical advice in an early stage of the disease, the TN duration will be shorter, which is beneficial for rTMS treatment (32, 33). Yet, there is no rTMS study explicitly analyzing patients with a VS-associated TN.

The aim of the present pilot study was to provide the first evidence for the feasibility and effectivity of low-frequency rTMS to the right DLPFC in a VS-associated TN. Here, we describe our first experience in nine patients indicating an acute effect or rTMS on TN perception as measured by questionnaires and TN matching.

Abbreviations: DHI, Dizziness Handicap inventory; DLPFC, dorsolateral prefrontal cortex; FU, follow-up; GR, Gardner & Robertson scale; HHI, Hearing Handicap Inventory; PTA, pure tone audiometry; RMT, resting motor threshold; rTMS, repetitive transcranial magnetic stimulation; SDS, speech discrimination; THI, Tinnitus Handicap inventory; TMT, tinnitus matching test; TN, tinnitus; VS, vestibular schwannoma.

METHODS

Patients

This prospective study enrolled nine patients (57.1 ± 10.6, four female) with a unilateral sporadic VS who were treated at the Neurosurgical Department of the University of Tuebingen, Germany (**Figures 1A,B**). The inclusion criteria covered an age range of 18–80 years old and the presence of a monoaural TN ipsilateral to the tumor. Exclusion criteria were pregnancy, contralesional hearing impairment, and the presence of additional neurological conditions (e.g., epilepsy). Patient characteristics are shown in **Table 1**. Patients gave a written informed consent to their participation. This study was approved by the ethics committee of the Eberhard Karls University Tuebingen and performed in accordance to the Declaration of Helsinki.

Clinical Evaluation

Hearing impairment was classified according to the Gardner & Robertson (GR) scale (34) based on the results of the pure tone audiometry (PTA) and speech discrimination (SDS) resulting in five classes: GR 1 (good, PTA 0–30 dB, and SDS 70–100%), GR 2 (serviceable, PTA 31–50 dB, and SDS 50–69%), GR 3 (non-serviceable, PTA 51–90 dB, and SDS 5–49%), GR 4 (poor, PTA 51–90 dB, and SDS 1–4%), GR 5 (deaf, PTA 0 dB, and SDS 0%). For statistical reasons, GR score was reclassified in (i) preserved hearing (GR 1–4) and (ii) no hearing (GR5). VS tumor size was graded according to the Hannover classification (5) into four classes: T1 (purely intrameatal), T2 (intra- and extrameatal), T3 (filling the cerebellopontine cistern), T4 (compressing the brain stem).

Study Design

The aim of the study was to prove the feasibility and effectivity of repetitive transcranial magnetic stimulation (rTMS) therapy in a VS-associated TN. The study covered a treatment period of 10 consecutive workdays on which rTMS was applied. All

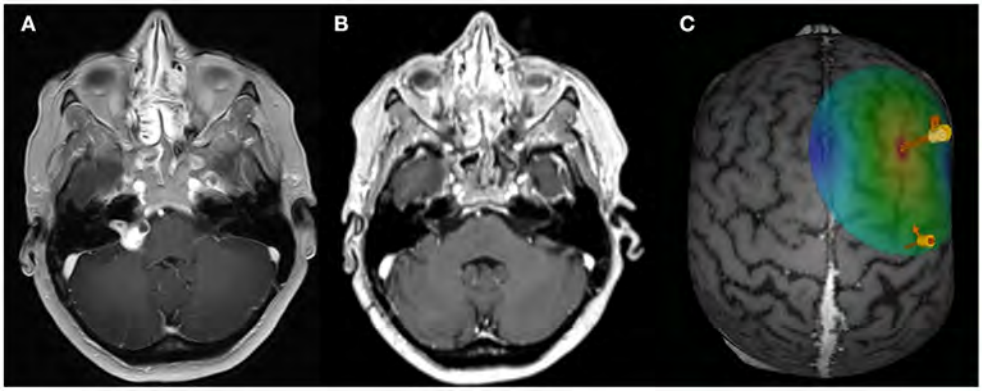

FIGURE 1 | rTMS paradigm. Exemplary axial MRI data (contrast-enhanced T1 sequence) of patient ID1 with a right-sided VS for the preoperative **(A)** and post-operative **(B)** situation. **(C)** Exemplary data of the rTMS application site. Arrows are indicating the APB hotspot and the rTMS on the DLPFC.

TABLE 1 | Data overview.

ID	1	2	3	4*	5	6	7	8	9	Sum
Age	60.0	51.3	67.6	71.6	44.3	33.6	60.3	47.5	67.4	57.1 ± 10.6
Gender	F	M	F	M	M	M	f	M	F	4:5
Tumor										
Size	T3	T3	T2	T2	T3	T3	T2	T2	T3	4:5
Side	Right	Left	Left	Right	Left	Right	Left	Left	Left	4:5
Hearing										
Ipsilateral	4	5	4	3	5	1	1	3	5	3.4 ± 1.6
Contralateral	1	1	1	1	1	1	1	1	1	
Tinnitus										
Type	T	N	T	N	N	T	N	N	T	4:5
Side	Right	Left	Left	Right	Left	Right	Left	Left	Left	4:5
Onset	Pre	Post	Post	Pre	Post	Post	Pre	Pre	Pre	5:4
Duration (y)	12.6	4.0	2.9	12.0	1.3	0.9	0.9	3.3	2.3	4.5 ± 4.6
rTMS										
Intensity (%)	38	36	50	30	45	29	32	40	30	37 ± 7
TMT										
Pre Freq (kHz)	7.0	–	3.0	–	–	5.4	–	–	4.0	4.8 ± 1.7
Pre Int (dB)	40	34	64	50	44	35	30	45	33	42 ± 11
Post Freq (kHz)	5.8	–	2.5	–	–	1.5	–	–	3.6	3.3 ± 1.3
Post Rel. int	0.39	0.67	0.1	1.0	0.43	0.05	0.25	0.53	0.20	
THI										
Pre	4	44	54	98	52	38	20	34	32	42.0 ± 26.0
Post	2	36	40	–	52	22	18	32	22	28.0 ± 15.3
FU	2	46	50	–	52	34	24	34	30	34.5 ± 16.9
HHI										
Pre	8	18	60	18	36	8	10	18	10	20.9 ± 17.1
Post	8	12	58	–	34	24	16	20	12	23.0 ± 16.4
FU	8	20	60	–	34	12	16	16	12	22.8 ± 17.0
DHI										
Pre	4	20	38	20	16	46	14	24	18	22.2 ± 12.7
Post	4	20	40	–	18	36	12	20	18	21.0 ± 11.8
FU	0	20	22	–	16	46	14	24	18	20.0 ± 12.8

*DHI, Dizziness Handicap Inventory; f, female; freq, TN frequency; HHI, Hearing Handicap Inventory; int, TN intensity; m, male; N, non-tonal; pre, pre-operative TN onset; post, post-operative TN onset; T, tonal; TTI, Tinnitus Handicap Inventory; *drop out.*

patients received a standardized evaluation of VS-associated audiovestibular symptoms (i.e., hearing impairment, tinnitus, dizziness) with questionnaires (i.e., Hearing Handicap Inventory, HHI; Tinnitus Handicap Inventory, THI; Dizziness Handicap Inventory, DHI) at the first day (PRE) and the last day (POST) of the treatment period. Questionnaires were also acquired after 4 weeks (follow-up, FU) to evaluate the long-term effects. In addition, we evaluated the patient's daily TN perception with a Tinnitus Matching Test (TMT) just prior and after the rTMS application. The primary endpoint of the study was a reduction of distress suffered by the TN patient as measured by the THI. Secondary endpoint of the study was the reduction of TN perception as measured by the TMT and the evaluation of factors predicting the rTMS effect (i.e., hearing impairment, tinnitus duration, type of tinnitus.).

Tinnitus Handicap Inventory

The Tinnitus Handicap Inventory (THI) is a self-administered test to determine the degree of distress suffered by the TN patient. The THI has been introduced in 1996 (35). It consists of 25 questions divided into three subgroups: functional, emotional, and catastrophic. Eleven items are included in the functional scale, nine in the emotional scale, and five in the catastrophic scale. A yes response yields a score of four points; sometimes, two points; and no, zero points. The total score ranges from zero (no disability) to 100 (severe disability). Studies have also indicated that the minimum change in the THI score that can be considered clinically relevant is a reduction of 6–7 points (35). It is widely used in medical offices and in clinical trials to determine the effectiveness of a given therapy (36, 37).

Hearing Handicap Inventory and Dizziness Handicap Inventory

The HHI (38) and the DHI (39) are constructed equivalent to the THI and designed as self-administered 25-item questionnaires to determine the degree of disability in relation to hearing impairment and dizziness. A *yes* response yields a score of four points; *sometimes*, two points; and *no*, zero points. The total score ranges from zero (no disability) to 100 (severe disability). The scales consist of a 7-item physical subscale, a 9-item emotional subscale, and a 9-item functional subscale.

Tinnitus Matching Test

The TMT was performed based on pure sinus waves (in tonal TN) or white gausian noise (wgn, in non-tonal/noise-like TN) provided by custom-written Matlab scripts and presented to both ears of the patient with headphones (HD4.30, Sennheiser, Wennebostel, Germany). In an iterative process, the patient was asked to provide feedback about the individual TN frequency (kHz, in tonal tinnitus) and TN intensity (in dB). Frequency and intensity were adjusted by the experimenter until the patient confirmed that the presented tone/noise matches to his/her individual TN. Frequency and/or intensity were noted for further analysis. The TMT was performed daily immediately prior and after the rTMS application. While TMT is an excellent way to objectify the subjective tinnitus sensation, it is subject to major problems which have been discussed elsewhere (40).

TMS-Mapping and rTMS Parameter

T1-weighted MRI brain scans preceded the experiment to obtain individual anatomical images in combination with an e-field guided neuronavigational rTMS system (NBS, Nexstim, Finland). First, a single standard motor mapping of the right primary motor cortex was performed with a bipulse eight-figure coil (41–44). After determining the "hotspot" yielding the largest motor-evoked potential (MEP) from the left abductor pollicis brevis muscle (APB), the resting motor threshold (RMT), defined as the minimum stimulus intensity to result in at least 5/10 trials a MEP $>50\ \mu V$, was obtained. The orientation of the induced current in the brain was posterior-anterior for the first phase and anterior-posterior for the second phase of the stimulus. The orientation of the electric field was kept perpendicular to the central sulcus. Subsequently, the cortex was mapped with 110% RMT starting at the primary motor cortex and then extending around this spot to cover the primary motor cortex, somatosensory cortex, and premotor cortex. The TMS coil was localized over the right DLPFC according to a standard algorithm by moving the coil from the APB hotspot 6 cm in the anterior direction (**Figure 1C**). The coordinates and direction of the e-field were saved and kept constant throughout the experiment. rTMS was applied with a bipulse eight-figure coil as a sequence of 1,200 pulses with a 1 Hz stimulation frequency and an intensity of 110% RMT (45).

Statistical Analysis

All analysis and statistical tests were performed using MATLAB (MathWorks, Inc., Natick, MA, USA) and SPSS (IBM SPSS Statistics for Windows, Version 26.0. Armonk, NY: IBM Corp.). Significance of rTMS related changes in THI, HHI, and DHI were evaluated with paired *t*-test. Changes in the TN frequency and intensity over the course of the therapy were linearly fitted by the Matlab "robustfit." To evaluate the impact of the hearing status (HEARING), TN duration (DURATION), and the TN type (TYPE) on the acute rTMS effect, an analysis of covariance was applied on the THI and the relative TN intensities. Pearson's regression analysis was performed to evaluate the correlation between the acute effect as measured by the THI and the TMT. Data are shown as the mean ± standard deviation (SD). $p < 0.05$ were considered significant. Finally, operative complications were evaluated, if detected in the postoperative CT scan.

RESULTS

There were no significant side effects of the rTMS stimulation in any of the patients. One patient (ID4) dropped-out of the study due to a subjective non-response to the treatment (see **Table 1**). There was a significant acute decrease of the THI scores at the end of the 10-day rTMS therapy (POST) in comparison to the baseline (PRE) values ($T = 3.33$, $p = 0.013$; paired *t*-test). The acute effect of rTMS on the THI values (PRE-POST) was approximated at -7.0 ± 6.0 [-16 0] points ($T = -3.33$, $p = 0.013$; one-sample *t*-test). As a reduction of 6–7 points in the THI are considered clinically relevant, only 4/9 (44.4%) are classified

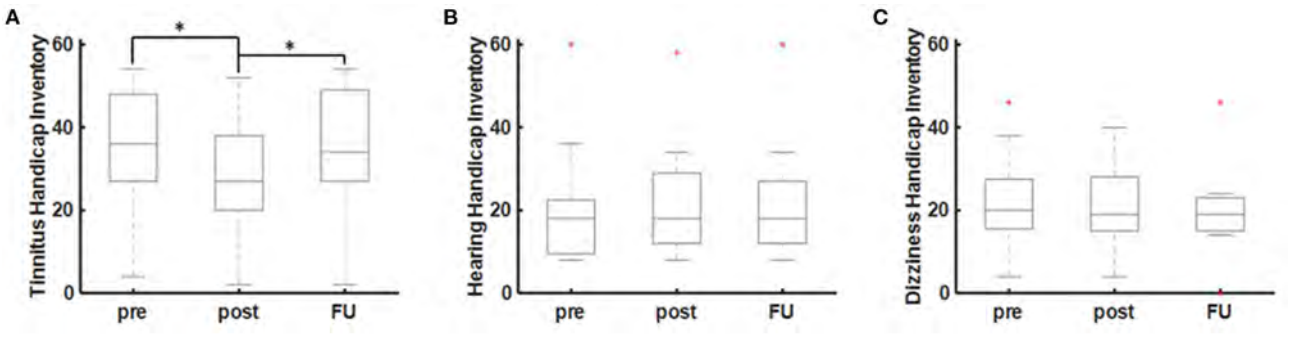

FIGURE 2 | rTMS effects on audiovestibular symptoms. **(A)** Tinnitus as measured by the Tinnitus Handicap Inventory (THI). **(B)** Hearing as measured by the Hearing Handicap Inventory (HHI) and **(C)** dizziness as measured by the Dizziness Handicap Inventory (DHI). Statistical significance is marked by an asterisk (*$p < 0.005$; paired *t*-test).

as good responders according to the THI. During the follow-up (FU) after 4 weeks, however, there was no sustained effect of rTMS ($T = 0.683$, $p = 0.516$; paired *t*-test) on the THI values (**Figure 2A**). In contrast, there was no short-term or long-term effect of rTMS on the HHI or DHI values (**Figures 2B,C**).

The acute effect of rTMS on tinnitus perception was confirmed by recordings of the TMT revealing a significant reduction of TN intensity ($b = -0.068$, $p < 0.001$; robust regression) over the course of the 10-day rTMS therapy (**Figure 3A**). The mean relative TN intensity after rTMS was 0.40 ± 0.30 [0.05–1.00] ($T = -5.95$, $p < 0.001$; one-sample *t*-test), indicating a reduction of TN intensity of ∼60%. As a reduction of 20% is considered clinically relevant, 8/9 (89%) of the patients are classified as good responders according to the TMT. Moreover, 6/9 (67%) of the patients showed a reduction of TN intensity for more than 50%. For patients with tonal tinnitus ($n = 4$), there was a tendency for a slight reduction of TN frequency ($b = -0.011$, $p = 0.009$; robust regression) over the course of the 10-day rTMS therapy (**Figure 3B**). Notably, there was a good correlation ($r = 0.43$; Pearson's) between the acute effect as measured by the THI and the TMT (**Figure 3C**). To evaluate the effect of the hearing status (HEARING), TN duration (DURATION), and the TN type (TYPE) on the acute rTMS effect, an analysis of covariance was applied on the THI and the relative TN intensities at the end of the 10-day rTMS therapy. In fact, we could not detect any significant main effect of HEARING [$F_{(1, 4)} = 1.56$; $p = 0.782$], TYPE [$F_{(1, 4)} = 4.01$; $p = 0.116$], or DURATION [$F_{(1, 4)} = 4.41$; $p = 0.104$] on the TN perception as measured by the THI questionnaire. Considering the TN matching results, however, we observed a significant effect of TYPE [$F_{(1, 4)} = 10.29$; $p = 0.024$] and DURATION [$F_{(1, 4)} = 17.81$; $p = 0.008$]. Patients with a tonal TN showed a higher benefit from therapy than patients with a noise-like TN (**Figure 3D**). Additionally, patients with a longer TN duration showed less TN intensity reduction after rTMS (**Figure 3E**). Basically, patients suffering from TN for <5 years showed a better response than patients suffering from tinnitus for more than 10 years. In contrast, there was no effect of HEARING [$F_{(1, 4)} = 0.25$; $p = 0.637$].

DISCUSSION

The present pilot study proves a significant acute effect of low-frequency rTMS to the right DLPFC on TN perception (THI and TMT) of nine VS patients. However, there was no significant long-term effect in the follow-up after 4 weeks. In contrast, rTMS had no effect on other audiovestibular complaints such as hearing impairment or dizziness. While the THI failed to detect any clinically relevant acute effect of rTMS in 56% of the patients, TMT revealed a reduction of TN intensity for more than 20 in 89% and for more than 50 in 56% of the patients. Notably, the acute effect of rTMS was influenced by the TN type and duration. In general, patients with a tonal TN and shorter TN duration showed a better response to rTMS therapy.

Considering the hypothesized pathophysiology of TN driven by a central maladaptation, rTMS has been suggested in TN treatment several years ago. However, the results have been divergent and even contradictory (21, 24, 26–29). rTMS applies a train of repetitive magnetic pulses to alter the excitability of the neurons and modulate cortical activity. High-frequency rTMS increases cortical excitability, while low-frequency rTMS is considered to inhibit the neural activity in stimulated regions (46, 47). In general, rTMS has been successfully applied for TN treatment at the primary auditory cortex (36, 37), temporoparietal junction (48), and dorsolateral pre-frontal cortex (DLPFC) (45, 49). Low-frequency rTMS to temporal stimulation sites is supposed to reduce the hyperexcitability of the auditory network (36, 37). However, a recent multicenter randomized controlled trial with a large sample size demonstrated that low-frequency (1 Hz) rTMS over the temporal cortex is not superior to sham rTMS in reducing TN severity (37). To the authors' opinion, the temporal lobe is not an optimal target candidate for rTMS application due to its coverage by the temporal muscle. Depending on the individual's anatomy, the temporal muscle might increase the distance to the cortex and thus, potentially decrease the strength of the magnetic field on the cortex to subthreshold levels. Additionally, involuntary muscle twitches related to the TMS pulses are limiting the applicable stimulation intensity. In contrast, stimulation to the

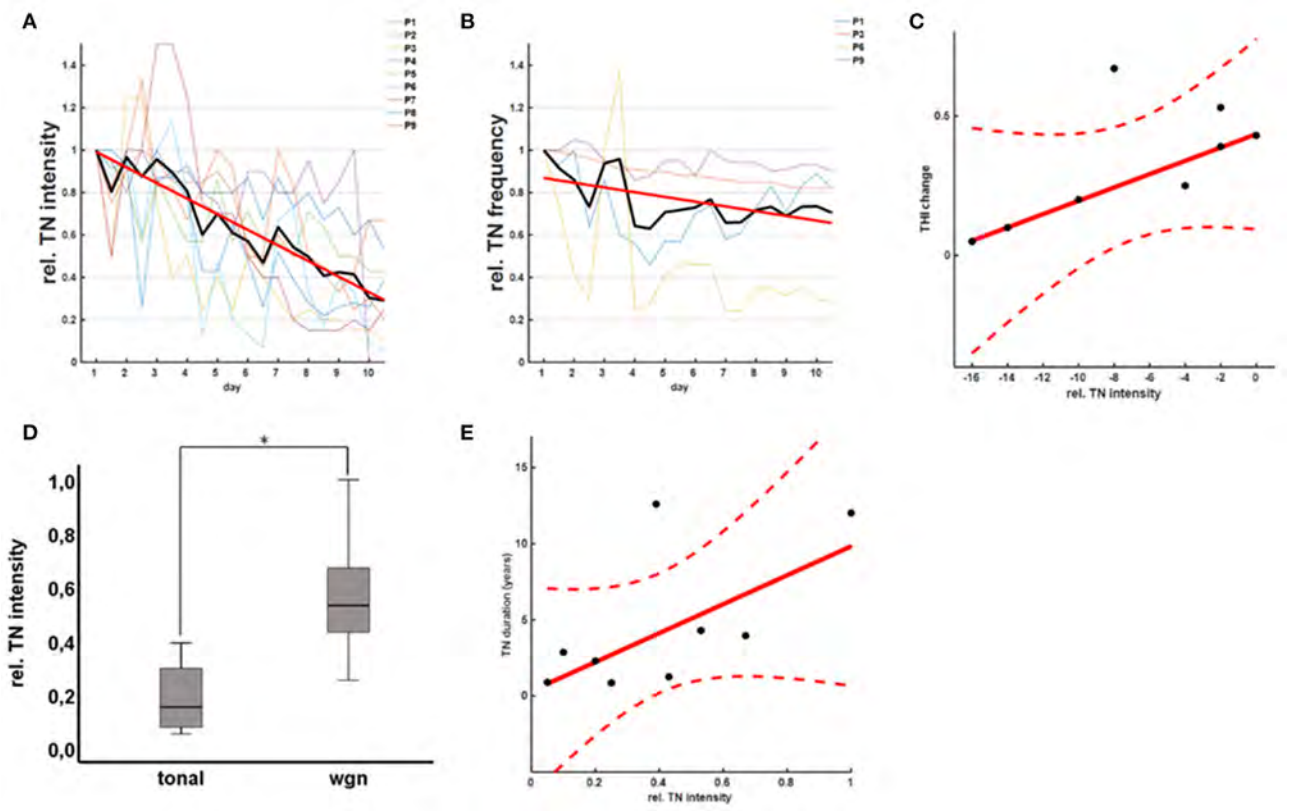

FIGURE 3 | rTMS effects on TN matching. rTMS therapy led to a significant reduction of the TN intensity as measured by the TN matching **(A)**. In patients with a tonal TN, there was an additional tendency for a reduction of the TN frequency **(B)**. Notably, there was a good correlation between the acute effect as measured by the THI and the TN matching test **(C)**. In general, patients with a tonal TN **(D)** and shorter TN duration **(E)** showed a better response to rTMS therapy.

DLPFC is easily accessible and thought to influence networks involved in auditory attention (50). Interestingly, TN suppression has been shown for either *high*-frequency stimulation of the *left* DLPFC (49) and *low*-frequency stimulation of the *right* DLPFC (45). Furthermore, combined multisite rTMS is hypothesized to improve treatment outcome (48). In a recent meta-analysis, however, concurrent high-frequency stimulation of the *left* DLPFC to the temporal cortex was not found to promote efficacy (23). Considering this evidence, we have decided on the application of *low*-frequency stimulation of the *right* DLPFC (45) for TN treatment. In fact, the present study represents the first study applying *low*-frequency rTMS on the *right* DLPFC in VS-associated TN.

Although being a more homogeneous patient cohort with a shorter TN duration than other published data (26), our response rates were quite comparable to other studies ranging around 50% of the treated patients (51). The application of rTMS in VS patients did not improve the treatment outcome substantially. However, the number of treated patients in this study is too low to draw final conclusions. Additionally, the sensitivity of the THI questionnaire might be—although widely used (21, 36, 37)—too low to detect slight rTMS-related TN improvements (52, 53). In contrast, there was a clear effect of rTMS on the TMT values. We hypothesize that the treatment duration might be too short to induce a clinically relevant effect measurable by the THI. In depression treatment, rTMS exerts a positive clinical effect after four rather than 2 weeks of treatment (54–56).

Notably, our findings indicate that patients with a tonal TN and shorter TN duration showed a better response to rTMS therapy. These findings are in good accordance with the previous publication indicating an impact of these factors on the treatment outcome (30–33). In particular, tonal TN in comparison to non-tonal/noise-like TN is suggested to benefit from rTMS therapy (32, 33). In contrast to the other studies showing an effect of hearing impairment on the treatment outcome (30, 31), our findings did not reproduce these observations. Due to statistical reasons, we have dichotomized hearing impairment in the present study, which might mask the actual effect. However, the number of patients is too low for more profound statistical evaluation. Finally, although our study indicates an acute rTMS effect on VS-associated TN, there is no evidence for a long-term effect after a period of 4 weeks (21, 24, 26–29). However, independent of the sustained long-term effect, rTMS might be useful for priming the cortex in chronic TN patients in order to increase the susceptibility for further treatment options, e.g., notched-noise therapy, pharmacological intervention, cognitive

behavioral therapy, TN masking, or music therapy (10, 11). Finally, there is an increasing literature indicating that TMS effects depend on the ongoing brain-state (57, 58). Thus, applying TMS in VS treatment in a closed-loop fashion depending on the ongoing brain state might improve the treatment outcome. Comparable observations have been made in the recruitment of additional corticospinal tracts (41, 59) for e.g., stroke therapy. In line with this, a dependency of rTMS-based TN therapy on cortical alpha oscillations has been described recently (60, 61).

Limitations of the Study

There are several limitations to the present study. First, the number of patients is too low to draw final conclusions about the effectivity of rTMS in VS-associated patients. However, our findings are comparable to the known results in literature.Second, there was no control group.Interventional studies should ideally be designed as randomized, double-blinded controlled studies (36, 37). However, considering the low incidence of VS-associated TN in comparison to other types of TN, it will be difficult to achieve an adequate sample size.

CONCLUSION

The present pilot study is the first one exclusively evaluating the effect of rTMS in VS-associated TN. Our results prove the feasibility and the efficacy of low-frequency rTMS to the right DLPFC in this patient cohort. The results were comparable to the available data with a significant acute but limited long-term effect. However, there is evidence that patients with a tonal TN and shorter TN duration might have the strongest benefit. A randomized controlled study with a larger sample size is necessary to prove these initial findings.

DATA AVAILABILITY STATEMENT

The raw data supporting the conclusions of this article will be made available by the authors, without undue reservation.

ETHICS STATEMENT

The studies involving human participants were reviewed and approved by Ethics committee of the Eberhard Karls University Tuebingen. The patients/participants provided their written informed consent to participate in this study.

AUTHOR CONTRIBUTIONS

MTL and GN were responsible for data acquisition, data analyses, statistical analysis as well as drafting and reviewing the manuscript. ML, JS, and KM were involved in data acquisition as well as drafting and reviewing the manuscript. MT and AS were involved in drafting and reviewing the manuscript. All authors contributed to the article and approved the submitted version.

FUNDING

This study was kindly supported by the Guido Fluri Foundation. We acknowledge the support by Open Access Publishing Fund of University of Tübingen.

REFERENCES

1. Baguley DM, Humphriss RL, Axon PR, Moffat DA. The clinical characteristics of tinnitus in patients with vestibular schwannoma. *Skull Base*. (2006) 16:49–58. doi: 10.1055/s-2005-926216
2. Lloyd SKW, Kasbekar AV, Baguley DM, Moffat DA. Audiovestibular factors influencing quality of life in patients with conservatively managed sporadic vestibular schwannoma. *Otol Neurotol*. (2010) 31:968–76. doi: 10.1097/MAO.0b013e3181e8c7cb
3. Naros G, Sandritter J, Liebsch M, Ofori A, Rizk AR, Del Moro G, et al. Predictors of preoperative tinnitus in unilateral sporadic vestibular schwannoma. *Front Neurol*. (2017) 8:378. doi: 10.3389/fneur.2017.00378
4. Trakolis L, Ebner FH, Machetanz K, Sandritter J, Tatagiba M, Naros G. Postoperative tinnitus after vestibular schwannoma surgery depends on preoperative tinnitus and both pre- and postoperative hearing function. *Front Neurol*. (2018) 9:136. doi: 10.3389/fneur.2018.00136
5. Matthies C, Samii M. Management of 1000 vestibular schwannomas (acoustic neuromas): clinical presentation. *Neurosurgery*. (1997) 40:1–9; discussion 9–10. doi: 10.1227/00006123-199701000-00001
6. Moffat DA, Baguley DM, Beynon GJ, Da Cruz M. Clinical acumen and vestibular schwannoma. *Am J Otol*. (1998) 19:82–7.
7. Myrseth E, Pedersen PH, Møller P, Lund-Johansen M. Treatment of vestibular schwannomas. Why, when and how? *Acta Neurochir*. (2007) 149:647–60; discussion 660. doi: 10.1007/s00701-007-1179-0
8. Del Río L, Lassaletta L, Díaz-Anadón A, Alfonso C, Roda JM, Gavilán J. Tinnitus and quality of life following vestibular schwannoma surgery. *B-ENT*. (2012) 8:167–71. Available online at: http://www.b-ent.be/en/tinnitus-and-quality-of-life-following-vestibular-schwannoma-surgery-13446
9. Grauvogel J, Kaminsky J, Rosahl SK. The impact of tinnitus and vertigo on patient-perceived quality of life after cerebellopontine angle surgery. *Neurosurgery*. (2010) 67:601–9. doi: 10.1227/01.NEU.0000374725.19259.EA
10. Baguley D, McFerran D, Hall D. Tinnitus. *Lancet*. (2013) 382:1600–7. doi: 10.1016/S0140-6736(13)60142-7
11. Langguth B, Kreuzer PM, Kleinjung T, De Ridder D. Tinnitus: causes and clinical management. *Lancet Neurol*. (2013) 12:920–30. doi: 10.1016/S1474-4422(13)70160-1
12. Chovanec M, Zvěrina E, Profant O, Balogová Z, Kluh J, Syka J, et al. Does attempt at hearing preservation microsurgery of vestibular schwannoma affect postoperative tinnitus? *Biomed Res. Int.* (2015) 2015:783169. doi: 10.1155/2015/783169
13. Kohno M, Shinogami M, Yoneyama H, Nagata O, Sora S, Sato H. Prognosis of tinnitus after acoustic neuroma surgery–surgical management of postoperative tinnitus. *World Neurosurg*. (2014) 81:357–67. doi: 10.1016/j.wneu.2012.09.008
14. Han BI, Lee HW, Kim TY, Lim JS, Shin KS. Tinnitus: characteristics, causes, mechanisms, and treatments. *J Clin Neurol*. (2009) 5:11. doi: 10.3988/jcn.2009.5.1.11
15. Møller AR. Pathophysiology of tinnitus. *Otolaryngol Clin North Am.* (2003) 36:249–66, v–vi. doi: 10.1016/S0030-6665(02)00170-6
16. O'Connor AF, France MW, Morrison AW. Perilymph total protein levels associated with cerebellopontine angle lesions. *Am J Otol*. (1981) 2:193–5.
17. Sahley T, Nodar R, Musiek F, Sahley TL, Nodar RH, Musiek FE. *Efferent Auditory System: Structure and Function, Singular Publishing Group Audiology series*. San Diego, CA: Singular Publishing Group (1997).
18. Henry JA, Roberts LE, Caspary DM, Theodoroff SM, Salvi RJ. Underlying mechanisms of tinnitus: review and clinical implications. *J Am Acad Audiol*. (2014) 25:5–22; quiz 126. doi: 10.3766/jaaa.25.1.2

19. Shore SE, Roberts LE, Langguth B. Maladaptive plasticity in tinnitus–triggers, mechanisms and treatment. *Nat Rev Neurol*. (2016) 12:150–60. doi: 10.1038/nrneurol.2016.12
20. Langguth B. Non-invasive neuromodulation for tinnitus. *J Audiol Otol*. (2020) 24:113–8. doi: 10.7874/jao.2020.00052
21. Dong C, Chen C, Wang T, Gao C, Wang Y, Guan X, et al. Low-Frequency repetitive transcranial magnetic stimulation for the treatment of chronic tinnitus: a systematic review and meta-analysis of randomized controlled trials. *Biomed Res Int*. (2020) 2020:3141278. doi: 10.1155/2020/3141278
22. Schoisswohl S, Arnds J, Schecklmann M, Langguth B, Schlee W, Neff P. Amplitude modulated noise for tinnitus suppression in tonal and noise-like tinnitus. *Audiol Neurotol*. (2020) 24:309–21. doi: 10.1159/000504593
23. Schoisswohl S, Agrawal K, Simoes J, Neff P, Schlee W, Langguth B, et al. RTMS parameters in tinnitus trials: a systematic review. *Sci Rep*. (2019) 9:12190. doi: 10.1038/s41598-019-48750-9
24. Theodoroff SM, Folmer RL. Repetitive transcranial magnetic stimulation as a treatment for chronic tinnitus: a critical review. *Otol Neurotol*. (2013) 34:199–208. doi: 10.1097/MAO.0b013e31827b4d46
25. May A, Hajak G, Gänßbauer S, Steffens T, Langguth B, Kleinjung T, et al. Structural brain alterations following 5 days of intervention: dynamic aspects of neuroplasticity. *Cereb Cortex*. (2007) 17:205–10. doi: 10.1093/cercor/bhj138
26. Liang Z, Yang H, Cheng G, Huang L, Zhang T, Jia H. Repetitive transcranial magnetic stimulation on chronic tinnitus: a systematic review and meta-analysis. *BMC Psychiatry*. (2020) 20:547. doi: 10.1186/s12888-020-02947-9
27. Meng Z, Liu S, Zheng Y, Phillips JS. Repetitive transcranial magnetic stimulation for tinnitus. *Cochrane Database Syst Rev*. (2011) 5:CD007946. doi: 10.1002/14651858.CD007946.pub2
28. Peng Z, Chen XQ, Gong SS. Effectiveness of repetitive transcranial magnetic stimulation for chronic tinnitus: a systematic review. *Otolaryngol Head Neck Surg*. (2012) 147:817–25. doi: 10.1177/0194599812458771
29. Soleimani R, Jalali MM, Hasandokht T. Therapeutic impact of repetitive transcranial magnetic stimulation (rTMS) on tinnitus: a systematic review and meta-analysis. *Eur Arch Oto-Rhino Laryngol*. (2016) 273:1663–75. doi: 10.1007/s00405-015-3642-5
30. De Ridder D, Verstraeten E, Van Der Kelen K, De Mulder G, Sunaert S, Verlooy J, et al. Transcranial magnetic stimulation for tinnitus: Influence of tinnitus duration on stimulation parameter choice and maximal tinnitus suppression. *Otol Neurotol*. (2005) 26:616–9. doi: 10.1097/01.mao.0000178146.91139.3c
31. Kleinjung T, Steffens T, Sand P, Murthum T, Hajak G, Strutz J, et al. Which tinnitus patients benefit from transcranial magnetic stimulation? *Otolaryngol Head Neck Surg*. (2007) 137:589–95. doi: 10.1016/j.otohns.2006.12.007
32. Astrid L, Martin S, Michael L, Michael KP, Timm BP, Elmar F, et al. Predictors for rTMS response in chronic tinnitus. *Front Syst Neurosci*. (2012) 6:11. doi: 10.3389/fnsys.2012.00011
33. Frank G, Kleinjung T, Landgrebe M, Vielsmeier V, Steffenhagen C, Burger J, et al. Left temporal low-frequency rTMS for the treatment of tinnitus: clinical predictors of treatment outcome-a retrospective study. *Eur J Neurol*. (2010) 17:951–6. doi: 10.1111/j.1468-1331.2010.02956.x
34. Gardner G, Robertson JH. Hearing preservation in unilateral acoustic neuroma surgery. *Ann Otol Rhinol Laryngol*. (1988) 97:55–66. doi: 10.1177/00034894880970 0110
35. McCombe A, Baguley D, Coles R, McKenna L, McKinney C, Windle-Taylor P. Guidelines for the grading of tinnitus severity: the results of a working group commissioned by the British association of otolaryngologists, head and neck surgeons, 1999. *Clin Otolaryngol Allied Sci*. (2001) 26:388–93. doi: 10.1046/j.1365-2273.2001.00490.x
36. Folmer RL, Theodoroff SM, Casiana L, Shi Y, Griest S, Vachhani J. Repetitive transcranial magnetic stimulation treatment for chronic tinnitus: a randomized clinical trial. *JAMA Otolaryngol Head Neck Surg*. (2015) 141:716–22. doi: 10.1001/jamaoto.2015.1219
37. Landgrebe M, Hajak G, Wolf S, Padberg F, Klupp P, Fallgatter AJ, et al. 1-Hz rTMS in the treatment of tinnitus: a sham-controlled, randomized multicenter trial. *Brain Stimul*. (2017) 10:1112–20. doi: 10.1016/j.brs.2017.08.001
38. Newman CW, Weinstein BE, Jacobson GP, Hug GA. Test-retest reliability of the hearing handicap inventory for adults. *Ear Hear*. (1991) 12:355–7. doi: 10.1097/00003446-199110000-00009
39. Kurre A, Van Gool CJAW, Bastiaenen CHG, Gloor-Juzi T, Straumann D, De Bruin ED. Translation, cross-cultural adaptation and reliability of the German version of the dizziness handicap inventory. *Otol Neurotol*. (2009) 30:359–67. doi: 10.1097/MAO.0b013e3181977e09
40. Klouse KP. Measurement procedures. *US Bur Mines Inf Circ*. (1975) 1:10–15.
41. Kraus D, Naros G, Bauer R, Leão MT, Ziemann U, Gharabaghi A. Brain-robot interface driven plasticity: distributed modulation of corticospinal excitability. *Neuroimage*. (2016) 125:522–32. doi: 10.1016/j.neuroimage.2015.09.074
42. Kraus D, Gharabaghi A. Projecting navigated TMS sites on the gyral anatomy decreases inter-subject variability of cortical motor maps. *Brain Stimul*. (2015) 8:831–7. doi: 10.1016/j.brs.2015.03.006
43. Leão MT, Naros G, Gharabaghi A. Detecting poststroke cortical motor maps with biphasic single- and monophasic paired-pulse TMS. *Brain Stimul*. (2020) 13:1102–4. doi: 10.1016/j.brs.2020.05.005
44. Mathew J, Kübler A, Bauer R, Gharabaghi A. Probing corticospinal recruitment patterns and functional synergies with transcranial magnetic stimulation. *Front Cell Neurosci*. (2016) 10:175. doi: 10.3389/fncel.2016.00175
45. De Ridder D, Song JJ, Vanneste S. Frontal cortex TMS for tinnitus. *Brain Stimul*. (2013) 6:355–62. doi: 10.1016/j.brs.2012.07.002
46. Hallett M. Transcranial magnetic stimulation: a primer. *Neuron*. (2007) 55:187–99. doi: 10.1016/j.neuron.2007.06.026
47. Hallett M. Transcranial magnetic stimulation and the human brain. *Nature*. (2000) 406:147–50. doi: 10.1038/35018000
48. Piccirillo JF, Kallogjeri D, Nicklaus J, Wineland A, Spitznagel EL, Vlassenko AG, et al. Low-frequency repetitive transcranial magnetic stimulation to the temporoparietal junction for tinnitus: four-week stimulation trial. *JAMA Otolaryngol Head Neck Surg*. (2013) 139:388–95. doi: 10.1001/jamaoto.2013.233
49. Vanneste S, De Ridder D. The involvement of the left ventrolateral prefrontal cortex in tinnitus: a TMS study. *Exp Brain Res*. (2012) 221:345–50. doi: 10.1007/s00221-012-3177-6
50. Vanneste S, De Ridder D. The auditory and non-auditory brain areas involved in tinnitus. An emergent property of multiple parallel overlapping subnetworks. *Front Syst Neurosci*. (2012) 6:31. doi: 10.3389/fnsys.2012.00031
51. Dornhoffer JL, Mennemeier M. Using repetitive transcranial magnetic stimulation for the treatment of tinnitus. *Hear J*. (2010) 63:16–20. doi: 10.1097/01.HJ.0000390816.71876.aa
52. Kamalski DM, Hoekstra CE, Van Zanten BG, Grolman W, Rovers MM. Measuring disease-specific health-related quality of life to evaluate treatment outcomes in tinnitus patients: a systematic review. *Otolaryngol Head Neck Surg*. (2010) 143:181–5. doi: 10.1016/j.otohns.2010.03.026
53. Meikle MB, Henry JA, Griest SE, Stewart BJ, Abrams HB, McArdle R, et al. The tinnitus functional index: development of a new clinical measure for chronic, intrusive tinnitus. *Ear Hear*. (2012) 33:153–76. doi: 10.1097/AUD.0b013e31822f67c0
54. Levkovitz Y, Isserles M, Padberg F, Lisanby SH, Bystritsky A, Xia G, et al. Efficacy and safety of deep transcranial magnetic stimulation for major depression: a prospective multicenter randomized controlled trial. *World Psychiatry*. (2015) 14:64–73. doi: 10.1002/wps.20199
55. Loo CK, Mitchell PB. A review of the efficacy of transcranial magnetic stimulation (TMS) treatment for depression, and current and future strategies to optimize efficacy. *J Affect Disord*. (2005) 88:255–67. doi: 10.1016/j.jad.2005.08.001
56. O'Reardon JP, Solvason HB, Janicak PG, Sampson S, Isenberg KE, Nahas Z, et al. Efficacy and safety of transcranial magnetic stimulation in the acute treatment of major depression: a multisite randomized controlled trial. *Biol Psychiatry*. (2007) 62:1208–16. doi: 10.1016/j.biopsych.2007.01.018
57. Khademi F, Royter V, Gharabaghi A. Distinct beta-band oscillatory circuits underlie corticospinal gain modulation. *Cereb Cortex*. (2018) 28:1502–15. doi: 10.1093/cercor/bhy016
58. Naros G, Lehnertz T, Leão MT, Ziemann U, Gharabaghi A. Brain state-dependent gain modulation of corticospinal output in the active motor system. *Cereb Cortex*. (2020) 30:371–81. doi: 10.1093/cercor/bhz093

59. Kraus D, Naros G, Guggenberger R, Leão MTMT, Ziemann U, Gharabaghi A. Recruitment of additional corticospinal pathways in the human brain with state-dependent paired associative stimulation. *J Neurosci*. (2018) 38:1396–407. doi: 10.1523/JNEUROSCI.2893-17.2017
60. Müller N, Lorenz I, Langguth B, Weisz N. rTMS induced tinnitus relief is related to an increase in auditory cortical alpha activity. *PLoS ONE*. (2013) 8:e55557 doi: 10.1371/journal.pone.0055557
61. Weisz N, Lüchinger C, Thut G, Müller N. Effects of individual alpha rTMS applied to the auditory cortex and its implications for the treatment of chronic tinnitus. *Hum Brain Mapp*. (2014) 35:14–29. doi: 10.1002/hbm.22152

Conflict of Interest: The authors declare that the research was conducted in the absence of any commercial or financial relationships that could be construed as a potential conflict of interest.

frontiers in Neurology

BRIEF RESEARCH REPORT
published: 14 May 2021
doi: 10.3389/fneur.2021.658025

Pre-surgical fMRI Localization of the Hand Motor Cortex in Brain Tumors: Comparison Between Finger Tapping Task and a New Visual-Triggered Finger Movement Task

Marco Ciavarro[1], Eleonora Grande[2], Luigi Pavone[1], Giuseppina Bevacqua[3], Michelangelo De Angelis[1], Paolo di Russo[1], Roberta Morace[1], Giorgia Committeri[2], Giovanni Grillea[1], Marcello Bartolo[1], Sergio Paolini[1,3] and Vincenzo Esposito[1,3]*

[1] *Istituto di Ricovero e Cura a Carattere Scientifico (IRCCS) Neuromed, Pozzilli, Italy,* [2] *Department of Neuroscience, Imaging and Clinical Sciences, University "Gabriele d'Annunzio" of Chieti-Pescara, Chieti, Italy,* [3] *Department of Human Neurosciences, University of Rome "La Sapienza", Rome, Italy*

OPEN ACCESS

Edited by:
Giovanni Raffa, University of Messina, Italy

Reviewed by:
Antonino Scibilia, Universitaire de Strasbourg, France
Enricomaria Mormina, Università degli Studi di Messina, Italy
Gianluca Scalia, Garibaldi Hospital, Italy
Gergely Orsi, Hungarian Academy of Sciences (MTA), Hungary

***Correspondence:**
Marco Ciavarro
marcociavarro@gmail.com

Specialty section:
This article was submitted to Applied Neuroimaging, a section of the journal Frontiers in Neurology

Received: *24 January 2021*
Accepted: *17 March 2021*
Published: *14 May 2021*

Citation:
Ciavarro M, Grande E, Pavone L, Bevacqua G, De Angelis M, di Russo P, Morace R, Committeri G, Grillea G, Bartolo M, Paolini S and Esposito V (2021) Pre-surgical fMRI Localization of the Hand Motor Cortex in Brain Tumors: Comparison Between Finger Tapping Task and a New Visual-Triggered Finger Movement Task. Front. Neurol. 12:658025. doi: 10.3389/fneur.2021.658025

Introduction: Pre-surgical mapping is clinically essential in the surgical management of brain tumors to preserve functions. A common technique to localize eloquent areas is functional magnetic resonance imaging (fMRI). In tumors involving the peri-rolandic regions, the finger tapping task (FTT) is typically administered to delineate the functional activation of hand-knob area. However, its selectivity may be limited. Thus, here, a novel cue-induced fMRI task was tested, the visual-triggered finger movement task (VFMT), aimed at eliciting a more accurate functional cortical mapping of the hand region as compared with FTT.

Method: Twenty patients with glioma in the peri-rolandic regions underwent pre-operative mapping performing both FTT and VFMT. The fMRI data were analyzed for surgical procedures. When the craniotomy allowed to expose the motor cortex, the correspondence with intraoperative direct electrical stimulation (DES) was evaluated through sensitivity and specificity (mean sites = 11) calculated as percentage of true-positive and true-negative rates, respectively.

Results: Both at group level and at single-subject level, differences among the tasks emerged in the functional representation of the hand-knob. Compared with FTT, VFMT showed a well-localized activation within the hand motor area and a less widespread activation in associative regions. Intraoperative DES confirmed the greater specificity (97%) and sensitivity (100%) of the VFMT in determining motor eloquent areas.

Conclusion: The study provides a novel, external-triggered fMRI task for pre-surgical motor mapping. Compared with the traditional FTT, the new VFMT may have potential implications in clinical fMRI and surgical management due to its focal identification of the hand-knob region and good correspondence to intraoperative DES.

Keywords: hand knob, gliomas, fMRI, pre-surgical planning, motor area

INTRODUCTION

Preservation of motor function in brain tumor surgery involving the peri-rolandic regions is a challenge for neurosurgeons. Surgical management remains the most successful strategy to date, although the resection of tumors in this region, more than in other eloquent areas, has been historically accompanied by considerable rates of incomplete resection and high risk of morbidity (1). Accurate localization of functional areas around the primary motor cortex (M1) is crucial to reduce negative outcomes while reaching the maximum resection (2). Intraoperative neurophysiological monitoring (IOM) through direct electrical stimulation (DES) is commonly employed. When this region is exposed, DES can be performed with a monopolar stimulation probe; otherwise, the positioning of a subdural strip electrode is required for continuous monitoring of motor evoked potentials (MEPs) during the resection (3). Preoperatively, the anatomical landmark such as the Ω-shaped structure has been traditionally used for the localization of the hand motor area (4). However, mass effects associated with brain tumors can distort these common relations; on the other hand, functional areas may be relocated to other brain regions, making anatomy-based localization of eloquent areas more challenging (5).

In this scenario, a variety of non-invasive pre-operative functional brain mapping techniques are nowadays successful in localizing motor function with a good correspondence with IOM (6). An emerging tool in pre-operative identification of the motor cortex (M1) is the navigated transcranial magnetic stimulation (nTMS) that, similarly to DES, establishes a causal link between the stimulation area and the observed motor outputs (7). Nevertheless, beyond the lack of availability in neurosurgery centers, a major disadvantage is that nTMS may not be employed in those cases in which, due to peritumoral edema and therapies necessary to prevent tumor-related seizures, it is necessary to increase the stimulation intensities to evoke MEPs, exposing the patient at risk for unfathomed events (stimulation-induced seizures and increased stimulation-related discomfort) (8).

By virtue of its non-invasiveness, fMRI is a widely available technique for mapping brain functions. It is considered a powerful tool in the pre-operative planning for surgical procedures involving M1, providing a 92% correspondence to DES mapping data (3, 9, 10) and high percentage of both sensitivity, ranging from 71 to 100%, and specificity, from 68 to 100% (11). It measures brain activity by recording concomitant changes in cerebral perfusion during task execution, and it is considered to be a quicker, less stressful and repeatable method in pre-operative brain mapping. Besides, fMRI allows a more detailed coregistration between structural and functional data (12) that may be useful both in pre-surgical planning, to determine the operative trajectories, and intraoperatively to guide subdural strip electrode positioning, especially in those cases in which the craniotomy does not allow to expose M1. The finger tapping task (FTT) is one of the easier tasks to be performed to investigate functional activation of the hand-knob area. The FTT requires a repetitive self-paced touch of thumb to each finger (13, 14) that is compared with a "no-task" control condition. Although FTT is widely used, the corresponding functional activation map involves not only those regions commonly associated with the execution of voluntary finger movements (i.e., the primary and supplementary motor cortices, basal ganglia, and cerebellum) but also other areas, such as the premotor and somatosensory motor cortices, which may play a more general role in motor tasks (15). In addition, the difficulties in executing the FTT in patients with partial motor deficits may determine poor functional imaging data (16).

In the light of these considerations, we developed a new task for pre-surgical motor mapping, the visual-triggered finger movement task (VFMT), with the aim of overcoming the weakness of FTT. VFMT was indeed designed by requiring simple finger movements without sensory feedback and an active control task during the rest period. We hypothesized that the VFMT, with respect to FTT, may provide a more focal and reliable functional localization of the hand motor region. Thus, it may be able to better predict the spatial relation between the lesion and the eloquent area, being useful in rating the surgical resection entities. We tested our hypothesis in a sample of patients who underwent tumor resection in central areas, by using both motor tasks during pre-surgical mapping.

MATERIALS AND METHODS

Subjects

Of 115 patients with a lesion involving central regions who underwent fMRI investigation of motor functions for pre-operative mapping between December 2017 and August 2020, 20 consecutive patients (M = 14; mean age 44; range 23–77 years) performed both FTT and VFMT with the hand contralateral to the lesion. We included in the study patients with evidence of glioma in peri-rolandic region and no contraindications to MRI, while we excluded patients who, for clinical reasons or poor compliance, performed FTT or VFMT exclusively. In 12 cases, tumors were localized in the right hemisphere. Seven patients presented tumor recurrence. All patients underwent surgical glioma resection by microsurgical subpial technique (17). The entire sample gave informed consent before the experiment, and the protocol was approved by the medical ethics committee of the I.R.C.C.S. Neuromed (Ethical Approval Code: 11/17 21-12-17). Clinical characteristics and histological diagnoses are shown in **Table 1**.

Magnetic Resonance Imaging

The MRI study was performed at the Neuroradiology Unit of IRCCS NEUROMED, Pozzilli (Is), Italy. MRI data were acquired on a 3T GE Signa HDxT scanner (General Electric Medical Systems, Milwaukee, WI). A high-resolution structural T1-weighted image was acquired using a 3D spoiled gradient recalled (SPGR) sequence [repetition time/echo time/inversion time (TR/TE/TI) = 10.26/4.192/400 ms, flip angle = 15°, field of view (FOV) = 256 mm, slice thickness = 1 mm, matrix size: 256 × 256]; then, an axial fast recovery fast spin echo (FRFSE) T2 scan (TR/TE/TI = 11,002/162.92/2,250 ms, FOV = 240 mm, slice thickness = 4 mm, matrix size: 320 × 224) and 3D Fast Spin Echo T2 image (TR/TE/TI = 6,000/140.524/1,824 ms, FOV = 256 mm, slice thickness = 1.6 mm, matrix size:

TABLE 1 | Demographic and clinical data: tumor type, localization and EOR.

Patients			Clinical information		Tumor location			fMRI activation localization		Concordance fMRI tasks—DES				Distance fMRI-lesion	
										Sensitivity		Sensitivity			
	Sex	Age	Histology (WHO grade)	Relapse	Emisphere	MNI AAL template	EOR	FTT	VMFT	FTT	VFMT	FTT	VFMT	FTT	VFMT
1	M	45	Oligodendroglioma (II)	Yes	R	S1, SPG, precuneus	93%	M1 R, SMA R, S1 R, MFG R	M1 R, SMA R	-	-	-	-	>1cm	>1cm
2	F	38	Diffuse astrocytoma (II)	Yes	R	SFG, SMA, ACC	88%	M1 R, SMA R/L, SFG R/L, MFG R	M1 R, SMA R	-	-	-	-	<5mm	<5mm
3	M	37	Anaplastic astrocytoma (II)	Yes	R	M1, PMd, SMG	86%	S1 R, SMA L/R, M1 L, S1 L, MFG L	M1 R, SMA L	-	-	-	-	<5mm	<5mm
4	M	46	Oligodendroglioma (II)	Yes	R	M1, SMA	92%	M1 R/L, S1 R, SMA L, MFG R	M1 R	50%	100%	75%	100%	<5mm	>1cm
5	F	70	Adenocarcinoma (II)	No	L	S1	90%	S1 L, M1 L, SMA L, SMA R, M1 R, PMd R, SPG R	M1 R, SMA R	-	-	-	-	>1cm	>1cm
6	M	40	Glioblastoma (IV)	No	R	SFG, IFG, CC	92%	MFG R	M1 R	-	-	-	-	none	>1cm
7	F	55	Oligoastrocytoma anaplastico (III)	Yes	R	M1, PMd, MFG, IFG	90%	M1 R, S1 R, M1 L, S1 L	M1 R, SMA L, S1 L	-	-	-	-	>1cm	>1cm
8	M	46	Glioblastoma (IV)	No	L	SM1, SMA, SPG	76%	M1 L, S1 L, PMd L, IFG L, SMA R, M1 L, S1 L, MFG L, SFG L	M1 R	28%	100%	100%	87%	<5 mm	<5 mm
9	F	52	Glioblastoma (IV)	No	R	M1, MFG, SFG	88%	M1 R, S1 R, SMA L, SMA R, M1 L, S1 L, MFG L	M1 R, SMA R	30%	100%	100%	100%	<5 mm	<5mm
10	F	34	Anaplastic astrocytoma (III)	No	R	M1, SMA, SFG, MFG	98%	M1 R, S1 R, SMA R, SMA L, MFG L, IFG R, M1 L	M1 R, SMA L, MFG L	50%	100%	100%	100%	<5mm	<1mm
11	M	23	Ganglioglioma (I)	No	L	SMA	95%	M1 R/L, S1 R/L, SMA R/L, PMd L, SPG R, SMG R/L	M1 L, SFG L	37%	100%	100%	100%	<5mm	<1mm
12	M	51	Diffuse astrocytoma (II)	No	L	M1, S1, CC, precuneus	86%	M1 L, S1 L, M1 R, SPG R, SMG L, AG L	M1 R/L	66%	100%	100%	100%	<5mm	<1 mm
13	M	42	Glioblastoma (II)	No	R	M1	88%	M1 R/L, S1 R/L, SMA R/L, CC L	M1 R/L, SMA R	57%	100%	50%	100%	<5 mm	<5mm
14	M	33	Anaplastic astrocytoma (IV)	No	L	Thalamus, hippocampus	77%	MFG L, preSMA L	M1 L, S1 R					>1cm	>1cm
15	M	45	Glioblastoma (IV)	Yes	L	M1	84%	M1 R/L, S1 L, SMA L, SPG R	M1 R/L	71%	100%	100%	100%	<5mm	<5mm
16	M	28	Glioblastoma (V)	Yes	R	M1, SFG, MFG, IFG, insula	91%	M1 R, S1 R, IPF R, M1 L, SMA L, SFG L, MFG L	M1 R, SMA L, MFG L	-	-	-	-	<5mm	<1mm
17	M	77	Radionecrosis (III)	No	R	SM1, SPG	70%	SFG R	M1 R, M1 L, SMA L	100%	100%	50%	100%	-	<5mm
18	F	42	Radionecrosis (III)	No	L	M1	85%	S1 L, SPG R/L, SMA R/L, M1 R	M1 R/L	50%	100%	66%	100%	<5mm	<5mm
19	M	46	Glioblastoma (IV)	No	L	M1	86%	M1 R/L, S1 L, SPG R/L, SMA L, PL R	M1 R/L, S1 R	57%	100%	100%	85%	<5mm	<5mm
20	M	30	Oligodendroglioma (II)	No	R	M1, MFG, IFG	88%	M1 R/L, S1 R/L, SMA R	M1 R/L, SMA R	-	-	-	-	<5mm	<5mm

Functional localization of fMRI maps, sensitivity, specificity and minimum distance between functional activation and lesion in both tasks. Tumor location and fMRI activation: M1, motor cortex; S1, sensory cortex; SM1, sensory-motor cortex; SMA, supplementary motor cortex; PMd, dorsal pre-motor cortex; SFG, superior frontal gyrus; MFG, middle frontal gyrus; IFG, inferior frontal gyrus; CC, cingulate cortex; SPG, superior parietal gyrus, IPG, inferior parietal gyrus; SMG, supramarginal gyrus; AG, angular gyrus.

320 × 320) were also acquired. Further, the same sequences were acquired post-surgery in order to evaluate the extent of resection (EOR). Blood oxygenation level-dependent (BOLD) contrast functional imaging was acquired using a whole-body radiofrequency coil for signal excitation and an eight-channel head coil for signal reception. The acquisition was performed utilizing T2*-weighted echo-planar imaging (EPI) sequences with the following parameters: TE 30 ms, matrix size 64 × 64, FOV 288 mm, flip angle 90°, and slice thickness 3 mm. For each subject, two different fMRI sessions were acquired, depending on the task performed by the subject. For the FTT, 100 functional volumes consisting of 39 transaxial slices parallel to the anterior commissure–posterior commissure (AC–PC) line were acquired with a TR of 3 s. For VFMT, 120 functional volumes consisting of 39 transaxial slices parallel to the AC–PC line were acquired with a TR of 2 s. All the images were anonymized. The whole acquisition period required about 35 min.

fMRI Task Design and Paradigm

For both tasks (FTT and VFMT), fMRI acquisition was performed using a block-design paradigm. The FTT was administered over 5 min 15 s (five dummy runs) with five cycles consisting of 30 s of active condition, in which the patients executed a repetitive self-paced touch of thumb to each finger, followed by 30 s of baseline condition, in which the patients were instructed to look at a fixation point without performing any movement. The instruction of "go" or "stop" was presented via a high-quality stereo headphone set. The VFMT was administered over 4 min 10 s (five dummy runs) with six cycles consisting of 20 s of active condition, in which they observed a green dot randomly appearing on each finger, requiring the execution of abduction of the corresponding finger for a total of 10 movements (twice for each finger), followed by 20 s of baseline condition in which a red dot appeared randomly twice on each finger, with patients instructed to passively observe without executing any movements (**Figure 1**). VFMT was administered using E-Prime presentation software (Psychology Software Tools; www.pstnet.com) and the Nordic Neurolab visual system (Nordic NeuroLab, Bergen, Norway). A dedicated neuropsychologist instructed the patients before entering in the scanner room and monitored the execution of each task during the scanning sessions. FTT and VFMT were run in random order across patients.

Single-Subject fMRI Data Analysis

Pre-surgical Planning

Real-time BOLD fMRI image processing was performed with BrainWaveRT (GE Medical Systems version 4.4). Data quality was monitored in real-time to alert the operator of poor data acquisition due to patient head movement and through task-performance monitoring with real-time activation maps. Moreover, an immediate post-processing of fMRI data was conducted on the scanner console using BrainWavePA software. An automatic pre-processing of functional scans was performed including images realignement using Woods AIR method (18, 19) to minimize movement artifact. Motion correction data indicated the magnitude and direction of rotations and translations detected and corrected during realignment. These data were extracted, and statistical comparison between the two tasks was run into R-studio software 1.3.1 performing Student's *t*-test. The fMRI image volumes were smoothed with a Gaussian spatial filter of full width at half maximum (FWHM) of 8.0 × 8.0 × 8.0 mm. A multiple regression analysis was then performed on the scans, and a *t*-test map was generated. To rate the temporal autocorrelations due to the smoothness of the hemodynamic response, the Worsley and Friston method was used, and the effective number of degrees of freedom estimated. Through the latter, the *t*-test maps were turned into an activation Z-map, and a p-value = 0.0001 was used for thresholding. Pre-processed functional volumes of patients were co-registered with the corresponding structural dataset, then the activation maps were created and visualized in the three orthogonal planes and in 3D rendering.

Intraoperative Mapping

In 11 patients (55% of the whole sample), craniotomy for resection allowed to expose M1. Before surgical resection, the motor cortex was stimulated through an anodal monopolar probe in order to map the cortical motor sites. DES consisted in a biphasic electrical current (60 Hz, 1 ms, 1–4 mA), which creates a "virtual transient lesion" on the cortex. When the stimulated site elicited a MEP, it was considered a positive site. We stimulated a mean of 11 sites that allowed to reach a complete cortical mapping. The DES results were compared with the 3D fMRI maps made with BrainWave for both tasks (as in **Figure 2**). The concordance between DES and fMRI maps was evaluated in terms of the percentage of true-positive rate (sensitivity) and true-negative rate (specificity).

Neuronavigation and Lesion Volume Estimation

fMRI raw data in DICOM format were imported into iPlannet server (version 3.0.1, Brainlab AG, Feldkirchen, Germany) for the neuronavigation planning. The default threshold (t-score) was set to a statistical significance of $p = 0.001$ and could be manually adapted. The proposed t-score was adjusted to reach an activation map overlapping to the one previously reconstructed in BrainWavePA software. Specifically, the threshold was increased until the cluster of activation in M1 reached the same extent obtained from BrainWave analysis.

iPlannet was also used to define tumor volume and postoperative tumor residual. These volumes were evaluated in all patients by using contrast T1-weighted or T2-weighted MR images in native space, acquired before and after tumor resection. In those cases of tumor recurrence, the previous resection cavities were estimated and not included in the lesion volume. Postoperatively, we estimated the EOR as the percentage of the resected volume compared with the pre-operative volume: EOR = (pre-operative tumor volume–postoperative tumor volume)/pre-operative tumor volume.

Anatomical Localization of fMRI Activation Maps

In order to find the anatomical localizations of fMRI activations, Formation of Burnt-In-Pixel (BIP) maps outlining the area of activation created with the BrainWave, together with the

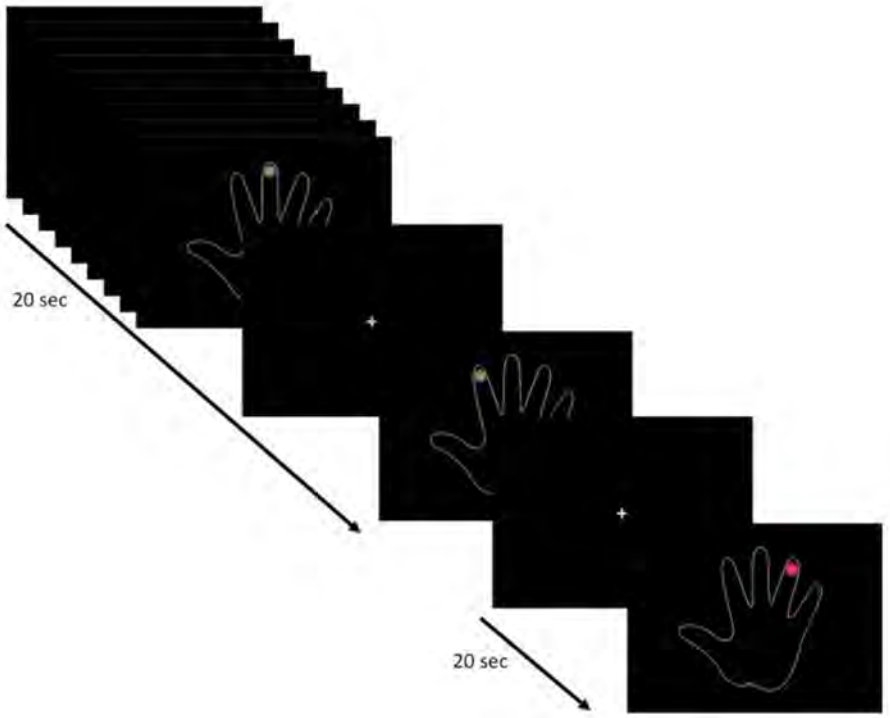

FIGURE 1 | Visual-triggered finger movement task (VFMT) protocol (e.g., right hand). Active condition (green dot): patients are instructed to move the corresponding finger when a green dot appears. Passive condition (red dot): patients are instructed to observe without making any movements.

corresponding 3D T1 images and the 3D T2 fluid-attenuated inversion recovery (FLAIR) images were exported in DICOM format and analyzed using a custom pipeline in SPM12 environment (https://www.fil.ion.ucl.ac.uk/spm/software/spm12/). The images were first converted from DICOM to NIFTI format; then each resulting image was normalized into Montreal Neurological Institute (MNI) space using the built-in function in SPM12. After the normalization, a co-registration between the structural and functional images, including also the Automated Anatomical Labeling (AAL) template, was performed using the normalized mutual information (20). Finally, the images were smoothed using the built-in function of SPM12, with a 6-mm Gaussian smoothing kernel. In order to anatomically localize the fMRI activations, the BIP image was loaded into xjView toolbox (https://www.alivelearn.net/xjview), and the peak coordinates of each cluster were extracted (**Table 1**).

fMRI Second-Level Analysis

Differences in fMRI activations maps between the two tasks (FTT and VFMT) were investigated through a second-level fMRI analysis implemented in SPM12. To examine the difference in neural activity between the two tasks, all the contrast images for each task created from the first-level analysis in SPM12 performed on raw data were entered into a second-level two-sample t-test model. According to the hand used for task execution, we divided the sample in two groups (left hand, $n = 8$; right hand, $n = 12$), and we examined which voxels survived by selecting a cluster-forming threshold of $p < 0.001$ and a cluster size of 10 voxels. Then, to localize the survived cluster of activation, they were superimposed on an AAL template in xjView.

RESULTS

Pre-operative Mapping

All patients completed both fMRI tasks successfully, although two patients (patients 6 and 17) showed poor task execution performance during FTT. In three cases, the task was re-performed due to poor data acquisition. **Table 1** shows the localization of single-subject fMRI activation clusters for both tasks, performed for pre-surgical planning purposes with BrainWavePA software using a conservative threshold of $p < 0.0001$. In 18 patients (90%), the activation maps of VFMT were more selective than FTT maps. Specifically, FTT revealed a widespread network of activation involving areas not closely related to motor processing, whereas VFMT was able to elicit a more focal cluster of activation in M1 and other motor regions (i.e., SMA). In the two cases mentioned above, the FTT was not able to provide activation in the sensory motor cortex at a fixed threshold due to motor coordination deficit. Conversely, in patients 9 and 13, while FTT produced widespread activation maps, VFMT required a reduction of the threshold ($p = 0.001$) to obtain a cluster of activation in the hand-knob region.

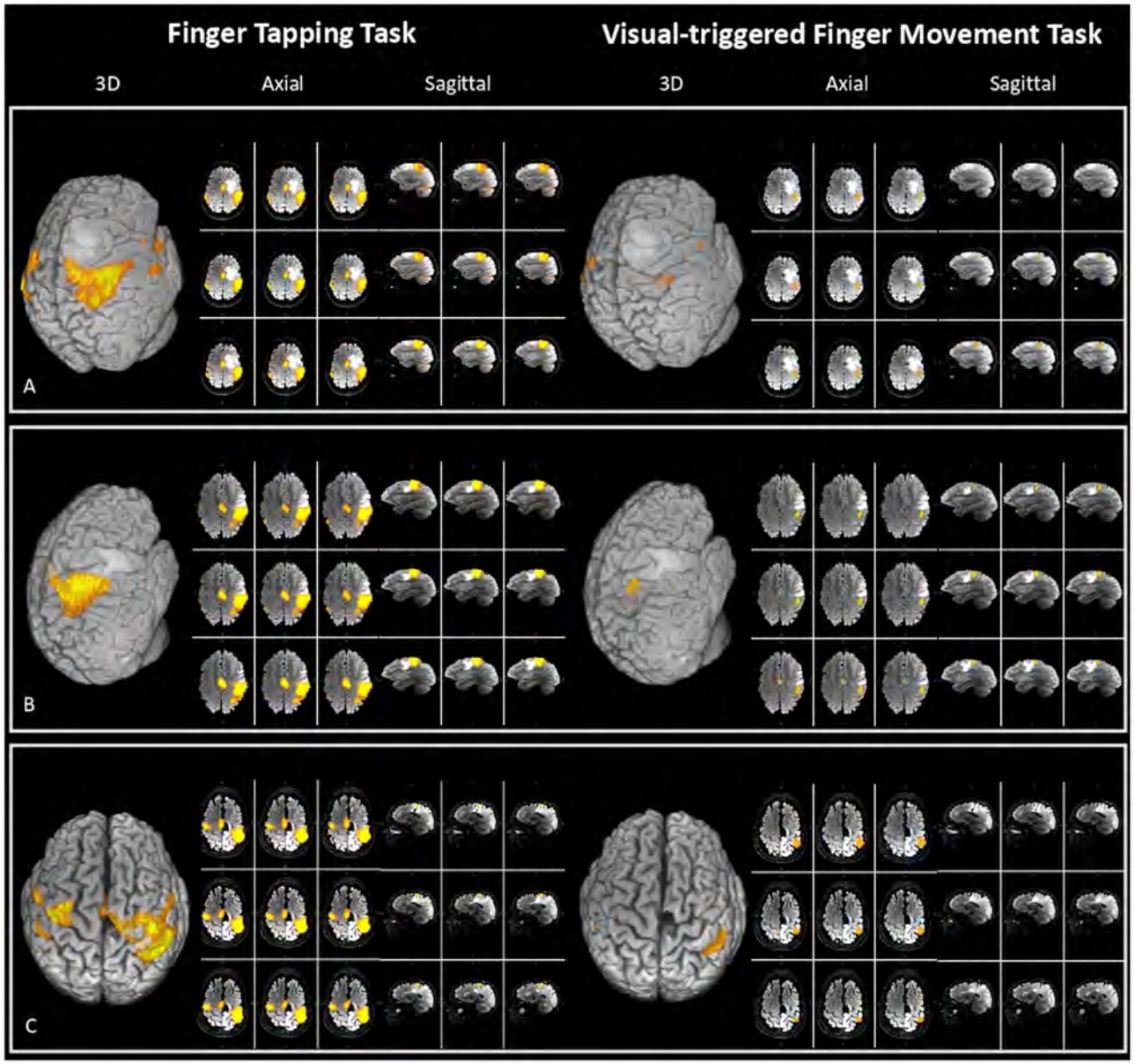

FIGURE 2 | Three-dimensional (3D), axial, and sagittal views of the activation maps for both fMRI tasks [finger tapping task (FTT) on the left and visual-triggered finger movement task (VFMT) on the right], elaborated at single-subject level in three exemplar patients for clinical purpose with BrainWave software on T2 MRI sequences. The figure also displays tumor position and its spatial relation with eloquent areas. **(A)** Patient 10: closer proximity between lesion and FTT vs. VFMT activation map [fMRI specificity: VFMT 100%; FTT 50%; extent of resection (EOR) 98%]. **(B)** Patient 20: close proximity between lesion and both fMRI maps <5 mm (EOR 88%). **(C)** Patient 4: a case of tumor recurrence in which VFMT compared with FTT maps has greater reliability (fMRI specificity: VFMT 100%; FTT 50%) and has a major predictive value on EOR (92%).

Intraoperative Mapping

Eleven patients underwent DES mapping. In the whole sample, the mean number of stimulation sites was 11 (±1.37). In VFMT, the mean sensitivity reached 100% and the specificity 97%, whereas in FTT, they were 54 and 86%, respectively (**Table 1**). In particular, the specificity was found to be poorer in FTT, in patients 13, 17, and 18 with tumors involving M1.

In addition, the EORs were compared with the distance from VFMT activation in M1. In nine cases (90%), the distance of the VFMT activation map from the lesion allows to achieve gross total resection (>80%). By contrast, in two cases, due to the close proximity between the lesion and eloquent hand-knob area, uncompleted resection was performed.

Taking these data together, VFMT maps showed a great predictive value in identifying functional areas than FTT (**Figure 2**).

fMRI-Based Neuronavigation

fMRI raw data of both tasks were imported in Brainlab suite, and the thresholds were manually defined based on BrainWave maps. We observed the previously described difference in the extension of the activation map between the two tasks. In addition, on the threshold (t-score) of both VFMT (13.3 $\pm$ 3.62) and FTT (18.9 $\pm$ 7.11), a *t*-test and Fishers' test were performed. They revealed a significant difference ($p < 0.05$) between the two fMRI tasks, with a higher threshold and greater variability in the FTT.

fMRI Second-Level Analysis

The clusters of activation surviving the second-level two-sample *t*-test model, run on opposite comparisons between FTT and VFMT, showed wider activation maps in FTT. Notably, in the right-hand group, the activation clusters spread into prefrontal regions (mean cluster size = 11 voxels), whereas in the left-hand group, the activation spread into inferior parietal regions (mean cluster size = 28 voxels). These statistical data confirmed the more focal cluster of activation in VFMT compared with FTT.

DISCUSSION

Pre-operative mapping techniques are routinely used to plan surgical resection of lesions located in the cerebral central region to identify eloquent cortical areas. fMRI is a well-established and a widely available technique to obtain a pre-operative functional cortical mapping. Traditionally, the block-design FTT is implemented to map the hand-knob region, although several methodological aspects may cause a loss of specificity in localizing this area. Here, we tested a novel, clinically based VFMT able to overcome the weaknesses of FTT in the fMRI environment. We compared the accuracy of these two tasks (i) in generating the 3D maps for pre-operative planning, (ii) in the overlap of fMRI data with DES during intraoperative mapping, and (iii) in neuronavigation for fMRI image guidance.

Preliminary data of 3D single-subject functional maps seemed to show a more focal cluster of activation in the hand-knob areas for VFMT compared with FTT. Moreover, results of FTT maps showed activations in cortical regions far beyond the hand-knob area, such as the prefrontal and inferior parietal regions (**Table 1**). The reduced activation in the sensory cortex in VFMT, consistent with our hypothesis, could be associated with the task execution framework (i.e., no touch among the fingers), thus generating a more focal activation map with accurate localization of the primary motor cortex. By contrast, the FTT execution framework requires the touch of the thumb to each finger. This may explain the more widespread map we obtained, which included the sensory cortex and may be confounding in the localization of the hand-knob area both during the pre-surgical planning and for neuronavigation purposes.

In addition, even in intraoperative mapping data, a major accuracy of VFMT was found by comparing fMRI activation maps of both tasks to DES. Even employing a low stimulation amplitude, we observed a good concordance between the fMRI technique and DES (3, 9, 10). Sensitivity and specificity rates (100 and 97%, respectively) of VFMT were greater than those of FTT and in accordance with previous data (11, 21). By contrast, the poorer FTT sensitivity rate, compared with that in previous studies (22, 23), might be due to the lower stimulation parameters applied.

In particular, beyond the low sample size, data concerning specificity showed a greater correspondence in the activation maps of VFMT compared with FTT (**Table 1**). This could be seen as a better overlap between intraoperative stimulated sites and the more focal VFMT functional activation maps, whereas poor correlation with FTT maps came out. Furthermore, the more precise VFMT activation maps correlated with the EOR: indeed, in those cases in which the clusters of activation were closer to the lesion, gross total resection could not be achieved (**Figures 2B,C**). By contrast, the FTT activation maps' proximity to the lesion had not a predictive value on EOR (**Figure 2A**).

Finally, during the integration of fMRI for neuronavigation purposes, the maps generated with Brainlab software showed less extension and variability in the threshold needed to obtain a more selective map in VFMT compared with FTT. Often, operators manually reach the threshold, finding a balance between spurious and expected activation (24). Our results suggest that the operator's influence may be reduced in the manually determined threshold of VFMT. Moreover, the more accurate maps obtained from VFMT could be useful when M1 is not exposed and strip positioning for IOM is required.

To summarize, all these data may be interpreted as an overall efficacy of VFMT in the accurate localization of the hand-knob area in pre-surgical mapping and during intraoperative phases. This accuracy could be explained by some crucial novelties in the task setting. FTT indeed requires a self-paced movement of the fingers, and although the frequency of a simple motor task has not been related to fMRI signal variability (25), it is worth noting that increasing frequencies of the finger movements have been related to greater cortical activation, especially in the sensory motor cortex (26–28). Thus, on the one hand, a lower movement frequency could be associated with a poorer activation, as what emerged in two of our cases in which patients showed poor task execution performance during FTT; on the other, a greater movement rate could explain those cases with widespread activity and lower accuracy. By contrast, VFMT execution requires a randomized time-constrained finger movement. In this view, the externally paced stimuli may remove the frequency bias and may reduce the fMRI signal variability. In addition, these differences in the task execution may underlie the significantly reduced head motion degree registered during VFMT execution. It could be argued that the head motion during FTT may be increased due to the rhythmic fingers movement or even it may be reduced in VFMT due to the visual stimulus that may work as a head "anchor" requiring the patients to fixate the screen. The quality of fMRI data is strongly hampered in the presence of substantial head movements (27). Thus, it is crucial to minimize head motion to reduce artifacts and increase fMRI accuracy.

At the same time, in VFMT, the active control condition collected with the same visual stimuli of the experimental

condition, but without movement execution, may allow to better isolate the primary motor cortex responses. By contrast, FTT offers a lower control due to a rest condition of "no task" (29). Moreover, beyond the voluntary movement activation *per se*, VFMT randomized cues require a continuous refresh of the movement plan, in contrast to the pacing task in FTT. Interestingly, the more widespread activation of FTT maps compared with the VFMT maps at a single-subject level emerged in our preliminary results and was confirmed by the second-level analysis run at the group level. Indeed, functional maps in FTT identified further areas in the prefrontal and inferior parietal regions within the right- and left-hand groups, respectively.

Either clinical results or ease of application could make VFMT a powerful tool in hand-knob localization for pre-surgical planning. The improvement of spatial relation knowledge about the tumor and eloquent areas may have a predictive value on EOR and be useful for ensuring safer surgery. Data acquisition is less time-consuming than other pre-operative mapping techniques, resulting in even less stress for the patients. Image processing in the clinical fMRI software is easy to perform and could be quickly implemented into clinical brain mapping routine of several neurological deficits, such as stroke, epilepsy, and Parkinson disease. Moreover, the clinical BrainWave software allows real-time monitoring of fMRI data quality, preventing poor data acquisition (30). Finally, co-registration between functional volumes and the corresponding structural dataset provides 3D maps with an accurate surface reconstruction to directly compare it with the anatomical landmarks on the exposed brain cortex intraoperatively.

LIMITATIONS

The small sample size represents one of the limitations of the research, not allowing to evaluate the influence of tumor type and lesion size on task accuracy and reliability. Moreover, VFMT, here presented for the first time, has not been already standardized on matched control populations. The differences between fMRI task protocols could represent another limitation. Nevertheless, we adopted FTT as standardized, commonly used paradigm for hand-knob localization and designed the new VFMT in order to properly overcome its limitations, including those related to the protocol. Further, the EPI series used for fMRI acquisition may have reduced the spatial resolution. At the same time, however, it allows to replicate our study and to implement VFMT routinely in pre-surgical mapping, with clinical low-field MRI scanners (1.5T) usually employed for clinical purposes. It is worth noting that both VFMT and FTT provided no hand-knob functional activation at a fixed threshold in two patients (10%). However, in VFMT, a minimal threshold variation was sufficient to obtain a good activation map. Additionally, despite that in our sample no patients faced difficulties during task execution, severe visual impairments may result as a major limitation. We are also aware that the lack of a clinical follow-up may represent a further limitation. Nevertheless, postoperative structural MRI showed a greater VFMT predictive value on EOR, with an accurate description of the spatial relationship between lesion and tumor, in order to reach safe resection.

We designed the study to present preliminary data on the efficacy and reliability of VFMT in identifying the hand-knob area in pre-surgical mapping. Further investigations need to be conducted in the future, extending the statistical analysis to perform a standardized direct comparison between tasks on larger groups of patients and including post-surgery clinical–radiological follow-ups in order to strengthen the current scientific evidence.

CONCLUSION

Pre-operative planning is a crucial step in determining surgical resection strategies of tumors involving motor cortical areas. fMRI is a widely available and well-established technique, and VFMT may represent a reliable task in localizing the hand-knob area. Thus, the more focal activation map obtained by VFMT may have a potential impact on the routine pre-surgical mapping, accurately disclosing the relationship between the lesion and the eloquent area and representing a powerful tool for surgical practice.

DATA AVAILABILITY STATEMENT

The original contributions presented in the study are included in the article/supplementary material, further inquiries can be directed to the corresponding author/s.

ETHICS STATEMENT

The studies involving human participants were reviewed and approved by Medical ethics committee of the I.R.C.C.S. Neuromed (Ethical Approval Code: 11/17 21-12-17). The patients/participants provided their written informed consent to participate in this study.

AUTHOR CONTRIBUTIONS

MC, MB, and VE: design and conceptualize the study. MC, EG, LP, and GC: major role in statistical analysis. MC, EG, LP, GB, and VE: interpretation and wrote the paper. MC, EG, LP, GB, MD, PR, RM, GG, MB, SP, and VE: data acquisition. MC, EG, LP, GB, GC, PR, SP, and VE: revised manuscript. All authors contributed to the article and approved the submitted version.

REFERENCES

1. Krishnan R, Raabe A, Hattingen E, Szelényi A, Yahya H, Hermann E, et al. Functional magnetic resonance imaging-integrated neuronavigation: correlation between lesion-to-motor cortex distance and outcome. *Neurosurgery.* (2004) 55:904–14. doi: 10.1227/01.NEU.0000137331.35014.5C
2. Fang S, Liang J, Qian T, Wang Y, Liu X, Fan X, et al. Anatomic location of tumor predicts the accuracy of motor function localization in diffuse

lower-grade gliomas involving the hand knob area. *AJNR Am J Neuroradiol.* (2017) 38:1990–7. doi: 10.3174/ajnr.A5342
3. Sagar S, Rick J, Chandra A, Yagnik G, Aghi MK. Functional brain mapping: overview of techniques and their application to neurosurgery. *Neurosurg Rev.* (2019) 42:639–47. doi: 10.1007/s10143-018-1007-4
4. Yousry TA, Schmid UD, Alkadhi H, Schmidt D, Peraud A, Buettner A, et al. Localization of the motor hand area to a knob on the precentral gyrus. A new landmark. *Brain.* (1997) 120:141–57 doi: 10.1093/brain/120.1.141
5. Cirillo S, Caulo M, Pieri V, Falini A, Castellano A. Role of functional imaging techniques to assess motor and language cortical plasticity in glioma patients: a systematic review. *Neural Plast.* (2019) 2019:4056436. doi: 10.1155/2019/4056436
6. Raffa G, Scibilia A, Conti A, Ricciardo G, Rizzo V, Morelli A, et al. The role of navigated transcranial magnetic stimulation for surgery of motor-eloquent brain tumors: a systematic review and meta-analysis. *Clin Neurol Neurosarg.* (2019) 180:7–17 doi: 10.1016/j.clineuro.2019.03.003
7. Krieg SM, Shiban E, Buchmann N, Meyer B, Ringel F. Presurgical navigated transcranial magnetic brain stimulation for recurrent gliomas in motor eloquent areas. *Clin Neurophysiol.* (2013) 124:522–7. doi: 10.1016/j.clinph.2012.08.011
8. Sollmann N, Zhang H, Kelm A, Schröder A, Meyer B, Pitkänen M, et al. Paired-pulse navigated TMS is more effective than single-pulse navigated TMS for mapping upper extremity muscles in brain tumor patients. *Clin Neurophysiol.* (2020) 131:2887–98. doi: 10.1016/j.clinph.2020.09.025
9. Mangraviti A, Casali C, Cordella R, Legnani FG, Mattei L, Prada F, et al. Practical assessment of preoperative functional mapping techniques: navigated transcranial magnetic stimulation and functional magnetic resonance imaging. *Neurol Sci.* (2013) 34:1551–7. doi: 10.1007/s10072-012-1283-7
10. Dimou S, Battisti RA, Hermens DF, Lagopoulos J. A systematic review of functional magnetic resonance imaging and diffusion tensor imaging modalities used in presurgical planning of brain tumour resection. *Neurosurg Rev.* (2013) 36:205–14. doi: 10.1007/s10143-012-0436-8
11. Castellano A, Cirillo S, Bello L, Riva M, Falini A. Functional MRI for Surgery of Gliomas. *Curr Treat Options Neurol.* (2017) 19:34. doi: 10.1007/s11940-017-0469-y
12. Esposito V, Paolini S, Morace R, Colonnese C, Venditti E, Calistri V, et al. Intraoperative localization of subcortical brain lesions. *Acta Neurochir.* (2008) 150:537. doi: 10.1007/s00701-008-1592-z
13. Maldjian J, Atlas SW, Howard 2nd RS, Greenstein E, Alsop D, Detre JA, et al. Functional magnetic resonance imaging of regional brain activity in patients with intracerebral arteriovenous malformations before surgical or endovascular therapy. *J Neurosurg.* (1996) 84:477–83. doi: 10.3171/jns.1996.84.3.0477
14. Hirsch J, Ruge MI, Kim KH, Correa DD, Victor JD, Relkin NR, et al. An integrated functional magnetic resonance imaging procedure for preoperative mapping of cortical areas associated with tactile, motor, language, and visual functions. *Neurosurgery.* (2000) 47:711–21. doi: 10.1227/00006123-200009000-00037
15. Witt ST, Laird AR, Meyerand ME. Functional neuroimaging correlates of finger-tapping task variations: an ALE meta-analysis. *Neuroimage.* (2008) 42:343–56. doi: 10.1016/j.neuroimage.2008.04.025
16. Krings T, Reinges MH, Erberich S, Kemeny S, Rohde V, Spetzger U, et al. Functional MRI for presurgical planning: problems, artefacts, and solution strategies. *J Neurol Neurosurg Psychiatry.* (2001) 70:749–60. doi: 10.1136/jnnp.70.6.749
17. Lavalle L, D'elia A, Ciavarro M, Esposito V. Subpial technique in supratentorial glioma resection: state of the art and analysis of costs and effectiveness in a single institute experience. *J Neurosurg Sci.* (2020). doi: 10.23736/S0390-5616.20.05046-8. [Epub ahead of print].
18. Woods RP, Cherry SR, Mazziotta JC. Rapid automated algorithm for aligning and reslicing PET images. *J Comp Assist Tomogr.* (1992) 16:620–33. doi: 10.1097/00004728-199207000-00024
19. Woods RP, Mazziotta JC, Cherry SR. MRI-PET Regis- tration with automated algorithm. *J Comp Assist Tomogr.* (1993) 17:536–46. doi: 10.1097/00004728-199307000-00004
20. Collignon A, Maes F, Delaere D, Vandermeulen D, Suetens P, Marchal G. Automated multi-modality image registration based on information theory. In: *Proc. Information Processing in Medical Imaging*. Dordrecht (1995).
21. Bizzi A, Blasi V, Falini A, Ferroli P, Cadioli M, Danesi U, et al. Presurgical functional MR imaging of language and motor functions: validation with intraoperative electrocortical mapping. *Radiology.* (2008) 248:579–89. doi: 10.1148/radiol.2482071214
22. Bartos R, Jech R, Vymazal J, Petrovický P, Vachata P, Hejcl A, et al. Validity of primary motor area localization with fMRI versus electric cortical stimulation: a comparative study. *Acta Neurochir.* (2009) 151:1071–80. doi: 10.1007/s00701-009-0368-4
23. Meier MP, Ilmberger J, Fesl G, Ruge MI. Validation of functional motor and language MRI with direct cortical stimulation. *Acta Neurochir.* (2013) 155:675–83. doi: 10.1007/s00701-013-1624-1
24. Rosazza C, Aquino D, D'Incerti L, Cordella R, Andronache A, Zacà D, et al. Preoperative mapping of the sensorimotor cortex: comparative assessment of task-based and resting-state FMRI. *PLoS ONE.* (2014) 9:e98860. doi: 10.1371/journal.pone.0098860
25. Diciotti S, Gavazzi C, Nave RD, Boni E, Ginestroni A, Paoli L, et al. Self-paced frequency of a simple motor task and brain activation. An fMRI study in healthy subjects using an on-line monitor device. *Neuroimage.* (2007) 38:402–12. doi: 10.1016/j.neuroimage.2007.07.045
26. Schlaug G, Sanes JN, Thangaraj V, Darby DG, Jäncke L, Edelman RR, et al. Cerebral activations covaries with movement rate. *NeuroReport.* (1996) 7: 879–83. doi: 10.1097/00001756-199603220-00009
27. Riecker A, Wildgruber D, Mathiak K, Grodd W, Ackermann H. Parametric analysis of rate-dependent hemodynamic response functions of cortical and subcortical brain structures durin auditorily cued finger tapping: a fMRI study. *NeuroImage.* (2003) 18: 731–9. doi: 10.1016/S1053-8119(03)00003-X
28. Lutz K, Koeneke S, Wustenberg T, Jancke L. Asymmetry of cortical activation during maximum and convenient tapping speed. *Neurosci Lett.* (2005) 373:61–6. doi: 10.1016/j.neulet.2004.09.058
29. Stippich C. *Clinical Functional MRI: Presurgical Functional Neuroimaging*. Springer (2015). doi: 10.1007/978-3-662-45123-6
30. Weiskopf N, Sitaram R, Josephs O, Veit R, Scharnowski F, Goebel R, et al. Real-time functional magnetic resonance imaging: methods and applications. *Magn Reson Imaging.* (2007) 25:989–1003. doi: 10.1016/j.mri.2007.02.007

Conflict of Interest: The authors declare that the research was conducted in the absence of any commercial or financial relationships that could be construed as a potential conflict of interest.

frontiers in Neurology

ORIGINAL RESEARCH
published: 19 May 2021
doi: 10.3389/fneur.2021.650830

Clinical Utility of Transcranial Magnetic Stimulation (TMS) in the Presurgical Evaluation of Motor, Speech, and Language Functions in Young Children With Refractory Epilepsy or Brain Tumor: Preliminary Evidence

Shalini Narayana[1,2,3], Savannah K. Gibbs[2], Stephen P. Fulton[1,2], Amy Lee McGregor[1,2], Basanagoud Mudigoudar[1,2], Sarah E. Weatherspoon[1,2], Frederick A. Boop[2,4,5] and James W. Wheless[1,2]*

[1] Division of Pediatric Neurology, Department of Pediatrics, University of Tennessee Health Science Center, Memphis, TN, United States, [2] Le Bonheur Children's Hospital, The Neuroscience Institute, Memphis, TN, United States, [3] Department of Anatomy and Neurobiology, University of Tennessee Health Science Center, Memphis, TN, United States, [4] Semmes Murphey Neurologic and Spine Institute, Memphis, TN, United States, [5] Department of Neurosurgery, University of Tennessee Health Science Center, Memphis, TN, United States

Accurate presurgical mapping of motor, speech, and language cortices, while crucial for neurosurgical planning and minimizing post-operative functional deficits, is challenging in young children with neurological disease. In such children, both invasive (cortical stimulation mapping) and non-invasive functional mapping imaging methods (MEG, fMRI) have limited success, often leading to delayed surgery or adverse post-surgical outcomes. We therefore examined the clinical utility of transcranial magnetic stimulation (TMS) in young children who require functional mapping. In a retrospective chart review of TMS studies performed on children with refractory epilepsy or a brain tumor, at our institution, we identified 47 mapping sessions in 36 children 3 years of age or younger, in whom upper and lower extremity motor mapping was attempted; and 13 children 5–6 years old in whom language mapping, using a naming paradigm, was attempted. The primary hand motor cortex was identified in at least one hemisphere in 33 of 36 patients, and in both hemispheres in 27 children. In 17 children, primary leg motor cortex was also successfully identified. The language cortices in temporal regions were successfully mapped in 11 of 13 patients, and in six of them language cortices in frontal regions were also mapped, with most children ($n = 5$) showing right hemisphere dominance for expressive language. Ten children had a seizure that was consistent with their clinical semiology during or immediately following TMS, none of which required intervention or impeded completion of mapping. Using TMS, both normal motor, speech, and language developmental patterns and apparent disease induced reorganization were demonstrated in this young cohort. The successful localization of motor, speech, and

OPEN ACCESS

Edited by:
Thomas Picht, Charité – Universitätsmedizin Berlin, Germany

Reviewed by:
Pantelis Lioumis, Aalto University, Finland
Sebastian Ille, Technical University of Munich, Germany
Maja Rogić Vidaković, University of Split, Croatia
Ali Jannati, Boston Children's Hospital, United States

***Correspondence:**
Shalini Narayana
snaraya2@uthsc.edu

Specialty section:
This article was submitted to Applied Neuroimaging, a section of the journal Frontiers in Neurology

Received: *08 January 2021*
Accepted: *25 March 2021*
Published: *19 May 2021*

Citation:
Narayana S, Gibbs SK, Fulton SP, McGregor AL, Mudigoudar B, Weatherspoon SE, Boop FA and Wheless JW (2021) Clinical Utility of Transcranial Magnetic Stimulation (TMS) in the Presurgical Evaluation of Motor, Speech, and Language Functions in Young Children With Refractory Epilepsy or Brain Tumor: Preliminary Evidence. Front. Neurol. 12:650830. doi: 10.3389/fneur.2021.650830

language cortices in young children improved the understanding of the risk-benefit ratio prior to surgery and facilitated surgical planning aimed at preserving motor, speech, and language functions. Post-operatively, motor function was preserved or improved in nine out of 11 children who underwent surgery, as was language function in all seven children who had surgery for lesions near eloquent cortices. We provide feasibility data that TMS is a safe, reliable, and effective tool to map eloquent cortices in young children.

Keywords: transcranial magnetic stimulation, motor mapping, language mapping, epilepsy, brain tumor, presurgical, children, speech mapping

INTRODUCTION

Presurgical mapping of the critical cortex in patients undergoing neurosurgery is critical in assisting surgical planning and minimizing post-operative deficits. Cortical stimulation mapping (CSM) has long been considered the "gold standard" for identifying motor and language cortices, much like intracarotid sodium amytal (Wada) testing, an invasive technique used to evaluate language dominance. The realization that CSM and Wada testing have a number of limitations (1, 2) has led to the emergence of safer non-invasive alternatives, including magnetoencephalography (MEG) (3), functional magnetic resonance imaging (fMRI) (4, 5), and more recently, transcranial magnetic stimulation (TMS) (6–10). Presently, these non-invasive methods are approved by the US Food and Drug Administration for use in presurgical functional mapping and are used alongside Wada and CSM to determine hemispheric dominance, to localize motor, speech, and language cortices in the vicinity of the lesion, and to plan the surgical approach. While these mapping methods can be readily administered in older children and adults (11–14), functional mapping in young children continues to be challenging. Neurological disorders such as tuberous sclerosis, perinatal stroke, hemimegaloencephaly, and pediatric tumors occur early in childhood and may result in refractory epilepsy. The optimal treatment for these disorders, especially in those who fail multiple antiepileptic drugs (AEDs), is often surgery. In such cases, precise mapping of brain function is paramount. However, the ability to perform functional mapping in this population, is limited, and may delay surgical treatments that could greatly improve cognitive function and the quality of life (15). In such young children, TMS could be uniquely suited to overcome challenges that other methods cannot, providing clinicians and patients with information critical to improved outcomes.

Abbreviations: AED, Antiepileptic drugs; APB, Adductor Pollicis Brevis; CSM, Cortical Stimulation Mapping; E-field, Electric Field; EEG, Electroencephalogram; EMG, Electromyography; fMRI, Functional MRI; FSPGR, Fast Spoiled Gradient-echo; GABA, γ-aminobutyric acid; HD, Hemispheric Dominance; LE, Lower Extremity; LH, Left Hemisphere; LI, Laterality Index; MEG, Magnetoencephalography; MEP, Motor Evoked Potentials; MRI, Magnetic Resonance Imaging; MT, Motor Threshold; RH, Right Hemisphere; SD, Standard Deviation; SO, Stimulator Output; TA, Tibialis Anterior; TMS, Transcranial Magnetic Stimulation; MRI-guided TMS; TSC-2, Tuberous Sclerosis Complex type 2; UE, Upper Extremity; VAS, Visual Analog Scale.

With respect to motor function, accurate localization of the motor cortex is challenging in patients under the age of 3 years, particularly if there is associated developmental delay. This is especially true for modalities like MEG and fMRI, and in such cases, mapping is typically attempted during natural sleep or sedation (16–19). Still, MEG and fMRI performed under these conditions are subject to unique limitations in this age group, including the indirect nature of motor cortex localization *via* sensorimotor tasks and the risks associated with sedation. In such situations, TMS has the advantage of directly mapping the motor cortex without the need for absolute patient cooperation (20). Since patients are not required to be still during TMS mapping, there is no need for sedation. Further, mapping using TMS is also possible in patients who are unable to perform motor tasks due to diseases such as paresis or plegia or due to behaviors such with autism or developmental delay. Therefore, TMS is singularly situated for use in non-invasively evaluating the motor system in young children under 3 years of age, including those with developmental delays, directly and without requiring sedation.

Like motor mapping in infants and toddlers, language mapping in pre-school children is often difficult. Children, particularly between 5 and 6 years old, make up one such group (21–23) in whom CSM poses significant risks (i.e., higher charge density (24) causing after-discharges and seizures) with only limited success. For instance, the success rate of CSM is reported to be under 50% in children under 10 years (age range 4.7–10 years) (25). Although fMRI and MEG modalities have gained widespread acceptance, pre-school children often are unable to cooperate with the testing demands of these procedures due to developmental delay, claustrophobia, or general anxiety. In fact, both fMRI and MEG do not yield language mapping results in ∼30% of cases (19, 26). Because children in this age group are sedated during fMRI and MEG and in instances when mapping is successful, it is limited to localization of receptive language areas (27). The lack of thorough speech and language localization for this group likely prevents timely surgeries that could significantly improve cognitive function (28) and quality of life (15, 23); in other cases, surgery proceeds without a precise language map, resulting in possible post-operative speech and language deficits (29) or inadequate resection. However, when compared to fMRI and MEG, TMS has many advantages. First, TMS does not require the patient to remain still. Second, unlike MEG and fMRI where task performance is covert, TMS requires overt speech, and therefore performance can be monitored for

accuracy. Third, expressive language mapping with TMS is also possible in young children who can only undergo receptive language mapping under sedation in MEG and fMRI (27). Fourth, because it is performed in the awake state, TMS language mapping can be performed across multiple sessions, or repeated for verification. Fifth, motor and language mapping with TMS are not impeded by contraindications from most intrinsic metals (unlike MEG and fMRI). Sixth, TMS results are not affected by potential signal artifacts from vascular anomalies and tumor-induced neurovascular uncoupling, as in the case of fMRI (30). Finally, the use of MRI guidance to visualize the cortical surface and accurately position TMS, also termed navigated TMS, has greatly facilitated the use of TMS in children. Henceforth in the manuscript, TMS refers to delivery of TMS under MRI guidance. For these reasons, in young children and other patients in whom alternative methods fail, functional mapping with TMS is especially promising.

At our institution, functional mapping with TMS is successful in nearly 90% of patients in whom MEG and fMRI are not able to provide a motor and/or language map. We have previously reported a small case-series of six children under the age of 3 years who underwent TMS motor mapping at our institution (20) and on the utility of TMS motor mapping in an infant with cortical dysplasia (31). We have also reported a case study of a 4-year 11-month-old child who underwent successful TMS language mapping (32). In this paper we aim to further assess whether reliable motor maps can be derived in very young children with neurological disorders and evaluate the safety and tolerability of TMS in a larger cohort of children younger than 3 years. Furthermore, we report here our experience of mapping speech and language functions in 5- and 6-year-old preschool children, an age group in whom both invasive and non-invasive methods are often unsuccessful. We describe challenges in mapping this population and strategies that have facilitated successful mapping. We also present post-surgical motor and language outcomes in children when available.

TABLE 1 | Demographic and clinical parameters in the motor and language mapping cohorts.

Demographic and clinical features	Upper extremity mapping	Lower extremity mapping	Language mapping
Number of patients	36	18	13
Average age ± SD (years)	1.68 ± 0.8	2.1 ± 0.5	5.6 ± 0.3
Age range	2 mo−3 y	1–3 y	5–6 y
Gender: Male/Female	19/17	11/7	8/5
Handedness: R/L/Ambi	9/8/1	8/3/1	8/3/2
Handedness: Too young/Not reported	16/2	5/1	0/0
Cortical dysplasia	8	3	2
Tuberous Sclerosis Complex type 2	8	5	1
Ischemia/Stroke	6	2	1
Infection	3	2	-
Brain tumor	4	1	7
Brain malformation	4	3	-
Other	3	2	-
Hippocampal sclerosis	–	–	1
Normal MRI	–	–	1
Lesioned Hemisphere: Left	12	3	7
Lesioned Hemisphere: Right	15	8	4
Lesioned Hemisphere: Bilateral	9	9	1
Number of AEDs (Average ± SD)	2.7 ± 1	2.9 ± 1	1.4 ± 0.5

SD, standard deviation; R, right; L, left; Ambi, ambidextrous; AED, Antiepileptic drugs.

METHODS

Patients

We performed a retrospective chart review of TMS motor and language mapping studies attempted between January 2013 and September 2020 at Le Bonheur Children's Hospital, Memphis TN. The institutional review boards at the University of Tennessee Health Science Center and Le Bonheur Children's Hospital approved the retrospective chart review. We identified 47 motor mapping sessions performed on 36 children under the age of 3 years. Six children were mapped twice, one child was mapped three times, and another child was mapped four times, while still under the age of 3. Motor mapping data from the seven children included here have been reported previously (20, 31). We also identified a separate cohort of 13 children between the ages of 5 and 6 years in whom TMS language mapping was attempted. In addition to TMS, most patients underwent continuous scalp video EEG monitoring, MEG for the localization of epileptiform discharges and somatosensory and language cortices, anatomical and functional MRI, and neuropsychological testing as part of the clinical evaluation (33). Wada or CSM were not attempted in this young cohort except in one child (2.3-year-old female) who underwent subdural grid placement for localization of epileptogenic focus. The details of the demographics and diagnoses of the children in the TMS motor and language mapping groups are listed in **Table 1**.

Structural MRI

Structural MR images were obtained on a 3 Tesla Siemens Verio scanner (Siemens AG, Munich, DE) or GE Signa HDxt scanner (General Electric, Milwaukee, WI) in all children utilizing sedation. In the Siemens Verio scanner, a T1-weighted 3D Stealth sequence was acquired using a 12-channel head coil (TR/TE/flip angle = 1900/2.93/9°) with slice-select inversion recovery pulses (TI = 900 ms), FOV = 512 x 512 x 176, and voxel size 0.5 × 0.5 × 1 mm. In the GE Signa HDxt scanner, a T1-weighted 3D Fast Spoiled Gradient-echo (FSPGR) sequence was acquired using an 8-channel head coil (TR/TE/flip angle = 7.95/3.56/12°), FOV = 512 × 512 × 220, and voxel size 0.5 × 0.5 × 0.8 mm. The anatomical MRI was used for neuro-navigation during TMS sessions. During the same MRI session, patients also

completed other clinical MRI and fMRI sequences as part of their epilepsy evaluation.

Transcranial Magnetic Stimulation (TMS)

Motor and language mapping were performed using an MRI-guided TMS system (NBS system 4.0; Nexstim, Inc., Atlanta, GA). The system uses a figure-of-eight coil with an outer winding of 70 mm that stimulates ∼1–2 cm^2 of the cortex beneath its central junction and had a maximum E-field of 172 Volts/meter at a distance of 25 mm from the coil surface (34, 35). The depth of stimulation is determined in each case by peeling the modeled scalp and skull until the cortical surface is visualized and ranged from 10 to 25 mm. The strength of the E-field is calculated taking into account the peeling depth, the size and shape of the individual's head, and the coil orientation parallel to the cortical columns (35) and is displayed for the chosen peeling depth. The high-resolution T1-weighted MRI of each patient was co-registered to the patient's head using anatomical landmarks and the surface matching procedure implemented in the Nexstim NBS system.

Motor Mapping

TMS motor mapping was performed while the children were seated on their parent's lap (see **Figure 1A** for example). The children were allowed to play with toys or to watch TV during the study. The motor evoked potentials (MEPs) elicited by TMS were recorded by surface electromyography (EMG) from bilateral adductor pollicis brevis (APB), brachioradialis, and tibialis anterior (TA) muscles using disposable electrodes (Neuroline 720, Ambu Inc., Maryland, USA) and sampled at 3 kHz and band-pass filtered from 10 to 500 Hz. In each hemisphere, the mapping procedure began with application of TMS at an intensity set at 100% of the stimulator output (SO) around the middle part of the precentral gyrus (i.e., the hand knob area). The starting TMS intensity was set at 100% SO to compensate for the decreased efficacy of the standard figure-of-eight TMS coil in infants and children due to their immature motor system, brain size, and brain tissue conductivity (36, 37) as well as to reduce testing time due to the limited cooperation expected in this cohort. In children with difficulty tolerating this stimulation intensity, SO was decreased gradually until adequate tolerability was achieved. At this point, if no MEPs or CSPs were elicited, the mapping session was ended. TMS stimulation was applied as one pulse at each location with stimulation repeated as needed to cover surrounding cortex, including the precentral and postcentral sulci. The leg motor cortex was mapped by applying TMS along the paracentral lobule and posterior medial frontal gyrus. As the patients could not maintain a true baseline or the incidence of MEP was variable, motor threshold determination (resting or active) was not attempted. The TMS time-locked EMG epochs were analyzed offline to determine the presence of MEP, and, when applicable, to calculate its latency and peak-to-peak amplitude. Since the patients could not maintain relaxed muscles and had ongoing muscle contractions during TMS stimulation, we also examined the EMG recordings for any interruption of this voluntary activity following TMS, i.e., the cortical silent period (CSP) (38). CSP has proven to be a useful diagnostic biomarker in many neurological disorders including epilepsy in adults (39–42). We and others have previously shown that CSP can also be used to localize the motor cortex in individuals including young children in whom the SO required to elicit an MEP is at or near 100% (12, 20, 43).

Language Mapping

TMS was used to localize the language-specific cortex by employing the "virtual lesion" paradigm (44) in 13 pre-school children between the ages of 5 and 6 years. Twelve of the 13 children also completed motor mapping prior to language mapping. The color-naming task was used in eight children (see **Figure 1B** for example) and an object-naming task was used in five children. We have previously shown that young and developmentally delayed children who could not consistently name objects could still name colors accurately and have successfully used the color-naming task to successfully map speech and language in this cohort (32, 45). In other children, pictures of objects included in the NexSpeech module was used (46). Since children were able to name common objects or colors used in this study, we did not individualize the stimuli based on their linguistic abilities.

The participants were seated in a chair and viewed the stimuli on a monitor. Colors (or objects) were displayed for 1,000 ms with an interstimulus interval adjusted according to the individual participant's ability ranging from 3.5 to 5 s. Patients were asked to correctly name the colors or the drawings of common objects as quickly as possible. Colors/pictures erroneously named were removed from the stimulus pool, so that all stimuli presented during TMS had a corresponding correct baseline recording. The TMS SO was adjusted to deliver an E-field of 80–100 V/m at the cortical surface based on previous reports (47, 48) and our own experience in older children and adults (45, 49). Patients were continuously monitored visually and by electromyography for signs of the intracortical spread of excitation or seizures (50). Discomfort during TMS was evaluated using the visual analog scale (VAS) for pain, recorded at baseline, four times throughout mapping, and whenever a patient spontaneously expressed discomfort. The intensity was decreased if participants rated pain $\geq$3 on the VAS but not below an E-field of 50 V/m. The mapping was discontinued if the pain persisted, and E-field fell below 50 V/m. Stimulus presentation and TMS onset were simultaneous with no delay to include early cortical activity (51) and decrease false negative results (52). The TMS train frequency was set at 5 Hz (five pulses). For mapping language cortices, TMS was applied from the supramarginal and angular gyri and extending to the superior, middle, and inferior temporal gyri, as anteriorly as the patient could tolerate. Then stimulation of the middle and inferior frontal gyri, including the pars opercularis and pars triangularis, as well as premotor regions was attempted. Baseline performance, stimuli presented, participant's response, and cortical locations of TMS were recorded for *post-hoc* analysis. Across compliance levels, the entire language mapping procedure was completed in ∼1 h. In each participant, the hemisphere to be stimulated first was decided by prioritizing clinical need and therefore, the lesional hemisphere was mapped first.

FIGURE 1 | Setup for TMS motor (A) and language (B) mapping studies in young children. **(A)**: During TMS motor mapping in infants and toddlers, the child is seated on the parent's lap. **(B)**: During TMS language mapping color naming task was used in some preschool children.

Data Analysis and Statistical Procedure

Motor Mapping

Motor mapping recordings of the EMG were reviewed, and cortical locations where MEPs were observed on the EMG were identified by comparing it with the patient's baseline EMG data, as well as with previously established criteria for identification of cortical motor cortex responses (50). For each MEP, peak-to-peak amplitude and corticomotor latency (time from TMS stimulation to MEP onset) were initially estimated using the automated algorithm included in Nexstim software and verified by visual inspection. The MEP amplitude was used as a threshold to determine whether TMS elicited a response or not. Since the EMG electrode positions were variable between children and the baseline EMG also varied greatly, from being quiet (asleep or paresis) to vigorously active (holding a toy, being agitated, etc.), the MEP amplitudes were not further analyzed. When present, the onset and offset of CSP were calculated by visual inspection. When CSP was observed following an MEP, the MEP onset was also considered to be the CSP onset. When isolated CSP was observed, its onset was determined to be the point when EMG became quiet, and its offset as when the EMG activity returned to baseline pre-TMS levels. Similar to MEPs, the presence of CSP was used to localize response to TMS, and no further analysis was carried out. Examples of TMS-elicited MEPs and CSPs in APB, brachioradialis, and TA muscles are shown in **Figure 2**. Cortical locations of identified MEPs and CSPs were then marked on the patient's MRI.

Language Mapping

Videos of patient performance during TMS language mapping were reviewed and potential speech and language errors were compared with the corresponding baseline response for the same item. Observed errors were independently categorized using the recommended criteria (9, 53) by two authors blinded to the site of stimulation. Any disagreement in categorization was resolved by consensus. The performance was coded as follows: *speech arrest errors*: when TMS resulted in an inability to produce any response; *semantic errors*: when a semantically related or associated word is substituted for the target word; and *performance errors*: form-based distortions, slurring, stuttering, imprecise articulation, or delayed response when compared to baseline recordings of the patient naming the same color or object. Speech errors attributed to discomfort or distraction were excluded from analysis. Further, speech errors resulting from the stimulation of primary mouth and laryngeal motor cortices or lips, jaw, and tongue muscles were also removed. The cortical location, type of error, and TMS intensity (%SO and E-field) for each TMS train were recorded. Similar to language mapping by fMRI (54, 55), we have previously shown that TMS-induced speech and language errors are also amenable to calculating a laterality index (LI) (45, 49). The LI was calculated as E_{left}-E_{right}/E_{left}+E_{right}, where E_{left} was the total number of speech and language errors in the left hemisphere, and E_{right} was the total number of speech and language errors in the right hemisphere. We also calculated LI by weighing the speech arrests (3x) and semantic errors (2x) more than the performance errors. Similar to LI thresholds used in fMRI (54, 55), TMS LI values 1.0–0.1 indicated left hemisphere dominance (HD), −1.0 to −0.1 indicated right HD, and values between −0.1 and +0.1 were considered a balanced bilateral representation of language.

RESULTS

Motor Mapping

Patients

The motor mapping cohort (n = 36 children, 47 total maps) consisted of 19 males and 17 females with a mean age (± SD) of 1.68 (± 0.8) years. The youngest child studied was a 2-month-old female, and 13 children were aged younger than 1 year. Nine children were reported to be right-handed, eight were left-handed, one was ambidextrous, two were not reported, and 16 were indeterminate due to their young age. Each child's

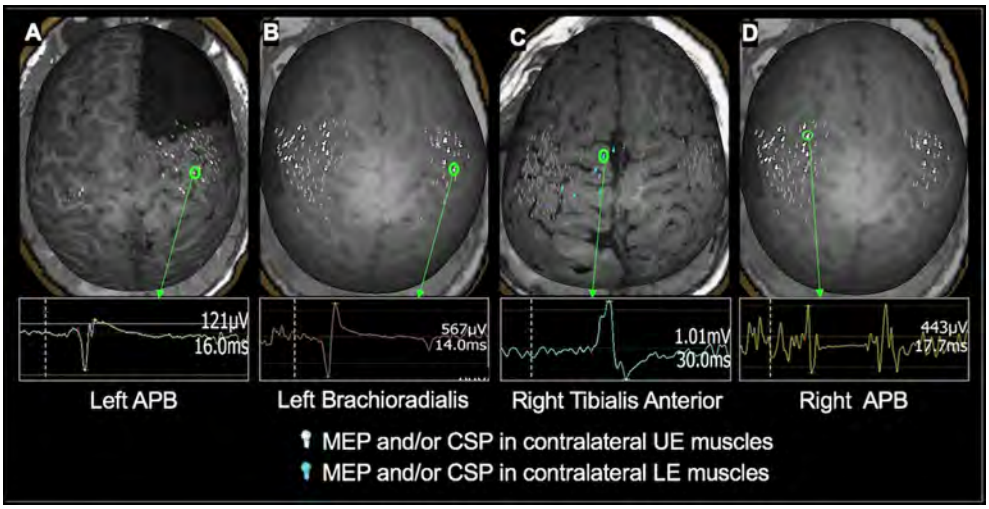

FIGURE 2 | Examples of TMS-evoked MEPs and CSP in children under 3 years of age. **(A)**: A 2.4-year-old male with right frontal lobe cortical dysplasia status post resection. MEP in the left APB muscle having an amplitude of 121 μV and a latency of 16 ms was evoked when TMS was applied to the right precentral gyrus. **(B)** An 18-month-old female with history of left hemisphere perinatal stroke involving left temporal lobe and subsequent infantile spasms demonstrating MEP evoked in the left brachioradialis muscle with an amplitude of 567 μV and a latency of 14 ms following TMS applied to the right precentral gyrus. **(C)** 1.7-year-old female with TSC- 2 demonstrating the MEP elicited in the right tibialis anterior muscle having an amplitude of 1.01 mV and a latency of 30 ms when TMS was applied to the left medial frontal lobe. **(D)** An 18-month-old female with history of left hemisphere perinatal stroke involving left temporal lobe and subsequent infantile spasms demonstrating CSP evoked in the right APB muscle following TMS applied to the left precentral gyrus. The left hemisphere is on the left side of the image.

handedness was determined *via* clinical evaluation by their attending neurologist. Patients were evaluated for refractory epilepsy ($n = 32$) or a brain tumor ($n = 4$). The most common etiologies for seizures were tuberous sclerosis complex type 2 (TSC-2, 22%), cortical dysplasia (22%), and perinatal stroke (17%). All children had an identifiable lesion on the MRI, with the lesion found in the left hemisphere in 33%, in the right hemisphere in 42%, and bilateral in 25% of the children. Thirty-two children were on AEDs (average 2.7 ± 1; range 1–5). The most common AEDs prescribed were levetiracetam (51% of children), clobazam (30%), oxcarbazepine (30%), and lacosamide (26%). The details of the demographic, clinical, and AED information of the motor mapping cohort are listed in **Table 1**.

Mapping Success

Upper extremity (UE) primary motor cortex localization was attempted in both hemispheres in 40 sessions, in only the hemisphere of clinical interest in four, and in the only intact hemisphere in three. Six children were mapped twice (range 2–13 months apart), one child mapped three times (at ages 0.4, 1, and 2 y), and another child mapped four times (at ages 0.5, 0.6, 0.9, and 2.4 y). Motor mapping was considered successful if MEP or CSP was observed even for one stimulation. Three children had only one clear response in each hemisphere, but most often, five or more clear responses were observed (average number of responses = 23; 14% of stimulations). On average, 167.2 stimulations were delivered per session with a range of 26–535 single pulses. Using these criteria, the motor representation for APB and brachioradialis muscles were successfully localized in at least one hemisphere in 44 sessions (33 children) and in both hemispheres in 33 sessions (27 children). In two children, a 5-month-old with cortical dysplasia and a 7-month-old with a tumor, TMS did not elicit any MEPs or CSPs in APB or brachioradialis muscles despite extensive stimulation of both hemispheres at 100% SO. In the 5-month-old infant, the repeat motor mapping at 11 months of age was successful. Finally, the hand/forearm motor cortex could not be identified in one 10-month-old infant with non-lesional refractory epilepsy who could not tolerate increasing TMS intensity > 70% SO.

The primary leg motor cortex localization was attempted in both hemispheres in 18 children (11 males, seven females; average age ± SD: 2.1 ± 0.5 y). Two children were mapped twice. The youngest child studied was a 1-year-old male, and nine children were younger than 2 years. The motor representation of TA was successfully localized in both hemispheres in eight children, with only one hemisphere successfully mapped in seven children. In five children (four males; average age ± SD: 2.0 ± 0.8 y), despite extensive stimulation of both hemispheres at 100% SO, TMS did not elicit any MEPs or CSPs in the lower extremity muscles.

Safety of TMS

All mapping sessions were completed under nursing supervision. We were able to accurately apply TMS in all children as they were seated in their parent's lap. In all children, except for the one child noted above, the loud TMS clicks and the sensation of tapping at an intensity of 100% SO was well-tolerated without any serious adverse effects. We did not use earplugs in an attempt to minimize exposure to TMS clicks as the children could not keep them in place. The entire motor mapping session, including placing EMG electrodes, registering to the MRI, and surveying brain areas, was completed most often in 30–45 min.

Five children (four males, age range 0.4–2.9 y) had seizures during the motor mapping procedure, and five (three males, age range 1.7–2.6 y) had seizures after the mapping procedure was completed, while being transferred to the wheelchair or transported to their inpatient room. In all children, the seizure semiology and duration during/following TMS were consistent with their clinical seizures observed at home and/or in the epilepsy monitoring unit, and all had a history of refractory epilepsy with frequent seizures. The seizures were either focal motor involving face and/or extremity twitching ($n = 5$) or generalized atonic seizures characterized by drop attacks ($n = 5$). In all children, seizures lasted <1 min (range 5 s−50 s) and did not require administration of rescue medication. In children who had seizures during mapping, the procedure was successfully completed, and meaningful data were derived.

TMS Parameters

Over 47 motor mapping sessions, an average of 167 ± 89 stimulations (range 26–532) with an intensity of 98 ± 8% SO was applied. The equivalent E-field in the UE motor cortex was 243 ± 97 V/m and in the leg motor cortex was 209 ± 73 V/m, both measured at a peeling depth of 17 ± 3 mm. There was no significant difference in the TMS E-field between the left and right hemispheres. The corticomotor latency from motor cortex to APB was 17.8 ± 3.1 ms; for brachioradialis, 16.6 ± 4.6 ms; for TA, 26 ± 4.5 ms. When isolated CSPs were observed, the latency for UE muscles was 34.1 ± 4.7 ms and for LE muscles 37.7 ± 6.7 ms. The details of the TMS parameters for upper and lower extremity mapping are listed in **Table 2**.

TABLE 2 | TMS parameters in the motor and language mapping cohorts.

TMS parameters	Upper extremity mapping	Lower extremity mapping	Language mapping
Number of sessions—attempted	47	20	13
Number of sessions—successful	44	15	12
Number of stimulations—single pulse	167 ± 89		191 ± 97
Number of stimulations—5 Hz	n/a		130 ± 52
TMS intensity—% MO	98 ± 8	98.5 ± 7	34 ± 3
TMS intensity—E field (V/m)	243 ± 97	209 ± 73	91 ± 14
Corticomotor latency—APB (ms)	17.8 ± 3.1	n/a	n/a
Corticomotor latency—Brachioradialis (ms)	16.6 ± 4.6	n/a	n/a
Corticomotor latency—TA (ms)	n/a	26 ± 4.5	n/a
Motor mapping: Normal localization	30	15	12
Motor mapping: Developmental variant	6	–	0
Motor mapping: Cortical reorganization	8	–	0
Language mapping task: Colors	n/a		8
Language mapping task: Objects	n/a		5
Number of speech arrests (Average ± SD)	n/a		4 ± 5
Number of semantic errors (Average ± SD)	n/a		2 ± 2
Number of performance errors (Average ± SD)	n/a		10 ± 7
LH dominance	n/a		-
RH dominance	n/a		5
Bilateral dominance	n/a		1
Dominance not determined	n/a		6
Adverse effects - pain at site of stimulation	1		6
Adverse effects - seizures	10		0

SO, stimulator output; E-field, Electric field; APB, Adductor pollicis brevis; TA, Tibialis anterior; SD, standard deviation; LH, left hemisphere; RH, right hemisphere; n/a, not applicable.

Localization of Motor Cortex

In the 33 children in whom motor mapping was successful, the UE primary motor cortex was localized to the central part of the precentral gyrus around the hand knob area (See **Figure 3** for examples). In five of these children (one with TSC-2, one with infection, and three with cortical dysplasia), stimulation of both hemispheres resulted in occasional MEPs in both UE muscles, representing intact uncrossed pyramidal neurons, a normal variant in this age group (see **Figure 3A**). In four out of six children with perinatal stroke, an interhemispheric pattern of motor reorganization was demonstrated with bilateral UE motor representation in the intact hemisphere (see **Figure 4B**). In two out of eight children with cortical dysplasia, an intrahemispheric pattern of motor reorganization was demonstrated with the UE representation displaced toward the lower extremity motor cortex (see **Figure 4A**) or the premotor cortex. In 15 children in whom LE mapping was successful, the primary leg motor cortex was localized to the paracentral lobule in the medial frontal gyrus in one or both hemispheres.

Comparison of TMS-Derived Motor Maps Against Other Mapping Modalities

Of the 36 patients who underwent TMS motor mapping, 20 children underwent somatosensory mapping with MEG, all under sedation. MEG was successful in only five children (four bilateral, and one in one hemisphere only). Twenty-five children underwent fMRI during passive hand movement, also under sedation. The sensorimotor cortex was successfully mapped in 20 children (18 bilateral, and two in one hemisphere only). These findings are consistent with our previous report in a smaller cohort of children under 3 years of age (20). When compared to TMS, which assesses motor cortices directly, MEG and fMRI under sedation primarily mapped the somatosensory cortex. Although the primary motor and sensory cortices are closely linked and findings of one modality can, to some extent, be generalized to the other, the comparison is not a direct

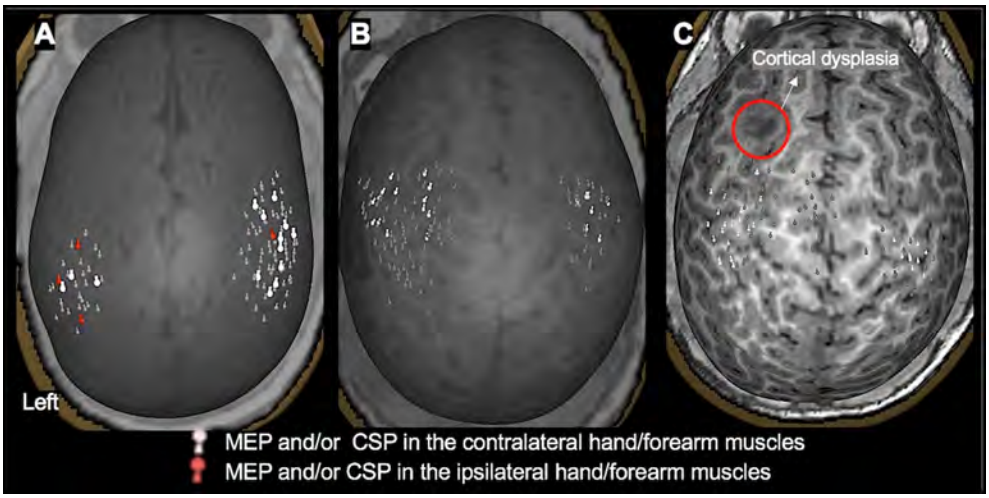

FIGURE 3 | TMS motor mapping demonstrating normal motor development in children under 3 years of age. **(A)**: A 3-month-old male with dysplasia along the inferior frontal sulcus involving the inferior aspect of the right precentral gyrus, inferior gyrus, frontal gyrus, and middle frontal gyrus and history of infantile spasms. The motor cortices were localized along the precentral gyrus with MEPs elicited in contralateral and ipsilateral hand muscles, representing a normal developmental variant. **(B)**: An 18-month-old female with history of left hemisphere perinatal stroke involving left temporal lobe and subsequent infantile spasms demonstrating a normal motor map. **(C)**: A 2.4-year-old female with history of left frontal lobe focal cortical dysplasia, type IIb. Motor representation was localized posterior to the dysplasia.

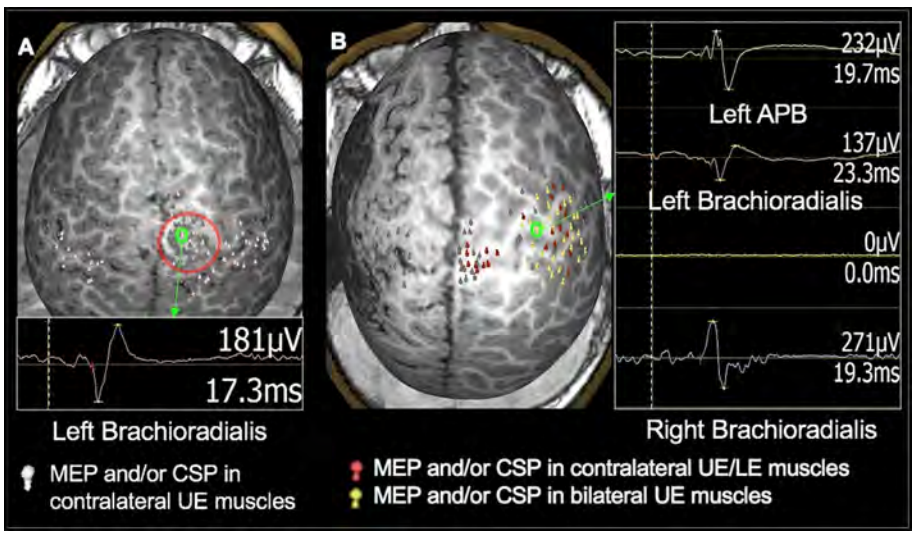

FIGURE 4 | TMS motor mapping demonstrating cortical reorganization in children under 3 years of age. **(A)**: TMS motor mapping in a 1.7-year-old male with history of refractory seizures involving left-sided tonic flexion with a cortical dysplasia in the medial frontal side of the right frontal lobe on the pre- and post-central gyrus. TMS localized left hand and forearm representation to the precentral gyrus. Additionally, MEPs in the hand and forearm muscles were elicited while stimulating the area of cortical dysplasia. No MEPs were elicited in the left lower extremity even at 100% of stimulator output. The child underwent surgical resection of the lesion. At 9 months follow up, he was seizure-free with intact left-hand function and mild left leg monoparesis. **(B)**: A 2-year-old male with history of left hemisphere perinatal stroke and right hemiparesis presenting with refractory epilepsy. TMS motor mapping demonstrated no motor representation for right upper extremity in the left hemisphere. Instead, both left and right upper extremities were represented around the precentral gyrus in the right hemisphere. The left hemisphere is on the left side of the image.

one. Therefore, we did not use fMRI or MEG somatosensory maps as controls for TMS motor results. One child (2.2 y/o female with TSC-2, see **Figure 5**) underwent subdural grid placement to confirm the epileptogenic focus. In this child, the CSM- and TMS-localized motor cortices showed excellent overlap (**Figure 5B**). None of the other children underwent invasive mapping. We therefore attempt to demonstrate the utility and accuracy of TMS presurgical motor mapping in this cohort through its use in surgical planning and the post-operative results.

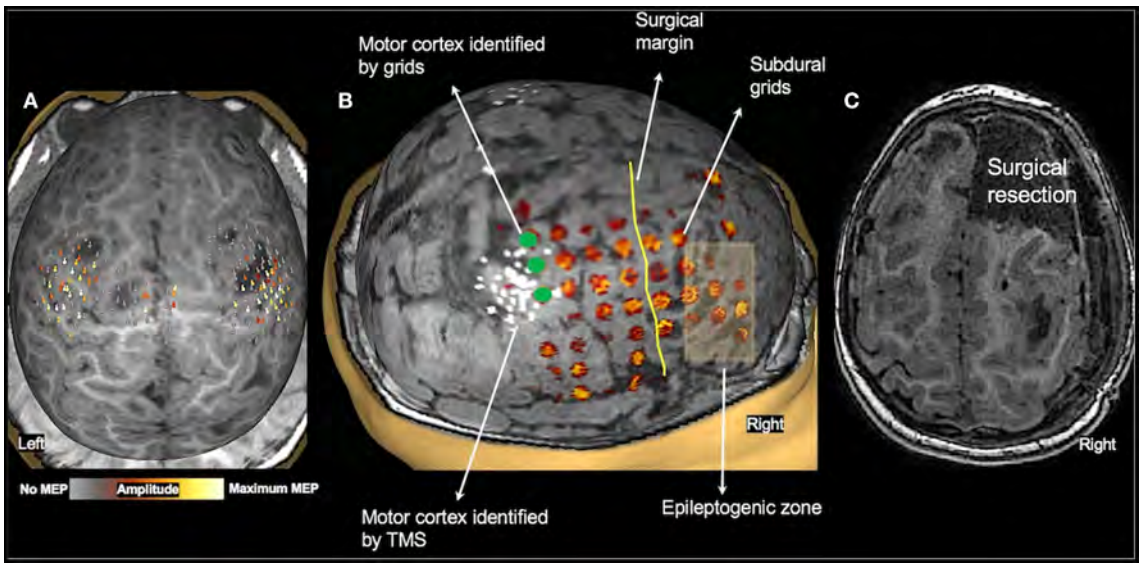

FIGURE 5 | Validation of TMS motor mapping by CSM. Presurgical TMS-derived motor mapping in a 2.3-year-old female with tuberous sclerosis complex type 2. **(A)**: TMS localized motor cortex in the right hemisphere in the precentral gyrus in the vicinity of a tuber. **(B)**: The child underwent subdural grid placement, and the epileptogenic focus was localized to be anterior to the motor cortex. **(C)**: The child underwent right anterior frontal lobectomy including the epileptogenic focus. Post-operatively, the child moves all extremities equally with normal bulk and strength and uses either hand to reach for an object.

Surgical Intervention

Of the children who underwent motor mapping only, many did not proceed to surgery. TMS mapping in these children provided the parents and physicians with information regarding the location of the child's motor cortices and also provided a baseline status of motor development. In children who returned for repeat motor mappings, TMS results were used to track motor function and development over time. Motor mapping was also used to assess the risks and benefits of surgical treatment in 11 children who had lesions in the vicinity of motor cortex. They included 2 children with brain tumor, 6 children with cortical dysplasia, 2 children with TSC-2, and one child with perinatal stroke. In all children who underwent surgery, the MRI with the TMS locations marked was transferred to the surgical navigation system, and the proximity of the anatomical lesion and/or the epileptiform focus to the primary motor cortex identified by TMS was estimated. The children were evaluated clinically at follow up and 7 children were found to have good motor function with no new motor deficits. The child with perinatal stroke, in whom motor representation in the lesioned hemisphere was shown to be reorganized to the intact hemisphere, demonstrated an improvement in preexisting hemiplegia following surgery. One child had slightly decreased movement in the contralateral UE with good muscle bulk, strength, and tone. Two children were found to have mild monoparesis at follow up; in one, the resected cortical dysplasia was within the primary leg motor cortex (**Figure 4A**), and in the other, the frontal lobectomy extended up to the precentral sulcus (**Figure 2A**).

Language Mapping

Patients

The TMS language mapping cohort consisted of eight males and five females with a mean age (± SD) of 5.6 (± 0.3) years, with all children being between 5 and 6 years of age. Eight patients were right-handed, three left-handed, and two ambidextrous. The patients were being evaluated for tumor (n = 7) or refractory epilepsy (n = 6). The causes of refractory seizures were cortical dysplasia (n = 2), tuberous sclerosis complex type 2 (n = 1), perinatal stroke (n = 1), and hippocampal sclerosis (n = 1). The lesion was in the left hemisphere in seven children, in the right hemisphere in four children, bilateral in one child, and no detectable lesion on MRI in one child. Ten children were on AEDs (average 1.4 ± 0.5; range 1–2). The most common AED prescribed was levetiracetam (50%). The details of demographic, clinical, and AED information of the language mapping cohort is listed in **Table 1**.

Mapping Success

The temporal and frontal lobes in both hemispheres were successfully mapped in six of 13 children. In five of the remaining children, bilateral temporal lobes were evaluated, but stimulation of frontal lobe language areas could not be tolerated. In one child, only the left hemisphere frontal lobe around the tumor was mapped. One child could not tolerate TMS stimulation and language mapping was discontinued. Twelve children also successfully completed motor mapping of the upper and lower extremities.

Safety of TMS

We were able to map at least part of the language areas in the two hemispheres in 92% of this cohort, with comprehensive language maps derived in 50% of children. The most common complaint was pain during stimulation. The TMS intensity was reduced when the pain reported on VAS was ≥3. Throughout the mapping procedure, we ensured that the pain score was below 3. No child had a seizure during or after completion of the TMS language study.

TMS Parameters

Eight children were mapped using the color-naming task and five using the object-naming task. The TMS parameters of rate and intensity used in this study were within the guidelines for safety (50). An average of 130 (± 52) trains of 5 Hz stimulation were applied. The TMS intensity was 34 ± 3 % SO (range 25–40% SO), equivalent to an E-field of 91 ± 14 V/m (range 58–107 V/m), measured at a peeling depth of 17 ± 3 mm. The hemisphere with the lesion was stimulated first (LH: 9; RH: 3). Mapping was considered successful if at least one convincing speech error was noted; however, the lowest number of errors noted in any child was six (both hemispheres included). On average, 13% of stimulations resulted in speech errors. Performance error (10 ± 7) was the most common type of speech error noted, followed by speech arrest (4 ± 5), and then semantic errors (2 ± 2). The average total number of errors in the left and right hemispheres were similar (LH: 8.1 ± 6.7; RH: 8.2 ± 7.8). The TMS intensities recorded were not significantly different for the three error types, indicating that the type of speech errors elicited by TMS were independent of TMS intensity. The details of the language mapping TMS parameters are listed in **Table 2**.

Localization of Language Cortices

TMS-elicited speech disruptions were noted following stimulation of the middle and posterior parts of the superior and middle temporal gyri and the supramarginal gyrus in both hemispheres (see **Figures 6**, **7** for examples). Critical language areas identified in the frontal lobe included the ventral premotor cortex, pars opercularis, and pars triangularis (see **Figures 6**, **7**). Across both hemispheres, language areas were primarily localized in the superior temporal lobe (83% of patients), the middle temporal gyrus (68% of patients), and the supramarginal gyrus (64% of patients). Language representation in the inferior frontal gyrus was identified in 94% of children in whom the frontal lobe was stimulated. Based on the localization of language cortices in the frontal and temporal lobes in the two hemispheres by TMS, the LI was estimated in 11 children. Two were deemed LH dominant, seven RH dominant, and two bilaterally dominant for language.

Comparison of TMS Derived Language Maps Against Other Mapping Modalities

Of the 13 patients who had TMS language mapping, 10 underwent MEG receptive language mapping under sedation, of which only three were successful. Of the eight children who underwent fMRI during passive listening under sedation, language cortices in the temporal lobes were successfully localized in only three patients. Because the sedation required for MEG (27) and fMRI (56) in this age group often precludes successful and reliable mapping, and even when successful, mapping primarily consists of receptive language, and the comparison against expressive language maps derived by TMS is not a viable option. None of the children in this group underwent invasive mapping. However, we feel that the utility and accuracy of TMS presurgical mapping in this cohort is best shown by its use in surgical planning and the post-operative results, presented below.

Surgical Intervention

Of the 13 children who underwent speech mapping with TMS, seven children underwent surgery to remove the tumor ($n = 6$) or tuber ($n = 1$). Due to the availability of TMS mapping, none underwent CSM. One child underwent placement of VNS, and the remaining five did not undergo surgery. Of those five, two declined surgery, two were experiencing adequate seizure control with medication management at that time, and one was not a surgical candidate due to non-localizable seizures. TMS mapping allowed neurosurgeons to demonstrate patient-specific functional areas and the proposed surgical approaches to patients' families, allowing both parties to accurately weigh the risks and benefits of proceeding with surgery at that time. Finally, for all children who underwent surgery, the TMS results provided a presurgical baseline of expressive language function which was used for comparison with post-operative language. In these children, the MRI with the TMS locations marked was transferred to the surgical navigation system, and the proximity of the anatomical lesion and/or the epileptiform focus to the language cortices identified by TMS was estimated. Post-operatively, the children were evaluated clinically, and none of the children were found to have speech or language deficits.

DISCUSSION

In this study, we demonstrate, successful localization of motor, speech, and language cortices in young children with refractory epilepsy or brain tumor using TMS. All children were tested in the awake state. Motor cortices were successfully mapped in 90% of children under 3 years of age, with TMS eliciting reliable MEPs and/or CSPs. In this young cohort, we were able to demonstrate normal developmental patterns as well as lesion-dependent cortical reorganization. In pre-school children aged between 5 and 6 years, language areas in the temporal lobes were localized in 92%, while language areas in the frontal lobes were successfully identified in 54%. To the best of our knowledge, this is the largest study reporting mapping of motor cortices in toddlers and language cortices in pre-school children using TMS. The successful TMS in these patients was in part due to the use of MRI-guided TMS and real-time localization of coil position and its orientation with respect to the cortical surface. As shown previously, when directly compared with TMS delivered without MRI guidance, navigated TMS leads to more accurate targeting of cortical areas which in turn results in more significant physiological and behavioral effects in both diagnostic and therapeutic TMS paradigms (57). The use of real-time

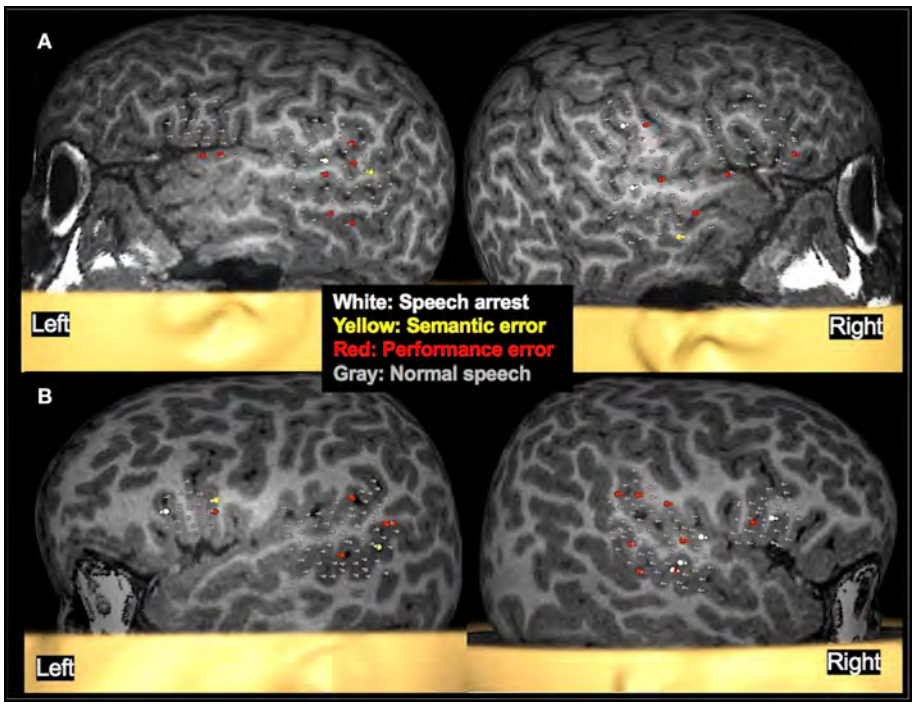

FIGURE 6 | Examples of language mapping with TMS. Speech errors in the form of speech arrest, semantic errors, and performance errors were elicited in both hemispheres. **(A)**: Language mapping with TMS in a 5.6-year-old female with refractory cryptogenic focal epilepsy and asymptomatic cervical and thoracic syringohydromyelia. Her brain MRI was normal. TMS language mapping was completed using a color naming task and showed bilateral dominance for expressive language. **(B)**: Language mapping with TMS in a 5.6-year-old male with right parietal cortical dysplasia that was in the inferior parietal lobule, predominantly superior to the marginal gyrus. TMS language mapping was completed using an object naming task and indicated a right hemisphere dominance for expressive language.

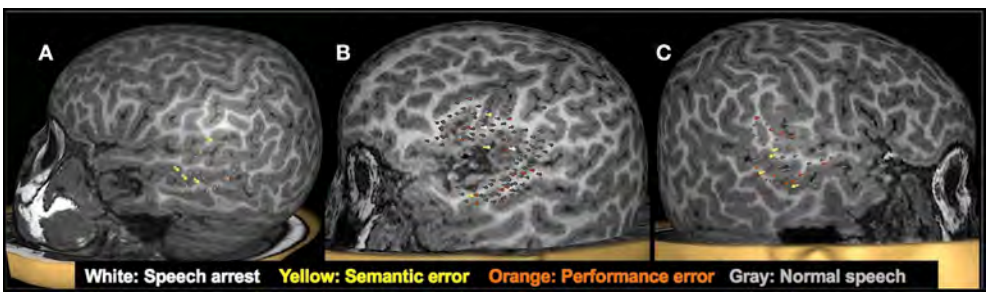

FIGURE 7 | Clinical utility of presurgical TMS-derived language mapping in preschool children with brain tumors. **(A)**: Left hemisphere temporal lobe language mapping in a 5.3-year-old female with recurrent pilomyxoid astrocytoma. She underwent a left temporal microsurgical subtotal (70%) tumor resection. Post-operatively, she had no speech deficits. **(B)**: TMS language map from a 5-year-old male with recurrent left sylvian anaplastic ependymoma. Critical language areas were found around the margin of the tumor. The tumor was resected in full without any postoperative language deficits. **(C)** Right hemisphere temporal lobe language mapping in a 5.9-year-old female with a lesion in the right temporal lobe. Critical language areas were identified in bilateral temporal lobes. She underwent a resection of the right anterior temporal lobe, right amygdala, and hippocampus. The pathology classified the specimen as grade I ganglioglioma and focal cortical dysplasia type IIIb. Post-operatively, she had no speech deficits.

visualization of the location and orientation of the coil along with the modeled E-field further facilitated TMS coil positioning (35).

Successful localization of motor and language cortices was helpful in optimizing risk-benefit evaluation in this population. For instance, TMS findings of bilateral language representation in the pre-school children and demonstration of the absence of motor function in the vicinity of lesions (cortical dysplasia/tumor/epileptogenic focus), respectively, increased confidence in recommending surgery. More importantly, TMS findings facilitated surgical planning aimed at preserving motor and language functions. If data from TMS were not available, the patients would have had CSM with intracranial electrodes. Due to the availability of TMS, the risks associated with placement of intracranial electrodes were avoided and the

children proceeded directly to surgery. Post-operatively, motor function was preserved in most children with only two children having mild, predicted weakness. Language was intact in all seven patients who had surgery for lesions near the language cortices. The data presented here provide preliminary evidence on the utility of presurgical TMS in preserving function and improving outcomes in toddlers and pre-school children with epilepsy or a brain tumor. Our findings add to the emerging evidence on the effectiveness of TMS alone, or in combination with functional mapping methods, in predicting postsurgical outcome in adults and adolescents with epilepsy and brain tumor (8, 11, 14, 47, 58–61). Finally, TMS mapping also provided a baseline to evaluate post-surgical changes in motor, speech, and language function.

Motor Mapping

While TMS motor mapping studies in healthy children as young as 0.2 years have demonstrated that reproducible MEP can be elicited in young children (62, 63), we demonstrate here that similar mapping is feasible in children of this age group with neurological disease. As demonstrated here, it is possible to localize primary hand and leg motor cortices and measure corticomotor latencies by eliciting MEPs and CSPs in hand and leg muscles. In this motor mapping cohort of children under 3 years of age, MEPs were elicited using maximum intensity of TMS, indicating increased activation thresholds in these children. This observation is consistent with previous studies in healthy young children, which have shown that the motor thresholds are high in the first few years of life (64) and remain high up to 10 years of age (65) due to the immature nature of motor system. Additionally, the relatively smaller head sizes and the different conductivity of brain tissues in young children influence the maximum E-field and decay over distance from the coil (36, 37). Another factor that can result in higher stimulation thresholds in this cohort is the presence of AEDs. Here, patients were on an average of 2.7 AEDs (up to 5 AEDs), ranging from sodium channel blockers or stabilizers, γ-aminobutyric acid (GABA) agonists, GABA analogs, and presynaptic calcium channel inhibitors.

One method through which we overcame the drawback of high thresholds to elicit MEP in this cohort, was the use of CSP to localize motor cortex (38, 66). The duration of the CSP is compatible with a long-lasting period of inhibition mediated by GABA receptors (67). The GABAergic interneurons mediating CSPs have lower thresholds than the pyramidal neurons that elicit MEPs (68, 69). Consistent with reports from our group (20, 31) and others (12, 70), in cases where the TMS intensity of $\geq$100% of SO is required to elicit MEPs, CSPs are more easily elicited. Using CSP, we were able to localize the motor cortex as well as assess the degree of inhibitory activity in the motor cortex.

The motor cortex localized by TMS has been validated against CSM-derived motor mapping in persons with a brain tumor (6, 71–73) and epilepsy (12). The mean distance between CSM- and TMS-motor locations were between 2 and 11 mm for hand muscles. Only one study has compared TMS and CSM results in children ($n = 8$; age range 9–17 years) (12). In one child in our cohort, who had subdural grid placement, we found the motor cortex identified by TMS and CSM had excellent agreement (**Figure 5B**). This finding provides preliminary evidence that TMS motor mapping is valid in young children and shows promise for use in children who cannot undergo invasive mapping. In our study, TMS-derived motor mapping informed in surgical planning in 11 children in whom the epileptogenic focus/tumor was in close proximity to the motor cortex. In the majority of these children, MEG and fMRI were unsuccessful and even when successful, these modalities provided information on the somatosensory cortex rather than the motor cortex. The localization of motor cortex helped facilitate the decision to operate and the planning of the surgery, in particular by defining the extent and the margins of the resection (see **Figures 2A**, **5** for examples). It also aided in educating parents regarding the planned surgery and providing reassurance that the motor function would be intact post-operatively.

TMS motor mapping is also useful in characterizing normal motor development in young children with neurological disorders. While TMS stimulation of the motor cortex usually elicited an MEP response in the contralateral muscles, we often observed responses in the ipsilateral muscles as well (see **Figure 3A**), indicative of the immature level of motor development in this age group. During normal development, crossed (contralateral) corticospinal tracts, projected to the spinal cord at birth, strengthen preferentially, and by 2 years of age, uncrossed (ipsilateral) tracts disappear (64). Our results indicate that similar motor developmental trajectory exists in many children with neurological diseases, as in this cohort, we did not observe MEPs in ipsilateral muscles in children older than 2 years with intact motor cortices.

However, we observed persistent ipsilateral MEPs in children with a history of perinatal injury leading to stroke. In such children, we observed robust representation of both upper extremities in the intact hemisphere (see **Figure 4B**). Such interhemispheric reorganization has previously been reported in children who had suffered perinatal brain injury (10, 20, 70, 74, 75), although the functional relevance of such interhemispheric reorganization is yet to be clearly understood. We also observed patterns of reorganization where the hand motor representation was noted in the putative leg area (See **Figure 4A**) or in the premotor cortex. This type of intrahemispheric reorganization was noted in children with cortical dysplasia. Since malformation of cortical development and neuronal migration disorder is observed in cortical dysplasia (76), the neurons destined to the hand motor cortex likely end up at aberrant locations in the same hemisphere. TMS is therefore a vital means to demonstrate the functionality of such dysplastic cortex, since the presence or absence of motor function in the lesion will influence the surgical decision.

Language Mapping

The language cortices in temporal and frontal regions were successfully mapped by TMS in both hemispheres in nine pre-school aged children. Most frequently, TMS identified critical language areas in both hemispheres. Findings of the presence of language cortices in both hemispheres (often R>L) in these children is consistent with previous reports and provides insight into language organization in this age group. For instance, onset

of epilepsy in young children has been shown to adversely affect language development (77, 78). Functional MRI studies have shown that many types of epilepsies alter the trajectory of maturation of language networks. Therefore, greater bilateral activation for language tasks is observed in children with epilepsy when compared to greater engagement of the left hemisphere in typically developing children (79–82). Thus, the bilateral representation and right hemisphere dominance for language in the study cohort, as identified by TMS, most likely represents a combination of ongoing development, false positives (discussed below), and the effects of refractory epilepsy or a brain tumor on the organization of language networks in this young cohort. Similar to our findings here, another recent TMS study has reported receptive language areas in the right hemisphere in children between 6 and 10 years of age with a brain tumor or epilepsy (83).

To date, few studies have compared the accuracy of TMS-derived language maps against regions identified by other invasive and non-invasive mapping methods. Studies comparing language localization by TMS and CSM have demonstrated TMS to have high sensitivity (63–97%), and a negative predictive value (74–99%), but with variable specificity (17–97%) stemming from high rates of false positive errors when compared to CSM (7, 13, 47, 48). But these studies are mainly in adults, and only a small number of children have been included (13, 47). In a small cohort of six patients (age range 14–37 years), we compared the HD estimated by TMS against that from Wada testing (45) and found the overall accuracy of TMS in identifying language in a hemisphere to be 79% with a diagnostic odds ratio of 14, indicating moderate agreement between the two modalities. In a primarily pediatric cohort, we have found that TMS-derived HD had high sensitivity and specificity with an overall accuracy of 80% when compared to non-invasive counterparts, MEG (49) and fMRI (45). Based on these reports, we expect the TMS-derived language mapping to have similar efficacy in this younger cohort as well. Only one other group has reported attempting speech and language mapping in children between 4 and 6 years of age, limited to the lesioned hemisphere (84, 85) and reporting a 40% success rate. Similar to our study, these researchers reduced the SO such that the children were comfortable with stimulation intensity used and the SO ranged from 24 to 36%, corresponding to an E-field of 39–66 V/m.

The findings from TMS language mapping in this cohort were used in surgical planning in seven children in whom the epileptogenic focus or brain tumor was in close proximity to the language cortices. In most cases, MEG and fMRI were unsuccessful, and even when successful, these modalities provided information on the receptive language areas only, as they were performed under sedation. The localization of the language cortex by TMS aided in the surgical decision to operate and in surgical planning, in particular by defining the extent and the margins of the resection. It also helped facilitate discussions with the family regarding the risks of language deficits and the likelihood of preserved language functions post-surgery. Consistent with our expectations, the seven patients had no deficits in language functions following surgery. Finally, TMS language mapping also provided a baseline with which to evaluate post-surgical changes in language function.

This study demonstrates the challenges of language mapping in young children. While, temporal lobe stimulation was well-tolerated, nearly half the children could not endure stimulation of frontal lobe language cortices, despite lower stimulation intensities used in this area. Since the stimulation intensity used for speech and language mapping was well below their UE motor threshold, it is very unlikely that speech errors observed during TMS were due to the stimulation of premotor, Broca's, or primary mouth/laryngeal motor cortices in the frontal lobe. More commonly, we found excessive stimulation of face and jaw muscles with frontal lobe TMS, which often caused discomfort, pain, and/or speech errors. Due to their young age, procedures used in adults to further delineate speech and language errors, such as neurophysiological recordings from laryngeal muscles (86, 87) or accelerometer-based voice onset detection (88), were not feasible. Therefore, we carefully reviewed the mapping session and discarded trials of speech arrest or hesitation observed with apparent discomfort or excessive muscle movement.

Patient compliance was another factor frequently affecting language mapping. Due to their young age, children often could not perform the task consistently, requiring frequent breaks and encouragement from the study team. The use of the color naming task was helpful in many of the children and improved their cooperation. Still, it was often challenging to differentiate TMS induced errors from baseline performance, likely leading to more false positive results than noted in older children and adults (45, 49). Moreover, the decreased compliance precluded extensive surveys of the temporal and especially frontal regions, and therefore, the findings might be biased due to incomplete sampling of critical language areas in this population. Another factor to be cognizant of is the anti-seizure medications taken by children. For example, topiramate and zonisamide have been shown to cause speech difficulties, including problems with word selection and slower response time, in children (89). The unpredictable nature of AED-induced apparent speech errors make analysis challenging both at baseline and during TMS. Finally, the influence of these patient parameters can only be fully deduced when TMS language mapping data in a comparable normative population is available. Despite these challenges, we believe meaningful information was provided by the TMS language mapping.

In addition to the aforementioned patient-related drawbacks, TMS parameters should also be taken into consideration to improve TMS language mapping in children. Key TMS parameters that affect language mapping results include task type, TMS onset relative to stimulus presentation, intensity, coil orientation, and rate. Our previous studies suggest that TMS intensities of 70–100 V/m independent of individual motor threshold (MT) successfully elicited speech errors while minimizing unsuccessful results from either patient discomfort due to too high an intensity or failure to elicit errors due to too low an intensity (45, 49). These findings support not basing TMS intensity on MT, as currently recommended (9), since MT is high in this age group. TMS applied at 100% of an

already high resting MT can be painful due to muscle stimulation and is likely to result in false positive responses. Moreover, we did not find that the stimulation intensity differed across types of speech errors or between hemispheres in each individual. Although we used a color/object-naming task consistently across patients in TMS, data from reported fMRI studies indicate that this task results in bilateral and variable patterns of activation (90, 91), making it impossible to dissociate the effects of task-induced engagement of bilateral language cortices from language reorganization. Therefore, task choice should be prioritized for optimization, with verb generation as a particularly promising task for study, as it is child-friendly, is already implemented in fMRI (92–94), and is suitable for performing during TMS.

TMS inaccuracies also result from issues of non-reproducibility of speech errors and over-reliance on non-specific errors. In our patient cohort, non-specific performance errors were the most common type of error elicited by TMS. However, these errors are more difficult to correctly identify by raters because they can resemble errors made during baseline speech performance. It has been generally assumed that higher TMS rates result in greater disruption of the stimulated region, and consequently in an increased number of specific errors. We used a fixed TMS rate of 5 Hz in all patients, but recent studies have found that rates $\geq$10 Hz resulted in an increased number of speech errors (95), and at 7 Hz, a greater percentage of elicited errors were speech arrests with fewer hesitation errors (96). While these findings suggest that higher rates may be more effective at inducing reliable speech errors, examining these parameters in young children is difficult due to decreases in compliance over time and the need to balance intensity-related discomfort with efficacy. Moreover, in order to allow a wider survey of brain areas while keeping the total number of stimulation within safety guidelines, we fixed the TMS frequency to 5 Hz. Another factor that can influence the error type is the timing of TMS stimulation in relation to the stimulus onset. We time-locked TMS to stimulus onset to ensure adequate coverage of the occipitotemporal or ventral pathway of object recognition (97) and early language processing occurring in the temporal cortex (51). TMS delivered with no delay has also been shown to result in fewer false negative results when compared to CSM (52). However, these findings have been reported in adults, and similar data are not available for young children. Indeed, the visual-language pathways and language-related processes could be delayed and/or longer in young children (98, 99) and therefore the TMS timing relative to the stimulus may have to be adjusted accordingly. Future work should be directed at optimizing the different TMS parameters and developing mapping strategies aimed at improving the accuracy of TMS language mapping in children.

SAFETY OF TMS

In this study, TMS was safely applied in young children with serious epilepsy syndromes. The most common side effect was mild and included local pain and discomfort during language mapping. Motor mapping using single-pulse TMS was usually well-tolerated and experienced by most children as painless. About 20% of the motor mapping cohort experienced seizures during or immediately following TMS. However, the seizures were consistent with their typical semiology and were deemed to not be directly caused by TMS. The occurrence of TMS-related seizures in patients with epilepsy is a known complication (100, 101), and the presence of medically intractable epilepsy has been known to increase the likelihood of a typical seizure occurring during TMS (102). However, in all reports of a seizure during TMS, the patients had their typical seizure followed by their typical recovery course (100, 101). The crude seizure risk for an adult with epilepsy is estimated to be 2.9% (103) to 3.6% (101) for single-, paired-pulse, and rTMS protocols. In our cohort, we performed a total of 60 sessions, with a seizure occurring in 10 of these; though the TMS-related seizure rate appears to be higher than previous reports, it is important to note that unlike other studies, our cohort primarily consisted of young children, and that children have lower seizure thresholds than adults. Furthermore, many conditions identified as associated with increased TMS-induced seizure risk in the TMS safety guidelines (50) were present in this clinical cohort at the time of testing; the patients had refractory epilepsy, were often sleep-deprived and anxious due to stressors associated with inpatient hospitalization, and had temporarily reduced or discontinued their anti-seizure medications for monitoring. Additionally, because this cohort consists of children who, in many cases, were already experiencing multiple seizures per day, the likelihood of seizure while in the TMS exam room was relatively high, regardless of stimulation. For instance, some children had seizures during transportation to the TMS lab or during initial setup before any TMS was applied. By comparing each child's TMS-related seizure timing, semiology, duration, and recovery to the child's own typical seizure, we were able to determine that the majority of seizures occurring during the TMS exams in this cohort were unlikely to be TMS-induced, but rather represent the patient's characteristic seizure pattern. Furthermore, at our institution, all TMS studies are performed in the presence of a nurse with immediate access to rescue medication. None of the children who had a seizure during or following TMS required administration of oxygen or intravenous AEDs. Finally, children's subjective experience of TMS places it in the middle of a spectrum of ordinary childhood experiences (104). Therefore, all available data so far indicate that the use of TMS in children is safe. However, it is recommended that safety precautions be taken during a TMS study in children, including having medical personnel and rescue medications at the ready during mapping. The rate and intensity parameters of TMS should be within the International Federation of Clinical Neurophysiology (IFCN) guidelines for safety (50). Patients should be continuously monitored visually and by EMG for signs of seizures or intracortical spread of excitation.

LIMITATIONS

This study does have some limitations. MEPs were elicited by applied TMS along the precentral gyrus, and due to the

challenges of performing a systematic examination, complete motor mapping was not possible in these young children. However, eliciting MEPs using TMS stimulation confirmed the presence of motor areas along the precentral gyrus. Although three children had only one clear response in each hemisphere, most children had five or more clear MEPs and/or CSPs. The 14% average response rate in this cohort, which was well below the average incidence of responses typically used to define MT (i.e., 50%), reflects the high MT of these children, which likely exceeded maximum SO. As such, even a single clear response in each hemisphere, isolated from background EMG noise and spontaneous activity, was considered representative of the motor cortex. Improvements in coil design to deliver greater E-fields should be considered in future studies to increase the response rate in this population.

The 70 mm figure-of-eight coil used in this study stimulates a large area of cortex under the coil, especially at 100% SO. There is therefore a possibility that MEPs could result from stimulation of the cortical area not directly beneath the coil center, leading to mislocalization. However, in all our patients, at each stimulation site, MEPs were elicited from only one muscle group, indicating that the stimulated area was most likely small. Nevertheless, care should be taken to keep the stimulation more focused, especially when performing pre-operative mapping prior to resection of a dysplasia or cortical neoplasm. With respect to language mapping, all the critical language areas were not surveyed in this young cohort and it is possible that the TMS intensity was too low to elicit reliable speech errors. It is also possible that the still-developing language networks in this young cohort may be less susceptible to lesioning and/or require a higher TMS intensity. The tradeoff between higher TMS intensity and pain during stimulation should be considered on an individual basis. Finally, the study lacks a direct comparison against other invasive and non-invasive mapping methods with respect to its efficacy in presurgical mapping or in predicting postoperative function. Future prospective studies should be designed to address this drawback.

CONCLUSIONS

In summary, we demonstrate the feasibility of using TMS to directly localize the motor, speech, and language systems without using conscious sedation and its utility in presurgical planning in a cohort of young children. We also provide evidence that TMS is well-suited to probe motor, speech, and language pathophysiology and plasticity in young children. Specifically, our data show that TMS can be a useful tool in mapping eloquent cortices in children with epilepsy or brain tumor, both on and off AEDs. Our experience indicates that TMS-derived motor and language maps are helpful in surgical planning, educating parents regarding the planned surgery, and providing a baseline to evaluate post-surgical changes in motor and language functions. Future large-scale studies are needed to confirm the effectiveness and reliability of TMS language mapping in this population.

DATA AVAILABILITY STATEMENT

The data analyzed in this study is subject to the following licenses/restrictions: Clinical data with patient HIPPA information cannot be shared with investigators outside of the institution. Requests to access these datasets should be directed to snaraya2@uthsc.edu.

ETHICS STATEMENT

The studies involving human participants were reviewed and approved by Institutional Regulatory Board, University of Tennessee Health Science Center, Memphis TN. Written informed consent to participate in this study was provided by the participants' legal guardian/next of kin. Written informed consent was obtained from the individual(s), and minor(s)' legal guardian/next of kin, for the publication of any potentially identifiable images or data included in this article.

AUTHOR CONTRIBUTIONS

SN and SG were responsible for the design and conceptualization of the study. SN oversaw the acquisition, analysis, and interpretation of the data and drafted and revised the manuscript. SG acquired and processed TMS data, assimilated clinical and imaging data, and revised the manuscript. SF, AM, BM, SW, FB, and JW oversaw the clinical care of patients and interpreted the clinical and imaging data. All authors provided critical revision of the manuscript for important intellectual content.

REFERENCES

1. Papanicolaou AC, Rezaie R, Narayana S, Choudhri AF, Babajani-Feremi A, Boop FA, et al. On the relative merits of invasive and non-invasive pre-surgical brain mapping: new tools in ablative epilepsy surgery. *Epilepsy Res.* (2018) 142:153–5. doi: 10.1016/j.eplepsyres.2017.07.002
2. Papanicolaou AC, Rezaie R, Narayana S, Choudhri AF, Wheless JW, Castillo EM, et al. Is it time to replace the Wada test and put awake craniotomy to sleep? *Epilepsia.* (2014) 55:629–32. doi: 10.1111/epi.12569
3. Papanicolaou AC, Simos PG, Castillo EM, Breier JI, Sarkari S, Pataraia E, et al. Magnetocephalography: a noninvasive alternative to the Wada procedure. *J Neurosurg.* (2004) 100:867–76. doi: 10.3171/jns.2004.100.5.0867
4. Bookheimer S. Pre-surgical language mapping with functional magnetic resonance imaging. *Neuropsychol Rev.* (2007) 17:145–55. doi: 10.1007/s11065-007-9026-x
5. Szaflarski JP, Gloss D, Binder JR, Gaillard WD, Golby AJ, Holland SK, et al. Practice guideline summary: use of fMRI in the presurgical evaluation of patients with epilepsy: report of the guideline development, dissemination, and implementation subcommittee of the American Academy of Neurology. *Neurology.* (2017) 88:395–402. doi: 10.1212/WNL.0000000000003532
6. Tarapore PE, Tate MC, Findlay AM, Honma SM, Mizuiri D, Berger MS, et al. Preoperative multimodal motor mapping: a comparison of magnetoencephalography imaging, navigated transcranial magnetic stimulation, and direct cortical stimulation. *J Neurosurg.* (2012) 117:354–62. doi: 10.3171/2012.5.JNS112124

7. Tarapore PE, Findlay AM, Honma SM, Mizuiri D, Houde JF, Berger MS, et al. Language mapping with navigated repetitive TMS: proof of technique and validation. *NeuroImage.* (2013) 82:260–72. doi: 10.1016/j.neuroimage.2013.05.018
8. Lefaucheur J-P, Picht T. The value of preoperative functional cortical mapping using navigated TMS. *Neurophysiol Clin.* (2016) 46:125–33. doi: 10.1016/j.neucli.2016.05.001
9. Krieg SM, Lioumis P, Mäkelä JP, Wilenius J, Karhu J, Hannula H, et al. Protocol for motor and language mapping by navigated TMS in patients and healthy volunteers; workshop report. *Acta Neurochir.* (2017) 159:1187–95. doi: 10.1007/s00701-017-3187-z
10. Narayana S, Papanicolaou AC, McGregor A, Boop FA, Wheless JW. Clinical applications of transcranial magnetic stimulation in pediatric neurology. *J Child Neurol.* (2015) 30:1111–24. doi: 10.1177/0883073814553274
11. Vitikainen A, Lioumis P, Paetau R, Salli E, Komssi S, Metsähonkala L, et al. Combined use of non-invasive techniques for improved functional localization for a selected group of epilepsy surgery candidates. *NeuroImage.* (2009) 45:342–8. doi: 10.1016/j.neuroimage.2008.12.026
12. Vitikainen A-M, Salli E, Lioumis P, Mäkelä JP, Metsähonkala L. Applicability of nTMS in locating the motor cortical representation areas in patients with epilepsy. *Acta Neurochir.* (2013) 155:507–18. doi: 10.1007/s00701-012-1609-5
13. Babajani-Feremi A, Narayana S, Rezaie R, Choudhri AF, Fulton SP, Boop FA, et al. Language mapping using high gamma electrocorticography, fMRI, and TMS versus electrocortical stimulation. *Clin Neurophysiol.* (2016) 127:1822–36. doi: 10.1016/j.clinph.2015.11.017
14. Babajani-Feremi A, Holder CM, Narayana S, Fulton SP, Choudhri AF, Boop FA, et al. Predicting postoperative language outcome using presurgical fMRI, MEG, TMS, and high gamma ECoG. *Clin Neurophysiol.* (2018) 129:560–71. doi: 10.1016/j.clinph.2017.12.031
15. Engel Jr. J, Wiebe S, Radhakrishnan K, Palmini A. Surgical treatment for epilepsy. *Neurologisch (Wien).* (2013) 2013:12–4.
16. Ogg RJ, Laningham FH, Clarke D, Einhaus S, Zou P, Tobias ME, et al. Passive range of motion functional magnetic resonance imaging localizing sensorimotor cortex in sedated children: clinical article. *PED.* (2009) 4:317–22. doi: 10.3171/2009.4.PEDS08402
17. Bercovici E, Pang EW, Sharma R, Mohamed IS, Imai K, Fujimoto A, et al. Somatosensory-evoked fields on magnetoencephalography for epilepsy infants younger than 4 years with total intravenous anesthesia. *Clin Neurophysiol.* (2008) 119:1328–34. doi: 10.1016/j.clinph.2008.02.018
18. Lauronen L, Nevalainen P, Pihko E. Magnetoencephalography in neonatology. *Neurophysiol Clin.* (2012) 42:27–34. doi: 10.1016/j.neucli.2011.08.006
19. Birg L, Narayana S, Rezaie R, Papanicolaou A. Technical tips: MEG and EEG with sedation. *Neurodiagnostic J.* (2013) 53:229–40. doi: 10.1080/21646821.2013.11079909
20. Narayana S, Rezaie R, McAfee SS, Choudhri AF, Babajani-Feremi A, Fulton S, et al. Assessing motor function in young children with transcranial magnetic stimulation. *Pediatric Neurol.* (2015) 52:94–103. doi: 10.1016/j.pediatrneurol.2014.08.031
21. Jayakar P. Cortical electrical stimulation mapping: special considerations in children. *J Clin Neurophysiol.* (2018) 35:106–9. doi: 10.1097/WNP.0000000000000451
22. de Ribaupierre S, Fohlen M, Bulteau C, Dorfmüller G, Delalande O, Dulac O, et al. Presurgical language mapping in children with epilepsy: clinical usefulness of functional magnetic resonance imaging for the planning of cortical stimulation: Pediatric Presurgical Language Mapping. *Epilepsia.* (2012) 53:67–78. doi: 10.1111/j.1528-1167.2011.03329.x
23. Arya R, Rutka JT. Pediatric epilepsy surgery: toward increased utilization and reduced invasiveness. *Neurology.* (2018) 90:401–2. doi: 10.1212/WNL.0000000000005036
24. Chou N, Serafini S, Muh CR. Cortical language areas and plasticity in pediatric patients with epilepsy: a review. *Pediatric Neurol.* (2018) 78:3–12. doi: 10.1016/j.pediatrneurol.2017.10.001
25. Schevon CA, Carlson C, Zaroff CM, Weiner HJ, Doyle WK, Miles D, et al. Pediatric language mapping: sensitivity of neurostimulation and wada testing in epilepsy surgery. *Epilepsia.* (2007) 48:539–45. doi: 10.1111/j.1528-1167.2006.00962.x
26. Yerys BE, Jankowski KF, Shook D, Rosenberger LR, Barnes KA, Berl MM, et al. The fMRI success rate of children and adolescents: typical development, epilepsy, attention deficit/hyperactivity disorder, and autism spectrum disorders. *Hum Brain Mapp.* (2009) 30:3426–35. doi: 10.1002/hbm.20767
27. Rezaie R, Narayana S, Schiller K, Birg L, Wheless JW, Boop FA, et al. Assessment of hemispheric dominance for receptive language in pediatric patients under sedation using magnetoencephalography. *Front Human Neurosci.* (2014) 8:657. doi: 10.3389/fnhum.2014.00657
28. Skirrow C, Cross JH, Owens R, Weiss-Croft L, Martin-Sanfilippo P, Banks T, et al. Determinants of IQ outcome after focal epilepsy surgery in childhood: a longitudinal case-control neuroimaging study. *Epilepsia.* (2019) 60:872–84. doi: 10.1111/epi.14707
29. Sherman EMS, Wiebe S, Fay-McClymont TB, Tellez-Zenteno J, Metcalfe A, Hernandez-Ronquillo L, et al. Neuropsychological outcomes after epilepsy surgery: systematic review and pooled estimates: cognitive change after epilepsy surgery. *Epilepsia.* (2011) 52:857–69. doi: 10.1111/j.1528-1167.2011.03022.x
30. Tieleman A, Deblaere K, Van Roost D, Van Damme O, Achten E. Preoperative fMRI in tumour surgery. *Eur Radiol.* (2009) 19:2523–34. doi: 10.1007/s00330-009-1429-z
31. Narayana S, Mudigoudar B, Babajani-Feremi A, Choudhri AF, Boop FA. Successful motor mapping with transcranial magnetic stimulation in an infant: a case report. *Neurology.* (2017) 89:2115–7. doi: 10.1212/WNL.0000000000004650
32. Narayana S, Embury LM, Shah N, Weatherspoon S, Choudhri AF, Boop FA. Noninvasive localization of language cortex in an awake 4-year-old child with rasmussen encephalitis: a case report. *Operative Neurosurg.* (2020) 18:E175–80. doi: 10.1093/ons/opz202
33. Gaillard WD, Jette N, Arnold ST, Arzimanoglou A, Braun KPJ, Cukiert A, et al. Establishing criteria for pediatric epilepsy surgery center levels of care: report from the ILAE pediatric epilepsy surgery task force. *Epilepsia.* (2020) 61:2629–42. doi: 10.1111/epi.16698
34. *Navigated Brain Stimulation System 5.0, User Manual*. Helsinki: Nexstim Plc. (2019).
35. Ruohonen J, Karhu J. Navigated transcranial magnetic stimulation. *Neurophysiol Clin.* (2010) 40:7–17. doi: 10.1016/j.neucli.2010.01.006
36. Garvey MA, Mall V. Transcranial magnetic stimulation in children. *Clin Neurophysiol.* (2008) 119:973–84. doi: 10.1016/j.clinph.2007.11.048
37. Cvetković M, Poljak D, Rogić Vidaković M, Đ*ogaš Z. Transcranial magnetic stimulation induced fields in different brain models. *J Electromagnetic Waves Applic.* (2016) 30:1820–35. doi: 10.1080/09205071.2016.1216807
38. Wolters A, Ziemann U, Benecke R. The cortical silent period. In: Wassermann EM, Epstein CM, Ziemann U, Walsh V, Paus T, Lisanby SH, editors. *The Oxford Handbook of Transcranial Stimulation*. New York, NY: Oxford University Press (2011). p. 91–102. doi: 10.1093/oxfordhb/9780198568926.013.0010
39. Kobayashi M, Pascual-Leone A. Transcranial magnetic stimulation in neurology. *Lancet Neurol.* (2003) 2:145–56. doi: 10.1016/S1474-4422(03)00321-1
40. Rossini PM, Burke D, Chen R, Cohen LG, Daskalakis Z, Di Iorio R, et al. Non-invasive electrical and magnetic stimulation of the brain, spinal cord, roots and peripheral nerves: Basic principles and procedures for routine clinical and research application. an updated report from an I.F.C.N. committee. *Clin Neurophysiol.* (2015) 126:1071–107. doi: 10.1016/j.clinph.2015.02.001
41. Cincotta M, Giovannelli F, Borgheresi A, Tramacere L, Viggiano MP, Zaccara G. A meta-analysis of the cortical silent period in epilepsies. *Brain Stimul.* (2015) 8:693–701. doi: 10.1016/j.brs.2015.04.008
42. de Goede AA, ter Braack EM, van Putten MJAM. Single and paired pulse transcranial magnetic stimulation in drug naïve epilepsy. *Clin Neurophysiol.* (2016) 127:3140–55. doi: 10.1016/j.clinph.2016.06.025
43. Tataroglu C, Ozkiziltan S, Baklan B. Motor cortical thresholds and cortical silent periods in epilepsy. *Seizure.* (2004) 13:481–5. doi: 10.1016/j.seizure.2003.11.003
44. Pascual-Leone A. Transcranial magnetic stimulation in cognitive neuroscience - virtual lesion, chronometry, and functional connectivity. *Curr Opinion Neurobiol.* (2000) 10:232–7. doi: 10.1016/S0959-4388(00)00081-7

45. Schiller K, Choudhri AF, Jones T, Holder C, Wheless JW, Narayana S. Concordance between transcranial magnetic stimulation and functional Magnetic Resonance Imaging (MRI) derived localization of language in a clinical cohort. *J Child Neurol.* (2020) 35:363–79. doi: 10.1177/0883073820901415
46. Snodgrass JG, Vanderwart M. A standardized set of 260 pictures. norms for name agreement, image agreement, familiarity, and visual complexity. *J Exp Psychol.* (1980) 6:174–215. doi: 10.1037/0278-7393.6.2.174-
47. Lehtinen H, Mäkelä JP, Mäkelä T, Lioumis P, Metsähonkala L, Hokkanen L, et al. Language mapping with navigated transcranial magnetic stimulation in pediatric and adult patients undergoing epilepsy surgery: comparison with extraoperative direct cortical stimulation. *Epilepsia Open.* (2018) 3:224–35. doi: 10.1002/epi4.12110
48. Picht T, Krieg SM, Sollmann N, Rösler J, Niraula B, Neuvonen T, et al. A comparison of language mapping by preoperative navigated transcranial magnetic stimulation and direct cortical stimulation during awake surgery. *Neurosurgery*. (2013) 72:808–19. doi: 10.1227/NEU.0b013e3182889e01
49. Rezaie R, Schiller KK, Embury L, Boop FA, Wheless JW, Narayana S. The clinical utility of transcranial magnetic stimulation in determining hemispheric dominance for language: a magnetoencephalography comparison study. *J Clin Neurophysiol.* (2020) 37:90–103. doi: 10.1097/WNP.0000000000000499
50. Rossi S, Antal A, Bestmann S, Bikson M, Brewer C, Brockmöller J, et al. Safety and recommendations for TMS use in healthy subjects and patient populations, with updates on training, ethical and regulatory issues: expert guidelines. *Clin Neurophysiol.* (2020) 132:269–306. doi: 10.1016/j.clinph.2020.10.003
51. Papanicolaou AC, Kilintari M, Rezaie R, Narayana S, Babajani-Feremi A. The role of the primary sensory cortices in early language processing. *J Cogn Neurosci.* (2017) 29:1755–65. doi: 10.1162/jocn_a_01147
52. Krieg SM, Tarapore PE, Picht T, Tanigawa N, Houde J, Sollmann N, et al. Optimal timing of pulse onset for language mapping with navigated repetitive transcranial magnetic stimulation. *NeuroImage.* (2014) 100:219–36. doi: 10.1016/j.neuroimage.2014.06.016
53. Corina DP, Loudermilk BC, Detwiler L, Martin RF, Brinkley JF, Ojemann G. Analysis of naming errors during cortical stimulation mapping: implications for models of language representation. *Brain Lang.* (2010) 115:101–12. doi: 10.1016/j.bandl.2010.04.001
54. Springer JA, Binder JR, Hammeke TA, Swanson SJ, Frost JA, Bellgowan PSF, et al. Language dominance in neurologically normal and epilepsy subjects. *Brain.* (1999) 122:2033–46. doi: 10.1093/brain/122.11.2033
55. Seghier ML. Laterality index in functional MRI: methodological issues. *Magn Reson Imaging.* (2008) 26:594–601. doi: 10.1016/j.mri.2007.10.010-
56. Guerin JB, Greiner HM, Mangano FT, Leach JL. Functional MRI in children: current clinical applications. *Semin Pediatr Neurol.* (2020) 33:100800. doi: 10.1016/j.spen.2020.100800
57. Bashir S, Vernet M, Najib U, Perez J, Alonso-Alonso M, Knobel M, et al. Enhanced motor function and neurophysiological correlates with navigated low-frequency repetitive transcranial magnetic stimulation over the contralesional motor cortex in stroke. *Brain Stimul.* (2015) 8:319–20. doi: 10.1016/j.brs.2015.01.037
58. Picht T, Frey D, Thieme S, Kliesch S, Vajkoczy P. Presurgical navigated TMS motor cortex mapping improves outcome in glioblastoma surgery: a controlled observational study. *J Neurooncol.* (2016) 126:535–43. doi: 10.1007/s11060-015-1993-9
59. Krieg SM, Picht T, Sollmann N, Bährend I, Ringel F, Nagarajan SS, et al. Resection of motor eloquent metastases aided by preoperative nTMS-Based motor maps-comparison of two observational cohorts. *Front Oncol.* (2016) 6:261. doi: 10.3389/fonc.2016.00261
60. Benjamin CFA, Li AX, Blumenfeld H, Constable RT, Alkawadri R, Bickel S, et al. Presurgical language fMRI: clinical practices and patient outcomes in epilepsy surgical planning. *Human Brain Mapping.* (2018) 39:2777–85. doi: 10.1002/hbm.24039
61. Sollmann N, Ille S, Hauck T, Maurer S, Negwer C, Zimmer C, et al. The impact of preoperative language mapping by repetitive navigated transcranial magnetic stimulation on the clinical course of brain tumor patients. *BMC Cancer.* (2015) 15:261. doi: 10.1186/s12885-015-1299-5
62. Nezu A, Kimura S, Uehara S, Kobayashia T, Tanaka M, Saito K. Magnetic stimulation of motor cortex in children: maturity of corticospinal pathway and problem of clinical application. *Brain Dev.* (1997) 19:176–80. doi: 10.1016/S0387-7604(96)00552-9
63. Fietzek UM, Heinen F, Berweck S, Maute S, Hufschmidt A, Schulte-Mönting J, et al. Development of the corticospinal system and hand motor function: central conduction times and motor performance tests. *Dev Med Child Neurol.* (2000) 42:220–7. doi: 10.1017/S0012162200000384
64. Eyre JA, Taylor JP, Villagra F, Smith M, Miller S. Evidence of activity-dependent withdrawal of corticospinal projections during human development. *Neurology.* (2001) 57:1543–54. doi: 10.1212/WNL.57.9.1543
65. Garvey MA, Ziemann U, Bartko JJ, Denckla MB, Barker CA, Wassermann EM. Cortical correlates of neuromotor development in healthy children. *Clin Neurophysiol.* (2003) 114:1662–70. doi: 10.1016/S1388-2457(03)00130-5
66. Cantello R, Gianelli M, Civardi C, Mutani R. Magnetic brain stimulation: the silent period after the motor evoked potential. *Neurology.* (1992) 42:1951–9. doi: 10.1212/WNL.42.10.1951
67. Connors B, Malenka R, Silva L. Two inhibitory postsynaptic potentials, and GABAA and GABAB receptor-mediated responses in neocortex of rat and cat. *J Physiol.* (1988) 406:443–68. doi: 10.1113/jphysiol.1988.sp017390
68. Rábago CA, Lancaster JL, Narayana S, Zhang W, Fox PT. Automated-parameterization of the motor evoked potential and cortical silent period induced by transcranial magnetic stimulation. *Clin Neurophysiol.* (2009) 120:1577–87. doi: 10.1016/j.clinph.2009.04.020
69. Narayana S, Rábago CA, Zhang W, Strickland C, Franklin C, Fox PT, et al. Thresholds and locations of excitation and inhibition in primary motor cortex: evidence from electromyography and imaging. *Soc Neurosci.* (2010).
70. Mäkelä JP, Vitikainen A-M, Lioumis P, Paetau R, Ahtola E, Kuusela L, et al. Functional plasticity of the motor cortical structures demonstrated by navigated TMS in two patients with epilepsy. *Brain Stimul.* (2013) 6:286–91. doi: 10.1016/j.brs.2012.04.012
71. Picht T, Schmidt S, Brandt S, Frey D, Hannula H, Neuvonen T, et al. Preoperative functional mapping for rolandic brain tumor surgery: comparison of navigated transcranial magnetic stimulation to direct cortical stimulation. *Neurosurgery.* (2011) 69:581–9. doi: 10.1227/NEU.0b013e3182181b89
72. Forster M-T, Hattingen E, Senft C, Gasser T, Seifert V, Szelényi A. Navigated transcranial magnetic stimulation and functional magnetic resonance imaging: advanced adjuncts in preoperative planning for central region tumors. *Neurosurgery.* (2011) 68:1317–25. doi: 10.1227/NEU.0b013e31820b528c
73. Krieg SM, Shiban E, Buchmann N, Gempt J, Foerschler A, Meyer B, et al. Utility of presurgical navigated transcranial magnetic brain stimulation for the resection of tumors in eloquent motor areas: clinical article. *JNS.* (2012) 116:994–1001. doi: 10.3171/2011.12.JNS111524
74. Staudt M, Grodd W, Gerloff C, Erb M, Jutta S, KraÈgeloh-Mann I. Two types of ipsilateral reorganization in congenital hemiparesis: a TMS and fMRI study. *Brain.* (2002) 125:2222–37. doi: 10.1093/brain/awf227
75. Staudt M. Brain plasticity following early life brain injury: insights from neuroimaging. *Semin Perinatol.* (2010) 34:87–92. doi: 10.1053/j.semperi.2009.10.009
76. Kabat J, Król P. Focal cortical dysplasia - review. *Polish J Radiol.* (2012) 77:35–43. doi: 10.12659/PJR.882968
77. Baumer FM, Cardon AL, Porter BE. Language dysfunction in pediatric epilepsy. *J Pediatrics.* (2018) 194:13–21. doi: 10.1016/j.jpeds.2017.10.031
78. Ibrahim GM, Morgan BR, Doesburg SM, Taylor MJ, Pang EW, Donner E, et al. Atypical language laterality is associated with large-scale disruption of network integration in children with intractable focal epilepsy. *Cortex.* (2015) 65:83–8. doi: 10.1016/j.cortex.2014.12.016
79. Lillywhite LM, Saling MM, Simon Harvey A, Abbott DF, Archer JS, Vears DF, et al. Neuropsychological and functional MRI studies provide converging evidence of anterior language dysfunction in BECTS. *Epilepsia.* (2009) 50:2276–84. doi: 10.1111/j.1528-1167.2009.02065.x
80. Datta AN, Oser N, Bauder F, Maier O, Martin F, Ramelli GP, et al. Cognitive impairment and cortical reorganization in children with benign epilepsy with centrotemporal spikes. *Epilepsia.* (2013) 54:487–94. doi: 10.1111/epi.12067
81. Vannest J, Szaflarski JP, Eaton KP, Henkel DM, Morita D, Glauser TA, et al. Functional magnetic resonance imaging reveals changes in language

localization in children with benign childhood epilepsy with centrotemporal spikes. *J Child Neurol.* (2013) 28:435–45. doi: 10.1177/0883073812447682
82. You X, Adjouadi M, Guillen MR, Ayala M, Barreto A, Rishe N, et al. Sub-patterns of language network reorganization in pediatric localization related epilepsy: a multisite study. *Hum Brain Mapp.* (2011) 32:784–99. doi: 10.1002/hbm.21066
83. Rejnö-Habte Selassie G, Pegenius G, Karlsson T, Viggedal G, Hallböök T, Elam M. Cortical mapping of receptive language processing in children using navigated transcranial magnetic stimulation. *Epilepsy Behav.* (2020) 103:106836. doi: 10.1016/j.yebeh.2019.106836
84. Rosenstock T, Picht T, Schneider H, Koch A, Thomale U-W. Left perisylvian tumor surgery aided by TMS language mapping in a 6-year-old boy: case report. *Child's Nerv Syst.* (2019) 35:175–81. doi: 10.1007/s00381-018-3944-1
85. Rosenstock T, Picht T, Schneider H, Vajkoczy P, Thomale U-W. Pediatric navigated transcranial magnetic stimulation motor and language mapping combined with diffusion tensor imaging tractography: clinical experience. *J Neurosurg.* (2020) 26:583–93. doi: 10.3171/2020.4.PEDS20174
86. Rogić M, Deletis V, Fernández-Conejero I. Inducing transient language disruptions by mapping of Broca's area with modified patterned repetitive transcranial magnetic stimulation protocol: clinical article. *JNS.* (2014) 120:1033–41. doi: 10.3171/2013.11.JNS13952
87. Rogić Vidaković M, Jerković A, Jurić T, Vujović I, Šoda J, Erceg N, et al. Neurophysiologic markers of primary motor cortex for laryngeal muscles and premotor cortex in caudal opercular part of inferior frontal gyrus investigated in motor speech disorder: a navigated transcranial magnetic stimulation (TMS) study. *Cognitive Process.* (2016) 17:429–42. doi: 10.1007/s10339-016-0766-5
88. Vitikainen A-M, Mäkelä E, Lioumis P, Jousmäki V, Mäkelä JP. Accelerometer-based automatic voice onset detection in speech mapping with navigated repetitive transcranial magnetic stimulation. *J Neurosci Methods.* (2015) 253:70–7. doi: 10.1016/j.jneumeth.2015.05.015
89. Kim SJ, Kim MY, Choi YM, Song MK. Effects of topiramate on language functions in newly diagnosed pediatric epileptic patients. *Pediatric Neurol.* (2014) 51:324–9. doi: 10.1016/j.pediatrneurol.2014.05.033
90. Rösler J, Niraula B, Strack V, Zdunczyk A, Schilt S, Savolainen P, et al. Language mapping in healthy volunteers and brain tumor patients with a novel navigated TMS system: Evidence of tumor-induced plasticity. *Clin Neurophysiol.* (2014) 125:526–36. doi: 10.1016/j.clinph.2013.08.015
91. Sollmann N, Tanigawa N, Ringel F, Zimmer C, Meyer B, Krieg SM. Language and its right-hemispheric distribution in healthy brains: an investigation by repetitive transcranial magnetic stimulation. *NeuroImage.* (2014) 102:776–88. doi: 10.1016/j.neuroimage.2014.09.002
92. Holland SK, Plante E, Weber Byars A, Strawsburg RH, Schmithorst VJ, Ball WS. Normal fMRI brain activation patterns in children performing a verb generation task. *NeuroImage.* (2001) 14:837–43. doi: 10.1006/nimg.2001.0875
93. Szaflarski JP, Holland SK, Schmithorst VJ, Byars AW. fMRI study of language lateralization in children and adults. *Hum Brain Mapp.* (2006) 27:202–12. doi: 10.1002/hbm.20177-
94. Szaflarski JP, Schmithorst VJ, Altaye M, Byars AW, Ret J, Plante E, et al. A longitudinal functional magnetic resonance imaging study of language development in children 5 to 11 years old. *Ann Neurol.* (2006) 59:796–807. doi: 10.1002/ana.20817
95. Sollmann N, Ille S, Obermueller T, Negwer C, Ringel F, Meyer B, et al. The impact of repetitive navigated transcranial magnetic stimulation coil positioning and stimulation parameters on human language function. *Eur J Med Res.* (2015) 20:47. doi: 10.1186/s40001-015-0155-z
96. Hauck T, Tanigawa N, Probst M, Wohlschlaeger A, Ille S, Sollmann N, et al. Stimulation frequency determines the distribution of language positive cortical regions during navigated transcranial magnetic brain stimulation. *BMC Neurosci.* (2015) 16:5. doi: 10.1186/s12868-015-0143-9
97. Ungerleider LG, Pasternak T. Ventral and dorsal cortical processing streams. In: Chalupa L, Werner J, editors. *The Visual Neurosciences*. Cambridge, MA: MIT Press (2004). p. 541–62.
98. D'Amico S, Devescovi A, Bates E. Picture naming and lexical access in italian children and adults. *J Cogn Dev.* (2001) 2:71–105. doi: 10.1207/S15327647JCD0201_4
99. Cycowicz YM, Friedman D, Rothstein M, Snodgrass JG. Picture naming by young children: norms for name agreement, familiarity, and visual complexity. *J Exp Child Psychol.* (1997) 65:171–237. doi: 10.1006/jecp.1996.2356
100. Bae EH, Schrader LM, Machii K, Alonso-Alonso M, Riviello JJ, Pascual-Leone A, et al. Safety and tolerability of repetitive transcranial magnetic stimulation in patients with epilepsy: a review of the literature. *Epilepsy Behav.* (2007) 10:521–8. doi: 10.1016/j.yebeh.2007.03.004
101. Schrader LM, Stern JM, Koski L, Nuwer MR, Engel J. Seizure incidence during single- and paired-pulse transcranial magnetic stimulation (TMS) in individuals with epilepsy. *Clin Neurophysiol.* (2004) 115:2728–37. doi: 10.1016/j.clinph.2004.06.018
102. Lerner AJ, Wassermann EM, Tamir DI. Seizures from transcranial magnetic stimulation 2012-2016: results of a survey of active laboratories and clinics. *Clin Neurophysiol.* (2019) 130:1409–16. doi: 10.1016/j.clinph.2019.03.016
103. Pereira LS, Müller VT, da Mota Gomes M, Rotenberg A, Fregni F. Safety of repetitive transcranial magnetic stimulation in patients with epilepsy: a systematic review. *Epilepsy Behav.* (2016) 57:167–76. doi: 10.1016/j.yebeh.2016.01.015
104. Garvey MA, Kaczynski KJ, Becker DA, Bartko JJ. Subjective reactions of children to single-pulse transcranial magnetic stimulation. *J Child Neurol.* (2001) 16:891–4. doi: 10.1177/088307380101601205

Conflict of Interest: The authors declare that the research was conducted in the absence of any commercial or financial relationships that could be construed as a potential conflict of interest.

frontiers in Oncology

ORIGINAL RESEARCH
published: 21 May 2021
doi: 10.3389/fonc.2021.676626

Preoperative nTMS and Intraoperative Neurophysiology - A Comparative Analysis in Patients With Motor-Eloquent Glioma

Tizian Rosenstock[1,2], Mehmet Salih Tuncer[1], Max Richard Münch[1], Peter Vajkoczy[1], Thomas Picht[1,3] and Katharina Faust[1]*

[1] Department of Neurosurgery, Charité – Universitätsmedizin Berlin, corporate member of Freie Universität Berlin and Humboldt-Universität zu Berlin, Berlin, Germany, [2] Berlin Institute of Health at Charité – Universitätsmedizin Berlin, Biomedical Innovation Academy, Berlin, Germany, [3] Cluster of Excellence: "Matters of Activity. Image Space Material", Humboldt University, Berlin, Germany

OPEN ACCESS

Edited by:
Marcos Vinicius Calfat Maldaun, Hospital Sirio Libanes, Brazil

Reviewed by:
Nico Sollmann, University of Munich, Germany
Jyrki Mäkelä, Hospital District of Helsinki and Uusimaa, Finland
Silvia Mazzali Verst, Hospital Sirio Libanes, Brazil

***Correspondence:**
Tizian Rosenstock
tizian.rosenstock@charite.de

Specialty section:
This article was submitted to Neuro-Oncology and Neurosurgical Oncology, a section of the journal Frontiers in Oncology

Received: *05 March 2021*
Accepted: *23 April 2021*
Published: *21 May 2021*

Citation:
Rosenstock T, Tuncer MS, Münch MR, Vajkoczy P, Picht T and Faust K (2021) Preoperative nTMS and Intraoperative Neurophysiology - A Comparative Analysis in Patients With Motor-Eloquent Glioma. Front. Oncol. 11:676626. doi: 10.3389/fonc.2021.676626

Background: The resection of a motor-eloquent glioma should be guided by intraoperative neurophysiological monitoring (IOM) but its interpretation is often difficult and may (unnecessarily) lead to subtotal resection. Navigated transcranial magnetic stimulation (nTMS) combined with diffusion-tensor-imaging (DTI) is able to stratify patients with motor-eloquent lesion preoperatively into high- and low-risk cases with respect to a new motor deficit.

Objective: To analyze to what extent preoperative nTMS motor risk stratification can improve the interpretation of IOM phenomena.

Methods: In this monocentric observational study, nTMS motor mapping with DTI fiber tracking of the corticospinal tract was performed before IOM-guided surgery for motor-eloquent gliomas in a prospectively collected cohort from January 2017 to October 2020. Descriptive analyses were performed considering nTMS data (motor cortex infiltration, resting motor threshold (RMT), motor evoked potential (MEP) amplitude, latency) and IOM data (transcranial MEP monitoring, intensity of monopolar subcortical stimulation (SCS), somatosensory evoked potentials) to examine the association with the postoperative motor outcome (assessed at day of discharge and at 3 months).

Results: Thirty-seven (56.1%) of 66 patients (27 female) with a median age of 48 years had tumors located in the right hemisphere, with glioblastoma being the most common diagnosis with 39 cases (59.1%). Three patients (4.9%) had a new motor deficit that recovered partially within 3 months and 6 patients had a persistent deterioration (9.8%). The more risk factors of the nTMS risk stratification model (motor cortex infiltration, tumor-tract distance (TTD) ≤8mm, RMT_{ratio} <90%/>110%) were detected, the higher was the risk for developing a new postoperative motor deficit, whereas no patient with a TTD >8mm deteriorated. Irreversible MEP amplitude decrease >50% was associated with worse motor outcome in all patients, while a MEP amplitude decrease ≤50% or lower SCS

intensities ≤4mA were particularly correlated with a postoperative worsened motor status in nTMS-stratified high-risk cases. No patient had postoperative deterioration of motor function (except one with partial recovery) when intraoperative MEPs remained stable or showed only reversible alterations.

Conclusions: The preoperative nTMS-based risk assessment can help to interpret ambiguous IOM phenomena (such as irreversible MEP amplitude decrease ≤50%) and adjustment of SCS stimulation intensity.

Keywords: navigated transcranial magnetic stimulation (nTMS), brain tumor surgery, glioma, motor outcome, diffusion tensor imaging, intraoperative neurophysiological monitoring (IOM), motor-evoked potential (MEP), subcortical stimulation

INTRODUCTION

When resecting a glioma, a gross total resection (GTR) is always aimed for since the extent of resection (EOR) is positively correlated with (progression free) survival (1, 2). A large multicenter trial demonstrated a benefit of supramarginal resections (= resection of both contrast-enhanced and noncontrast-enhanced tumor parts) especially for patients with Isocitrate dehydrogenase (IDH)-wild-type glioblastoma (3). However, it is important to note that patients with eloquently located brain lesions require careful consideration of tumor resection versus functional preservation, as new functional deficits lead not only to reduced quality of life but also to reduced survival (4).

The gold standard for surgical treatment of motor-eloquent brain lesions is resection guided by intraoperative neurophysiological monitoring (IOM) (5). Yet, different techniques, stimulation intensities, concepts, and warning signs can be found in the literature, making interpretation of IOM phenomena difficult (6, 7). In addition, there are reports of false-positive and false-negative monitoring phenomena affecting intraoperative motor outcome prediction as well (8–10). Navigated transcranial magnetic stimulation (nTMS) has been established as a reliable preoperative motor mapping method with very high concordance to direct cortical stimulation (11, 12). A meta-analysis demonstrated the clinical benefit of nTMS motor mapping and showed improvement in motor outcome and extent of resection (13). We developed a risk stratification model based on nTMS and tractography data with which patients with motor-eloquent tumor can be used to stratify into low and high-risk cases (14). High-risk cases (with higher likelihood of postoperative motor deterioration) are characterized by 3 risk parameters: 1.) nTMS-verified motor cortex infiltration, 2.) tumor distance to the diffusion tensor imaging (DTI)-derived corticospinal tract (CST) ≤8mm or 3.) a ratio <90%/>110% of the resting motor threshold (RMT) of both hemispheres (indicating individual and interhemispheric excitability).

A comparison between preoperative nTMS motor mapping/tractography and phenomena of IOM has not been done so far. One can hypothesize that preoperative nTMS assessment can support the interpretation of ambiguous IOM changes (such as reversible MEP amplitude alterations or irreversible MEP amplitude decrease ≤50%) that might be examined more meticulously and carefully in high-risk cases. The aim of this study was to investigate the extent to which preoperative nTMS motor risk stratification and diffusion analysis can help relate ambiguous IOM phenomena to surgical outcome and therefore improve IOM interpretation.

MATERIALS AND METHODS

Study Design

Retrospective analysis of a prospectively collected cohort from 01/2017 to 10/2020 was performed in accordance with the STROBE-Guidelines (15) and the ethical standards of the Declaration of Helsinki. The Ethics Commission approved the study (#EA1/016/19) and the patients provided written informed consent. Our workflow is exemplarily shown in **Figure 1**.

Patients

Sixty-six patients (age ≥ 18 years) with a motor-eloquent glioma (affecting the motor cortex and/or the CST) who received preoperative nTMS motor mapping and underwent IOM-guided resection were included. Intracranial implants are exemplary contraindications for nTMS (16), however no patient had to be excluded. Patient characteristics such as age, sex and the Karnofsky Performance Scale (17) were assessed in a purpose made database. The motor status was assessed preoperatively, on the day of discharge and after 3 months by the attending neurosurgeon according to the British Medical Research Council [BMRC]) (18) (a scale ranging between 0-5 where BMRC grade 5 represents full strength and 0 representing no muscle activation). The motor outcome was defined as worsened or not worsened, with motor worsening defined as decreased postoperative muscle strength compared with preoperative status. Tumor grading (according to WHO classification of 2016) was performed by the department of neuropathology (19).

MR Imaging

The MRI scans were performed on a 3 Tesla MRI scanner (Siemens 3T Skyra system, Erlangen, Germany), with technical details published elsewhere (20). A contrast-enhanced 3D

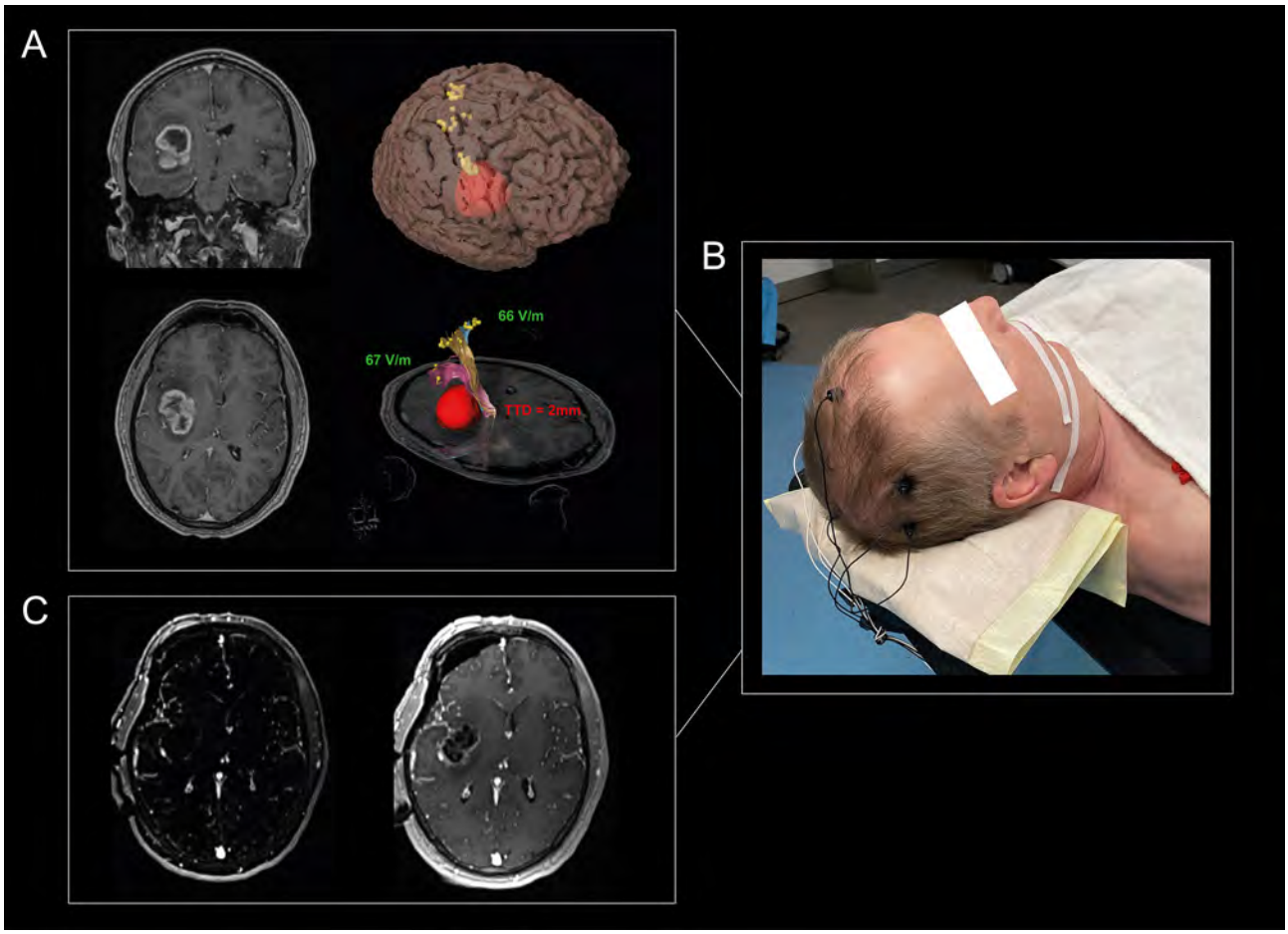

FIGURE 1 | Visualization of our workflow. A 65-year-old man suffered from headache and personality changes. Cerebral MRI showed an insular, contrast-enhancing tumor in the right hemisphere **(A)**. An nTMS motor mapping was performed for the upper extremity, lower extremity, and facial muscles to define the individual cortical motor representation and to investigate the individual excitability level of the patients, which showed a normal RMT_{ratio} between 90% and 110%. Standardized nTMS-based tractography revealed a TTD of 2 mm, so that a total of 1 of 3 risk factors was detectable. Tumor resection was performed using MEPs, SSEPs, and SCS, with SCS guided by the mapping suction probe at a minimum intensity of 2mA. The MEPs showed changes two times, so resection was paused each time and irrigated with papaverine until the MEPs recovered **(B)**. MRI resection control showed a good result with no evidence of residual tumor **(C)**. The patient did not suffer a new motor deficit.

gradient echo sequence with a slice thickness of 1mm was used as reference sequence for the nTMS mapping. Preoperative tumor volume was calculated by tumor segmentation with the clinical planning software Elements (Brainlab AG, Munich, Germany) using the T1-weighted sequences with contrast agent in contrast-enhanced tumors and fluid-attenuated inversion recovery (FLAIR) sequences in cases without contrast enhancement. In each patient, DTI sequences were acquired for fiber tracking and analysis of diffusion tensor-based metrics (2-mm isotropic resolution; TR/TE 7500/95ms; 1 shell b-value = 1300 s/mm^2 with 60 directions per shell) with details published previously (20). The postoperative MRI scan (acquired within 72h postoperatively) was carefully evaluated for ischemia and residual tumor tissue by an interdisciplinary board of neurosurgeons and neuroradiologists based on diffusion weighted imaging (DWI) sequences for ischemia, subtraction sequences (T1 with contrast agent subtracted by T1) for contrast agent enhancing tumors or otherwise based on the FLAIR sequence. The EOR was defined as follows: GTR: complete removal, subtotal resection: residual tumor volume ≤ 15ml and partial resection: > 15ml (21).

nTMS Mapping

An nTMS motor mapping (NBS 5.1; Nexstim, Helsinki, Finland) was performed in all patients for both hemispheres in accordance with the consensus protocol of an international expert panel (22). Based on the exact localization of the coil and the respective stimulation intensity (measured in V/m as the resulting electric field strength), we performed somatotopic mapping for the following muscles:

- upper extremity: abductor pollicis brevis, first digital interosseus and extensor carpi radialis

- lower extremity: tibialis anterior and abductor hallucis brevis.

A stimulation site was considered positive if the amplitude of the resulting motor evoked potential (MEP) was at least 50μV. The mapping data could also be visualized intraoperatively by implementation into the neuronavigation system so that the motor cortex could be identified. The RMT of each hemisphere (RMT_{tumor}, $RMT_{healthy}$) and the ratio (RMT_{ratio} = RMT_{tumor} divided by $RMT_{healthy}$) as surrogate parameters for the cortical excitability were determined based on an adaptive threshold-hunting algorithm (23). We verified whether the tumor infiltrated the gyrus which was identified as motor cortex (= in which MEPs were elicited) on the basis of a 3D MRI reconstruction.

Tractography

The data of the nTMS motor mapping were then imported *via* DICOM format into our planning software Elements (Brainlab AG, Munich, Germany), followed by image fusion with the MRI data and cranial distortion correction to optimize the planning accuracy (24). Deterministic "*fiber assignment by continuous tracking*" and "*tensor deflection*" algorithms were used to visualize the CST for the upper and the lower extremity in a highly reliable and user-independent manner. We combined an anatomically seeded region of interest in the anterior-inferior pontine level with the nTMS stimulation points as seeding regions (20, 25). Intraoperative validation of the nTMS-based tracking algorithm showed to be superior to other algorithms, specifically visualizing peritumoral tracts while avoiding aberrant fibers (25–28). Finally, the minimum distance between the CST and the tumor was measured and the mean as well as the peritumoral diffusion values fractional anisotropy (FA) and apparent diffusion coefficient (ADC) were calculated (FA_{avg} and the ADC_{avg} [mm^2/s] of the entire tracts, FA_{tumor} and ADC_{tumor} at the tumor level).

Intraoperative Neurophysiological Monitoring

All patients received standard anesthesia (total venous anesthesia and short-acting relaxants for intubation) with weight-adjusted use of propofol, fentanyl and remifentanil. IOM was applied in all cases with the ISIS system (Inomed, Emmendingen, Germany), with the treating neurosurgeon deciding individually on the monitoring techniques used:

-MEPs (n = 61) (train of 5, pulse duration: 0.2 msec, interstimulus interval: 2 msec) with corkscrew electrodes placed at C_3 and C_4 according to the 10–20 electroencephalography (EEG) system (29)

-continuous subcortical stimulation (SCS) (n = 53) using a monopolar mapping suction probe at a frequency of 2 Hz with a stimulation intensity of 10-15 mA initially, which was reduced depending on the individual case (7)

-recordings of the somatosensory evoked potential (SSEP) (n = 29) of the medianus and posterior tibial nerve with computer-assisted averaging and corkscrew electrodes additionally placed at F_z, C_z', C_3' and C_4' (stimulating intensities: 15-25 mA; current pulses: 0.2 msec; filter settings: 7 Hz–5 kHz) (30)

MEPs were recorded by pairs of needle electrodes inserted in the same muscles as mentioned above. Continuous EEG monitoring (using the corkscrew scalp electrodes) was performed to detect seizures and to keep the depth of anesthesia constant.

A decrease in MEP or SSEP amplitude >50% was considered a warning sign and the resection was paused immediately. Nonsurgical reasons for the decrease such as hypotension, altered anesthetic regimen (anesthetic use/ventilation parameters), or hypothermia were immediately evaluated (7, 31). Papaverine was applied aiming for full recovery of MEP and SSEP amplitude. It was recorded whether an amplitude decrease was transient or permanent and whether the permanent decrease was ≤50% or >50%. Resection was terminated when there was an irreversible MEP decrease >50% or subcortical stimulation indicated a very close location of the CST. We documented the (minimal) stimulation intensity of the mapping suction probe.

Statistical Analysis

Statistics were performed with IBM SPSS Statistics 25.0 (IBM Corp., Armonk, N.Y., USA). A two-sided statistical significance level of $\alpha = 0.05$ was used. Descriptive analyses were performed by reporting the mean and standard deviation (SD) for normally distributed parameters or the median and interquartile range (IQR) otherwise. Standardized mean differences (SMD) and the contingency coefficient (cc) were calculated to indicate sample size independent magnitude of group differences. The Pearson's Chi-Square Test, two sample t-Test or Mann-Whitney-U Test were used depending on the scaling and distribution of the variables. Correlation analyses of metric parameters were performed by calculating Pearson correlation coefficient r.

RESULTS

Patients Sample

This consecutive cohort consisted of 66 patients with a median age of 48 years whose characteristics are detailed in **Table 1**. Most patients suffered from a glioblastoma (59.1% of cases). The preoperative clinical examination revealed a motor deficit in 12 patients (18.2%). A new/an agravated postoperative paresis was found in 11 patients (16.7%) at the day of discharge. One patient (1.5%) showed an improvement in motor function postoperatively. A persistent paresis at 3-month follow-up occurred in 6 patients (9.1%) and 3 patients showed a partial recovery (4.5%) with a BMRC grade ≥ 3. The proportion of patients who developed a new postoperative motor deficit was the same in patients with preoperative paresis (16.7%) and without preoperative paresis (16.7%). Five patients (7.6%) were lost to follow-up for the following reasons: 3 patients with tumor progression, 1 patient died, and 1 patient moved to another city.

Postoperative ischemia was detected in 20 patients (30.3%), of whom 3 (4.5%) were subcortically located in the course of CST and one (1.5%) was partially located in the motor cortex (**Table 1**). Subcortical ischemic injury resulted in a persistent motor deficit in all 3 cases.

TABLE 1 | Patient sample.

	n = 66
Age in years, median (IQR)	48y (28)
Sex	
Female	27 (40.9%)
Male	39 (59.1%)
KPS, median (IQR)	90 (13)
$BMRC_{preop}$.	
0-3	5 (7.6%)
4	7 (10.6%)
5	54 (81.8%)
Hemisphere	
R	37 (56.1%)
L	29 (43.9%)
Tumor Location	
Frontal	23 (34.8%)
Parietal	18 (27.3%)
Temporo-insular	22 (33.3%)
Multilocular	3 (4.5%)
Histology	
WHO II°	10 (15.2%)
WHO III°	17 (25.8%)
WHO IV°	39 (59.1%)
Tumor Recurrency	22 (33.3%)
Tumor Volume in ml, median (IQR)	23.35 (32.58)
Edema within CST	36 (54.5%)
IOM	
MEP	61 (92.4%)
SSEP	29 (43.9%)
SCS	53 (80.3%)
Motor Outcome	
Day of Discharge	
Worsening	11 (16.7%)
No Worsening	55 (83.3%)
3 Months postop.	
missings[1]	5 (7.6%)
Persistent Worsening	6 (9.1%)
Partial Recovery	3 (4.5%)
No Worsening	52 (78.8%)
Extent of Resection	
GTR	46 (65.7%)
STR	20 (28.6%)
PR	4 (5.7%)

[1]*3 patients with tumor progression, 1 patient died, and 1 patient lived in another city; KPS, Karnofsky Performance Scale; BMRC, motor status according to the British Medical Research Counsil; CST, corticospinal tract; MEP, motor evoked potentials; SSEP, somatosensory evoked potentials; SCS, subcortical stimulation; GTR, gross total resection; STR, subtotal resection; PR, partial resection.*

nTMS Risk Stratification

The cortical mapping verified a tumorous motor cortex infiltration in 16 cases of which 7 patients (43.8%) suffered from a new motor deficit postoperatively. In contrast, only 4 out of 50 patients (8%) without motor cortex infiltration showed a postoperative deteriorated motor status (p = .002).

Descriptive statistics of the nTMS parameters (RMT, MEP latency, MEP amplitude) are outlined in **Supplementary 1**. Patients with a worse motor outcome had a higher preoperative RMT_{tumor} (worsening: 73.89 V/m, SD: 30.143 vs. no worsening: 62.27 V/m, SD: 16.743; p = .101, SMD = 0.62) and a higher $RMT_{healthy}$ (worsening: 75.89 V/m, SD: 23.513 vs. 63.90, SD: 19.438; p = .096, SMD = 0.60). Only one patient with an RMT_{ratio} between 90% and 110% had a worsened motor status after surgery, but this paresis recovered, whereas all other patients with a new deficit had an RMT_{ratio} <90% or >110% (**Figure 2**; sensitivity: 88.9%, specificity: 15.4%).

Fiber-tracking of CST showed a median tumor-tract distance (TTD) of 4.5 mm (IQR: 10.0), and no patient suffered from a new deficit when the TTD was greater than 8 mm (short-term motor outcome: cc = .302, p = .010; long term motor outcome: cc = .289, p = .019). Interestingly, the two patients with a partial recovery had a low TTD < 8mm but no tumorous infiltration of the CST (**Figure 2**). The proportion of patients with a GTR was higher in the group with TTD > 8mm (81.8%) than in the group with TTD 1-8mm (69.2%) and in the group with TTD = 0mm (44.4%) (cc = .296, p = .044).

The number of patients with a new motor deficit depending on the number of nTMS risk factors is shown in **Figure 2**. The more risk factors (motor cortex infiltration, TTD ≤ 8mm, RMT_{ratio} <90%/ >110%) were detected, the higher was the risk for a worse motor outcome (cc = .506, p <.001). Postoperative imaging revealed ischemia within the motor cortex in 2 patients (3%) and within the CST in another 2 patients (3%). Subcortical ischemia resulted in permanent new motor deficits which was not the case with cortical ischemia.

The distribution of FA_{avg}, FA_{tumor}, ADC_{avg}, and ADC_{tumor} are shown in **Supplementary 2**. Lower FA_{avg} values (worsening: mean: 0.38 (SD: 0.09), no worsening mean: 0.47 (SD: 0.07), p = .008, SMD = 1.07) and higher ADC_{tumor} (worsening: mean: 12.47 * 10^{-4} (SD: 7.99 * 10^{-4}), no worsening mean: 8.91 * 10^{-4} (SD: 6.93 * 10^{-4}) p = .045, SMD = 0.48) were associated with a deteriorated postoperative motor status.

IOM

An overview of the used IOM techniques is presented in **Table 2**. Only one patient (2.9%) of 34 with stable MEP amplitude suffered from a new motor deficit postoperatively (p = .001, cc = .403) and recovered in long-term motor outcome (p = .003, cc = .408). An irreversible MEP amplitude decrease resulted in a new motor deficit postoperatively in the majority of cases (**Table 2**, p = .003, cc = .544), however patients with a decrease ≤50% of the baseline MEP amplitude were more likely to have a recovery in long-term motor outcome (**Table 2**, p = .011, cc = .601). No patient with a completely reversible MEP amplitude alteration showed postoperative motor worsening.

Patients whose resection was performed at lower stimulation intensities ≤4mA during the SCS had the highest risk of suffering a new motor deficit, in contrast to an intensity ≥8mA, which was found to be safe from postoperative motor deterioration (**Table 2**, p = .003, cc = .422). In the cases in which SSEP monitoring was performed, there was no correlation with postoperative motor status (shot-term motor outcome: p = .658, cc = .082; long-term motor outcome: p = .437, cc = .245).

Comparative Analysis of nTMS/DTI and IOM

In patients with preoperatively verified tumorous motor cortex infiltration, intraoperative MEP alterations occurred more frequently (**Figure 3**; 33.3% with infiltration vs. 14.7% without; p = .086, cc = .215). In 3 of 4 patients with motor cortex infiltration (75%) a permanent decrease of the MEP amplitude ≤50% resulted in a permanent deficit and in one patient (25%) in a transient

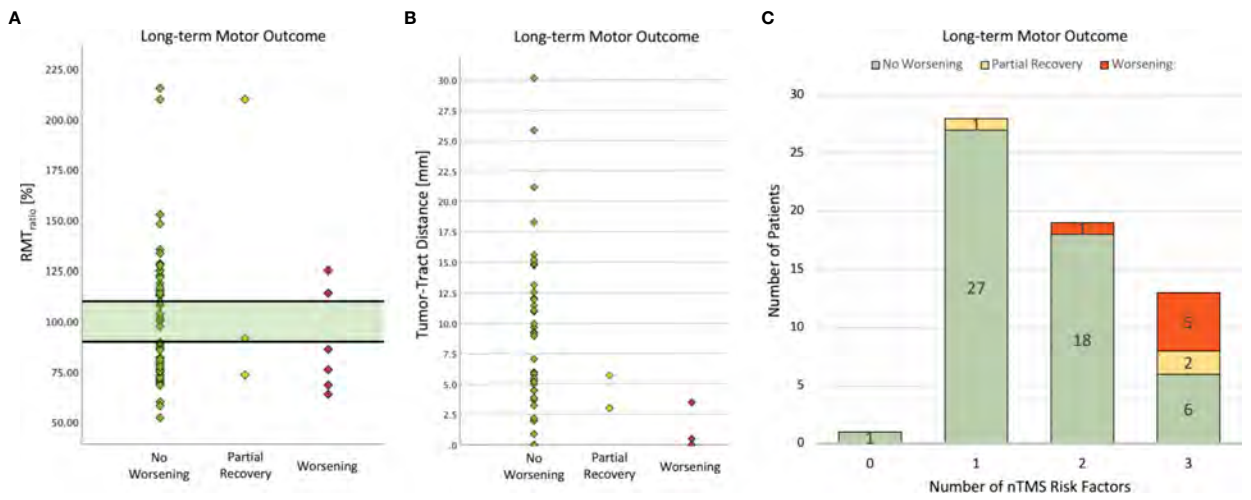

FIGURE 2 | Analysis of nTMS risk factors and long-term motor outcome. No patient suffered a new permanent motor deficit when the RMT_{ratio} was between 90% and 110% **(A)**. Only one patient developed a postoperative paresis which recovered partially within 3 months. The lower the TTD was, the higher was the risk of postoperative motor deterioration **(B)**. Note that 4 patients in the worsening group had a TTD of 0 mm. Thus, in addition to the recently proposed safe TTD of 8mm, the entire nTMS risk stratification was confirmed in this cohort **(C)**.

deficit. In contrast, no postoperative deterioration occurred in 4 of 5 patients (80%) without verified motor cortex infiltration, although MEP amplitude was also decreased by ≤ 50%. One patient (20%) had a new motor deficit which recovered partially.

A subgroup analysis of patients with TTD >8mm revealed that MEP amplitude alterations were detected in 6 of 27 patients (22.2%), 2 of whom had an irreversible MEP amplitude decrease ≤50%, although no patient within this group deteriorated (**Figure 3**). An irreversible MEP decrease >50% was only found in the patients with a TTD ≤8mm. In a further analysis of patients with an irreversible MEP amplitude decrease ≤50%, two patients with a TTD of 0mm (100%) suffered a permanent motor deficit, whereas 1 of 5 patients (20%) with a TTD between 0 and 8mm had a new persistent motor deficit, 2 (40%) had a new paresis with partial recovery within 3 months, and 2 (40%) had no postoperative motor deterioration (**Figure 3**).

The TTD measured preoperatively and the minimum used intensity of intraoperative SCS were significantly correlated (Pearson's r = 0.5; p <.001). An SCS intensity ≤4mA and a TTD of 0mm resulted in a permanent deficit in 2 of 4 patients (50%). In contrast, a TTD between 0 and 8mm led to a new permanent paresis in 1 of 7 patients (14.3%) and to a postoperative deterioration in 2 of 7 patients (28.6%) which partially recovered within 3 months (**Figure 3**).

Neither the $RMT_{tumor}/RMT_{healthy}$ nor the RMT_{ratio} were associated with specific findings of the IOM.

DISCUSSION

Main Finding of the Study

To the best of our knowledge, this is the first study to analyze findings from nTMS motor mapping and DTI fiber tracking and IOM with respect to the short- and long-term motor outcome, which we have illustrated in a flow chart (**Figure 4**). The motor outcome of patients with an irreversible MEP amplitude decrease ≤50% or used SCS intensities ≤7mA depends on the nTMS risk stratification. The more risk factors (motor cortex infiltration, TTD ≤8mm, RMT_{ratio} <90%/>110%) were found, the higher was the risk for a new motor deficit. An irreversible MEP amplitude decrease >50% was always associated with worse motor outcome whereas patients with reversible MEP amplitude alterations and used SCS intensities >7mA always showed preserved motor function. The same was true when the TTD was >8mm as described before by our group (14).

Preoperative Assessment by nTMS and DTI

The use of nTMS data for DTI fiber tracking of CST proved to be a superior technique, as peritumoral tracts in particular could be visualized in a user-independent manner and robust to peritumoral edema (25, 28). The highly significant correlation between the TTD and the minimal SCS intensity is consistent with a previously published validation study of nTMS-derived tractography (32). Our analysis also confirmed the recent risk stratification model that no new postoperative motor deficit occurred in patients with a TTD > 8 mm (14). The results of which were also confirmed externally with a similar TTD threshold of 12 mm (33, 34). In addition to the TTD, nTMS-verified tumorous infiltration of the motor cortex was also confirmed as a risk for postoperative motor deficit, which must be emphasized because tumor mass effect, peritumoral edema, and tumor-induced plasticity often confound accurate landmark-based assessment (34, 35). The nTMS mapping not only provides topographic data but also allows neurophysiological assessment whereby an unbalanced

TABLE 2 | Evaluation of the IOM.

	Short-Term Motor Outcome			Long-Term Motor Outcome				Extent of Resection		
	n = 66	No Worsening	Worsening	n = 61	No Worsening	Partial Recovery	Persistent Worsening	GTR	STR	PR
MEP Monitoring	61 (92.4%)	50 (82%)	11 (18%)	57 (93.4%)	48 (84.2%)	3 (5.3%)	6 (10.5%)	42 (68.9%)	16 (26.2%)	3 (4.9%)
MEP amplitude stable	34 (55.7%)	33 (97.1%)	1 (2.9%)	34 (59.6%)	33 (97.1%)	1 (2.9%)	0	27 (79.4%)	6 (17.6%)	1 (2.9%)
MEP amplitude alteration	27 (44.3%)	17 (63%)	10 (37%)	23 (40.4%)	15 (65.2%)	2 (8.7%)	6 (26.1%)	15 (55.6%)	10 (37%)	2 (7.4%)
completely reversible	11 (40.7%)	11 (100%)	0	10 (43.5%)	10 (100%)	0	0	7 (63.6%)	4 (36%)	0
irreversible + ≤50% decrease	9 (33.3%)	4 (44.5%)	5 (55.6%)	9 (39.1%)	4 (44.4%)	2 (22.2%)	3 (33.3%)	7 (77.8%)	2 (22.2%)	0
irreversible + >50% decrease	7 (25.9%)	2 (28.6%)	5 (71.4%)	4 (17.4%)	1 (25%)	0	3 (75%)	1 (14.3%)	4 (57.1%)	2 (28.6%)
SCS Monitoring	53 (80.3%)	44 (83%)	9 (17%)	48 (78.7%)	41 (85.4%)	3 (6.3%)	4 (8.3%)	33 (62.3%)	19 (35.8%)	1 (1.9%)
≤4mA	13 (24.5%)	7 (53.8%)	6 (46.2%)	11 (22.9%)	6 (54.5%)	2 (18.2%)	3 (27.3%)	7 (53.8%)	6 (46.2%)	0
5-7mA	24 (45.3%)	21 (87.5%)	3 (12.5%)	22 (45.8%)	20 (90.9%)	1 (4.5%)	1 (4.5%)	15 (62.5%)	8 (33.3%)	1 (4.2%)
>7mA	16 (30.2%)	16 (100%)	0	15 (31.3%)	15 (100%)	0	0	11 (68.8%)	5 (31.3%)	0
SSEP Monitoring	29 (43.9%)	24 (82.8%)	5 (17.2%)	26 (42.6%)	22 (84.6%)	1 (3.8%)	3 (11.5%)	21 (72.4%)	7 (24.1%)	1 (3.4%)
SSEP amplitude reversible decrease	25 (86.2%)	21 (84%)	4 (16%)	23 (88.5%)	20 (87%)	1 (4.3%)	2 (8.7%)	18 (72%)	6 (24%)	1 (4%)
SSEP amplitude irreversible decrease	4 (13.8%)	3 (75%)	1 (25%)	3 (11.5%)	2 (66.7%)	0	1 (33.3%)	3 (75%)	1 (25%)	0

MEP, motor evoked potentials; SCS, subcortical stimulation; SSEP, somatosensory evoked potentials; GTR, gross total resection; STR, subtotal resection; PR, partial resection.

interhemispheric excitability (RMT_{ratio} <90%/>110%) was associated with worse postoperative motor outcome (14, 36). Our analysis shows RMT_{ratio} to be a sensitive (sensitivity: 88.9%) but nonspecific (specificity: 15.4%) parameter for predicting motor outcome. On the one hand, only one patient with an RMT_{ratio} between 90% and 110% suffered a motor deficit that partially recovered within 3 months. On the other hand, 44 of 52 patients (84.6%) with an impaired RMT_{ratio} <90%/>110% maintained their motor function postoperatively. Previous studies indicated that worsened motor status was associated with higher RMT_{tumor} values, a trend that was also evident in this cohort (33). The RMT_{ratio} seems to have a limited significance in this cohort because of its low specificity. However, in combination with the other risk factors, the likelihood of motor deterioration is further increased or decreased depending on the RMT_{ratio}.

IOM – Transcranial MEP Monitoring

There is evidence from a meta-analysis that resection of eloquent brain tumors should be guided by intraoperative stimulation to increase the extent of resection and reduce the incidence of new motor deficit (5). In addition, innovative techniques such as nTMS and IOM enable surgical treatment of patients whose brain tumors were previously deemed unresectable (37). A European multicenter survey raised the (still unanswered) question which stimulation parameters and which warning criteria should be used (38).

Different thresholds regarding irreversible MEP amplitude decrease and postoperative motor deterioration have been discussed (from any irreversible change to 50% decrease and up to 80% decrease), where the studies analyzed MEPs induced by both transcranial electrical stimulation and direct cortical stimulation (9, 39–41). Reversible MEP amplitude alterations were rather associated with transient motor deficits (8, 9, 41). More recently, MEP latency prolongation was less considered for motor outcome prediction because of its low sensitivity and specificity (8, 9, 31). In agreement with the literature, no patient suffered a new postoperative paresis if the MEP amplitude was stable or showed a completely reversible change, so there were no false-negative events. On the other hand, an irreversible MEP amplitude decrease >50% led to a permanent deficit in 75% of patients, which is also in accordance with the literature. Interestingly, irreversible MEP amplitude decrease ≤50% was associated with worse motor outcome in high-risk nTMS cases, which was not true for patients without motor cortex infiltration or a TTD >8 mm. Thus, the preoperative nTMS risk stratification not only correlates with MEP amplitude alterations but also provides information that can improve the interpretation of IOM findings, especially for identifying false-positive amplitude changes. This is particularly important because recent studies have reported various neurosurgical as well as anesthesiologic causes that may affect MEP amplitude and could not be distinguished from phenomena induced by direct tissue lesions (39, 42–44). To our knowledge, our analysis is the first one that can help to distinguish true-positive from false-positive MEP amplitude alterations.

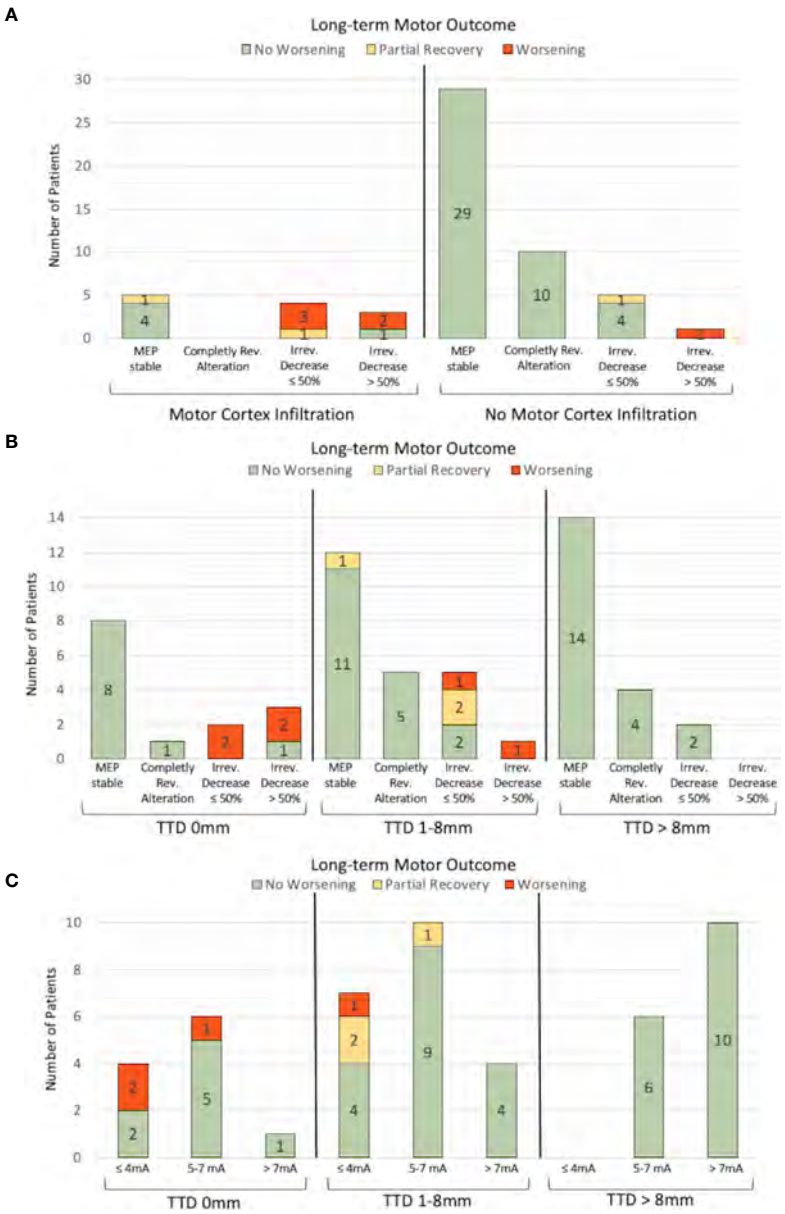

FIGURE 3 | Analysis of IOM and long-term motor outcome. An irreversible MEP amplitude decrease >50% resulted in worse motor outcome in 3 of 4 patients **(A)**. An irreversible MEP amplitude decrease ≤50% resulted in a new postoperative motor deficit, particularly in patients with nTMS-verified motor cortex infiltration, that was not present in patients without motor cortex infiltration. A similar correlation could be found for the analysis of the TTD **(B)**. No patient with a TTD >8mm suffered a new motor deficit, independently of whether MEP changes were detected or not. The motor outcome of patients with an irreversible MEP decrease ≤50% is worse, especially in patients with a TTD of 0mm than in patients with a TTD between 1 and 8mm. This phenomenon is also observed for the minimum SCS intensity, where the postoperative motor outcome was worse in the group of patients with a TTD of 0 mm than in the group with a TTD between 1 and 8mm, while the same SCS intensities were used **(C)**.

IOM – Continuous Subcortical Mapping

The usefulness and accuracy of continuous SCS for detecting and preserving the CST have been demonstrated, since MEP alterations are rather suitable for outcome prediction than as warning system (7, 45, 46). However, MEP monitoring and continuous SCS remained as standard of care to enhance safety during low stimulation thresholds (45).

Earlier studies aimed to find a safe limit for SCS intensities (e.g., 5-6mA) with which tumor resection can be performed without risk for the motor system (31, 47–49). Raabe et al. showed that SCS intensities <5mA only causes transient motor deficits in their case series – except two patients with detected ischemia on postoperative imaging who suffered a permanent motor deterioration (7). This and other studies promoted

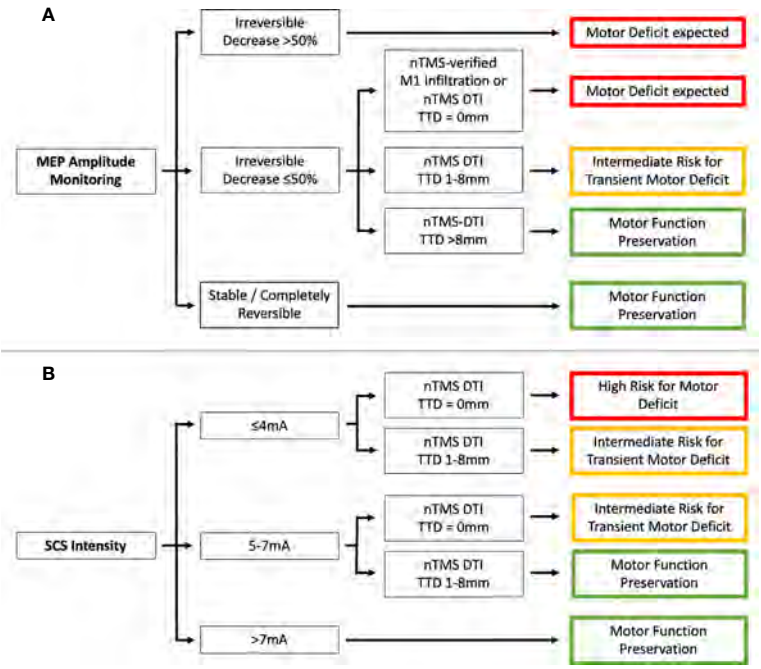

FIGURE 4 | Flowchart showing the association between preoperative nTMS assessment (motor cortex [M1] infiltration and tumor-tract distance [TTD]) and IOM (**A** - MEP amplitude monitoring and **B** - SCS intensity).

lowering stimulation intensities to 2-3mA (7, 50, 51) but the question of which patients are appropriate for this approach has yet to be answered, as lower SCS intensities were associated with a higher risk of CST injury in our study. In our patients with a tumorous subcortical infiltration of the CST (TTD = 0mm), lowering the stimulation intensity ≤4mA was associated with a higher risk of a new permanent motor deficit. This tendency was much less pronounced in the group of patients with TTD between 1 and 8mm. Thus, the minimal SCS intensity should always be adjusted to whether a GTR is realistically possible and oncologically appropriate. We observed for the first time that the risk for a new motor deficit depends on the TTD despite the same SCS intensity. Thus, the nTMS risk stratification may additionally help to optimize the tumor resection and monitoring strategy to further minimize the risk for motor deterioration.

IOM – Somatosensory Evoked Potentials

SSEPs were used less frequently in our cohort and showed no correlation that could contribute to the improvement of motor outcome or intraoperative guidance of resection. There is one study showing very low sensitivity with low positive predictive value of SSEP monitoring in brainstem surgery, stating that incautious interpretation may lead to unnecessary termination of tumor resection (52). However, SSEPs in brain tumor surgery have been studied more in terms of identifying the motor cortex by phase reversal of the somatosensory evoked potential and not for monitoring the integrity of the motor system (53).

Limitations

We performed a retrospective analysis of a prospectively collected cohort of patients with motor-eloquent glioma in whom the treating neurosurgeon individually decided on the exact IOM techniques. Therefore, we cannot exclude the occurrence of selection bias. Because of our very detailed analysis of motor-eloquent brain tumors and of abnormal IOM phenomena, the resulting subgroups are small, which did not permit statistical testing for group differences. On the other hand, this allowed us to provide a sound comparative analysis of nTMS and IOM findings that has not been investigated before. Multicentric, prospectively designed studies are needed to further improve the treatment algorithm of motor-eloquent tumors.

Deterministic DTI has been used in routine clinical practice to determine TTD in a validated and user-independent approach with robustness to peritumoral edema (25, 32). New techniques such as probabilistic tractography capable of visualizing areas of complex fiber architecture have been investigated, however, these approaches have not yet been established in clinical practice (54). For visualization of the CST, we used deterministic DTI as the established clinical routine. This technique has limitations, especially in the situation of crossing/kissing fibers (55).

CONCLUSIONS

An irreversible MEP amplitude decrease >50% was associated with higher risk of developing a new postoperative paresis in all

cases. The motor outcome of patients with an irreversible MEP amplitude decrease ≤50% or used SCS intensities ≤7mA depends on the nTMS risk stratification: high-risk cases (motor cortex infiltration, TTD <8mm, RMT_{ratio} <90%/>110%) had a higher risk for postoperative motor deterioration which was not the case in low-risk patients. Thus, the preoperative nTMS-based risk assessment can improve the interpretation of IOM phenomena and the adjustment of SCS stimulation intensity. These observations warrant a prospective interventional study to address the potential impact of nTMS informed IOM interpretation on clinical outcomes.

DATA AVAILABILITY STATEMENT

The datasets presented in this article are not readily available because of restrictions due to the Data Protection Act. Requests to access the datasets should be directed to TR.

ETHICS STATEMENT

The studies involving human participants were reviewed and approved by The ethics committee of the Charité – Universitätsmedizin Berlin (#EA1/016/19). The patients/participants provided their written informed consent to participate in this study. Written informed consent was obtained from the individual(s) for the publication of any potentially identifiable images or data included in this article.

AUTHOR CONTRIBUTIONS

Substantial contributions to the conception or design of the work, or the acquisition, analysis or interpretation of data for the work: TR, MS, MM, PV, TP, and KF. Drafting the work or revising it critically for important intellectual content: TR and TP. Providing approval for publication of the content: TR, MS, MM, PV, TP, and KF. Agree to be accountable for all aspects of the work in ensuring that questions related to the accuracy or integrity of any part of the work are appropriately investigated and resolved: PV, TP, and KF. All authors contributed to the article and approved the submitted version.

FUNDING

The authors acknowledge the support of the Cluster of Excellence Matters of Activity. Image Space Material funded by the Deutsche Forschungsgemeinschaft (DFG, German Research Foundation) under Germany´s Excellence Strategy – EXC 2025. TR is participant in the BIH-Charité Junior Digital Clinician Scientist Program funded by the Charité – Universitätsmedizin Berlin and the Berlin Institute of Health.

ACKNOWLEDGMENTS

We acknowledge support from the German Research Foundation (DFG) and the Open Access Publication Fund of Charité – Universitätsmedizin Berlin.

SUPPLEMENTARY MATERIAL

The Supplementary Material for this article can be found online at: https://www.frontiersin.org/articles/10.3389/fonc.2021.676626/full#supplementary-material

Supplementary 1 | Analysis of neurophysiological data. The distribution of the RMT stimulator output **(A)**, the RMT electric field strength **(B)**, the MEP latency **(C)** and the MEP amplitude **(D)** is shown for the tumor and the healthy hemisphere.

Supplementary 2 | Analysis of the diffusion parameters. The distribution of the FA_{avg}, FA_{tumor} **(A)**, ADC_{avg} and ADC_{tumor} in mm^2/s **(B)** is shown.

REFERENCES

1. Brown TJ, Brennan MC, Li M, Church EW, Brandmeir NJ, Rakszawski KL, et al. Association of the Extent of Resection With Survival in Glioblastoma: A Systematic Review and Meta-Analysis. *JAMA Oncol* (2016) 2(11):1460–9. doi: 10.1001/jamaoncol.2016.1373
2. Xia L, Fang C, Chen G, Sun C. Relationship Between the Extent of Resection and the Survival of Patients With Low-Grade Gliomas: A Systematic Review and Meta-Analysis. *BMC Cancer* (2018) 18(1):48. doi: 10.1186/s12885-017-3909-x
3. Molinaro AM, Hervey-Jumper S, Morshed RA, Young J, Han SJ, Chunduru P, et al. Association of Maximal Extent of Resection of Contrast-Enhanced and Non-Contrast-Enhanced Tumor With Survival Within Molecular Subgroups of Patients With Newly Diagnosed Glioblastoma. *JAMA Oncol* (2020) 6 (4):495–503. doi: 10.1001/jamaoncol.2019.6143
4. McGirt MJ, Mukherjee D, Chaichana KL, Than KD, Weingart JD, Quinones-Hinojosa A. Association of Surgically Acquired Motor and Language Deficits on Overall Survival After Resection of Glioblastoma Multiforme. *Neurosurgery* (2009) 65(3):463–9; discussion 9-70. doi: 10.1227/01.NEU.0000349763.42238.E9
5. De Witt Hamer PC, Robles SG, Zwinderman AH, Duffau H, Berger MS. Impact of Intraoperative Stimulation Brain Mapping on Glioma Surgery Outcome: A Meta-Analysis. *J Clin Oncol Off J Am Soc Clin Oncol* (2012) 30 (20):2559–65. doi: 10.1200/JCO.2011.38.4818
6. Saito T, Muragaki Y, Maruyama T, Tamura M, Nitta M, Okada Y. Intraoperative Functional Mapping and Monitoring During Glioma Surgery. *Neurol Med Chir (Tokyo)* (2015) 55(1):1–13. doi: 10.2176/nmc.ra.2014-0215
7. Raabe A, Beck J, Schucht P, Seidel K. Continuous Dynamic Mapping of the Corticospinal Tract During Surgery of Motor Eloquent Brain Tumors: Evaluation of a New Method. *J Neurosurg* (2014) 120(5):1015–24. doi: 10.3171/2014.1.JNS13909
8. Krieg SM, Shiban E, Droese D, Gempt J, Buchmann N, Pape H, et al. Predictive Value and Safety of Intraoperative Neurophysiological Monitoring With Motor Evoked Potentials in Glioma Surgery. *Neurosurgery* (2012) 70(5):1060–70; discussion 70-1. doi: 10.1227/NEU.0b013e31823f5ade
9. Szelenyi A, Hattingen E, Weidauer S, Seifert V, Ziemann U. Intraoperative Motor Evoked Potential Alteration in Intracranial Tumor Surgery and Its Relation to Signal Alteration in Postoperative Magnetic Resonance Imaging.

Neurosurgery (2010) 67(2):302–13. doi: 10.1227/01.NEU.0000371973.46234.46
10. Moiyadi A, Velayutham P, Shetty P, Seidel K, Janu A, Madhugiri V, et al. Combined Motor Evoked Potential Monitoring and Subcortical Dynamic Mapping in Motor Eloquent Tumors Allows Safer and Extended Resections. *World Neurosurg* (2018) 120:e259–e68. doi: 10.1016/j.wneu.2018.08.046
11. Picht T, Schmidt S, Brandt S, Frey D, Hannula H, Neuvonen T, et al. Preoperative Functional Mapping for Rolandic Brain Tumor Surgery: Comparison of Navigated Transcranial Magnetic Stimulation to Direct Cortical Stimulation. *Neurosurgery* (2011) 69(3):581–8; discussion 8. doi: 10.1227/NEU.0b013e3182181b89
12. Tarapore PE, Tate MC, Findlay AM, Honma SM, Mizuiri D, Berger MS, et al. Preoperative Multimodal Motor Mapping: A Comparison of Magnetoencephalography Imaging, Navigated Transcranial Magnetic Stimulation, and Direct Cortical Stimulation. *J Neurosurg* (2012) 117(2):354–62. doi: 10.3171/2012.5.JNS112124
13. Raffa G, Scibilia A, Conti A, Ricciardo G, Rizzo V, Morelli A, et al. The Role of Navigated Transcranial Magnetic Stimulation for Surgery of Motor-Eloquent Brain Tumors: A Systematic Review and Meta-Analysis. *Clin Neurol Neurosurg* (2019) 180:7–17. doi: 10.1016/j.clineuro.2019.03.003
14. Rosenstock T, Grittner U, Acker G, Schwarzer V, Kulchytska N, Vajkoczy P, et al. Risk Stratification in Motor Area-Related Glioma Surgery Based on Navigated Transcranial Magnetic Stimulation Data. *J Neurosurg* (2017) 126(4):1227–37. doi: 10.3171/2016.4.JNS152896
15. von Elm E, Altman DG, Egger M, Pocock SJ, Gotzsche PC, Vandenbroucke JP, et al. The Strengthening the Reporting of Observational Studies in Epidemiology (STROBE) Statement: Guidelines for Reporting Observational Studies. *Lancet* (9596) 2007) 370:1453–7. doi: 10.1016/S0140-6736(07)61602-X
16. Tarapore PE, Picht T, Bulubas L, Shin Y, Kulchytska N, Meyer B, et al. Safety and Tolerability of Navigated TMS for Preoperative Mapping in Neurosurgical Patients. *Clin Neurophysiol Off J Int Fed Clin Neurophysiol* (2016) 127(3):1895–900. doi: 10.1016/j.clinph.2015.11.042
17. Schag CC, Heinrich RL, Ganz PA. Karnofsky Performance Status Revisited: Reliability, Validity, and Guidelines. *J Clin Oncol Off J Am Soc Clin Oncol* (1984) 2(3):187–93. doi: 10.1200/JCO.1984.2.3.187
18. Compston A. Aids to the Investigation of Peripheral Nerve Injuries. Medical Research Council: Nerve Injuries Research Committee. His Majesty's Stationery Office: 1942; Pp. 48 (Iii) and 74 Figures and 7 Diagrams; With Aids to the Examination of the Peripheral Nervous System. by Michael O'Brien for the Guarantors of Brain. Saunders Elsevier: 2010; Pp. [8] 64 and 94 Figures. *Brain* (2010) 133(10):2838–44. doi: 10.1093/brain/awq270
19. Wesseling P, Capper D. WHO 2016 Classification of Gliomas. *Neuropathol Appl Neurobiol* (2018) 44(2):139–50. doi: 10.1111/nan.12432
20. Fekonja L, Wang Z, Bahrend I, Rosenstock T, Rosler J, Wallmeroth L, et al. Manual for Clinical Language Tractography. *Acta Neurochirurg* (2019) 161(6):1125–37. doi: 10.1007/s00701-019-03899-0
21. Berger MS, Deliganis AV, Dobbins J, Keles GE. The Effect of Extent of Resection on Recurrence in Patients With Low Grade Cerebral Hemisphere Gliomas. *Cancer* (1994) 74(6):1784–91. doi: 10.1002/1097-0142(19940915)74:6<1784::AID-CNCR2820740622>3.0.CO;2-D
22. Krieg SM, Lioumis P, Makela JP, Wilenius J, Karhu J, Hannula H, et al. Protocol for Motor and Language Mapping by Navigated TMS in Patients and Healthy Volunteers; Workshop Report. *Acta Neurochirurg* (2017) 159(7):1187–95. doi: 10.1007/s00701-017-3187-z
23. Engelhardt M, Schneider H, Gast T, Picht T. Estimation of the Resting Motor Threshold (RMT) in Transcranial Magnetic Stimulation Using Relative-Frequency and Threshold-Hunting Methods in Brain Tumor Patients. *Acta Neurochirurg* (2019) 161(9):1845–51. doi: 10.1007/s00701-019-03997-z
24. Gerhardt J, Sollmann N, Hiepe P, Kirschke JS, Meyer B, Krieg SM, et al. Retrospective Distortion Correction of Diffusion Tensor Imaging Data by Semi-Elastic Image Fusion - Evaluation by Means of Anatomical Landmarks. *Clin Neurol Neurosurg* (2019) 183:105387. doi: 10.1016/j.clineuro.2019.105387
25. Rosenstock T, Giampiccolo D, Schneider H, Runge SJ, Bahrend I, Vajkoczy P, et al. Specific DTI Seeding and Diffusivity-Analysis Improve the Quality and Prognostic Value of TMS-Based Deterministic DTI of the Pyramidal Tract. *NeuroImage Clin* (2017) 16:276–85. doi: 10.1016/j.nicl.2017.08.010
26. Forster MT, Hoecker AC, Kang JS, Quick J, Seifert V, Hattingen E, et al. Does Navigated Transcranial Stimulation Increase the Accuracy of Tractography? a Prospective Clinical Trial Based on Intraoperative Motor Evoked Potential Monitoring During Deep Brain Stimulation. *Neurosurgery* (2015) 76(6):766–75; discussion 75-6. doi: 10.1227/NEU.0000000000000715
27. Weiss C, Tursunova I, Neuschmelting V, Lockau H, Nettekoven C, Oros-Peusquens AM, et al. Improved Ntms- and DTI-Derived CST Tractography Through Anatomical ROI Seeding on Anterior Pontine Level Compared to Internal Capsule. *NeuroImage Clin* (2015) 7:424–37. doi: 10.1016/j.nicl.2015.01.006
28. Frey D, Strack V, Wiener E, Jussen D, Vajkoczy P, Picht T. A New Approach for Corticospinal Tract Reconstruction Based on Navigated Transcranial Stimulation and Standardized Fractional Anisotropy Values. *NeuroImage* (2012) 62(3):1600–9. doi: 10.1016/j.neuroimage.2012.05.059
29. Szelenyi A, Kothbauer KF, Deletis V. Transcranial Electric Stimulation for Intraoperative Motor Evoked Potential Monitoring: Stimulation Parameters and Electrode Montages. *Clin Neurophysiol Off J Int Fed Clin Neurophysiol* (2007) 118(7):1586–95. doi: 10.1016/j.clinph.2007.04.008
30. MacDonald DB, Dong C, Quatrale R, Sala F, Skinner S, Soto F, et al. Recommendations of the International Society of Intraoperative Neurophysiology for Intraoperative Somatosensory Evoked Potentials. *Clin Neurophysiol Off J Int Fed Clin Neurophysiol* (2019) 130(1):161–79. doi: 10.1016/j.clinph.2018.10.008
31. Ottenhausen M, Krieg SM, Meyer B, Ringel F. Functional Preoperative and Intraoperative Mapping and Monitoring: Increasing Safety and Efficacy in Glioma Surgery. *Neurosurg Focus* (2015) 38(1):E3. doi: 10.3171/2014.10.FOCUS14611
32. Forster MT, Hoecker AC, Kang JS, Quick J, Seifert V, Hattingen E, et al. Does Navigated Transcranial Stimulation Increase the Accuracy of Tractography? A prospective clinical trial based on intraoperative motor evoked potential monitoring during deep brain stimulation. *Neurosurgery* (2015) 76(6):766–76. doi: 10.1227/NEU.0000000000000715
33. Sollmann N, Wildschuetz N, Kelm A, Conway N, Moser T, Bulubas L, et al. Associations Between Clinical Outcome and Navigated Transcranial Magnetic Stimulation Characteristics in Patients With Motor-Eloquent Brain Lesions: A Combined Navigated Transcranial Magnetic Stimulation-Diffusion Tensor Imaging Fiber Tracking Approach. *J Neurosurg* (2018) 128(3):800–10. doi: 10.3171/2016.11.JNS162322
34. Sollmann N, Zhang H, Fratini A, Wildschuetz N, Ille S, Schroder A, et al. Risk Assessment by Presurgical Tractography Using Navigated TMS Maps in Patients With Highly Motor- or Language-Eloquent Brain Tumors. *Cancers* (2020) 12(5):1264. doi: 10.3390/cancers12051264
35. Ius T, Angelini E, Thiebaut de Schotten M, Mandonnet E, Duffau H. Evidence for Potentials and Limitations of Brain Plasticity Using an Atlas of Functional Resectability of WHO Grade II Gliomas: Towards a "Minimal Common Brain". *NeuroImage* (2011) 56(3):992–1000. doi: 10.1016/j.neuroimage.2011.03.022
36. Picht T, Strack V, Schulz J, Zdunczyk A, Frey D, Schmidt S, et al. Assessing the Functional Status of the Motor System in Brain Tumor Patients Using Transcranial Magnetic Stimulation. *Acta Neurochirurg* (2012) 154(11):2075–81. doi: 10.1007/s00701-012-1494-y
37. Krieg SM, Schnurbus L, Shiban E, Droese D, Obermueller T, Buchmann N, et al. Surgery of Highly Eloquent Gliomas Primarily Assessed as Non-Resectable: Risks and Benefits in a Cohort Study. *BMC Cancer* (2013) 13:51. doi: 10.1186/1471-2407-13-51
38. Spena G, Schucht P, Seidel K, Rutten GJ, Freyschlag CF, D'Agata F, et al. Brain Tumors in Eloquent Areas: A European Multicenter Survey of Intraoperative Mapping Techniques, Intraoperative Seizures Occurrence, and Antiepileptic Drug Prophylaxis. *Neurosurg Rev* (2017) 40(2):287–98. doi: 10.1007/s10143-016-0771-2
39. Suess O, Suess S, Brock M, Kombos T. Intraoperative Electrocortical Stimulation of Brodman Area 4: A 10-Year Analysis of 255 Cases. *Head Face Med* (2006) 2:20. doi: 10.1186/1746-160X-2-20
40. Kombos T, Suess O, Ciklatekerlio O, Brock M. Monitoring of Intraoperative Motor Evoked Potentials to Increase the Safety of Surgery in and Around the Motor Cortex. *J Neurosurg* (2001) 95(4):608–14. doi: 10.3171/jns.2001.95.4.0608
41. Neuloh G, Bien CG, Clusmann H, von Lehe M, Schramm J. Continuous Motor Monitoring Enhances Functional Preservation and Seizure-Free

Outcome in Surgery for Intractable Focal Epilepsy. *Acta Neurochirurg* (2010) 152(8):1307–14. doi: 10.1007/s00701-010-0675-9

42. Journee HL, Berends HI, Kruyt MC. The Percentage of Amplitude Decrease Warning Criteria for Transcranial MEP Monitoring. *J Clin Neurophysiol Off Publ Am Electroencephalographic Soc* (2017) 34(1):22–31. doi: 10.1097/WNP.0000000000000338
43. Ohtaki S, Akiyama Y, Kanno A, Noshiro S, Hayase T, Yamakage M, et al. The Influence of Depth of Anesthesia on Motor Evoked Potential Response During Awake Craniotomy. *J Neurosurg* (2017) 126(1):260–5. doi: 10.3171/2015.11.JNS151291
44. Benuska J, Plisova M, Zabka M, Horvath J, Tisovsky P, Novorolsky K. The Influence of Anesthesia on Intraoperative Neurophysiological Monitoring During Spinal Surgeries. *Bratisl Lek Listy* (2019) 120(10):794–801. doi: 10.4149/BLL_2019_133
45. Seidel K, Beck J, Stieglitz L, Schucht P, Raabe A. The Warning-Sign Hierarchy Between Quantitative Subcortical Motor Mapping and Continuous Motor Evoked Potential Monitoring During Resection of Supratentorial Brain Tumors. *J Neurosurg* (2013) 118(2):287–96. doi: 10.3171/2012.10.JNS12895
46. Szelenyi A, Senft C, Jardan M, Forster MT, Franz K, Seifert V, et al. Intra-Operative Subcortical Electrical Stimulation: A Comparison of Two Methods. *Clin Neurophysiol Off J Int Fed Clin Neurophysiol* (2011) 122(7):1470–5. doi: 10.1016/j.clinph.2010.12.055
47. Keles GE, Lundin DA, Lamborn KR, Chang EF, Ojemann G, Berger MS. Intraoperative Subcortical Stimulation Mapping for Hemispherical Perirolandic Gliomas Located Within or Adjacent to the Descending Motor Pathways: Evaluation of Morbidity and Assessment of Functional Outcome in 294 Patients. *J Neurosurg* (2004) 100(3):369–75. doi: 10.3171/jns.2004.100.3.0369
48. Mikuni N, Okada T, Enatsu R, Miki Y, Hanakawa T, Urayama S, et al. Clinical Impact of Integrated Functional Neuronavigation and Subcortical Electrical Stimulation to Preserve Motor Function During Resection of Brain Tumors. *J Neurosurg* (2007) 106(4):593–8. doi: 10.3171/jns.2007.106.4.593
49. Sanai N, Berger MS. Intraoperative Stimulation Techniques for Functional Pathway Preservation and Glioma Resection. *Neurosurg Focus* (2010) 28(2):E1. doi: 10.3171/2009.12.FOCUS09266
50. Seidel K, Schucht P, Beck J, Raabe A. Continuous Dynamic Mapping to Identify the Corticospinal Tract in Motor Eloquent Brain Tumors: An Update. *J Neurol Surg A Cent Eur Neurosurg* (2020) 81(2):105–10. doi: 10.1055/s-0039-1698384
51. Shiban E, Krieg SM, Haller B, Buchmann N, Obermueller T, Boeckh-Behrens T, et al. Intraoperative Subcortical Motor Evoked Potential Stimulation: How Close is the Corticospinal Tract? *J Neurosurg* (2015) 123(3):711–20. doi: 10.3171/2014.10.JNS141289
52. Shiban E, Zerr M, Huber T, Boeck-Behrends T, Wostrack M, Ringel F, et al. Poor Diagnostic Accuracy of Transcranial Motor and Somatosensory Evoked Potential Monitoring During Brainstem Cavernoma Resection. *Acta Neurochirurg* (2015) 157(11):1963–9; discussion 9. doi: 10.1007/s00701-015-2573-7
53. Kombos T, Picht T, Derdilopoulos A, Suess O. Impact of Intraoperative Neurophysiological Monitoring on Surgery of High-Grade Gliomas. *J Clin Neurophysiol Off Publ Am Electroencephalographic Soc* (2009) 26(6):422–5. doi: 10.1097/WNP.0b013e3181c2c0dc
54. Wende T, Hoffmann KT, Meixensberger J. Tractography in Neurosurgery: A Systematic Review of Current Applications. *J Neurol Surg A Cent Eur Neurosurg* (2020) 81(5):442–55. doi: 10.1055/s-0039-1691823
55. Conti Nibali M, Rossi M, Sciortino T, Riva M, Gay LG, Pessina F, et al. Preoperative Surgical Planning of Glioma: Limitations and Reliability of Fmri and DTI Tractography. *J Neurosurg Sci* (2019) 63(2):127–34. doi: 10.23736/S0390-5616.18.04597-6

Conflict of Interest: The authors declare that the research was conducted in the absence of any commercial or financial relationships that could be construed as a potential conflict of interest.

frontiers in Oncology

ORIGINAL RESEARCH
published: 25 June 2021
doi: 10.3389/fonc.2021.677172

Mapping and Preserving the Visuospatial Network by repetitive nTMS and DTI Tractography in Patients With Right Parietal Lobe Tumors

Giovanni Raffa[1], Maria Catena Quattropani[2], Giuseppina Marzano[2], Antonello Curcio[1], Vincenzo Rizzo[3], Gabriella Sebestyén[4], Viktória Tamás[4], András Büki[4] and Antonino Germanò[1]*

[1] Division of Neurosurgery, BIOMORF Department, University of Messina, Messina, Italy, [2] Department of Clinical and Experimental Medicine, University of Messina, Messina, Italy, [3] Division of Neurology, Department of Clinical and Experimental Medicine, University of Messina, Messina, Italy, [4] Department of Neurosurgery, Medical School, University of Pécs, Pécs, Hungary

OPEN ACCESS

Edited by:
Alireza Mansouri, Pennsylvania State University (PSU), United States

Reviewed by:
Alexandra Golby, Harvard Medical School, United States
Carlos Velásquez, Marqués de Valdecilla University Hospital, Spain

***Correspondence:**
Giovanni Raffa
giovanni.raffa@unime.it

Specialty section:
This article was submitted to Neuro-Oncology and Neurosurgical Oncology, a section of the journal Frontiers in Oncology

Received: *07 March 2021*
Accepted: *17 May 2021*
Published: *25 June 2021*

Citation:
Raffa G, Quattropani MC, Marzano G, Curcio A, Rizzo V, Sebestyén G, Tamás V, Büki A and Germanò A (2021) Mapping and Preserving the Visuospatial Network by repetitive nTMS and DTI Tractography in Patients With Right Parietal Lobe Tumors. Front. Oncol. 11:677172. doi: 10.3389/fonc.2021.677172

Introduction: The goal of brain tumor surgery is the maximal resection of neoplastic tissue, while preserving the adjacent functional brain tissues. The identification of functional networks involved in complex brain functions, including visuospatial abilities (VSAs), is usually difficult. We report our preliminary experience using a preoperative planning based on the combination of navigated transcranial magnetic stimulation (nTMS) and DTI tractography to provide the preoperative 3D reconstruction of the visuospatial (VS) cortico-subcortical network in patients with right parietal lobe tumors.

Material and Methods: Patients affected by right parietal lobe tumors underwent mapping of both hemispheres using an nTMS-implemented version of the Hooper Visual Organization Test (HVOT) to identify cortical areas involved in the VS network. DTI tractography was used to compute the subcortical component of the network, consisting of the three branches of the superior longitudinal fasciculus (SLF). The 3D reconstruction of the VS network was used to plan and guide the safest surgical approach to resect the tumor and avoid damage to the network. We retrospectively analyzed the cortical distribution of nTMS-induced errors, and assessed the impact of the planning on surgery by analyzing the extent of tumor resection (EOR) and the occurrence of postoperative VSAs deficits in comparison with a matched historical control group of patients operated without using the nTMS-based preoperative reconstruction of the VS network.

Results: Twenty patients were enrolled in the study (Group A). The error rate (ER) induced by nTMS was higher in the right vs. the left hemisphere (p=0.02). In the right hemisphere, the ER was higher in the anterior supramarginal gyrus (aSMG) (1.7%), angular gyrus (1.4%) superior parietal lobule (SPL) (1.3%), and dorsal lateral occipital gyrus (dLoG)

(1.2%). The reconstruction of the cortico-subcortical VS network was successfully used to plan and guide tumor resection. A gross total resection (GTR) was achieved in 85% of cases. After surgery no new VSAs deficits were observed and a slightly significant improvement of the HVOT score (p=0.02) was documented. The historical control group (Group B) included 20 patients matched for main clinical characteristics with patients in Group A, operated without the support of the nTMS-based planning. A GTR was achieved in 90% of cases, but the postoperative HVOT score resulted to be worsened as compared to the preoperative period (p=0.03). The comparison between groups showed a significantly improved postoperative HVOT score in Group A vs. Group B (p=0.03).

Conclusions: The nTMS-implemented HVOT is a feasible approach to map cortical areas involved in VSAs. It can be combined with DTI tractography, thus providing a reconstruction of the VS network that could guide neurosurgeons to preserve the VS network during tumor resection, thus reducing the occurrence of postoperative VSAs deficits as compared to standard asleep surgery.

Keywords: brain tumors, diffusion tensor imaging tractography, navigated transcranial magnetic stimulation (nTMS), superior longitudinal fasciculus (SLF), visuospatial abilities, visuospatial network, parietal lobe, Hooper visual organization test

INTRODUCTION

The modern goal of brain tumor surgery is to achieve the so-called "maximal safe resection", consisting in the maximal resection of neoplastic tissue while respecting adjacent eloquent tissue to preserve brain functions (1–3). Traditionally, motor and language functions can be confidentially assessed by neurosurgeons both pre- and postoperatively, therefore great attention is usually paid to the preservation of cortico-subcortical networks involved in these functions before and during brain tumor surgery (3–7). Conversely, complex cognitive functions, including visuospatial abilities (VSAs), usually require a specific neuropsychological expertise for their assessment, and therefore are usually undervalued by neurosurgeons when facing with surgery of brain neoplasms (8). Nevertheless, many cognitive functions are equally important than motor and language functions for an optimal quality of life, and should be preserved during brain tumor surgery to ensure, as much as possible, a normal postoperative familial, social, and even professional life to patients (8). Nevertheless, the neuroanatomical correlates of these brain functions are not well known or understood in all cases, and therefore the preservation of the involved cortico-subcortical networks cannot be easily achieved during brain tumor surgery.

Among these functions, VSAs deserves a great consideration, since it consists of a heterogeneous group of cognitive processes involved in the visual interaction with the environment and objects, essential for visual perception and finalistic behavior (9). VSAs impairment can result in a variety of neurological manifestations, including hemispatial neglect, visuospatial agnosia, etc. that severely affect the everyday life of patients, their quality of life (9, 10), and potentially their Karnofsky performance status, thus potentially also influencing their eligibility to adjuvant oncological care. The neuroanatomical correlate of VSAs has been identified mainly in right hemisphere, consisting in a fronto-parietal network mainly represented by the posterior parietal cortex and its connections with the prefrontal cortex by the superior longitudinal fasciculus (SLF), and in particular its three branches, namely the SLF-I, SLF-II, and SLF-III (11–16). Such a hemispheric asymmetry results in the fact that the right hemisphere controls attentional orienting in both left and right hemispaces, while the left hemisphere controls the direction of attention only in the right hemispace (17–21).

The visuospatial (VS) network can be successfully indentified and preserved during brain tumor surgery by expert neurosurgeons in collaboration with neuropsychologists during awake surgery (8, 10). Nevertheless, not all patients are eligible to undergo awake surgery (22, 23), and unfortunately to date many neurosurgical centers does not possess the expertise and resources to perform intraoperative brain mapping of the VS network (8). The final result is that, still nowadays, the attention paid to the VS network during brain tumor surgery is poor, and the occurrence of postoperative VSAs defictis is underestimated (8).

An alternative to intraoperative mapping is represented by advanced functional and structural imaging. Functional MRI (fMRI) can be used to identify the fronto-parietal cortical areas of the VS network (24). Nevertheless, fMRI has the limitation to

Abbreviations: RH, Right Hemipsher; RMT, resting motor threshold; HVOT, Hooper visual organization test; KPS, Karnofsky Performance Status; LBT, Line Bisection Task; LH, Left Hemisphere; VS, Visuospatial; WHO, World Health Organization.

show wide activation regions that reflect all the cognitive processes involved in the execution of a specific task, but not necessarily essential for it (25–28). Moreover, the phenomenon of dissociation between neural activation and BOLD signal has been widely reported and represents a serious potential risk for misinterpretation of fMRI results (29), even when using visual tasks in experimental models (30). Therefore, in the past years, several studies have tried to map cortical areas of the VS network by using different technologies, including repetitive navigated transcranial magnetic stimulation (nTMS) (31–33). nTMS has a higher spatial resolution (few millimeters) as compared to fMRI (34–36), and, unlike fMRI that relies on a positive-activation model, repetitive nTMS is based on a virtual-lesion model, consisting in a transient disruption of neuronal activity through a repetitive stimulation during the execution of a specific task (37, 38). Preliminary reports demonstrated repetitive nTMS is a feasible technique to successfully map cortical areas of the VS network in healthy subjects (31–33). On the other hand, diffusion tensor imaging (DTI) tractography can be successfully used to compute the three major branches of the SLF (SLF-I, SLF-II, SLF-III), and to visualize their connections to the right parietal and frontal lobe, thus enabling the identification of subcortical white matter fibers of the VS network (39).

Despite the combination of nTMS and DTI tractography can help neurosurgeons to identify and visualize the cortico-subcortical components of the VS network, to our knowledge no studies have ever analyzed the potential benefit of using such information to identify and preserve the VS network during brain tumor surgery, so far.

Here we report our preliminary experience using a preoperative planning based on nTMS cortical mapping and DTI tractography for the 3D reconstruction and visualization of the VS network. We also analyze how the use of this planning could help neurosurgeons in preserving the network during surgery of brain tumors in the right parietal lobe, as well as in reducing the occurrence of new postoperative visuospatial deficits. Finally, we compared findings achieved in patients treated using our new protocol for preoperative mapping of the VS network with findings observed in a matched historical control group of patients operated using standard asleep surgery without the help of any preoperative functional mapping and planning.

MATERIALS AND METHODS

Study Design

We retrospectively collected clinical, neurological, neuropsychological, and neuroradiological data of all patients admitted at the Department of Neurosurgery of the University of Messina, Italy, between January 2019 and December 2020 harboring a brain tumors located mainly in the right parietal lobe, and submitted to preoperative nTMS mapping of VS cortical areas and DTI tractography of the three SLF branches (SLF-I, SLF-II, SLF-III) to plan and guide tumor resection (Group A). Inclusion criteria were: age ≥ 18 years old, native Italian-language speakers, brain tumors mainly located in the right parietal lobe and therefore suspected to involve the VS network. Exclusion criteria were: age < 18 years old, bilingual speaking, the presence of any contraindication to undergo MRI and/or nTMS mapping (e.g., subjects harboring pacemakers, cochlear implants, non-MRI-compatible prosthesis, severe epilepsy). The information provided by nTMS cortical mapping and DTI tractography enabled the reconstruction of the VS network that was used to plan and guide the maximal tumor resection as well as to preserve the VS cortical and subcortical structures.

We also collected data from a historical control group including 20 patients affected by brain tumors mainly located in the right parietal lobe and operated at the same Neurosurgical Center in the period between January 2016 and December 2020 using a standard asleep microneurosurgical treatment without the use of any preoperative mapping and reconstruction of the VS network (Group B). Patients in Group B were matched for main clinical characteristics with patients in Group A (**Table 1**).

In Group A, we first analyzed the cortical distribution of errors induced by nTMS mapping during the execution of a specific neuropsychological test investigating VSAs to disclose cortical areas involved in the VS network (i.e., the Hooper Visual Organization Test, HVOT) in the right vs. left hemisphere. We also analyzed the eventual different intra-hemispheric distribution of errors induced by nTMS mapping in each hemisphere.

Finally, we analyzed the impact of the use of the preoperative planning based on the advanced reconstruction of the VS network on tumor extent of resection (EOR) and postoperative preservation of visuospatial abilities. We also compared the EOR, the postoperative visuospatial performance and functional outcome in Group A vs. Group B.

All participants signed a written informed consent for collection and use of clinical data for scientific purposes, according to the IRB at our Institution (Comitato Etico Messina).

Repetitive nTMS Cortical Mapping of the VS Network in Group A

All participants (Group A and B) underwent brain MRI scan by using a 3 Tesla scanner (Achieva 3T, Philips Medical Systems, The Netherlands). T1-weighted multiplanar reconstruction (MPR) sequences (TR/repetition time=8.1, TE/echo time = 3.7) were acquired after gadolinium i.v. administration, as a part of the routine preoperative diagnostic assessment. In case of non contrast-enhancing lesions (i.e., low grade gliomas) FLAIR sequences (TR = 8000, TE = 331.5/7) were also acquired.

The MRI scan of patients in Group A was imported into the nTMS system for mapping cortical areas involved in the VS network. The nTMS mapping was performed by using the NexSpeech module of the Nexstim NBS 4.3 system (Nexstim Oy, Helsinki, Finland), and basically consisted in the use of repetitive nTMS delivered through a figure-of-eight coil over the scalp of the patient during the execution of the HVOT test. Initially, the resting motor threshold (RMT) for the first dorsal

TABLE 1 | Salient demographic and clinical characteristics of patients in Group A and B, as well as nTMS mapping features of patients in Group A.

N°	Sex	Age	Handedness	Histology	Location	RH RMT (μV)	LH RMT (μV)	Eloquence for VS network	EOR	HVOT T score (pre-OP)	HVOT T score (post-OP 1 month)	KPS score (pre-OP)	KPS score (post-OP 1 month)	LBT score (pre-OP)	LBT score (post-OP)
nTMS Group (Group A)															
#1	F	73	Right	Glioblastoma WHO IV	Fronto-parietal, Right	41	35	N	GTR	68	71	90	90	8	7
#2	M	56	Right	Glioblastoma WHO IV	Parietal, Right	35	38	N	GTR	81	80	80	80	6	7
#3	M	54	Right	Glioblastoma WHO IV	Temporo-parietal, Right	32	36	N	GTR	66	64	80	90	7	8
#4	M	67	Right	Glioblastoma WHO IV	Fronto-parietal, Right	36	29	Y	STR	77	78	70	70	7	7
#5	F	78	Right	Glioblastoma WHO IV	Fronto-parietal, Right	39	38	N	GTR	58	54	80	80	8	9
#6	F	70	Right	Glioblastoma WHO IV	Temporo-parietal, Right	59	41	N	GTR	77	70	90	90	7	7
#7	F	73	Right	Glioblastoma WHO IV	Parieto-occipital, Right	32	31	N	GTR	75	71	80	80	7	7
#8	M	46	Right	Metastases from Lung Cancer	Parietal, Right	30	28	Y	GTR	80	80	80	80	6	6
#9	M	55	Right	Diffuse Astrocytoma WHO II	Fronto-temporo-parietal, right	34	32	N	GTR	71	70	90	90	6	7
#10	M	77	Right	Glioblastoma WHO IV	Parieto-temporo-occipital, right	35	31	N	GTR	76	77	90	80	6	6
#11	M	48	Right	Glioblastoma WHO IV	Parietal, Right	35	34	Y	GTR	80	78	80	90	7	7
#12	F	44	Right	Glioblastoma WHO IV	Parietal, Right	32	32	N	GTR	54	56	90	90	9	9
#13	F	44	Right	Glioblastoma WHO IV	Parietal, Right	38	39	N	GTR	62	60	90	80	9	9
#14	F	53	Right	Glioblastoma WHO IV	Parietal, Right	40	41	N	GTR	74	72	90	90	8	9
#15	F	41	Right	Diffuse Astrocytoma WHO II	Parietal, Right	39	39	Y	GTR	80	80	80	80	7	7
#16	M	66	Right	Glioblastoma WHO IV	Fronto-parietal, Right	34	36	Y	STR	60	60	90	90	7	8
#17	F	65	Right	Glioblastoma WHO IV	Fronto-parietal, Right	41	39	Y	GTR	64	61	80	90	7	7
#18	M	66	Right	Glioblastoma WHO IV	Parietal, Right	31	32	N	GTR	76	74	80	60	7	7
#19	M	25	Right	Diffuse Astrocytoma WHO II	Fronto-parietal, Right	35	36	Y	STR	70	70	90	90	7	7
#20	F	66	Right	Glioblastoma WHO IV	Fronto-parietal, Right	39	39	Y	GTR	68	66	70	80	7	7

(Continued)

TABLE 1 | Continued

N°	Sex	Age	Handedness	Histology	Location	RH RMT (μV)	LH RMT (μV)	Eloquence for VS network	EOR	HVOT T score (pre-OP)	HVOT T score (post-OP 1 month)	KPS score (pre-OP)	KPS score (post-OP 1 month)	LBT score (pre-OP)	LBT score (post-OP)
Historical Matched Control Group (Group B)															
#1	M	57	Right	Glioblastoma WHO IV	Temporo-parietal, Right	/	/	/	GTR	70	72	80	90	7	7
#2	M	52	Right	Glioblastoma WHO IV	Parieto-occipital, Right	/	/	/	GTR	78	76	80	80	7	7
#3	F	68	Right	Glioblastoma WHO IV	Parietal, Right	/	/	/	GTR	68	74	90	90	8	7
#4	F	70	Right	Glioblastoma WHO IV	Fronto-parietal, Right	/	/	/	STR	75	80	70	70	6	6
#5	F	50	Right	Metastases from Breast Cancer	Parietal, Right	/	/	/	GTR	70	72	90	90	6	6
#6	M	71	Right	Glioblastoma WHO IV	Parietal, Right	/	/	/	GTR	67	67	90	90	7	7
#7	F	72	Right	Glioblastoma WHO IV	Fronto-parietal, Right	/	/	/	GTR	72	74	80	80	7	7
#8	M	41	Right	Diffuse Astrocytoma WHO II	Fronto-parietal, Right	/	/	/	STR	84	85	70	60	6	6
#9	M	35	Right	Diffuse Astrocytoma WHO II	Temporo-parietal, Right	/	/	/	GTR	80	80	90	90	6	6
#10	M	50	Right	Glioblastoma WHO IV	Parietal, Right	/	/	/	GTR	70	72	80	90	7	6
#11	M	49	Right	Diffuse Astrocytoma WHO II	Temporo-parietal, Right	/	/	/	GTR	78	74	80	80	7	7
#12	F	50	Right	Glioblastoma WHO IV	Fronto-parietal, Right	/	/	/	GTR	70	70	90	70	7	6
#13	F	55	Right	Glioblastoma WHO IV	Fronto-parietal, Right	/	/	/	GTR	71	72	80	80	7	7
#14	M	75	Right	Metastases from Lung Cancer	Parietal, Right	/	/	/	GTR	68	70	90	80	8	7
#15	M	58	Right	Anaplastic Astrocytoma WHO III	Temporo-parieto-occipital, Right	/	/	/	GTR	72	75	90	90	7	7
#16	M	60	Right	Glioblastoma WHO IV	Parietal, Right	/	/	/	GTR	65	76	90	80	7	5
#17	M	66	Right	Glioblastoma WHO IV	Fronto-parietal, Right	/	/	/	GTR	60	80	80	70	9	6
#18	F	67	Right	Glioblastoma WHO IV	Fronto-parietal, Right	/	/	/	GTR	72	70	80	90	8	8
#19	F	75	Right	Glioblastoma WHO IV	Parietal, Right	/	/	/	GTR	68	69	90	90	8	8
#20	M	52	Right	Diffuse Astrocytoma WHO II	Temporo-parietal, Right	/	/	/	GTR	74	78	90	90	7	6

RH, Right Hemipsher; RMT, resting motor threshold; HVOT, Hooper visual organization test; KPS, Karnofsky Performance Status; LBT, Line Bisection Task; LH, Left Hemisphere; VS, Visuospatial; WHO, World Health Organization.

"/" means not available.

interosseus (FDI) muscle using single-pulse stimulation of the primary motor cortex was defined as previously described (40–42). Then, a repetitive stimulation was applied over both the hemispheres, with particular regard to the parietal lobe and the adjacent frontal, temporal and occipital gyri, during the execution of an nTMS-implemented version of the HVOT test. The HVOT is a standardized test for measuring the individual ability to integrate visual stimuli, and is commonly used during routine neuropsychological assessment for the investigation of visuospatial processing (43). It consists of 30 line drawings depicting simple objects, which have been cut into pieces and rearranged in a puzzle-like fashion (**Figure 1**). The subject is asked to identify what each object would be if all pieces were put back together correctly. All the HVOT drawings were imported into the nTMS system and displayed into a LCD screen in front of the subject. Pictures were presented to subjects for a fixed time (4 s) and with a fixed inter-picture interval (IPI; 4 s). Each participant underwent a baseline task without nTMS stimulation three times, in order to eliminate unrecognized/misnamed drawings, to induce a learning-effect, and therefore to reduce as much as possible false-positive results. Then, the task was administered during the repetitive stimulation. As already reported in literature regarding nTMS mapping of VSAs, the stimulation protocol consisted in a train of 10 pulses with a 5 hz frequency at 100% of the RMT intensity (32, 33). Stimulation intensity was reduced to 90% or 80% of the RMT if the patient complained some discomfort during the mapping procedure. The repetitive stimulation was triggered with the picture presentation by using an onset delay of 0 ms (44). The nTMS coil was randomly moved in about 10-mm steps over the parietal cortex and the adjacent frontal, temporal and occipital gyri. The coil was placed perpendicular to the sulcus posterior to the stimulated point to achieve the maximum field induction (45). During the mapping procedure, about 100 cortical sites in both hemispheres were stimulated 3 times each. Since repetitive nTMS is able to temporarily disrupt brain functions according to a "virtual lesion" model (37, 38), the nTMS mapping induced specific errors during the execution of the HVOT when stimulating cortical areas involved in the VS network. A stimulated cortical site was considered involved in the VS network if an nTMS-induced error at the HVOT was obtained at least during 2 of 3 stimulations. All the procedure was video-recorded and used for the off-line analysis.

Off-Line Analysis of nTMS Mapping in Group A

The recorded videos of the HVOT performance during both the baseline and the stimulation procedures were accurately analyzed and compared by two experienced neuropsychologists in order to identify nTMS-induced errors. According to the literature, HVOT errors were categorized into performance, part, and language-based errors (46). Performance errors include: 1) *perseverative errors*, consisting in repeating a previous correct or incorrect response on a later item, providing category responses that are unrelated to the current stimulus item but that are related to a previous item; 2) *unformed/unassociated errors*, consisting of a response that is unassociated to the current item, for example, "knife" for "dog"; 3) *don't know/no response errors*, consisting in providing no response or in do not understand the item. Part errors consist in naming only one part of the current stimulus, for example, "finger" for "hand". Language-based errors consist of 1) semantically related or

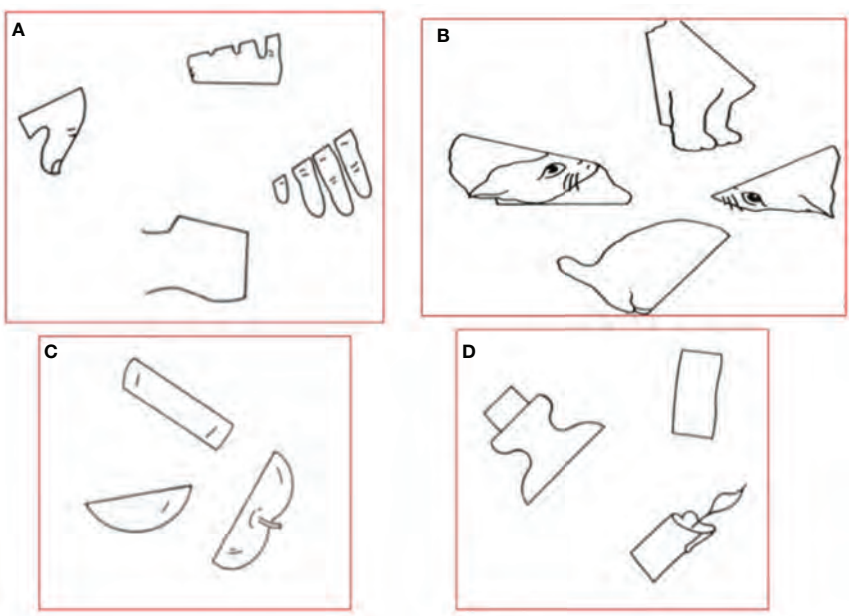

FIGURE 1 | Example of classical drawings showed during the HVOT. **(A)** Hand; **(B)** Cat; **(C)** Apple; **(D)** Candle.

unrelated name for an object; 2) circumlocutory response; 3) neologistic response; 4) agrammatic response; 5) incorrect phonemically related response.

Performance and part errors specifically regard visual analytic and synthetic abilities, whereas language-based errors regard the verbal representation of visual stimuli. When an error response occurred during nTMS mapping, the corresponding cortical site was marked as visual-organization related and tagged according to the observed error type (performance, or language-based, or part error).

After the offline analysis of responses was accomplished, the nTMS cortical spots corresponding to HVOT errors were automatically merged over the patient's MRI scan and exported as DICOM images (i.e., Fusion MRI scan). Then, the anatomical localization over the brain cortex of each nTMS-induced error was defined. The Fusion MRI scan was used to perform an automatic MRI reconstruction and volumetric segmentation of the brain cortical surface using the Freesurfer image analysis suite, which is documented and freely available for download online (http://surfer.nmr.mgh.harvard.edu/) (**Figure 2**). Then, the Freesurfer surface reconstruction and segmentation of each hemisphere was further segmented according to the cortical parcellation system described by Corina et al. (47, 48). Thereafter, the location of each single nTMS-induced error/spot was identified in a specific Corina's cortical area.

We analyzed the inter- and intra-hemispheric cortical distribution of the nTMS-induced errors. The errors' distribution was expressed as error rate % (ER) per single area (number of errors/total stimulation trials) and analyzed in both the right and left hemisphere. As well, the ER distribution was also analyzed according to the different classification of errors (performance, language-based and part errors) in both the hemispheres.

DTI Tractography of the SLF branches in Group A

During MRI scan acquisition, also diffusion weighted imaging (DWI, 64 directions, TR/repetition time = 2383.9, TE/echo time = 51.9) sequences were acquired for the successive DTI computation. DWI sequences were imported together with the Fusion MRI scan into the Medtronic Planning Station (Medtronic Navigation, Coal Creek Circle Louisville, CO, USA). All the tractography workflow was performed using the StealthViz software (Medtronic Navigation, Coal Creek Circle Louisville, CO, USA). After co-registration of the different sequences, the tensor was calculated, and the software created the Apparent Diffusion Coefficient (ADC) map and the Directionally Encoded Colors (DEC) map. The DEC map was therefore used to choose the ROI for the tractography of the SLF branches. When possible, all the three different components of the SLF (SLF-I, SLF-II, SLF-III) were computed. Otherwise, only the branch closer to the tumor was reconstructed. It is important to highlight that, according to the current literature, the SLF-III is the most ventral portion of the SLF and is synonym of the anterior segment of the arcuate fascicle (49). The tractographic reconstruction was performed choosing a multiple region-of-interest (ROI)-based approach, according to the literature (39, 50), and using a deterministic approach (fiber assignment by continuous tracking algorithm, FACT) with the following parameters: fractional anisotropy (FA) threshold = 0.20; vector step length = 1 mm; minimum fiber length = 50 mm; seed density = 1.0; and max directional change = 55°. In case of massive perilesional edema that could hamper the fiber tracking of the SLF branches, the FA threshold value to stop tracking is progressively reduced in 0.01 steps from the standard 0.20 value up to reach the minimum value of 0.10. If no fibers are visualized, the computation of the specific SLF branch is stopped to avoid

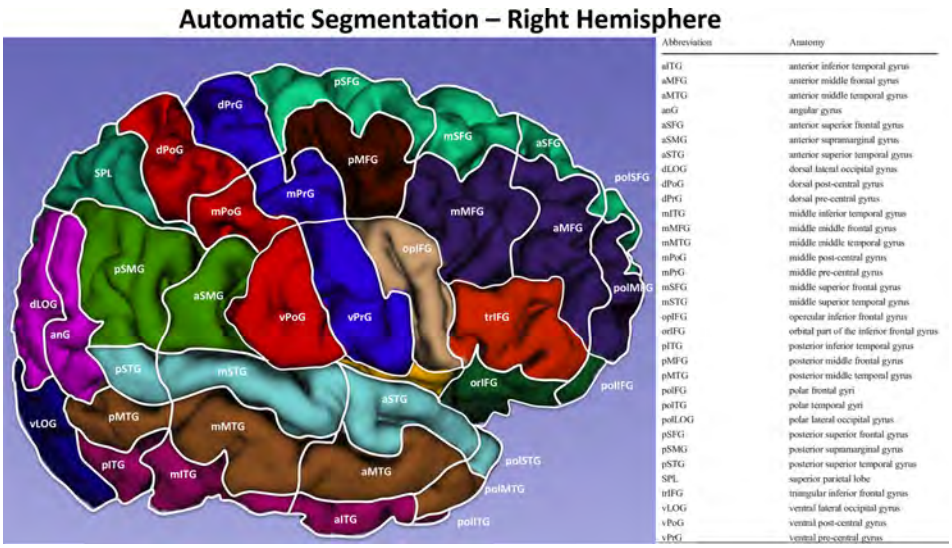

FIGURE 2 | Automatic segmentation of the cortical surface of the right hemisphere according to Corina et al (47). with the relative legend.

false-positive results. Patients were included in the study if at least one of the three SLF branches was successfully computed.

Preoperative Planning in Group A and Surgical Treatment in Group A and B

In Group A, the nTMS mapping of the VS network and the DTI fiber tracking of the SLF branches were simultaneously visualized into the Neuronavigation System, thus providing a 3D reconstruction of the VS cortico-subcortical network. Such a 3D reconstruction was used by neurosurgeon to plan the best surgical corridor to achieve the maximal tumor resection as well as to preserve as much as possible the VS network. Once the surgical strategy was defined, the 3D reconstruction of the VS network was still displayed during surgery into the neuronavigation system and guided neurosurgeon during tumor resection. The 3D reconstruction of the VS network helped neurosurgeons to spare, as much as possible, the nTMS spots at the cortical level and the SLF branches at the subcortical level.

Surgery was performed under general anesthesia in Group A and B. Nevertheless, in Group B patients, surgical resection was not guided by any preoperative nTMS mapping neither reconstruction of the VS network. In both groups, whenever lesions were located in the anterior parietal lobe and invaded also the frontal lobe, the intraoperative neurophysiological mapping and monitoring of the motor pathway was performed to preserve the motor cortex and corticospinal tract, as previously described (42). Moreover, in case of contrast-enhancing brain tumors, the surgical resection was further guided by intraoperative fluorescence thanks to the administration of intravenous sodium-fluoresceine as we reported elsewhere (51, 52).

Postoperative Outcome Assessment in Group A and B

In both Group A and B we assessed patients' outcome by evaluating and comparing the EOR, and the preoperative vs. postoperative 1) functional status expressed through the Karnofsky Performance Status (KPS) score, and 2) visuospatial performances through the HVOT as well as the traditional line bisection task (LBT).

The EOR was assessed in both groups on an early postoperative MRI scan (within 48 hours from surgery). Tumor segmentation and EOR calculation were performed on T1-enhanced sequences or, on FLAIR sequences in case of non-enhancing lesions, using OsiriX Imaging Software© (Pixmeo SARL, Bernex, Switzerland) (53). Segmentation of the tumor was manually performed across all MRI slices (54, 55). The EOR was defined as the difference between the preoperative and postoperative tumor volumes (ml) (56). The EOR was defined as follows: gross total resection (GTR) = no residual pathological tissue; subtotal resection (STR) = less than 10 ml of pathological tissue residue; partial resection (PR) ≥ 10 ml of tissue residue; biopsy ≥ of 95% of tumor residue (42, 57, 58).The EOR was expressed describing the percentage of GTR in both groups.

The KPS was evaluated before surgery and after one month from surgical treatment.

The preoperative neuropsychological evaluation was performed before surgery by two experienced neuropsychologists and included a general assessment of the VSAs by administering the standard LBT and HVOT. Moreover, during the preoperative evaluation, the hemispheric language dominance was assessed according to the handedness defined through the Edinburgh Handedness Inventory (EHI) (59). Post-operative visuospatial outcome was assessed at discharge and at one month from surgery during a standard neuropsychological evaluation including the assessment of VSAs through the administration of the standard LBT and HVOT. The HVOT and LBT scores at the one month follow-up were compared with the corresponding preoperative scores. The HVOT performance was expressed as a T-score (range 41-104) (43, 46, 60). The higher is the T-score, the higher is the probability of VSAs impairment. The LBT score was expressed according to the current literature (61).

Statistical Analysis

The paired Student T-test was used for the analysis and comparison of the inter- and intra-hemispheric distribution of the ER, as well as for the comparison of the pre- vs. postoperative KPS, HVOT, and LBT scores in each group. The unpaired Student T-test was used to compare different quantitative parameters, including clinical characteristics and outcome findings in Group A vs. Group B. The one-way ANOVA with Tukey post-hoc correction for multiple comparisons was used to compare the mean ER in each hemisphere according to the different error type (performance, language-based, part). Finally, contingency table with Chi-square or Fisher test were used to compare qualitative parameters in Group A vs. Group B, as well as to investigate the association between the eloquence defined by the nTMS-based planning and the EOR in group A. Statistical significance was defined as a p value < 0.05. Data analysis was realized by using GraphPad Prism version 6.00 for Windows, GraphPad Software, La Jolla, California, USA, www.graphpad.com.

RESULTS

Demographic and Clinical Characteristics of Patients in Group A and B

The Group A included a total of 20 patients (10 males, 10 females, mean age 58.35 ± 14.03). All patients were monolingual (native-language: Italian) and right-handed. Tumors were mainly located in the right parietal lobe in all cases. Nevertheless, in 8 cases the neoplastic tissue invaded also the ipsilateral frontal lobe, in 4 the temporal lobe, and in 2 cases the occipital lobe. Pathological examinations revealed that 16 patients were affected by glioblastoma (GBM), 3 by diffuse astrocytomas, and 1 by lung cancer metastases. The mean preoperative KPS was 83.5 ± 6.7. The preoperative neuropsychological evaluation showed that the mean T-score computed through the HVOT was 70.85 ± 8.08, while the mean LBT score was 7.15 ± 0.87.

The Group B included 20 patients (12 males, 8 females, mean age 58.65 ± 11.47). As well as in Group A, all patients were monolingual, Italian native speakers, and right-handed. Tumors were all manly located in the right parietal lobe, and involved also

the frontal lobe in 7 cases, the temporal lobe in 5, and the occipital lobe in 2. The histological diagnosis was GBM in 13 cases, diffuse astrocytoma in 4, anaplastic astrocytoma in 1, metastases from lung cancer in 1, and from breast cancer in the remaining one. The mean preoperative KPS was 84 ± 6.8. The mean T-score at the HVOT was 71.6 ± 5.49, and the mean LBT score was 7.1 ± 0.78.

Table 1 shows salient demographic and clinical characteristics of patients in Group A and B, as well as nTMS mapping features of patients in Group A. Statistical analysis showed no significant differences in Group A vs. Group B for all the preoperative demographic and clinical characteristics.

nTMS Cortical Mapping of VSAs in Group A

In Group A, the nTMS mapping of cortical areas involved in the VS network was feasible and well tolerated in all cases. The mean RMT was 36.85 ± 6.2 μV in the right hemisphere and 35.3 ± 3.97 μV in the left hemisphere (**Table 1**). The difference was not statistically significant.

The offline analysis of the nTMS-induced errors showed that the ER was significantly higher in the right hemisphere vs. the left one (0.77% ± 0.44 vs. 0.55%± 0.31, p=0.02) (**Figure 3C**).

In the right hemisphere, the ER was higher in the anterior supramarginal gyrus (aSMG, 1.7%), angular gyrus (anG, 1.4%), superior parietal lobule (SPL) (1.3%), and dorsal lateral occipital gyrus (dLoG) (1.2%)(**Figure 3A**). The analysis of the intra-hemispheric ER distribution according to the different type of errors showed that performance errors were significantly more frequent then language-based and part errors (respectively, 0.34% ± 0.31 vs. 0.15% ± 0.15 vs. 0.28% ± 0.12, p=0.02).

Conversely, in the left hemisphere, the ER was higher in the SPL (1.14%), posterior supramarginal gyrus (pSMG, 1.12%), and middle superior temporal gyrus (mSTG, 1.04%). (**Figure 3B**). The intra-hemispheric analysis of the cortical distribution of errors showed the language-based errors were induced more frequently than performance and part errors (respectively, 0.29% ± 0.17 vs. 0.16% ± 0.17 vs. 0.09% ± 0.09, p=0.001).

The analysis of the inter-hemispheric cortical distribution of the ER showed that performance and part errors were significantly higher in the right hemisphere as compared to the left one (respectively, 0.34% ± 0.31 vs. 0.16% ± 0.17, p=0.01; 0.28% ± 0.12 vs. 0.09% ± 0.09, p=0.0001). Conversely, language-based errors were significantly more frequent in the left hemisphere (0.29% ± 0.17 vs. 0.15% ± 0.15, p=0.003) (**Figure 4**).

Preoperative Planning and Surgical Resection in Group A

In Group A patients, the nTMS cortical mapping (**Figure 5**) and the DTI tractography of the SLF (one or more of the three major branches) were successfully combined in all cases, thus providing a 3D representation of the VS network. The preoperative reconstruction of the VS network and the analysis of its spatial

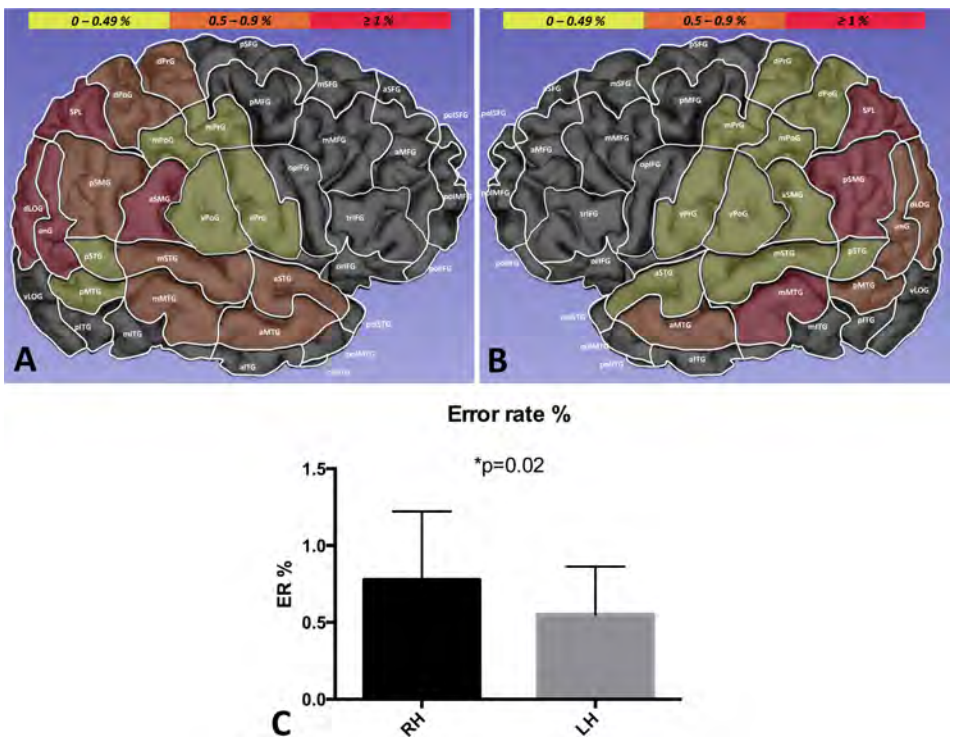

FIGURE 3 | Distribution of the global ER in the right **(A)** vs. left hemisphere **(B)**. The ER (%) in each single area is identified by a growing color intensity (yellow, orange, red). The ER was significantly higher in the right hemisphere (RH) as compared to the left hemisphere (LH), suggesting a lateralization of VSAs **(C)**.

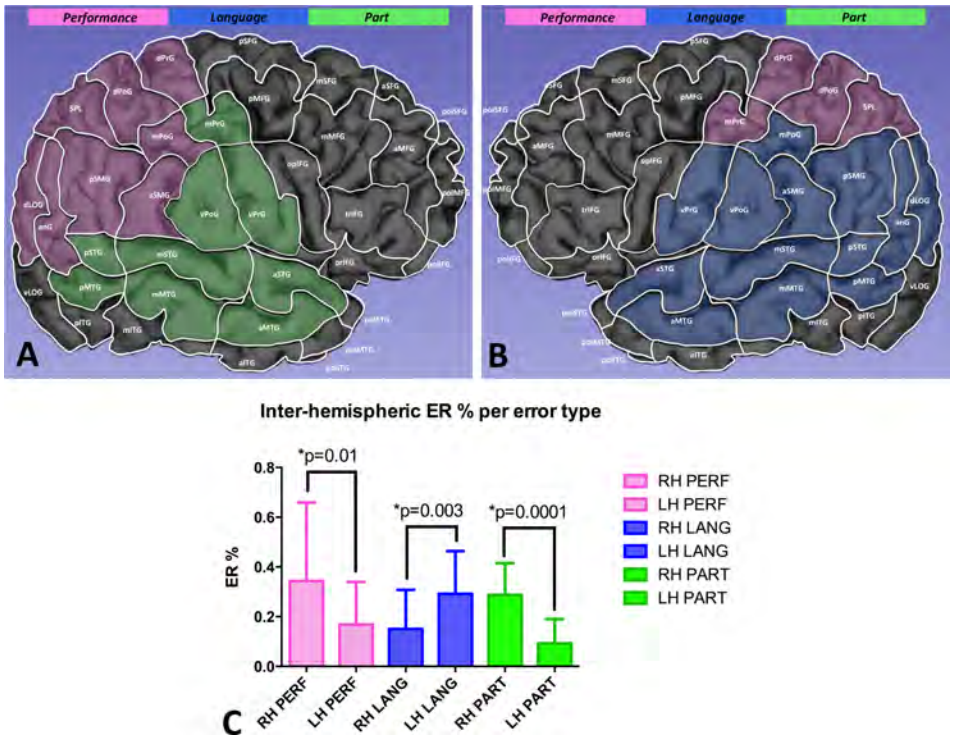

FIGURE 4 | Comparison of the ER per error type between the right **(A)** and the left hemisphere **(B)**. Performance and part errors were significantly more frequent in the right hemisphere, while language-based errors occurred more frequently in the left hemisphere **(C)**.

relationship with brain tumors enabled to identify a concrete risk for injury to the network during surgery in 8 out of 20 cases (40%). Such a risk was considered concrete because of the proximity of the tumor (≤10mm) (42, 58) to the nTMS cortical spots and/or the SLF branches. Eight lesions close (≤10mm) to the VS network were considered true-eloquent; the remaining 12 were defined as false-eloquent (12 out of 20). Such a preoperative risk stratification of patients was used to plan the best-customized surgical approach to preserve the components of the VS network (**Figure 6**). In some cases, the visualization of the preoperative reconstruction of the VS network induced a change of the original surgical strategy hypothesized before by neurosurgeons (**Figure 7**). After a definitive surgical plan had been established, surgery was performed under the guidance of the 3D reconstruction of the VS network in all cases. Indeed, it was continuously visualized into the neuronavigation system and guided the neurosurgeon in performing tumor resection and preserving the nTMS spots and the SLF (**Figure 8**).

Comparison of Outcome Variables in Group A vs. Group B

In Group A the GTR was achieved in 17 out of 20 patients (85%). In all cases the neurosurgeon performed the resection under the neuronavigation guidance up to the complete removal of the neoplastic tissue close to the structures of the VS network. Only in three cases 3 cases (15%) a STR was obtained because of the proximity of the tumor to the corticospinal tract and the primary motor cortex. In one of these 3 cases, the tumor infiltrated also the SLF and the neurosurgeon decided to plan a subtotal resection and to leave a small portion of the SLF-infiltrating neoplastic tissue (**Figure 9**). In the remaining 19 cases the proximity of the tumor to the nTMS spots and/or the SLF branches never required the interruption of resection. Statistical analysis through the Fisher test documented a slightly significant association between the eloquence defined by the nTMS-based planning (true vs. false) and the EOR (GTR vs. STR) (p=0.04).

At discharge, no new deficits of VSAs were observed in the study population during the standard neuropsychological evaluation. At one month from surgery, we observed a significant reduction of the T-score at the HVOT (69.60 ± 8.21 vs. 70.85 ± 8.08; p=0.02), and an improvement of the LBT score (7.15 ± 0.87 vs. 7.4 ± 0.94; p=0.05) suggesting an improvement of VSAs as compared to the preoperative period (**Figure 10A**). After one month from surgery, we recorded a stable KPS score as compared to the preoperative period (83.5 ± 8.1 vs. 83.5 ± 6.7; ns).

In Group B, the GTR was achieved in 18 out of 20 patients (90%). No preoperative stratification of the risk for the VS network was available before surgery. After one month from surgery, the T-score at the HVOT was significantly increased (74.3 ± 4.53 vs. 71.6 ± 5.49; p = 0.03), while the LBT score was significantly reduced (6.6 ± 0.75 vs. 7.1 ± 0.78; p=0.01),

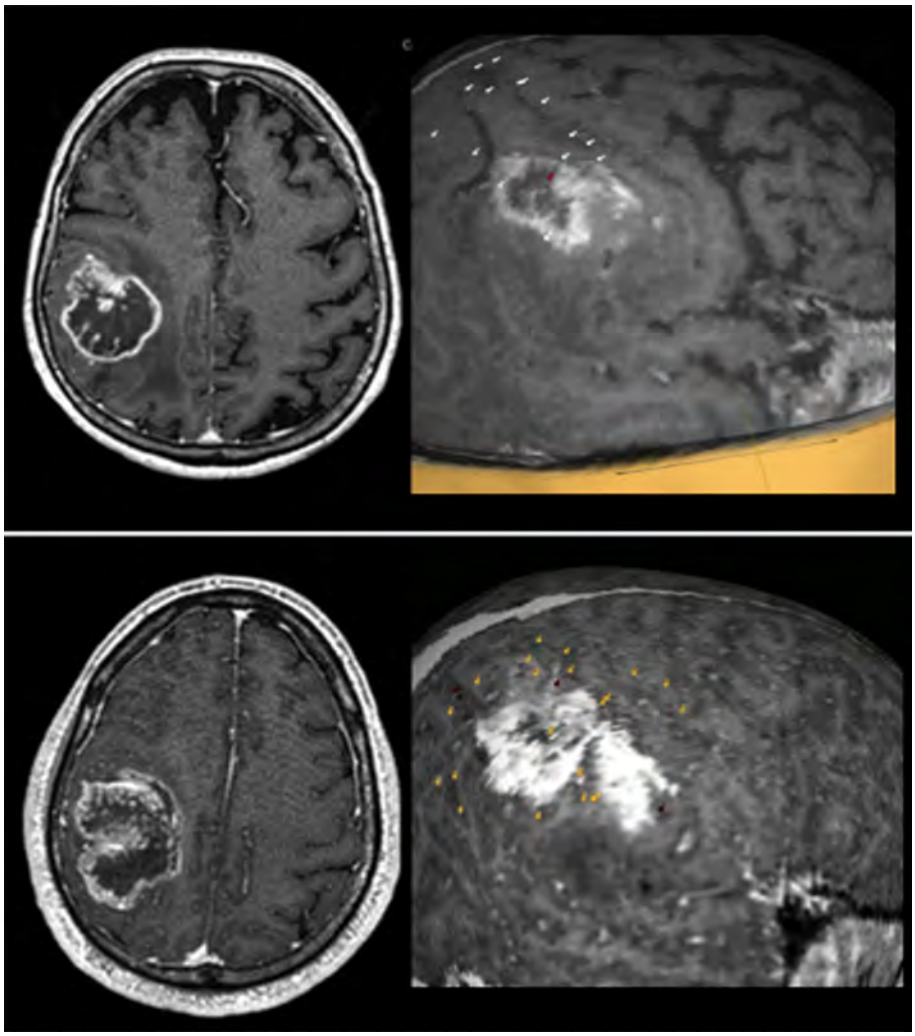

FIGURE 5 | Some examples of the nTMS mapping of VSAs in patients with tumors involving the right parietal lobe. In all three cases some nTMS spots are overlapped to the lesions, suggesting a high risk for postoperative VSAs deficits. Spots are color-coded: white = performance errors; red = language-based errors; yellow = part errors.

suggesting a worsening of VSAs as compared to the preoperative period (**Figure 10B**). Finally, at one month from surgery, we observed also a non-significant worsening of the KPS score (82.5 ± 9.1 vs. 84 ± 6.8; ns).

The comparison of outcome parameters between the two groups, documented a significant improvement of the postoperative T-Score at the HVOT ($p = 0.03$) and of the LBT score ($p = 0.005$) in Group A as compared to Group B (**Figure 10C**). No significant differences were found for the EOR and KPS score comparing the two groups.

DISCUSSION

Surgical treatment of brain intrinsic tumors aims to the maximal resection of the neoplastic tissue and to the simultaneous preservation of the adjacent functional brain networks to reduce postoperative morbidity that could seriously affect the functional independence and quality of life of patients (62). Such an objective has been translated in an increasing ability of neurosurgeons to preserve especially the motor and language network, thanks also to the availability of innovative technologies and surgical strategies. Nevertheless, in the recent years a growing attention has been paid also to the preservation of other complex brain functions, including VSAs (8). In fact, a surgical damage to the brain networks involved in these functions during brain tumor resection could seriously affect the patients' quality of life. VSAs rely on a complex fronto-parietal network that shows a significant lateralization to the right hemisphere (19, 46). Accordingly, brain tumors located within the right parietal lobe can cause a VASs impairment (24, 63). Nevertheless, VSAs impairment is usually underestimated or

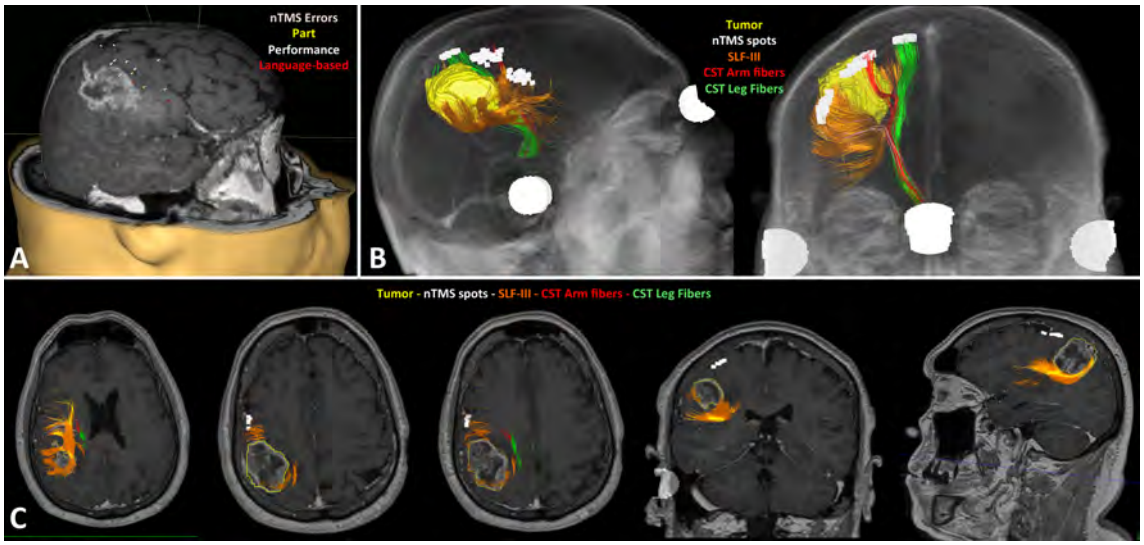

FIGURE 6 | Case example of the preoperative planning in a right fronto-parietal glioblastoma. The nTMS mapping of VSAs identified several eloquent cortical sites of the VS network **(A)**; the DTI tractography showed the tumor (yellow) was very close to the SLF-III (orange), but also to the corticospinal tract (CST; arm fibers in red, leg fibers in green) **(B)**; the fusion MRI scan confirmed the SLF-III was infiltrated by the posterior part of the tumors, as visible in the different axial, coronal and sagittal slices; conversely, the nTMS cortical spots are far away from the tumor **(C)**.

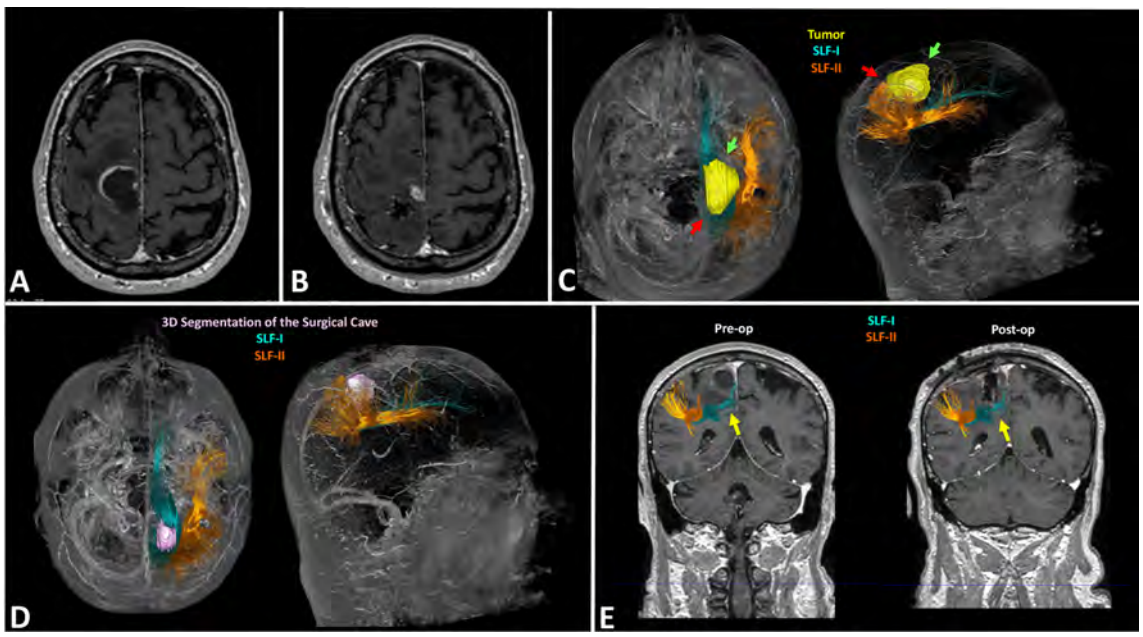

FIGURE 7 | Case example of the planning in a case of right fronto-parietal GBM (case 4 in **Table 1**). Preoperative MRI scan documenting the lesion is located in the anterior portion of the right parietal lobe and infiltrates also the primary motor cortex **(A)**; postoperative MRI scan documenting the subtotal resection of the lesion: neurosurgeons removed only the portion located in the right parietal lobe, while they didn't resect the portion infiltrating the motor cortex **(B)**; preoperative reconstruction of the VS network showing the posterior portion of the lesion is close to the blue fibers of the SLF-I indicated by the red arrows: this induced a change of surgical strategy leading neurosurgeons to start resection from the antero-lateral portion of the tumor indicated by the green arrows, just medially to the orange fibers of the SLF-II **(C)**; postoperative DTI fiber tracking showing the 3D rendering of the surgical cave in pink, and the preserved blue fibers of the SLF-I and orange fibers of the SLF-II **(D)**; coronal section showing the preservation of the SLF-I and II, especially the blue fibers of the SLF-I running medial to the surgical cave **(E)**.

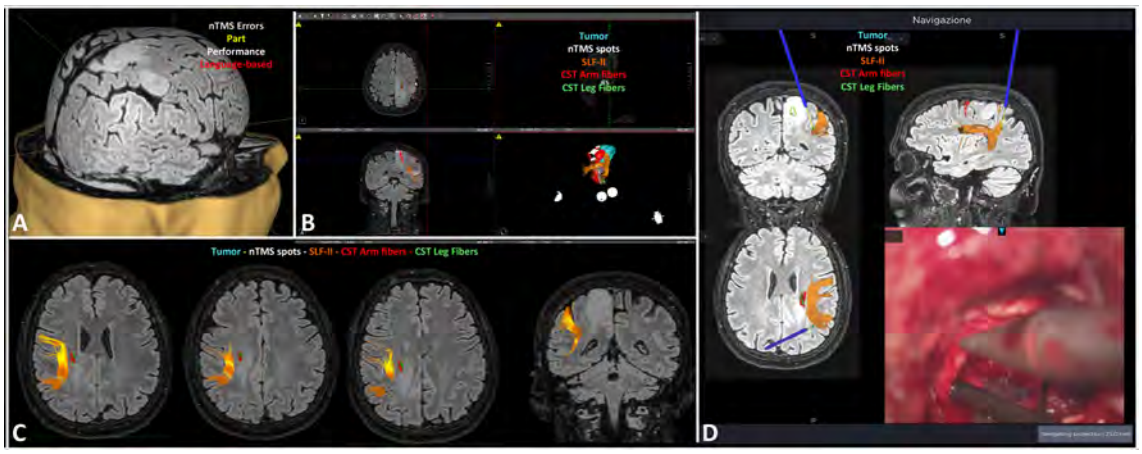

FIGURE 8 | Case-example of the intraoperative use of the 3D reconstruction of the VS network in a case of right parietal diffuse astrocytoma. The nTMS mapping documented some spots surrounding the lesion, and two overlapped to it **(A)**; a snapshot of the preoperative planning describing the relationship between the tumor and the VS network **(B)**; the axial and coronal slices show the proximity of the tumor (light blue) to the SLF-II (orange) and the corticospinal tract (CST; arm fibers in red, leg fibers in green) **(C)**; example of the intraoperative verification of the distance between the tumor, the navigation pointer (blue stylet) and the SLF-II (orange) **(D)**.

not properly evaluated in neurosurgical patients because of the need of a specific neuropsychological expertise (8). Many neurosurgical departments have recently developed new strategies for the assessment of VSAs in brain tumor patients, trying to reduce the occurrence of new postoperative deficits. Among these, the intraoperative neurophysiological mapping (IONM) of the VS network during awake surgery seems to be the most effective (10). As a matter of fact, IONM is considered the gold standard technique for resection of CNS tumors (64–67). Nevertheless, not all patients are eligible for awake surgery (22, 23). A good alternative is represented by the preoperative mapping of the VS network using advanced neuroimaging techniques. Among these, nTMS has recently gained great favor in the neurosurgical community (68). It allows for a non-invasive identification of eloquent cortex prior to surgery, including motor and language areas. Several studies reported that nTMS mapping improves surgical treatment and outcome of patients affected by brain tumors in eloquent areas (34, 58, 69,

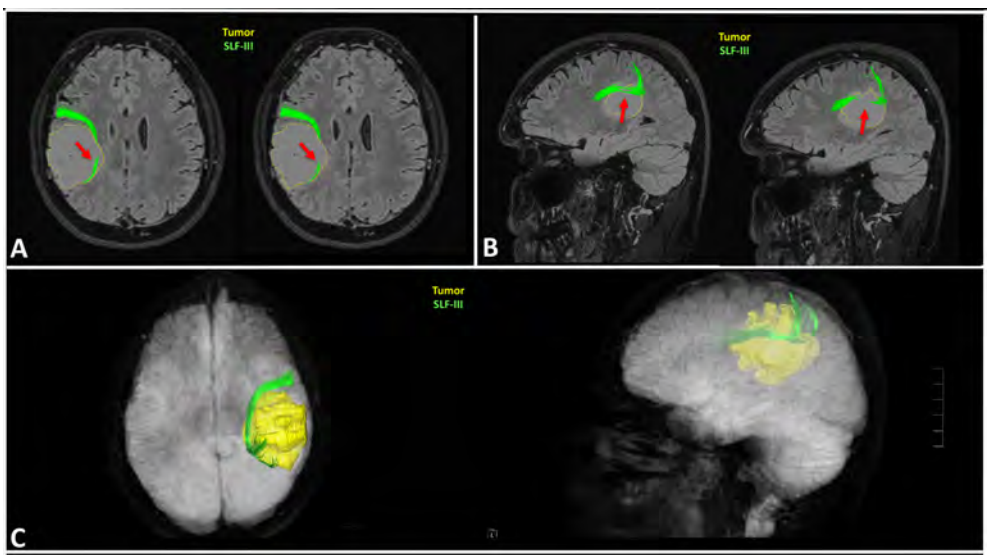

FIGURE 9 | Case example of the planning in a case of right fronto-parietal diffuse astrocytoma. The preoperative 3D reconstruction of the SLF-III showed it was infiltrated by the tumor. The green fibers of the SLF-III are infiltrated by the medial **(A)** and superior **(B)** portion of the tumor as indicated by the red arrows; the 3D reconstruction confirmed the infiltration of the SLF-III, thus inducing neurosurgeon to plan a subtotal resection to preserve the VS network **(C)**.

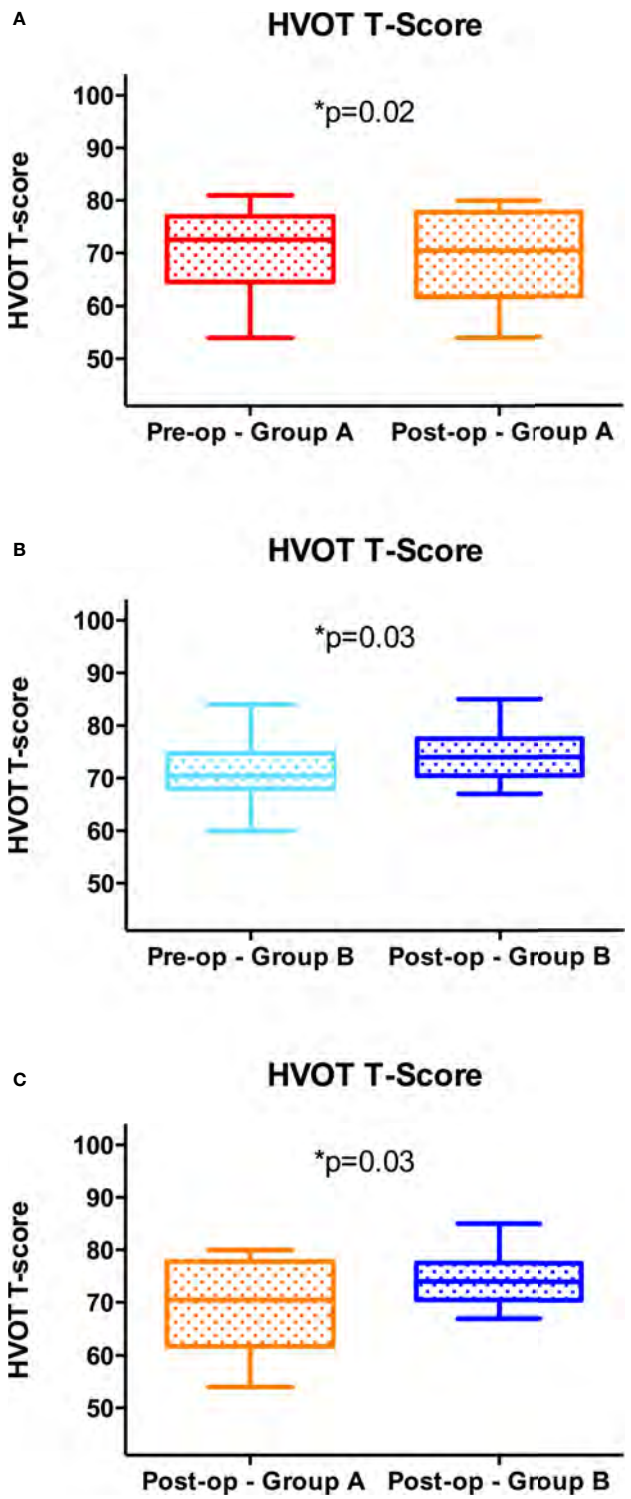

FIGURE 10 | Visuospatial outcome at one month from surgery. Significant reduction of the postoperative vs. preoperative T Score at the HVOT in Group A **(A)**; significant increase of the postoperative vs. preoperative T Score at the HVOT in Group B **(B)**; significant reduction (improved VSA) of the postoperative T Score at the HVOT in Group A vs. Group B **(C)**.

70). Moreover, nTMS can be successfully combined with DTI tractography in the clinical practice, thus enabling the visualization of eloquent networks and the analysis of their spatial relationship with the tumor: that allows for a customized preoperative planning that guides neurosurgeons to achieve the maximal safe resection of brain tumors in critical areas (34, 71, 72). Nevertheless, to our knowledge no studies have ever reported the use of nTMS mapping in combination with DTI tractography for the reconstruction of the VS network, with the final aim to improve surgical treatment of brain tumors involving such a network and reduce the occurrence of postoperative impairment of VSAs.

In the present study, we reported our preliminary experience using the nTMS cortical mapping of the VS network, in combination with the DTI tractography of the SLF branches. Previous studies reported the possibility to use repetitive nTMS for mapping VSAs. Giglhuber K. et al. in a first paper in 2016 reported a novel approach to evoke neglect-like symptoms in healthy subjects using repetitive nTMS. They implemented a line bisection judgement task (the landmark task) in the nTMS system to map cortical areas involved in the VS network. They found a higher nTMS-induced error rate in the aSMG, dLOG, and SPL (32). In a second paper from the same authors, in 2018, repetitive nTMS was used in healthy subjects to map visuospatial attention (33). In this study, using the greyscale task (73), the authors found that nTMS was able to induce leftward or rightward deviations of the VS attention by stimulating the right hemisphere, especially the pSMG, SPL, anG, vLOG, several temporal (mSTG, pMTG mMTG) and frontal areas (mSFG, mMFG, pMFG, mMFG, trIFG, opIFG). The most interesting finding reported is that repetitive nTMS is a feasible technique to map the cortical component of the VS network. Nevertheless, these experimental studies were performed only in healthy subjects. The most important result of our study is the confirmation of preliminary results reported by Giglhuber K. et al. in patients affected by tumors located in the right parietal lobe. As a matter of fact, we found a higher ER in the same areas of the right hemisphere reported in previous studies: the aSMG, anG, SPL, and dLOG. However, many error responses were also evoked by stimulating the temporal lobe, in particular the superior temporal gyrus (aSTG, mSTG, pSTG), like it has been reported in previous nTMS studies (32). Since we performed mapping in brain tumor patients, we explored only the parietal lobe and the adjacent temporal, frontal and occipital gyri: we didn't applied nTMS over the most anterior portion of the frontal lobe and therefore we cannot confirm or deny the ability of repetitive nTMS to map the frontal cortical areas involved in the VS network as reported in the second study by Giglhuber et al. (33).

The results of our nTMS-based mapping of cortical regions belonging to the VS network are also concordant with previous studies based on lesional models or intraoperative brain mapping that indicated the right inferior and superior parietal, angular, and middle occipital cortices are key anatomical structures in the visuoconstruction processes (17–20). Furthermore, evidence from previous standard TMS studies in healthy subjects

showed that the right posterior parietal cortex (rPPC), right supramarginal gyrus, and medial SPL are involved in visuospatial localization (74), visual search tasks (75, 76), and general visual selection mechanisms (77).

Interestingly, we achieved similar results using the same repetitive nTMS protocol of Giglhuber K. et al. but a different neuropsychological task, that is the HVOT. HVOT is commonly used during the routine neuropsychological examination to measure visuospatial processing (78–83). The cognitive processes investigated by HVOT are multifactorial, including mental rotation, visual working memory, object identification and name retrieval (78). Although some authors suggested the HVOT is not a pure visuospatial test, but implicates other functions such as language (84), it has been reported that it clearly loads on a global dimension called *non-verbal cognitive ability* which encompasses a large variety of attentional and visuospatial measures (85). Nadler J. et al. reported a simply method for qualitative analysis of HVOT results that is based on the distinction between errors related to visuospatial processing (performance and part errors) and errors related to language functions (language-based errors) (46). In their paper the authors clearly documented a lateralization of different error types, being part and performance errors more common in patients with lesions in the right hemisphere, while language-based errors occurring more frequently in patients with left hemisphere lesions. Interestingly, using the nTMS-implemented version of the HVOT we observed a significant different inter-hemispheric distribution of the nTMS-induced errors: performance and part errors occurred more frequently in the right hemisphere (p=0.0001), while language-based were more commonly induced by stimulating the left one (p=0.003). Such findings exactly confirm results of Nadler et al. in their lesional model, and are concordant with the current knowledge about the location of the visuospatial and language networks (19, 25, 46). Therefore, the qualitative analysis of the HVOT error responses (even those nTMS-induced) allow to discriminate language-based errors related to the impairment (permanent, like in cases of stroke, or transient, like in case of nTMS stimulation) of the language network from part and performance errors due to the impairment of the VS network. Accordingly, in our study, cortical areas showing a higher nTMS-induced ER of language-based errors were exclusively located in the left hemisphere (**Figure 4**).

The neuroanatomic correlates of the HVOT have been investigated by Moritz C.H. et al. (78) using an fMRI-implemented version of the test in a cohort of healthy subjects. The authors found fMRI activation of the bilateral SPL,bilateral lateral occipital and posterior medial temporal lobes, bilateral middle frontal gyri and left anterior cingulate gyrus, with a strong right lateralization. These findings are concordant with the results of our study and with those of Giglhuber K. et al (32, 33), thus demonstrating that nTMS is able to accurately map cortical areas involved in the VS network in the posterior parietal, occipital and frontal cortex.

Nevertheless, the identification of cortical areas involved in the VS network is not enough to preserve the network during brain tumor surgery, thus avoiding the occurrence of postoperative VSAs impairment. Tractography studies largely demonstrated the role of the SLF in the VS network (11–14, 39, 86). The different branches namely SLF-I, SLF-II and SLF-III connect the posterior parietal cortex to the dorsal and ventral frontal cortex, thus creating a complex fronto-parietal VS network (13, 39). Such a subcortical network must be preserved during brain tumor surgery to avoid the occurrence of new postoperative VSAs deficits. In the literature, there are few reports on the use of IONM during awake surgery to preserve VSAs during brain tumor surgery (10, 20, 87). Nevertheless, to our knowledge, there are no reports about the use of preoperative functional imaging techniques that could be useful to preserve VSAs in patients operated for brain tumors located within the right parietal lobe. In the present study, we report for the first time the combination of nTMS cortical mapping and DTI tractography for the preoperative 3D reconstruction of the cortico-subcortical structures of the VS network in patients affected by right parietal lobe brain tumors. Such a reconstruction was successfully used to plan and guide a safe surgical strategy to achieve the maximal tumor resection while respecting the cortico-subcortical component of the VS network (**Figure 7**). In the present study, the first result of the availability of the 3D reconstruction of the VS network for preoperative planning was that neurosurgeons were able to identify true-eloquent lesions (40% of cases) characterized by their proximity/infiltration of nTMS spots (indicating cortical eloquent sites for VSAs) and/or the SLF branches: in this cases a more careful tumor resection was planned to preserve the VS network. On the other hand, false-eloquent tumors (60%) located far from the VS network were approached more aggressively. Resection was stopped in 3 cases because the infiltration of the motor pathway, and in 1 of these cases the infiltration of the SLF induced a further, small limitation of the extent of tumor resection. Nevertheless, in this case the EOR would have been anyway subtotal because of the infiltration of the motor pathway.

The final result of such a surgical strategy based on a specific attention paid to the VS network during tumor resection was that no cases of worsened performance at the HVOT or at a standard VS test such as the LBT were observed after one month from surgery. Moreover, the comparison with a matched historical control group documented that the availability of the preoperative reconstruction of the VS network for planning and guiding surgical resection led to a significant improved postoperative VS performance at the HVOT and LBT in comparison with the standard microneurosurgical resection during asleep surgery. Nevertheless, no significant differences were found comparing the EOR, thus suggesting that our proposed strategy could be helpful specifically to preserve the VS network during surgery without reducing the possibility to achieve the GTR of the tumor. Such a strategy could also potentially have a positive impact on the postoperative KPS score, although we were not able to document any significant difference between the two study groups. However, patients treated without using the nTMS-based mapping and planning showed a non-significant reduction of the postoperative KPS score as compared to the preoperative period.

Similar surgical strategies have been already reported for resection of tumor close to the motor or language networks: several studies (including some from our group) reported that the use of a preoperative planning based on nTMS cortical mapping and nTMS-based DTI tractography is associated to a tailored less-invasive surgical approach, and to an improved EOR and functional outcome (23, 42, 58, 69, 88, 89). Since this is the first study evaluating the impact of such an advanced preoperative planning for the 3D reconstruction of the VS network in brain tumor patients, it is plausible to speculate that this approach could lead to those encouraging results in terms of improvement of surgical treatment and outcome already observed for the nTMS-based planning in patients with motor- or language-eloquent brain tumors. Nevertheless, although the results of our study are encouraging, further larger prospective studies are needed to confirm or deny our preliminary observations.

Limitations of the Study

The single-center retrospective design, the small number of patients enrolled, and the comparison with a matched historical control group limit the strength of our conclusions. Moreover, this study suffers from the common intrinsic limitations of nTMS, such as the different mapping accuracy due to the use of different stimulation parameters (44, 90, 91), but also the inaccuracy of the nTMS navigation during both the registration and the stimulation phases (92, 93).

Moreover, we must consider the intrinsic limitations of DTI tractography in cases of excessive peritumoral edema that, in some cases, could seriously hamper the possibility to perform a correct DTI fiber tracking (94, 95), as well as the possible occurrence of brain shift during surgery: the latter is another unavoidable limitation of image-guided surgery, unless intraoperative imaging is employed (96–98). Nevertheless, the use of tailored approaches with minimal brain exposure, and the continuous verification of established superficial anatomical landmarks may reduce inaccuracy due to the brain shift (99).

Finally, we must acknowledge that postsurgical deficits, including VSAs impairment, may be due to other causes than a direct damage during surgery, such as vascular injury to the structures of functional brain networks (100–105). In these cases, the intraoperative visualization of VS network cannot preserve its cortical and/or subcortical structures from indirect ischemic damage caused by surgical damage to vascular structures or postoperative hemodynamic changes. Nevertheless, this aspect is difficult to analyze and is poorly considered in the literature.

However, the present study aims to simply describe a new technique for the advanced visualization of the VS network prior to surgery as well as to report preliminary data about its potential usefulness in the treatment of patients affected by right parietal lobe tumors. It sheds a light on the possibility to use really up-to-date technologies for the non-invasive mapping of brain areas involved in visuospatial processing. This could increase the awareness and the confidence of neurosurgeons with VSAs and VS network, whose importance for patients' quality of life is still underestimated.

CONCLUSIONS

Cortical mapping using the repetitive nTMS-implemented HVOT is a feasible technique and can be successfully combined with DTI tractography of the SLF branches to achieve a 3D reconstruction of the most important cortico-subcortical components of the brain visuospatial network. Such a reconstruction can be used by neurosurgeons for a customized presurgical planning in patients affected by right parietal lobe tumors with the aim to better assess the risk of surgical damage to the VS network. Moreover, through neuronavigation it could also guide neurosurgeons to identify and preserve the VS network during tumor resection, thus avoiding the occurrence of new subtle postoperative deficits of VSAs. Further larger prospective studies are warranted to confirm our preliminary results.

DATA AVAILABILITY STATEMENT

The raw data supporting the conclusions of this article will be made available by the authors, without undue reservation.

ETHICS STATEMENT

Ethical review and approval was not required for the study on human participants in accordance with the local legislation and institutional requirements. According to the Italian law, this retrospective observational study was notified to the Comitato Etico Messina. The patients/participants provided their written informed consent to participate in this study.

AUTHOR CONTRIBUTIONS

GR: Conception and design of the work, analysis and interpretation of data, drafting the work, revision of the paper for important intellectual content, final approval of the version to be published, agreement to be accountable for all aspects of the work. MQ: Conception and design of the work, interpretation of data, final approval of the version to be published, agreement to be accountable for all aspects of the work. GM: Design of the work, acquisition of data, final approval of the version to be published, agreement to be accountable for all aspects of the work. AC: Design of the work, acquisition of data, final approval of the version to be published, agreement to be accountable for all aspects of the work. VR: Design of the work, acquisition of data, final approval of the version to be published, agreement to be accountable for all aspects of the work. GS: Design of the work, interpretation of data, revision of the paper for important intellectual content, final approval of the version to be published, agreement to be accountable for all aspects of the work. VT: Design of the work, interpretation of data, revision of the paper for important intellectual content, final approval of the version to be published, agreement to be accountable for all aspects of the work. AB: Design of the work, interpretation of data, revision

of the paper for important intellectual content, final approval of the version to be published, agreement to be accountable for all aspects of the work. AG: Conception of the work, interpretation of data, revision of the paper for important intellectual content, final approval of the version to be published, agreement to be accountable for all aspects of the work. All authors contributed to the article and approved the submitted version.

FUNDING

The study has been funded by the 1) Department of Clinical and Experimental Medicine of the University of Messina, Italy, recipient MQ, and by the 2) European Social Fund (FSE), Call "PON Ricerca e Innovazione 2014-2020 - AIM Attraction and International Mobility", Activity AIM1839117-3, Line 1, Area SNSI Salute (CUP J44I18000280006), recipients BIOMORF Department of the University of Messina, and GR.

ACKNOWLEDGMENTS

We would like to thank Prof. Francesco Tomaiuolo for his support to interpretation of results and to the writing of the draft of the paper.

REFERENCES

1. D'Amico RS, Englander ZK, Canoll P, Bruce JN. Extent of Resection in Glioma–a Review of the Cutting Edge. *World Neurosurg* (2017) 103:538–49. doi: 10.1016/j.wneu.2017.04.041
2. Berger MS, Hadjipanayis CG. Surgery of Intrinsic Cerebral Tumors. *Neurosurgery* (2007) 61:275–9. doi: 10.1227/01.NEU.0000255489.88321.18
3. Duffau H. Introduction. Surgery of Gliomas in Eloquent Areas: From Brain Hodotopy and Plasticity to Functional Neurooncology. *Neurosurg Focus* (2010) 28:1–2. doi: 10.3171/2009.12.FOCUS.FEB2010.INTRO
4. Skirboll SS, Ojemann GA, Berger MS, Lettich E, Winn HR. Functional Cortex and Subcortical White Matter Located Within Gliomas. *Neurosurgery* (1996) 38:675–8. doi: 10.1227/00006123-199604000-00008
5. Berger MS, Ojemann GA. Intraoperative Brain Mapping Techniques in Neuro-Oncology. *Stereotact Funct Neurosurg* (1992) 58:153–61. doi: 10.1159/000098989
6. Berger MS. Lesions in Functional ("Eloquent") Cortex and Subcortical White Matter. *Clin Neurosurg* (1994) 41:444–63.
7. Hervey-Jumper SL, Berger MS. Role of Surgical Resection in Low- and High-Grade Gliomas. *Curr Treat Options Neurol* (2014) 16:284. doi: 10.1007/s11940-014-0284-7
8. Duffau H. New Philosophy, Clinical Pearls, and Methods for Intraoperative Cognition Mapping and Monitoring "À La Carte" in Brain Tumor Patients. *Neurosurgery* (2021) 88(5):919–30. doi: 10.1093/neuros/nyaa363
9. Buening J, Brown RD. "Visuospatial Cognition,". In: *Neuroscience of Mathematical Cognitive Development: From Infancy Through Emerging Adulthood*. New York: Springer International Publishing (2018). p. 79–96. doi: 10.1007/978-3-319-76409-2_5
10. Duffau H. Awake Surgery for Nonlanguage Mapping. *Neurosurgery* (2010) 66:523–9. doi: 10.1227/01.NEU.0000364996.97762.73
11. Carter AR, McAvoy MP, Siegel JS, Hong X, Astafiev SV, Rengachary J, et al. Differential White Matter Involvement Associated With Distinct Visuospatial Deficits After Right Hemisphere Stroke. *Cortex* (2017) 88:81–97. doi: 10.1016/j.cortex.2016.12.009
12. Lunven M, Bartolomeo P. Attention and Spatial Cognition: Neural and Anatomical Substrates of Visual Neglect. *Ann Phys Rehabil Med* (2017) 60:124–9. doi: 10.1016/j.rehab.2016.01.004
13. Bartolomeo P, Thiebaut de Schotten M, Chica AB. Brain Networks of Visuospatial Attention and Their Disruption in Visual Neglect. *Front Hum Neurosci* (2012) 6:110. doi: 10.3389/fnhum.2012.00110
14. Thiebaut De Schotten M, Tomaiuolo F, Aiello M, Merola S, Silvetti M, Lecce F, et al. Damage to White Matter Pathways in Subacute and Chronic Spatial Neglect: A Group Study and 2 Single-Case Studies With Complete Virtual "in Vivo" Tractography Dissection. *Cereb Cortex* (2014) 24:691–706. doi: 10.1093/cercor/bhs351
15. Doricchi F, Thiebaut de Schotten M, Tomaiuolo F, Bartolomeo P. White Matter (Dis)Connections and Gray Matter (Dys)Functions in Visual Neglect: Gaining Insights Into the Brain Networks of Spatial Awareness. *Cortex* (2008) 44:983–95. doi: 10.1016/j.cortex.2008.03.006
16. Doricchi F, Tomaiuolo F. The Anatomy of Neglect Without Hemianopia: A Key Role for Parietal-Frontal Disconnection? *Neuroreport* (2003) 14:26–36. doi: 10.1097/00001756-200312020-00021
17. Gazzaniga MS, Bogen JE, Sperry RW. Observations on Visual Perception After Disconnexion of the Cerebral Hemispheres in Man. *Brain* (1965) 88:221–36. doi: 10.1093/brain/88.2.221
18. Szczepanski SM, Kastner S. Shifting Attentional Priorities: Control of Spatial Attention Through Hemispheric Competition. *J Neurosci* (2013) 33:5411–21. doi: 10.1523/JNEUROSCI.4089-12.2013
19. Biesbroek JM, van Zandvoort MJ, Kuijf HJ, Weaver NA, Kappelle LJ, Vos PC, et al. The Anatomy of Visuospatial Construction Revealed by Lesion-Symptom Mapping. *Neuropsychologia* (2014) 62:68–76. doi: 10.1016/j.neuropsychologia.2014.07.013
20. Vallar G, Bello L, Bricolo E, Castellano A, Casarotti A, Falini A, et al. Cerebral Correlates of Visuospatial Neglect: A Direct Cerebral Stimulation Study. *Hum Brain Mapp* (2014) 35:1334–50. doi: 10.1002/hbm.22257
21. Mesulam MM. "Functional Anatomy of Attention and Neglect: From Neurons to Networks,". In: H-OAD Karnath Milner, G Vallar, editors. *The Cognitive and Neural Bases of Spatial Neglect*. Oxford, UK: Oxford University Press (2002). p. 35–45.
22. Nossek E, Matot I, Shahar T, Barzilai O, Rapoport Y, Gonen T, et al. Failed Awake Craniotomy: A Retrospective Analysis in 424 Patients Undergoing Craniotomy for Brain Tumor. *J Neurosurg* (2013) 118:243–9. doi: 10.3171/2012.10.JNS12511
23. Raffa G, Quattropani MC, Scibilia A, Conti A, Angileri FF, Esposito F, et al. Surgery of Language-Eloquent Tumors in Patients Not Eligible for Awake Surgery: The Impact of a Protocol Based on Ntms on Presurgical Planning and Language Outcome, With Evidence of Tumor-Induced Intra-Hemispheric Plasticity. *Clin Neurol Neurosurg* (2018) 168:127–39. doi: 10.1016/j.clineuro.2018.03.009
24. Charras P, Herbet G, Deverdun J, de Champfleur NM, Duffau H, Bartolomeo P, et al. Functional Reorganization of the Attentional Networks in Low-Grade Glioma Patients: A Longitudinal Study. *Cortex* (2015) 63:27–41. doi: 10.1016/j.cortex.2014.08.010
25. Chang EF, Raygor KP, Berger MS. Contemporary Model of Language Organization: An Overview for Neurosurgeons. *J Neurosurg* (2015) 122:250–61. doi: 10.3171/2014.10.JNS132647
26. Scibilia A, Conti A, Raffa G, Granata F, Abbritti RV, Priola SM, et al. Resting-State Fmr Evidence of Network Reorganization Induced by Navigated Transcranial Magnetic Repetitive Stimulation in Phantom Limb Pain. *Neurol Res* (2018) 40:241–8. doi: 10.1080/01616412.2018.1429203
27. Jacobs J, Korolev IO, Caplan JB, Ekstrom AD, Litt B, Baltuch G, et al. Right-Lateralized Brain Oscillations in Human Spatial Navigation. *J Cognit Neurosci* (2010) 22:824–36. doi: 10.1162/jocn.2009.21240
28. Orringer DA, Vago DR, Golby AJ. Clinical Applications and Future Directions of Functional MRI. *Semin Neurol* (2012) 32:466–75. doi: 10.1055/s-0032-1331816

29. Ekstrom A. How and When the Fmri BOLD Signal Relates to Underlying Neural Activity: The Danger in Dissociation. *Brain Res Rev* (2010) 62:233–44. doi: 10.1016/j.brainresrev.2009.12.004
30. Maier A, Wilke M, Aura C, Zhu C, Ye FQ, Leopold DA. Divergence of Fmri and Neural Signals in V1 During Perceptual Suppression in the Awake Monkey. *Nat Neurosci* (2008) 11:1193–200. doi: 10.1038/nn.2173
31. Maurer S, Giglhuber K, Sollmann N, Kelm A, Ille S, Hauck T, et al. Non-Invasive Mapping of Face Processing by Navigated Transcranial Magnetic Stimulation. *Front Hum Neurosci* (2017) 11:4. doi: 10.3389/fnhum.2017.00004
32. Giglhuber K, Maurer S, Zimmer C, Meyer B, Krieg SM. Evoking Visual Neglect-Like Deficits in Healthy Volunteers – an Investigation by Repetitive Navigated Transcranial Magnetic Stimulation. *Brain Imaging Behav* (2017) 11:17–29. doi: 10.1007/s11682-016-9506-9
33. Giglhuber K, Maurer S, Zimmer C, Meyer B, Krieg SM. Mapping Visuospatial Attention: The Greyscales Task in Combination With Repetitive Navigated Transcranial Magnetic Stimulation. *BMC Neurosci* (2018) 19(1):40. doi: 10.1186/s12868-018-0440-1
34. Raffa G, Quattropani MC, Germanò A. When Imaging Meets Neurophysiology: The Value of Navigated Transcranial Magnetic Stimulation for Preoperative Neurophysiological Mapping Prior to Brain Tumor Surgery. *Neurosurg Focus* (2019) 47(6):10. doi: 10.3171/2019.9.FOCUS19640
35. Ro T, Cheifet S, Ingle H, Shoup R, Rafal R. Localization of the Human Frontal Eye Fields and Motor Hand Area With Transcranial Magnetic Stimulation and Magnetic Resonance Imaging. *Neuropsychologia* (1999) 37:225–31. doi: 10.1016/S0028-3932(98)00097-9
36. Mangraviti A, Casali C, Cordella R, Legnani FG, Mattei L, Prada F, et al. Practical Assessment of Preoperative Functional Mapping Techniques: Navigated Transcranial Magnetic Stimulation and Functional Magnetic Resonance Imaging. *Neurol Sci* (2013) 34:1551–7. doi: 10.1007/s10072-012-1283-7
37. Pascual-Leone A, Bartres-Faz D, Keenan JP. Transcranial Magnetic Stimulation: Studying the Brain-Behaviour Relationship by Induction of "Virtual Lesions."*Philos Trans R Soc L B Biol Sci* (1999) 354:1229–38. doi: 10.1098/rstb.1999.0476
38. Pascual-Leone A, Walsh V, Rothwell J. Transcranial Magnetic Stimulation in Cognitive Neuroscience–Virtual Lesion, Chronometry, and Functional Connectivity. *Curr Opin Neurobiol* (2000) 10:232–7. doi: 10.1016/S0959-4388(00)00081-7
39. De Schotten MT, Dell'Acqua F, Forkel SJ, Simmons A, Vergani F, Murphy DGM, et al. A Lateralized Brain Network for Visuospatial Attention. *Nat Neurosci* (2011) 14:1245–6. doi: 10.1038/nn.2905
40. Conti A, Raffa G, Granata F, Rizzo V, Germanò A, Tomasello F. Navigated Transcranial Magnetic Stimulation for "Somatotopic" Tractography of the Corticospinal Tract. *Neurosurgery* (2014) 10:542–54. doi: 10.1227/NEU.0000000000000502
41. Rizzo V, Terranova C, Conti A, Germanò A, Alafaci C, Raffa G, et al. Preoperative Functional Mapping for Rolandic Brain Tumor Surgery. *Neurosci Lett* (2014) 583:136–41. doi: 10.1016/j.neulet.2014.09.017
42. Raffa G, Conti A, Scibilia A, Cardali SM, Esposito F, Angileri FF, et al. The Impact of Diffusion Tensor Imaging Fiber Tracking of the Corticospinal Tract Based on Navigated Transcranial Magnetic Stimulation on Surgery of Motor-Eloquent Brain Lesions. *Neurosurgery* (2018) 83:768–82. doi: 10.1093/neuros/nyx554
43. Hooper HE. *Hooper Visual Organization Test (Vot) - Manual. 1983*. Los Angeles, CA, USA: Western Psycological Services (1983).
44. Krieg SM, Tarapore PE, Picht T, Tanigawa N, Houde J, Sollmann N, et al. Optimal Timing of Pulse Onset for Language Mapping With Navigated Repetitive Transcranial Magnetic Stimulation. *Neuroimage* (2014) 100:219–36. doi: 10.1016/j.neuroimage.2014.06.016
45. Krieg SM, Lioumis P, Makela JP, Wilenius J, Karhu J, Hannula H, et al. Protocol for Motor and Language Mapping by Navigated TMS in Patients and Healthy Volunteers; Workshop Report. *Acta Neurochir* (2017) 159:1187–95. doi: 10.1007/s00701-017-3187-z
46. Nadler JD, Grace J, White DA, Butters MA, Malloy PF. Laterality Differences in Quantitative and Qualitative Hooper Performance. *Arch Clin Neuropsychol* (1996) 11:223–9. doi: 10.1093/arclin/11.3.223
47. Corina DP, Gibson EK, Martin R, Poliakov A, Brinkley J, Ojemann GA. Dissociation of Action and Object Naming: Evidence From Cortical Stimulation Mapping. *Hum Brain Mapp* (2005) 24:1–10. doi: 10.1002/hbm.20063
48. Corina DP, Loudermilk BC, Detwiler L, Martin RF, Brinkley JF, Ojemann G. Analysis of Naming Errors During Cortical Stimulation Mapping: Implications for Models of Language Representation. *Brain Lang* (2010) 115:101–12. doi: 10.1016/j.bandl.2010.04.001
49. Nakajima R, Kinoshita M, Shinohara H, Nakada M. The Superior Longitudinal Fascicle: Reconsidering the Fronto-Parietal Neural Network Based on Anatomy and Function. *Brain Imaging Behav* (2020) 14:2817–30. doi: 10.1007/s11682-019-00187-4
50. Giampiccolo D, Howells H, Bährend I, Schneider H, Raffa G, Rosenstock T, et al. Preoperative Transcranial Magnetic Stimulation for Picture Naming is Reliable in Mapping Segments of the Arcuate Fasciculus. *Brain Commun* (2020) 2(2):fcaa158. doi: 10.1093/braincomms/fcaa158
51. Raffa G, Scibilia A, Conti A, Cardali SM, Rizzo V, Terranova C, et al. Multimodal Surgical Treatment of High Grade Gliomas in the Motor Area: The Impact of the Combination of Navigated Transcranial Magnetic Stimulation and Fluorescein-Guided Resection. *World Neurosurg* (2019) 128:e378-90. doi: 10.1016/j.wneu.2019.04.158
52. Raffa G, Picht T, Angileri FFFFF, Youssef M, Conti A, Esposito F, et al. Surgery of Malignant Motor-Eloquent Gliomas Guided by Sodium-Fluorescein and Navigated Transcranial Magnetic Stimulation: A Novel Technique to Increase the Maximal Safe Resection. *J Neurosurg Sci* (2019) 63(6):670–8. doi: 10.23736/S0390-5616.19.04710-6
53. Rosset A, Spadola L, Ratib O. Osirix: An Open-Source Software for Navigating in Multidimensional DICOM Images. *J Digit Imaging* (2004) 17:205–16. doi: 10.1007/s10278-004-1014-6
54. Ius T, Isola M, Budai R, Pauletto G, Tomasino B, Fadiga L, et al. Low-Grade Glioma Surgery in Eloquent Areas: Volumetric Analysis of Extent of Resection and its Impact on Overall Survival. A Single-Institution Experience in 190 Patients: Clinical Article. *J Neurosurg* (2012) 117:1039–52. doi: 10.3171/2012.8.JNS12393
55. Skrap M, Mondani M, Tomasino B, Weis L, Budai R, Pauletto G, et al. Surgery of Insular Nonenhancing Gliomas: Volumetric Analysis of Tumoral Resection, Clinical Outcome, and Survival in a Consecutive Series of 66 Cases. *Neurosurgery* (2012) 70:1081–4. doi: 10.1227/NEU.0b013e31823f5be5
56. Bloch O, Han SJ, Cha S, Sun MZ, Aghi MK, McDermott MW, et al. Impact of Extent of Resection for Recurrent Glioblastoma on Overall Survival: Clinical Article. *J Neurosurg* (2012) 117:1032–8. doi: 10.3171/2012.9.JNS12504
57. Berger MS, Deliganis AV, Dobbins J, Keles GE. The Effect of Extent of Resection on Recurrence in Patients With Low Grade Cerebral Hemisphere Gliomas. *Cancer* (1994) 74:1784–91. doi: 10.1002/1097-0142(19940915)74:6<1784::AID-CNCR2820740622>3.0.CO;2-D
58. Frey D, Schilt S, Strack V, Zdunczyk A, Rosler J, Niraula B, et al. Navigated Transcranial Magnetic Stimulation Improves the Treatment Outcome in Patients With Brain Tumors in Motor Eloquent Locations. *Neuro Oncol* (2014) 16:1365–72. doi: 10.1093/neuonc/nou110
59. Oldfield RC. The Assessment and Analysis of Handedness: The Edinburgh Inventory. *Neuropsychologia* (1971) 9:97–113. doi: 10.1016/0028-3932(71)90067-4
60. Hooper HE. The Hooper Visual Organization Test. *West Psychol Serv* (1958).
61. Wilson B, Cockburn J, Halligan PW. *The Behavioural Inattention Test*. Bury St. Edmunds, UK: Thames Valley Test Company.
62. Krivosheya D, Prabhu SS, Weinberg JS, Sawaya R. Technical Principles in Glioma Surgery and Preoperative Considerations. *J Neurooncol* (2016) 130:243–52. doi: 10.1007/s11060-016-2171-4
63. Russell SM, Elliott R, Forshaw D, Kelly PJ, Golfinos JG. Resection of Parietal Lobe Gliomas: Incidence and Evolution of Neurological Deficits in 28 Consecutive Patients Correlated to the Location and Morphological Characteristics of the Tumor. *J Neurosurg* (2005) 103:1010–7. doi: 10.3171/jns.2005.103.6.1010
64. Sanai N, Berger MS. Intraoperative Stimulation Techniques for Functional Pathway Preservation and Glioma Resection. *Neurosurg Focus* (2010) 28:E1. doi: 10.3171/2009.12.FOCUS09266

65. Duffau H. Contribution of Cortical and Subcortical Electrostimulation in Brain Glioma Surgery: Methodological and Functional Considerations. *Neurophysiol Clin* (2007) 37:373–82. doi: 10.1016/j.neucli.2007.09.003
66. Scibilia A, Terranova C, Rizzo V, Raffa G, Morelli A, Esposito F, et al. Intraoperative Neurophysiological Mapping and Monitoring in Spinal Tumor Surgery: Sirens or Indispensable Tools? *Neurosurg Focus* (2016) 41 (2):E18. doi: 10.3171/2016.5.FOCUS16141
67. Scibilia A, Raffa G, Rizzo V, Quartarone A, Visocchi M, Germanò A, et al. Intraoperative Neurophysiological Monitoring in Spine Surgery: A Significant Tool for Neuronal Protection and Functional Restoration. *Acta Neurochir Suppl* (2017) 128:263–70. doi: 10.1007/978-3-319-39546-3_38
68. Picht T, Mularski S, Kuehn B, Vajkoczy P, Kombos T, Suess O. Navigated Transcranial Magnetic Stimulation for Preoperative Functional Diagnostics in Brain Tumor Surgery. *Neurosurgery* (2009) 65:93–9. doi: 10.1227/01.NEU.0000348009.22750.59
69. Raffa G, Scibilia A, Conti A, Ricciardo G, Rizzo V, Morelli A, et al. The Role of Navigated Transcranial Magnetic Stimulation for Surgery of Motor-Eloquent Brain Tumors: A Systematic Review and Meta-Analysis. *Clin Neurol Neurosurg* (2019) 180:7–17. doi: 10.1016/j.clineuro.2019.03.003
70. Raffa G, Picht T, Scibilia A, Rösler J, Rein J, Conti A, et al. Surgical Treatment of Meningiomas Located in the Rolandic Area: The Role of Navigated Transcranial Magnetic Stimulation for Preoperative Planning, Surgical Strategy, and Prediction of Arachnoidal Cleavage and Motor Outcome. *J Neurosurg* (2019) 1:1–12. doi: 10.3171/2019.3.JNS183411
71. Raffa G, Bährend I, Schneider H, Faust K, Germanò A, Vajkoczy P, et al. A Novel Technique for Region and Linguistic Specific Ntms-Based DTI Fiber Tracking of Language Pathways in Brain Tumor Patients. *Front Neurosci* (2016) 10:552. doi: 10.3389/fnins.2016.00552
72. Raffa G, Scibilia A, Germanò A, Conti A. "Ntms-Based DTI Fiber Tracking of Motor Pathways,". In: SM Krieg, editor. *Navigated Transcranial Magnetic Stimulation in Neurosurgery*. New York, USA: Springer International Publishing (2017). p. 97–114. doi: 10.1007/978-3-319-54918-7_6
73. Mattingley JB, Bradshaw JL, Nettleton NC, Bradshaw JA. Can Task Specific Perceptual Bias be Distinguished From Unilateral Neglect? *Neuropsychologia* (1994) 32:805–17. doi: 10.1016/0028-3932(94)90019-1
74. Wright JM, Krekelberg B. Transcranial Direct Current Stimulation Over Posterior Parietal Cortex Modulates Visuospatial Localization. *J Vis* (2014) 14(9):5. doi: 10.1167/14.9.5
75. Ellison A, Ball KL, Moseley P, Dowsett J, Smith DT, Weis S, et al. Functional Interaction Between Right Parietal and Bilateral Frontal Cortices During Visual Search Tasks Revealed Using Functional Magnetic Imaging and Transcranial Direct Current Stimulation. *PloS One* (2014) 9:e93767. doi: 10.1371/journal.pone.0093767
76. Bocca F, Tollner T, Muller HJ, Taylor PC. The Right Angular Gyrus Combines Perceptual and Response-Related Expectancies in Visual Search: TMS-EEG Evidence. *Brain Stimul* (2015) 10(1):171. doi: 10.1016/j.brs.2015.02.001
77. Capotosto P, Tosoni A, Spadone S, Sestieri C, Perrucci MG, Romani GL, et al. Anatomical Segregation of Visual Selection Mechanisms in Human Parietal Cortex. *J Neurosci* (2013) 33:6225–9. doi: 10.1523/JNEUROSCI.4983-12.2013
78. Moritz CH, Johnson SC, McMillan KM, Haughton VM, Meyerand ME. Functional MRI Neuroanatomic Correlates of the Hooper Visual Organization Test. *J Int Neuropsychol Soc* (2004) 10:939–47. doi: 10.1017/S1355617704107042
79. Lopez MN, Lazar MD, Oh S. Psychometric Properties of the Hooper Visual Organization Test. *Assessment* (2003) 10:66–70. doi: 10.1177/1073191102250183
80. Lopez MN, Lazar MD, Imperio SM. A Qualitative Analysis of Inaccurate Responses on the Hooper Visual Organization Test. *Percept Mot Ski* (2005) 100:695–702. doi: 10.2466/pms.100.3.695-702
81. Whiteside D, Wald D, Busse M. Classification Accuracy of Multiple Visual Spatial Measures in the Detection of Suspect Effort. *Clin Neuropsychol* (2011) 25:287–301. doi: 10.1080/13854046.2010.538436
82. Giannakou M, Kosmidis MH. Cultural Appropriateness of the Hooper Visual Organization Test? Greek Normative Data. *J Clin Exp Neuropsychol* (2006) 28:1023–9. doi: 10.1080/13803390591004374
83. Su CY, Lin YH, Wu YY, Wuang YP. Development of the Chinese Version of the Hooper Visual Organization Test: Normative Data. *Int J Rehabil Res* (2013) 36:56–67. doi: 10.1097/MRR.0b013e3283588b95
84. Merten T, Volkel L, Dornberg K. What do Hooper-Like Tests Measure? *Appl Neuropsychol* (2007) 14:275–83. doi: 10.1080/09084280701719252
85. Merten T. Factor Structure of the Hooper Visual Organization Test: A Cross-Cultural Replication and Extension. *Arch Clin Neuropsychol* (2005) 20:123–8. doi: 10.1016/j.acn.2004.03.001
86. Corbetta M, Shulman GL. Control of Goal-Directed and Stimulus-Driven Attention in the Brain. *Nat Rev Neurosci* (2002) 3:201–15. doi: 10.1038/nrn755
87. Bartolomeo P, Thiebaut de Schotten M, Duffau H. Mapping of Visuospatial Functions During Brain Surgery: A New Tool to Prevent Unilateral Spatial Neglect. *Neurosurgery* (2007) 61:E1340. doi: 10.1227/01.neu.0000306126.46657.79
88. Hendrix P, Senger S, Simgen A, Griessenauer CJ, Oertel J. Preoperative Rtms Language Mapping in Speech-Eloquent Brain Lesions Resected Under General Anesthesia: A Pair-Matched Cohort Study. *World Neurosurg* (2017) 100:425–33. doi: 10.1016/j.wneu.2017.01.041
89. Sollmann N, Giglhuber K, Tussis L, Meyer B, Ringel F, Krieg SM. Ntms-Based DTI Fiber Tracking for Language Pathways Correlates With Language Function and Aphasia - a Case Report. *Clin Neurol Neurosurg* (2015) 136:25–8. doi: 10.1016/j.clineuro.2015.05.023
90. Hauck T, Tanigawa N, Probst M, Wohlschlaeger A, Ille S, Sollmann N, et al. Task Type Affects Location of Language-Positive Cortical Regions by Repetitive Navigated Transcranial Magnetic Stimulation Mapping. *PloS One* (2015) 10:e0125298. doi: 10.1371/journal.pone.0125298
91. Hauck T, Tanigawa N, Probst M, Wohlschlaeger A, Ille S, Sollmann N, et al. Stimulation Frequency Determines the Distribution of Language Positive Cortical Regions During Navigated Transcranial Magnetic Brain Stimulation. *BMC Neurosci* (2015) 16:5. doi: 10.1186/s12868-015-0143-9
92. Kaus M, Steinmeier R, Sporer T, Ganslandt O, Fahlbusch R. Technical Accuracy of a Neuronavigation System Measured With a High-Precision Mechanical Micromanipulator. *Neurosurgery* (1997) 41:1431–7. doi: 10.1097/00006123-199712000-00046
93. Orringer DA, Golby A, Jolesz F. Neuronavigation in the Surgical Management of Brain Tumors: Current and Future Trends. *Expert Rev Med Devices* (2012) 9:491–500. doi: 10.1586/erd.12.42
94. Lu S, Ahn D, Johnson G, Cha S. Peritumoral Diffusion Tensor Imaging of High-Grade Gliomas and Metastatic Brain Tumors. *AJNR Am J Neuroradiol* (2003) 24:937–41.
95. Yen PS, Teo BT, Chiu CH, Chen SC, Chiu TL, Su CF. White Matter Tract Involvement in Brain Tumors: A Diffusion Tensor Imaging Analysis. *Surg Neurol* (2009) 72:464–9. doi: 10.1016/j.surneu.2009.05.008
96. Nimsky C, Ganslandt O, Hastreiter P, Wang R, Benner T, Sorensen AG, et al. Preoperative and Intraoperative Diffusion Tensor Imaging-Based Fiber Tracking in Glioma Surgery. *Neurosurgery* (2005) 56:130–7. doi: 10.1227/01.NEU.0000144842.18771.30
97. Bozzao A, Romano A, Angelini A, D'Andrea G, Calabria LF, Coppola V, et al. Identification of the Pyramidal Tract by Neuronavigation Based on Intraoperative Magnetic Resonance Tractography: Correlation With Subcortical Stimulation. *Eur Radiol* (2010) 20:2475–81. doi: 10.1007/s00330-010-1806-7
98. Romano A, D'Andrea G, Calabria LF, Coppola V, Espagnet CR, Pierallini A, et al. Pre- and Intraoperative Tractographic Evaluation of Corticospinal Tract Shift. *Neurosurgery* (2011) 69:695–6. doi: 10.1227/NEU.0b013e31821a8555
99. Bello L, Castellano A, Fava E, Casaceli G, Riva M, Scotti G, et al. Intraoperative Use of Diffusion Tensor Imaging Fiber Tractography and Subcortical Mapping for Resection of Gliomas: Technical Considerations. *Neurosurg Focus* (2010) 28:E6. doi: 10.3171/2009.12.FOCUS09240
100. Bette S, Wiestler B, Wiedenmann F, Kaesmacher J, Bretschneider M, Barz M, et al. Safe Brain Tumor Resection Does Not Depend on Surgery Alone - Role of Hemodynamics. *Sci Rep* (2017) 7:5585. doi: 10.1038/s41598-017-05767-2
101. Jakola AS, Berntsen EM, Christensen P, Gulati S, Unsgård G, Kvistad KA, et al. Surgically Acquired Deficits and Diffusion Weighted MRI Changes After Glioma Resection - a Matched Case-Control Study With Blinded Neuroradiological Assessment. *PloS One* (2014) 9:e101805. doi: 10.1371/journal.pone.0101805

102. Bette S, Wiestler B, Kaesmacher J, Huber T, Gerhardt J, Barz M, et al. Infarct Volume After Glioblastoma Surgery as an Independent Prognostic Factor. *Oncotarget* (2016) 7(38):61945–54. doi: 10.18632/oncotarget.11482
103. Germanò A, Priola S, Angileri FF, Conti A, La Torre D, Cardali S, et al. Long-Term Follow-Up of Ruptured Intracranial Aneurysms Treated by Microsurgical Wrapping With Autologous Muscle. *Neurosurg Rev* (2013) 36:123–32. doi: 10.1007/s10143-012-0408-z
104. Merlo L, Cimino F, Scibilia A, Ricciardi E, Chirafisi J, Speciale A, et al. Simvastatin Administration Ameliorates Neurobehavioral Consequences of Subarachnoid Hemorrhage in the Rat. *J Neurotrauma* (2011) 28:2493–501. doi: 10.1089/neu.2010.1624
105. Kamiya-Matsuoka C, Cachia D, Yust-Katz S, Rodriguez YA, Garciarena P, Rodarte EM, et al. Ischemic Stroke in Patients With Gliomas at the University of Texas-M.D. Anderson Cancer Center. *J Neurooncol* (2015) 125:143–8. doi: 10.1007/s11060-015-1880-4

Conflict of Interest: The authors declare that the research was conducted in the absence of any commercial or financial relationships that could be construed as a potential conflict of interest.

frontiers in Neurology

OPINION
published: 28 June 2021
doi: 10.3389/fneur.2021.687030

Novel Asleep Techniques for Intraoperative Assessment of Brain Connectivity

Francesco Sala[1]*, *Davide Giampiccolo*[1] and *Luigi Cattaneo*[2]

[1] Section of Neurosurgery, Department of Neuroscience, Biomedicine and Movement Sciences, University of Verona, Verona, Italy, [2] CIMeC - Center for Mind/Brain Sciences, University of Trento, Trento, Italy

Keywords: intraoperative neurophysiological monitoring, motor evoked potentials, cortico-cortical evoked potentials, neuro-oncology – surgical, brain mapping

OPEN ACCESS

Edited by:
Antonino F. Germano',
University of Messina, Italy

Reviewed by:
Giuseppe Maria Della Pepa,
Fondazione Policlinico Universitario Agostino Gemelli IRCSS, Italy
domenico D'Avella,
University of Padua, Italy

***Correspondence:**
Francesco Sala
francesco.sala@univr.it

Specialty section:
This article was submitted to Neuro-Oncology and Neurosurgical Oncology, a section of the journal Frontiers in Neurology

Received: *28 March 2021*
Accepted: *26 May 2021*
Published: *28 June 2021*

Citation:
Sala F, Giampiccolo D and Cattaneo L (2021) Novel Asleep Techniques for Intraoperative Assessment of Brain Connectivity. Front. Neurol. 12:687030. doi: 10.3389/fneur.2021.687030

INTRODUCTION

State of the Art in Intraoperative Monitoring for Neurosurgery and Current Limitations

From the pioneering work of neurosurgeon-neuroscientists such as Otfried Foerster and Wilder Penfield, mapping of brain function using electrical stimulation has allowed to identify and spare motor behavior and language during awake surgery, producing the first cartographies of the brain cortex (1, 2). This has been refined in the early 2000s as neurosurgeons started routine subcortical awake mapping using white matter tracts as subcortical boundaries (3), with subsequent improvement in both functional (4) and surgical outcome (5, 6). The advantages of performing awake surgery when cognitive functions are at risk, should not be questioned, and we remark this should be performed whenever feasible. However, patients with pre-existing neurological deficits and/or inadequate neuropsychological profiles are not good candidates for awake surgery, and therefore must undergo asleep procedures. Notably, pediatric patients cannot undergo awake surgery, on one hand because of their scarce compliance (7), on the other hand because the immaturity of their motor system makes the cortex almost inexcitable using the traditional bipolar Penfield's 50/60 Hz technique (8, 9).

In patients who are poor candidates for awake surgery, developing methods to map cortico-cortical and cortico-subcortical connectivity under anesthesia is of primary importance since otherwise surgery will be performed blind to function, with higher risk of incurring into neurological deficits. Since the adoption of somatosensory evoked potentials (SEPs) in the '70s (10) and particularly with the development of the train-of-five motor evoked potential (MEP) technique (11), the field of intraoperative neurophysiological monitoring (IONM) has specifically addressed the issue of mapping and monitoring during asleep anesthesia. Standard protocols for motor mapping are nowadays available, offering reproducible, and reliable parameters to qualitatively and quantitatively predict outcome (12). This somehow differed from awake surgery, where neuropsychological tests and mapping protocols have a greater degree of variability. In brain tumor surgery IONM is particularly well-established for preservation of the corticospinal tract (13, 14), but asleep mapping and monitoring outside the corticospinal system is lacking. The aim of this opinion paper is to discuss two novel potential IONM techniques allowing to map and monitor functions beyond corticospinal motor function in the anesthetized setting, namely, (A) conditioning of motor output (15, 16) and (B) cortico-cortical evoked potentials (17, 18). These have been performed under total intravenous anesthesia using Propofol (100–150 μg/kg/min) and Fentanyl (1 μg/kg/min) in continuous infusion, and avoiding muscle relaxants after intubation.

Potential Novel Intraoperative Measures of Brain Connectivity in the Anesthetized Patient

Conditioning of Corticospinal Output

The conditioning stimulus (CS)/test stimulus (TS) paradigms have been used widely in experimental and clinical neurophysiology to investigate functional connectivity between two regions of the nervous system. In CS/TS paradigms (illustrated in panel A of **Figure 1**), a suprathreshold stimulus (TS) is delivered to the motor cortex, thus evoking a motor potential (MEP) of a given amplitude. The CS, of intensity comparable to that of the TS, is delivered to a region that is supposedly connected to the motor cortex but is not itself a source of corticospinal output. Therefore, the CS alone does not produce a MEP. However, when the CS precedes the TS, the MEP obtained by the conditioned TS may be different (i.e., increased or decreased MEP amplitude) from that obtained by TS alone. Whenever such remote effects of CS on TS occur, they are taken as evidence of functional connectivity between the site of application of the CS and that of the TS. The CS-TS interactions are generally specific for given inter-stimulus intervals (ISI), i.e., the time interval between CS and TS. Conditioning effects of the CS over the TS at short ISIs is generally thought to be informative of the underlying anatomical connections: interactions at short ISIs indicate direct cortico-cortical connections.

CS/TS paradigms are commonly explored using non-invasive brain stimulation, namely transcranial magnetic stimulation (TMS) applied with two different coils over the scalp, one delivering the CS and the other delivering the TS over the motor cortex (20). These paradigms have been extensively reviewed by Koch (21). The modulatory effect of CS can be excitatory or inhibitory, therefore increasing or decreasing MEP amplitude compared to TS alone. However, as MEP amplitude can physiologically vary between two identical stimuli, it is important to repeat both TS stimulations and CS+TS stimulation. Therefore, the comparison between CS+TS MEPs and MEPs to TS alone cannot be done between single MEPs, but must be performed between groups of conditioned (CS+TS) MEPs and of baseline (TS alone) MEPs.

The descending corticospinal volley evoked by stimulation of the motor cortex has different components, separated in time. The earliest volley is referred to as direct, or "D" wave and is due to direct activation of corticospinal axons. The later components, known as indirect or "I" waves originate from stimulation of neurons that in turn project onto the corticospinal neurons, which are therefore activated trans-synaptically (22).

Abbreviations: AF, arcuate fasciculus; CCEPs, Cortico-cortical evoked potentials; CS, conditioning stimulus; CST, cortico-spinal tract; DES, direct electrical stimulation; DTI, diffusion tensor imaging; DWI, diffusion weighted imaging; ECoG, electrocorticography; EEG, electroencephalography; EMG, electromyography; HARDI, high angular resolution diffusion imaging; ISI, interstimulus interval; IONM, intraoperative neurophysiological monitoring; MEPs, motor evoked potentials; MFG, middle frontal gyrus; mFUSA, middle fusiform gyrus; MTG, middle temporal gyrus; pOP, pars opercularis; pTRI, pars triangularis; STG, superior temporal gyrus; TOj, temporo-occipital junction; To5, train-of-five stimulation; TS, test stimulus; vPM, ventral premotor cortex; ITG, inferior temporal gyrus.

It is important to note that for the TS to be susceptible to modulation by the CS, it must produce a corticospinal volley containing I-waves, as the D-wave cannot be modulated by any afferents to the corticospinal neuron because it is generated downstream of any point of integration of inputs from cortico-cortical afferents. Indeed, direct cortical stimulation and intraoperative transcranial electrical stimulation are known to produce I-waves (23–25).

We propose that the CS/TS approach can be successfully performed also by means of direct cortical stimulation in the intraoperative setting, and therefore potentially be used for assessing and potentially monitoring the integrity of specific brain and spine connections, as demonstrated by two recent works from our group, on parietal-motor connectivity (15) and on cerebello-motor connectivity (16).

In the first **work** we described the successful use of a CS/TS paradigm in the intraoperative setting to explore putative direct parietal-motor connectivity (15) (**Figure 1B**). Briefly, two strip electrodes were deployed, one over the parietal cortex (CS) and one over the motor cortex (TS). Conditioning stimuli in the parietal cortex were always delivered in a short train of 2 stimuli at 250 Hz and of 0.5 ms duration while test stimulus varied from a single stimulus to a train of 3 stimuli at 250 Hz and 0.5 ms duration according to the individual patient's cortical excitability. Stimulation intensity for conditioning and test stimulation was always the same (15–35 mA). Prior to all experimental stimulations we acquired blocks of conditioning stimuli alone, verifying that no MEP could be observed from test stimulation

Such functional connectivity has been abundantly described by means of dual coil TMS in healthy participants (20, 26). In our study we highlighted the presence of conditioning effects from CS applied *directly* to the posterior parietal cortex on the TS applied *directly* to the ipsilateral upper limb motor cortex, in 17 anesthetized oncological patients during surgical resection. The conditioning effects on the TS were specific for both timing and anatomical localization of the CS. The effects appeared at short ISIs (4–20 ms) with the earliest effective ISI depending on the anatomical proximity of the parietal stimulation electrode to the motor cortex: short ISIs were efficient when the CS was delivered near to the motor cortex. The use of trains of stimuli to stimulate the motor cortex renders timing of the CS/TS ISI difficult. In general we considered, for the sake of timing, the last stimulus of the train as the one that is effective in triggering the efferent corticofugal volley (27). Anatomical specificity was clearly evident in the spatial clustering of CS sites with excitatory effects in the inferior parietal lobule and of CS sites with inhibitory effects in the superior parietal lobule. Note that focality of CS stimulation was granted by the use of bipolar stimulation between adjacent electrodes of a stimulating strip.

In the second **work** we tested the effects of CS applied to the cerebellar cortex onto corticospinal excitability (16), tested by TS applied *transcranially* to target the upper limb motor cortex (**Figure 1C**) in 10 anesthetized patients undergoing posterior fossa tumor surgery. Our experimental paradigm is inspired by a well-established CS+TS technique referred to as

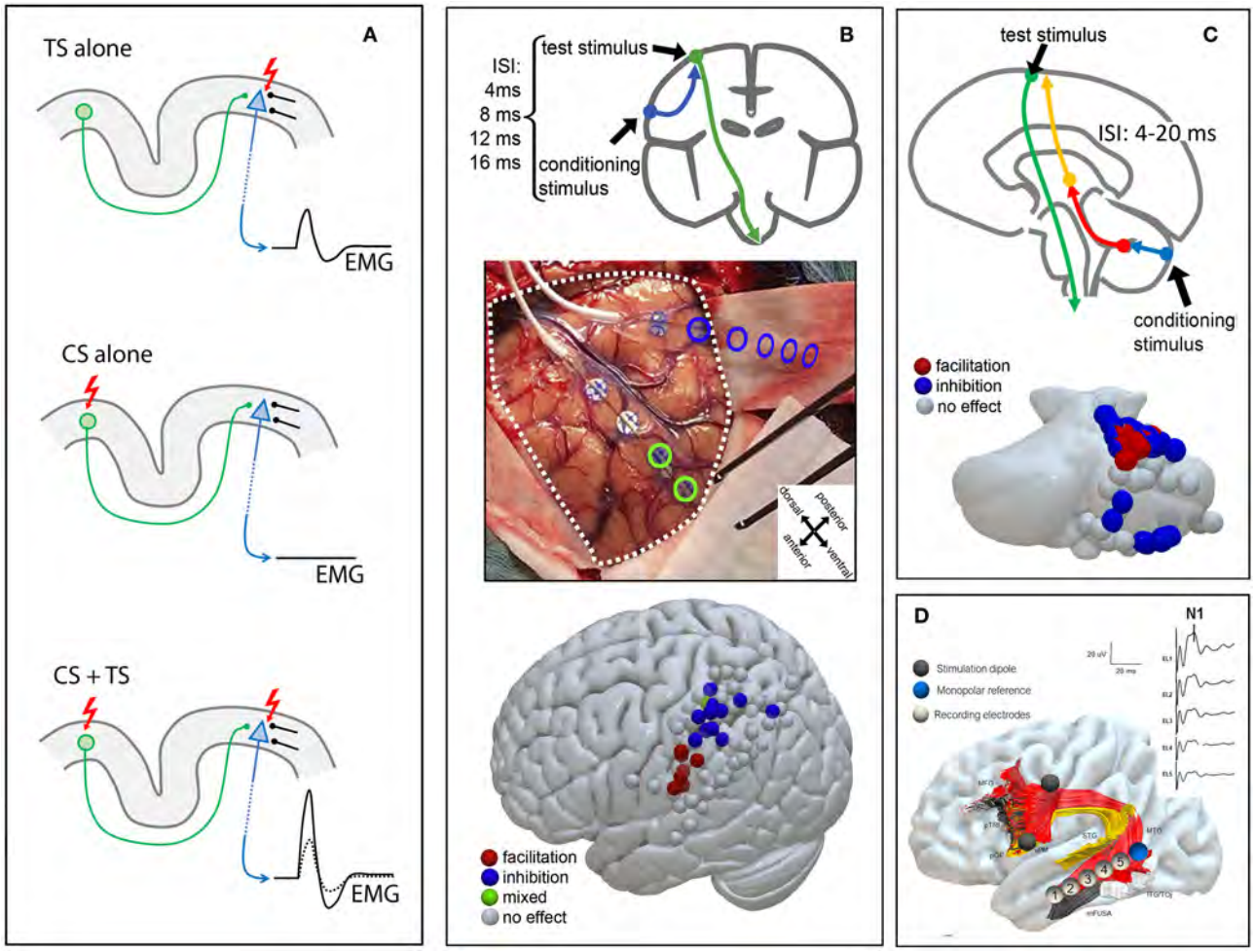

FIGURE 1 | Schematic CS/TS and ccEP paradigms. **(A)** *Upper panel* TS stimulation alone induces an MEP; *middle panel* CS stimulation alone does not evoke an MEP; *lower panel* combined CS + TS stimulation leads to increased MEP amplitude. *CS, conditioning stimulus; TS, test stimulus* **(B)** Parieto-motor stimulation protocol: a CS stimulus is applied over the posterior parietal cortex from 4 to 16 ms before a TS on M1. A dorso-ventral posterior parietal distinction between MEP inhibition (dorsal) and MEP facilitation (ventral) is shown. The picture is modified from (15) with permission *CS, conditioning stimulus; TS, test stimulus* **(C)** Cerebello-motor stimulation protocol: direct cerebellar precedes transcranial electrical stimulation with an inter-stimulus interval (ISI) of 4–20 ms, causing MEP inhibition (blue) or facilitation (red). **(D)** ccEPs for the arcuate fasciculus: strip electrodes are placed intraoperatively at cortical termination of the arcuate fasciculus after preoperative testing. ccEPs are recorded from the middle temporal cortical termination of the arcuate fasciculus (shown on the right side). Segments of the arcuate fasciculus are dissected according to cortical termination (19). *MFG, middle frontal gyrus; pTRI, pars triangularis; pOP, pars opercularis; vPM, ventral premotor cortex; STG, superior temporal gyrus; MTG, middle temporal gyrus; ITG, inferior temporal gyrus; TOj, temporo-occipital junction; mFUSA, middle fusiform gyrus*.

"cerebellar inhibition" in which the cerebellum and the motor cortex are stimulated by TMS (28, 29). Briefly, conditioning stimuli on the cerebellar cortex were delivered in a short train of 2–5 stimuli at 250 Hz and of 0.5 ms duration with an intensity of 15–25 ms. Test stimuli varied from a train of 2–5 stimuli at 250 Hz and 0.5 ms duration with stimulation intensity of 15–35 mA. Our results showed that CS cerebellar stimuli conditioned at short ISIs the corticospinal excitability, with a significant anatomical specificity: cerebellar CS exerted conditioning effects on the hand corticospinal system when applied to regions of the cerebellar cortex in the anterior and posterior lobule that are known to contain hand representations (30, 31).

Cortico-Cortical Evoked Potentials in the Anaesthetized Patient

While the rationale for describing brain connectivity by means of ccEPs was first discussed by Lord Adrian (32), the clinical use of cortico-cortical evoked potentials was first pioneered by Matsumoto (33). In ccEPs, one of two cortical terminations of a white matter tract is stimulated electrically, and cortical evoked activity is recorded at the other termination in the form of evoked potentials. Twenty to 120 raw traces are conventionally averaged, similarly to cortically recorded somatosensory evoked potentials. ccEPs show two components, an N1 between 20 and 30 ms (33, 34) and a second, later component peaking at 100–150 ms (33), though some authors claim this later component

could represent epileptogenic activity instead (35). CcEPs latency should reflect fiber myelination and length (33, 36). Moreover, there is strong evidence for directionality in the evoked potentials (37, 38). The recording of ccEPs is potentially applicable to the whole cerebral cortex and transcends language function (39, 40). However, clinical use of this technique has been historically mainly related to language function.

The recording of ccEPs is generally limited to awake patients, because of (a) the suppression of neural activity due to anesthesia (41), and (b) the chance to identify location for strip electrodes placement using functional mapping (33, 42). However, their use is of potential interest in monitoring white matter integrity also in the asleep patient. In a recent work in a cohort of 9 patients with tumors in the left perisylvian area who could not undergo awake surgery, we recorded ccEPs of the arcuate fascicle in anesthetized patients undergoing tumor surgery (18). Results indicated that (a) reliable potentials of small amplitude can be obtained from the arcuate fasciculus also under anesthesia and that (b) strip electrode placement can be made more effective by combining tractographic MR information and presurgical neuronavigated TMS (nTMS). Results in the asleep setting resembled those in the awake setting: an N1 potential with a latency of 21 ms was shown, together with an earlier positive potential peaking at 12 ms. In our series, evoked potentials clustered in the middle temporal gyrus while stimulation mainly covered the ventral premotor cortex. Although the arcuate fasciculus has cortical terminations over superior, middle and inferior temporal gyri (43, 44), such selectivity may be justified by a layered distribution of its components, particularly in a ventral/dorsal fashion (19, 44). Indeed, ccEP responses for this tract may support this, since location for optimal recorded responses varies according to the stimulated gyrus in the frontal lobe (45). Moreover, the inferior temporal gyrus components of the arcuate fasciculus have not been extensively investigated in this study, which is another limitation to be taken into account.

CONCLUSION AND LIMITATIONS

Asleep surgery without mapping is blind to function and therefore at highest risk of inducing neurological deficits. We believe it is an ethical responsibility to raise awareness of this issue. Therefore, the work presented here lies on this foundation and the attempt to predict, and therefore prevent, neurological deficits in patients who are not good candidates to an awake craniotomy.

However, to be useful in clinical practice these techniques require to (a) be standardized; (b) be deterministic, i.e., allow predictions in individual patients; (c) have a strong predictive value of a given clinical/behavioral aspect. The phenomena that we have described do not satisfy any of the above criteria, therefore further research is needed before a clinical use, if any, can be proposed. Points (a) and (b) require extensive tests for standardization and reproducibility. Regarding point (c), we believe that cortico-motor CS/TS paradigms should be tested also from a constellation of other areas that project the motor cortex, namely the premotor, supplementary motor and somatosensory cortices and their perioperative changes need to be correlated with behavior such as skilled movement and sensorimotor behavior in general. The cerebello-motor CS/TS paradigm's predictive value should be tested specifically on the pediatric population undergoing posterior fossa surgery. This is of overriding importance, as individual age-associated myelination and axonal length (9) may imply significant changes in the optimal parameters (ISI, stimulation intensity) for cerebello-cortical modulation. Similarly, ccEPs for language connectivity should be tested for their predictive value in perioperative language disorders.

AUTHOR CONTRIBUTIONS

FS, DG, and LC: conceptualization and writing - original draft. FS: funding acquisition. FS and LC: supervision. All authors contributed to the article and approved the submitted version.

FUNDING

This work was supported by the grant NEUROCONNECT issued to FS by the Fondazione Cassa di Risparmio di Verona.

REFERENCES

1. Vogt C, and Vogt O. Die vergleichend-architektonische und die vergleichend-reizphysiologische Felderung der Großhirnrinde unter besonderer Berücksichtigung der menschlichen. *Naturwissenschaften* (1926) 14:1190–4.
2. Foerster O, Penfield W. The structural basis of traumatic epilepsy and results of radical operation. *Brain*. (1930) 53:99–119. doi: 10.1093/brain/53.2.99n
3. Duffau H, Capelle L, Denvil D, Sichez N, Gatignol P, Lopes M, et al. Functional recovery after surgical resection of low grade gliomas in eloquent brain: hypothesis of brain compensation. *J Neurol Neurosurg Psychiatry*. (2003) 74:901–7. doi: 10.1136/jnnp.74.7.901n
4. De Witt Hamer PC, Robles SG, Zwinderman AH, Duffau H, Berger MS. Impact of intraoperative stimulation brain mapping on glioma surgery outcome: a meta-analysis. *J Clin Oncol*. (2012) 30:2559–65. doi: 10.1200/JCO.2011.38.4818n
5. Darlix A, Rigau V, Fraisse J, Gozé C, Fabbro M, Duffau H. Postoperative follow-up for selected diffuse low-grade gliomas with WHO grade III/IV foci. *Neurology*. (2020) 94:e830–41. doi: 10.1212/WNL.0000000000008877n
6. Rossi M, Gay L, Ambrogi F, Nibali MC, Sciortino T, Puglisi G, et al. Association of supratotal resection with progression-free survival, malignant transformation, and overall survival in lower-grade gliomas. *Neuro Oncol*. (2020) 23:812–26. doi: 10.1093/neuonc/noaa225n
7. Gallentine WB, Mikati MA. Intraoperative electrocorticography and cortical stimulation in children. *J Clin Neurophysiol*. (2009) 26:95–108. doi: 10.1097/WNP.0b013e3181a0339dn
8. Ojemann SG, Berger MS, Lettich E, Ojemann GA. Localization of language function in children: results of electrical stimulation mapping. *J Neurosurg*. (2003) 98:465–70. doi: 10.3171/jns.2003.98.3.0465n
9. Sala F, Manganotti P, Grossauer S, Tramontanto V, Mazza C, Gerosa M. Intraoperative neurophysiology of the motor system in children: a tailored approach. *Child's Nerv Syst*. (2010) 26:473–90. doi: 10.1007/s00381-009-1081-6n
10. Tamaki T, Yamashita T, Kobayashi H. Spinal cord monitoring. *Jpn J Electroenceph Electromyogr*. (1972) 1:196n
11. Taniguchi M, Cedzich C, Schramm J. Modification of cortical stimulation for motor evoked potentials under general anesthesia: technical description. *Neurosurgery*. (1993) 32:219–26. doi: 10.1227/00006123-199302000-00011n

12. Seidel K, Beck J, Stieglitz L, Schucht P, Raabe A. The warning-sign hierarchy between quantitative subcortical motor mapping and continuous motor evoked potential monitoring during resection of supratentorial brain tumors. *J Neurosurg.* (2013) 118:287–96. doi: 10.3171/2012.10.JNS12895n
13. Neuloh G, Pechstein U, Schramm J. Motor tract monitoring during insular glioma surgery. *J Neurosurg.* (2007) 106:582–92. doi: 10.3171/jns.2007.106.4.582n
14. Giampiccolo D, Parisi C, Meneghelli P, Tramontano V, Basaldella F, Pasetto M, et al. Long-term motor deficit in brain tumor surgery with preserved intraoperative motor evoked potentials. *Brain Commun.* (2021) 3:fcaa226. doi: 10.1093/braincomms/fcaa226n
15. Cattaneo L, Giampiccolo D, Meneghelli P, Tramontano V, Sala F. Cortico-cortical connectivity between the superior and inferior parietal lobules and the motor cortex assessed by intraoperative dual cortical stimulation. *Brain Stimul.* (2020) 13:819–31. doi: 10.1016/j.brs.2020.02.023n
16. Giampiccolo D, Basaldella F, Badari A, Squintani M, Cattaneo L, Sala F. Feasibility of cerebello-cortical stimulation for intraoperative neurophysiological monitoring of cerebellar mutism. *Child's Nerv Syst.* (2021) 37:1505–14. doi: 10.1007/s00381-021-05126-7n
17. Yamao Y, Matsumoto R, Kunieda T, Arakawa Y, Kobayashi K, Usami K, et al. Intraoperative dorsal language network mapping by using single-pulse electrical stimulation. *Hum Brain Mapp.* (2014) 35:4345–61. doi: 10.1002/hbm.22479n
18. Giampiccolo D, Parmigiani S, Basaldella F, Russo S, Pigorini A, Rosanova M, et al. Recording cortico-cortical evoked potentials of the human arcuate fasciculus under general anaesthesia. *Clin Neurophysiol.* (2021) 132:1332–3 doi: 10.1016/j.clinph.2021.03.044n
19. Fernández-Miranda JC, Wang Y, Pathak S, Stefaneau L, Verstynen T, Yeh FC. Asymmetry, connectivity, and segmentation of the arcuate fascicle in the human brain. *Brain Struct Funct.* (2015) 220:1665–80. doi: 10.1007/s00429-014-0751-7n
20. Koch G, Fernandez Del Olmo M, Cheeran B, Ruge D, Schippling S, Caltagirone C, et al. Focal stimulation of the posterior parietal cortex increases the excitability of the ipsilateral motor cortex. *J Neurosci.* (2007) 27:6815–22. doi: 10.1523/JNEUROSCI.0598-07.2007n
21. Koch G. Cortico-cortical connectivity: the road from basic neurophysiological interactions to therapeutic applications. *Exp Brain Res.* (2020) 238:1677–84. doi: 10.1007/s00221-020-05844-5n
22. Patton HD, Amassian VE. Single- and multiple-unit analysis of cortical stage of pyramidal tract activation. *J Neurophysiol.* (1954) 17:345–63. doi: 10.1152/jn.1954.17.4.345n
23. Yamamoto T, Katayama Y, Nagaoka T, Kobayashi K, Fukaya C. Intraoperative monitoring of the corticospinal motor evoked potential (D-wave): clinical index for postoperative motor function and functional recovery. *Neurol Med Chir.* (2004) 44:170–82. doi: 10.2176/nmc.44.170n
24. Fujiki M, Furukawa Y, Kamida T, Anan M, Inoue R, Abe T, et al. Intraoperative corticomuscular motor evoked potentials for evaluation of motor function: a comparison with corticospinal D and I waves. *J Neurosurg.* (2006) 104:85–92. doi: 10.3171/jns.2006.104.1.85n
25. Deletis V, Sala F. Intraoperative neurophysiological monitoring of the spinal cord during spinal cord and spine surgery: a review focus on the corticospinal tracts. *Clin Neurophysiol.* (2008) 119:248–64. doi: 10.1016/j.clinph.2007.09.135n
26. Hallett M, Di Iorio R, Rossini PM, Park JE, Chen R, Celnik P, et al. Contribution of transcranial magnetic stimulation to assessment of brain connectivity and networks. *Clin Neurophysiol.* (2017) 128:2125–39. doi: 10.1016/j.clinph.2017.08.007n
27. Deletis V, Rodi Z, Amassian VE. Neurophysiological mechanisms underlying motor evoked potentials in anesthetized humans. Part 2. relationship between epidurally and muscle recorded MEPs in man. *Clin Neurophysiol.* (2001) 112:445–52. doi: 10.1016/S1388-2457(00)00557-5n
28. Ugawa Y, Uesaka Y, Terao Y, Hanajima R, Kanazawa I. Magnetic stimulation over the cerebellum in humans. *Ann Neurol.* (1995) 37:703–13. doi: 10.1002/ana.410370603n
29. Daskalakis ZJ, Paradiso GO, Christensen BK, Fitzgerald PB, Gunraj C, Chen R. Exploring the connectivity between the cerebellum and motor cortex in humans. *J Physiol.* (2004) 557:689–700. doi: 10.1113/jphysiol.2003.059808n
30. Grodd W, Hülsmann E, Lotze M, Wildgruber D, Erb M. Sensorimotor mapping of the human cerebellum: fMRI evidence of somatotopic organization. *Hum Brain Mapp.* (2001) 13:55–73. doi: 10.1002/hbm.1025n
31. Manni E, Petrosini L. A century of cerebellar somatotopy: a debated representation. *Nat Rev Neurosci.* (2004) 5:241–9. doi: 10.1038/nrn1347n
32. Adrian ED. The spread of activity in the cerebral cortex. *J Physiol.* (1936) 88:127–61. doi: 10.1113/jphysiol.1936.sp003427n
33. Matsumoto R, Nair DR, LaPresto E, Najm I, Bingaman W, Shibasaki H, et al. Functional connectivity in the human language system: a cortico-cortical evoked potential study. *Brain.* (2004) 127:2316–30. doi: 10.1093/brain/awh246n
34. Keller CJ, Bickel S, Entz L, Ulbert I, Milham MP, Kelly C, et al. Intrinsic functional architecture predicts electrically evoked responses in the human brain. *Proc Natl Acad Sci USA.* (2011) 108:10308–13. doi: 10.1073/pnas.1019750108n
35. Valentin A, Anderson M, Alarcon G, Seoane JG, Selway R, Binnie CD, et al. Responses to single pulse electrical stimulation identify epileptogenesis in the human brain *in vivo*. *Brain.* (2002) 125:1709–18. doi: 10.1093/brain/awf187n
36. Silverstein BH, Asano E, Sagiura A, Sonoda M, Lee, M.-H, Jeong J.-W. Dynamic tractography: integrating cortico-cortical evoked potentials and diffusion imaging. *Neuroimage.* (2020) 215:116763. doi: 10.1016/j.neuroimage.2020.116763n
37. Entz L, Tóth E, Keller CJ, Bickel S, Groppe DM, Fab,ó D, et al. Evoked effective connectivity of the human neocortex. *Hum Brain Mapp.* (2014) 35:5736–53. doi: 10.1002/hbm.22581n
38. Shine JM, Kucyi A, Foster BL, Bickel S, Wang D, Liu H, et al. Distinct patterns of temporal and directional connectivity among intrinsic networks in the human brain. *J Neurosci.* (2017) 37:9667–74. doi: 10.1523/JNEUROSCI.1574-17.2017n
39. Matsumoto R, Nair DR, LaPresto E, Bingaman W, Shibasaki H, Lüders HO. Functional connectivity in human cortical motor system: a cortico-cortical evoked potential study. *Brain.* (2007) 130:181–97. doi: 10.1093/brain/awl257n
40. Enatsu R, Gonzalez-Martinez J, Bulacio J, Kubota Y, Mosher J, Burgess RC, et al. Connections of the limbic network: a corticocortical evoked potentials study. *Cortex.* (2015) 62:20–33. doi: 10.1016/j.cortex.2014.06.018n
41. Suzuki Y, Enatsu R, Kanno A, Yokoyama R, Suzuki H, Tachibana S, et al. The Influence of anesthesia on corticocortical evoked potential monitoring network between frontal and temporoparietal cortices. *World Neurosurg.* (2019) 123:e685–92. doi: 10.1016/j.wneu.2018.11.253n
42. Saito T, Tamura M, Muragaki Y, Maruyama T, Kubota Y, Fukuchi S, et al. Intraoperative cortico-cortical evoked potentials for the evaluation of language function during brain tumor resection: initial experience with 13 cases. *J. Neurosurg.* (2014) 121:827–38. doi: 10.3171/2014.4.JNS131195n
43. Martino J, De Witt Hamer PC, Berger MS, Lawton MT, Arnold CM, De Lucas EM, et al. Analysis of the subcomponents and cortical terminations of the perisylvian superior longitudinal fasciculus: a fiber dissection and DTI tractography study. *Brain Struct Funct.* (2013) 218:105–21. doi: 10.1007/s00429-012-0386-5n
44. Yagmurlu K, Middlebrooks EH, Tanriover N, Rhoton AL. Fiber tracts of the dorsal language stream in the human brain. *J Neurosurg.* (2016) 124:1396–405. doi: 10.3171/2015.5.JNS15455n
45. Nakae T, Matsumoto R, Kunieda T, Arakawa Y, Kobayashi K, Shimotake A, et al. Connectivity gradient in the human left inferior frontal gyrus: intraoperative cortico-cortical evoked potential study. *Cereb Cortex.* (2020) 30:4633–50. doi: 10.1093/cercor/bhaa065n

Conflict of Interest: The authors declare that the research was conducted in the absence of any commercial or financial relationships that could be construed as a potential conflict of interest.

frontiers in Neurology

ORIGINAL RESEARCH
published: 26 August 2021
doi: 10.3389/fneur.2021.673836

Cortical Excitability and Connectivity in Patients With Brain Tumors

Vincenzo Rizzo[1], Carmen Terranova[1], Giovanni Raffa[2], Salvatore Massimiliano Cardali[2], Filippo Flavio Angileri[2], Giuseppina Marzano[1], Maria Catena Quattropani[1], Antonino Germanò[2], Paolo Girlanda[1] and Angelo Quartarone[3]*

[1] Department of Clinical and Experimental Medicine, University of Messina, Messina, Italy, [2] Division of Neurosurgery, BIOMORF Department, University of Messina, Messina, Italy, [3] Department of Biomedical Science and Morphological and Functional Images, University of Messina, Messina, Italy

Background: Brain tumors can cause different changes in excitation and inhibition at the neuronal network level. These changes can be generated from mechanical and cellular alterations, often manifesting clinically as seizures.

Objective/Hypothesis: The effects of brain tumors on cortical excitability (CE) have not yet been well-evaluated. The aim of the current study was to further investigate cortical–cortical and cortical–spinal excitability in patients with brain tumors using a more extensive transcranial magnetic stimulation protocol.

Methods: We evaluated CE on 12 consecutive patients with lesions within or close to the precentral gyrus, as well as in the subcortical white matter motor pathways. We assessed resting and active motor threshold, short-latency intracortical inhibition (SICI), intracortical facilitation (ICF), short-latency afferent inhibition (SAI), long-latency afferent inhibition, cortical silent period, and interhemispheric inhibition.

Results: CE was reduced in patients with brain tumors than in healthy controls. In addition, SICI, ICF, and SAI were lower in the affected hemisphere compared to the unaffected and healthy controls.

Conclusions: CE is abnormal in hemispheres affected by brain tumors. Further studies are needed to determine if CE is related with motor impairment.

Keywords: cortical excitability, brain tumors, transcranial magnetic stimulation, motor function, recovery

OPEN ACCESS

Edited by:
Pierpaolo Peruzzi, Brigham and Women's Hospital and Harvard Medical School, United States

Reviewed by:
Claudia Katharina Petritsch, Stanford University, United States
Tomofumi Yamaguchi, Juntendo University, Japan

****Correspondence:***
Vincenzo Rizzo
enzo.rizzo@gmail.com

Specialty section:
This article was submitted to Neuro-Oncology and Neurosurgical Oncology, a section of the journal Frontiers in Neurology

Received: *28 February 2021*
Accepted: *29 June 2021*
Published: *26 August 2021*

Citation:
Rizzo V, Terranova C, Raffa G, Cardali SM, Angileri FF, Marzano G, Quattropani MC, Germanò A, Girlanda P and Quartarone A (2021) Cortical Excitability and Connectivity in Patients With Brain Tumors. Front. Neurol. 12:673836. doi: 10.3389/fneur.2021.673836

INTRODUCTION

The "maximal safe resection" represents the goal standard of the modern surgical treatment of brain tumors located in eloquent areas. Various techniques supply important anatomical and functional information regarding the brain functional organization. Different neuroimaging and neurophysiological techniques can be used to plan a surgical strategy to preserve functional networks and to increase the maximal safe resection. Navigated transcranial magnetic stimulation (nTMS) is a helpful tool for preoperative cortical mapping and planning before surgery of brain tumors located in eloquent areas (1–5). Brain tumors like brain trauma, hematoma, and focal cerebral ischemia can cause brain parenchyma compression that can produce changes in excitation and inhibition, even in the absence of histologically significant cell injury, often manifesting clinically as seizures. The precise mechanism producing seizures after cortical compression remains elusive (6). Recent studies used preoperative nTMS as a

predictor of motor outcome in patients with brain tumors. Rosenstock et al. showed that an abnormal interhemispheric resting motor threshold (RMT) ratio was related to a higher risk for poor postoperative outcome in the 1st week, but not in the following 3 months (7). This proposed stratification model, based on functional–anatomical and neurophysiological measures, could allow quantification of the functional impairment or recovery potential. Several parameters of cortical excitability have been studied in patients with traumatic brain injury (8) and stroke (9). In a recent paper, Neville et al. (10) described an increase in motor threshold (MT) that was paralleled by an alteration in short-latency intracortical inhibition (SICI) and intracortical facilitation (ICF) (10). However, the authors did not check other important parameters of cortical excitability such as short-latency afferent inhibition (SAI), long-latency afferent inhibition (LAI), cortical silent period (CSP), recruitment curve (RC), and interhemispheric inhibition (IHI). The aim of the current study was to further investigate cortical–cortical and cortical–spinal excitability in patients with brain tumors using a more extensive TMS protocol.

MATERIALS AND METHODS

The present study was conducted in accordance with the ethics committee of the University of Messina and the Declaration of Helsinki. Informed consent was obtained from every patient.

Patient Population

The cortical excitability measurements by transcranial magnetic stimulation (TMS) were carried out on 12 consecutive patients with lesions involving the primary motor cortex (M1) and corticospinal tract (CST). Not all 12 patients participated in all cortical excitability measurements (see below). **Table 1** reports all nosographic data and neurological status of patients. Exclusion criteria for brain stimulation were the same as for magnetic resonance imaging (MRI). Patients were examined for handedness, motor impairment, medical history, and use of medication (see **Table 1**). The WHO classification was used for tumor histology (11).

Measures of Cortical Excitability

Patients and controls were seated in a "comfortable reclining chair and surface EMG was recorded from the right or left first dorsal interosseus (FDI) muscle using disposable disc electrodes with a belly-tendon montage. EMG was filtered by Neurolog System supplied by Digitimer with a time constant of 3 ms, and a high pass filter set a 3 kHz." Single or paired pulses were given to the right or left M1 using a standard figure-of-eight coil connected with a single (for single-pulse TMS) or two (for paired-pulse TMS) high-power Magstim 200 stimulators. "Signals were collected via a CED 1401 laboratory interface (Cambridge Electronic Design, Cambridge, UK) and fed to a personal computer for offline analysis" (12).

Threshold Measurements

In 10 patients, we evaluated RMT and active MT (AMT). "RMT was defined as the minimum intensity that evoked a peak-to-peak motor evoked potential (MEP) of 50 μV in at least 5 out of 10 consecutive trials in the relaxed FDI muscle. AMT was defined as the minimum intensity that elicited a reproducible MEP of at least 200 μV in the tonically contracting FDI muscle in at least 5 out of 10 consecutive trials" (13).

Recruitment Curve

In 12 patients, we evaluated input–output RC. "Motor evoked potentials (MEPs) input–output recruitment curve was performed at stimulus intensities ranging from 100 to 150% RMT (in steps of 10%). Fifteen peak-to-peak MEP at each stimulation intensities were averaged" (12).

Intracortical Paired-Pulse Excitability

In 10 patients, we studied SICI and ICF. SICI and ICF were determined according to the paired-pulse method described by Kujirai et al. (14). The intensity of the conditioning stimulus was set at 80% of AMT, while the test stimulus was adjusted to elicit MEPs with amplitudes of 0.5–1.0 mV at baseline (115–125% of RMT in healthy subjects, and ∼140–150% of the RMT in patients with brain tumors). SICI and ICF were assessed at ISIs of 2 and 12 ms, respectively. The mean amplitude of the conditioned MEP was expressed as percentage of the amplitude of the unconditioned MEP. This characterized the strength of SICI and ICF.

Cortical Silent Period

In eight patients, we evaluated CSP. CSP was measured during slight tonic contraction of the right or left FDI muscle at ∼10–15% of maximum force level measurements. The intensity of the test stimulus was 130% of resting MT. The duration of the CSP was measured in each trial (15).

Sensorimotor Intracortical Inhibition

In nine patients, we studied SAI and LAI, which were studied using the conditioning test protocol described by Tokimura et al. (16). The median nerve was stimulated through bipolar electrodes at the wrist (cathode proximal). The intensity was set just approximately three times the perceptual threshold. The intensity of the transcranial test stimulus was adjusted to evoke a muscle response in relaxed abductor pollicis brevis (APB) with a peak-to-peak amplitude of ∼0.5–1 mV (115–125% of RMT in healthy subjects, and ∼140–150% of RMT in patients with brain tumors). SAI and LAI were probed at ISIs of 20, 25, and 200 ms, respectively. The relative change in MEP amplitude induced by the peripheral stimulus was taken as a measure of SAI and LAI.

Interhemispheric Inhibition

"A conditioning-test protocol as described by Ferbert et al. (17) was used to evaluate IHI of the right or left M1. IHI was studied in 8 patients. A conditioning stimulus was applied to the left or right M1, and the test stimulus was applied to the homologous right or left M1. We set the intensity of the first (conditioning) stimulus to obtain an inhibition of the test MEP to about 50% at an ISI of 10 ms. The second (test) stimulus was set at an intensity that, when given alone, would evoke an EMG response of 0.5–1 mV peak-to-peak amplitude (115–125% of RMT in healthy subjects,

TABLE 1 | Summary of patients' epidemiological data.

	Age, sex	Handedness	Tumor location	Neurological examination	Histology	AEDs
#1, DM	51, F	R	MC l, right	Moderate left upper limb weakness	Oligodendroglioma IDH-mutant 1p/19q-codeleted	LEV
#2, BA	38, M	R	MC l left	No deficit	Oligodendroglioma IDH-mutant 1p/19q-codeleted	//
#3, FT	69, F	R	Fronto-temporo-insular, left	No deficit	Glioblastoma IDH-wildtype	//
#4, CS	35, M	R	Fronto-temporo-insular, right	No deficit	Diffuse astrocytoma IDH-wildtype	LEV
#5, CG	46, M	R	Fronto-insular, left	No deficit	Glioblastoma IDH-mutant	//
#6, CT	70, F	R	Fronto-opercular, left	No deficit	Gliobastoma IDH-wildtype	LEV
#7, VA	67, M	R	Fronto-temporal, right	No deficit	Gliobastoma IDH-wildtype	//
#8, CG	46, M	L	Fronto-temporal, right	No deficit	Diffuse astrocytoma IDH-wildtype	//
#9, PN	53, F	R	Fronto-temporal, right	No deficit	Oligodendroglioma NOS	//
#10, MR	60, F	R	Temporo-parietal, left	No deficit	Gliobastoma IDH-wildtype	LEV
#11, MW	36,M	L	Fronto-temporo-insular, right	No deficit	Diffuse astrocytoma IDH-wildtype	LEV
#12, BAG	55,M	R	Temporo-parietal, right	No deficit	Gliobastoma IDH-wildtype	LEV

Nosographic data and neurological status for all 12 consecutive patients with lesions within or close to the precentral gyrus.
MC, motor cortex; LEV, levetiracetam.

∼140–150% of the RMT in patients with brain tumors). IHI was tested at three conditioning-test intervals (8, 9, 10 ms)" (18).

Statistical Analysis

Factorial ANOVA was computed to show differences in RMT; SAI 20 and 25 ms; LAI; SICI; ICF; IHI at 8, 9, and 10 ms; and CSP between the affected hemisphere, unaffected hemisphere, and controls. MEP RCs were evaluated in separate repeated-measures ANOVA in the different sets of subjects. We performed a two-way repeated-measures ANOVA with intensity (six levels: 100, 110, 120, 130,140, 150% of MT) as within-subject factor, and group (three levels: affected hemisphere, unaffected hemisphere, and controls) as between-subjects factor. If appropriate, *post hoc t*-tests were performed. *Post hoc* Fisher's PLSD analysis was executed for RC. Significance was set at $p < 0.05$. Data are given as mean ± standard error of the mean.

RESULTS

No participants reported any adverse effects during or after the study.

Motor Threshold

RMT and AMT were significantly higher in patients than in controls [RMT: $F_{(2,26)} = 4.03$, $p = 0.029$; power = 0.66; AMT: $F_{(2,26)} = 4.1$, $p = 0.028$, power = 0.65] (**Figure 1**). *Post hoc t*-tests revealed relative change only between controls and the affected hemisphere of patients [for RMT: $t_{(1,9)} = 2.6$, $p = 0.017$; for AMT: $t_{(1,9)} = 2.2$, $p = 0.03$].

Recruitment Curve

MEP amplitudes increased with increasing stimulus intensity in controls and patients. However, MEP RC was significantly less steep in patients in both hemispheres compared to controls (**Figure 2**). Indeed, repeated ANOVA indicated a significant effect for intensity [$F_{(2,29)} = 50.9$, $p < 0.0001$; power = 1.0] with a significant interaction between intensity and groups [$F_{(2,29)} = 18.780$, $p < 0.0001$; power = 1.0]. *Post hoc* Fisher's PLSD analysis showed that MEP amplitudes were significantly higher in control subjects compared to the affected ($p < 0.001$) and unaffected hemispheres of patients ($p < 0.001$). On the contrary, there were no differences between the RCs of both affected and unaffected hemispheres ($p = 0.9$) of patients.

Intracortical Paired-Pulse Excitability

Paired-pulse stimulation consistently produced SICI at an ISI of 2 ms and ICF at an interval of 12 ms in controls, but not so well in patients. The data showed a lower degree of inhibition and facilitation in brain tumor patients (**Figure 3**). ANOVA showed a main effect between patients (affected and unaffected hemispheres) and controls for ICI [$F_{(2,27)} = 3.87$, $p = 0.03$; power = 0.65] and ICF [$F_{(2,27)} = 3.58$, $p = 0.042$; power = 0.58]. *Post hoc t*-tests revealed relative change only between controls and affected hemisphere of patients for ICI [$t_{(1,9)} = 4.10$, $p = 0.0006$] and ICF [$t_{(1,9)} = 2.13$, $p = 0.046$], but none between controls and unaffected hemisphere of patients [ICI: $t_{(1,9)} = 1.8$, $p = 0.08$; ICF: $t_{(1,9)} = 1.7$, $p = 0.1$].

Sensorimotor Intracortical Inhibition

ANOVA showed a selective reduction in SAI (20 and 25 ms) but not in LAI (200 ms) (see **Figure 4**). For SAI, there was a

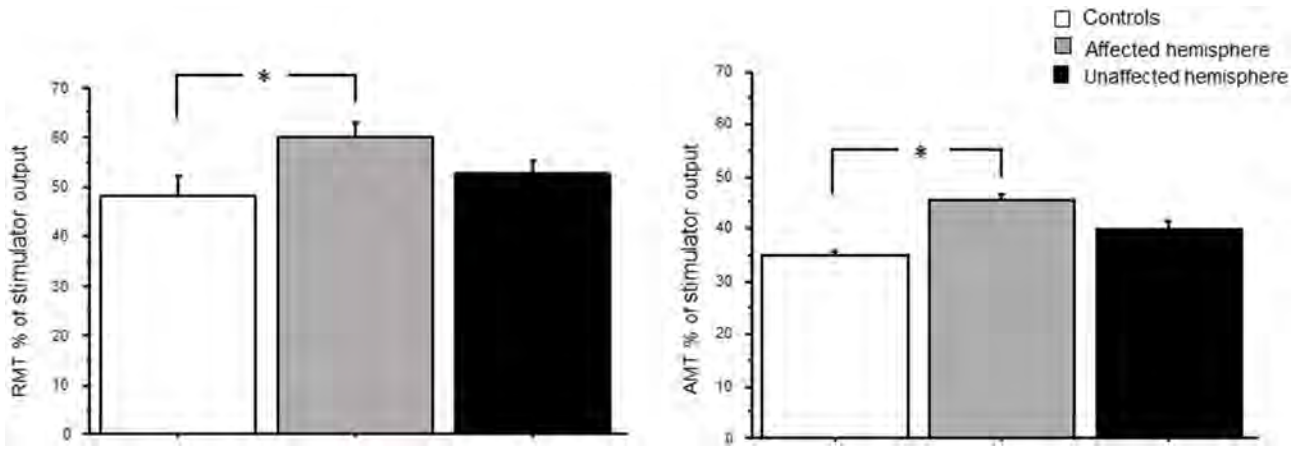

FIGURE 1 | RMT and AMT levels in controls and patients with brain tumors (affected and unaffected hemispheres). RMT and AMT are expressed as % of max output. *$p < 0.05$.

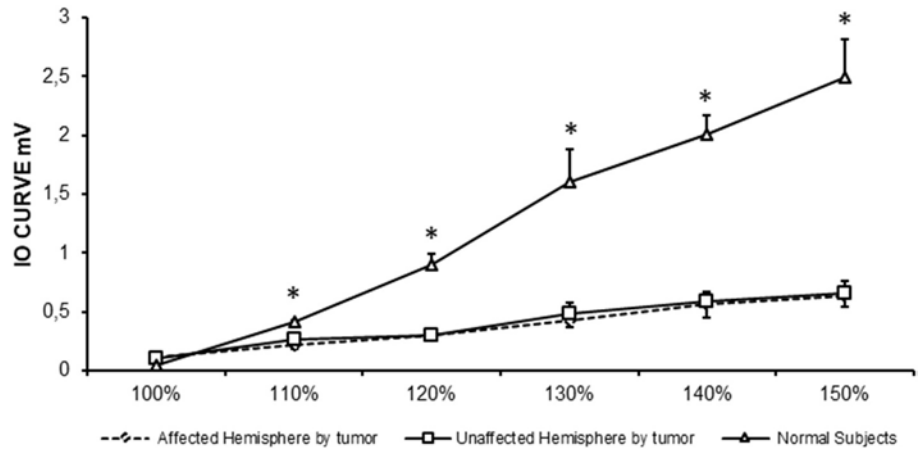

FIGURE 2 | RC in controls and patients with brain tumors (affected and unaffected hemispheres). Stimulus intensities ranging from 100 to 150% RMT (in steps of 10%). *$p < 0.05$.

prominent main effect for ISI at 25 ms [$F_{(2,29)} = 5.33$; $p = 0.01$; power = 0.8] and 20 ms [$F_{(2,29)} = 4.29$; $p = 0.02$; power = 0.7]. *Post hoc t*-tests revealed significant change only between controls and affected hemisphere of patients for SAI at 25 ms [$t_{(1,9)} = 3.6$, $p = 0.0015$] and 20 ms [$t_{(1,9)} = 2.7$, $p = 0.011$]. For LAI, ANOVA demonstrated no main effect [$F_{(2,29)} = 2.7$; $p = 0.08$].

Cortical Silent Period

The duration of CSP did not differ between patients (affected and unaffected hemispheres) and controls [$F_{(2,21)} = 0.75$; $p = 0.48$] (see **Figure 5**).

Interhemispheric Inhibition

Figure 5 shows also the time course of IHI in patients (affected and unaffected hemispheres) and controls. Repeated-measures ANOVA did not reveal a significant interaction between the two main factors of ISI and population for no interval [8 ms: $F_{(2,23)} = 3.17$; $p = 0.07$; 9 ms: $F_{(2,23)} = 2.34$; $p = 0.11$; 10 ms: $F_{(2,23)} = 2.82$; $p = 0.08$].

DISCUSSION

Our data yielded three main findings. First, affected and unaffected hemisphere excitability in patients with brain tumors was reduced compared to healthy controls. Second, SICI, ICF, and SAI were lower in the affected hemisphere. Third, IHI, LAI, and CSP showed no differences between patients and healthy controls. These findings indicate that the effects of brain tumors on cortical excitability are mostly localized to the affected hemisphere.

Effects on Corticospinal Excitability

MT is an indicator of cortical excitability reflecting membrane excitability (19). In our study, RMT and AMT were significantly

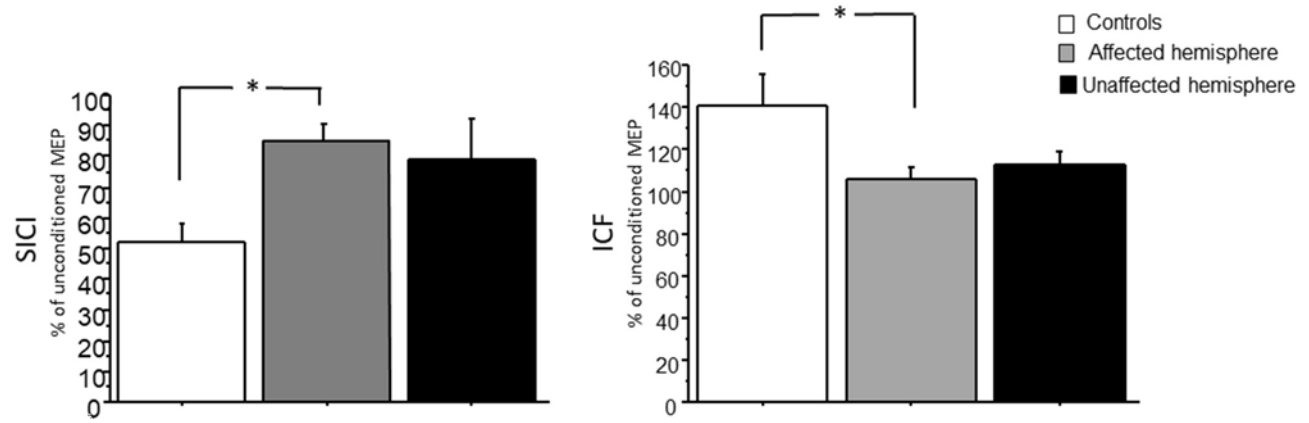

FIGURE 3 | SICI and ICF in controls and patients with brain tumors (affected and unaffected hemispheres). Mean amplitude of the conditioned MEP was expressed as percentage of the amplitude of the unconditioned MEP. The relative change in MEP amplitude induced by the conditioning stimulus characterized the strength of SICI and ICF. *$p < 0.05$.

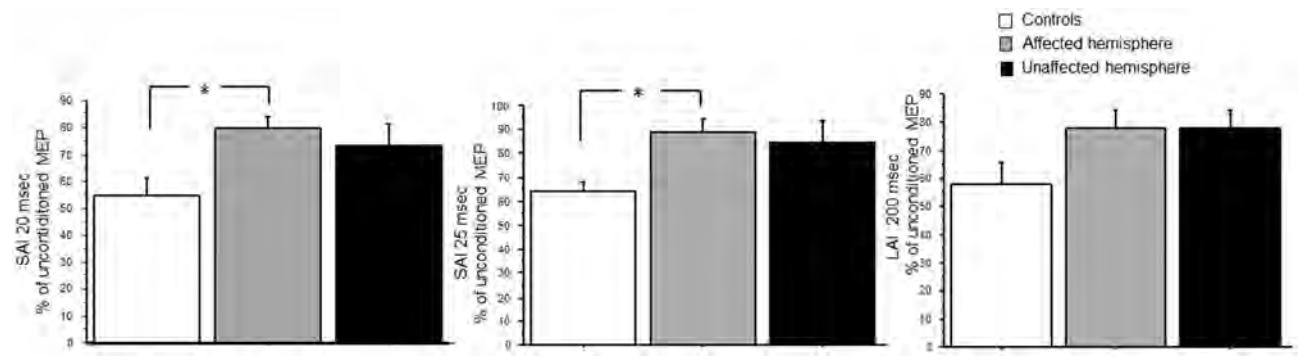

FIGURE 4 | SAI at 20 and 25 ms, LAI at 200 ms in controls and patients with brain tumors (affected and unaffected hemispheres). The relative change in MEP amplitude induced by the peripheral stimulus was taken as a measure of SAI and LAI. *$p < 0.05$.

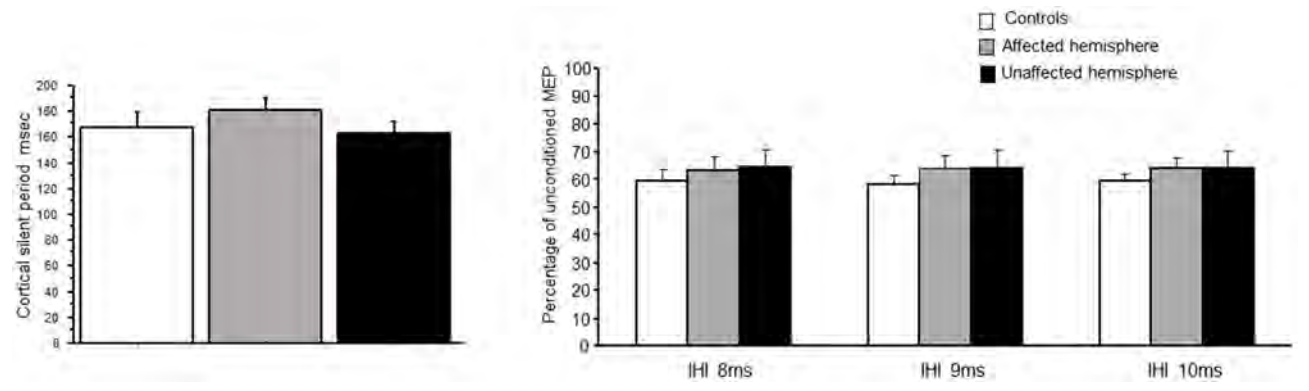

FIGURE 5 | CSP and IHI at 7, 8, and 9 ms in controls and patients with brain tumors (affected and unaffected hemispheres).

higher in patients, especially in the affected hemisphere, than in healthy controls. This result may be due to a reduced density and number of corticospinal neurons in relation to motor impairment. However, in our study, only one patient had a moderate left upper limb weakness. In addition, higher MT may predict a poor motor outcome in patients with brain tumors (20). Picht et al. speculated that patients initially without hemiparesis but with high RMT were at a higher risk in the

long term of a decline in motor function (20). Rosenstock et al. studied abnormal RMT interhemispheric ratio was related to a higher risk for poor postoperative outcome in the 1st week, but not in the following 3 months (7). Similar to previous findings, Neville et al. reported an increase in MT in patients with brain tumors (10). Furthermore, in stroke patients, Swayne et al. (21) demonstrated that corticospinal excitability of the affected hemisphere, measured as AMT and RMT, increased in the acute phase, but this increment became weaker at 3 months and it continued for 6 months (chronic phase of stroke). The authors concluded that, in the chronic phase of stroke, the motor function could be dependent on the reorganization of alternative cortical networks (21). Moreover, our data show that MEP RC was significantly less steep in patients in both hemispheres compared to controls. RC illustrates a graded profile of cortical spinal tract (CST) function, providing a more global measure of cortical excitability than MT (22). Alterations in the slope of the RC can predict more substantial CST damage, motor impairment, and poor recovery in patients with brain injury (23). RCs are widely used in stroke because they are believed to reflect CST gain and output from the primary motor cortex (24). In our study, MEP RC was significantly less steep in patients in both hemispheres compared to controls. Experimental data in animal model suggest that glioma cells release high amounts of glutamate resulting in excitotoxicity and tumor invasion (25, 26). Therefore, it is likely that excitotoxicity at a chronic stage may result in a significant loss of motor neurons within primary motor area and a loss of CSTs as indexed by the increase in RMT and AMT and by the reduced slope of RC. The excitotoxicity promoted by infiltrating glioma cells may also in turn affect fast-spiking $GABA_A$ interneurons, and a reduced GABA availability may create a vicious circle where increased pyramidal neurons firing amplify glutamate excitotoxicity (27), producing neuronal cell death (see below).

Effects on Cortical Excitability

We showed that SICI, ICF, and SAI are reduced in the affected hemisphere compared to the unaffected and healthy controls. On the other hand, there were no significant differences of LAI and CSP between patients and healthy controls. SICI is mediated by $GABA_A$ receptors, while CSP is a marker for the excitability of long-lasting (presumably $GABA_B$) intracortical interneurons. Conversely, ICF is mediated by glutamate and is associated with excitatory cortical circuits (28–30). In a case report, only the lack of inhibition, assessed by SICI, had been demonstrated in two patients with focal motor seizures caused by a circumscribed glioblastoma or metastasis (31). The results of our study are in agreement with similar findings of Neville et al., who reported an alteration of SICI and ICF in the affected hemisphere (10). The novel finding of a reduced SICI and ICF in the affected hemisphere could be caused by the simultaneous selective reduction in $GABAergic_A$ inhibition and glutamatergic excitation because of either reduced excitability or loss of inhibitory/excitatory neurons or changes in GABAergic/glutamatergic receptor function. The presence of a disruption of $GABA_A$ mechanisms in the affected hemisphere could explain the high percentage of seizures (50%) in our population. On the other hand, this disinhibition could also be an adaptive plastic mechanism recruited by the affected hemisphere to counteract the reduced overall excitability caused by tumor-related brain edema and swelling (see above). These findings parallel evidences in stroke patients where SICI is reduced in the affected hemisphere in the first 6 months with normal CSP and may contribute to cortical reorganization and recovery (32).

This reduced $GABA_A$ intracortical inhibition is in line with several findings coming from the bench side. The largest class (40–50%) of GABAergic interneurons is represented by fast-spiking, parvalbumin-positive cells, which are present in all layers and form synapses on the soma and proximal dendrites of pyramidal cells (33). Several pieces of evidence in animal models have demonstrated a loss of fast-spiking interneurons, and more in general a reduced firing rate in the peritumoral glioma area (34). This dysfunction of fast-spiking GABAa interneurons is critically involved in tumor-associated epileptic seizures (34).

Interestingly, it has been demonstrated that the selective optogenetic stimulation of parvalbumin-positive $GABA_A$ interneurons induces a significant reduction in glioma cell proliferation (27). Human glioblastoma cells may express functional $GABA_A$ receptors, and that endogenous GABA release may attenuate tumor proliferation (35). On the other hand, pyramidal cell stimulation enhances cell proliferation in tumor mass (36). It is likely that fast-spiking $GABA_A$ interneuron vulnerability to tumor-induced excitotoxicity may trigger a vicious circle where reduced GABA availability may increase pyramidal neuron firing, producing an enhanced tumor growth. Future studies in humans are needed to better understand the relationship of SICI with tumor proliferation.

Another important finding was a selective reduction in SAI (20 and 25 ms) but not in LAI (200 ms) in the affected hemisphere. LAI and SAI are mediated through different sensorimotor circuits. SAI is controlled by muscarinic neurotransmission (37). LAI is significantly understudied compared to SAI, and the neural circuitries underlying these phenomena are unclear (38). SAI has been used to assess and predict functional recovery following ischemic stroke, where larger SAI reductions correlate with improved long-term recovery 6 months following injury (39). The presence of a reduced SAI in the affected hemisphere of patients with brain tumor needs to be better investigated in future longitudinal studies, especially in low-grade glioma, to see if SAI reduction is heralding a good recovery after surgical operation.

Effects on IHI

Our study demonstrates no differences in IHI between patients and controls. The normalcy of IHI confirms previous evidence suggesting that a physiological interplay between the two primary motor cortices is required to maintain a good motor function in patients with brain tumor (40). In a very elegant study, brain connectivity was measured in patients with glioma using task-free functional MRI to probe motor networks. Patients with motor weakness showed reduced interhemispheric and left primary motor cortex and the right premotor area connectivity compared to healthy controls. Conversely, in patients without motor deficit, motor performance assessed on the grooved

pegboard was not related to interhemispheric connectivity, which was unchanged but correlated with ipsilateral connectivity between the premotor area and supplementary motor area (40).

The absence of motor impairment in our cohort of patients could be explained by the normalcy of transcallosal connection evaluated using the IHI. Indeed, Otten et al. showed that an integrity of transcallosal pathway between the two motor areas is needed to maintain a normal motor function (40). Since TMS is a non-invasive technique, future longitudinal studies are warranted to explore the role of IHI to predict motor outcome in patients with brain tumor.

CONCLUSIONS

This study investigates cortical–cortical and cortical–spinal excitability in patients with brain tumors using a more extensive TMS protocol. Different measurements of cortical excitability are abnormal in brain hemispheres affected by tumors, but further studies are needed to determine their relationship to motor impairment and subsequent motor recovery. Finally, it will be important to explore the correlation between brain tumor molecular features and the impairment of cortical excitability in a lager sample population.

DATA AVAILABILITY STATEMENT

The raw data supporting the conclusions of this article will be made available by the authors, without undue reservation.

ETHICS STATEMENT

The studies involving human participants were reviewed and approved by AOU G. Martino. The patients/participants provided their written informed consent to participate in this study.

AUTHOR CONTRIBUTIONS

CT, GR, GM, SC, and FA contributed to the acquisition, analysis and interpretation of data, and writing of the first draft. VR and AQ were responsible for the conception and design, data acquisition, analysis and interpretation as well as the review, and critique of the manuscript. MQ, PG, and AG contributed to interpretation of data and the review and critique of the final manuscript. All authors contributed to the article and approved the submitted version.

REFERENCES

1. Hervey-Jumper SL, Berger MS. Role of surgical resection in low- and high-grade gliomas. *Curr Treat Options Neurol.* (2014) 16:284. doi: 10.1007/s11940-014-0284-7
2. Rizzo V, Terranova C, Crupi D, Sant'angelo A, Girlanda P, Quartarone A. Increased transcranial direct current stimulation after effects during concurrent peripheral electrical nerve stimulation. *Brain Stimul.* (2014) 7:113–21. doi: 10.1016/j.brs.2013.10.002
3. Raffa G, Scibilia A, Conti A, Ricciardo G, Rizzo V, Morelli A, et al. The role of navigated transcranial magnetic stimulation for surgery of motor-eloquent brain tumors: a systematic review and metaanalysis. *Clin Neurol Neurosurg.* (2019) 180:7–17. doi: 10.1016/j.clineuro.2019.03.003
4. Raffa G, Scibilia A, Conti A, Cardali SM, Rizzo V, Terranova C, et al. Multimodal surgical treatment of high grade gliomas in the motor area: the impact of the combination of navigated transcranial magnetic stimulation and fluorescein-guided resection. *World Neurosurg.* (2019) 128:e378–90. doi: 10.1016/j.wneu.2019.04.158
5. Raffa G, Quattropani MC, German,ò A. When imaging meets neurophysiology: the value of navigated transcranial magnetic stimulation for preoperative neurophysiological mapping prior to brain tumor surgery. *Neurosurg Focus.* (2019) 47:E10. doi: 10.3171/2019.9.FOCUS19640
6. Ming-Chieh D, Wang Q, Lo EH, Stanley GB. Cortical excitation and inhibition following focal traumatic brain injury. *J Neurosci.* (2011) 31:14085–94. doi: 10.1523/JNEUROSCI.3572-11.2011
7. Rosenstock T, Grittner U, Acker G, Schwarzer V, Kulchytska N, Vajkoczy P, et al. Risk stratification in motor area-related glioma surgery based on navigated transcranial magnetic stimulation data. *Neurosurg.* (2017) 126:1227–37. doi: 10.3171/2016.4.JNS152896
8. Hayashi CY, Neville IS, Rodrigues PA, Galhardoni R, Brunoni AR, Zaninotto AL, et al. Altered intracortical inhibition in chronic traumatic diffuse axonal injury. *Front Neurol.* (2018) 9:189. doi: 10.3389/fneur.2018.00189
9. McDonnell MN, Stinear CM. TMS measures of motor cortex function after stroke: A meta-analysis. *Brain Stimul.* (2017) 10:721–34. doi: 10.1016/j.brs.2017.03.008
10. Neville IS, Gomes Dos Santos A, Almeida CC, Hayashi CY, Solla DJF, Galhardoni R, et al. Evaluation of changes in preoperative cortical excitability by navigated transcranial magnetic stimulation in patients with brain tumor. *Front Neurol.* (2021) 11:582262. doi: 10.3389/fneur.2020.582262
11. Louis DN, Perry A, Reifenberger G, von Deimling A, Figarella-Branger D, Cavenee WK, et al. The 2016 world health organization classification of tumors of the central nervous system: a summary. *Acta Neuropathol.* (2016) 131:803–20. doi: 10.1007/s00401-016-1545-1
12. Rizzo V, Crupi D, Bagnato S, Quartarone A, Benvenga S, Bartolone L, et al. Neural response to transcranial magnetic stimulation in adult hypothyroidism and effect of replacement treatment. *J Neurol Sci.* (2008) 266:38–43 doi: 10.1016/j.jns.2007.08.031
13. Rizzo V, Terranova C, Conti A, Germanò A., Alafaci C, Raffa G, et al. Preoperative functional mapping for rolandic brain tumor surgery. *Neurosci Lett.* (2014) 583:136–41. doi: 10.1016/j.neulet.2014.09.017
14. Kujirai T, Caramia MD, Rothwell JC, Day BL, Thompson PD, Ferbert A,Wroe S, et al. Corticocortical inhibition in human motor cortex. *J Physiol.* (1993) 471:501–19. doi: 10.1113/jphysiol.1993.sp019912
15. Orth M, Rothwell JC. The cortical silent period: intrinsic variability and relation to the waveform of the transcranial magnetic stimulation pulse. *Clin Neurophysiol.* (2004) 115:1076–82. doi: 10.1016/j.clinph.2003.12.025
16. Tokimura H, Di Lazzaro V, Tokimura Y, Oliviero A, Profice P, Inolsa A, et al. Short latency inhibition of human hand motor cortex by somatosensory input from the hand. *J Physiol.* (2000) 523:503–13. doi: 10.1111/j.1469-7793.2000.t01-1-00503.x
17. Ferbert A, Priori A, Rothwell JC, Day BL, Colebatch JG, Marsden CD. Interhemispheric inhibition of the human motor cortex. *J Physiol.* (1992) 453:525–46. doi: 10.1113/jphysiol.1992.sp019243
18. Gilio F, Rizzo V, Siebner HR, Rothwell JC. Effects on the right motor hand-area excitability produced by low-frequency rTMS over human contralateral homologous cortex. *J Physiol.* (2003) 551:563–73. doi: 10.1113/jphysiol.2003.044313
19. Wassermann EM. Variation in the response to transcranial magnetic brain stimulation in the general population. *Clin Neurophysiol.* (2002) 113:1165–71. doi: 10.1016/S1388-2457(02)00144-X
20. Picht T, Strack V, Schulz J, Zdunczyk A, Frey D, Schmidt S, et al. Assessing the functional status of the motor system in brain tumor patients using transcranial magnetic stimulation. *Acta Neurochir (Wien).* (2012) 154:2075–81. doi: 10.1007/s00701-012-1494-y

21. Swayne OB, Rothwell JC, Ward NS, Greenwood RJ. Stages of motor output reorganization after hemispheric stroke suggested by longitudinal studies of cortical physiology. *Cereb Cortex.* (2008) 18:1909–22. doi: 10.1093/cercor/bhm218
22. Thickbroom GW, Byrnes ML, Archer SA, Mastaglia FL. Motor outcome after subcortical stroke: MEPs correlate with hand strength but not dexterity. *Clin Neurophysiol.* (2002) 113:2025–9. doi: 10.1016/S1388-2457(02)00318-8
23. Talelli P, Greenwood RJ, Rothwell JC. Arm function after stroke: neurophysiological correlates and recovery mechanisms assessed by transcranial magnetic stimulation. *Clin Neurophysiol.* (2006) 117:1641–59. doi: 10.1016/j.clinph.2006.01.016
24. Devanne H, Lavoie BA, Capaday C. Input-output properties and gain changes in the human corticospinal pathway. *Exp Brain Res.* (1997) 114:329–38. doi: 10.1007/PL00005641
25. Marcus HJ, Carpenter KL, Price SJ, Hutchinson PJ. In vivo assessment of high-grade glioma biochemistry using microdialysis: a study of energy-related molecules, growth factors and cytokines. *J Neurooncol.* (2010) 97:11–23. doi: 10.1007/s11060-009-9990-5
26. Sontheimer HJ. A role for glutamate in growth and invasion of primary brain tumors. *Neurochem.* (2008) 105:287–95. doi: 10.1111/j.1471-4159.2008.05301.x
27. Tantillo E, Vannini E, Cerri C, Spalletti C, Colistra A, Mazzanti CM, et al. Differential roles of pyramidal and fast-spiking, GABAergic neurons in the control of glioma cell proliferation. *Neurobiol Dis.* (2020) 141:104942. doi: 10.1016/j.nbd.2020.104942
28. Bowden JL, Taylor JL, McNulty PA. Voluntary activation is reduced in both the more-and less-affected upper limbs after unilateral stroke. *Front Neurol.* (2014) 5:239. doi: 10.3389/fneur.2014.00239
29. Di Lazzaro V, Restuccia D, Oliviero A, Profice P, Ferrara P, Insola A, et al. Magnetic transcranial stimulation at intensities below active motor threshold activates intracortical inhibitory circuits. *Exp Brain Res.* (1998) 119:265–8. doi: 10.1007/s002210050341
30. Nakamura H, Kitagawa H, Kawaguchi Y, Tsuji H. Intracortical facilitation and inhibition after transcranial magnetic stimulation in conscious humans. *J Physiol.* (1997) 498:817–23. doi: 10.1113/jphysiol.1997.sp021905
31. Irlbacher K, Brandt SA, Meyer BU. In vivo study indicating loss of intracortical inhibition in tumor-associated epilepsy. *Ann Neurol.* (2002) 52:119–22. doi: 10.1002/ana.10229
32. Honaga K, Fujiwara T, Tsuji T, Hase K, Ushiba J, Liu M. State of intracortical inhibitory interneuron activity in patients with chronic stroke. *Clin Neurophysiol.* (2013) 124:364–70. doi: 10.1016/j.clinph.2012.08.005
33. Lim L, Mi D, Llorca A, Marín O. Development and functional diversification of cortical interneurons. *Neuron.* (2018) 100:294–313. doi: 10.1016/j.neuron.2018.10.009
34. Tewari BP, Chaunsali L, Campbell SL, Patel DC, Goode AE, Sontheimer H. Perineuronal nets decrease membrane capacitance of peritumoral fast spiking interneurons in a model of epilepsy. *Nat Commun.* (2018) 9:4724. doi: 10.1038/s41467-018-07113-0
35. Blanchart A, Fernando R, Häring M, Assaife-Lopes N, Romanov RA, Andäng M, et al. Endogenous GABAA receptor activity suppresses glioma growth. *Oncogene.* (2017) 36:777–86. doi: 10.1038/onc.2016.245
36. Venkatesh HS, Johung TB, Caretti V, Noll A, Tang Y, Nagaraja S, et al. Neuronal activity promotes glioma growth through neuroligin-3 secretion. *Cell.* (2015) 161:803–16. doi: 10.1016/j.cell.2015.04.012
37. Di Lazzaro V, Oliviero A, Profice P, Pennisi,MA., Di Giovanni S, Zito G, et al. Muscarinic receptor blockade has differential effects on the excitability of intracortical circuits in the human motor cortex. *Exp Brain Res.* (2000) 135:455–61. doi: 10.1007/s002210000543
38. Turco CV, El-Sayes J, Savoie MJ, Fassett HJ, Locke MB, Nelson AJ. Short- and long-latency afferent inhibition; uses, mechanisms and influencing factors. *Brain Stimul.* (2018) 11:59–74. doi: 10.1016/j.brs.2017.09.009
39. Di Lazzaro V, Profice P, Pilato F, Capone F, Ranieri F, Florio L, et al. The level of cortical afferent inhibition in acute stroke correlates with long-term functional recovery in humans. *Stroke.* (2012) 43:250–2. doi: 10.1161/STROKEAHA.111.631085
40. Otten ML, Mikell CB, Youngerman BE, Liston C, Sisti MB, Bruce JN, et al. Motor deficits correlate with resting state motor network connectivity in patients with brain tumours. *Brain.* (2012) 135:1017–26. doi: 10.1093/brain/aws041

Conflict of Interest: The authors declare that the research was conducted in the absence of any commercial or financial relationships that could be construed as a potential conflict of interest.

Advantages of publishing in Frontiers

OPEN ACCESS
Articles are free to read for greatest visibility and readership

FAST PUBLICATION
Around 90 days from submission to decision

HIGH QUALITY PEER-REVIEW
Rigorous, collaborative, and constructive peer-review

TRANSPARENT PEER-REVIEW
Editors and reviewers acknowledged by name on published articles

Frontiers
Avenue du Tribunal-Fédéral 34
1005 Lausanne | Switzerland

Visit us: www.frontiersin.org
Contact us: frontiersin.org/about/contact

REPRODUCIBILITY OF RESEARCH
Support open data and methods to enhance research reproducibility

DIGITAL PUBLISHING
Articles designed for optimal readership across devices

FOLLOW US
@frontiersin

IMPACT METRICS
Advanced article metrics track visibility across digital media

EXTENSIVE PROMOTION
Marketing and promotion of impactful research

LOOP RESEARCH NETWORK
Our network increases your article's readership